NASA Conference Publication 2052
Part II

Helicopter Acoustics

Proceedings of an International
Specialists Symposium held at
NASA Langley Research Center
Hampton, Virginia
May 22-24, 1978
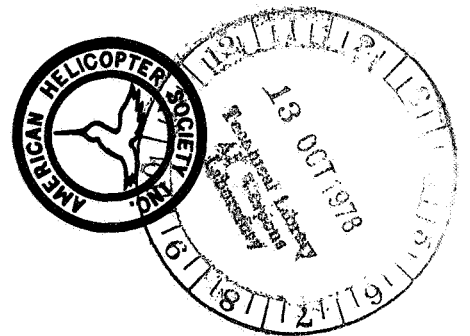
NASA Conference Publication 2052
Part II

Helicopter Acoustics

Proceedings of an International
Specialists Symposium sponsored
by the American Helicopter Society,
Washington, D.C.; the U.S. Army
Research Office, Durham, North
Carolina; and the Langley Research
Center, Hampton, Virginia, and
held at Langley Research Center
May 22-24, 1978

NASA

National Aeronautics
and Space Administration

Scientific and Technical
Information Office

1978

PREFACE

The papers included herein were presented at the International Specialists Symposium on Helicopter Acoustics which was held at the NASA Langley Research Center on May 22-24, 1978. The symposium was jointly sponsored by the American Helicopter Society, the U.S. Army Research Office, and the NASA Langley Research Center. Exterior and interior noise problems were addressed both from the physics and engineering as well as the human factors points of view.

The objective of the symposium was to explore the role of technology in closing the gap between what the customers and the regulating agencies would like to have and what is currently available. In this regard, papers were presented on noise regulation concepts, human factors and criteria, rotor noise generation and control, design, operations and testing for noise control, helicopter noise prediction and research tools and measurements. There was active participation by attendees from a number of foreign countries.

The included papers are largely as submitted as camera-ready copy at the time of the symposium. Only minor editorial changes have been performed and a title page and abstract have been added. The assistance of the Scientific and Technical Information Programs Division of the NASA Langley Research Center in publishing these proceedings is gratefully acknowledged.

Use of manufacturers or identification of commercial products in this report does not constitute an official endorsement of such manufacturers or products, either expressed or implied, by the National Aeronautics and Space Administration.

CONTENTS

Part I*

*Papers 1 to 19 are presented under separate cover.

PART II

HUMAN FACTORS AND CRITERIA

STATE OF THE ART

SESSION REVIEWS

SUBJECTIVE EVALUATION OF HELICOPTER

BLADE SLAP NOISE

William J. Galloway
Bolt Beranek and Newman Inc.

SUMMARY

Several methods for adjusting EPNL to account for its underestimate of judged annoyance are applied to eight helicopter flyover noise signatures having various degrees of blade slap. A proposal from an ISO working group for making such adjustments is investigated for these data as well as two sets of data submitted by France to the ICAO Committee on Aircraft Noise, Working Group B. When all data are combined, the ISO proposal is little better than simply adding an arbitrary fixed adjustment of 3 decibels to EPNL.

INTRODUCTION

Means for measurement of the physical characteristics of impulsive noise produced by helicopter blade slap and accounting for the underestimate of judged annoyance by EPNL have been studied by a number of groups in Europe and the USA over the last few years. Working Group 2 on Aircraft Noise of ISO TC43/SC1, Acoustics/Noise, has considered a number of possible measurement and assessment procedures at the request of ICAO/CAN/WGB for use in its development of noise certification procedures for helicopters. A draft proposal for an impulsive noise correction procedure emerged from ISO in January 1978 and has been circulated for comment. The procedure is based on a digital analysis of the flyover signal.

The basic psychoacoustical data used to derive the ISO proposal were obtained from a combination of steady state and simulated helicopter blade slap noises. This paper describes the investigation of the ability of an analog analysis of a number of simulated noises and eight recorded noise signatures from actual helicopters, as well as the use of the ISO and other digitally based procedures, to account for the results of psychoacoustical judgments of these signals. Comparisons of the application of the ISO procedures to the eight recorded helicopter noise signals and to two sets of French data on simulated helicopters are made for the separate data sets and to the aggregated data.

ABBREVIATIONS AND SYMBOLS

Abbreviations

ISO   International Standardization Organization

ICAO   International Civil Aviation Organization

EPNL   effective perceived noise level

PNLT   tone-corrected perceived noise level

Rep.   repetition

TSC   Transportation Systems Center

Symbols

CF   crest factor, decibels

CF_M maximum value of CF over an event, decibels

$\overline{CF}_{0.5}$ logarithmic average over an event of crest factors
              obtained for each 0.5 second of the event, decibels

CI   French impulse coefficient

I   ISO impulse factor derived from sampled voltages

r   product moment correlation coefficient

V_i voltage sampled at ith time increment

Δ_C calculated additive adjustment to EPNL, decibels

Δ_S subjective difference between judged and measured
              EPNL, decibels

MEASURES OF IMPULSIVENESS

The psychoacoustical study reported in reference 1 investigated the use of several analog and digital measures of impulsiveness that had been proposed in the ISO working group. Since the time of that report the ISO proposal has emerged as a coalescence of two proposals, one from the National Physical Laboratory in England and the other from France. The two computational procedures results in impulse measures that differ only by a subtractive constant of unity when based on the same digital sampling intervals and integration times. In this paper both the ISO proposal and the last French proposal are used, since the transfer functions between the impulsiveness measures and the subjective corrections to EPNL are different. In addition to the digital techniques, several analog measures of crest factor were used in the analysis of the subjective data in reference 1.

In all the procedures the basic concept is to derive an adjustment factor, for each 0.5 second interval of the flyover, which is added to the measured value of tone-corrected perceived noise level (PNLT) for that 0.5 second interval, before integrating (summing) over the event to obtain EPNL. The differences between the impulse adjustment procedures lie in how the adjustment increment is determined for each 0.5 second interval.

Digital Analyses

The noise signal voltage is A-weighted, passed through a 2000 Hz low pass anti-aliasing filter, then digitally sampled at 5000 (or an integer multiple of 5000) samples per second. In the French proposal the 2500 samples in each 0.5 second interval are combined to determine an impulsiveness coefficient CI (ref. 2):

$$CI = \frac{\frac{1}{2500} \sum_{i=1}^{2500} V_i^4}{\left[\frac{1}{2500} \sum_{i=1}^{2500} V_i^2\right]^2} \tag{1}$$

Note that the denominator is the square of the mean-square voltage during the time interval, denoted in the ISO procedure as "S". In the ISO procedure, the impulsiveness quality I is calculated from the same sampled data (ref. 3):

$$I = \frac{1}{2500} \sum_{i=1}^{2500} \left[\frac{V_i^2 - S}{S} \right]^2 \qquad (2)$$

Thus, $CI = I + 1$.

The values of CI and I are converted through transfer functions to decibel adjustments, Δ, which are added to the PNLT values in the same time interval. The form of these transfer functions has varied at different times during their evolution. In each case the aim was to develop a function that would empirically fit the then available subjective data and, at the same time, have a zero adjustment for "non-impulsive" noise, such as that produced by conventional jet aircraft. The current forms (refs. 2 and 3) of the transfer functions may be expressed as:

$$\text{French:} \quad \Delta = -6.875 + 13.75 \log_{10} CI$$

$$\text{ISO:} \quad \Delta = -2.4 + 8 \log_{10} I \qquad (3)$$

where Δ is restricted to $0 \leq \Delta \leq 5.5$.

Analog Analysis

A classical way to describe the impulsiveness of a signal is through its crest factor, its peak-to-rms ratio. Expressed in decibels, where L_{pk} is the peak sound pressure level, and L is the mean square sound pressure level, crest factor $CF = L_{pk} - L$. For random noise CF is of the order of 12 decibels and, for severe helicopter blade slap, may be as high as 20 or more decibels, depending upon what, if any, frequency-weighting is employed. As a measure of helicopter blade slap, Leverton has proposed the crest factor measured in the 250 Hz octave band, while a number of different investigators have used A-weighted sound level crest factors.

In this study A-weighted sound level crest factor in decibels is used, as measured with a B&K 2209 sound level meter. In making peak measurements the instrument uses a 10 microsecond RC detector with a resetable peak hold circuit and provides accurate sound level measurements for crest factors of more than 30 decibels. Two different crest factors have been used in the study. The simplest is the maximum crest factor measured during a flyover, irrespective of when it occurred, and is abbreviated as CF_M. A more complex measure is the mean-square average of the separate maximum crest factors obtained in each 0.5 second interval of the flyover, abbreviated as $\overline{CF}_{0.5}$.

SUMMARY OF SUBJECTIVE TESTS

A complete description of these experiments is provided in reference 1. A brief summary is provided here.

Steady-State Synthesized Signals

Eight different signals were constructed for judgement against two different non-impulsive signals. All signals had durations of 10 seconds at constant level, with 0.5 second on and off ramps. Three different non-impulsive noise spectra were used to represent different helicopter spectra. The first non-impulsive noise was a replica of the signal reported by Fuller in experiments at the National Physical Laboratory (NPL), in England (ref. 4). The other two were representative of the spectra of large multi-bladed and smaller two-bladed helicopters. Impulsive noise simulations were made by mixing single sine wave pulses, repeated at a specified repetition rate, with the broad-band non-impulsive "background" spectra. The signals may be described by the "background" non-impulsive spectrum, the fundamental frequency of the sine pulse, the frequency of the pulse repetition rate, and the level difference in decibels between the peak sound pressure level of the sine pulses to the overall sound pressure level of the non-impulsive spectrum. (Note that this is not the crest factor for the combined signals.)

Time-Varying Synthesized Signals

Six of the steady-state signals were modified to become time varying simulations of flyover signals by use of a variable gain amplifier to provide a trapezoidal time pattern in which the overall signal level was increased at a rate of 2 decibels per second to a maximum level, held for 2 seconds, then decreased in level at a decay rate of 2 decibels per second (providing signals 12 seconds wide at the points in the time pattern that are 10 decibels below the maximum level).

In order to simulate the effect of directivity on impulse noise during a flyover, two of the signals were further modified to fadeout the impulsive part of the signal during the 2 second maximum level portion of the time pattern. Thus these signals had impulsive content on the increasing level portion of the signal and no impulses on the decaying portion of the signal, as in the case with most actual helicopter noise signatures.

Recorded Helicopter Noise Signals

Nine recorded helicopter signals were selected from those obtained in a comprehensive measurement program conducted by FAA/TSC to define the noise characteristics produced by a variety of helicopters during level flyover and approach maneuvers under consideration for noise certification. The signals used in the psychoacoustical tests were chosen to represent the range of helicopter designs and sizes currently in operation that produce significantly audible blade slap, with one signal having negligible blade slap chosen as a comparison signal (S-61 in level flight). The general characteristics of the signals selected and the operational conditions under which they were produced are described in detail in reference 5. The events used in this study are listed in table 1.

Experimental Facilities

All stimuli were presented to subjects seated, one at a time, in an anechoic chamber. The individual test signals were recorded on individual magnetic tape loops that could be selected at will through computer control. The playback system frequency response was equalized so that the signal as measured at the listener's head position reproduced the signal spectrum of the original recording. The signal levels used in all presentations were measured in EPNL, as calculated from real-time analyses of the signals obtained at the listener's head position, using the procedures of FAR Part 36/ICAO Annex 16. Particular attention was paid to insure that the analysis system properly measured the rms levels of the signals with high crest factors.

Test Subjects

Twenty college students between the ages of 18 and 32 were used as subjects. Half of these were women and half were men. All subjects were audiometrically screened to assure that they were within 20 decibels of ISO defined normal hearing.

Test Procedure

Each listener was asked to choose which of two sequentially reproduced signals was more annoying. For each test stimulus the experimental procedure, called PEST (Parameter Estimation of Sequential Testing), in an iterative manner controlled by a computer, varied the level of a comparison stimulus in a succession of trials until the subject's responses indicated that the test stimulus was subjectively equal to the standard

stimulus. The computer program randomizes the order of presentation of the two signals and varies the level of the test stimulus in both increasing and decreasing fashion to obtain a convergence in the judgements from the subject. The convergence criterion used in these tests was 1 decibel, and the allowed upper limit in number of trials was 30. The 20 subjects used an average of approximately 10 trials each to reach stable judgements for the subjective equality between the test and standard stimuli. The difference in EPNL between the test and comparison stimuli, averaged over all subjects, was used as the measure of the subjective underestimate of blade slap by EPNL.

Although the order of presentation of the different test stimuli was randomized between subjects, all subjects were given a pretest training session during which they were asked to judge one of the NPL test noises against itself. The average difference in judgements for this test was 0.4 decibels, with a standard error in the mean of 0.3 decibels.

In all tests the fixed level signal was reproduced at a nominal EPNL value of 80 decibels. The comparison signal level could be varied as much as 30 decibels above and below this level.

SUMMARY OF RESULTS

The subjects, on average, judged impulsive signals to be more annoying than non-impulsive signals by up to 7 decibels. On the other hand, non-impulsive signals of substantially different spectral shape were equated on an EPNL basis within 0.1 to 0.4 decibel, on average. The standard errors in the mean (20 subjects) ranged from 1.0 to 1.8, for all signals, and from 1.0 to 1.4 for just the helicopters. For the small number of subjects, these standard errors are very acceptable.

A physical analysis of each signal was made to calculate the various impulsiveness measures. Adjustment factors for PNLT were computed according to the proposed transfer functions, added to PNLT values, and EPNL re-computed for each signal. The difference in EPNL with and without the impulse adjustment was then compared to the judged differences. The differences between EPNL computed with crest factors added to PNLT and without were compared directly with the judgements.

The results of the comparisons between calculated and judged values were discouraging when all signals were compared as a set. In essence, the comparisons were uncorrelated, with the best measure accounting for less than 20 percent of the variance

in a linear regression analysis ($r^2 = 0.18$). When only the eight helicopters were considered as a subset the picture improved, for the French CI proposal, with $r^2 = 0.69$. The crest factor measures did not improve, with $r^2 = 0.17$. Scatter diagrams and the regression lines of Δ_S on Δ_C are shown in figure 1 for the French procedure and in figure 2 for $\overline{CF}_{0.5}$.

In some other tests on the judged annoyance of impulsive sounds we have found preliminary evidence that annoyance increases with crest factor when pulse repetition rate is held constant, while with crest factor held constant annoyance varies with repetition rate. The shape of the sensitivity curve is very much like a visual flicker sensitivity curve, little sensitivity at low (≈ 5 Hz) and high (≈ 80 Hz) repetition frequencies (flicker fusion in the case of vision) with a maximum in sensitivity of repetition frequencies of the order of 30 to 40 Hz. Using the zero airspeed blade passage frequency as a measure, the product moment correlation between Δ_S and frequency accounts for 65% of the variance in the eight helicopter signals ($r^2 = 0.65$); however, for the entire signal set little correlation resulted ($r^2 = 0.10$).

In an attempt to improve the picture, multiple regressions of Δ_S on a linear combination of calculated adjustments, Δ_C (or CF) and repetition frequency were computed. Typical results for the helicopters were improvement in r^2 for the French adjustment from 0.69 to 0.87 and improvement in r^2 for $CF_{0.5}$ from 0.17 to 0.77. Standard errors for the regression improved from 0.8 decibels to 0.5 decibels for the French adjustment, and from 1.4 to 0.7 decibels for $\overline{CF}_{0.5}$.

CONFLICTING VIEWS

The possible use of analog measures of crest factor to assess impulsiveness has not met with much enthusiasm in ISO, particularly on the basis of analyses reported from France. Wright and Damongeot (ref. 6) argue that crest factor is a poor measure since, in their tests, it provided poor resolution for low impulsiveness signals. Our contention is that they did not follow the specified measurement procedure, since in their paper they determined crest factor from visual analysis on an oscilloscope.

In another analysis Berry and Robinson (ref. 7) found good correlation with their data using a crest factor determined from the largest value of their digitally sampled voltages used to compute CI or I. In the one case where we can compare their analysis directly with one of ours, their digital method

correlates well (r^2 of 0.91), for seven samples of synthesized blade slap noise, with our analog analysis. Further, the slope of the regression line is 1.01, although there is a 1.7 decibel offset at CF = 0.

A more basic disagreement exists over the use of repetition rate in an adjustment process. The primary issue is the repetition rate to be attributed to a helicopter with dual main rotors. If one takes the repetition rate as that due to the blade passage rate of one rotor only, the correlation with repetition rate is low. If one takes the repetition rate as twice this number, the correlation is retained. The fact is, a dual set of pulses exists, not quite uniformly spaced (constant repetition time overlap of two sets), with one set somewhat weaker than the other, their relative crest factors varying with operating conditions.

The second fact is that this kind of helicopter is judged to be twice, in decibels, as annoying as other helicopters having essentially the same degree of impulsiveness as calculated by any of the impulsiveness measures. See figures 1 and 2 for examples.

ISO ADJUSTMENTS AND COMPARISONS OF DATA

Of major interest at this time is how well the proposed ISO adjustment procedure works on judged data. Analyses of two sets of French data and of a dubbed recording of our eight helicopter signals, provided by us, have been reported by Aerospatialle in an ICAO working paper (ref. 8). The following discussion is based on the data reported in reference 8.

Consider first the ISO procedure applied to the eight helicopters. The scatter diagram showing the relationship between Δ_S and Δ_C is plotted in figure 3, along with the regression line. A positive correlation exists, with r^2 of 0.60, intercept of 0.2, and slope of 1.23.

The French judgement data are derived from one set of time-varying signals and from one set of steady-state signals. Consider first the data for the time-varying signals, as plotted in figure 4. In this case, $r^2 = 0.38$, but the values of Δ_S are negatively correlated, the regression line slope being $- 0.49$. Combining these data with the eight helicopters to obtain all the time-varying signals results in the plot of figure 5. Here the correlation is meaningless, with $r^2 = 0.04$.

The relationship between Δ_S and Δ_C for the French steady-state signals provides a better picture, as seen in figure 6. This should be better, since these data are basically those used to derive the CI and ISO transfer functions in the first place. Here $r^2 = 0.85$ and the slope is 1.04.

Finally, combining the three sets of data, as in reference 8, the plot in figure 7 results. In this figure the 6 signals used as comparison standards have been omitted since the subjective differences for the impulsive signals are judged relative to these standards. In this combined case $r^2 = 0.34$ and the slope is 0.69.

CONCLUDING REMARKS

It seems clear that at this point our knowledge of a good general predictor of subjective response to impulsive noise is poor. It is also clear that EPNL does underestimate annoyance due to blade slap. For these data the average underestimate is about 3 decibels for single main rotor aircraft and about 6 for the dual main rotor aircraft. Considering the variability in the data, one might arbitrarily use these constant values and ignore any more elaborate approach. One could simply apply these additive values to any helicopter that had a maximum A-weighted crest factor of more than 14 decibels.

REFERENCES

1. Galloway, W. J., "Subjective Response to Simulated and Actual Helicopter Blade Slap Noise," BBN Report No. 3573, December 1977.

2. Anon., "Impulsivity Indicators—Effect of Integration Time on NPL Indicator," ICAO/CAN/WG B WP 16 (France), June 1977.

3. "First Draft Proposal for Amendment to ISO 3891 'Acoustics-Procedure for Describing Aircraft Noise Heard on the Ground' Measurement of Noise From Helicopters," ISO/TC43/SC1 (Secretariat-254) 356, January 1978.

4. Fuller, H. C., "Rating Helicopter Noise: A Study of Subjective Reaction to Impulsive Sound," ISO/TC43/SC1/WG2 N 77, November 1976 (B&R 3).

5. True, H. C. and Rickley, E. J., "Noise Characteristics of Eight Helicopters," Report No. FAA-RD-77-94, July 1977.

6. Wright, S. E. and Damongeot, A., "Psychoacoustic Studies of Impulsive Noise," Paper No. 55, Third European Rotorcraft and Powered Lift Aircraft Forum," September 1977.

7. Berry, B. F. and Chew, A. J., "Helicopter Noise: Analysis of Various Descriptors of Impulsiveness," ISO/TC43/SC1/WG2 N 81, February 1977 (B&R 4).

8. Anon., "Analysis of the Effect of "Pulse Repetition Rate' on the Annoyance of Helicopter Impulsive Noise," ICAO/CAN/WGB WP 8 (France), April 1978.

TABLE 1

HELICOPTER SIGNALS USED IN
SUBJECTIVE RESPONSE STUDY

BBN No.	Aircraft Type	TSC Event	Operating Condition	Static Rep. Rate, Hz
214	S-61 (ref.)	34	115 knot level	17
215	S-64	50	60 knot level	18.6
216	CH-47C	28	150 knot level	25
217	CH-47C	18	60 knot level	25
218	212	36	105 knot level	11
219	212	31	61 knot level	11
220	47 G	19	6° Approach	12
221	S-61	20	6° Approach	17
222	206 L	46	6° Approach	13

414
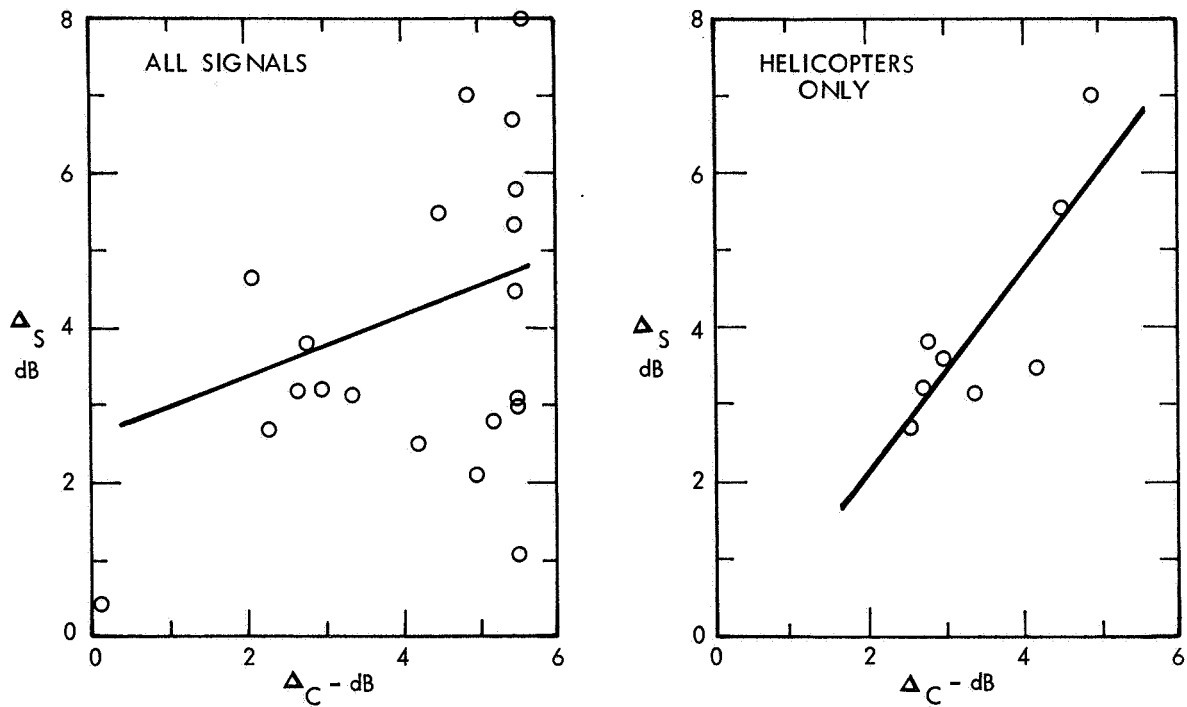
Figure 1.- Comparison of judged difference in EPNL between impulsive and non-impulsive signals and calculated impulse adjustment using French measure CI_A.
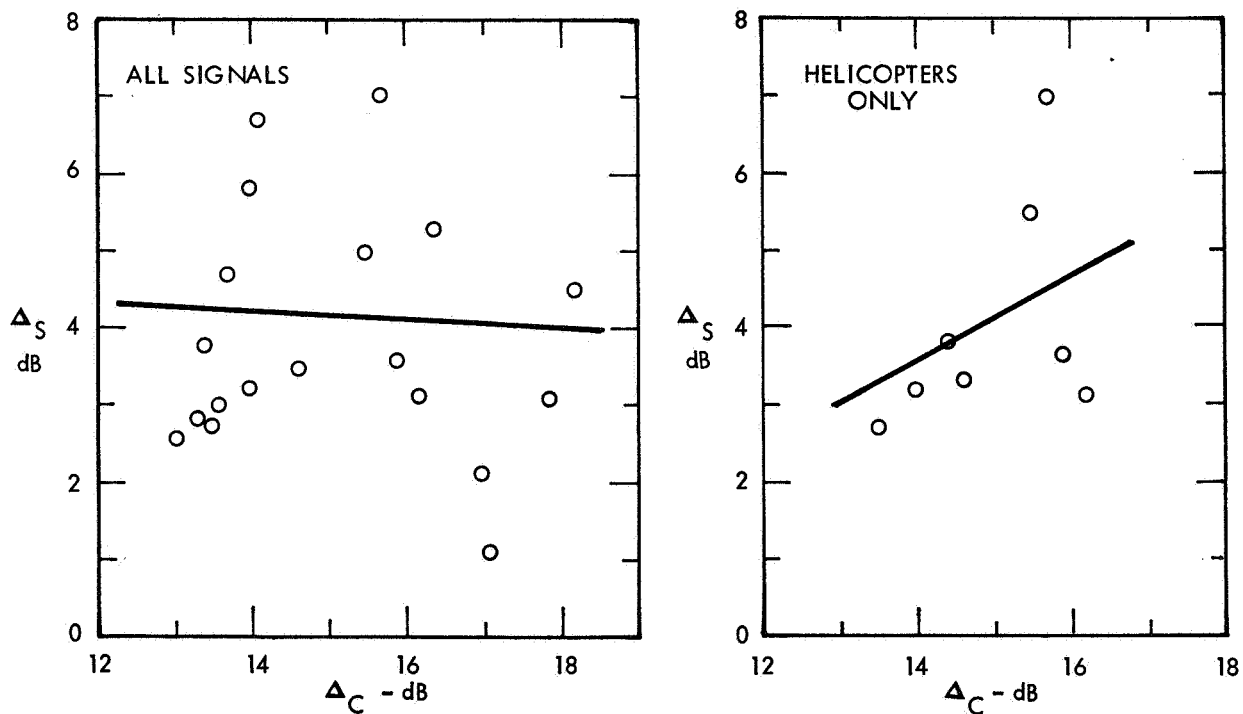
Figure 2.- Comparison of judged difference in EPNL between impulsive and non-impulsive signals and calculated impulse adjustment using $\overline{CF}_{0.5}$.
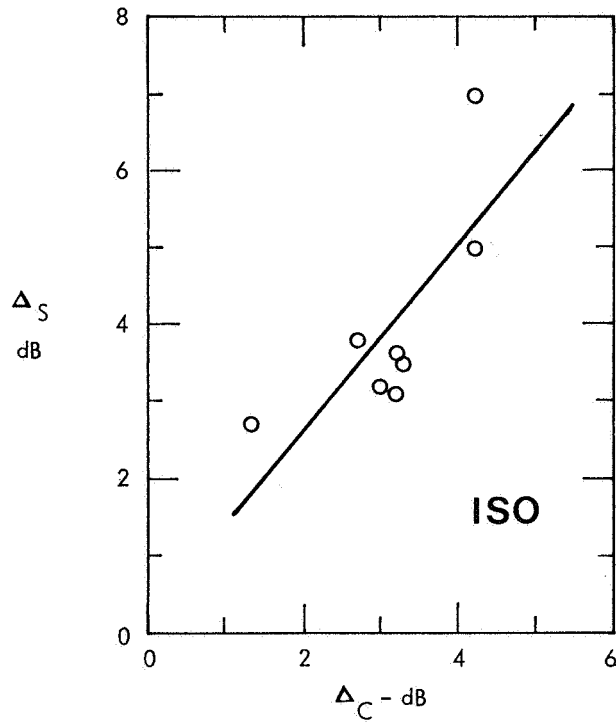
Figure 3.- Correlation between judged and calculated
adjustment to EPNL for BBN helicopters.
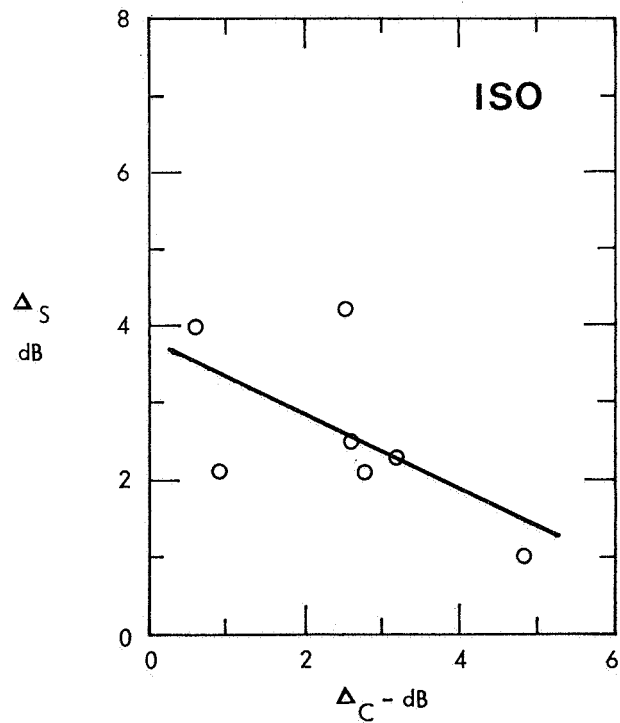
Figure 4.- Correlation between judged and calculated adjustment
to EPNL for French time-varying simulations.
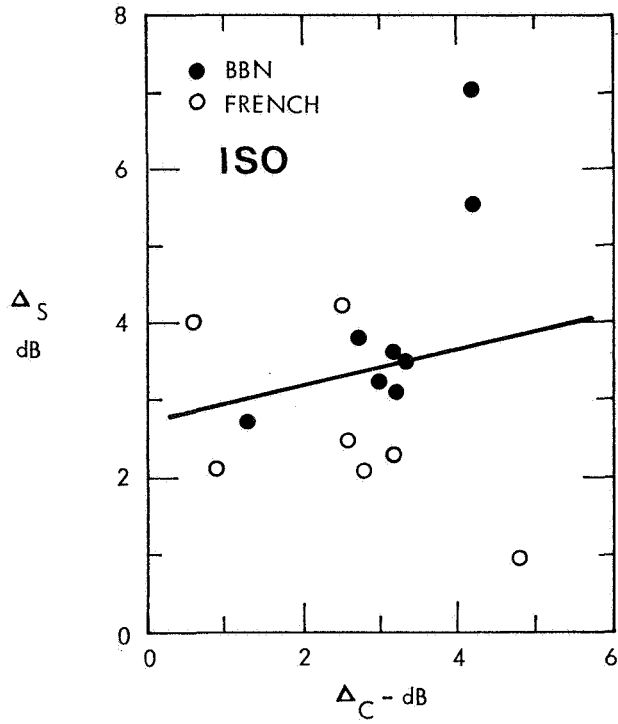
Figure 5.- Correlation between judged and calculated adjustment to EPNL for BBN and French time-varying signals.
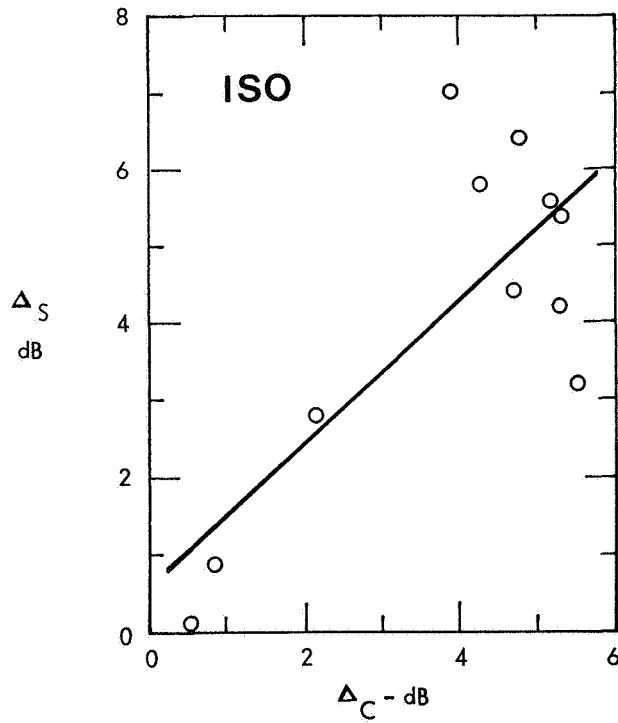
Figure 6.- Correlation between judged and calculated adjustment to EPNL for French steady-state signals.
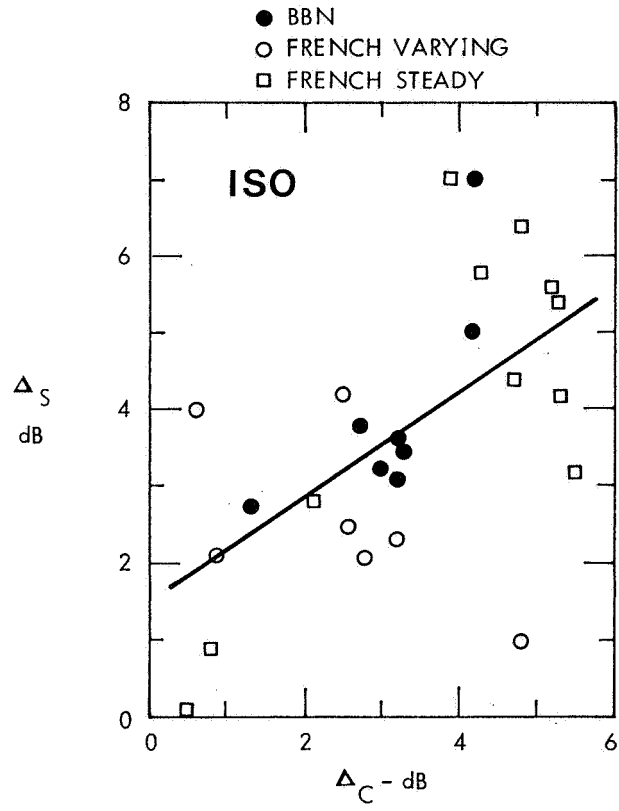
Figure 7.- Correlation between judged and calculated adjustment
to EPNL for combined signals.

RATING HELICOPTER NOISE

John W. Leverton, B. J. Southwood,
and A. C. Pike
Westland Helicopters Limited

SUMMARY

In the case of helicopters the main problem from the community point of view is the noise heard on the approach. This is particularly true in the case of helicopters with high levels of blade slap and/or tail rotor noise. The EPNL concept does not appear particularly well suited on quantifying helicopter noise since it is insensitive to the noise heard on approach some distance from the flyover position. Blade slap and tail rotor noise both need an additional correction. The former is now readily agreed and preliminary evidence is presented to show that a similar correction is required in the case of tail rotor noise. The impact of the use of such corrections is examined and although they improve the correlation, with the practical situation there is still considerable difficulty due to the inherent characteristics of the EPNL procedure.

INTRODUCTION

The use of helicopters for general commercial purposes has continued to increase and although in many instances they operate from remote sites on specialist operations, their use within built up areas has continued to grow. As a natural consequence overflights over many areas far from heliport sites have showed a significant increase. In urban areas, well-defined flight paths have been established for safety and ATC reasons and, as a result, there has been a tendency to concentrate flights over particular locations. This wider use of helicopters has given rise to concern over noise and although the number of complaints are still small, they have tended to increase over the last few years. The noise levels of helicopters have also shown a tendency to increase as modern technology has allowed high speed rotors to be employed and helicopters with higher forward flight speeds. Noise certification for helicopters has now been under consideration by the ICAO Working Group B for a number of years and certification proposals are expected shortly. There appears to be a need, therefore, to re-examine the whole topic of external helicopter noise and the results of such a survey conducted by Westland Helicopters Ltd. (WHL) are presented in this paper. In this context it is worth noting that in addition to manufacturing helicopters, WHL operates the London (Battersea) Heliport and has been involved in helicopter/community interface problems encountered by the British Army of the Rhine in West Germany. The WHL airfield is also situated within the boundaries of a small town; thus, considerable experience has been gained from the operators, manufacturers, and community point of view. The author has also been closely involved, as an adviser to the United Kingdom (UK) delegation, with the ICAO Working Group B.

HELICOPTER NOISE - THE REAL PROBLEM

In the case of helicopters the main noise problem from the community point of view is the noise heard on approach. This is particularly true in the case of helicopters with high levels of blade slap and/or tail rotor noise. It is the noise heard at distance which is of main concern. If this noise is impulsive (blade slap) or contains a distinctive whine (tail rotor noise), then it readily attracts attention, becomes disturbing, and, because it can be heard for a relatively long period as the helicopter approaches, gives rise to complaints. In many cases, but not always, blade slap decreases rapidly in level as the overflight position is approached. Similarly, on practically all helicopters with a high degree of tail rotor noise, the noise dies away well before the overflight point is reached. This is due to the directional characteristics of these two noise sources.

The effects discussed above are illustrated in figures 1, 2, and 3 which show time histories (amplitude - time traces). Figure 1 shows results for a two-bladed single rotor helicopter with and without blade slap where the blade slap decreases just prior to the overhead position; as can be seen, there is a marked difference in the duration of the noise. Also indicated on this figure is the blade slap region and the "peak levels" determined using a peak detector developed within WHL. This, in effect, gives a measure of the blade slap and a true representation of the duration associated with this helicopter. The data on this figure, like that on figures 2 and 3, are unfortunately limited in the sense that the recordings were not taken over a sufficient time period, (the data were collected as a part of other studies) and, as a result, the true duration above the background noise cannot be shown. The general implications are, however, clear. Figure 2 shows results again for a helicopter with blade slap but in this case the blade slap occurs during the complete flight. These data were obtained from a tandem rotor helicopter and are typical of the noise levels generated by this type of helicopter. Indicated on the figure is the 'peak' level for the blade slap case and the dB(A) level for the same helicopter when flown (during special tests) with no blade slap. Figure 3 shows the corresponding results for a helicopter with a high degree of tail rotor noise compared with a helicopter which has a low level of tail rotor noise. As can be seen, the duration is increased when tail rotor noise is present.

From a review of test data and a brief review of complaints and observation of helicopter noise, it has been concluded that although in many cases the absolute level of helicopter noise is highest at the overflight position, the annoying characteristics have decreased and there is little notice taken of the maximum overflight noise. This is not to imply that the complaints against helicopter noise are completely independent of the level since obviously a low altitude flyover which generates a very high level will prompt an adverse reaction. In the real environment helicopters are typically 500 ft (150 m) or more from the nearest residence and then it would appear that the character of the noise is equally, or more, important than the absolute level. There has, however, been little or no technical studies into these aspects, although experience gained from helicopter flights over London and generally within the UK supports these general observations.

420

According to Greater London Council there is in London "a small but steady flow of complaints about noise" (ref. 1). Yet, when 230 occupiers of properties within the vicinity of the London Battersea Heliport were contacted, only 3 objections on noise were received. In fact, there appears to be more objections from locations well away from the heliport; this result agrees with the conclusion from the WHL review that the main problems arise from the noise generated on approach. In this context it is also worth noting that in addition to the absolute level of helicopter noise decaying rapidly after the overflight point is reached, neither blade slap nor tail rotor noise is thereafter subjectively detectable.

In the practical situation, high noise levels are generated during "bank turns", manoeuvres etc. prior to landing and take-off at heliports. These are obviously a function of the specific flight procedures used or the ATC constraints and thus should not be included in any certification scheme. They can, and do, however, have a major influence on the subjective reaction to helicopter noise and it would appear from the available evidence that it is such aspects which define the acceptability to the general public of a particular helicopter near a heliport. The details of the flight path are important in this context and if they are chosen such that a helicopter has to turn sharply to avoid overflying a particular location, this can often generate higher noise levels than would occur if the helicopter was allowed to fly overhead.

RATING HELICOPTER NOISE

It follows from the points outlined previously that since the annoyance of a helicopter is largely dependent on the noise heard on approach that any rating or certification scheme for helicopters should be completely different from that derived for fixed wing (CTOL) aircraft. This should take into account the subjective character of the helicopter noise on approach some distance from the flyover point and the time associated with the noise, as well as the maximum level measured during the overflight. It is often argued that it is not the role of certification to control the "operational noise situation", but blade slap noise and tail rotor noise are of fundamental importance in the case of the helicopter, particularly since these noise sources can occur during "straight and level" cruise flight. This is a very different situation from that associated with fixed wing aircraft and therefore, by implication, the traditional method of rating aircraft noise is basically inappropriate. It is difficult, however, to imagine how a "new scheme" for helicopters could be formulated particularly since the various certification authorities place significant emphasis on developing a scheme which is, as far as possible, compatible with 'fixed wing' procedures. As a consequence, the helicopter noise certification concept currently being considered with the International Civil Aviation Organization (ICAO) and by the Federal Aviation Administration (FAA) are based on the EPNL method which is dependent mainly on the absolute level of the noise and the duration between the '10 dB down' points.

The EPNL method also takes into consideration the tonal content of the noise and thus it would be expected that it would take account of the subjective

impact of tail rotor noise as well as the high frequency engine 'whine.' Preliminary studies within WHL suggested that this is not the case and that the 'tone corrections' are often, to a first order, independent of the level of tail rotor noise. This is a complex subject and there has been very little work on this topic to date, but it would appear from analysis made by the author that problems arise from the fact that helicopter noise, particularly below 500 Hz, contains many discrete frequencies from the main and tail rotor and the one-third octave band spectra is not a true reflection of the annoying characteristics of the tail rotor noise. To remove the uncertainties of applying the tone correction procedure, ICAO Working Group B suggested at one stage that tone corrections should be applied only above 500 Hz, but recently this approach has been dropped and the latest view appears to be that tone corrections should be applied over the complete frequency range as in the standard EPNL procedure (Annex 16).

As mentioned previously, blade slap is the most annoying source associated with the helicopter. There is ample evidence to show the inadequacies of the standard EPNL procedure and that an additional correction factor is required to account for this source. There is, however, some opposition to this procedure and, although the International Organization for Standardization (ISO) has proposed a procedure for accounting for blade slap, this has not received wide acceptance in the U.S.A. In fact, it would appear that even some groups, which have accepted in principle that a blade slap correction is necessary, are more concerned with developing alternative schemes rather than assessing the relative merits of those already proposed.

The concern over the suitability of the use of the EPNL concept for rating helicopter noise will still apply even if a blade slap correction is finally accepted. The adoption of such a correction will, however, significantly improve the rating of helicopter noise relative to the use of an unmodified EPNL.

RATING UNITS

It is not proposed in this paper to review the various units for rating helicopter noise since it is clear that for a number of reasons the perceived noise level (PNL) will be used as the basic unit with possibly the dB(A) in some situations. Intuitively, it would be expected that the PNL method should adequately account for helicopter noise providing the signal is relatively broadband in nature and without any pronounced discrete noise sources. Also, since it is used for rating CTOL aircraft, it should also be equally applicable for rating helicopter engine noise. It follows, therefore, that with the exception of the cases when the signal is dominated by blade slap and/or tail rotor noise, the PNL unit, and by implication the dB(A), should be suitable for rating helicopter noise. For blade slap and tail rotor noise, some additional correction terms are required and this is discussed in the following sections.

422

BLADE SLAP

Correcting for Blade Slap

It is clear from the studies conducted within the UK by the National Physical Laboratory (NPL) and WHL (refs. 2 and 3), by Aerospatiale in France (ref. 4) and from some of the work conducted in the States (refs. 5 and 6) that a subjective correction is required to account for blade slap. There is very little disagreement between the results and there is a general consensus that the penalty associated with severe blade slap is 6 dB. This is illustrated in figure 4 which shows the results of psychoacoustic tests conducted within WHL (ref. 7). The figure shows the subjective correction in terms of dB(A) against a measure of the impulsive nature of the signal based on the crest factor developed by WHL some years ago (refs. 3 and 7). The subjective rating of blade slap, from none to severe, is indicated on the figure, together with a proposed correction curve. For all practical purposes, the results would be identical if, instead of dB(A), the corrections had been determined in terms of PNL values. Since the analogue crest factor method developed by WHL was proposed, NPL and Aerospatiale have developed impulsive noise descriptors which are based on digital analysis of the signals. Recently, the rating of blade slap has been reviewed by the International Standards Organization (ISO) and they have recommended the use of a method based on that originally devised by NPL (ref. 8).

The NPL and Aerospatiale CI descriptors are compared in general terms on figure 5 which shows the results for a 250-Hz sine wave pulse as a function of repetition rate. Also indicated on this figure is the true crest factor and, as can be seen, providing the integration time employed in the NPL method is small, then for all practical purposes the results of the NPL and the CI descriptor follows closely those given by the crest factor. Thus, from a fundamental point of view, there is little to choose between the methods (assuming the integration is 0.2 ms) and determination of the crest factor of the signal as originally proposed by WHL. The ISO, when it adopted the NPL descriptor, chose an integration time of 0.2 ms which is identical to the value used in the WHL analogue peak detector (ref. 9).

It is not proposed in this paper to discuss the relative merits of these methods but, since in practical terms they result in the same order of correction, to review implications which result from their use. There is, however, one exception to this general trend in that the method proposed by Galloway (ref. 6) contains a crest factor and repetition rate term and can give very different results. Firstly, the crest factor, by definition, already contains a repetition rate term and secondly, if this procedure is adopted, then helicopters with a high blade passing frequency (repetition rate) will have a high subjective penalty or correction even if the impulsive content of the signal is small (ref. 10). This result is opposite to what occurs in practice, where there is a marked tendency for the severity of blade slap to decrease with an increase in the number of blades; hence, the blade passing frequency is increased. There is a number of other difficulties associated with the use of this method and thus it would not seem to be a suitable descriptor for blade slap.

The blade slap correction was originally based on steady state (hover) recordings, although recently Aerospatiale (ref. 11) and Galloway (ref. 6) have conducted physcoacoustic tests using flyover recordings. These have shown to a first order that the steady state and flyover tests give for all practical purposes identical results. The flyovers used appear, however, in general to be of shorter duration than signals commonly encountered in the real environment. Even so, it has been argued that the results are equally applicable to hover and flyover signals.

The blade slap correction factor, as currently proposed by ISO, is added to the PNLT time history, in a similar manner to the tone correction, every half second to give the PNLT(I) time history from which the EPNL(I) is calculated using the normal approach. The difference between the EPNL(I) and the standard EPNL is a measure of the overall impulsiveness of the helicopter noise or in other words the magnitude of the annoyance associated with the blade slap.

Use of the Blade Slap Correction

A number of studies have been conducted within WHL on the effect of using the various proposed blade slap correction procedures. These have been based on the NPL, the Aerospatiale CI and/or the WHL analogue crest factor detector methods since, as mentioned previously, the results are essentially independent of the method used. Real helicopter and simulated helicopter signals have been used and the impact of the time at which the blade slap dies away, relative to the time of the maximum noise level, established. The general trends are illustrated in figures 6 and 7. Two cases are shown on figure 6 which gives results of a theoretical analysis. In the first the maximum correction of 6 dB, which corresponds to severe blade slap, is assumed to apply over the blade slap range whilst in the other a lower intensity blade slap with a correction of 4 dB was considered. As will be observed, the impact, as expected, of applying the correction is decreased as the time from overhead position is increased. Figure 7 shows similar results for a simulated flyover with blade slap and results of real helicopter analysis.

It is difficult from this analysis to draw specific conclusions, although, if blade slap occurs during the complete flight, the correction is more likely to be in the order of 5.5 PNdB rather than the theoretical 6 dB. From a review of a wide range of helicopters, it would appear that for the helicopter with severe blade slap on approach which "dies away" 2 or 3 seconds prior to the overhead position that the correction will be in the order of 4.5 EPNdB. Another difficulty associated with the blade slap descriptors currently being proposed by ISO is that nonimpulsive helicopters give rise to a correction in terms of EPNL of 1 to 2 EPNdB. This results from the fact that although subjectively they are not impulsive, they are more impulsive than the broadband white noise signal used as a reference in determination of the impulsive descriptor. The practical effect of this is that the difference between the impulsive and non-impulsive helicopter is further decreased.

Based on experience obtained within WHL from evaluating public reaction to helicopter noise, it seems fair to conclude, therefore, that the EPNL(I)

concept as currently being proposed still underestimates, in relation to a non-slapping helicopter, the impact of helicopter blade slap. This is not meant to imply that the correction procedure is inappropriate but rather that basic EPNL concept is inadequate.

TAIL ROTOR NOISE

Characteristics

Tail rotor noise, like blade slap, shows up on analysis as a series of pulses spaced at the blade passing interval. Thus, except for the differences in pulse frequency and blade passing frequency, the signals, which subjectively are classed "whine", are very similar to those associated with blade slap. This is illustrated diagrammatically in figure 8 which shows representative blade slap and tail rotor noise pulse chains. Thus, from a rating point of view, tail rotor noise is impulsive in character and hence "rated" by the various blade slap descriptors discussed previously. This is a very important point which is over-looked by many investigators who simply associated tail rotor noise with a dis-crete frequency spectrum.

The Tone Correction Procedure

Tail rotor noise, as discussed previously, is very dominant on approach, but unlike blade slap, it dies away well before the overhead position, as illus-trated in figure 3. When tail rotor noise is pronounced, then it can be detec-ted on a one-third octave band plot; a typical result is shown on figure 9. The EPNL procedure is, however, relatively insensitive to such tones as can be seen from results indicated on the figure. If the flyovers shown in figure 3 are exami-ned, then it can be shown that the EPNL for the Scout with the high level of tail rotor noise is only 2 EPNdB higher than that for the Wessex. Part of this is due to the difference in the duration correction arising from the slightly different flight speeds between the two helicopters. If this is taken into consideration, then the calculated difference is less than 1 EPNdB. In an attempt to highlight this problem further, the equivalent continuous noise level (Leq) has been calculated for a Scout flyover when the tail rotor noise is very pronounced and compared with the prediction of the Leq for an equivalent flight with no tail rotor noise. This is illustrated in figure 10 and it will be noted that the tail rotor 'hump' is within 3 dB(A) of the maximum dB(A) level. The difference between the two Leq values, based on the levels within the region covered by the 'maximum - 25 dB(A), is 1.9 dB(A) - yet obviously the two conditions sound very different.

When analysing flyover signals, it has also been observed that tone corrections result in a constant difference between the PNLT and PNL values, being typically 1.5 dB. Owing to the variability of the one-third octave band spectra, the band which is responsible for the correction does not appear to be represen-tative of the real situation. This is considered to be due to the complex nature of helicopter noise.

425

It is concluded therefore from the analysis outlined above and detailed reviews of a wide range of flight conditions that tone corrections in the EPNL procedure bear little relation to the true annoyance of helicopter tail rotor noise.

Rating by Impulsive Noise Descriptors

Since tail rotor noise takes the same form as blade slap, then any impulsive descriptor will be equally sensitive to both of these sources of noise and, of course, to any other impulsive sources of noise. This can be seen on figure 5 which, in addition to values for idealised blade slap pulses (low repetition rates), shows results for idealised tail rotor noise. As discussed previously, values are shown for the NPL (ISO) and Aerospatiale CI descriptors and the crest factor. The main difference between the two sets of results is that whereas the NPL (ISO) method gives a measure of blade slap when an integration time of 10 ms is used, it effectively rejects tail rotor noise. This effect can be better appreciated from the plot for idealised signals shown in figure 11. It may appear from these plots that if a 10 ms integration time was used, then tail rotor noise would be rejected and the measured value in practice would depend solely on the level of the impulsive (blade slap) noise. There are, however, a number of major objections to this. Firstly, the relationship between the NPL descriptor (10 log I) and the crest factor varies with repetition rate — in other words, on figure 5, the values are not parallel to those of the crest factor. More importantly, however, is the fact that use of such a method would give a result independent of the pulse frequency, and hence crest factor, as indicated in figure 12. Thus, such a solution is not practical.

In the method originally proposed by WHL for rating blade slap, which was based on the use of the crest factor, this problem was overcome by passing the signal through a band pass filter centered on 250 Hz in order that all impulsive signals except those associated with blade slap were rejected (ref. 3). Such a method is used within WHL for assessing the magnitude of blade slap, but objections were raised against this method on the grounds that since the widest standard filter which could be used was an octave band (177 to 354 Hz), some helicopters could generate blade slap with the main energy above the upper frequency limit. An example often quoted is the Bolkow BO 105 which appears to have the blade slap energy maximum centered on 600 Hz (ref. 12), while on most other helicopters it is around 250 to 300 Hz (ref. 13). It is considered that the WHL proposal could possibly be further developed to take account of such cases and it is questionable whether a signal with a repetition rate, as is the case of the BO 105, of 28 Hz and "pulse frequency" of 600 Hz will subjectively sound the same as the blade slap generated by other helicopters. It has also not yet been shown whether the standard PNL/dB(A) method fails to penalize such blade slap in a similar manner to that found for blade slap of the type used in the studies summarized in figure 4. WHL has, however, not pursued this method recently since current proposals by ISO provide an adequate descriptor for blade slap and there is an intuitive feeling — recently confirmed by preliminary subjective tests — that the ISO method could be used to account for both tail rotor noise and blade slap.

If figures 5 and 11 are examined in detail, it will be observed that the crest factor associated with tail rotor noise is less than that for blade slap. This is a genuine effect and agrees well with the real practical situation in that severe blade slap is always more pronounced and annoying than the corresponding high level of tail rotor noise.

Subjective Evaluation

Preliminary physchoacoustic tests have been conducted within WHL using simulated and real helicopter steady state (hover) recordings (ref. 14). The results obtained to date are shown in terms of dB(A) values in figure 13. This figure is directly comparable to the blade slap results shown in figure 4 and, as will be noted, it suggests that pronounced tail rotor noise requires an additional correction of 4 dB(A). It follows that, to a first order, this is similar to blade slap and therefore, by taking into account that tail rotor noise gives slightly lower crest factor than associated with blade slap, it can be argued that an impulsive descriptor of the type proposed by ISO can adequately account for both sources of impulsive noise. If this approach was adopted, then obviously the conventional tone corrections would not be required. The impulsive rating procedures, as currently envisaged, have a 'cut off' at around 2 kHz and the level of tail rotor noise is very low above 1 kHz. It would seem appropriate, therefore, to limit the tone correction procedure in the present EPNL procedure to, say, 1 kHz and above. This would provide, assuming an impulsive noise descriptor was used, a good measure of both sources of impulsive noise, while ensuring that high frequency discretes tones from the engine etc. were adequately covered and that tail rotor noise was not penalized twice.

THE REQUIREMENTS FOR NOISE STANDARDS

From the experience within the UK it would seem reasonable to assume that the aim of 'noise certification' should be, in general, to contain the current situation since, unlike CTOL aircraft, helicopters do not cause any major noise disturbance. There are, of course, a number of noisy helicopters which are exceptions to this general rule and hence 'certification' limits should be such as to prohibit their development and ensure that they are phased out of civil use. Even so, there does not appear to be any case for setting standards which would require a dramatic reduction in the noise generated by the majority of helicopters.

The helicopters in the subjectively 'noisy' category are usually those which generate high levels of 'blade slap' (impulsive main rotor noise) or to a lesser extent those with a high level of tail rotor noise. It has been established that the standard dBA and PNL (PNdB) units do not adequately account for blade slap and 'corrections' are required. The position relating to the subjective impact of tail rotor noise has not been studied in such depth, but it appears from the available evidence that the standard procedures do not fully quantify this source even if the 'tone correction procedure' in the EPNL procedure is applied. It follows, therefore, that it is completely false to

use a unit which does not take these aspects into account when setting the appropriate limit.

Noise certification is an important issue and it is vital that care should be taken in both the selection of the flight test conditions and the rating unit since certification will have a long term effect on the helicopter industry and the community. It seems essential that a method and a rating unit which takes into account the subjective impact are derived or otherwise public reaction will be based on the feeling that certification is inadequate and then numerous local rules will be applied. These could be more severe than the certification requirements and the industry would be burdened by the need to meet conflicting requirements. It is, therefore, considered that the certification scheme should be based on a full technical evaluation of all the issues involved including those outlined in this paper.

CONCLUDING REMARKS

Helicopter noise is not the major problem often suggested, although obviously there are a number of noisy helicopters which give rise to complaints. Thus, it would appear that although there is a need to limit, and possibly lower slightly, the noise levels associated with current helicopters, there is little justification in attempting to obtain a dramatic reduction. This is particularly true if the economic penalties involved in obtaining noise reductions on helicopters and the likely gains in real noise terms in a real environment are taken into account. Furthermore, it would appear from the experience of WHL that many of the problems that occur in practice are associated almost entirely with blade slap and/or high levels of tail rotor noise which occur on approach during cruise flight. In simple terms there is ample evidence to suggest that a blade slap correction is required and that when the blade slap is severe, this should be 6 dB. A similar situation occurs in the case of the tail rotor noise and although preliminary results indicate this can be tackled in a similar manner to blade slap, it is recognized that it will be some time before such a correction is accepted. The main problem appears to be, however, that if these corrections are taken into account on a "half second" basis, then since the rating methods are being based on the EPNL concept, they will not account for the annoyance caused by helicopters in practice. There is also the possibility that even if certification results in a reduction of the maximum noise emitted by a helicopter during flyover, the character (crest factor) of the noise generated on approach due to blade slap and/or a high level of tail rotor noise will remain the same. Thus, it is possible that the annoyance to the public will, for all practical purposes, be the same even though the absolute level is reduced. Added to this is the fact that near a heliport transient manoeuvre noise (bank turns, etc.) may still occur and since to some extent these are independent of the maximum noise generated by the helicopter, the impact of noise certification in this case may again be small. This particular aspect can, however, be controlled in practice by local heliport or ATC rules.

A review has been made of possible alternative methods of rating helicopter noise and to date WHL freely admits that it has not yet been able to

devise a completely acceptable scheme. Aspects considered have included, in the EPNL procedure, changing the calculating time to the 'maximum level - 20 dB' but this does not give any marked improvement and a method in which a correction based on the crest factor of the signal in the far field (approach condition) is added to the computed PNLM or EPNL value. Use of the Leq concept has also been evaluated, together with a number of 'ad hoc' approaches where different allowances have been taken into account for blade slap and/or tail rotor noise.

Since there is obviously difficulty at the present time with the overall rating procedure to be used, this again gives support to the view that certification should essentially provide a scheme which limits the use and development of very noisy "slapping" type helicopters or those with high levels of tail rotor noise, rather than attempt an overall reduction of helicopter noise. In this context it is also worth noting that the prediction of 'total helicopter' noise is relatively inaccurate and less precise than commonly associated with fixed wing aircraft. This is understandable since the research effort both in terms of manpower and financial resources has been significantly less than in the case of CTOL aircraft. The main sources of rotor noise are, however, relatively well understood and it is the interaction effects which cause problems during predictions. It also implies that the configuration (layout) of the helicopter has a significant impact in the resulting overall noise. It follows, therefore, that it is not possible to design, within the required accuracy, to a specific level.

REFERENCES

1. Greater London Council: Report (11.6.75) by the Controller of Planning and Transportation. Item 11 P847.

2. Fuller H.C.: Rating Helicopter Noise - A Study of Subjective Reaction to Impulsive Sound. National Physical Laboratory Report, November 1976.

3. Southwood B.J., Pike, A.C.: The Rating and Subjective Assessment of Helicopter Blade Slap. Westland Helicopters Ltd. (WHL) Applied Acoustics Department Note 1147, May 1976.

4. Damongest A: Gene Produit par les Bruits de Nature Impulsive. Aerospatiale Report H/DE - ER 351-67, November 1976.

5. Noise Certification Considerations for Helicopters Based on Laboratory Investigations - Man Acoustics Report. FAA-RD-76-116, July 1976.

6. Galloway W.J.: Subjective Response to Simulated and Actual Helicopter Noise. BBN Report 3573, December 1977.

7. Leverton J.W., Southwood B.J. - A Correction for Helicopter Blade Slap. WHL Applied Acoustics Department Note 1163, November 1976.

8.   First Draft Proposal for Amendment to ISO 3891 "Acoustics – Procedure for Describing Aircraft Noise Heard on the Ground" – Measurement of Noise from Helicopters. ISO/TC 43/SC 1 (Secretariat – 254) 356.

9.   Pike A.C., Leverton J.W.: An Analogue Method for Quantifying Impulsive Noise. Paper presented at Internoise – 77. Conference in Zurich, Switzerland, March 1977.

10. Southwood B.J.: Comments on BBN Report 3573 – Subjective Response to Simulated and Actual Helicopter Noise. WHL Applied Acoustics Department Note 1216, March 1978.

11. Wright Dr. S.E., Damongeot A: Psychoacoustic Studies of Impulsive Noise. Paper No.55 presented at the Third European Rotorcraft and Powered Lift Aircraft Forum, Aix en Provence, France, September 1977.

12. Laudien E, Huber H.: Impulsive Helicopter Rotor Noise. Paper No. 2.4 presented at the GARTEur – 5 Specialist Meeting on Propeller and Helicopter Noise, Paris, 1–2nd June 1977.

13. Leverton J.W.: Helicopter Noise – Blade Slap Part 2: Experimental Results NASA Report CR-1983 (Prepared by ISVR, Southampton), March 1972.

14. Southwood B.J., Leverton J.W., Pike A.C.: Rating Tail Rotor Noise. Paper presented at the IOA Spring Conference, Cambridge, April 1978.
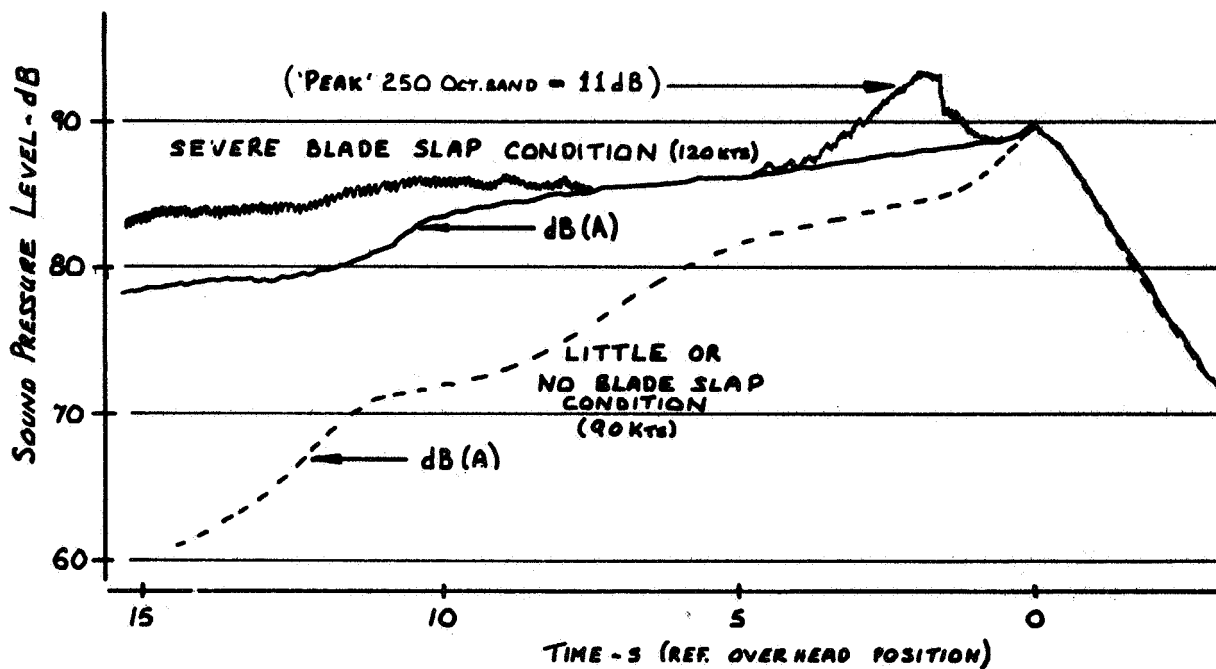
Figure 1.- Flyover time history - 2 bladed main rotor helicopter (UH-1B).
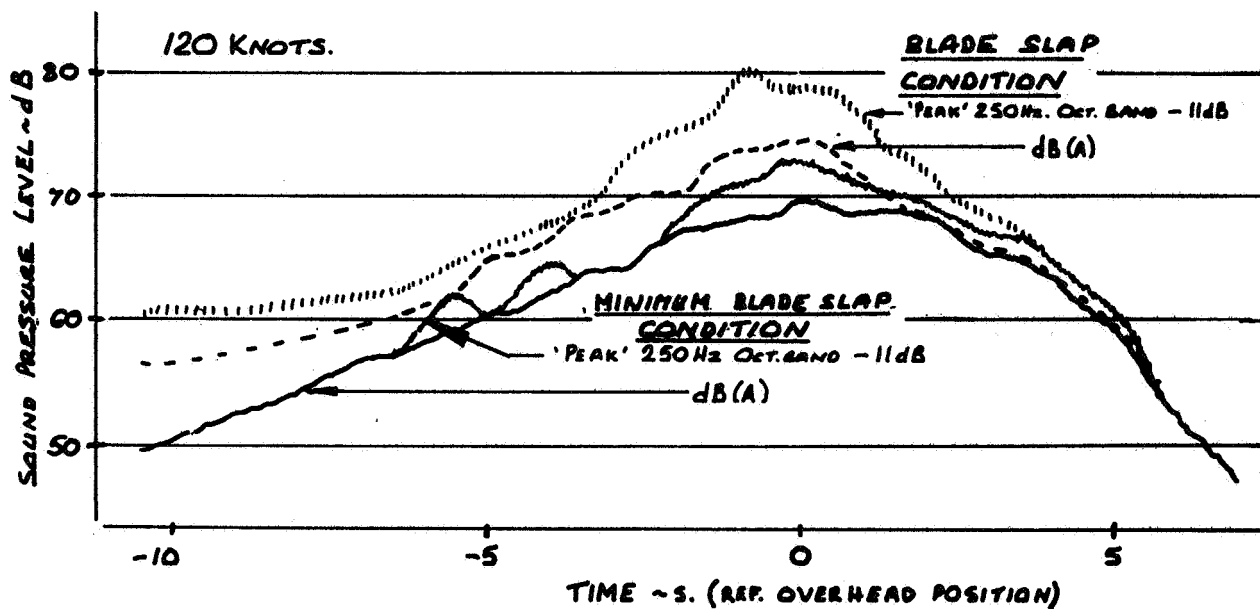
Figure 2.- Flyover time history - tandem rotor helicopter (V107).

SCOUT: (70 KNOTS): HIGH TAIL ROTOR NOISE

WESSEX (S58): (90 KNOTS) LOW TAIL ROTOR NOISE

TIME ~S.

OVERHEAD POSITION
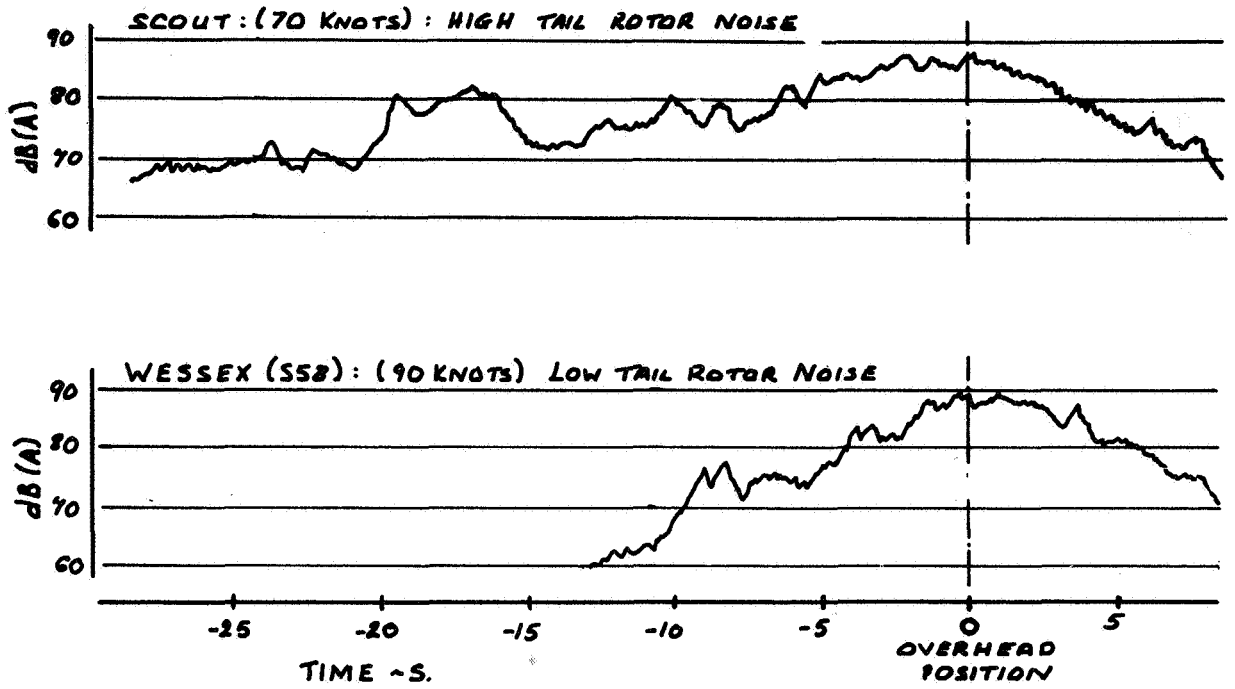
Figure 3.- Flyover time history - Scout and Wessex.

BLADE SLAP SUBJECTIVE RATINGS

NONE   MARGINAL   MILD   SEVERE

CHINOOK/WESSEX COMPARISON

SIMULATED IMPULSE SUBJECTIVE TESTS

PROPOSED CORRECTION

CREST FACTOR ~ "PEAK' 250 OCT. BAND - dB(A) SLOW "
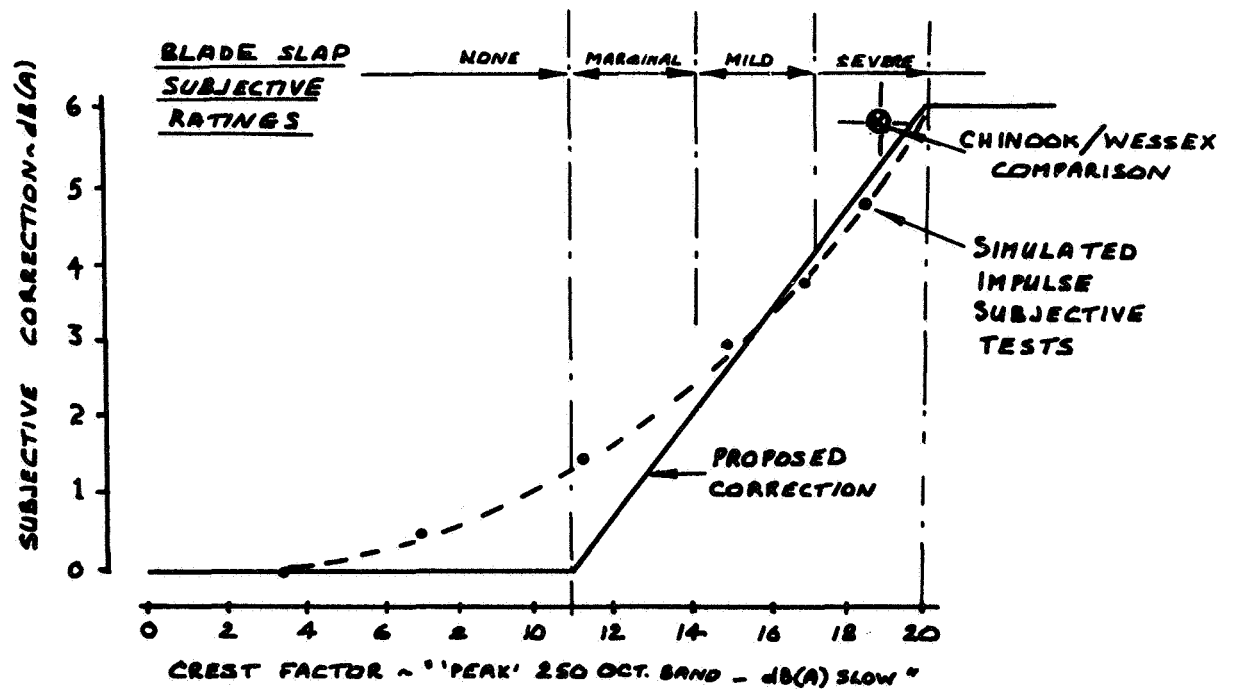
Figure 4.- Blade slap: subjective correction.

432
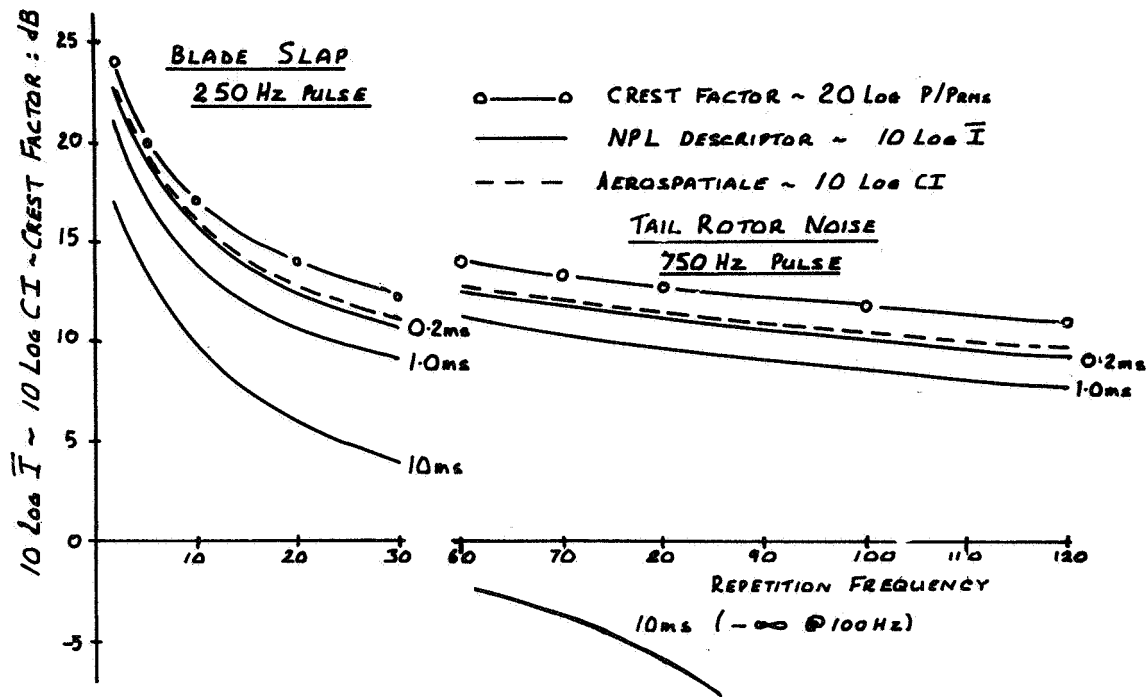
Figure 5.- Characteristics of impulse descriptors - variation
with repetition rate.
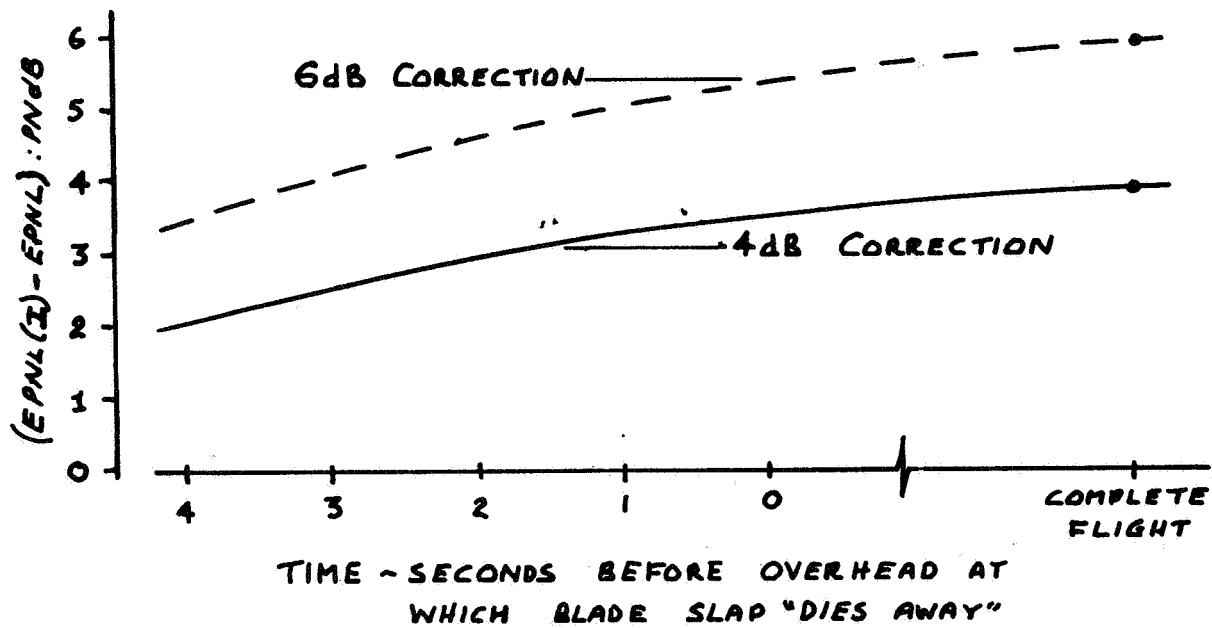
Figure 6.- Impact of blade slap descriptors on EPNL
(idealised signals).
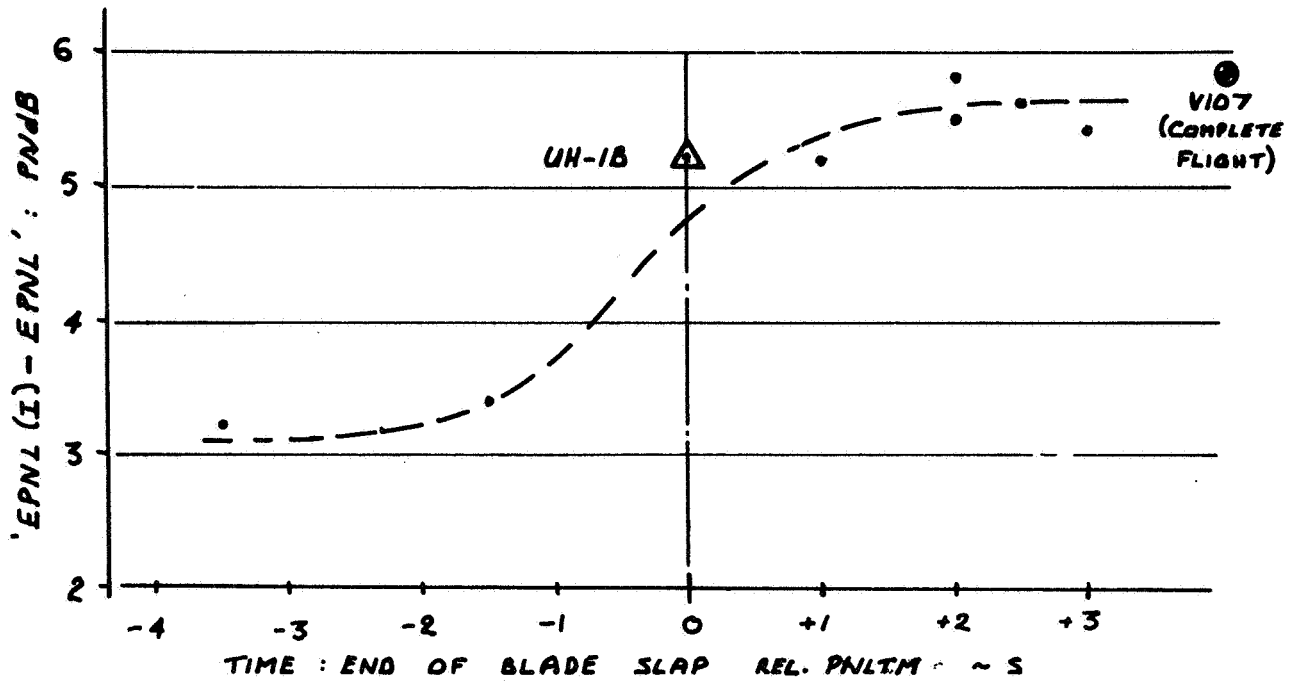
Figure 7.- Impact of blade slap descriptors on EPNL - simulated
and real helicopter results.
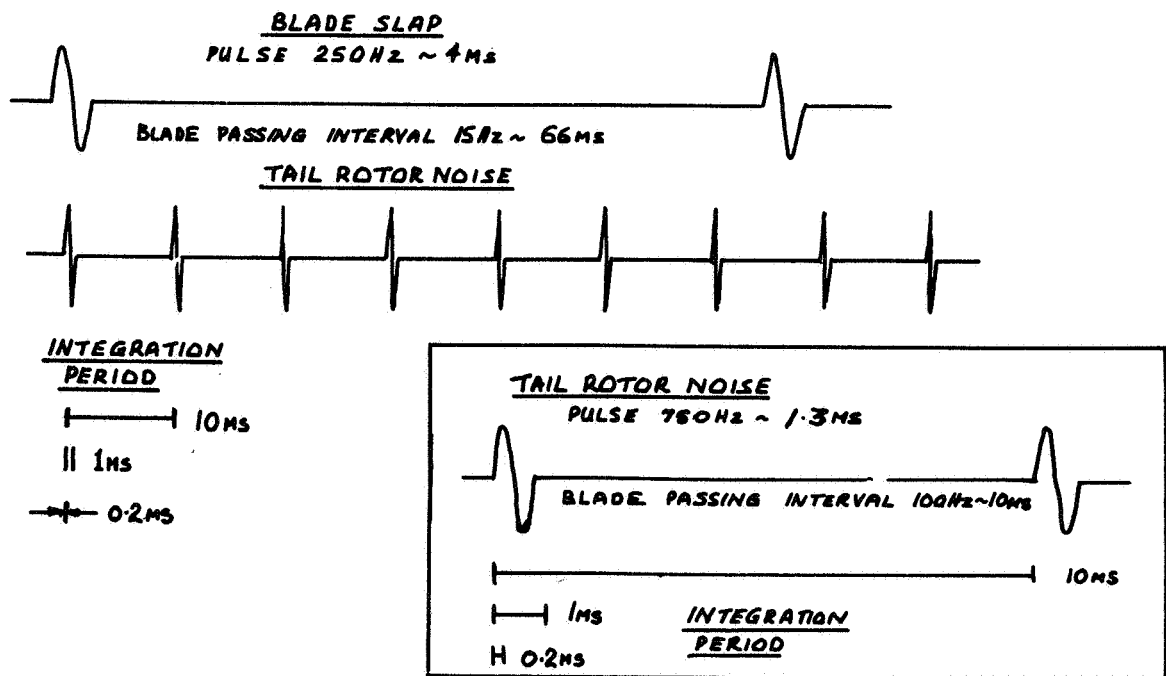
Figure 8.- Diagrammatic representation of blade slap and tail
rotor noise.

434
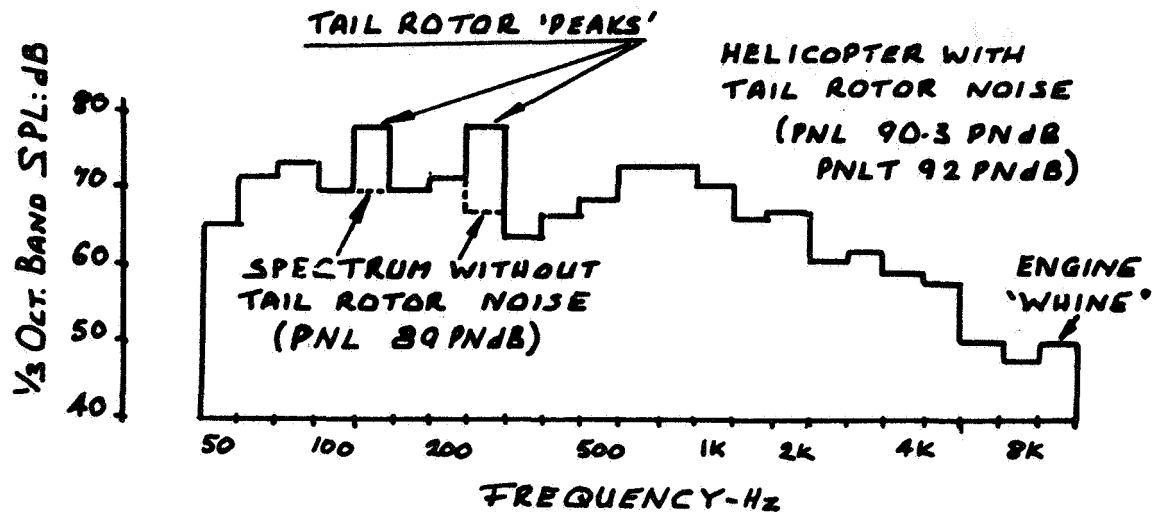
Figure 9.- $\frac{1}{3}$ octave band of helicopter noise.
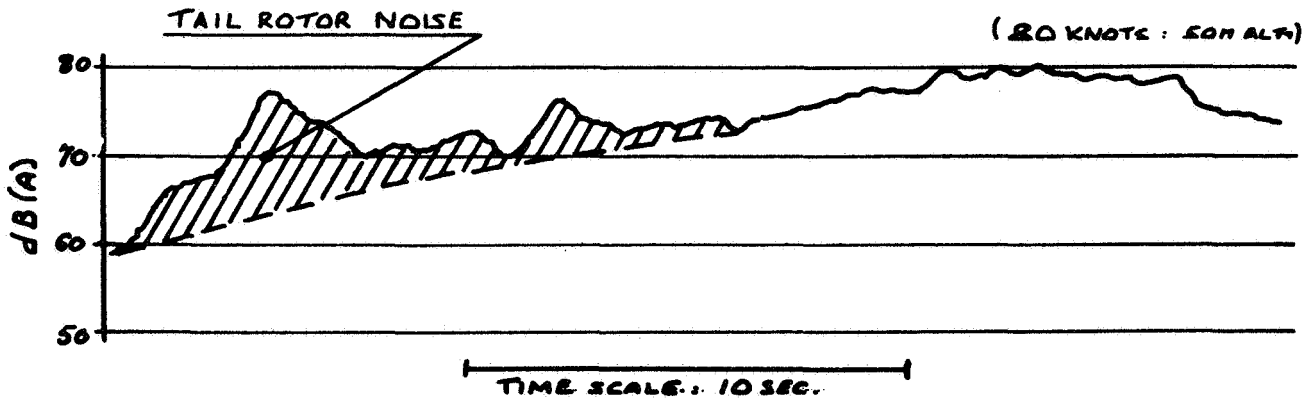
Figure 10.- Flyover time history. Scout helicopter
with high level of tail rotor noise.
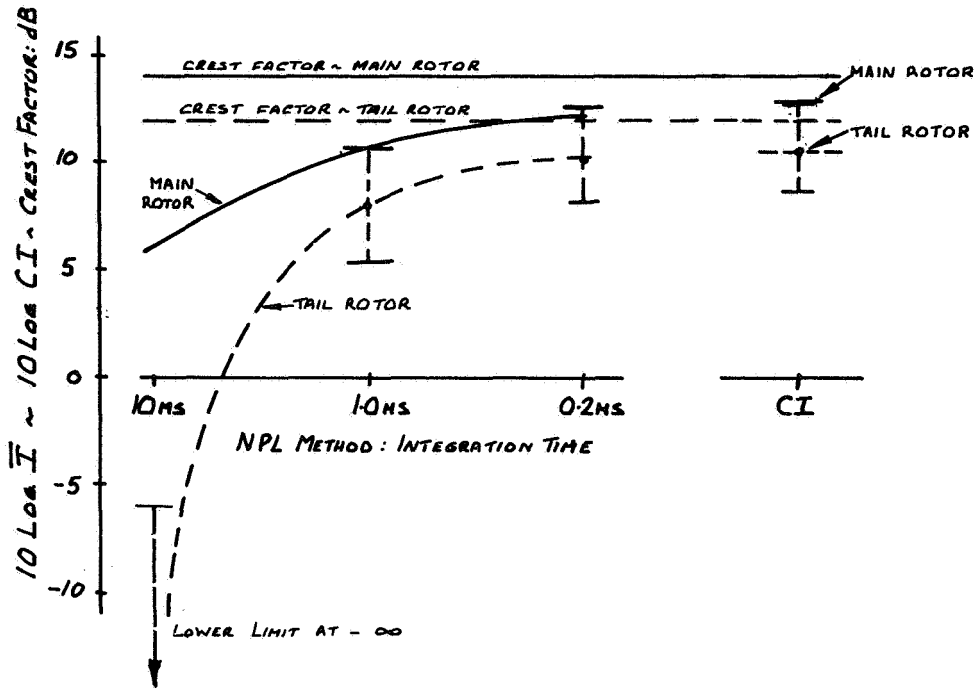
Figure 11.- Variation of main and tail rotor noise
with integration time and descriptor.
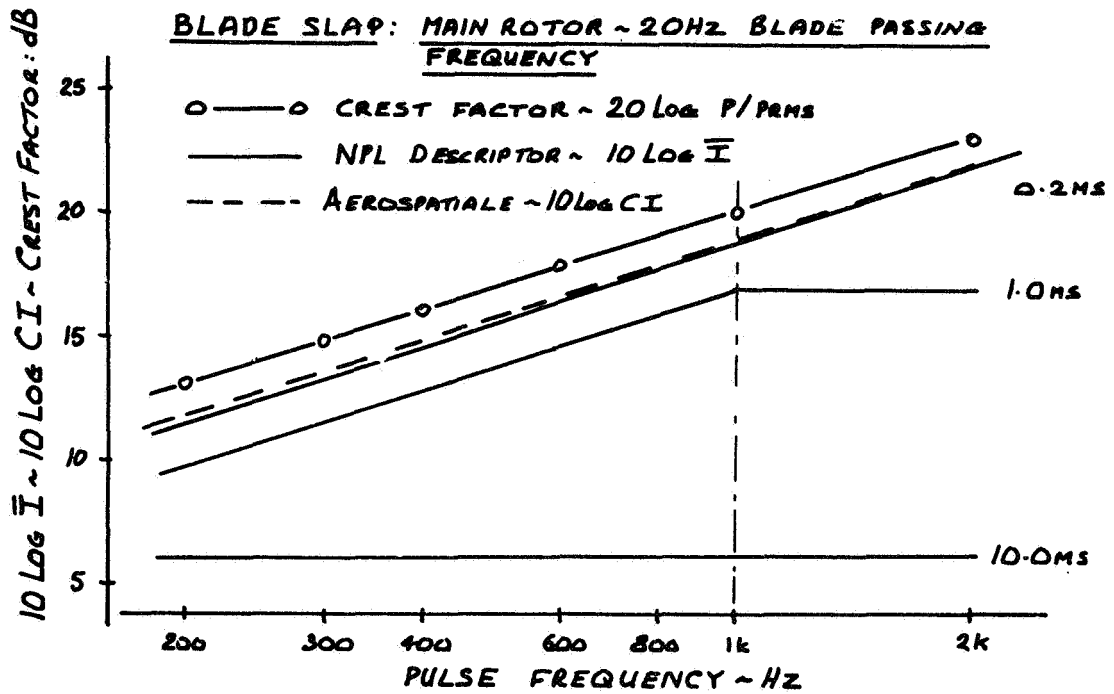
Figure 12.- Characteristics of impulse descriptors - variation
with pulse frequency.
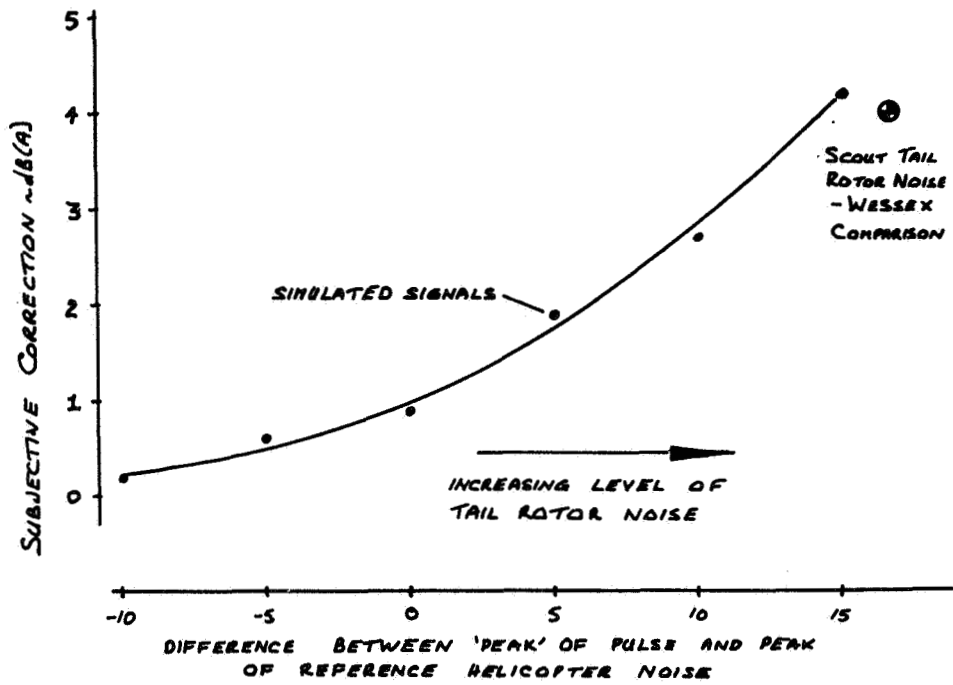
Figure 13.- Tail rotor noise. Subjective correction - preliminary
results.

ANNOYANCE OF HELICOPTER

IMPULSIVE NOISE

F. d'Ambra and A. Damongeot
S.N.I. Aerospatiale

SUMMARY

Psychoacoustic studies of helicopter impulsive noise have been conducted in order to qualify additional annoyance due to this feature and to develop physical impulsiveness descriptors to develop impulsivity correction methods.

The paper reviews the explored impulsiveness parameters and the subjective evaluation data. The currently proposed descriptors and methods of impulsiveness correction are compared using a multilinear regression analysis technique. It is shown that the presently ISO recommended descriptor and correction method provides the best correlation with the subjective evaluations of real helicopter impulsive noises. The equipment necessary for data processing in order to apply the correction method is discussed.

INTRODUCTION

During the last few years, environmental agencies of different countries have expressed a need to establish and enforce a certification rule for all types of flying vehicles and in particular for helicopters. Among the different problems to be solved in order to promote such a certification rule, the question of representative noise unit is of utmost importance.

Indeed it should obviously:

- Reflect the true annoyance felt by the public

- Allow comparisons with the annoyance due to operations of other types of flying machines

- Reflect truly the efforts that the aircraft manufacturer and operator put in the design and operations of their vehicle to fly more quietly

- Not affect the present units used for aircraft

- Be as simple as possible for data processing

In view of this forthcoming certification scheme of helicopter noise, several countries have undertaken some work on the particular features of helicopter noise in order to assess representative noise units based on corrections to the presently accepted aeronautical noise units. These units already take into account the effect of particular distribution of acoustic energy in the audio frequency range (Noy) and the effect of tone and duration of the noise (EPNL). A new feature which has not yet been taken into account in the noise signature of flying machines is the impulsive type of pressure signals which the majority of helicopter shows in some flight configurations. This impulsive feature is also found in other noise sources of day to day life, like repetitive hammer blows, pneumatic drills, and motorcycles.

The work reported in this paper was supported by the "Ministère de la Culture et de l'environnement," the "Service technique Aéronautique – Section Moteurs" and S.N.I. Aérospatiale.

For the motivations previously stated, the work has been conducted in such a way to promote possible correction methods to already existing aeronautical, and to a lesser degree, civil engineering, noise units. A large part of the subjective data which are analyzed originates from psychoacoustic tests performed in France by a joint team of the Helicopter and Aircraft Division of Aerospatiale. Other subjective data and magnetic tape recordings used for psychoacoustic tests performed in other countries have been kindly made available in the framework of ISO and ICAO-WG.B working sessions. These data have also been incorporated to this study.

The paper is divided into four main sections:

(I)   Physical impulsiveness parameters: Subjective evaluation methods and results

(II)   Data Interpretation: Impulsiveness descriptors and possible methods of corrections

(III) Multilinear Regression Analysis: Quality criteria of the proposed methods

(IV)   Instrumentation and data processing

Some aspects of this report have already been presented at the third European Rotorcraft and Powered Lift Aircraft Forum by Dr. S. E. Wright and A. Damongeot (ref. 1). They pertained mainly to the above mentioned sections I and II.

I   Impulsive noise signal

R_n Nonimpulsive noise signal

(I)   Impulsive noise level; PNdB, TPNdB, EPNdB units

(NI)   Nonimpulsive noise level; PNdB, TPNdB, EPNdB units

CF_{Max}, CF_M Maximum Crest Factor $\dfrac{(peak)}{(r.m.s)}$

$CF_{0.5}$ Crest Factor during a 0.5 sec time interval

$\overline{CF}_{0.5}$ Mean 0.5 sec Crest Factor during a transient signal

P, P_A Pressure and "A" weighted pressure time history

$x, \bar{x}$ 0.5 sec and mean value of the ISO descriptor

A,B,C   Coefficients of the regression law in dB,
dB per unit value of the impulsive descriptor,
dB per unit value of the repetition rate

SA,SB,SC   Standard deviation of A,B,C

r, r_e Multiple correlation coefficients

Se   Overall standard deviation

ΔS Subjective correction (dB)

ΔC Computed correction (dB)

f   Pulse repetition rate (Hz)

IMPULSIVENESS PARAMETERS AND SUBJECTIVE EVALUATION METHODS

It has been shown elsewhere (ref. 2) by careful recordings of helicopter noise signals performed either with microphones on the ground and aircraft in hover or in flight (descent or flyover at high speed) or with microphones set in the same reference frame as the helicopter in motion that the impulsiveness content of helicopter noise signals is mainly linked to aerodynamic phenomena on the main rotor and to a lesser extent to the tail rotor. This impulsive character arises when there is either a strong interaction between the main rotor blades and the wake vortices (flight of descent or hover) or when a high aerodynamic speed relative to the tip of the advancing blade is reached (compressibility and/or thickness effect).

Physical Impulsiveness Parameters

The main physical parameters which describe the pressure trace of stationary noise signal in these circumstances are shown in figure 1.

(a) The impulse shape may be different, as illustrated for a light or a heavy helicopter.

(b) The degree of impulsivity can vary widely from a pure random noise to a weak, a medium, and a strong impulsive noise.

(c) The pulse repetition rate - which is equal to the rotor angular frequency times the number of blades - can also vary in a wide range depending on the helicopter weight (rotor diameter and tip speed) and the number of blades used (two to six in present design).

(d) Finally the noise levels, expressed in the presently agreed noise units of PNdB, can vary to a lesser extent at the distances which are actually sought for possible certification scheme. Figure 2, which reproduces noise traces taken at different times during the flyover of a heavy helicopter, shows that, for transient noise signals, there is in addition to the previously stated parameters an _evolution_ of the _degree_ of impulsivity of the noise signal, the trend being that this degree increases before the maximum noise level is obtained, then decreases sharply afterward.

Subjective Evaluation Methods

The principle of a subjective evaluation experiment is to submit to a certain jury the noise signal to be qualified and a reference noise of known annoyance. Broad band noise has been the subject of many subjective evaluations from which the unit of PNdB (Perceived Noise decibel) has been derived. Therefore, it can represent a very good reference, especially if it is taken as the broad band noise of a helicopter.

Elaboration of Impulsive Noise Recordings

In order to be able to change at will the different parameters which were pointed out in the previous paragraph, it is necessary to elaborate the impulsive noise signal to qualify in such a way that one can separate these parameters, while using as much as possible the actual helicopter noise traces. In the French psychoacoustic tests performed, this has been achieved by electrically mixing helicopter broad band noise signals with real helicopter impulse signals, as shown in figure 3. This allows the pulse amplitude and repetition rate to be varied at will so that the four physical parameters, shape, degree, repetition rate, and overall noise levels, could be tested separately.

442

The same technique has been applied to elaborate the transient impulsive noise signals to be tested. The same pulse shape is maintained during the time history of the pressure signal but with a variation of the degree of impulsivity according to the previously mentioned trend: increasing degree before maximum PNL, sharp decrease thereafter.

Method of Comparisons by Pairs

In the French study, the method used to subjectively evaluate impulsive noise is the method of comparison by pairs, illustrated in figure 4. To evaluate given impulsive noise I, five levels of nonimpulsive noise R_n are played twice. The ten pairs (I,R_n) and (R_n,I) are compared at random. For each comparison, the Jury is asked simply "Which noise is the most annoying?" The percentage of the Jury who finds the nonimpulsive noise more annoying is then plotted against the difference in level between the nonimpulsive (NI) and the impulsive noise (I) measured in present subjective noise units: ΔPNdB and ΔTPNdB for stationary signals, ΔEPNdB for transient signals. Two "sensitivity curves" are obtained as shown in figure 5: one relative to (NI) being played before (I), the other relative to (NI) being played after (I). The mean curve is chosen to be the characteristic response curve. The annoyance correction ΔS is then considered to be such that 50% of the Jury find the (I) and (NI) levels equally annoying.

One can notice from figure 5 that the impulsive noise (I) is found more annoying when it is played _after_ the nonimpulsive noise (NI). This trend, constantly noticed throughout the complete study, shows that there is a memory effect which tends to emphasize the last event felt by the Jury as compared to the previous event.

This method of comparison by pairs needs an anechoic chamber and a large jury. But it does not require subjects acquainted to the specific problem to be studied. It qualifies in some way the annoyance felt by a general public not specifically motivated to exaggerate some special features of a noise signal which they would resent due to previous exposures as it could be the case for inhabitants located in the immediate vicinity of a heliport.

Details on the number and selection procedure of the French Jury are specified in reference 1 (about 60 persons retained after audiometer tests).

Method of Pairs Adjustment

It is based on the same principle of comparison between a reference noise and a noise to be qualified, but the subject is allowed to change the reference noise level and play back and forth the two noises to be compared until the equal annoyance of the two noises is reached. The iteration procedure followed by the subject can be recorded and allows a better statistical interpretation of the results obtained.

The subjective evaluation of the impulsive content of noise signals has been evaluated by this method of adjustment in several research centers: Westland Helicopters Ltd., National Physical Laboratory (U.K.), and Bolt Beranek and Newman (U.S.A.). The application of the method does not require an anechoic chamber and it can be conducted with a jury of smaller size. During the course of the experiments, the subjects acquire more experience in the particular features of the noise signals to be tested. In some way, the corrections found for impulsive signals could be closer to the opinion of inhabitants located in the immediate vicinity of an heliport.

Subjective Evaluation Results

Tables I and II provide the subjective results obtained in the French study. The impulse shape used is identified, together with the value of the different impulse parameters previously discussed. The CF_M, $\overline{CF}_{0.5}$, and $\bar{x}$ columns, which specify the degree of impulsivity, will be discussed and identified in the section entitled "Impulsiveness Descriptors and Possible Methods for Corrections."

Table III provides the subjective results of real helicopter transient noise which have been kindly provided by Bolt Beranek and Newman Inc., together with a duplicate of the recordings of the tested noise signals. Parameters pertaining to the degree of impulsivity (CF_M, $\overline{CF}_{0.5}$, $\bar{x}$) have been computed from this tape.

Both types of experimental results show that corrections of 0 to 7 dB have to be added to conventional units of PNdB or EPNdB to reflect the annoyance effect of impulsive noises. As shown in reference 1, the jury responses are statistically meaningful, giving a 90% confidence level of ± 1.3 dB.

IMPULSIVENESS DESCRIPTORS AND POSSIBLE METHODS FOR CORRECTIONS

An "impulsive descriptor" is a mathematical expression which is as simple as possible for ease of data processing and which could, as much as possible, provide a good correlation between the value of the descriptor and the subjective correction ΔS.

Stationary Noise Signals: Impulsiveness Descriptors

For stationary subjective data, examination of the jury corrections ΔS as a function of noise levels (90 and 100 PNdB) shows practically no influence of this parameter within this short range of variation. The three other parameters, namely shape, degree, and pulse repetition rate, have been combined into one single descriptor through use of:

- An "A" filtered signal which tends to decrease the effect of the low frequency content of the impulse

- An impulsivity coefficient $\overline{P_A^4}\Big/\Big(\overline{P_A^2}\Big)^2$ where P_A is the A filtered sound pressure time history

As shown in reference 1, for a pure periodic pulse train of pulse width a and period T, the unweighted coefficient $\overline{P^4}\Big/\Big(\overline{P^2}\Big)^2$ turns out to be equal to be equal to $k\,\dfrac{T}{a}$,

where k depends on the pulse shape (rectangle, k = 1; triangle, k = 1.8). If T increases, i.e., if the pulse repetition rate decreases, or if a decreases (i.e., if the "spikyness" increases), then this impulsivity coefficient increases.

Thus shape, degree, and pulse repetition rate are indeed taken into account in this $\overline{P_A^4}\Big/\Big(\overline{P_A^2}\Big)^2$ descriptor.

In the framework of the International Standard Organization (ISO) Working Group 2, this topic of impulsiveness descriptor has been brought forth and several impulsiveness descriptors have been submitted for examination. Among the different proposals (Westland Helicopters Ltd., South Africa National Research Institute, France SNI Aerospatiale, U.K. National Physical Laboratory) submitted before their last meeting date (Dec. 5, 1977), the NPL proposal[*] has been retained and recommended for application to ICAO - Working Group B.

The NPL descriptor is based on the variance of the square of the "A" weighted sound pressure signal divided by the square value of the r.s. "A" weighted sound pressure signal:

$$I = \frac{1}{\left(\overline{P_A^2}\right)^2} \cdot \left(P_A^2 - \overline{P_A^2}\right)^2$$

It can be shown that the I descriptor is identical to the French descriptor minus one. So this descriptor does take also into account the shape, degree, and pulse repetition rate parameters of impulsive noise. The other descriptors proposed were mainly based on the Crest Factor concept $\left(\dfrac{peak}{r.m.s}\right)$. As shown in figure 6, where comparisons are made on the same noise signals between x = 10 Log I and CF = 20 Log $\left(\dfrac{peak}{r.m.s}\right)$, the latter descriptor presents a lack of sensitivity.

[*]With a "short integration time" $\leq$ 200 µs.

Stationary Noise Signals: Correction Methods

Once an impulsiveness descriptor has been chosen, a correction method can be easily built using a best fit technique between the subjective corrections ΔS and the computed corrections ΔC. In the ISO N 356 proposal, the recommended correction law is

$$\Delta C_{(dB)} = 0.8 \ (x - 3)$$

where x = 10 Log I

This correction is limited to the range of

$$0. < \Delta C. < 5.5 \ dB$$

and held constant at 5.5 dB for larger values of x. It is to be noted that for x = 3 and I ≈ 2, the noise signal is purely broad band.

This correction method applied to the French subjective data provides a standard deviation of ±1.3 dB.

Transient Noise Signals: Impulsiveness Descriptors and Correction Methods

In the ISO N 356 recommended procedure, the impulsiveness descriptor remains the same as in the stationary case. The I Descriptor is computed at each 0.5 sec time interval, the correction $\Delta C_{0.5}$ is added to the L_{TPN} giving a L_{ITPN} time history from which the corrected EPNL is computed. This procedure is synthetically presented in figure 7.

At the last ISO Working Group 2 meeting, another procedure has been proposed to ISO members (ref. 3). As presented synthetically in figure 8, the impulsiveness descriptor is based on a "A" weighted Crest Factor CF, and the impulse repetition rate (f) is taken as a complementary descriptor.

Two possible impulsiveness correction methods were presented which are briefly sketched in figure 9.

In the first one, the "A" weighted Crest Factor is computed every 0.5 sec of the transient signal and a correction law is applied to L_{TPN}, giving a L_{ITPN} time history from which the corrected EPNL is computed.

An alternate method presented was to compute an overall correction Δ_0 to the EPNL which is based on the "A" weighted maximum Crest Factor CF_{Max}* measured during the transient noise signal.

The correction laws proposed in the two cases are linear as function of Crest Factor and pulse repetition frequency (f):

$$\Delta_{dB} = A + B \cdot (CF) + C \cdot f$$

---

*[Max (peak)]/[Max (r.m.s)], each factor measured independently.

446

and the A, B, and C coefficients are obtained in each case by a multilinear regression analysis using the subjective corrections ΔS of table III (nine experiments) as input data.

Procedures Discussion

The use of a multilinear regression technique to obtain a best fit correction method is indeed a very good approach, provided that a large number of experiments is taken into account in the computation process of the coefficients of the regression law. Otherwise, the correction law obtained may very well fit the experimental data which are used as input, while putting, on some parameter, a weight through the regression law coefficient which does not reflect its true importance. More precisely, at a time when manufacturers are trying to increase the number of blades of their rotors (ex., Hughes Aircraft Company, Quiet Helicopter Program) in order to decrease the noise, it is very important to know if the pulse repetition rate (f) has to be an independent parameter, and if it is the case, what values should be chosen for its regression coefficient C and its accuracy.

In order to answer these questions, a multilinear regression analysis has been performed on the complete set of available data presented in tables I, II, and III, using as possible descriptors the two previous Crest Factors $CF_{0.5}$ and CF_{Max}, the ISO descriptor x together with the pulse repetition rate f.

MULTILINEAR REGRESSION ANALYSIS

The method used in this analysis is briefly sketched in figure 10. The method is identical to the multilinear regression analysis used in appendix A of reference 3. Regression coefficients A, B, and C are computed using on one hand the subjective corrections ΔS as stated by the juries and impulsiveness parameters (I.D. = x, $CF_{0.5}$, CF_M) and pulse repetition rate f on the other hand. That is to say, the correction law assumed is

$$\Delta C = A + B \cdot (I.D.) + C \cdot f$$

and A, B, and C are computed to minimize

$$|\Delta C - \Delta S|$$

In addition to the overall standard deviation S_e which results from the best fit technique, and of the multiple correlation coefficient r, the present study defines also the standard deviation SA, SB, and SC for the coefficients A, B, and C.

These standard deviations on the regression coefficients define the accuracy provided on these coefficients A, B, and C by the method of analysis. They show, in a simple manner, the confidence level that one can grant to each parameter (I.D., f) taken into account. For example, it is possible that the multiple correlation coefficient r be statistically significant for a given confidence level, and that, at the same time, one obtains a standard deviation on one of the coefficients as large as the value of this coefficient itself. Obviously, in this case the parameter related to this coefficient has no real significance. These quality criteria have been summarized in figure 10.

Application of the Regression Analysis

- For the CF_{Max} and $CF_{0.5}$ descriptors, the procedure underlined in reference 3 has been followed. It is first necessary for a transient signal to define a mean value of the descriptor $CF_{0.5}$. For this purpose, $CF_{0.5}$ is computed at each 0.5 sec time interval from the "A" weighted noise signal, and a "first" correction $\Delta CF_{0.5}$ is computed

$$\Delta CF_{0.5} = CF_{0.5} - 12 \quad (\Delta CF_{0.5} > 0)$$

- A corrected PNLT is then computed

$$PNLT_{corr.} = PNLT + \Delta CF_{0.5}$$

which is used in the integration process to compute the $EPNL_{corr.}$

A mean 0.5 sec Crest Factor for the complete signal is obtained by the following expression:

$$\overline{CF}_{0.5} = (EPNL_{corr.} - EPNL) + 12$$

- A mean value of the ISO impulsiveness descriptor x has also to be computed in order to conduct the regression analysis. This mean descriptor $\bar{x}$ is computed following the same procedure as in the case of the $CF_{0.5}$ descriptor.

The EPNL correction is first computed following the ISO N 356 recommended method. Then $\bar{x}$ is deduced from this correction setting.

$$EPNL_{corr.} - EPNL = 0.8 \ (\bar{x} - 3)$$

- The values of CF_{Max}, $\overline{CF}_{0.5}$, and $\bar{x}$ are indicated for each recording used in the subjective evaluation methods in tables I, II, and III. It is to be noted that throughout this regression analysis a good consistency has been maintained in the hypothesis in order to get comparable results:

448

- The corrections at each 0.5 sec are applied from x = 3 (ΔC = 0) and $CF_{0.5}$ = 12 which represent the values of a pure broad band noise signal.

- The maximum correction at each 0.5 sec is 5.5 dB in each case.

- The regression analysis is conducted for the three descriptors in two cases:

(a) Taking into account the pulse repetition rate (f) as an independent parameter.

(b) Discarding the pulse repetition rate f in the regression law.

Regression Analysis Results

Table IV summarizes the results obtained in this regression analysis. The following remarks can be drawn from this table.

(a) The overall standard deviation is minimum (1.4 dB) when the ISO recommended method is used.

(b) The multiple correlation coefficient r is much higher (>0.75) when the ISO recommended method is used, while it is barely significant at 1% confidence level with the CF_{Max} or $\overline{CF}_{0.5}$ descriptor.

(c) Discarding the pulse repetition rate – which has a low regression coefficient C with a very high (44 to 75%) relative standard deviation (SC/C) – improves very much the standard deviation SA which influences directly (dB) the level of the correction ΔC.

Table V provides a direct comparison of the quality criteria of the regression analysis in the six cases treated. From this table one can conclude that:

- The pulse repetition rate should be discarded as an independent parameter

- The ISO recommended procedure provides on a statistical basis the best available method at the present time

These conclusions are more clearly illustrated in table VI which represents the computed results obtained from application of the regression laws without repetition rate dependency on the psychoacoustic tests conducted on the real helicopter noise signals of reference 3. Comparing computed corrections ΔC with the Jury subjective evaluations lead to the following remarks:

- CF_M and $\overline{CF}_{0.5}$ give high penalties (2.3 and 1.8 dB) for the reference noise supposedly nonimpulsive

- Overall standard deviation between the computed and the subjective results is 1.1 dB for the ISO method, 1.5 dB for the $CF_{0.5}$ method, and 1.7 dB for the CF_M method of correction

INSTRUMENTATION AND DATA PROCESSING

Procedure

In the ISO N 356 recommended method, the impulsiveness descriptor I is defined as follows:

1. The acoustic signal is weighted through a filter "A," then sampled at a frequency of 5000 Hz.

2. The digital values "v_i" thus obtained are processed, every 0.5 sec, in two steps:

- The mean square "s" of v_i at each 0.5 sec (i.e., the square of the signal r.m.s value), is first computed.

$$s = \frac{1}{n} \sum_{i=1}^{n} v_i^2 \qquad n = 2500$$

- The impulsivity descriptor I is then

$$(1) \quad I = \frac{1}{n} \sum_{i=1}^{n} \left(\frac{v_i^2 - s}{s} \right)^2 = \frac{1}{n} \frac{1}{s^2} \sum_{i=1}^{n} \left(v_i^2 - s \right)^2$$

It has been proved mathematically in reference 4 that this procedure leads to the value of the previously proposed French descriptor minus one, the latter descriptor being defined as:

$$(2) \quad CI = \frac{\overline{v_i^4}}{\left(\overline{v_i^2} \right)^2} \qquad I = CI - 1$$

So in principle, either expressions 1 or 2 can be used for the impulsivity descriptor computation process.

Instrumentation and Cost

The procedure previously underlined implies the use of:

450

- the "A" weighting and antialiasing (0 to 2000 Hz) filters

- an analog/digital converter ($\pm$10 volts; 11 bits + sign) associated with a 5000-Hz timer controlling the signal sampling

These instruments are quite inexpensive ($\approx$\$400).

The timer is synchronized with the 1/3 octave analyzer used to compute each 0.5 sec the 24 levels of the 1/3 octave spectrum needed for PNL computation.

Two cases have then to be considered (see fig. 11):

Case 1: The laboratory in which the data processing is to be performed uses a 1/3 octave analyzer coupled to a 5000 Hz real time computer for the I task in normal operations of PNL and EPNL computations. In this case, the computer has enough storage capacity to store 5000 sampled values (two time intervals of 0.5 sec, ΔT_{i-1}, and ΔT_i with 2500 values v_i at each time interval) and enough performance to compute the I value (5000 multiplications, 2500 subtractions, and few divisions) of the ΔT_{i-1} time interval during the time allowed (0.5 sec) for the "v_i" acquisition of the next ΔT_i time interval.

Case 2: The 1/3 octave analyzer is coupled to a lower performance computer not allowing real time computation of the I task at the frequency of 5000 Hz. In this case a complementary "mini computer" is necessary to store the 5000 sampled values and compute at each 0.5 sec the I value of the previous 0.5 sec time interval. This type of mini computer is at the present time available commercially at a low price compared to the other equipment necessary for pure EPNL computations. For example, in France, the AMSI type ALPHA LSI 4/90 which has the floating point computation capability (2 K - RAM, 8 K ROM - PROM) is sold in France at approximately \$5000 which is to be compared with the \$20 to 30 000 needed for a 1/3 octave analyzer.

GENERAL CONCLUSIONS

This study has essentially shown that:

(1) Impulsive noise needs to be corrected in order to represent the annoyance really felt by the public.

(2) Corrections up to 7 PNdB or EPNdB have been found by representative Juries in several countries, with a standard deviation of $\pm$1.3 dB.

(3) Among the proposed impulsiveness descriptors and correction methods, the recommended ISO N 356 procedure provides the best correlation between subjective and computed corrections.

(4) There is no special need to add to the proposed ISO N 356 procedure an additional correction term based on pulse repetition rate.

(5) The standard deviation obtained between computed and subjective annoyance of real helicopter noises is +1.1 dB which is comparable to the standard deviation of the jury subjective responses.

(6) The instrumentation and computing hardware necessary for data processing are available on the market at a small price compared to the cost of the equipment needed for EPNL data processing.

REFERENCES

1. Wright, S. E.; and Damongeot, A.: Psychoacoustic Studies of Impulsive Noise. 3rd European Rotorcraft Forum.

2. Schmitz, F. H.; Boxwell, A. A.; and Yu, Y. H.: A Simple Theoretical Model of High Speed Helicopter Noise. 3rd European Rotorcraft Forum.

3. Galloway, W. J.: Subjective Response to Simulated and Actual Helicopter Blade Slap Noise. BBN Report No. 3573.

4. Damongeot, A.: Instrumentation for Measuring the Impulsivity Indicator, ISO/TC-43/SC-1/WG2, proposed by N.P.L. or France.

PULSE SHAPE   **DEGREE OF IMPULSIVITY**

LIGHT HELICOPTER SIGNATURE

100 ms

WEAK IMPULSIVITY

HEAVY HELICOPTER SIGNATURE

100 ms

REPETITION RATE
10 Hz → 58 Hz

STRONG IMPULSIVITY

NOISE LEVELS
90 and 100 PNdB
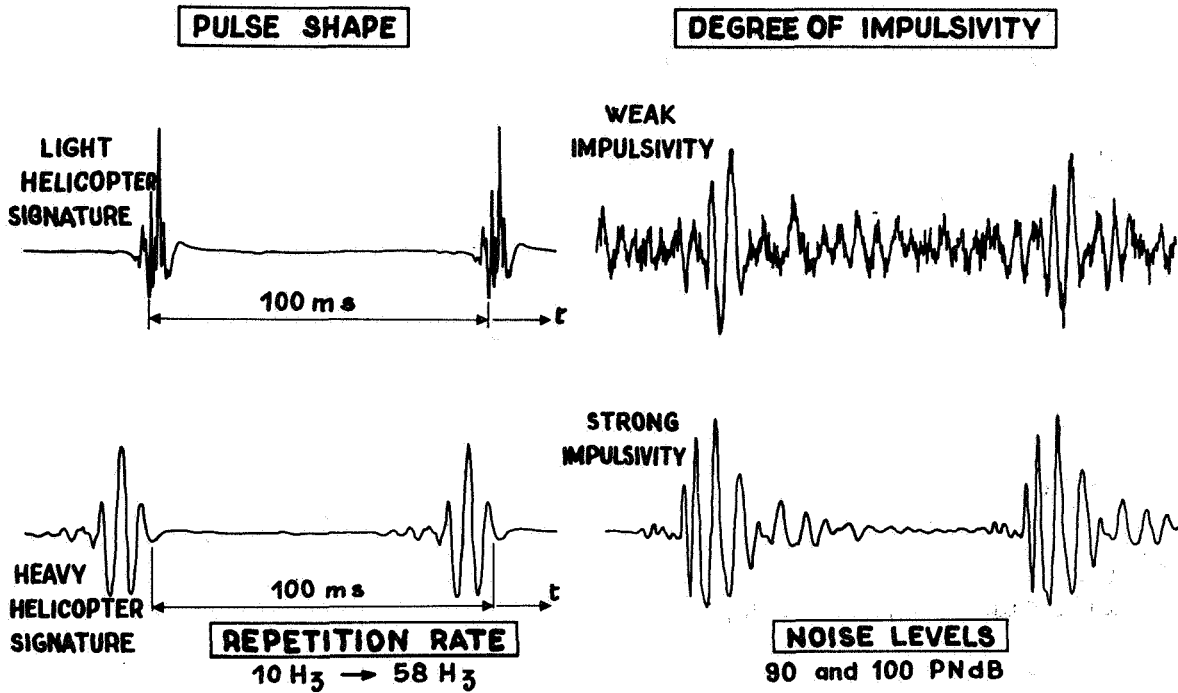
Figure 1.- Impulsiveness parameters.

SPEED 60 kts - HEAVY HELICOPTER

PRESSURE

0.2 seconds

10 SEC BEFORE PNL MAX
$x \simeq 7$ TO 8
STRONG IMPULSIVITY

AT PNL MAX
$x \simeq 6$ TO 7
MEDIUM IMPULSIVITY

10 SEC AFTER PNL MAX
$x \simeq 3$ TO 4
WEAK IMPULSIVITY
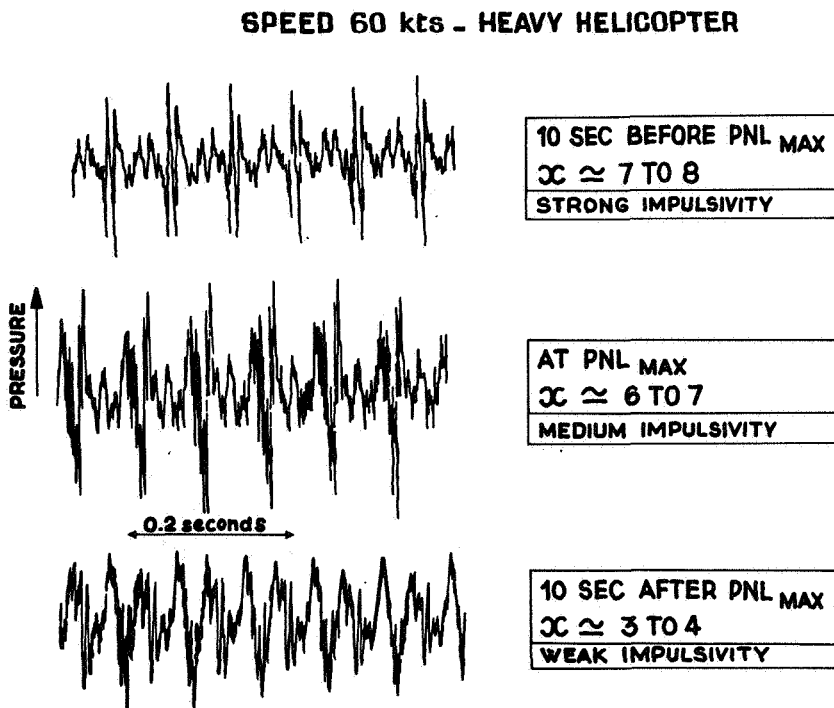
Figure 2.- Evolution of impulsiveness degree during helicopter flyover.

453
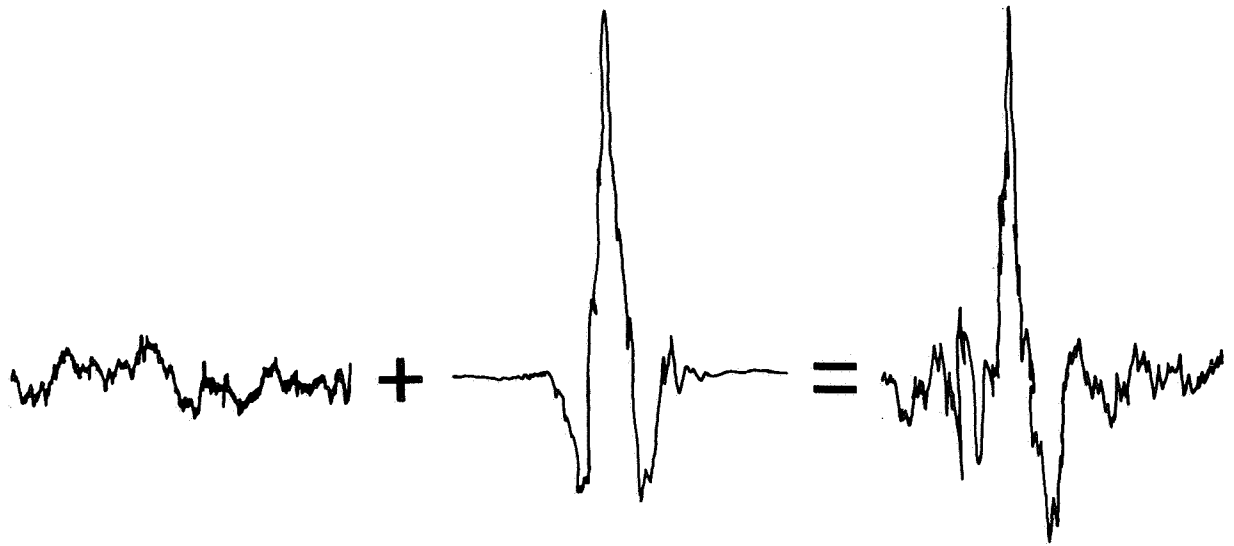
Figure 3.- Generation of helicopter noise signal.
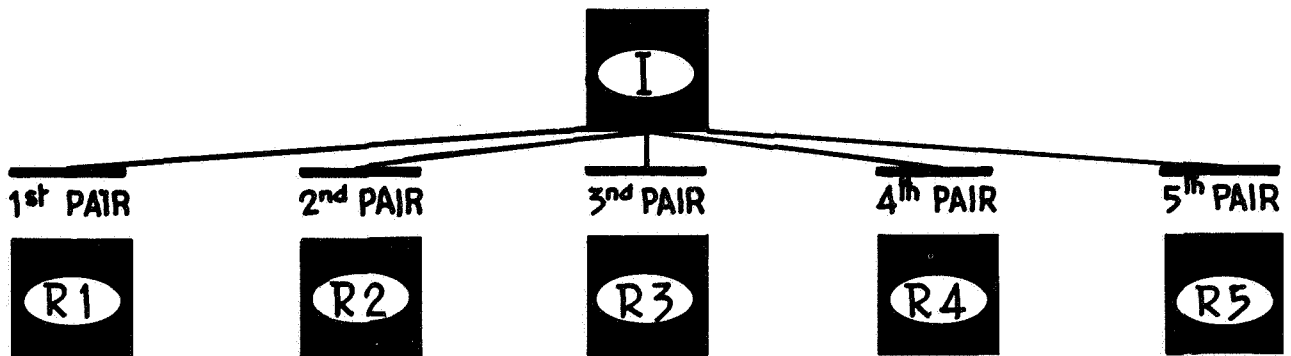
I : IMPULSIVE NOISE TO EVALUATE
   FIXED CONDITIONS : NOISE LEVEL, DEGREE OF IMPULSIVITY(x),PULSE
                     SHAPE, PULSE REPETITION RATE

R : NONIMPULSIVE COMPARISON NOISE AT 5 DIFFERENT NOISE LEVELS
    R1 TO R5 EACH PAIR(I, R_n) EVALUATED TWICE : ORDER (I,R_n) and (R_n,I)

Figure 4.- Subjective evaluation method comparison by pairs.
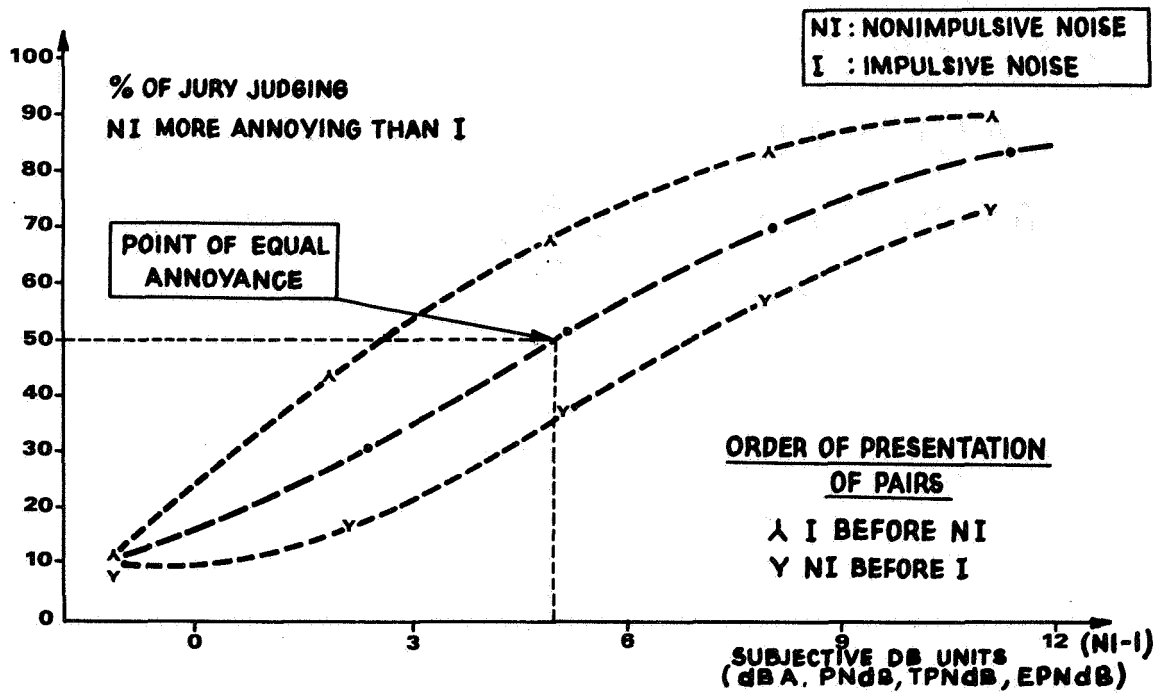
Figure 5.- Jury response curve.

$$CF = 20 \log \frac{PEAK}{RMS} \quad ; \quad x = 10 \log I \quad \text{with} \quad I = \frac{\overline{v_i^4}}{\left(\overline{v_i^2}\right)^2} - 1$$
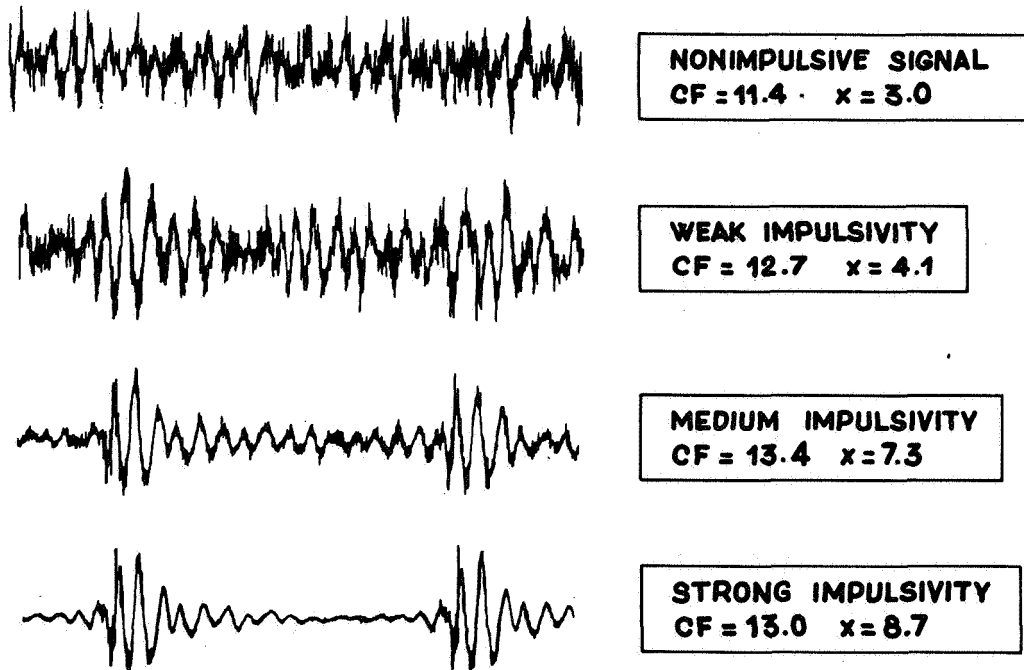
Figure 6.- Impulsiveness descriptors comparison.

■ ISO N 356 RECOMMENDED METHOD

- ● COMPUTE I DESCRIPTOR AT EACH 0.5 SEC.

- ● APPLY AT EACH 0.5 SEC. A CORRECTION ΔC TO THE L_{TPN}.

$$\Delta C_{(dB)} = .8(x - 3) \quad 0 \leq \Delta C \leq 5.5$$

WHERE $x = 10 \, \text{Log} \, I$

- ● COMPUTE THE EPLN FROM THE CORRECTED L_{ITPN} TIME HISTORY

Figure 7.- Impulsiveness correction methods.

● ISO RECOMMENDED DESCRIPTOR

$I \longrightarrow$ BASED ON THE VARIANCE OF THE SQUARE OF THE "A" WEIGHTED TIME HISTORY.

● DESCRIPTOR MENTIONED TO ISO

$-$ CF $\longrightarrow$ BASED ON THE CREST FACTOR OF THE "A" WEIGHTED PRESSURE TIME HISTORY.

$-$ IMPULSE REPETITION RATE (f) MENTIONED AS A POSSIBLE COMPLEMENTARY DESCRIPTOR

Figure 8.- Impulsiveness descriptor.

■ CORRECTION METHOD MENTIONED TO ISO

- COMPUTE $CF_{0.5}$ DESCRIPTOR AT EACH 0.5 SEC.
- APPLY AT EACH 0.5 SEC. A CORRECTION Δ TO THE L_{TPN}

$$\Delta_{dB} = A + B \ CF_{0.5} + \ Cf \qquad 0 \leftarrow \Delta \leq 5.5$$

  A, B, C OBTAINED FROM REGRESSION ANALYSIS OF PSYCHOACOUSTIC DATA.

- COMPUTE THE EPNL FROM THE CORRECTED L_{ITPN} TIME HISTORY

ALTERNATE METHOD

- OVERALL CORRECTION Δ_O APPLIED TO EPNL BASED ON CF_{MAX}

- $\Delta_O = A + B \ CF_M + Cf$

  WHERE A, B, C ARE COMPUTED FROM PSYCHOACOUSTIC DATA BY REGRESSION ANALYSIS TECHNIQUES

Figure 9.- Impulsiveness correction methods.

INPUT

- SET OF PSYCHOACOUSTIC DATA
    JUDGED RESPONSE : (ΔS)
    IMPULSE DESCRIPTOR (I.D.)
    IMPULSE REPETITION RATE (f)
- LINEAR CORRECTION LAW ASSUMED :

    $\Delta C = A + B(ID) + C \ (f)$

COMPUTE

    A, B, C. REGRESSION LAW COEFFICIENTS
    TO MINIMIZE $|\Delta C - \Delta S|$

QUALITY CRITERIA

- MULTIPLE CORRELATION COEFFICIENT $r > r_e$ FOR
    SIGNIFICANCE AT 1% LEVEL
- OVERALL STANDARD DEVIATION S_e : MINIMUM
- STANDARD DEVIATION ON COEFFICIENTS A, B, C : SMALL

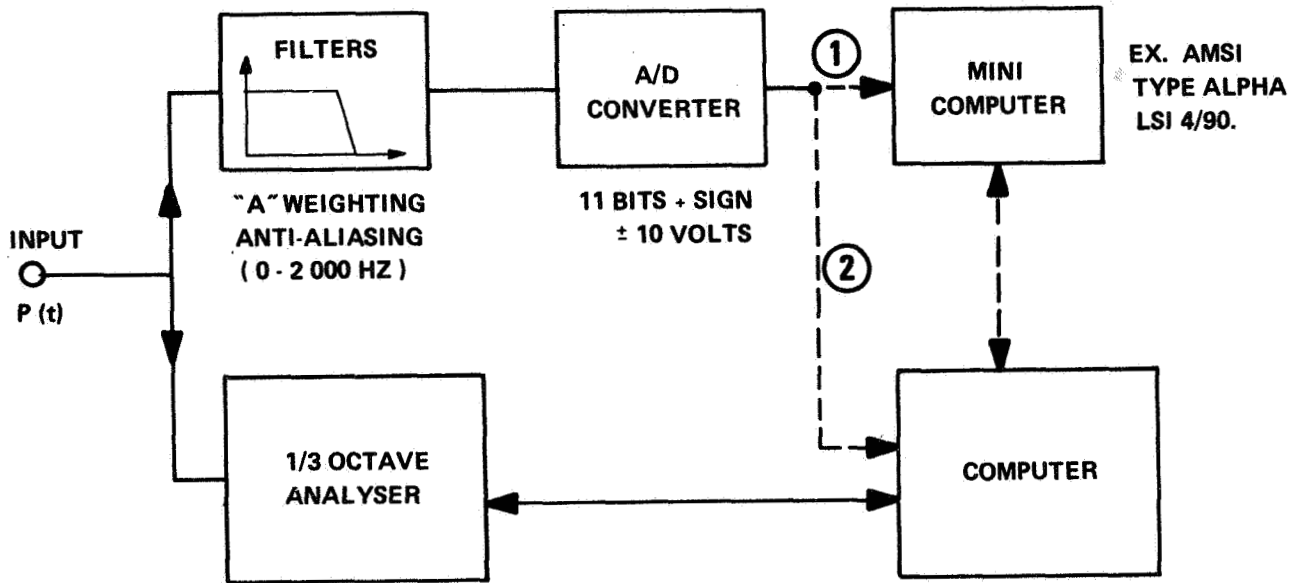Figure 10.- Multilinear regression analysis.

Figure 11.- PNL, EPNL computer system with impulsivity corrections.

TABLE I.- PSYCHOACOUSTIC TEST DATA - STATIONARY NOISE SIGNALS*

TEST N°	TYPE OF HELICOPTER	FREQ. HZ	CF_M	$CF_{0.5}$	$\bar{x}$	ΔS PNdB
201	HEAVY - N.I. (REF.)	17.5	12.9	12.4	3.3	0
202	LIGHT - N.I. (REF.)	17.5	15.2	12.9	3.6	0
206	HEAVY - 100 PNdB	10	14.7	14.8	9.5	5.6
210	LIGHT - 100 PNdB	10	14.9	13.8	4.0	0.9
211	LIGHT - 100 PNdB	10	19.4	20.3	9.6	4.2
212	LIGHT - 100 PNdB	10	20.3	22.	9.6	5.4
213	LIGHT - 90 PNdB	10	15.4	14.7	5.6	2.8
214	HEAVY - 90 PNdB	10	14.1	12.4	3.6	0.1
215	LIGHT - 90 PNdB	17.5	16.1	14.9	8.8	4.4
216	LIGHT - 90 PNdB	25	14.7	15.9	9.0	6.4
217	LIGHT - 90 PNdB	35	16.7	14.8	8.4	5.8
218	MOTORCYCLE - N.I. (REF.)	30	13.9	13.7	4.0	0
220	MOTORCYCLE 1	58	14.6	13.2	7.9	7.0
221	MOTORCYCLE 2	24	19.4	16.6	9.8	3.2

* FRENCH STUDIES, COMPARISON BY PAIRS

TABLE II.- PSYCHOACOUSTIC TEST DATA - TRANSIENT NOISE SIGNALS*

TEST N°	TYPE OF HELICOPTER	FREQ. HZ	CF_M	$\overline{CF}_{0.5}$	$\bar{x}$	ΔS EPNdB
101	FLYOVER - 70 Kt - N.I. (REF.)	17.5	12.5	12.3	3.5	0
102	H. LIGHT - 70 Kt - 95 EPNdB	10	15.8	15.2	6.1	4.2
103	HEAVY - 70 Kt - 95 EPNdB	17.5	14.3	14.5	4.1	2.1
104	FLYOVER - 148 Kt. N.I. (REF.)	17.5	13.8	13.5	4.1	0
105	H. HEAVY - 148 Kt - 95 EPNdB	17.5	15.8	17.8	9.0	1
106	H. HEAVY - 70 Kt - 95 EPNdB	17.5	13.7	13.1	3.8	4
107	H. HEAVY - 70 Kt - 95 EPNdB	17.5	14.8	15.6	7.0	2.3
108	H. HEAVY - 70 Kt - 95 EPNdB	17.5	15.7	15.7	6.2	2.5
109	H. HEAVY - 70 Kt - 100 EPNdB	17.5	15.9	15.8	6.5	2.1

• FRENCH STUDIES, COMPARISON BY PAIRS

TABLE III.- PSYCHOACOUSTIC TEST DATA - TRANSIENT NOISE SIGNALS*

B.B.N. N°	TYPE OF HELICOPTER	FREQ. HZ	CF_M	$\overline{CF}_{0.5}$	$\overline{x}$	ΔS EPNdB
214	S.61 (REF.) - 115 Kt - LEVEL	17	14.3	12.7	3.5	0
215	S.64 - 60 Kt - LEVEL	18.6	14.4	14.1	4.6	2.7
216	CH47.C. - 150 Kt - LEVEL	12.5	17.6	15.8	8.3	7.0
217	CH47.C. - 60 Kt - LEVEL	12.5	17.3	16.9	8.3	5.5
218	B.212 - 105 Kt - LEVEL	11	14.3	15.0	6.8	3.2
219	B.212 - 61 Kt - LEVEL	11	19.4	15.8	7.0	3.1
220	47.G. - 6° APPR.	12	17.7	16.1	7.1	3.5
221	S.61 - 6° APPR.	17	15.6	14.6	6.4	3.8
222	B.206 L - 6° APPR.	13	21.4	15.8	7.0	3.6

* B.B.N. STUDIES, METHOD OF ADJUSTMENT

DATA COMPUTED FROM B.B.N. MAGNETIC TAPE COPY.

TABLE IV.- REGRESSION ANALYSIS RESULTS - 32 PSYCHOACOUSTIC TEST DATA

I.D. IMPULSE DESCRIPTOR		A ± SA		B ± SB		C ± SC		S_e dB	r
CF_M	(a)	− 6.50	2.77	0.52	0.16	0.08	0.04	1.9	0.55
	(b)	− 4.01	0.36	0.44	0.16	—	—	2.0	0.44
$\overline{CF}_{0.5}$	(a)	− 7.14	2.71	0.57	0.16	0.09	0.04	1.8	0.58
	(b)	− 4.12	0.35	0.47	0.17	—	—	2.0	0.46
$\overline{x}$ (ISO)	(a)	− 2.43	0.90	0.74	0.12	0.04	0.03	1.4	0.77
	(b)	− 1.84	0.26	0.75	0.12	—	—	1.4	0.75

* CH47C PULSE RATE (f) AT 12.5 HZ

ΔS = A + B (I.D.) + C.f

r > 0.46 SIGNIFICANT AT 1 % LEVEL

(a) PULSE REPETITION RATE TERM INCLUDED

(b) PULSE REPETITION RATE TERM DROPPED

460

TABLE V.- QUALITY CRITERIA OF DIFFERENT IMPULSIVENESS DESCRIPTORS

DESCRIPTORS (I.D.)		SA dB	SB/B %	SC/C %	S_e dB	r
CF_M	(a)	2.8	31	50	1.8	0.55
	(b)	0.4	36	—	2.0	0.44
$\overline{CF}_{0.5}$	(a)	2.7	28	44	1.8	0.58
	(b)	0.4	36	—	2.0	0.46
$\overline{x}$ (ISO)	(a)	0.9	16	75	1.4	0.77
	(b)	0.3	16	—	1.4	0.75

$\Delta S = A + B \ (I.D.) + C.f$

SIGNIFICANCE AT 1 % LEVEL ⟶ r > 0.46

(a) PULSE REPETITION RATE TERM INCLUDED

(b) PULSE REPETITION RATE TERM DROPPED

TABLE VI.- COMPARISONS BETWEEN COMPUTED AND SUBJECTIVE IMPULSIVENESS
CORRECTION - TRANSIENT NOISE SIGNALS*

B.B.N. N°	TYPE OF HELICOPTER	FREQ.	ΔC EPNdB			ΔS JURY
			CF_M	$\overline{CF}_{0.5}$	$\overline{x}$ (ISO)	
214	S.61 (REF.) - 115 Kt - LEVEL	17	2.3	1.8	0.8	0
215	S.64 - 60 Kt - LEVEL	18.6	2.3	2.5	1.6	2.7
216	CH47.C. - 150 Kt - LEVEL	12.5	3.7	3.3	4.4	7.0
217	CH47.C. - 60 Kt - LEVEL	12.5	3.6	3.8	4.4	5.5
218	B.212 - 105 Kt - LEVEL	11	2.3	2.9	3.3	3.2
219	B.212 - 61 Kt - LEVEL	11	4.5	3.3	3.4	3.1
220	47.G. - 6° APPR.	12	3.8	3.4	3.5	3.5
221	S.61 - 6° APPR.	17	2.9	2.7	3.0	3.8
222	B.206 L - 6° APPR.	13	5.4	3.3	3.4	3.6
STANDARD DEVIATION			1.7	1.5	1.1	

* B.B.N. STUDIES, METHOD OF ADJUSTMENT.

462

ANNOYANCE DUE TO SIMULATED BLADE-SLAP NOISE

Clemans A. Powell
NASA Langley Research Center

SUMMARY

A study conducted at the NASA Langley Research Center was previously
reported in which the effects of several characteristics of blade-slap noise
on annoyance response were studied concurrently. These characteristics or
parameters were the sound pressure level of the continuous noise used to
simulate helicopter broadband noise, the ratio of impulse peak to
broadband noise or crest factor, the number of pressure excursions
comprising an impulse event, the rise and fall time of the individual
impulses, and the repetition frequency of the impulses. Forty subjects
made repeated judgments on a set of 36 noise stimuli which included 32
simulated helicopter blade-slap noises characterized by the above five
parameters and four nonimpulsive broadband noises. Each parameter was found
to have a significant effect on the annoyance judgments.

In the present study, additional analyses were conducted to determine the
correlation between subjective response and various physical measures for the
range of parameters studied. A small but significant improvement in the
predictive ability of PNL was provided by an A-weighted crest factor correction.
No significant improvement in predictive ability was provided by a rate
correction.

INTRODUCTION

Human reaction to helicopter noise, in general, cannot be quantified or
predicted as well as the noise from conventional take-off and landing aircraft.
It is generally agreed that the discrepancy in prediction, usually an under-
estimation of annoyance response, is caused by factors associated with the
pulsative nature of helicopter noise. Depending on the particular helicopter
and flight conditions, the impulsiveness of helicopter noise can range from
marginally perceptible modulation to severe repetitive bands or slapping
sounds.

Because of the underestimation of annoyance of helicopter noise by
various aircraft noise-rating scales, some researchers have suggested
modifying the noise-rating scales or adding an impulse noise correction.
Although considerable research has been conducted to determine the appropriate
modifications or corrections, these efforts have been generally unsuccessful
or inconclusive. Field annoyance studies suffer from a lack of control over

the physical parameters affecting the intensity of blade slap. It is generally not possible to separate the subjective effects of changes in blade slap from subjective effects of changes in other acoustical parameters which result from using different helicopter types or the same type under different operating conditions. Laboratory annoyance studies using recordings of actual helicopter noises, while suffering from a similar confounding of effects, also suffer from inadequacy of reproduction of the complex and phase sensitive time histories of helicopter flyover noise. To solve many of the problems associated with subjective tests using actual helicopter noises or recordings, some researchers have resorted to using simulations of helicopter noises. Most of these studies, however, have been confined to testing only one out of many characteristics of blade-slap noise which could be responsible for the reported discrepancies in prediction of annoyance response to such noises.

The study described in this paper was conducted to examine the subjective effects of several characteristics of repetitive impulse noise. Five variables were chosen to characterize helicopter blade slap and these characteristics or parameters were varied concurrently to investigate possible interactive effects. Human subjects listened to and rated the annoyance of short bursts of the simulated blade-slap noises. Some results of this study have been previously reported in reference 1, which indicated that each of the parameters had a significant effect on annoyance response. Additional analyses have been conducted which indicated that various objective measures such as PNL and L_A were also sensitive to changes in the parameters. The results of these analyses and the correlation between subjective and objective measures are reported herein. Comparisons are made between the results of this experiment and a study conducted by Boeing Vertol (ref. 2).

DESIGN AND PRELIMINARY RESULTS

A detailed description of the experimental design, procedures, and equipment used in the experiments is given in reference 1. The following paragraphs will summarize the design and present the preliminary results as presented in that reference.

Experimental Design

The following five parameters were chosen to characterize helicopter blade-slap noise consisting of a series of repeated impulses upon a continuous noise:

1. The sound pressure of the continuous noise used to simulate helicopter broadband noise.

2. The ratio of impulse peak to broadband noise sound pressure levels (idealized crest factor).

3. The number of pressure excursions making one complete impulse, ideally the number of sine waves in a single impulse.

464

4. The frequency of sine waves used to synthesize the individual impulses.

5. The repetition rate of the impulses.

A set of 32 simulated blade-slap noises was created which included each of these parameters in a high or low condition in the manner of a 2^5 factorial design. The high and low conditions for each parameter are given in table I. In addition to the impulsive noises, four samples of the nonimpulsive, broadband noise were included in the set for judgments by the subjects. The 36 noise stimuli were randomly ordered into four groups of nine stimuli each. The order of presentation of the stimuli groups was counterbalanced between groups of test subjects.

Special precautions were taken to reduce the influence of room reflections and to insure that the subjects experienced the desired waveforms. Sound-absorbing panels which can be seen in figure 1 were used to reduce room reflections. The impulsive and continuous portions of the stimuli were synthesized and recorded on separate channels of a stereo tape recorder. A specially modified low-frequency loudspeaker was used to reproduce the impulsive waveforms. During stimuli preparation, the impulsive signals were monitored at the test subject's head location and the recorded signals modified to reproduce the waveforms called for in the experimental design. The stimuli heard by the subjects were constant level 10-sec bursts of noise with 0.5 sec on ramp and off ramp.

Twenty male and twenty female subjects made judgments on each of the complete sets of noise stimuli and a complete replication of the stimuli. Each judgment was made on a continuous numerical scale from 0 to 9, from "no annoyance" to "maximum annoyance."

Data Analysis and Results

The 2560 annoyance judgments made on the impulsive noises were analyzed using an analysis of variance procedure, an abbreviated version of which is presented in table II. Each of the five parameters was found to have a significant effect at the 0.01 level on the annoyance response of the impulsive blade-slap noises. Figure 2 illustrates the magnitude and direction of the effect of each of the five parameters on the mean annoyance response. For example, the mean annoyance rating for the impulsive noises with one sine wave per impulse was less than the mean annoyance rating for the impulsive noises with three sine waves per impulse. From this figure, it can be seen that the level of continuous noise and the idealized crest factor had large, positive effects on mean annoyance. The number of sine waves, the frequency of sine waves, and the repetition frequency had much smaller, positive effects although each was statistically significant.

These findings, although of academic interest, do not resolve the question of whether or not the present noise-rating scales underestimate the annoyance potential of impulsive noises as compared with nonimpulsive noises.

465

To provide some information on this question, the author of reference 1 performed correlation analyses between the subjective ratings of both the impulsive and nonimpulsive noises and various noise-rating scales. These analyses indicated that the perceived noise level scale underestimated by about 2 dB the annoyance potential of the impulsive noises.

The next section of this report will present the results of additional analyses which were performed on the data from reference 1 to determine whether or not this underestimation of the annoyance potential of the impulsive noises was related in any systematic way with the five parameters varied in the experiment.

ADDITIONAL ANALYSES AND RESULTS

Analyses

The first step of additional analyses was to determine which of the noise-rating scales examined in the experiment provided the best overall correlation with the mean response data for each noise condition. Linear least square regression analyses were performed with the mean response data as the dependent variable and with the physically measured data for each rating scale as independent variables. The correlations in terms of the Pearson product moment correlation coefficients for the mean response and each rating scale are presented in table III. In addition, the correlations between the various rating scales are also presented. The mean data were obviously highly correlated with the measured values of each rating scale, as were the measured values between rating scales. Because of the high correlation between rating scales, the differences in correlation for the different rating scales with the mean response are not significant. However, since PNL was more highly correlated than the other rating scales and since it forms the basic measure for the accepted standard measure (EPNL) for conventional aircraft noise, the further analyses were conducted using PNL as the primary physical measure.

The results of the regression analysis of the mean response on the PNL values for the stimuli are presented in figure 3. The nonimpulsive noise stimuli are represented by the solid circular symbols and the impulsive noise stimuli by the open circular symbols. The least squares linear regression for these points is indicated by the solid line. As is typical for this type judgment scale, there appears to be some slight curvature in trend of the data points at the ends of the range. In order to reduce this nonlinear behavior, the following procedure was used to convert the mean subjective data into subjectively equivalent noise levels for further comparison between the various noise conditions. A polynomial regression was performed in the form

$$X_i = a + by_i + cy_i^2 + dy_i^3$$

where X_i is the PNL value for the ith stimulus and y_i is the corresponding mean subjective response. The resulting best fit regression was found to be

$$X = 64.76 + 6.874y - 0.670y^2 + 0.044y^3$$

The predicted or subjectively equivalent noise level for each stimulus was calculated by substituting the respective mean response value into the regression relationship. For further discussion, the subjectively equivalent noise levels will be designated simply as equivalent levels. The equivalent level (Eq.L.) of each stimulus is plotted in figure 4 against the respective measured PNL values. A close comparison of the data in figures 3 and 4 indicates the improvement in linearity between the subjective response and noise level in PNL.

The difference in annoyance between the impulsive noise stimuli and the continuous noise which served as simulated helicopter broadband noise was determined by subtracting the equivalent levels of the nonimpulsive noise stimuli from those of the respective impulsive noise stimuli. The values thus obtained (ΔEq.L.) represent the increase in annoyance due to the addition of the impulsive noise on the continuous background noise. Similarly, the difference in the PNL values of the impulsive noise stimuli and the respective nonimpulsive noise stimuli (ΔPNL) represents the increase in PNL attributed to the addition of the impulsive noise. A comparison of these two sets of values is presented in figure 5. The open symbols represent those data with a continuous noise level of 65 dB (OASPL) and the solid symbols represent those with a continuous level of 80 dB (OASPL). From this figure, it can be seen that, in general, the addition of the impulsive noise produced a greater increase in annoyance than was accounted for by the increase in PNL. The excess annoyance did not appear to be strongly related to the level of continuous noise.

The same data are reproduced in figures 6 to 9 with the other factors of the experimental design as separable parameters. The data in figure 6 are separated by the different symbols into the conditions of high and low idealized crest factor. Although the data are clearly grouped by this parameter, the change in PNL mirrors the change in effective noise level equally as well for the high idealized crest factor as for the low idealized crest factor conditions. In figure 7, the data are separated by the repetition rate of the impulses. No clear separation of the data is provided by the repetition rate factor. In figure 8, the data are separated by the number of sine waves in the impulse events. Based on the greater number of data points below the line of equality for the 3-sine wave condition as compared with the 1-sine wave condition, there appears to be some relationship between the annoyance of the impulsive noises and the number of sine waves that is not accounted for by PNL. Figure 9 presents the data separated by the frequency of sine waves in the impulse events. There appears to be no consistent effect of the frequency of sine waves on the increase in annoyance due to impulsiveness which is not accounted for by a change in PNL.

In order to more accurately quantify the effects of the various factors of the experiment, a correlation analysis was performed between the factors, subjective measures, and objective measures previously described. Two additional correlates were considered in the analysis and are defined as follows. The underestimation of PNL to account for the subjective differences between the impulsive and nonimpulsive noise annoyance was defined as

$$\Delta S = \Delta Eq.L. - \Delta PNL$$

where $\Delta Eq.L.$ was the difference between the equivalent level for the impulsive and nonimpulsive noises and ΔPNL was the difference between the perceived noise levels of the impulsive and nonimpulsive noises. An A-weighted impulsive correction was defined as

$$\Delta CF_A = L_A(peak) - L_A(rms) - 12$$

The correlation matrix for the subjective measures, objective measures, and experimental factors is presented in table IV.

The high correlation of the effective level with PNL is indicative that, in general, PNL predicted the subjective response very well, the unexplained error being only 4 percent of the total variation in subjective response over a wide range (28 PNdB) of noise levels. The standard error of estimate using PNL as a predictor of effective noise level was 1.72 dB. The only experimental factor which was found to be significantly correlated with the equivalent level was the idealized crest factor. The idealized crest factor, however, was also found to be significantly correlated with PNL to approximately the same degree.

Similarly, the change in equivalent level between the impulsive and nonimpulsive noises was found to be significantly correlated with the change in PNL and the idealized crest factor. Again, however, the idealized crest factor was found to be significantly correlated with a change in PNL.

The difference (ΔS) between the change in equivalent level and the change in PNL was found to be significantly correlated with the crest factor correction but not with the idealized crest factor. There was, however, a significant negative correlation of ΔS and the number of sine waves comprising the impulse events. Qualitative indications of this trend were presented in figure 8 and in previous discussions. The number of sine waves was also sufficiently and negatively correlated with ΔCF_A so that it is doubtful that any improvement in prediction beyond that afforded by ΔCF_A would be realized.

Least square regression analyses (fig. 10) were performed with the underestimation of PNL for impulsive noises ΔS as the dependent variable and the impulsive correction ΔCF_A as the independent variable. The regression

468

equation thus obtained was

$$\Delta S = -0.04 + .400 \times \Delta CF_A$$

The standard error of estimate (SEE) for the regression was 1.52 dB. It should be pointed out, however, that this value is only 0.2 dB improvement in the predictive ability of PNL with no impulsive correction.

There has been recent evidence (ref. 3) that the rate of the impulse events correlates equally as well with the underestimate of PNL or EPNL as does various impulsive corrections. This trend has not been confirmed with the results of the present experiment.

Comparison With Other Research

In a recent experiment conducted by Boeing Vertol and reported in reference 2, subjects adjusted the impulsiveness of simulated blade-slap noises until they were as equally annoying as continuous noises with spectra simulative of helicopter broadband noise. The impulsive noises were presented simultaneously with broadband noise with the same spectra as the reference noises but at a lower fixed level. The subjects' task was to vary the level of the impulsive portion of the test stimuli to match the annoyance of the reference stimuli. The experiment was factorial in design and consisted of 108 pairs of stimuli comprised of three different broadband spectra, three levels of reference broadband noise, three impulsiveness conditions, and four impulse repetition rates. At the completion of each adjustment for equality of annoyance, the level of the impulsive noises in terms of various physical measures was recorded. The average of these levels over subjects provided measures of the level for equal annoyance for the impulsive stimuli. The difference in level between the reference broadband stimuli and the test impulsive stimuli at the point of equality thereby represented the underestimation of the physical measure. Regression analyses were performed with the underestimation (in terms of PNL) as the dependent variable and with ΔCF_A and rate as independent variables. Significant correlation was found only for the crest factor correction. The relationship was found to be

$$\Delta S = -3.37 + 0.113 \Delta CF_A$$

with a correlation coefficient of 0.265, which for 106 degrees of freedom is significant at the 0.99 level. The standard error of estimate was 2.65 dB.

Although a significant dependence was found on the A-weighted crest factor correction, the slope for the dependence was considerably less than was found in the NASA experiment.

One possible reason for the differences in results could be the differences in the manner of presentation of the noise stimuli. The stimuli for the NASA experiment were presented via loudspeaker whereas those for the Boeing Vertol experiment were presented over headphones. The differences in results, thereby, could have been the result of the difference in whole-body response and auditory response.

CONCLUDING REMARKS

Additional analyses have been conducted on data obtained from a previously reported experiment which was conducted to systematically investigate the effects of various parameters of helicopter blade-slap noise. Five parameters were chosen to synthesize blade-slap noise. These were the sound pressure level of the continuous broadband noise, the idealized crest factor of the impulses above the continuous noise, the number of sine waves in a single impulse, the frequency of the sine waves, and the impulse repetition frequency. Forty subjects judged the annoyance of each of the noises.

Although each of the parameters was found to have a positive and significant effect on judged annoyance, each parameter was found in the analysis reported herein to produce a similar change in measured noise level in terms of PNL.

A slight but significant improvement in the predictive ability of PNL was provided by the addition of an A-weighted crest factor correction. No significant improvement was provided by the addition of a correction proportional to the rate of impulses.

Further analysis of a recent experiment conducted by Boeing Vertol under NASA contract indicated a similar lack of need for a rate correction. Results from this experiment, however, indicated a significant but smaller crest factor correction than was indicated in the NASA experiment.

REFERENCES

1. Lawton, Ben William: Subjective Assessment of Simulated Helicopter Blade-Slap Noise. NASA TN D-8359, 1977.

2. Sternfeld, Harry, Jr.; and Doyle, Linda Bukowski: Evaluation of the Annoyance Due to Helicopter Rotor Noise. NASA CR-3001, 1978.

3. Galloway, William J.: Subjective Evaluation of Helicopter Blade-Slap Noise. Helicopter Acoustics, NASA CP-2052, Pt. II, 1978. (Paper no. 20 of this compilation.)

TABLE I.- VALUES ASSIGNED TO FIVE PARAMETERS CHOSEN TO

SIMULATE HELICOPTER BLADE SLAP

Parameter	Value of Parameter	
	Low	High
Number of sine waves in impulse	1	3
Sine wave frequency, Hz	200	400
Repetition frequency of impulses, Hz.	8	20
Level of continuous noise, dB[a].	65	80
Idealized crest factor[b] of impulsive noise, dB. . .	15	25

[a]SPL dB referenced to 20 µPa.

[b]Crest factor is defined as ratio of peak to root-mean-square pressure for an acoustic signal.

$$\text{Crest factor} = \frac{\text{Peak pressure}}{\text{rms pressure}}$$

When converted to dB scale, crest factor is peak SPL minus rms SPL. For purposes of defining noises used in this study, an idealized crest factor was specified, peak SPL of impulses minus rms SPL of continuous noise.

TABLE II.- RESULTS OF ABBREVIATED ANALYSIS OF VARIANCE

Source	Degrees of freedom	Sum of squares	Mean square	F-ratio[a]
Number of sine waves	1	77.006	77.006	22.510
Frequency of sine waves	1	104.248	104.248	30.473
Impulse repetition frequency	1	55.460	55.460	16.212
Level of continuous noise	1	9307.838	9307.838	2720.795
Idealized crest factor	1	1460.170	1460.170	426.825
Error	2554	8737.289	3.421	--------
Total	2559	19742.011		

[a]These F-ratio values are significant at 0.01 level. For one and infinite degrees of freedom at this level, the critical F-value equals 6.63.

TABLE III.- CORRELATION MATRIX OF MEAN SUBJECTIVE RESPONSE

AND PHYSICAL DESCRIPTORS

	OASPL, rms	OASPL, peak	L_A, rms	L_A, peak	L_A, impulse	PNL
Mean response	0.965	0.972	0.976	0.954	0.966	0.978
OASPL, rms		.975	.976	.921	.964	.990
OASPL, peak			.974	.969	.974	.977
L_A, rms				.968	.993	.994
L_A, peak					.925	.947
L_A, impulse						.984

TABLE IV.- CORRELATION MATRIX OF SUBJECTIVE MEASURES,

OBJECTIVE MEASURES, AND EXPERIMENTAL FACTORS

	ΔEq.L.	PNL	ΔPNL	ΔS	ΔCF_A	Idealized crest factor	Rate	Number	Frequency
Eq.L.	[b]0.547	[b]0.980	[a]0.417	0.268	0.005	[a]0.370	0.076	0.079	0.107
ΔEq.L.		[b].499	[b].890	.202	.112	[b].842	.172	.180	.244
PNL			[b].457	.073	-.103	[a].372	.115	.166	.052
ΔPNL				-.267	-.129	[b].860	.266	[a].383	.119
ΔS					[b].513	-.065	-.206	[a]-.441	.259
ΔCF_A						.203	[b]-.454	[b]-.522	[b].559

[a]Correlation coefficient significant at 0.05 level.

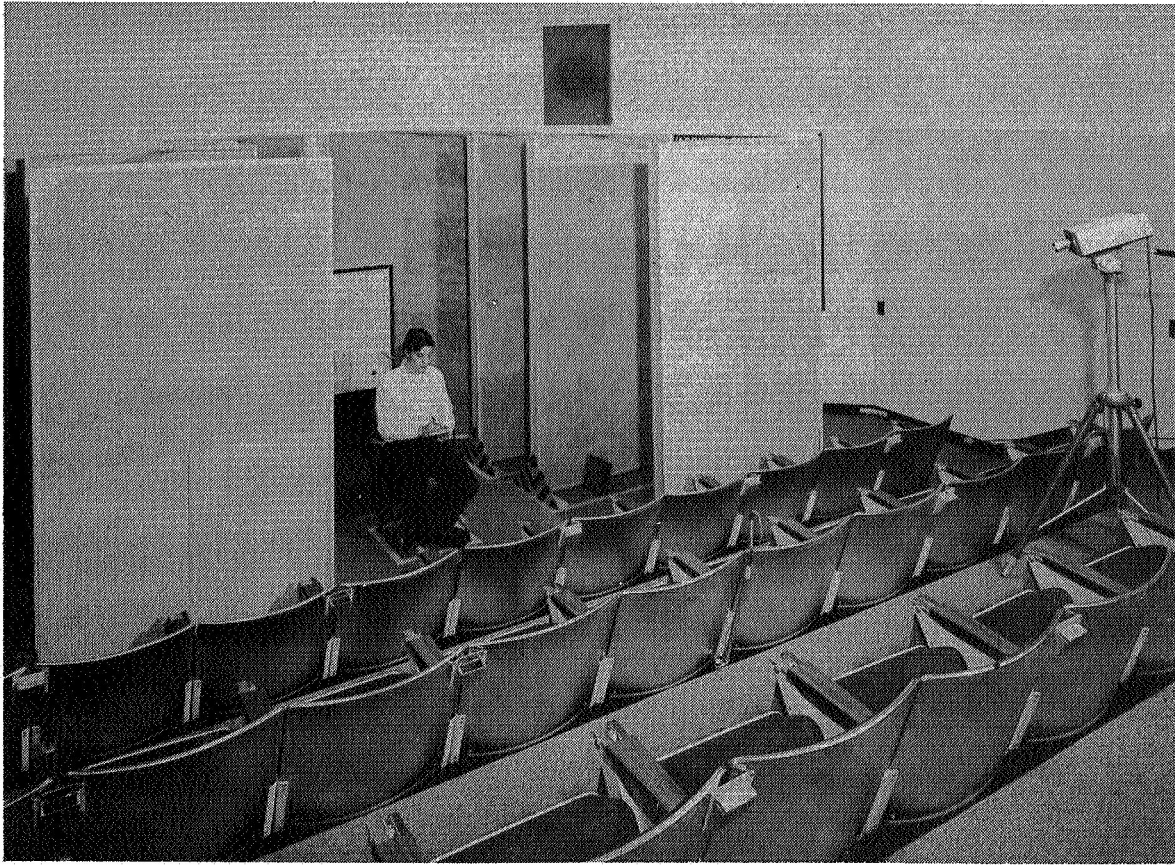[b]Correlation coefficient significant at 0.01 level.

Figure 1.- Photograph of test chamber showing orientation of subject and loudspeakers.
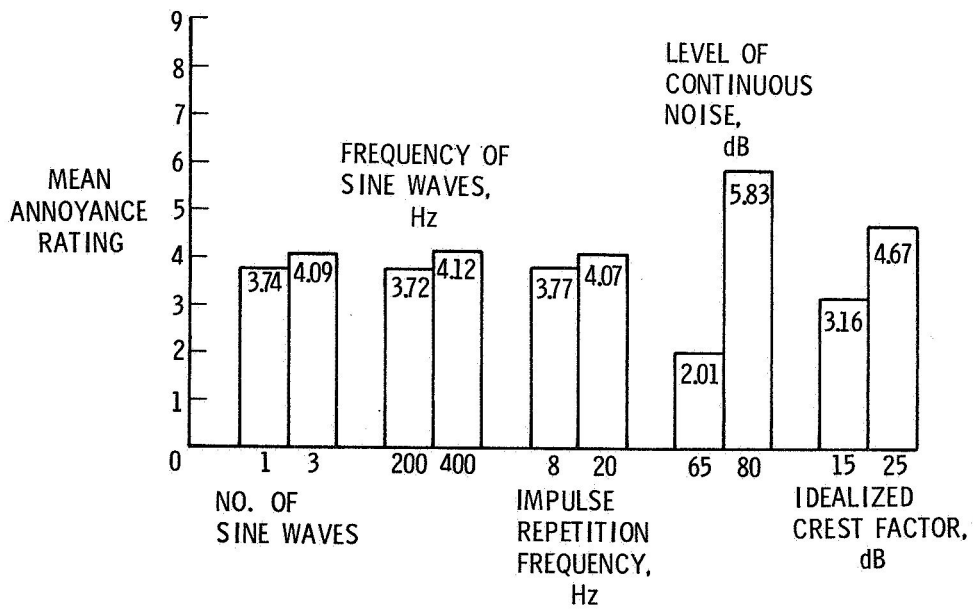

Figure 2.- Annoyance effects of five parameters used to synthesize impulsive test noises.
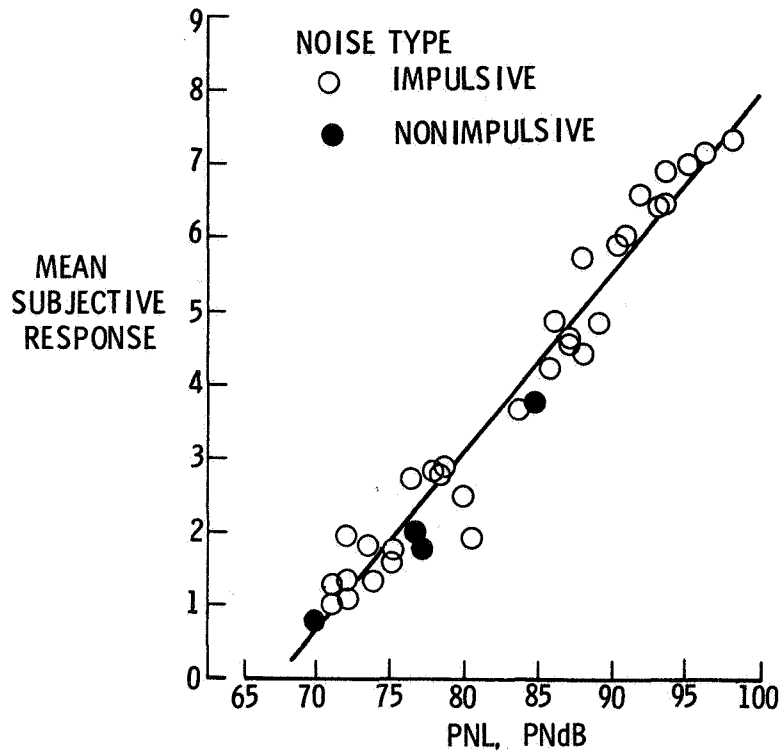
Figure 3.- Mean subjective response to impulsive and nonimpulsive noises.
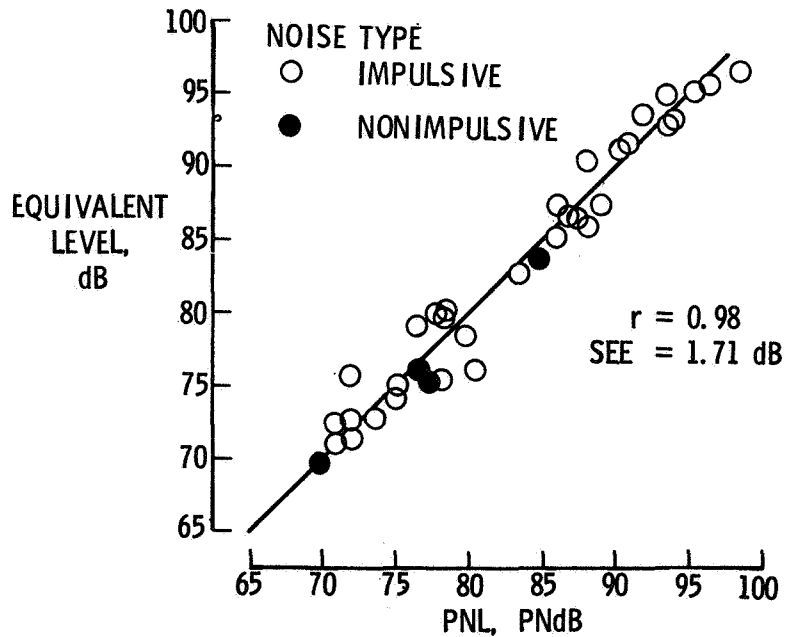
Figure 4.- Correlation of equivalent noise level with PNL for impulsive and nonimpulsive noises.
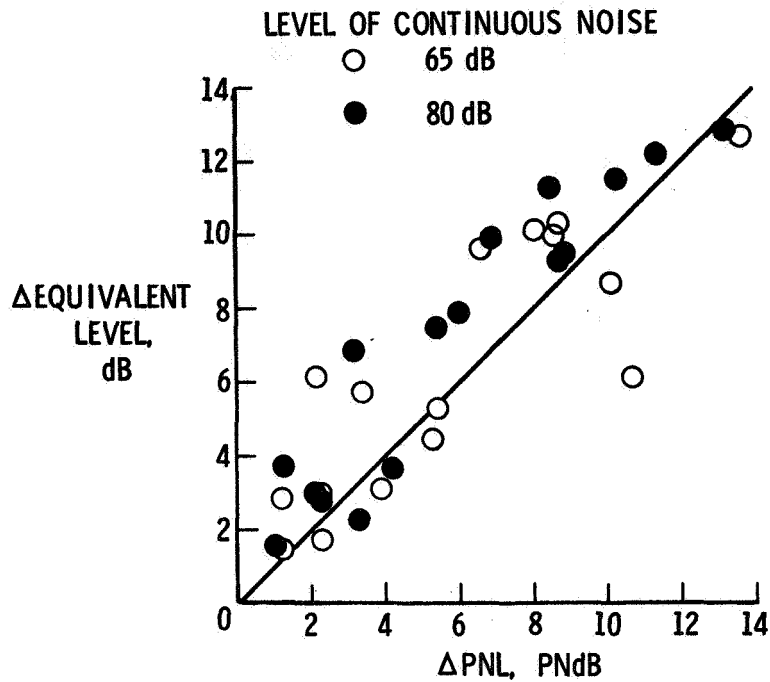
Figure 5.— Effects of impulsiveness for two levels of continuous noise.

Figure 6.— Effects of impulsiveness for two levels of idealized crest factor.

Figure 7.- Effects of impulsiveness for two repetition rates
of impulsive events.

Figure 8.- Effects of impulsiveness for two numbers of sine waves
comprising an impulse event.

Figure 9.- Effects of impulsiveness for two frequencies of sine waves comprising an impulse event.

Figure 10.- Underestimation of PNL for impulsive noises.

HUMAN RESPONSE TO AIRCRAFT-NOISE-INDUCED BUILDING VIBRATION

Jimmy M. Cawthorn, Thomas K. Dempsey, and Richard DeLoach
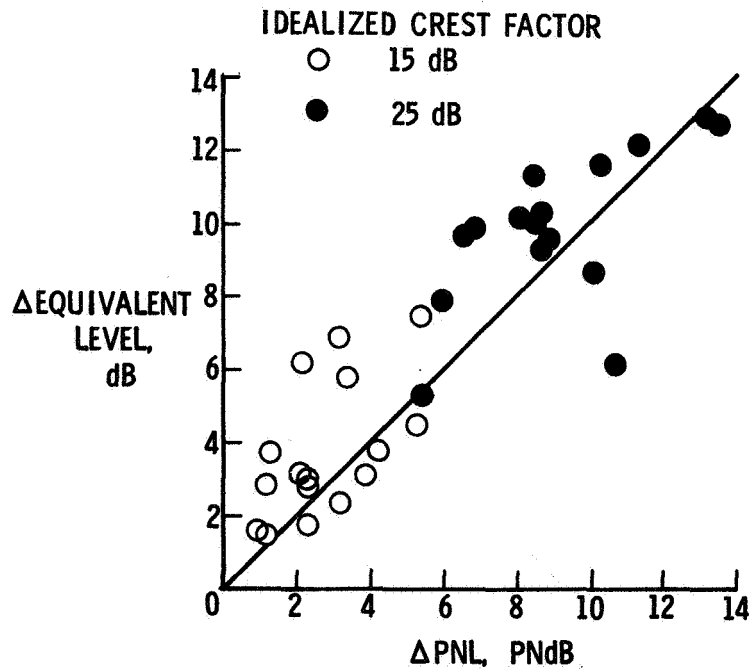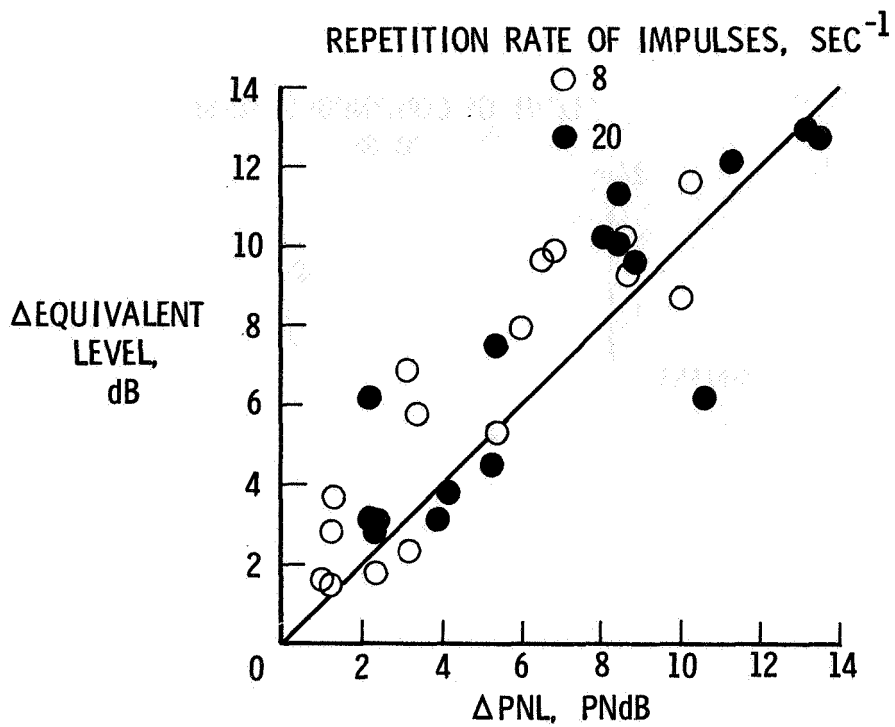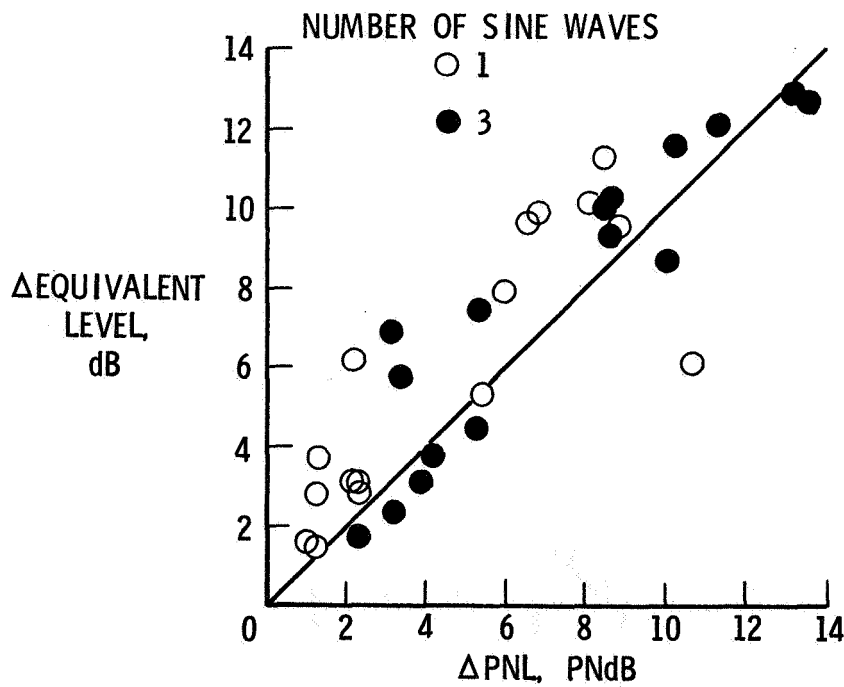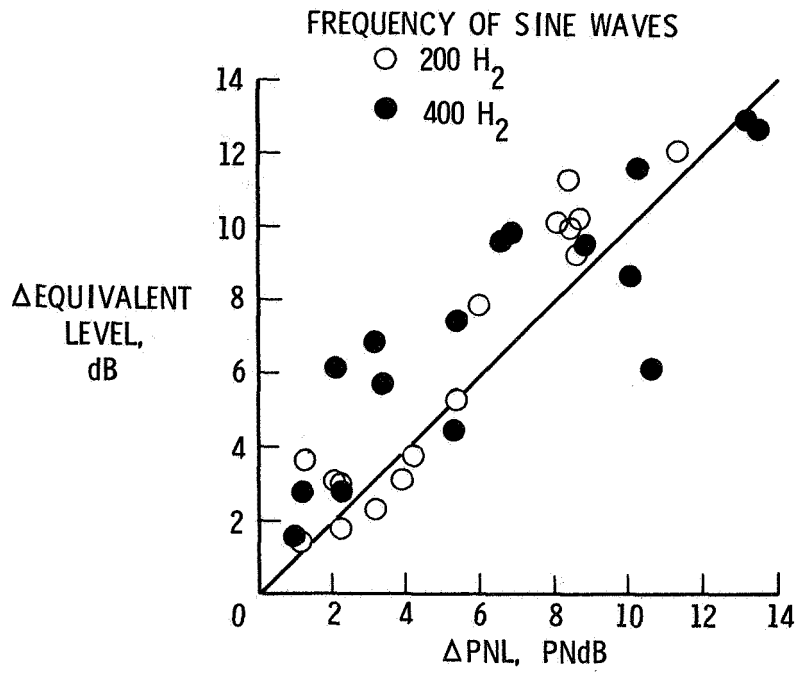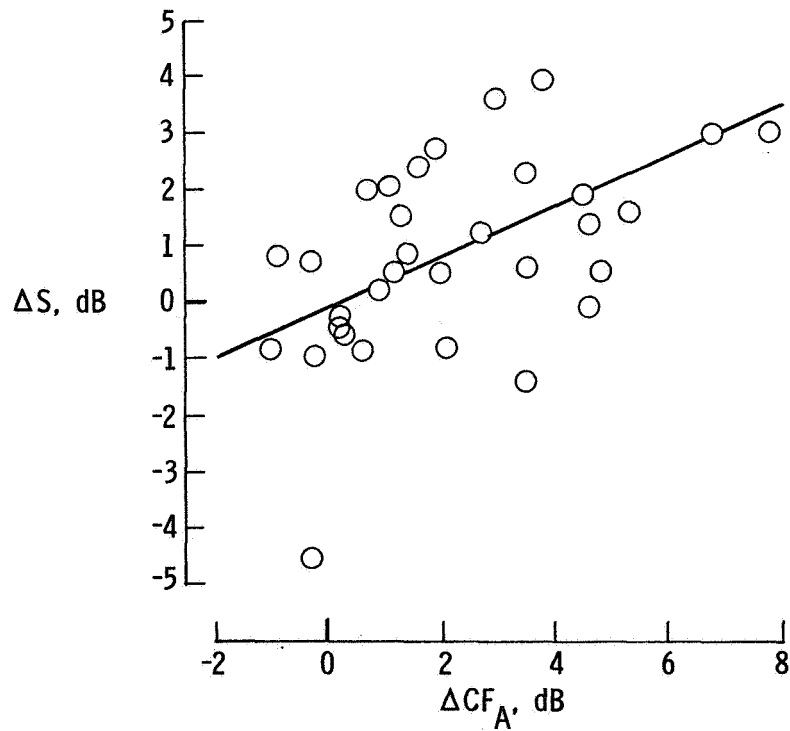NASA Langley Research Center

SUMMARY

A series of pilot studies has been conducted in both the field and the
laboratory to investigate the effects of noise-induced building structure
vibration and the rattle of objects 'on human response to aircraft flyover
noise. The field studies were conducted in actual airport communities,
and the specific objectives included the determination of subjective detection
thresholds for vibration and rattle, as well as the effect of vibration and
rattle upon aircraft noise annoyance. The laboratory study, conducted at
Langley Research Center, was concerned primarily with the factor of rattle.
The specific objectives included the determination of rattle detection thres-
holds, rattle annoyance thresholds, and the effect of rattle on the overall
annoyance response to an aircraft flyover noise event.

As a result of these studies, the vibration detection threshold was
determined and building structural vibration was found to increase the annoyance
response produced by an aircraft noise event. The rattle of objects was
observed very infrequently in the field study and in the laboratory study
rattle was found to be of no significance and not important.

INTRODUCTION

Airport community noise surveys (ref. 1) and complaint records (ref. 2)
have often highlighted building vibrations and associated rattle of objects
within buildings as a source of annoyance to residents living in airport
communities. This vibration/rattle may be a potential detriment to helicopter
development and operations because of the low frequency and impulsive nature
of helicopter noise signals. The impact of aircraft noise (inclusive of
helicopter noise) on people who are exposed to the noise while indoors can be
illustrated as shown schematically in figure 1. Aircraft operations generate
noise which impinges upon the exterior of a house and is then transmitted
through the house structure to the interior where it is perceived by the
resident. In some cases, the noise impingement and sound transmission process
will produce structural vibration and/or the rattle of objects within the home.
If the magnitude of any (or all three) of these physical stimuli are above an
individual's detection threshold, it is likely that the individual will not only
perceive them but will combine them in some way to produce a total annoyance
response. The resultant annoyance response of a community resident to an air-
craft noise is, therefore, dependent upon some type of integration of the three
physical stimuli. The noise generation and propagation into the interior of
the house together with the associated building vibration and rattle constitute
the major physical aspects of this environment. The subjective response to the

physical environment, however, involves a determination of separate noise, vibration, and rattle detection thresholds and the manner in which these separate physical factors combine to produce a total annoyance. This paper presents the results of a series of field and laboratory studies that were conducted to (1) obtain detailed measurements of the noise/vibration/rattle environment, (2) obtain subjective annoyance responses to the combined environment, and (3) attempt to define the psychophysical relationship between the subjective responses and the physical environment.

The field studies were conducted in actual airport communities. Specific objectives of the community studies included the determination of subjective detection thresholds for vibration and rattle, as well as the effect of vibration/rattle upon aircraft noise annoyance. The laboratory study conducted at Langley Research Center was concerned primarily with investigating the relative importance or influence of the factor of rattle upon subjective annoyance. The laboratory setting was selected for the rattle investigation since it is very difficult to define and measure rattle in the complex environment of a field study. Specific objectives of the laboratory study were to determine, under controlled conditions, the rattle detection threshold, rattle annoyance threshold, and the effect of rattle on aircraft noise annoyance.

COMMUNITY STUDY

Procedure

The community study reported herein was conducted in the communities surrounding John F. Kennedy International Airport (New York City) in conjunction with the government's assessment program of the Concorde supersonic transport (ref. 2). A number of homes in the Kennedy Airport area were utilized for this study, and the subjects who participated included both residents and members of the NASA monitoring team. The test procedures can be best described in conjunction with the photograph of figure 2. This photograph shows a typical group of subjects participating in the subjective response tests as well as some of the instrumentation used to obtain the physical noise and vibration measurements. Microphones were located both indoors and outdoors (not shown) for recording the aircraft noise levels. Accelerometers were used to measure the acceleration levels of the window, wall, and floor (vertical and horizontal). All the physical data were recorded on magnetic tape in a mobile acoustic van (located outside the residence) for later analysis. Since this was a community study utilizing aircraft flyover events as they naturally occurred, no control over the sound sources was possible. Consequently, both subjective ratings and physical measurements were obtained for each flyover event that occurred during a test session which nominally lasted about 1/2 to 1 hour at each site.

The technique used to obtain the subjective response ratings for each flyover is illustrated by the sample flyover event rating form of figure 3. Each flyover event was assigned a flyover number by the test director, and the number was written on the rating form in the appropriate space by each subject. At the conclusion of each event, the test director instructed the subjects to

480

rate the flyover at which time the subjects would indicate on their rating form whether or not they had detected vibration, rattle, or noise; whether or not the vibration, rattle, or noise was annoying; and finally an overall annoyance rating of the flyover on a numerical category scale which ranged from 0 to 9, where "0" was defined as "zero annoyance" and "9" was defined as "maximum annoyance." Since many of the resident subjects had difficulty in differentiating between noise, vibration, and rattle and in properly using the rating form, only the data from the NASA "trained" subjects of the assessment team are utilized in this paper.

Test Results

A total of 109 aircraft flyover events at 8 houses were experienced by a total of 16 test subjects. With regard to rattle detection, the subjective ratings indicated that on only three occasions did one half or more of the subjects detect rattle. This implies that rattle may exert only a minor influence upon a person's annoyance response to aircraft noise. However, due to the scarcity of data, it was determined that a final conclusion with respect to the importance of rattle should await the results of a laboratory investigation in which this factor was studied under controlled conditions. These results are presented later in this paper.

Vibration was detected by 50 percent or more of the subjects on 21 occasions at 3 of the 8 houses. All three of these houses were located inside the 40 NEF contour, and each had conventional wooden floors above a crawl space. The results of this phase of the experiment are shown in figure 4 in which the percent of subjects detecting vibration is plotted as a function of the level of vertical floor vibration in dB units (ref. 1 μg). The threshold of vibration detection is defined as the level at which 50 percent of the observers feel the vibration. Consequently, for these data, the threshold of detection is seen to be in the range of from 62 to 68 dB, vertical floor acceleration. The range of 62 to 68 dB corresponds approximately to 100 to 105 dB, outside sound pressure level. Thus, it appears that aircraft-generated outside sound pressure levels greater than 100 dB are capable of inducing vibrations of a magnitude sufficient to exceed the threshold of vibration detection of the occupants within.

Figure 5 presents the results of the category scaling experiment of the overall annoyance rating of the flyover events. Average annoyance ratings are shown as a function of outside A-weighted sound pressure level for two categories of events, namely for aircraft flyovers in which the threshold of vibration detection was achieved, and for those aircraft flyover events for which the threshold of vibration detection was not achieved. The lines shown in the figure were drawn based on a least-square linear fit of the two sets of data. The figure and "paired t-tests" (based on the actual data of one curve versus the predicted data of the other curve) show that aircraft flyovers for which there was vibration detection were evaluated as significantly more annoying than aircraft flyovers for which vibration was not detected. An implication of these data is that structural building vibration does have a significant and detrimental effect on the annoyance response of people to aircraft flyover noise. Since most studies of the effects of aircraft noise on people have not considered building

vibration, these results may explain some of the subjective response variation that occurs within and between various studies,

LABORATORY STUDIES

Rattle Detection and Annoyance Thresholds

The laboratory study of rattle detection, rattle annoyance, and rattle effects on aircraft noise annoyance was conducted in the Langley aircraft noise reduction laboratory. The facility used in the study was the interior effects room (IER) which is shown in figure 6. This room is configured to resemble a typical residential living room, and its construction is considered representative of that found in a standard residential house. It consists of painted dry wall over 50.8-mm by 101.6-mm (2 by 4) studs on 406.4-mm (16 in) centers. The dimensions of the room are approximately 4 by 6 by 2.5 meters. Noise stimuli are presented in the room by means of four loud-speakers which are located outside and above each corner of the room.

Experimental design.- The experimental design of the rattle detection and the rattle annoyance experiments involved presentation of an aircraft noise at a constant level with varying amounts of rattle. As shown in figure 7, the peak A-weighted sound pressure level of the aircraft flyover noise was held constant at 71 dB while the rattle level was varied from 45 to 61 dB(A) (measured at the subjects' seating positions). For control and repeatability, the rattle level was produced by tape recording the sound of drinking glasses rattling when excited by an electromechanical shaker mounted to a china cabinet containing the glasses and which was driven by a tape recording of the aircraft flyover. For playback, the tape recording of the rattle was synchronized with the aircraft flyover noise and was introduced into the IER through a small loudspeaker located under a china cabinet while the aircraft noise was played through the overhead, outside speakers. The level of the rattle noise was adjusted by changing the gain setting of the tape recorder playback.

A total of 24 paid, volunteer subjects participated in this experiment. Each noise and rattle level combination was randomized and repeated once and each subject heard every combination. As further shown in figure 7, the determination of detection and annoyance thresholds was addressed in two separate tasks. For detection, the subjects were asked to rate whether or not they detected the objects in the china cabinet rattling. For the annoyance threshold task, subjects were asked to rate whether or not the rattling sounds they heard were annoying. In either case, the expected results would be an increasing number of yes responses with increasing rattle level. The thresholds for detection and for annoyance are defined as the level for which 50 percent of the subjects detected the rattle.

Results.- The results of the threshold determination tasks are shown in figure 8 which displays the percent of "yes" responses for both tasks as a function of rattle level in dB(A) units. The results shown in figure 8 indicate that the threshold of annoyance occurred at approximately 56 dB(A) which is

482

about 9 dB higher than the threshold of detection which occurred at 47 dB(A).
That is, the threshold of annoyance is 9 dB higher than the threshold of
detection and probably represents an important result. Also, the 56 dB(A)
required to achieve rattle annoyance threshold is believed to be abnormally
high in a household setting. Therefore, if rattle is important as a factor
to evaluation of aircraft noise, its effects could operate only through
detection since rattle levels needed to achieve annoyance are not believed to
occur.

Effect of Rattle on Aircraft Noise Annoyance

Experimental design.- In order to determine if the perception of rattle
affects subjective response to aircraft flyover noise, an additional experiment
was conducted based upon the experimental design shown in figure 9. Tape
recorded aircraft noise was presented to the subjects at four different
A-weighted sound pressure levels, both with and without accompanying rattle.
A total of 24 subjects participated in the test. Twelve of the subjects were
exposed to noise/rattle combinations, whereas the remaining 12 subjects were
exposed to noise only. The subjects used the magnitude estimation procedure
to provide subjective evaluations of the aircraft noises with or without
accompanying rattle. For this task, all subjects were presented with an
aircraft noise at a level of 76 dB with no rattle. This standard sound was
assigned an annoyance value of 100 and was presented periodically throughout
testing. The evaluation task for the subjects was to assign numbers to
successive comparison aircraft noises (given in fig. 9) to reflect how much
greater or less the annoyance of the comparison noise was relative to the
standard noise. For example, if the annoyance of the comparison noise was felt
to be twice, three times, one-tenth, or one-half the annoyance of the standard
noise, the subject would assign 200, 300, 10 or 50 to the comparison noise,
respectively.

If rattle has an adverse effect on a person's annoyance of aircraft noise,
then a noise with rattle would be rated as subjectively more annoying than a
noise without rattle. This determination could be made since, as mentioned
earlier, only half of the subjects were exposed to combined noise and rattle.

Results.- The results of this study are presented in figure 10. This
figure shows the magnitude estimations of subjective annoyance obtained from
the various subject groups (both with and without rattle) as a function of
aircraft A-weighted noise level. Figure 10 indicates that increases of noise
level produces increased magnitude estimations of annoyance regardless of
whether or not rattle was present. However, the most important implication of
the data of figure 10 is the fact that there is no appreciable difference
between the "rattle" and "no rattle" conditions. That is, the presence of
rattle did not, in a practical sense, affect the subjective response to
aircraft noise.

The implications from these laboratory studies are that any rattle produced
by aircraft flyover noise should not, of itself, produce annoyance in a
listener. Furthermore, the presence of rattle does not increase the annoyance

caused by aircraft flyover noise. Caution should be exercised, however, in extrapolating these laboratory findings to the real-world environment of the airport community where the noise impact is confounded by complicating factors not present in the laboratory such as proprietorship, intrusion into relaxation time, etc.).

HELICOPTER FLYOVER STUDY

A helicopter flyover subjective response study has very recently been conducted at Wallops Flight Center, and data analysis is currently underway. This study utilized approximately 100 test subjects (fig. 11) in four groups; two indoors and two outdoors. Two types of house structures were utilized (one brick veneer and one wood siding) and extensive physical measurements of structural vibration were obtained in the same mammer as the Kennedy Airport study. In the data analysis of this study, acceleration levels of building structural elements will be quantified as a function of the helicopter noise level and will be compared with the similar data from CTOL aircraft. A primary question of this study is to determine if the helicopter noise data correlates with CTOL noise data, or if some characteristic of the helicopter noise signal (rotor bang, low frequency, etc.) causes it to be unique. In addition, the subjective response data will be analyzed to determine if it is related to amount of helicopter caused building vibration in a fashion analogous to the way the subjective data were related to the CTOL noise data for the study conducted at John F. Kennedy International Airport.

CONCLUDING REMARKS

Based on an extensive physical measurement program and a limited subjective response pilot study conducted in the J. F. Kennedy International Airport communities of New York City (in conjunction with the government's assessment program of the Concorde SST), the following concluding remarks can be made:

1. A vibration detection threshold was determined for CTOL aircraft and was found to correspond to an outside overall sound pressure level of approximately 100 to 105 dB. This implies that aircraft-generated noises of this level can produce perceivable structural vibrations.

2. The perception of vibration was found to produce an increase in the annoyance associated with an aircraft flyover event giving the implication that vibration is an important factor which should be considered in the assessment of aircraft flyover noise.

3. The results of the community study and a laboratory pilot study suggested that the effects of rattle upon subjective aircraft noise annoyance are negligible. This is based upon the fact that the phenomenon of rattle was observed for less

484

than 3 percent of the aircraft noise events during the field study, and in the
laboratory study, the presence of rattle did not appreciably influence
subjective evaluations of annoyance to flyover noise.

REFERENCES

.. Second Survey of Aircraft Noise Annoyance Around London (Heathrow)
   Airport. H.M.S.O., London, 1971.

:. Staff-Langley Research Center: Concorde Noise-Induced Building Vibrations
   International Airport Dulles - Final Report. NASA TM 74083, 1977.
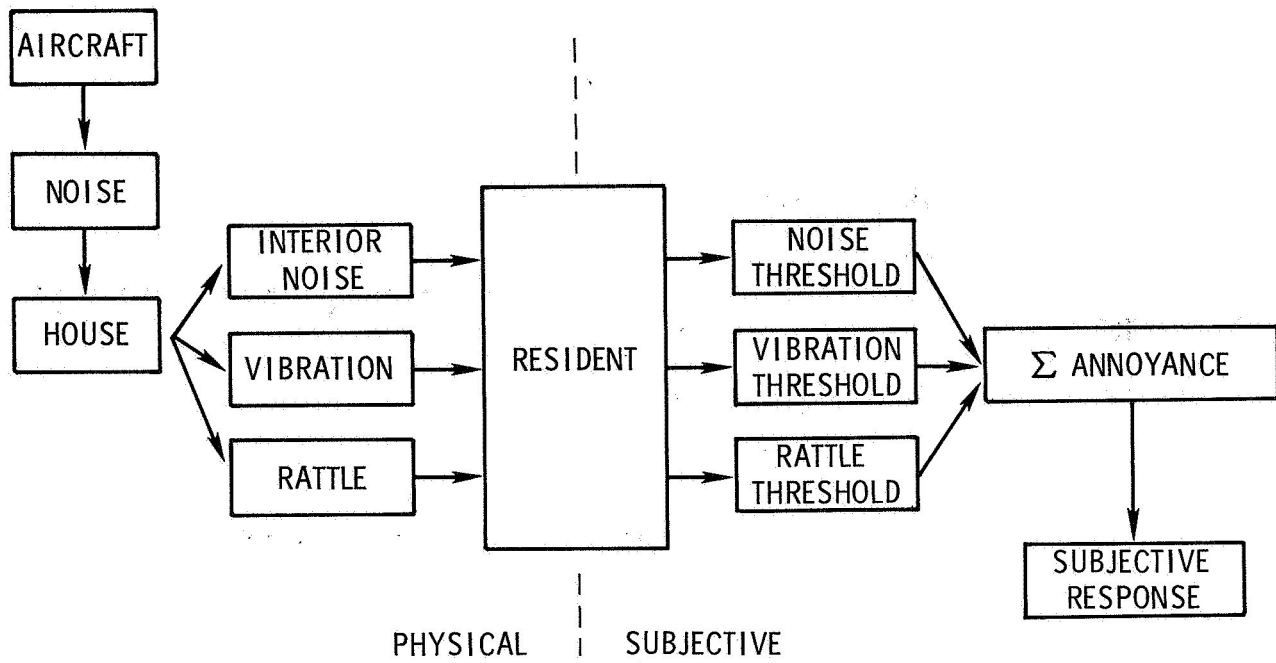
Figure 1.- Schematic illustration of impact of aircraft noise on people exposed to noise while indoors.

Figure 2.- Community noise study; human response to noise, vibration and rattle.

FLYOVER NO.	DETECTION		ANNOYANCE	
	YES	NO	YES	NO
—— VIBRATION	——	——	——	——
RATTLE	——	——	——	——
NOISE	——	——	——	——

ANNOYANCE RATING OF FLYOVER

```
|  |  |  |  |  |  |  |  |  |  |
0  1  2  3  4  5  6  7  8  9
```

ANNOYANCE RATING: 0 - ZERO ANNOYANCE
                   9 - MAXIMUM ANNOYANCE

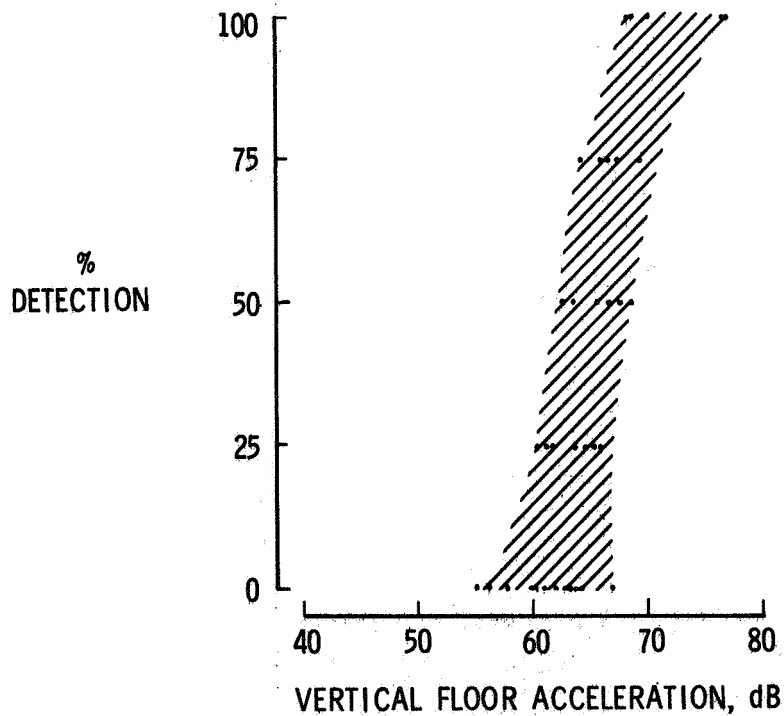Figure 3.- Sample flyover event rating form used in
community noise study.

Figure 4.- Results of experiment to determine
vibration detection threshold.
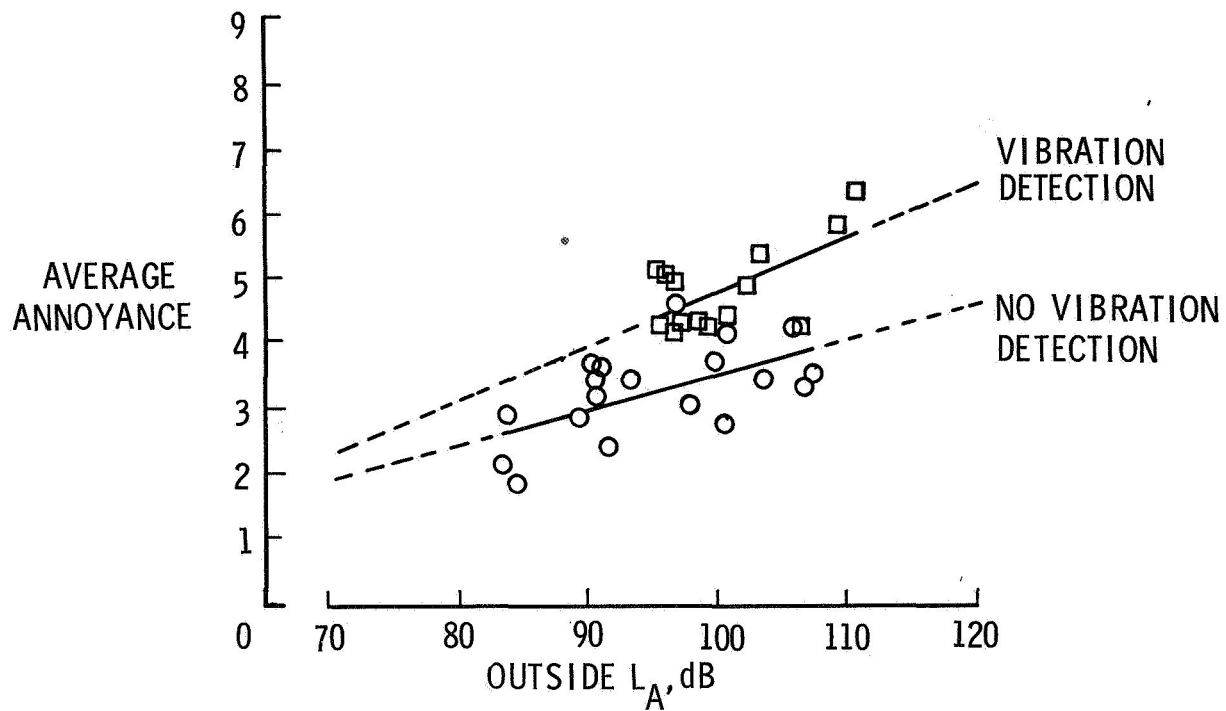
Figure 5.- Effect of vibration on overall subjective annoyance to aircraft flyover noise.
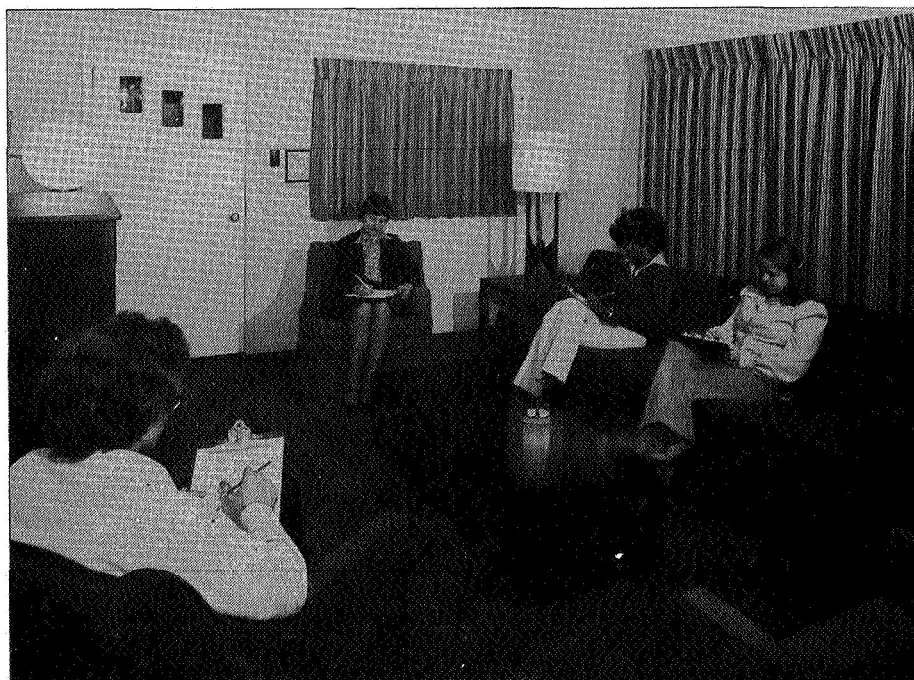
Figure 6.- Interior effects room of Langley aircraft noise reduction laboratory.

NOISE LEVEL, dB (A)	RATTLE LEVEL, dB (A)						
71	45	47	51	54	56	59	61

NO. OF SUBJECTS: 24

TASK: I YES/NO DETECTION II YES/NO ANNOYANCE

EXPECTED RESULTS:
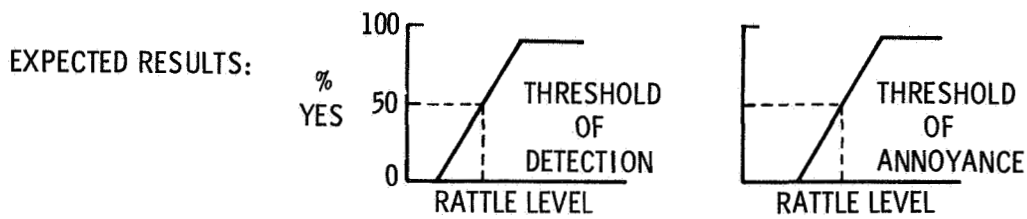
Figure 7.- Experimental design of determination of rattle detection threshold and rattle annoyance threshold.
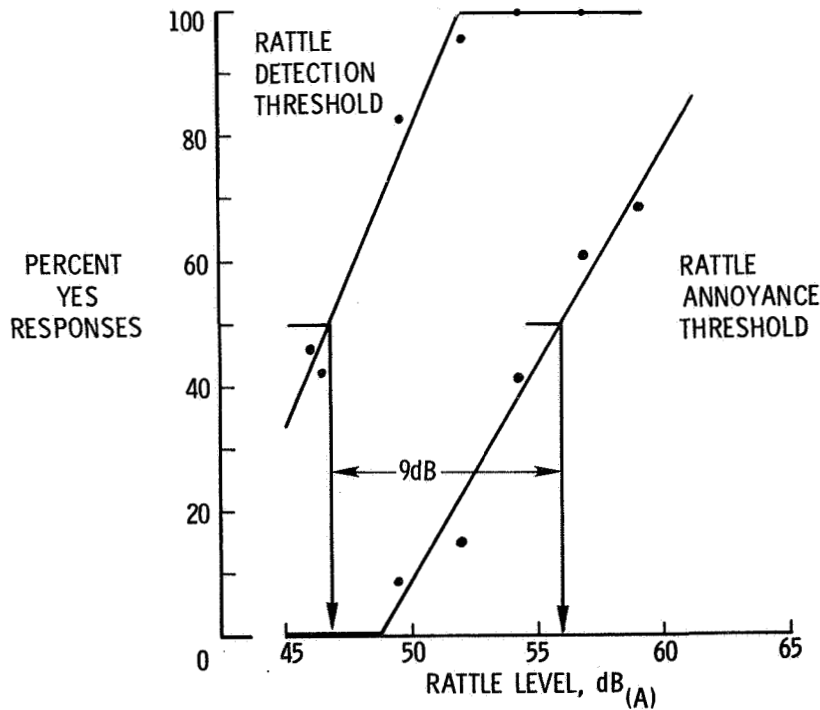
Figure 8.- Comparison of rattle detection and rattle annoyance thresholds.

	RATTLE LEVEL, dB (A)	
	RATTLE	NO RATTLE
NOISE LEVEL, dB (A) 71	62	—
74	62	—
78	62	—
81	62	—

NO. OF SUBJECTS: 24

TASK: MAGNITUDE ESTIMATION
ANNOYANCE TO AIRCRAFT

EXPECTED RESULTS

SUBJECT ANNOYANCE

RATTLE
NO RATTLE

AIRCRAFT NOISE LEVEL
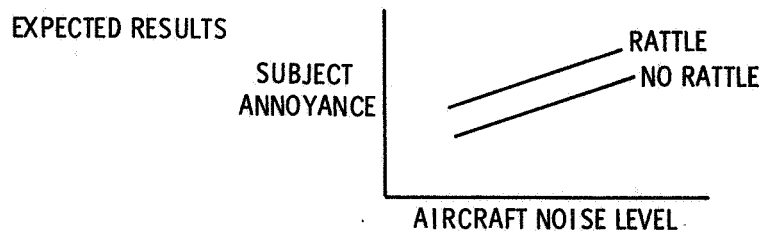
Figure 9.- Experimental design of determination of effect
of rattle on aircraft noise annoyance.
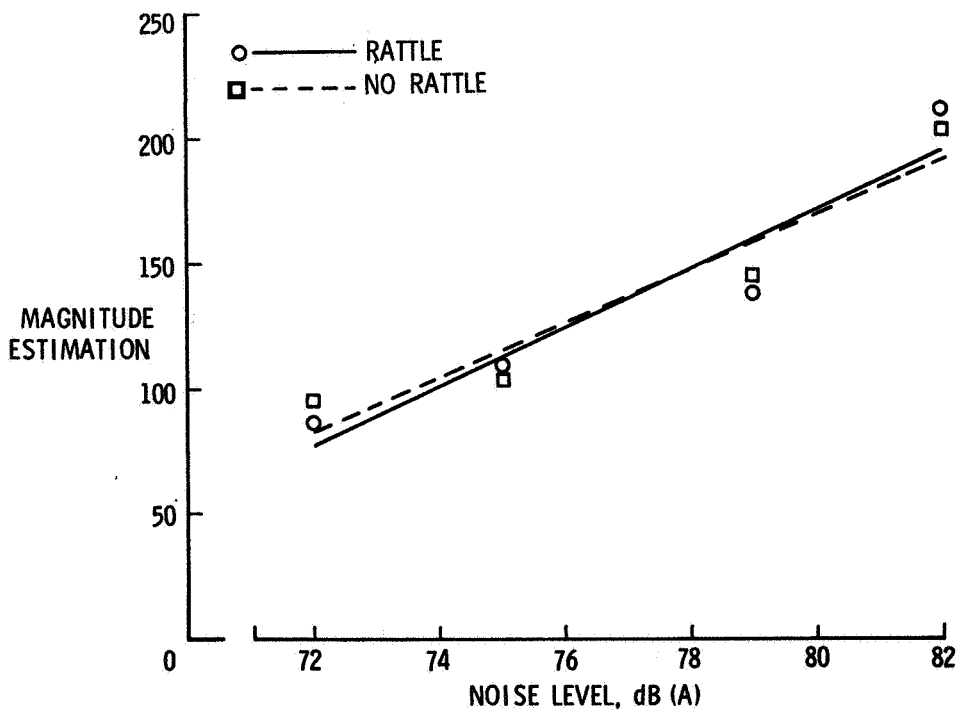
Figure 10.- Effect of rattle on aircraft noise annoyance.

490

NUMBER OF SUBJECTS: ≈ 100
SUBJECT LOCATION: INDOORS AND OUTDOORS
PHYSICAL MEASUREMENTS: STRUCTURAL VIBRATION
SOURCE DIFFERENCES: AMOUNT OF ROTOR BANG

ACCELERATION LEVEL

HELICOPTER

CTOL

ΔdB?

NOISE LEVEL

SUBJECT ANNOYANCE

HIGH VIBRATION

LOW/NO VIBRATION

ΔdB

?

HELICOPTER = CTOL

NOISE LEVEL

Figure 11.- Subjective response to helicopter flyover noise study.

491

A METHOD FOR DETERMINING INTERNAL NOISE CRITERIA

BASED ON PRACTICAL SPEECH COMMUNICATION

APPLIED TO HELICOPTERS*

Harry Sternfeld, Jr., and Linda Bukowski Doyle
Boeing Vertol Company

SUMMARY

The objective of this study was to provide information regarding the relationship between the internal noise environment of helicopters and the ability of personnel to understand commands and instructions. A test program was conducted to relate speech intelligibility to a standard measurement called Articulation Index. An acoustical simulator was used to provide noise environments typical of Army helicopters. Speech material ("Command" sentences and Phonetically Balanced Word Lists) were presented at several voice levels in each helicopter environment. Recommended helicopter internal noise criteria, based on speech communication, were derived and the effectiveness of hearing protec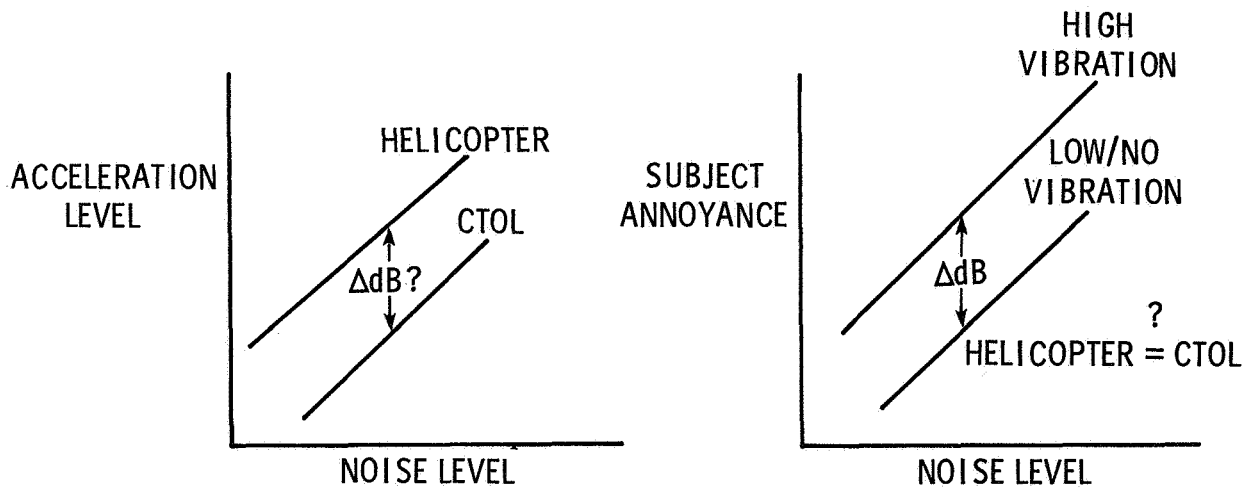tion devices were evaluated. Similar limits to satisfy other types of criteria can be developed using the methods presented in this paper.

INTRODUCTION

An investigation being conducted by the Army's Working Group on Aircraft Noise indicates that speech communication requirements, as well as hearing damage risk criteria, are important factors in determining interior noise level criteria for helicopters and that the speech communication requirements are especially important in troop carrying helicopters where misunderstood instructions in combat situations may lead to serious consequences.

Speech communication in the current generation of Army helicopters is known to be inadequate but little information has been quantified in order to assist in developing adequate criteria. Although several studies have been conducted in the general area of speech communication in office-type environments, no predictive method had been validated as being completely adequate for all types of noise environments and all types of speech content. In the helicopter both of these factors are somewhat unique. The ambient noise is generally of higher level and more dominated by both low frequency noise (from rotors) and pure tones (from transmissions and turbines) than most environments previously tested; while the speech tends to be simple sentences of limited content, also quite different in structure than the material used in more generalized speech testing.

In order to provide the needed information the Army (AVSCOM) has sponsored the study which is described in this paper to assist in establishing the relationship between the internal noise environment of helicopters and the ability of troops flying in helicopters to understand commands and instructions. Information of this type, which was not previously available, can be used as a basis for reevaluating and, if necessary, revising Specification MIL-A-8806-A, "Acoustical Noise Level in Aircraft, General Specification For."

The program, therefore, applied standard speech communication test procedures as specified in Reference 1, but added noise environments and speech material typical of those encountered in troop-carrying helicopter operations in order to assess Army requirements. The same techniques can also be applied to develop criteria for application to other purposes such as passenger carrying civil helicopters.

TEST PROGRAM

Speech Intelligibility Testing

Any test involved with speech communication is called speech intelligibility testing. Two measurements which frequently come up in tests regarding speech intelligibility are Articulation Index and Speech Intelligibility Scores. Intelligibility refers to those units of speech material which are complete and meaningful words, phrases, or sentences. Test subjects are asked to listen to noise and speech simultaneously; they then record, in writing, what has been spoken. The subjects are scored on the percentage of speech recorded correctly. These scores are called their Speech Intelligibility Scores.

Articulation Index, developed by French and Steinberg (Reference 2), is a rather powerful tool for measuring speech intelligibility. The Articulation Index (AI) is a weighted number representing, for a given set of speech and noise conditions, the effective proportion of the normal speech intelligibility. AI is computed from acoustical measurements (or estimates) of the speech spectrum and of the effective masking spectrum. The detailed method for calculating Articulation Index may be found in Reference 1 which also gives suggestions for refinements to AI to take into account such things as interruption in the noise, the reverberation in the listening situation, the vocal effort used by the talker and face to face talking.

Figure 1, from Reference 1, shows the correlation between the speech intelligibility scores and articulation index in certain noise and speech environments. By use of this figure AI can be used to predict speech intelligibility.

In intelligibility testing there are four main categories of test materials (i.e., speech material) used most often (Reference 3):

        (1)   nonsense syllables
        (2)   monosyllabic words
        (3)   spondiac words
        (4)   sentences

(1) Nonsense syllables are superior to words or sentences as test items when it is desired to determine accurately the effectivenss of a device in transmitting particular speech sounds. Two practical disadvantages are the speaker must pronounce the speech sounds very precisely and the test subjects must record the sound they hear in phonetic symbols.

(2) A standard monosyllabic list contains words so chosen that all speech sounds are approximately according to their frequency of occurrence in normal speech; hence, they are termed "Phonetically Balanced (PB)." There are 20 such lists of 50 words each, the spread of difficulty being approximately the same in each list and each list having nearly the same average difficulty. Rare and unfamiliar words have been avoided as much as possible.

Two variations on the monosyllabic word lists are the rhyme test and the modified rhyme test which are tests of phonemic differentiation. The rhyme test vocabulary consists of 50 monosyllabic word sets of five rhyming words each; the modified rhyme test consists of 50 monosyllabic word sets of six rhyming words each (Reference 4 and 5). Within a given set, the rhyming words differ in a consonantal spelling. The subjects are scored on whether they supplied the correct consonant. Reference 5 contains more information on the differences between the rhyme and modified rhyme tests.

(3) Spondiac lists contain words of homogenous audibility, i.e., lists in which each individual word is as difficult as each other word. Such words are most easily selected from those which have the syllables spoken with equal stress on each syllable; e.g., railroad, horseshoe, airplane. They are especially useful in tests whose design is to establish accurately the amplification or power level at the threshold of hearing.

(4) There are different forms of sentence lists. In one form, the test subject is required to respond to questions or commands by an appropriate word or phrase. A sentence would then be either "right" or "wrong," depending on whether or not it was clear that the subject understood the meaning.

In another type of test, the listener is required to record in writing the sentence that is read to him. In sentences of this type, there are "key words" that are to be marked as right or wrong. An effort is made to avoid clichés, proverbs, and other stereotyped constructions, as well as the too frequent use of any one word.

Noise Simulation

One of the obvious problems in conducting a speech intelligibility program involving helicopter noise is that of providing enough different helicopter interior environments (and systematic variations in environment), which

495

are stable and repeatable enough to permit the required testing. Prior to this program, Boeing Vertol had developed a useful capability for synthesis of internal noise. This simulator (Figure 2) consists of a full-scale mockup of a 15-passenger helicopter cabin and cockpit. Loudspeakers and horns are mounted at various locations on and around the fuselage in order to provide an independent sound source for each noise component. Each speaker receives its signal from a separate amplifier which, in turn, is input from a separate track of a 14-track tape playback. There are three fundamental types of signals which are employed in the simulation, broadband noise, continuous pure tones and pulsed harmonic sets.

The broadband noise, such as engine and boundary layer, are produced by random noise generators and then shaped through a one-third octave band filter set to achieve the desired spectrum.

Pure tone components, such as transmission gears, occur in harmonic sets. Initially an oscillator is used to generate each harmonic and that signal, at its required level, is put on a separate track of a magnetic tape. This tape is then dubbed so that the desired harmonic combinations are recorded on a single track of the final tape.

The pulsed harmonic combinations are used for main and tail rotors. In this case each harmonic is stored in the memory of a digital averager until the entire required combination is in memory. The averager, which had been especially modified, was then instructed to read the stored signal out at a rate corresponding to the blade passage period. The key to making this system work lies in .the use of on-line real-time data analysis of signals sensed by microphones at desired locations in the aircraft as the signals are generated. In this manner the input is adjusted so that the desired output is obtained, thereby automatically accounting for electronic component frequency characteristics and for "room" acoustics.

In any finite size enclosure with directive sources, the sound field, especially of pure tone components, will not be uniform. Anyone who is familiar with helicopters knows that substantial differences in transmission noise level can be experienced by merely moving one's head. Therefore any meaningful sound pressure level data must be obtained by space averaging both during simulation development and final analysis. To achieve this, occupancy was limited to four test subjects sitting in a rather tight square. During simulation development a microphone on a rotating turntable was used. Each noise component was provided from the appropriate loudspeaker and its level adjusted so that its average level during rotation reached the desired value.

A preliminary review was conducted of available data on internal noise in current Army helicopters. This compilation resulted in the scatter shown in Figure 3. Also shown is the level defined by specification MIL-A-8806-A indicating that most procurement, to date, has deviated from established requirements.

Since the main concern of this study is directed at current Army troop-carrying helicopters, this constraint limits the field to two models: the

496

Bell UH-1 (Huey) and the Boeing Vertol CH-47 (Chinook) series. Accordingly, the following were selected as representative for the test program:

1. CH-47C at 22 680 kg (50 000 lb) gross weight (Current Army configuration).

2. CH-47A at 14 969 kg (33 000 lb) gross weight (Original Army Chinook configuration which contained more acoustical treatment in the aft cabin than the CH-47C).

3. A "Paper Design" CH-47 which is a predicted spectrum of a Chinook designed to meet MIL-A-8806-A. This will be referred to as CH-47 'MIL Spec.'

4. UH-1H at 4309 kg (9500 lb) gross weight.

5. UH-1H with doors open which is a configuration often used to permit rapid egress of troops when approaching landing zones.

In order to develop the required simulations, the aircraft noise must be studied in detail in order to identify individual components by means of narrow band spectra shown in Figures 4 and 5. Analyses of this type of data from several locations in each aircraft was done to develop the spectra which were the basis for preparation of the test samples. A typical simulation consisting of two broadband and thirty harmonic components is presented in Figure 6.

Speech Material

This program, after much consideration of the available speech materials, used both standard Phonetically Balanced (PB) word lists and non-standard "Military Jargon" sentence lists. The 1000 PB word list is from Reference 6. The purpose of the PB testing is to provide continuity between this program and the results of other speech communication studies.

Since this program is concerned with determining the effect of helicopter noise on communication with troops, the "Military Jargon" sentence lists were developed as samples designed to reflect somewhat typical commands and questions which might occur in an assault helicopter. Some typical sentences were:

Hold it - move now.
Advance to the northeast sector.
Out the front door.

Sentences of this type are more pertinent to actual Army usage than the more theoretical PB word lists. There were five different military sentence lists, each one composed of twenty sentences. Each of the five lists was randomly scrambled once; hence, there was a total of ten lists (two hundred sentences) of the military type employed in the program. The two hundred sentences contained a total of 300 key words on which scoring was based. It will be noted that the military sentences on the whole are much shorter than the standard sentences of Reference 3 of the type whose test results are shown in Figure 1. Also, they are limited to fewer words; whereas the standard sentences avoid cliches and stereotyped expressions, the military sentences are

composed mainly of these.

The PB word lists and "Military Jargon" sentence lists were tape recorded for playback through a loudspeaker located so that the sound came from the front of the cabin. The individual selected as the speaker had no strong regional accent and had clear diction. As the data was recorded the peak levels were monitored on a graphic level recorder to assist in maintaining a constant voice level. A raised voice was used rather than a conversational tone to produce the type of compressed range associated with higher voice levels. A calibration tone was included on each tape for the purpose of providing a constant reference for setting the desired playback volume levels. The use of this procedure ensured repeatability of data between test sessions.

Test Procedures

The subjects in this program were twelve males who were members of various engineering staffs of the Boeing Vertol Company. Potential candidates were screened by audiograms, conducted by the Boeing Vertol Medical Department.

Prior to the start of the test program, the twelve test subjects were divided into three groups, consisting of four subjects each (the subjects were allowed to form their own groups of four). At a pre-test session, the subjects were given their instructions, they familiarized themselves with the military sentences and a practice session was held. Since testing with phonetically balanced words is a much more rigorous procedure which requires training to a level where other subjects score at least 90% in a quiet environment, these practice sessions were held at each test session scheduled for military jargon testing. By the time PB word testing all subjects had exceeded the minimum requirements.

Each subject was equipped with writing utensils, a lap board and answer sheets. During a particular test (a test is defined as one aircraft level and one speech level), the helicopter noise was continuous; one word and/or sentence at a time was played with a finite time interval for each subject to write what he heard or what he thought he heard. Minor rests of about 1 minute were given at approximately 5-minute intervals with longer rest periods at every 15 minutes.

In order to ensure that each test would produce a meaningful range of results, a pretest was performed for each aircraft noise environment. In this pretest the voice playback level was varied until, in the opinion of the Test Director, only a few of the messages could be understood. The level was then readjusted until it was judged that most of the messages could be understood. At each of these levels the value of the 1000 Hz reference tone was measured. These calibration levels and one additional level which was the average of the above two were then used to set the voice levels prior to each test.

In addition to the full aircraft spectra discussed above, additional variations were obtained by completely eliminating individual components by disconnecting the appropriate tape track from the simulation system during playback. This not only provided more test environments but was also used to evaluate the

498

relative importance of the various noise sources in affecting speech communication.

Additional testing was conducted in one single rotor and one tandem rotor configuration to evaluate the effect of hearing protective devices.

RESULTS

Data Analysis

The phonetically balanced word lists were simply scored as correct or incorrect for each individual word. Phonetic spelling and/or misspellings were counted as correct providing the word was recognizable. Failure to fill in any word was counted as incorrect. In the sentence lists, failure to correctly recognize any key word was scored as not understanding the sentence, hence there was usually more than one chance to miss a sentence.

The principles of calculating A.I., which are fully described in Reference 1, require measurement of both the ambient noise and speech levels at the observer's location. In order to define the aircraft noise levels, one-third octave band measurements were made at the left and right ear position of each subject for each separate environment tested. The left and right ear spectra were arithmetically averaged to obtain a single spectrum for each seat location for each test.

Reference 1 recommends the use of long-term rms spectra for speech measurement. Accordingly four sections of the PB tape were played through the speaker system and analyzed in a manner which provided one-third octave band spectra integrated over 32 seconds for each sample. Averaging these samples thus produced a 128 second rms spectrum. Since different playback levels were used for each test, a curve of absolute level against calibration tone level was made in order to assign amplitude values to the long term rms spectrum shape.

Articulation Index (A.I.) was calculated as defined in Reference 1. Of the three methods (full octave, one-third octave and 20 band) described in that reference, the one-third octave band method was used due to compatibility with available analyzing equipment. Speech peaks were determined by adding 12 dB to the measured long-term rms values of the speech actually used in preference to use of the idealized voice of Reference 1.

Speech Communication

The fundamental results of this program are shown in Figure 7 for all the combinations of aircraft noise condition and speech levels tested. Since we are concerned with evaluating the general situation in the cabin of military helicopters and not the characteristics of specific locations, the data for each of the four test locations has been combined to give a single value representative of the aircraft/speech combination tested. Each PB data point of Figure 8 is based on 1200 and each Military Jargon data point on 720 separate evaluations.

499

Comparison of these results with the more general data of Reference 1 is illustrated in Figure 8 and indicates that these latter criteria would be too conservative if applied to the helicopter. Since this difference appears to be true of both the sentences and PB words it does not seem that the type of speech material used is responsible, therefore the difference probably is due to the particular characteristic of helicopter cabin noise. Although the scope of this program cannot rigorously define the reason, a possible explanation may lie in the fact that in the speech interference range the helicopter noise is often predominated by pure tones generated by dynamic components. In this case the value of a one-third octave band of noise may be set by only a very narrow portion of the bandwidth, leaving the rest of the band available for much better speech communication than would be indicated by an Articulation Index calculated on the basis of the one-third octave band (or even the twenty band method). This implies that the use of an equivalent band level concept (by adjusting the measured band level by $10 \log \frac{b_t}{B}$ (where b_t is the bandwidth of the tone and B the bandwidth of the one-third octave band in question) might be applicable. Such a procedure would have to be applied exercising great judgment in cases where a particular level is set by several tones, or a combination of tones and broadband noise. A more practical approach is to assume the data developed in this program as being more correct than the Reference 1 curves for application to helicopter internal noise.

In evaluating speech communication in a given aircraft, there are essentially three parameters which must be considered:

(1) The voice level which may be used.

(2) The distance over which communication must take place.

(3) The reliability of understanding which must be achieved.

In order to perform the required evaluations, it was necessary to assume some voice levels and spectra. For the greatest general applicability, the spectrum shape used was the ideal voice spectrum of Reference 1 as opposed to the specific spectrum of the talker used in this program. The rms overall sound pressure levels corresponding to the descriptions were obtained using a simple test in which three males (who had helicopter experience) used voice levels which were felt to be typical of those employed in military helicopters. The levels were measured using a one-third octave band analyzer with a graphic level recorder set such that the response was an rms level corresponding to a standard sound level meter set for "slow" response. (This corresponds to a pen decay rate of about 40 dB/sec at a writing speed of 80 mm/sec or a 1-second time constant.)

For discussion purposes, three voice levels were evaluated:

"Loud Shout" (90 dB rms at speech peak value at 1 meter) was a level which could be used to issue command sentences to troops and was not unlike those employed in addressing ground troops during military drill.

"Short Duration Shout" (100 dB rms at 1 meter) was a level which could be sustained for up to about ten continuous words without rest.

500

"Maximum Effort" (110 dB rms at 1 meter) was a level which could only be sustained for a few words and resulted in some vocal strain; this level might be expected in emergency situations.

Having defined the voice spectra as just described, the Articulation Index can be calculated for each aircraft by using the appropriate internal noise data and the method of Reference 1. The "Military Jargon" curve of Figure 7, which was developed by this study, can then be used to convert the abstract Articulation Index to a more applicable speech intelligibility percent.

In order to assess the adequacy of speech recognition in Army helicopters, it is necessary to establish requirements which will permit troops to perform their mission. Unfortunately, no such standard has been established. Lacking any published guidelines, two interim criteria are suggested.

A minimum requirement should be based on communication essential to safety. For example, when using maximum vocal effort (110 dB rms at 1 meter), it should be possible to achieve 50% intelligibility which would at least attract the attention of a person anywhere in the cabin even if he cannot accurately understand the message content.

Although maintenance of a minimum communication in emergency communication in emergency situations is of first priority, this does not in itself ensure a comprehension which will permit troops to adequately follow instructions necessary to successful completion of their required missions. A reasonable suggestion might be based on 80% communication using a "Loud Shouting" level (90 dB rms at a distance of 1 meter). This would ensure that a troop commander, using the type of voice which might be used to instruct a platoon on the drill field, could achieve good simultaneous communication with personnel located within a radius of 1 meter of the speaker.

If it is desired to improve the speech communication reliability by increasing A.I. in an aircraft in an efficient manner, the reductions should be made in the frequency bands which contribute most directly to the A.I. Figure 9 illustrates the relative A.I. weighting factors normalized to their maximum value and suggest that noise reduction outside the frequency range of 100 Hz to 5 kHz will have relatively little payoff. Coupled with the above is the fact that it generally requires less weight to attenuate high frequency noise than low frequency. Pure mass attenuation, for example, provides 5-dB increased attenuation per doubling of frequency for the same surface density, while materials such as fiberglass greatly exceed that rate at the higher frequencies.

The procedure for establishing an internal noise level to meet a given communication requirement in an efficient manner is illustrated in Figure 10. The A.I. is calculated as described in Reference 1. The score of the aircraft noise limit required to obtain a desired value of the A.I. is found by trial and error solution.

At frequencies below 500 Hz, the aircraft noise levels need not be dictated by speech communication requirements but rather by hearing damage risk criteria.

Application of the above procedures to the suggested conditions results in the helicopter noise criteria curve of Figures 11 and 12. Other criteria based on other assumed requirements can be constructed in a similar manner.

Hearing Protection

The noise levels in helicopters not only affect communication but may, if high enough, cause temporary threshold shift, hearing damage, or at least discomfort. For these reasons, the use of protective devices may be recommended. It is important, however, to know if these devices have any adverse effect on understanding of spoken commands. To investigate this, testing was repeated in the CH-47C and UH-1H (doors open) configurations with the following protective devices:

1) Army SPH-4 flight crew helmets.

2) Disposable ear plug (a spongy material which was compressed, inserted in the ears and then allowed to expand).

3) A non-disposable fitted ear plug (size for each person based on ear canal measurement).

The results which are shown in Figure 13 reveal that no adverse effect on speech communication can be attributed to the use of ear plugs and, in fact, they even enhance understanding. In the case of the SPH-4 helmet when evaluated in the UH-1H, a significant deterioration occurred. Although no measurements of noise inside the helmets were made, spontaneous comments from several of the test subjects indicated that with the helmet on, the tail rotor noise was extremely annoying. It is therefore suspected that the SPH-4 helmet may have a resonance in the tail rotor frequency range and may be amplifying one or more harmonics of UH-1 tail rotor noise.

The disposable ear plugs tested slightly better than the fitted ones, probably due to being uncritical with regard to fit. They were also judged to be more comfortable.

CONCLUDING REMARKS

In order to assure adequate speech communication in military helicopters, internal noise standards should provide for noise levels which will result in Articulation Index(es) in accordance with the following sketch (which is replotted from Figure 7):

502
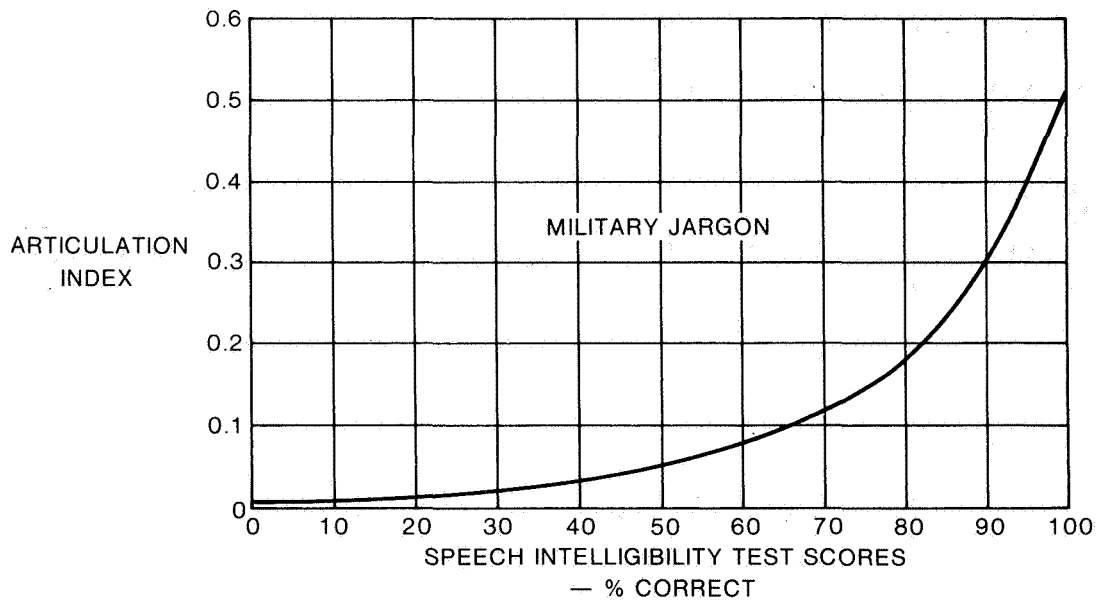
In order to relate the Articulation Index to a sound pressure level spectrum, it will be necessary to further define

(a)   the voice level to be required

(b)   the distance over which communication is required

(c)   the required reliability of communication

Additional investigation of Army requirements is needed to establish these parameters.

Ear plugs can be used to protect hearing with little or no degradation in speech communication.

The procedures developed during this program can be used to develop internal noise criteria for other applications such as civil transports.

REFERENCES

1. Anonymous: METHODS FOR THE CALCULATION OF THE ARTICULATION INDEX, ANSI S3.5-1969, American National Standards Institute, New York.

2. Kryter, Karl D.: THE EFFECTS OF NOISE ON MAN, Academic Press, New York, 1970.

3. Beranek, Leo L.: ACOUSTIC MEASUREMENTS, John Wiley and Sons, Inc., New York, 1962.

4. Fairbanks, Grant: TEST OF PHONEMIC DIFFERENTIATION: THE RHYME TEST, Journal of the Acoustical Society of America, Vol. 30, No. 7, July 1958, pp. 596-600.

5. Kryter, Karl D., and Whitman, Edward C.: SOME COMPARISONS BETWEEN RHYME AND PB-WORD INTELLIGIBILITY TESTS, Letters to the Editor, Journal of the Acoustical Society of America, Vol. 37, No. 6, June 1965, p. 1146.

6. Anonymous: METHOD FOR MEASUREMENT OF MONOSYLLABIC WORD INTELLIGIBILITY, ANSI S3.2-1960 (Revised 1971), American National Standards Institute, New York.
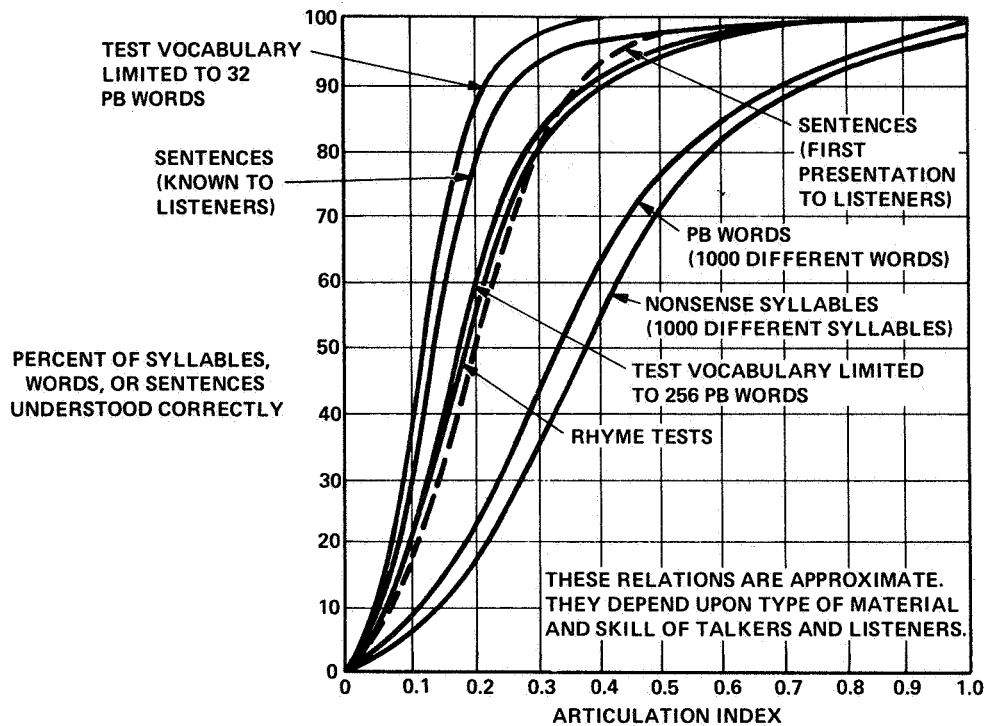
TEST VOCABULARY
LIMITED TO 32
PB WORDS

SENTENCES
(KNOWN TO
LISTENERS)

SENTENCES
(FIRST
PRESENTATION
TO LISTENERS)

PB WORDS
(1000 DIFFERENT WORDS)

PERCENT OF SYLLABLES,
WORDS, OR SENTENCES
UNDERSTOOD CORRECTLY

NONSENSE SYLLABLES
(1000 DIFFERENT SYLLABLES)

TEST VOCABULARY LIMITED
TO 256 PB WORDS

RHYME TESTS

THESE RELATIONS ARE APPROXIMATE.
THEY DEPEND UPON TYPE OF MATERIAL
AND SKILL OF TALKERS AND LISTENERS.

ARTICULATION INDEX

Figure 1.- Relationship between articulation index and
speech intelligibility (ref. 1).

SOURCES   GENERATION   RECORD/PLAYBACK   SIMULATOR

MAIN ROTOR NOISE

TAIL ROTOR NOISE

TRANSMISSION NOISE

ENGINE NOISE

BOUNDARY LAYER
NOISE

DIGITAL AVERAGER
(VARIABLE RATE)

OSCILLATOR
(PURE TONES)

NOISE GENERATOR
(BROAD BAND)

MAIN ROTOR
AMPLIFIER

TAIL ROTOR
AMPLIFIER

TRANSMISSION
AMPLIFIER

ENGINE
AMPLIFIER

BROADBAND NOISE
AMPLIFIER
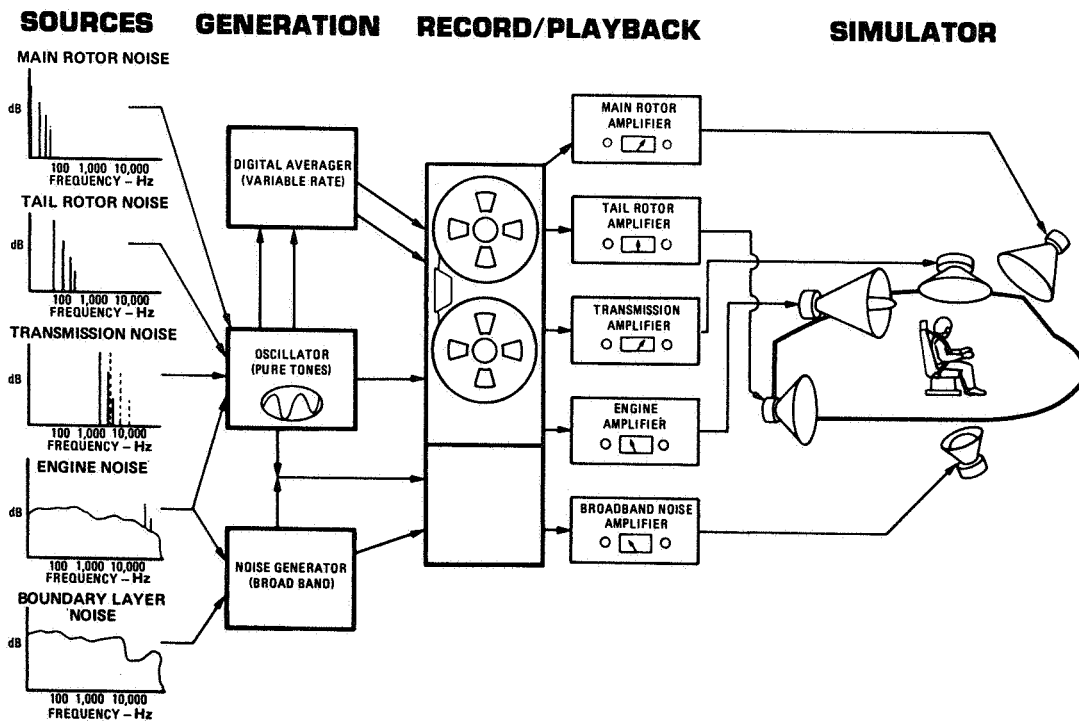
Figure 2.- Noise simulation.
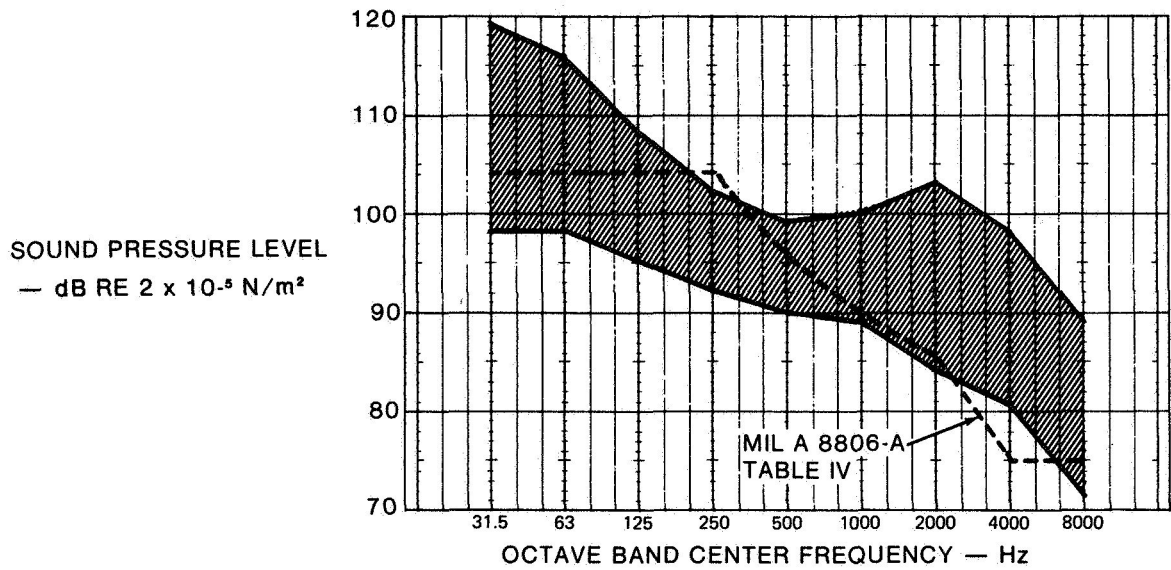
505

SOUND PRESSURE LEVEL — dB RE 2 x 10⁻⁵ N/m²

OCTAVE BAND CENTER FREQUENCY — Hz

(DATA INCLUDES CH-47C, CH-47A, UH-1H, AND OH-58)

Figure 3.- Scatter of center cabin noise data in army helicopters.

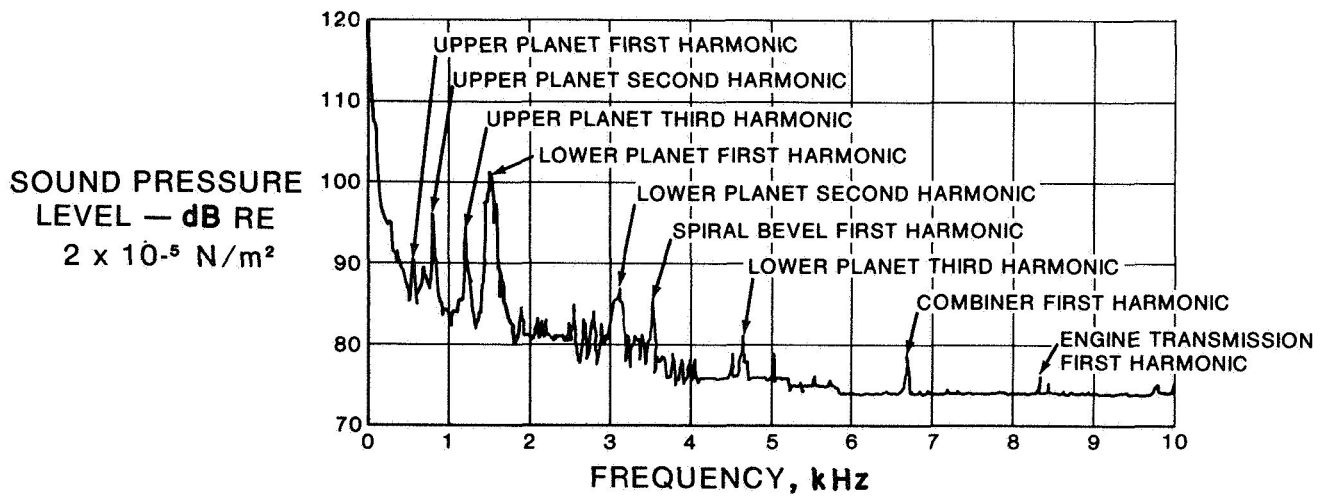

SOUND PRESSURE LEVEL — dB RE 2 x 10⁻⁵ N/m²

FREQUENCY, kHz

Figure 4.- Noise spectrum of CH-47C interior at station 320 (20 Hz bandwidth).

506
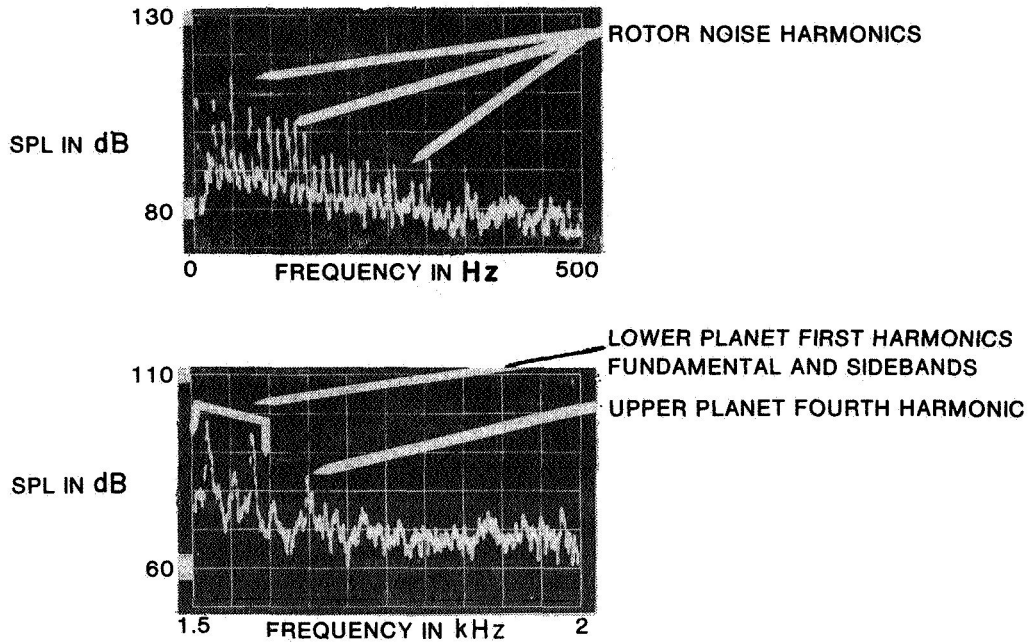
Figure 5.- High resolution noise spectra, CH-47C cabin.
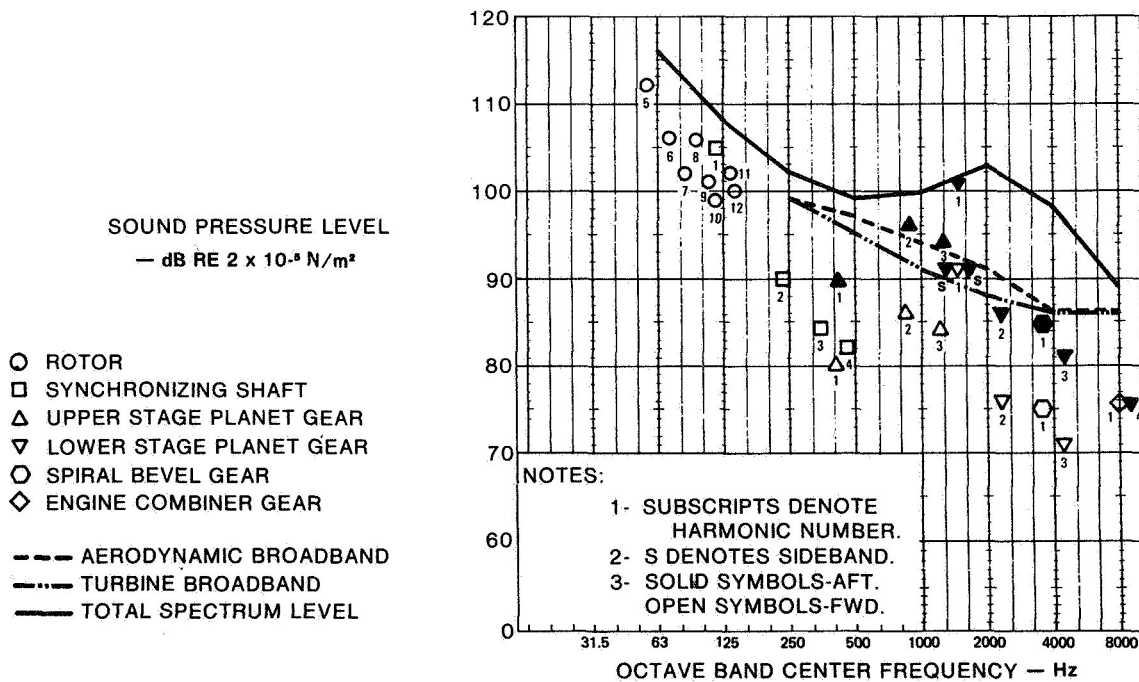
SOUND PRESSURE LEVEL
— dB RE 2 x 10⁻⁵ N/m²

○ ROTOR
□ SYNCHRONIZING SHAFT
△ UPPER STAGE PLANET GEAR
▽ LOWER STAGE PLANET GEAR
○ SPIRAL BEVEL GEAR
◇ ENGINE COMBINER GEAR

━ ━ ━ AERODYNAMIC BROADBAND
━ ··· ━ TURBINE BROADBAND
━━━━ TOTAL SPECTRUM LEVEL

NOTES:
1- SUBSCRIPTS DENOTE HARMONIC NUMBER.
2- S DENOTES SIDEBAND.
3- SOLID SYMBOLS-AFT. OPEN SYMBOLS-FWD.

Figure 6.- Noise components of the CH-47C.

507
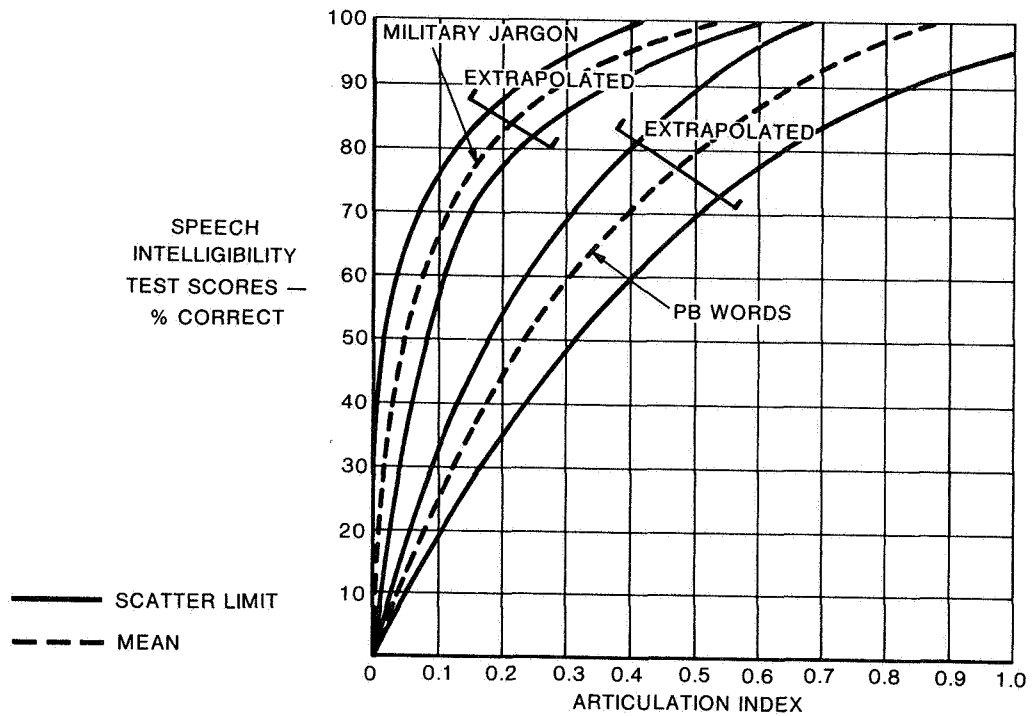
Figure 7.- Test results - relation between speech intelligibility and articulation index in helicopters.
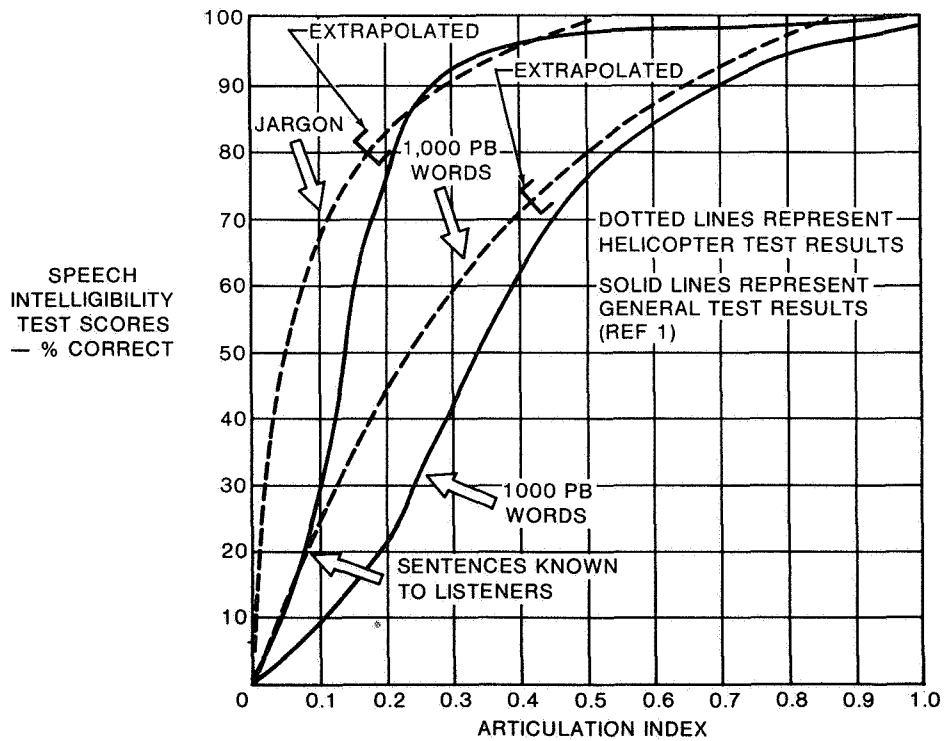
Figure 8.- Comparison of helicopter and general test results.
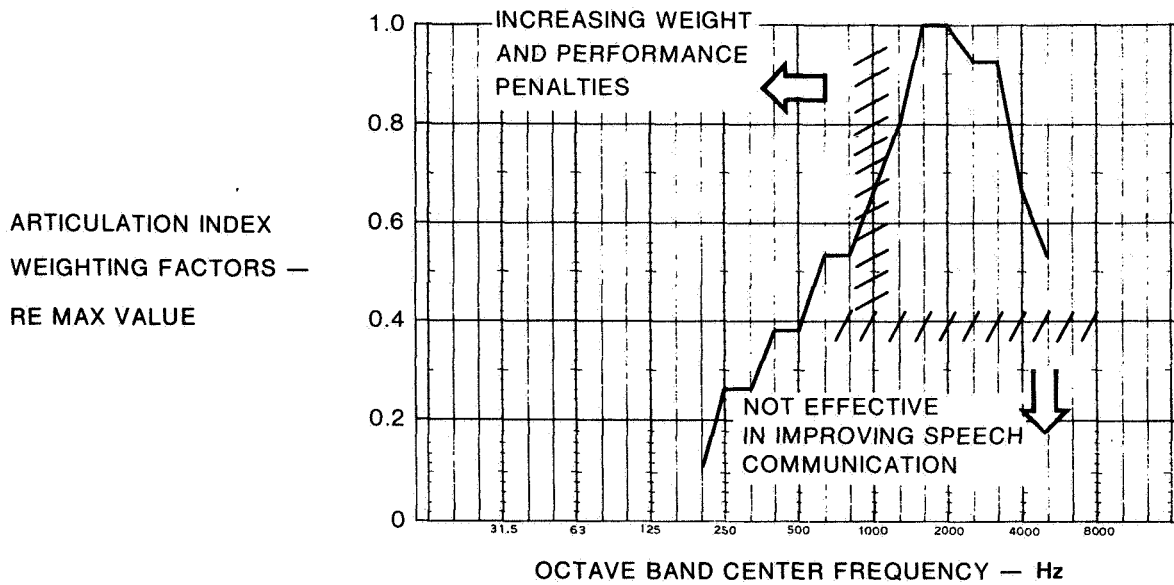
508
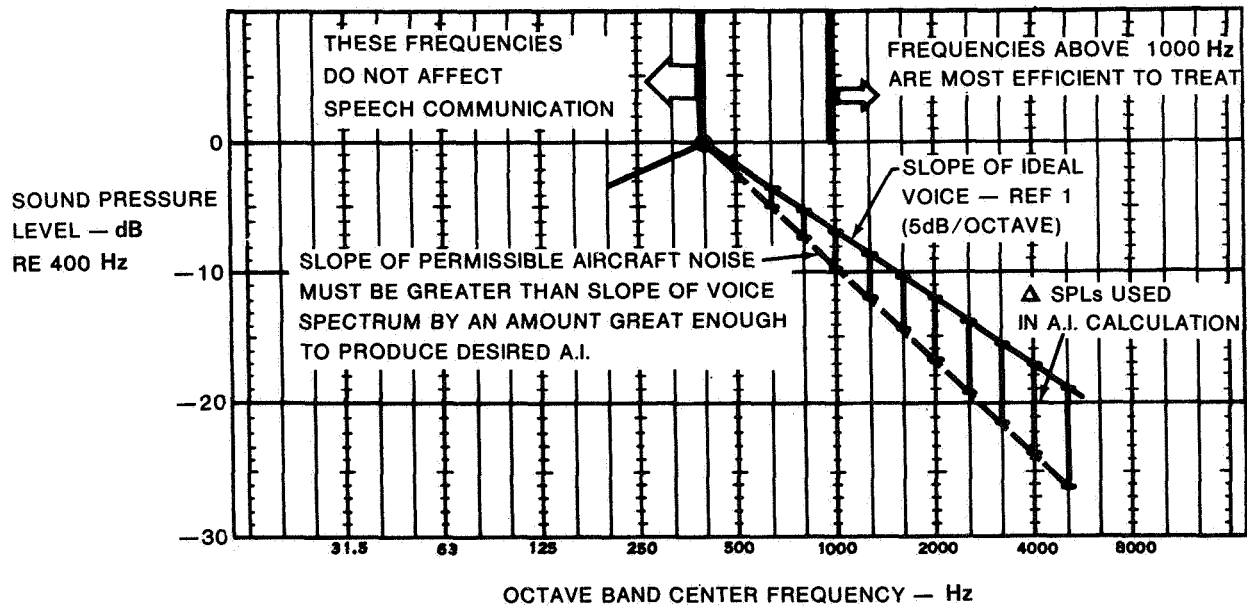
Figure 9.- Articulation index weighting factors.

Figure 10.- Principles involved in construction of an aircraft noise criterion which results in minimum weight penalty.
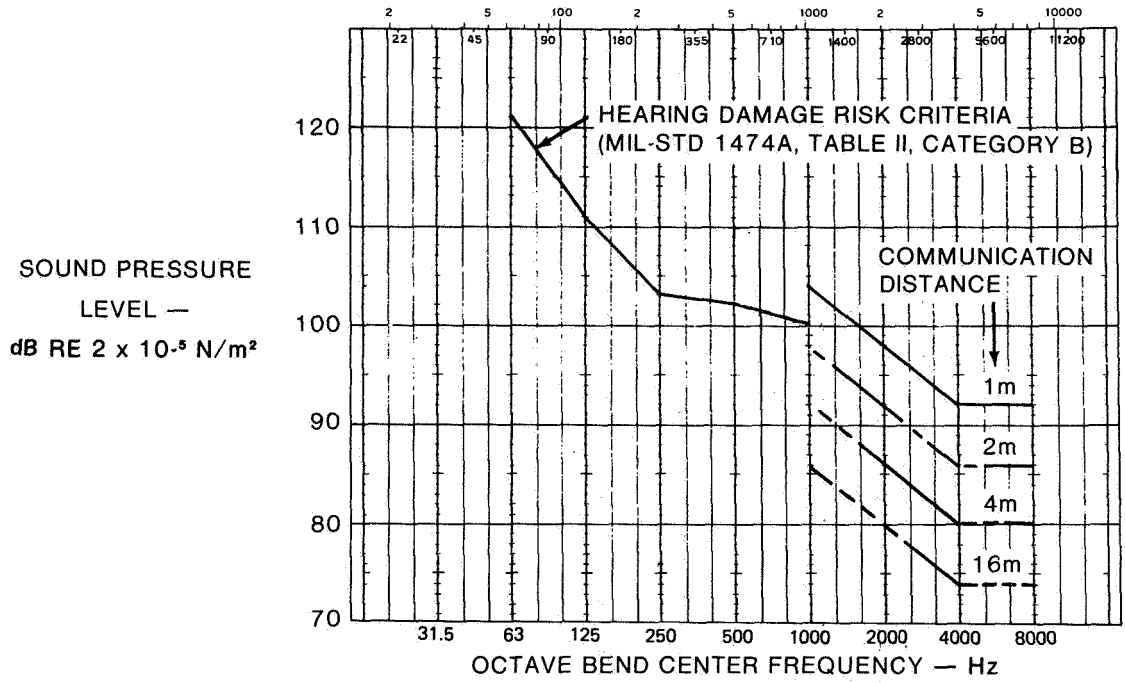
509

Figure 11.- Helicopter interior noise levels for required emergency commands, 50% speech intelligibility using a maximum effort voice, 110 dB rms at 1 meter.
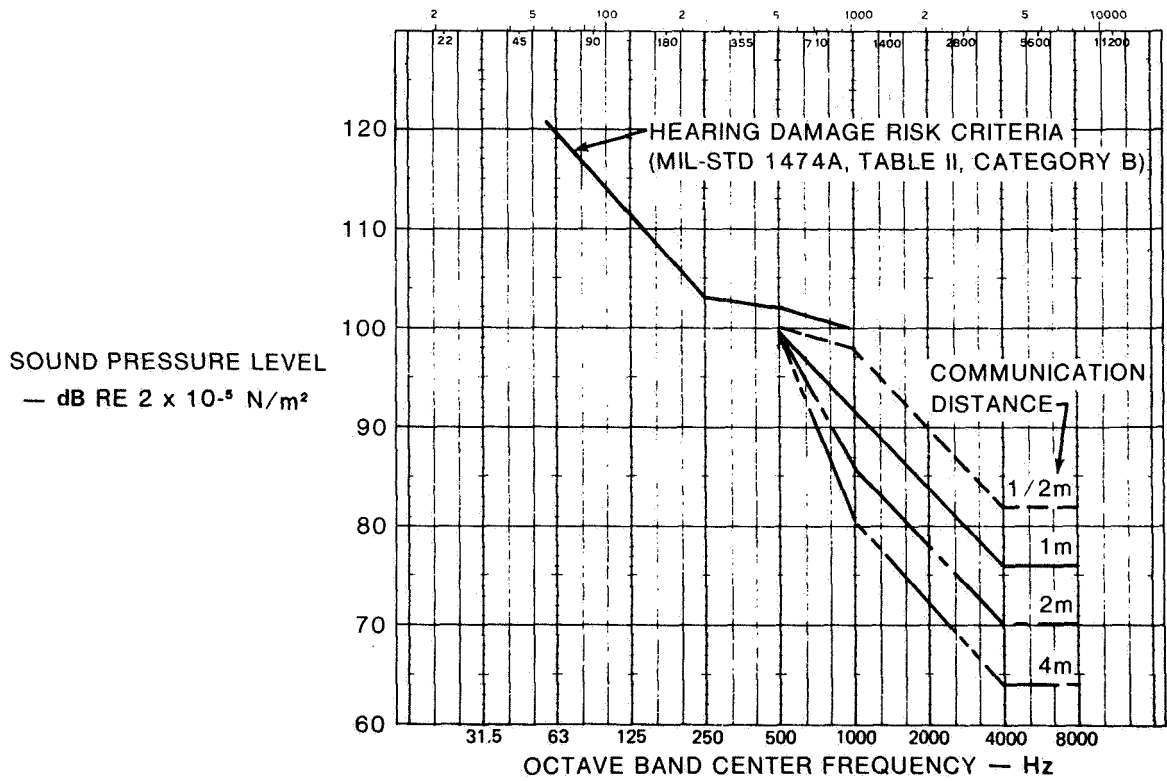

Figure 12.- Helicopter interior noise levels for troop instruction, 80% speech intelligibility using a loud shouting voice, 100 dB rms at 1 meter.
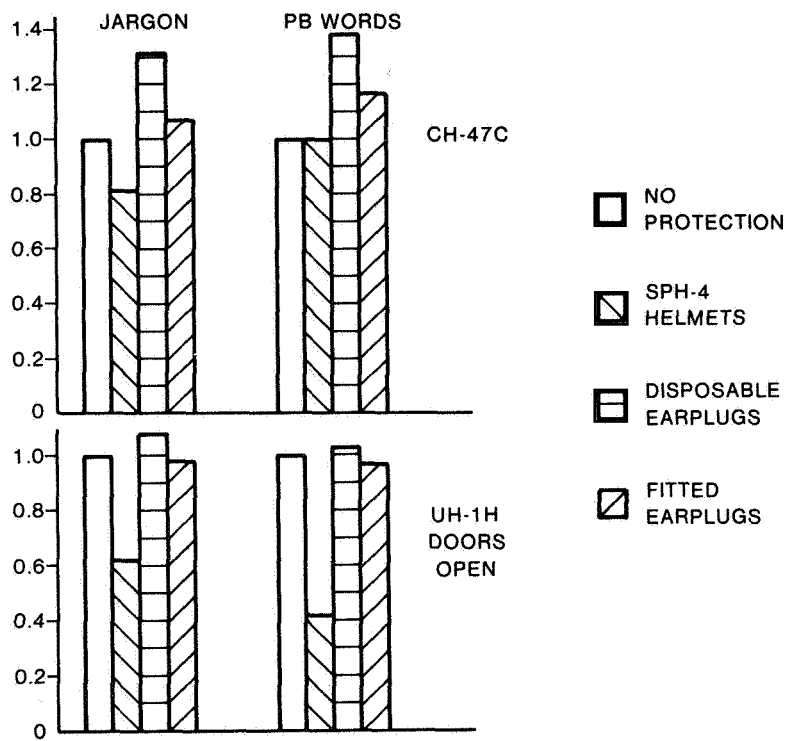
510

Figure 13.- Effect of hearing protection on speech intelligibility.

THE EFFECTIVE ACOUSTIC ENVIRONMENT OF HELICOPTER CREWMEN

Robert T. Camp, Jr., and Ben T. Mozo
Bioacoustics Division
US Army Aeromedical Research Laboratory

SUMMARY

Internal and external noise levels of helicopters are usually measured to determine the acoustic environment of the crewmen. These types of measurements alone are inadequate for assessing the real acoustic hazards of personnel. The attenuation characteristics of helmets and hearing protectors and the variables of the physiology of the human ear must be taken into account in determining the effective acoustic environment of Army helicopter crewmen. Also, the acoustic hazards of voice communications systems noise may influence the overall acoustic environment of the personnel. The composite acoustic environment can be determined only with complex acoustic measurements that are necessary to quantify the effective acoustic environment of the crewmen.

INTRODUCTION

Noise characteristics of helicopters should be given consideration in the design and purchase of aircraft for several reasons. The high sound pressure levels associated with the operation of military aircraft are hazardous to hearing by most damage risk criteria. Also, the high level sounds may interfere with communications and operational efficiency of crewmen.

The traditional approach to the task of ascertaining the acoustic environment that may affect the personnel is to measure sound pressure levels at various crewmen's positions under various operational conditions. In discussions of helicopter noise problems in popular and scientific articles, it is often assumed that the sound pressure levels within the aircraft are the actual pressure level values that impinge on the ears of the personnel who operate the aircraft. It is assumed that the ambient sound pressure levels are the same as the effective acoustical environment of the crewmen. The effective acoustical environment is defined as the actual acoustic energy that is received by the hearing system.

Measuring the effective acoustic environment of helicopter crewmen is a complex process. The purpose of this paper is to discuss the differences between the ambient acoustic level environment of the aircraft and the actual acoustic levels that affect the aircraft crewmen's ears.

HUMAN AUDITORY SYSTEM EFFECTS

The human ear is divided into three sections: the external, middle, and inner ear. The inner ear contains a complex system of membranes, nerves, and hair cells that may be damaged by noise. The amount of noise-induced hearing loss is determined by the effective acoustic environment or the actual energy transmitted into the inner ear.

The middle ear is a pathway to the inner ear and is equipped with certain protective mechanisms that affect the acoustic input. It contains two muscles that limit the input to the inner ear.

The external canal is shaped as an irregular tube. There are various forms and sizes. The variations of sizes and shapes may produce various amounts of protection, especially in the high frequencies. Unpredictable limiting characteristics of the middle ear plus the variations of sizes and shapes of the external ear canal make it difficult to measure the actual acoustic stimuli traveling through the system to the inner ear.

HEARING PROTECTOR AND VOICE COMMUNICATIONS SYSTEMS EFFECTS

The human auditory system just discussed is not the only source of variables that may affect the actual sound transmitted to the ear. Hearing protective devices, earplugs, headsets, and helmets contribute to the transformation of the acoustic environment to sound spectrum characteristics and sound pressure levels that may be vastly different from the values obtained using free field measurements in the cockpit. In general, all types of hearing protectors, both insert and circumaural, attenuate high frequencies much more efficiently than they attenuate low frequencies.

Let us take, for example, the case of a typical pilot flying an Army CH-47 helicopter wearing the standard SPH-4 helmet. One would expect that the change of sound characteristics beneath the helmet when fitted on the head of the aircrewman would be the original sound spectrum on the outside of the helmet minus the attenuation characteristics of the helmet. If the pilot were flying with no voice communication system or warning signals activated, the resultant spectrum at the external ear would be approximately the values as determined by this method. One must remember that the helmet earcups are sealed tightly over the ears of the crewmen and contain earphones that generate a sound source beneath the helmet. One normally does not associate very high sound pressure levels with an earphone. Coupled to small volumes such as the canal of the human ear, earphones are capable of generating up to 120 dB sound pressure level. Our investigations of sound sources from communication systems, warning signals and navigation signals, have revealed that a very significantly high sound pressure level may be transmitted from the earphone. These levels are much greater than the ambient noise that is transmitted through the helmet.

Another source of noise that may enter in the total effective acoustic environment is the distortion created by the design of voice communications electronic systems. It is well-known that military voice communication systems are designed with distortion. Some military specifications require only 70% intelligibility and specify certain various amounts of peak clipping which yield harmful distortion harmonics. The effects of peak clipping have been thoroughly discussed in some of my previous presentations to this group. Peak clipping may cause a decrement of intelligibility and also creates unnecessary harmonics that add to the total excessive energy that is transmitted to the ears and thereby the contributor to hearing loss. Added to these harmonics, often we have found inverter power-line noise that yields very high acoustic signals through the earphones and therefore is a significant source of acoustic hazard.

TRANSDUCER CHARACTERISTICS EFFECTS

Another aspect of the problem that one should note is the characteristics of transducers. Ideally, microphones and earphones should have flat response within the audio range. If either the microphone or the earphones have peaks, the crewmen may set gains of voice communications and other signals emitted through the earphones that are unnecessarily high level. By some evaluations the M-87 microphone has been considered one of the best military type noise cancelling microphones available. The response characteristics contain a very large peak in the 4000 Hz range. So when one receives messages transmitted through this microphone, there is an unnecessarily high emphasis of the 4000 Hz range. With our present-day knowledge of hearing loss causes, it is well established that this is the most vulnerable portion of the audio spectrum for hearing damage. If this microphone were used in low ambient noise conditions and if the reception were in quiet environments, there would probably be no significant amounts of hearing loss. However, in its application in high noise environments where gain settings are very high, the net result is that the ear is subjected to large quantities of energy which, for long periods of time, may cause significant hearing loss for some personnel.

Earphones should also have flat response. If they produce peak response, one would expect the same potential hearing damaging spectra in high level noise for much the same reason that peak microphones cause problems. The recent trend to change to lighter earphones should be watched carefully to avoid regression of headphone response. Some of the small earphones may produce high distortion when driven at the levels required in the military noise environment.

With the excess energy caused by variables of transducer response plus the many other signals such as voice communication messages, warning signals, navigation signals, and special instrumentation, there are significantly high acoustic levels generated beneath the helmet earcups.

515

SPECIAL PROBLEMS OF LOW FREQUENCY NOISE

One other aspect of the helicopter noise problem that may affect the effective acoustic environment of the crewmen is extremely low rotary blade passing frequency which is usually below the octave bands traditionally given ir the analyses of survey data. In this region of the audio spectrum, measurement is seldom made of the aircraft noise spectra. The attenuation characteristics of the hearing protectors that are also worn in helicopters are not usually reported. The questions arise: Are these low frequencies passing through the helmets? Do they cause high frequency harmonic distribution that contributes to the total noise in the effective acoustic environment?

Our laboratory is presently engaged in the investigation of the effects of low frequencies on animal ears. We have found significant temporary threshold shift in the high frequencies when the animals were exposed to long periods of low frequency band centered at 63 Hz.

CONCLUDING REMARKS

In summary, the purpose of our presentation is to call attention to the fact that the ambient sound pressure level measurements often made in helicopter cockpits with sound level meters will not yield essential information about the noise characteristics that truly affect the helicopter crewmen. We should be aware of the difference between these levels and the actual effective acoustic environment that must be determined by other means. We have shown how the ambient acoustics level transmitted through the helmets is transformed by the attenuation characteristics of the helmet or other hearing protective devices that the crewmen may be wearing. In addition to these transformations, there are added signals caused by the design of microphones, earphones, hearing protective devices, and electronic systems. In a word, the actual acoustic energy at the eardrums of the crewmen is usually totally different from the acoustic environment measured around the various positions inside the aircraft. We have also discussed the variables of the middle ear that limit and modify the acoustic spectrum that is produced at the eardrum. All of these variables and unknowns make it very difficult to assess the real energy that reaches the inner ear, the locale of hearing damage. We have methods by which we measure the output of earphones and the magnitudes of various warnings and navigation signals necessary in the operation of helicopters.

Precise narrow band measurements are necessary, and in addition, standard real-ear attenuation characteristics of helmets and hearing protective devices must be accomplished. A better estimate of the total acoustic input to the crewmen is made by the insertion of a tiny microphone in the ear with small

516

wires that will not affect the attenuation characteristics of the helmets. Also, we have developed a portable cement chamber that is very useful in estimating the output of earphones as used in the helicopter operations.

It is recommended that future helicopters voice communication systems, auditory warning systems, and other special instrumentation with auditory signals be designed with consideration for the total systems output so as to minimize the acoustic hazards that presently exist. This approach is necessary for realizing the most efficient operation of the crewmen. The evaluation of this low frequency problem can be done only after sufficient research has been accomplished. The recent findings about the significance of low frequency noise spectra cast doubt about the present universal application of dBA for reporting helicopter noise measurements. It is also recommended that as more sophisticated instrumentation is obtained for the measurement of helicopter noise, more attention be given to the extremely low frequency of the rotary blade.

THE EFFECT OF OPERATIONS ON THE GROUND NOISE FOOTPRINTS

ASSOCIATED WITH A LARGE MULTIBLADED,

NONBANGING HELICOPTER

David A. Hilton, Herbert R. Henderson
and Domenic J. Maglieri
NASA Langley Research Center

William B. Bigler II
University of Virginia

INTRODUCTION

Pending noise certification of helicopters has focused attention on the effects of their operations on ground noise exposure. Knowledge of the effects of helicopter configurations (blade numbers, airfoil configuration, etc.) and operations plays an important role in the evolution of final procedures to be utilized for the noise certification of helicopters. In addition, as noted in reference 1, the prediction of realistic and representative ground noise contours, or footprints, caused by various aircraft operations, including helicopters, can aid significantly in minimizing the noise intrusion.

Considerable effort has been expended in an attempt to better understand helicopter operational effects so that improved noise prediction techniques can be developed (ref. 2). Measurements made to date are providing a better understanding of the physical phenomenon involved. However, the results from single point measurement programs suggest that the determination of true ground exposure necessitates the use of numerous ground noise measurements at multiple locations along, and perpendicular to, the aircraft ground track. The recently developed remotely operated multiple array acoustics range (ROMAAR) at NASA Wallops Flight Center, reference 3, was designed to provide an arrangement for obtaining noise measurements along the aircraft ground track and at various lateral positions simultaneously along with information on aircraft position, operating parameters, and local meteorological information.

In order to expand the data base of helicopter external noise characteristics, NASA conducted a flyover noise measurement program utilizing the NASA Civil Helicopter Research Aircraft. In these studies, both the ROMAAR and a 2560-m linear microphone array, laid out along a runway at NASA Wallops Flight Center, were utilized for the purpose of documenting the noise characteristics of the test helicopter during flyby and landing operations. By utilizing both the ROMAAR concept and the linear array, the data necessary to plot the ground noise footprints and noise radiation patterns were obtained.

The purpose of this paper is to present examples of the measured noise signature of the test helicopter, the ground noise footprint or contours, and the directivity patterns measured during level flyby and landing operations of a large, multibladed, nonbanging helicopter, the CH-53.

APPARATUS AND METHODS

Test Site

The NASA Wallops Flight Center on the Eastern Shore of Virginia was chosen as the test site of these acoustics tests. The sketch of figure 1 indicates the geographical relationship between the Wallops Flight Center and the Langley Research Center. The insert in the figure, an aerial photograph of the airfield at Wallops Flight Center, gives an indication of the general runway layout and the type of terrain surrounding the test area.

The Wallops Flight Center offers a number of desirable characteristics that are necessary for flyover noise testing. The ROMAAR (ref. 3) is located at the Wallops Flight Center and was made available for this series of acoustics tests. The ROMAAR is located in an area south of the airfield where ambient noise is low and where aircraft other than the one under test do not operate routinely. The microphone array is located in relatively flat, open areas which tend to minimize shielding, reflection, and shadow-zones, etc. The range is supported by aircraft tracking and weather observation facilities.

The general ROMAAR and linear-array concept combines the basic elements of flyover noise testing, which include acoustic measurements, aircraft position measurements, and weather measurements. The noise measurement elements of the range consist of analog stations (manned) and/or digital stations (unmanned) For these tests, aircraft positions over the range and over the linear microphone array were determined by radar, and the aircraft operating parameters were read from the standard instrument panel aboard the test aircraft. Data from all of the above sources were time correlated using a time signal generated by WWVB.

Test Helicopter

The test aircraft for this series of noise experiments was a modified CH-53A turbine-powered transport helicopter that is being utilized as a test bed in the NASA Civil Helicopter Technology Program. The test helicopter has uprated engines and drive systems and has a normal gross weight of 16 330 kg (the uprated engines and drive system make this machine comparable to the later D model). The test aircraft has also been outfitted with a 16 seat passenger compartment for ride quality research. A photograph of the helicopter utilized for these tests is shown at the top of figure 2. The general dimensions of the CH-53 are shown in the drawing at the bottom of the figure. Briefly, the main rotor has six blades and has a 22-m diameter, and the tail rotor contains four blades and is 4.9 m in diameter.

520

Aircraft Operations

ROMAAR.- As indicated by the schematic drawings of figures 3(a) and (b), .anding and level flyby operations were performed over the ROMAAR. The ROMAAR consisted of 38 measurement positions which were located to the south of runway 04 and covered an area approximately 500 m to either side of the extended centerline of runway 04 and approximately 10 km downrange. The circles in the sketches indicate the approximate deployment of the microphones.

For the landing approach measurements, the aircraft approached the range at an altitude of approximately 457 m until the six-degree glide slope was intercepted; at that point a descent was made to a full stop landing at a point approximately 40 m inside the approach end of runway 04/22. For these operations the approach was always made from the south, directly over the ROMAAR.

For the level flyby noise measurements, constant altitude flyovers were made along the extended centerline of runway 04/22, directly over the ROMAAR. The helicopter was flown at a nominal altitude of approximately 152 m at an airspeed of 49 m/s. For this particular series of tests, the helicopter was flown on reciprocal headings over the ROMAAR. The helicopter flight path and power conditions were stable approximately 1 km prior to range entry and 1 km after leaving the range.

During these operations, the spatial position of the test aircraft was determined by utilizing a precision radar; the general specifications are listed in reference 3. For both the landing approach operations and the level flyby operations over the ROMAAR range, the onboard flight parameters were read from pilot display instruments.

Linear microphone array.- As indicated in figure 3(c), a linear microphone array was established along the centerline of runway 04/22. Utilizing the standard analog measurement systems, microphone positions were established at distances indicated in the sketch. For this series of flights, the flight track was established perpendicular to the array and overhead of the center microphone. Flights were made on reciprocal headings at airspeeds of 47 and 82 m/s and at altitudes of 76 and 152 m. For this series of tests, the aircraft was in stabilized condition approximately 1 km before passing over the microphone array and these conditions were maintained approximately 1 km after passing overhead.

Shown in figures 4(a) to (c) are radar data concerning the altitude, lateral displacement, and velocity time histories associated with the flight operations over ROMAAR for the six-degree approach and level flight conditions and for level flight operations over the linear array. It can be noted from these figures that slight variations in altitude, lateral displacement, and velocity existed from flight to flight. These variations in the flight path and velocity could have resulted in some minor variations in the noise level values from flight to flight. Corrections can be made for these variations; however, in this case they were felt to be so small that no attempt was made to include such corrections for the data of this paper.

METEROLOGICAL CONDITIONS

Shown in figures 5(a) and (b) are the measured variations in selected meterological quantities for the two time periods during which the subject test were conducted. Temperature, relative humidity, wind direction, and wind speed are plotted as functions of altitude. The hatched region represents the ranges and measured values at altitudes up to and beyond the test altitudes. These data were obtained by means of standard rawinsondes. Data concerning altitude, temperature, and relative humidity are telemetered to a receiver on the ground, and dual theodolities are used to track the lifting balloon in order to obtain the wind information. Alternating temperature and humidity sondes were release at approximately 1/2-hour intervals throughout the test period. These data are presented for information only and no corrections have been made to the measure noise data of this paper to reference day conditions.

TEST RESULTS

Noise Characteristics

Typical noise characteristics of the test helicopter during a level fly-over operation at an airspeed of 49 m/s and an altitude of 152 m are illustrate in figure 6. Presented in the left-hand portion of the figure is a sound pressure level time history measured on the ground track directly under the test aircraft. The time of overhead passage of the helicopter is noted on the figure, and it can be seen that for this particular helicopter the maximum sound pressure level occurs at approximately overhead passage. A frequency spectrum of the noise at the time of maximum sound pressure level is shown in the right-hand portion of the figures. It can be seen that the spectrum is dominated by the relatively low frequency components associated with the main- and tail-rotor blade rotational noise. For all of the measurements made at the analog station, data of the type illustrated in figure 6 are available. For the digital stations, the dB(A) descriptor was selected for the purpose of reporting and dB(A) time histories are available from each of these measurement stations.

Noise Level Variability

The data of figures 7, 8, and 9 are included to indicate the data spread and variability experienced for this series of tests. An indication of the noise variability can be obtained by examining the histograms of figures 7 and 8. Shown in these figures are histograms which indicate the variations in maximum dB(A) for six flights of the test aircraft over the 2560-m linear array at an altitude of 152 m and an airspeed of 49 m/s and during an approach operation over the ROMAAR. Data are grouped in intervals of 5 dB(A). In general, these figures indicate that less scatter is associated with stations located under the aircraft, along the flight track than at the lateral locations. As distance increases and/or as look angle β decreases, the variability in the noise measurements increases.

Presented in figure 9 are average data from four passes of the test helicopter over the ROMAAR at an altitude of 152 m and an airspeed of approximately

49 m/s. The data, presented at the top of the figure, are for the on-track microphones only. The average levels from these microphones are shown as functions of position on the track; as an aid to interpretation, a line has been drawn at a nominal level of 80 dB(A). It is interesting to note that, over the entire 10-km length of the ROMAAR, the on-track variations are on the order of approximately 3 dB(A).

Utilizing the average dB(A) levels from all measurement stations in the ROMAAR array for the same four level flybys, data are presented in the lower portion of figure 9 which indicate the extent of the ground noise footprint of the helicopter. For each measurement station, the average dB(A) level for the four flights is shown at the measurement station location. Based on these average levels, the 75-dB(A) and 70-dB(A) noise contours, or footprints, were developed. These contours were obtained by appropriate cross-plotting and extrapolation of the average values of the measured noise level parallel to and perpendicular to the aircraft ground track. Inspection of the contour indicates that the pattern is quite symmetrical in nature around the aircraft ground track.

Ground Noise Contour and Directivity Patterns

Six-degree landing approach operations.- The ground noise contours for a six-degree landing approach of the test helicopter are shown in figure 10. These contours were constructed utilizing the average of the maximum dB(A) levels measured at each of the 38 ground noise meaurement stations during five 6° landing operations over the ROMAAR. Again, these contours were constructed by cross-plotting and extrapolation of the average of the values of the measured levels parallel and perpendicular to the aircraft ground track. Again, it should be noted that the ordinate and abscissa are plotted to the same scale. One can see that during the approach the contours are parallel to the flight track and are symmetrical in nature. As the helicopter begins its descent other contours appear and, due to the descending flight, these contours close. These closed contours are also symmetrical about the flight track which suggests that this particular helicopter does not exhibit any sharply directional noise pattern.

Further insight into the noise radiation patterns for the test helicopter can be obtained by examining the results from the level flybys over the linear microphone array.

Level flybys.- The data of figure 11 represent aircraft noise directivity patterns obtained as a result of analyzing the noise data for six passes of the test aircraft over the linear microphone array. The aircraft was frozen over-head of the center microphone of the linear array and at several locations during the approach to and the departure from the array. The aircraft was frozen at five-second intervals along the flight track, and the dB(A) levels were read from the time histories at each measurement location for that partic-ular time. In this manner a grid of dB(A) values was established for each pass. These data were then extrapolated and cross-plotted; one could then choose a particular dB(A) value and a constant dB(A) contour or line drawn through the intercept points. The data of figure 11 show that the radiation pattern is

symmetrical about the flight path axis; however, the levels seem to be somewhat higher to either side of the aircraft than those to the front and rear of the aircraft. These data graphically illustrate the symmetrical patterns that were suggested by the previous figure.

The variation in the directivity patterns for the test helicopter as a function of altitude and airspeed are illustrated in figure 12. It can be seen that increasing altitude results in very small changes in the shape or size of the radiation patterns. This suggests that a uniform radiation pattern exists below the helicopter. On the other hand radiation patterns developed from data measured at the same altitude but at two airspeeds show an increase in the radiation pattern size in addition to a change in shape. The increase in level is thought to be due to the increase in disc loading at the higher speeds, while the shape is thought to be modified by a change in the tilt to the blade tip path.

CONCLUDING REMARKS

A field measurement program was conducted utilizing the NASA Civil Helicopter Research Aircraft. In these studies both the remotely operated multiple array acoustic range (ROMAAR) and 2560-m linear microphone array laid out along a runway at the NASA Wallops Flight Center were utilized for the purpose of documenting the noise characteristics of the test helicopter during flyby and landing operations. By utilizing both the ROMAAR concept and the linear array, the data necessary to plot ground noise footprints and noise radiation patterns were obtained.

The results of these tests indicate that both the ground noise contours and the radiation patterns for this particular helicopter are symmetrical about the flight axis of the helicopter. It was also shown that increasing altitude did not significantly modify the radiation pattern while increasing speed caused higher levels and a distinct change in the radiation pattern.

REFERENCES

1. Stepniewski, W. Z.; and Schmitz, F. H.: Possibilities and Problems of Achieving Community Noise Acceptance of VTOL. Presented at Eight Congress of International Council of Aeronautical Sciences, ICAS Paper No. 72-34, Amsterdam, The Netherlands, Aug. 1972.

2. Maglieri, Domenic J.; Henderson, Herbert R.; and Hilton, David A.: Observed Variability of Aircraft Noise Footprint Measurements. NOISE-CON 77, Proceedings, George C. Maling, Jr., ed., Noise Control Found. c.1977, pp. 443-458.

3. Hilton, David A.· and Henderson, Herbert R.: A Remotely Operated Multiple Array Acoustic Range (ROMAAR) and Its Application for the Measurement of Airplane Flyover Noise Footprints. NASA TM X-73986, 1976.

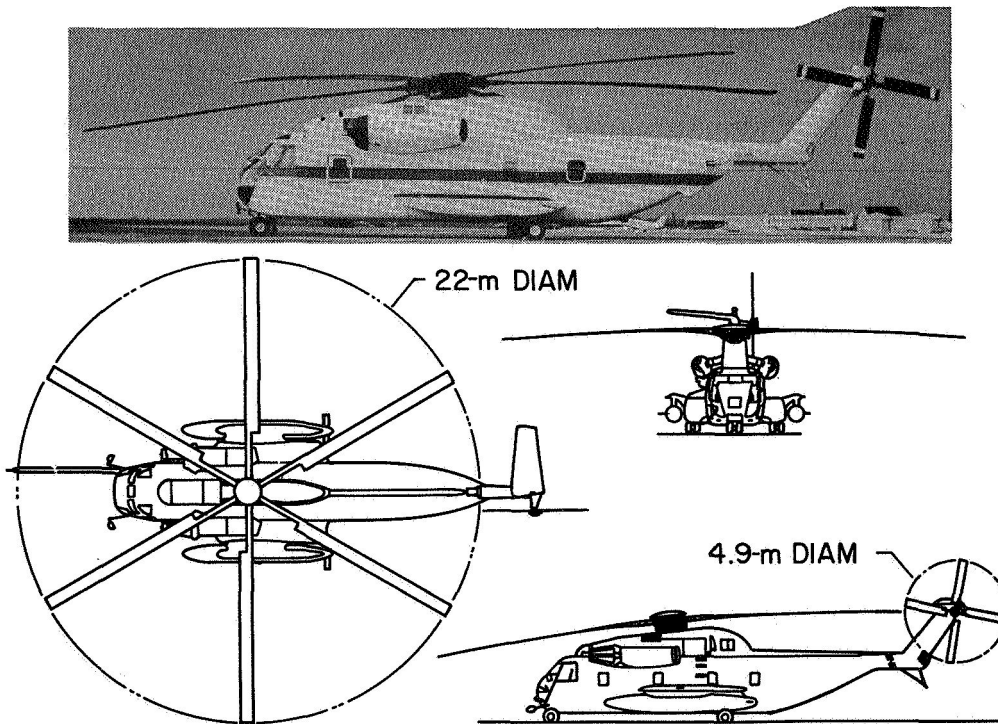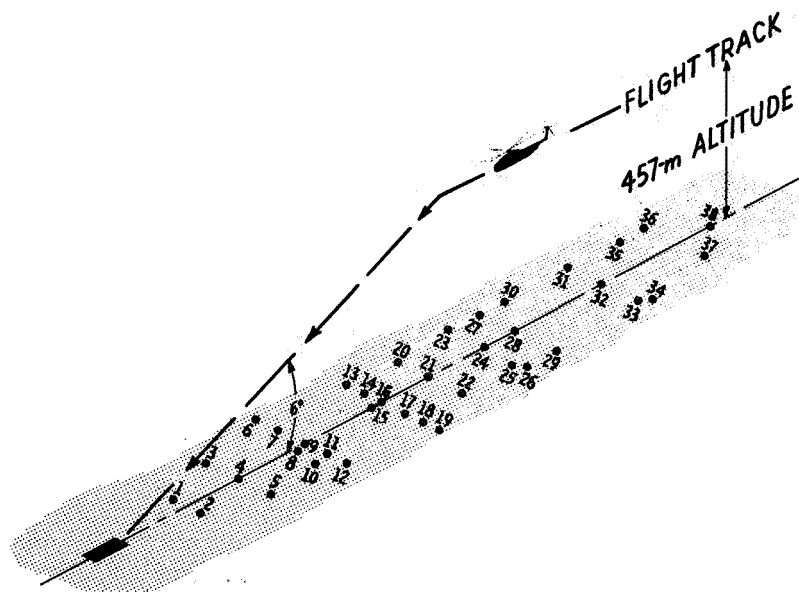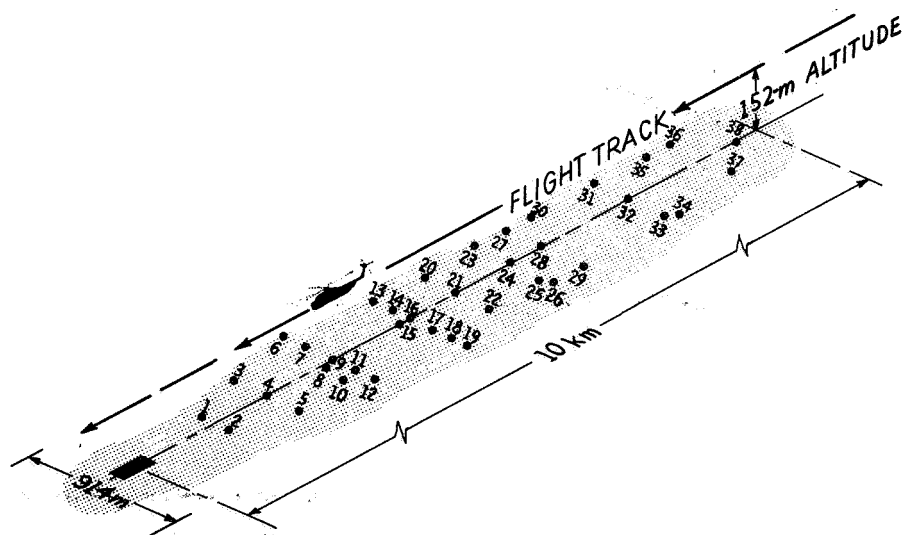Figure 1.- Schematic illustration of geographical relationship between Wallops and Langley.

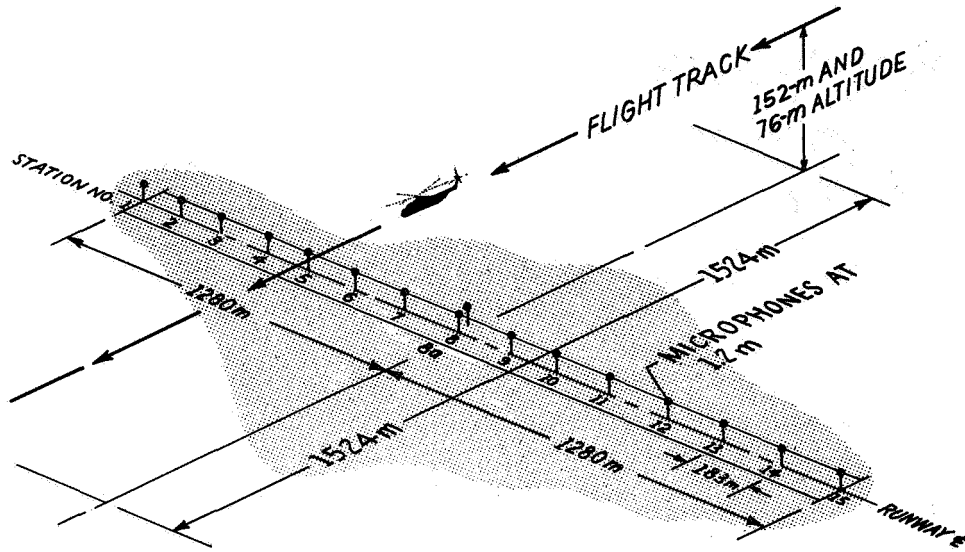Figure 2.- Turbine-powered helicopter used in tests.

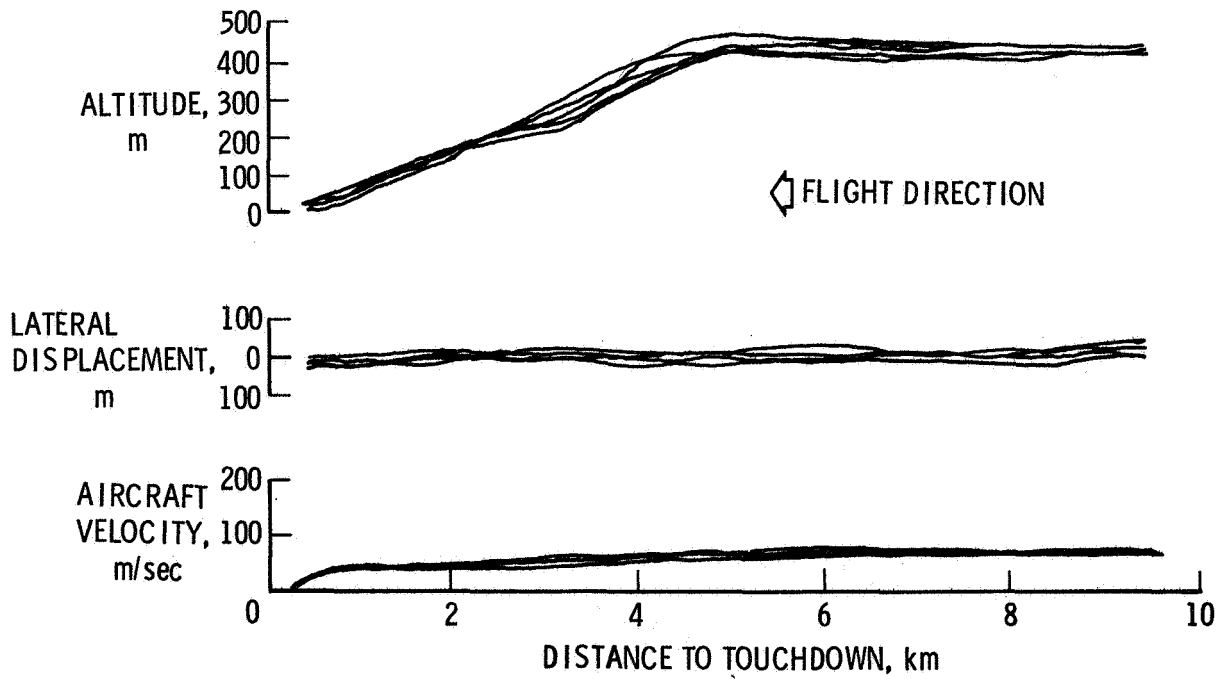(a) Six-degree landing approach over ROMAAR.

(b) Level flyby over ROMAAR.

Figure 3.- Schematic drawings of landing and level flyby operations performed by test helicopter.
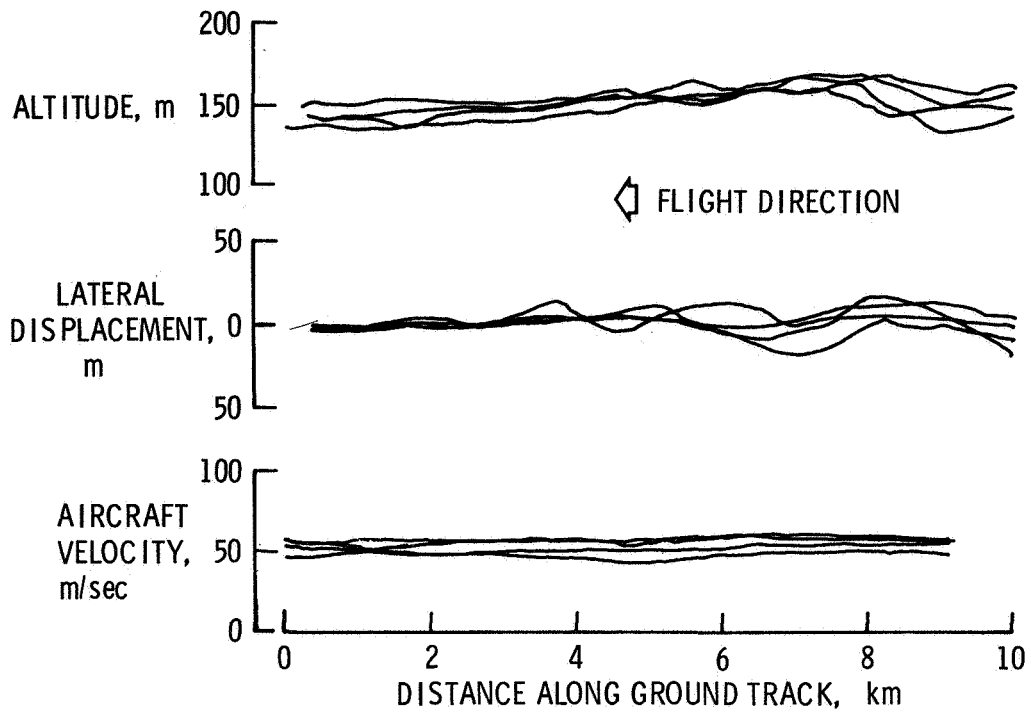
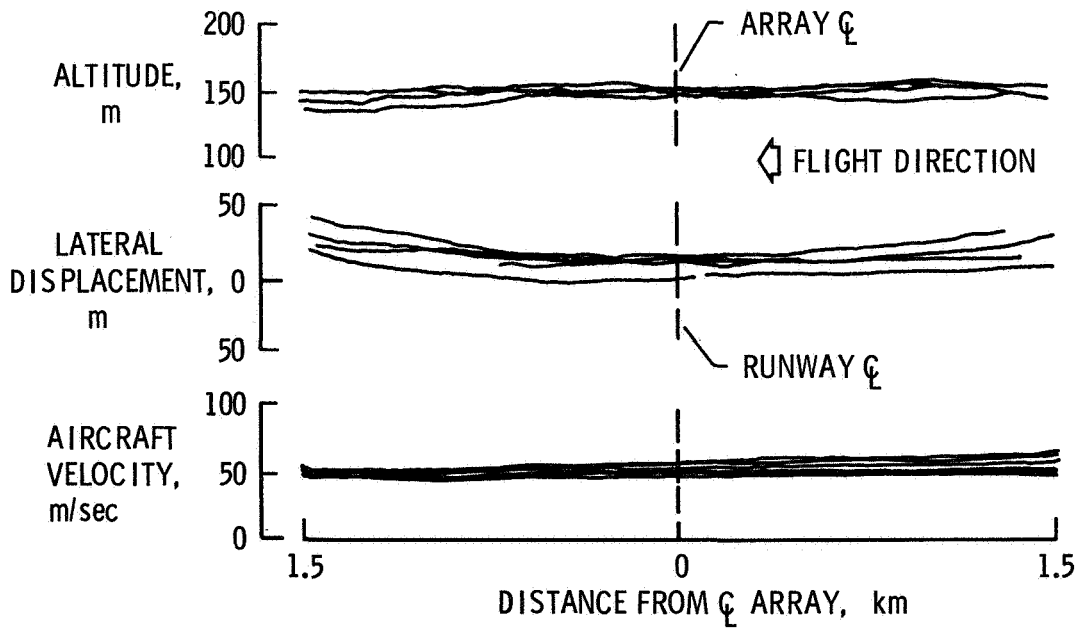(c) Level flyby over linear array.

Figure 3.- Concluded.

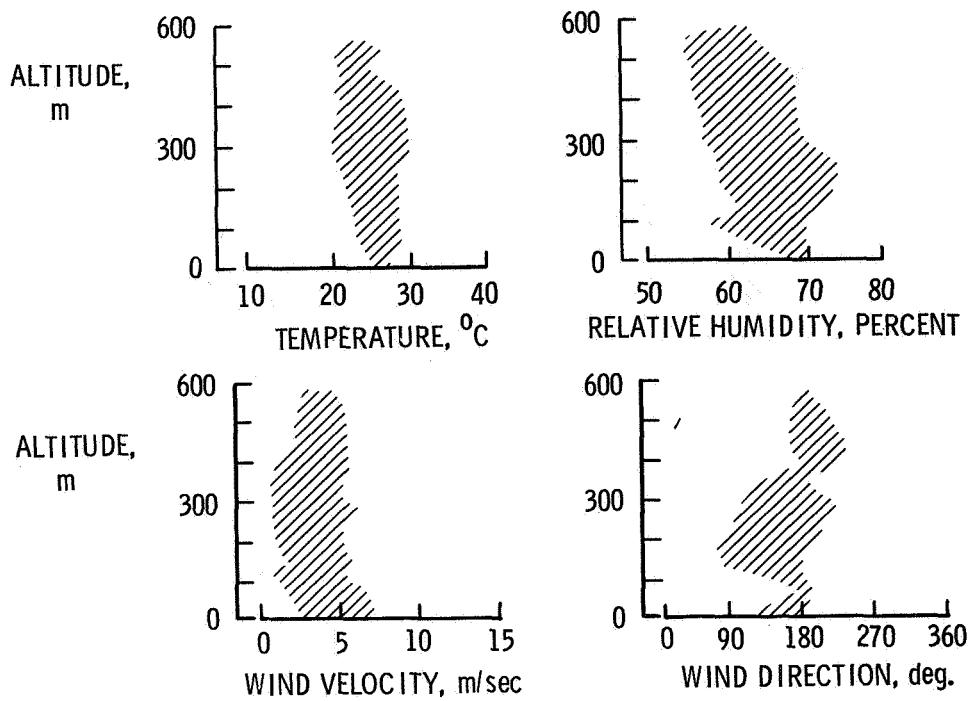(a) Six-degree landing approach over ROMAAR.

Figure 4.- Radar tracking and aircraft velocity information.
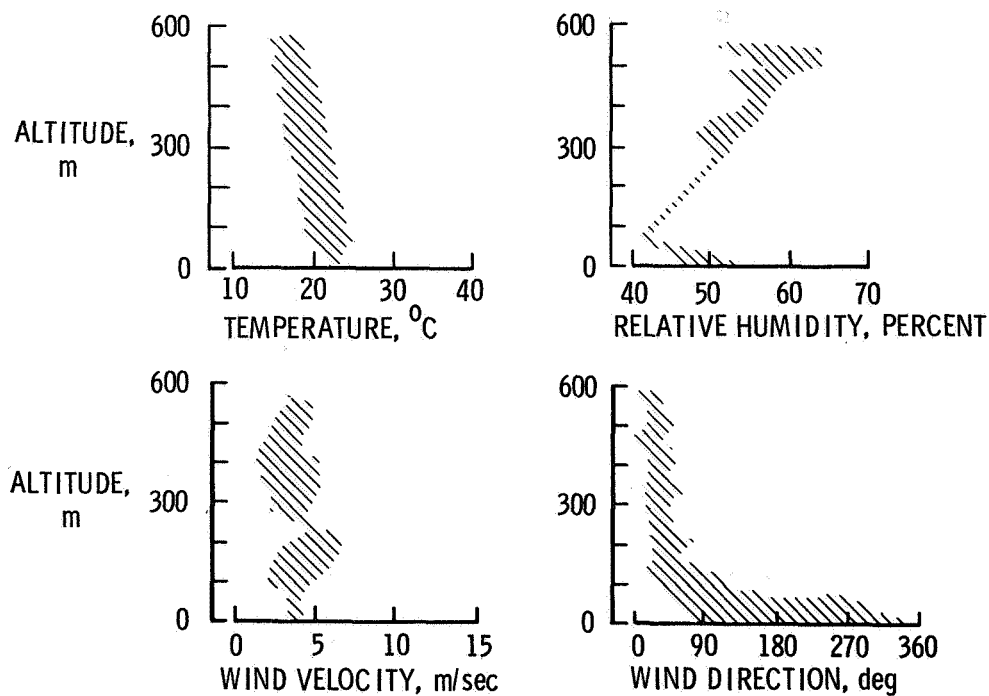
(b) Level flyby over ROMAAR.

(c) Level flyby over linear array.

Figure 4.- Concluded.

(a) ROMAAR operations.

(b) Linear array operations.

Figure 5.- Variations in meteorological conditions for two test periods.
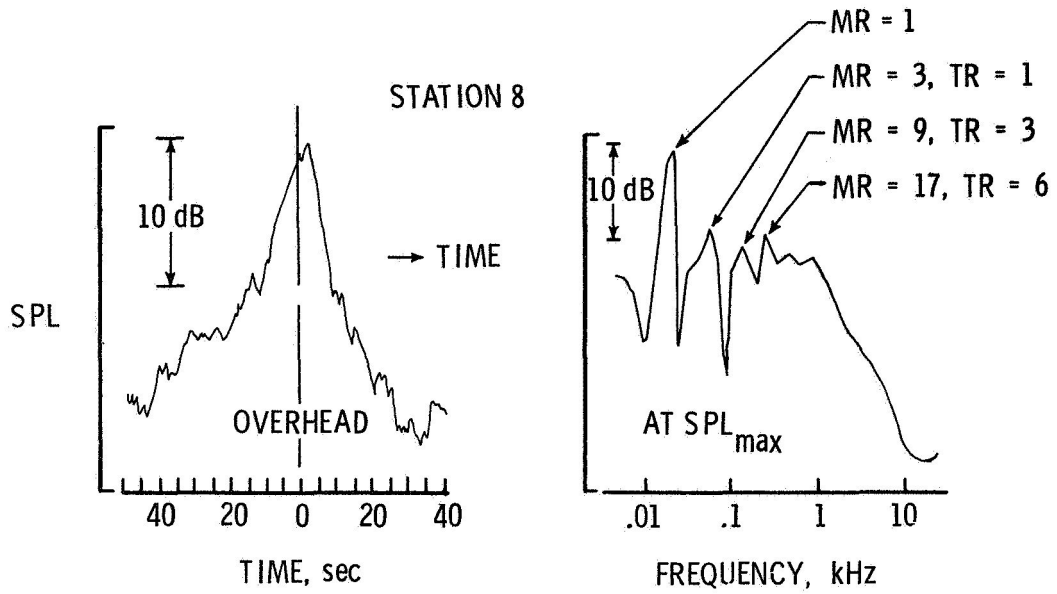
ROTOR rpm = 100 PERCENT TORQUE= 40 PERCENT

Figure 6.- Typical noise characteristics of test helicopter
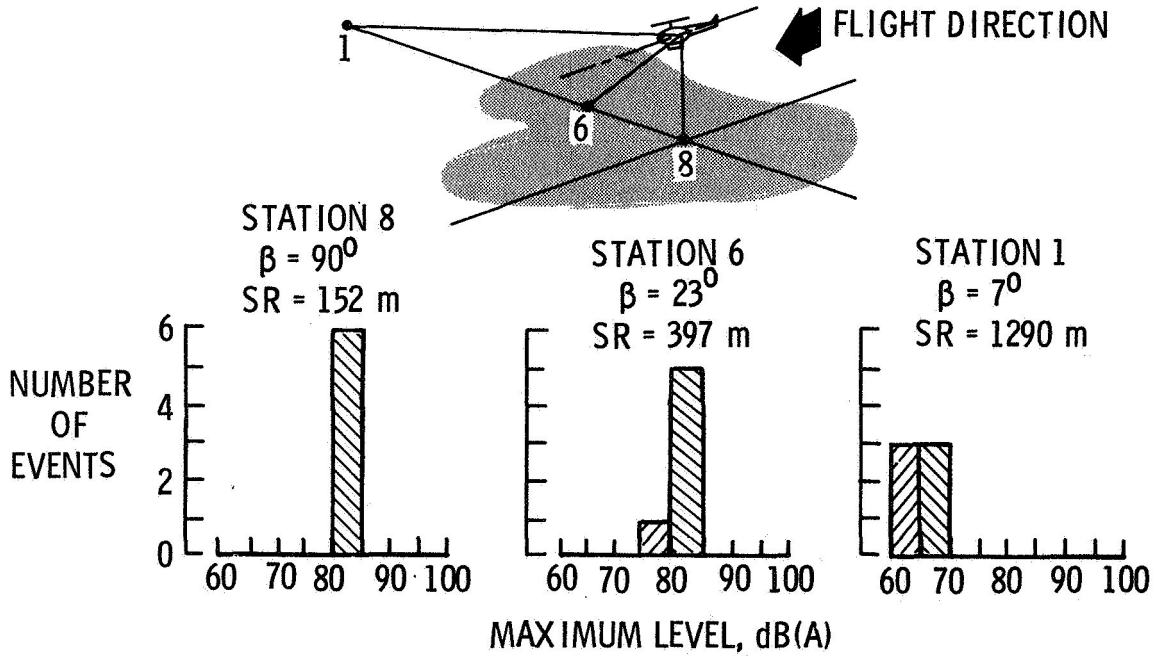during level flyby. Altitude = 152 m, airspeed = 49 m/sec.

Figure 7.- Variation in maximum dB(A) levels over linear microphone
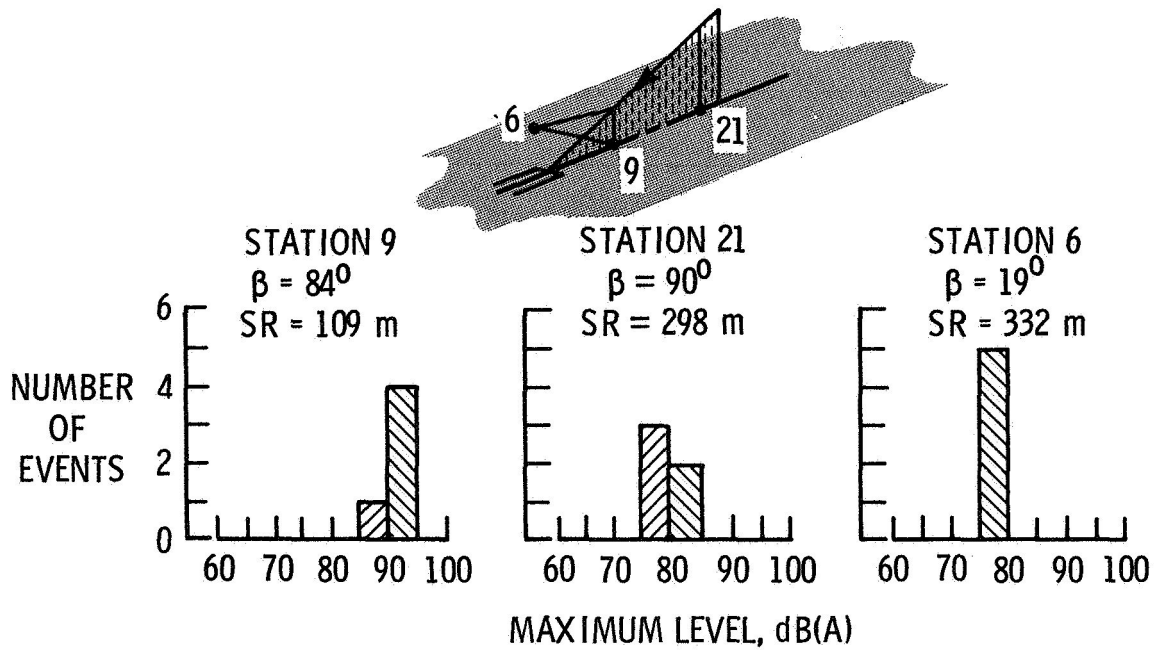array for six flights at 152-m altitude at speed of 49 m/sec.

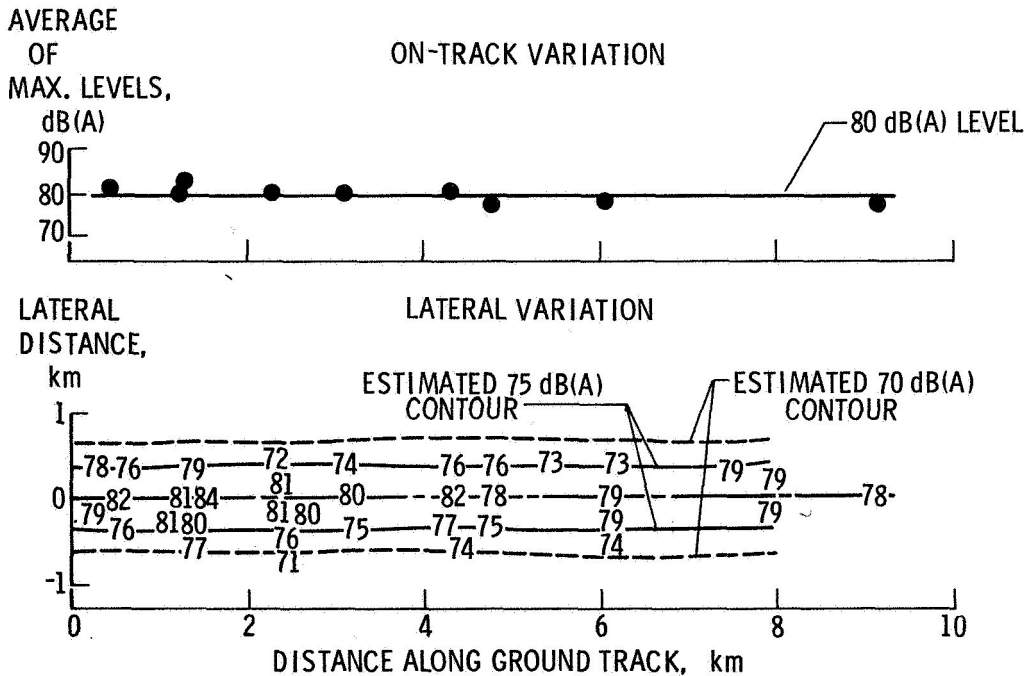Figure 8.- Variation in maximum dB(A) levels for five six-degree landing approach flights over ROMAAR.

Figure 9.- Noise variability along ground track using ROMAAR for four level flybys at 152-m altitude and 49-m/sec airspeed.
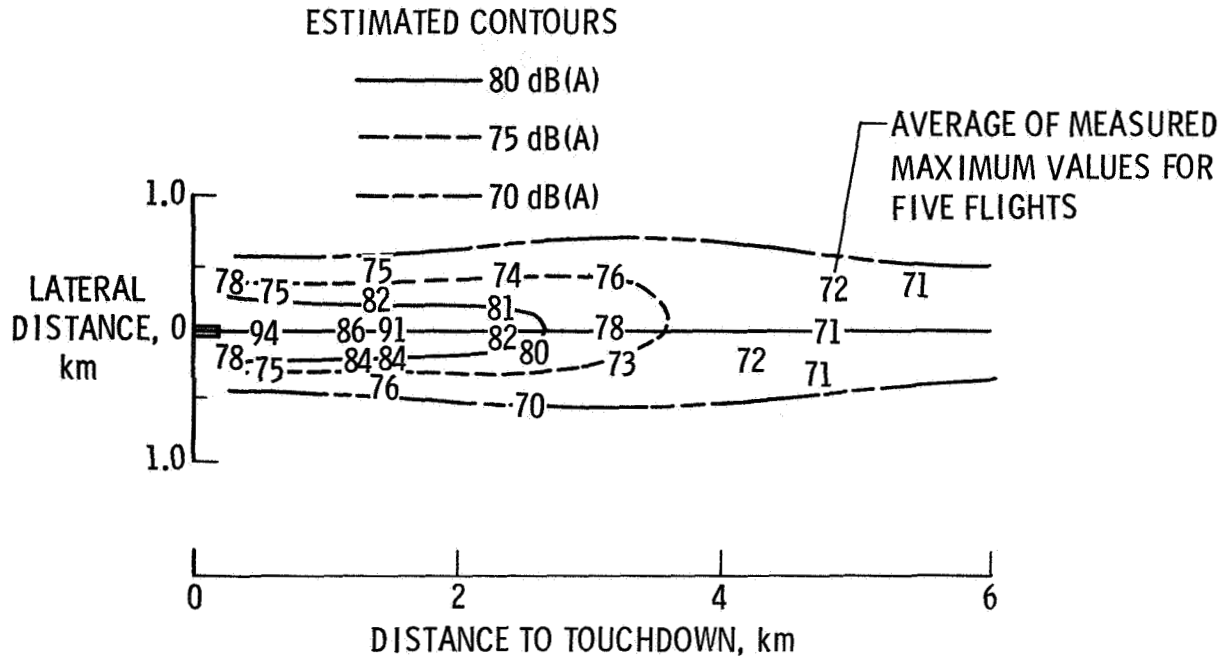
ESTIMATED CONTOURS

——————— 80 dB(A)

– – – – – 75 dB(A)

– – – – 70 dB(A)

AVERAGE OF MEASURED
MAXIMUM VALUES FOR
FIVE FLIGHTS

1.0

LATERAL
DISTANCE, 0
km

1.0

0   2   4   6
DISTANCE TO TOUCHDOWN, km

Figure 10.- Ground noise contours from five flights utilizing
six-degree approach over ROMAAR.

FLIGHT DIRECTION

| 60 | 60 | 61 | 62 | 63 | 63 | 65 | 67 | 65 | 64 | 64 | 62 | 60 | 60 | 60 |

| 62 | 62 | 63 | 64 | 65 | 66 | 67 | 66 | 67 | 66 | 66 | 64 | 62 | 61 | 61 |

| 63 | 63 | 65 | 66 | 69 | 71 | 71 | 71 | 68 | 65 | 64 | 63 | 63 |

| 65 | 65 | 67 | 68 | 72 | 77 | 77 | 77 | 72 | 67 | 67 | 66 | 65 |

| – 65 | – 66 | – 67 | – 69 | 72 | 78 | 82 | – 83 | – 82 | 78 | 73 | 69 | – 68 | – 66 | – 65 |

| 65 | 65 | 67 | 71 | 77 | 77 | 77 | 71 | 67 | 65 | 65 |

| 64 | 64 | 65 | 68 | 68 | 71 | 71 | 70 | 68 | 68 | 66 | 64 | 64 |

| 62 | 64 | 66 | 66 | 65 | 64 | 66 | 68 | 66 | 65 | 65 | 66 | 64 | 64 | 62 |

| 61 | 62 | 62 | 64 | 62 | 61 | 64 | 67 | 64 | 62 | 62 | 64 | 63 | 62 | 61 |

ESTIMATED NOISE
PATTERNS

——●—— 80 dB(A)

– –■– – 75 dB(A)

–·▲·– 70 dB(A)

"FROZEN" POSITION OF HELICOPTER

RUNWAY ₵

70 dB(A) GROUND
INTERSECTION POINTS

← 1 km →

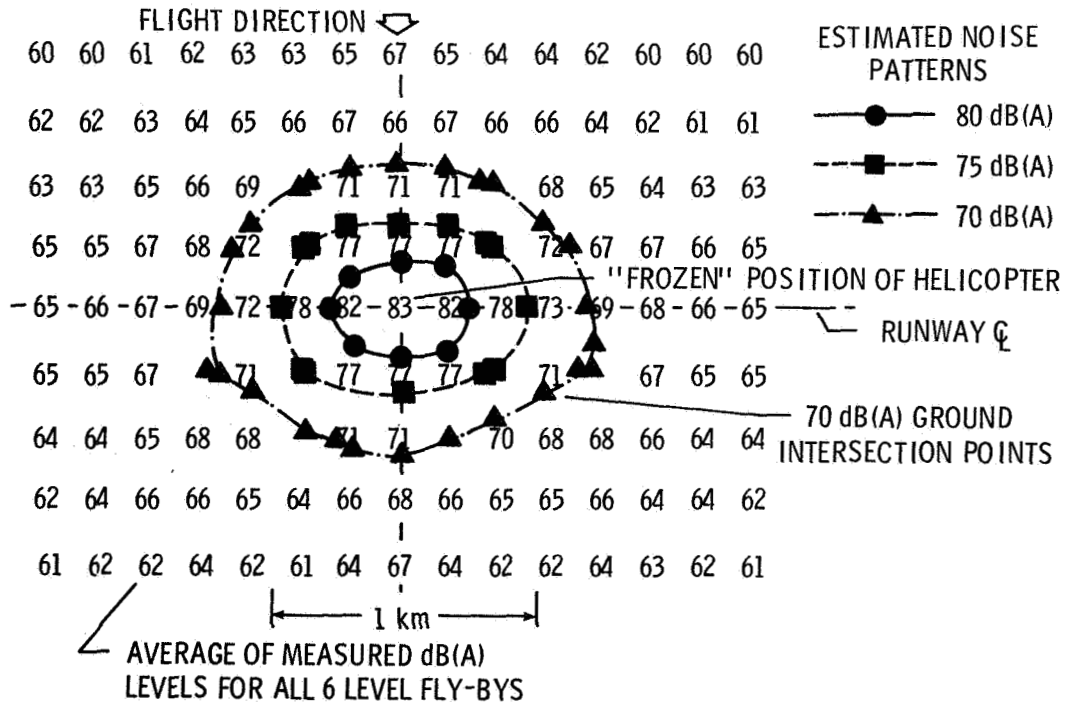AVERAGE OF MEASURED dB(A)
LEVELS FOR ALL 6 LEVEL FLY-BYS

Figure 11.- Ground noise directivity patterns for six level flybys over
linear array at 152-m altitude and 49-m/sec airspeed.
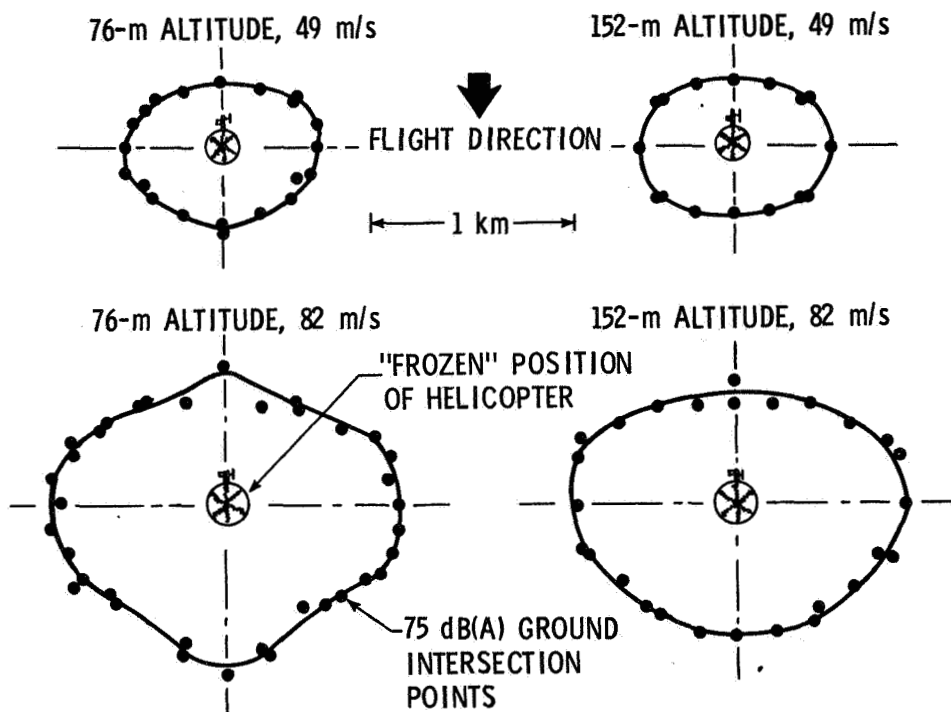
532

Figure 12.– Variations in 75-dB(A) noise directivity patterns over linear array for altitudes of 76 and 152 m and airspeeds of 49 and 82 m/sec.

A STATIC ACOUSTIC SIGNATURE SYSTEM FOR

THE ANALYSIS OF DYNAMIC FLIGHT INFORMATION

DANIEL J. RAMER
U.S. ARMY ARMAMENT RESEARCH AND DEVELOPMENT COMMAND

SUMMARY

The Army family of helicopters was analyzed to measure the polar octave band acoustic signature in various modes of flight. A static array of calibrated microphones was used to simultaneously acquire the signature and differential times required to mathematically position the aircraft in space. The signature was then reconstructed, mathematically normalized to a fixed radius around the aircraft.

INTRODUCTION

A number of years ago, this organization was asked to measure the polar octave band output of each of the Army family of helicopters in various modes of flight. The intent was to, first, model the perception, based on this signature study, of an unsophisticated enemy force who would be expected to fire on friendly aircraft with small arms and, second, predict and minimize attrition based on flight tactics. Since each aircraft was to be traveling at some considerable velocity during data acqusition, some means of measuring the output through 360 degrees had to be devised. Emplacing a circular array of microphones was rejected as was towing a microphone behind a lead aircraft. It was decided to combine this organization's sound ranging techniques with signature analysis to mathematically construct the desired family of polar signatures.

This paper, then, will describe the application of a measurement technique normally restricted to transient phenomena to that signature task.

c   velocity of sound

L   distance between any two adjacent microphones

n_1 differential propagation distance between first and second excited microphones

n_2 differential propagation distance between first and third excited microphones

R   radial distance between origin microphone and sound source

V_s velocity of propagation

V_w vector average of wind velocity during sound propagation

x   one cartesian distance between origin microphone and sound source

y   remaining cartesian distance between origin microphone and sound source

δ propagation medium shift

Δt_{12} differential time between first and second excited microphones

Δt_{13} differential time between first and third excited microphones

THE THEORY AND APPLICATION OF SOUND RANGING

Sound ranging is a technique which can be used to accurately determine the location of an impulsive sound source in three-dimensional space. This technique was developed to measure munition performance in jungle canopy where radar and optical techniques are impractical.

To implement sound ranging data acquisition, a geometric array of microphones is emplaced in a surveyed position at a target site. The shape of the array was determined by error analysis of various mathematical models.

A typical array consists of from 3 to 6 microphones, although any number greater than three could be used. Sound emanating from the source propagates through the air at a relatively constant velocity, and the wave-front arrives at each microphone at a specific time after the sound has occurred. The differences in arrival time among the various microphones are accurately determined. Equations, derived from the Euclidean geometry, the velocity of sound, and the differential times between the microphones, will yield the position coordinates of the sound source.

A typical two-dimensional sound ranging transducer array is shown in figure 1. For this transducer system, the mathematical solution can be obtained from the geometry as follows:

$$R^2 = x^2 + y^2 \tag{1}$$

$$(R + n_1)^2 = x^2 + (L - y)^2 \tag{2}$$

$$(R + n_2)^2 = x^2 + (2L - y)^2 \tag{3}$$

expanding (2) and (3) and substituting (1) for x,

$$R^2 + 2Rn_1 + n_1^2 = R^2 - y^2 + L^2 - 2Ly + y^2 \tag{4}$$

$$R^2 + 2Rn_2 + n_2^2 = R^2 - y^2 + 4L^2 + y^2 - 4Ly \tag{5}$$

which reduces to

$$2Rn_1 + n_1^2 = L^2 - 2Ly \tag{6}$$

$$2Rn_2 + n_2^2 = 4L^2 - 4Ly \tag{7}$$

solving for R from (6)

$$R = \frac{(L^2 - 2Ly - n_1^2)}{2n_1} \tag{8}$$

substituting in (7)

$$\frac{2 (L^2 - 2Ly - n_1^2)}{2n_1} n_2 + n_2^2 = 4L^2 - 4Ly$$

solving for y

$$y = \frac{L^2 (4n_1 - n_2) (n_1 n_2) + (n_1 n_2)}{2L (2n_1 - n_2)} \tag{9}$$

Substituting this value of y in (8) yields R and substituting R and y in (1) yields x.

A second array, either parallel or perpendicular to the first, yields a second set of coordinates which are combined with the first set to derive the third dimensional distance, z.

There are significant sources of error with this approach, however. Signal-to-noise and resolution errors can be a problem but, since these are related to the nature of the specific acoustic signature produced by the test item, for the purposes of this paper will not be discussed. That leaves the assumption that the velocity of sound is constant, which of course, it is not. Wind and wind gradients and, to a lesser extent, temperature gradients will all distort the velocity of propagation. Wind, more properly, represents the migration of the total medium during propagation, but for the purposes of error analysis can be considered a propagation velocity shift (figure 2).

In figures 3 and 4, the errors in x and y induced by a 1% error in the velocity of propagation are shown. After a first glance, there is a tendency to structure the test to place the microphones at several times the microphone array dimension from the test item to minimize this type of error; however, in reality, the larger this distance, the more appreciable velocity gradients will become. Thus the trade-off must be made between improved accuracy in constant wind velocity, against reduced accuracy caused by topographically induced wind gradients.

An error correcting scheme for wind has been devised; computer modeling indicates accuracy improvements of up to an order of magnitude result. Briefly, this technique involves the storage of total vector anemometer history, the computation of position coordinates based on a constant propagation velocity, the reconstruction of propagation velocity based on wind data over the computed distance, the recomputation of coordinates based on the new velocity of sound, and the reconstruction and recomputation repeated until the result is converged upon. The tolerance between successive recomputations determines the exit from the algorithm.

The hardware necessary to execute this technique include total vector anemometers, microphones, line drivers, transient recorders, time code generator and digital processor (figure 5). This system is designed to store data and compute the coordinates of a transient forcing function. The techniques, however, are applicable to repetitive transient producing vehicles, such as helicopters.

APPLYING SOUND RANGING TO HELICOPTERS

Having been given the task of measuring the polar signature around an aircraft in flight, it was decided to fly the aircraft by a sound ranging array of calibrated microphones to simultaneously acquire the signature and position information. A magnetic tape medium was selected since the Real-Time Sound Ranging System was incapable of keeping up with the data rates. A data processing scheme was devised to compute the position of the aircraft in polar coordinates, measure the rms amplitude of each octave band, correct those amplitudes for spreading loss and absorption, and finally, list the polar distributions of octave band energy.

538

Clearly, this methodology depended on the ability to distinguish a long wavelength repetitive phenomenon in the acoustic signature of each aircraft to utilize sound ranging; and, conveniently, the helicopter blade slap provided just such a waveform. A Huey Cobra, for example, will typically produce a blade slap rate of 14Hz, a Huey approximately 12Hz. Thus, with fundamental wavelengths in excess of 23 meters, a substantially sized microphone array could be surveyed in place. This permitted acceptable accuracies over the distances required to measure the aircraft signatures at low angles of incidence. Further, those long wavelengths avoided the necessity of keeping track of multiple cycles when the wavelength is exceeded by the inter-microphone distances.

This data acquisition and reduction task was greatly simplified by the funding organization's request to operate in still air, for in addition to the instrumentation, accompanying personnel took part in simultaneous threshold perception tests.

Figure 6 illustrates the reduction hardware. To accurately range the aircraft during data reduction, it was necessary to insure differential time measurements between the same point on each succeeding cycle of acoustic signature. Thus, phase lock loops were utilized to lock onto the fundamental blade slap frequency transduced by each microphone. Each channel from the magnetic tape recorder drove a phase lock loop; the lock range was adjusted to a reasonable range around the fundamental blade slap frequency for each aircraft and the loop time constant made long, approximately 1 sec, to "flywheel" over dropouts caused by topographical multipath, the tape medium or air turbulence. The square wave output of each phase lock loop was differentiated to yield a pulse of 100 µsec in width which, in turn, drove both the stop and start enable ports of each counter and the first-in start logic.

The first-in start logic generated a start pulse for each counter only when it received a pulse from the first arrival microphone circuitry. It then counted the remaining microphone outputs and started over again; since this circuit produced a 50 µsec wide pulse, the counter associated with the first excited microphone always read zero. The start logic also contained sequencing logic that would permit the selection of the identity of the first excited microphone (this was predictable since the aircraft flew a prescribed path); this avoided getting locked into an improper data acquisition sequence.

Thus, at the end of one multimicrophone cycle, each counter would be stopped at some time with respect to the first counter stimulated. The busy bit was generated when any counter was counting. The transition to busy cued the Analog-to-Digital Converter to converge and the transition to not busy cued the computer to first, accept the data from the counters and, second, test end-of-conversion until the digitization was ready for transfer.

539

The computer sampled the data asynchronously, buffering sufficient data to reform the polar signatures. The computer terminal was used to periodically enter the aircraft type, flight mode and temperature (to calculate the velocity of sound). The program did the rest, listing the results on the line printer as per the funder's preference.

CONCLUSION

Figure 7 illustrates the format of the data as reported and figure 8, the graphical representation. It was found that this technique worked extremely well on a variety of aircraft whether the blade slap was particularly audible or not. To date, it isn't clear whether a wind correcting algorithm will be possible for this technique but one will be persued with the interest of a funding organization. It was found, however, that in relatively still air, this signature technique is both cost effective and timely.

$$n_1 = c\Delta t_{12}$$
$$n_2 = c\Delta t_{13}$$

WHERE $c \equiv$ VELOCITY OF SOUND

$$R^2 = x^2 + y^2$$
$$(R+n_1)^2 = x^2 + (L-y)^2$$
$$(R+n_2)^2 = x^2 + (2L-y)^2$$
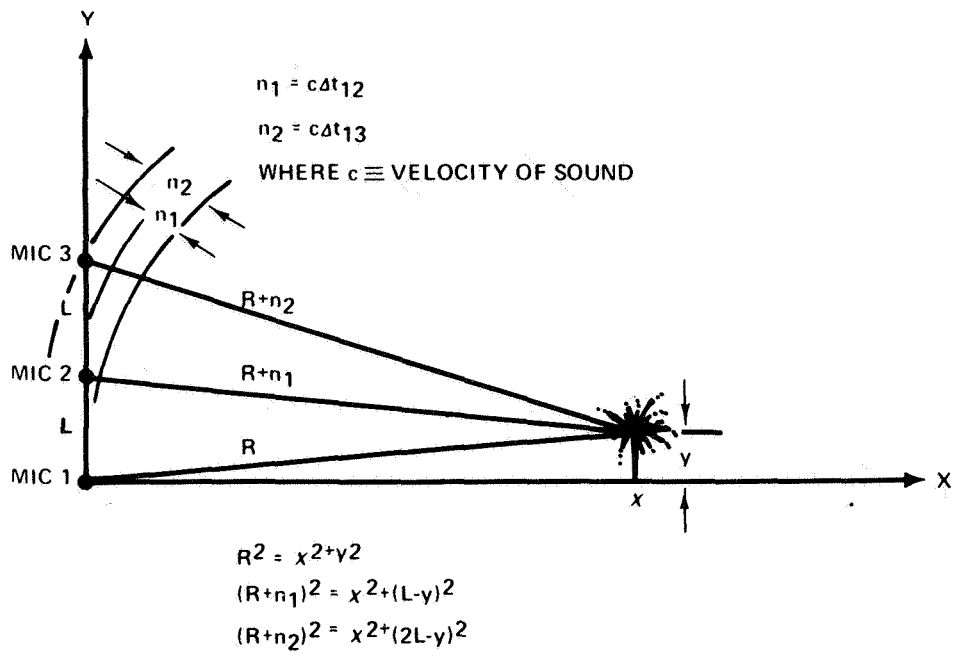
Figure 1.- 3 microphone vertical array.

$$T_{PROPAGATION} = R_{MEASURED}/V_S$$
$$\zeta = (V_w)(T_{PROPAGATION})$$
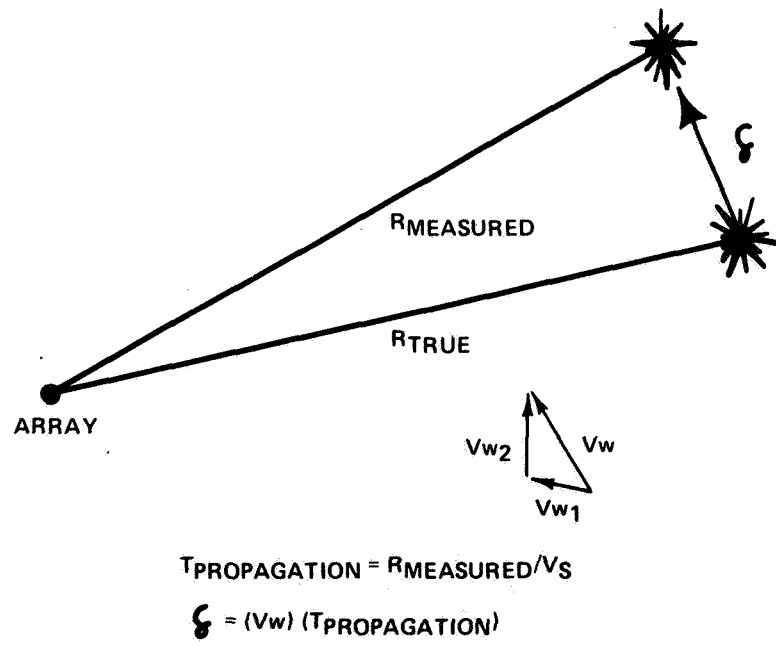
Figure 2.- Plan view of 3 microphone array in wind.
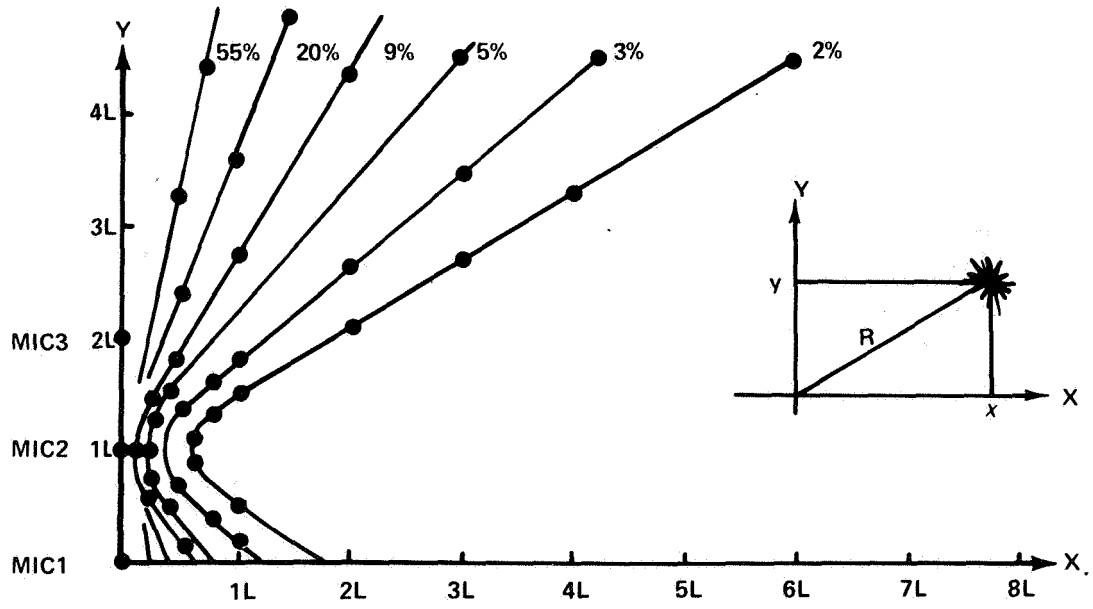
Figure 3.- Error in x caused by 1% error in V_s.
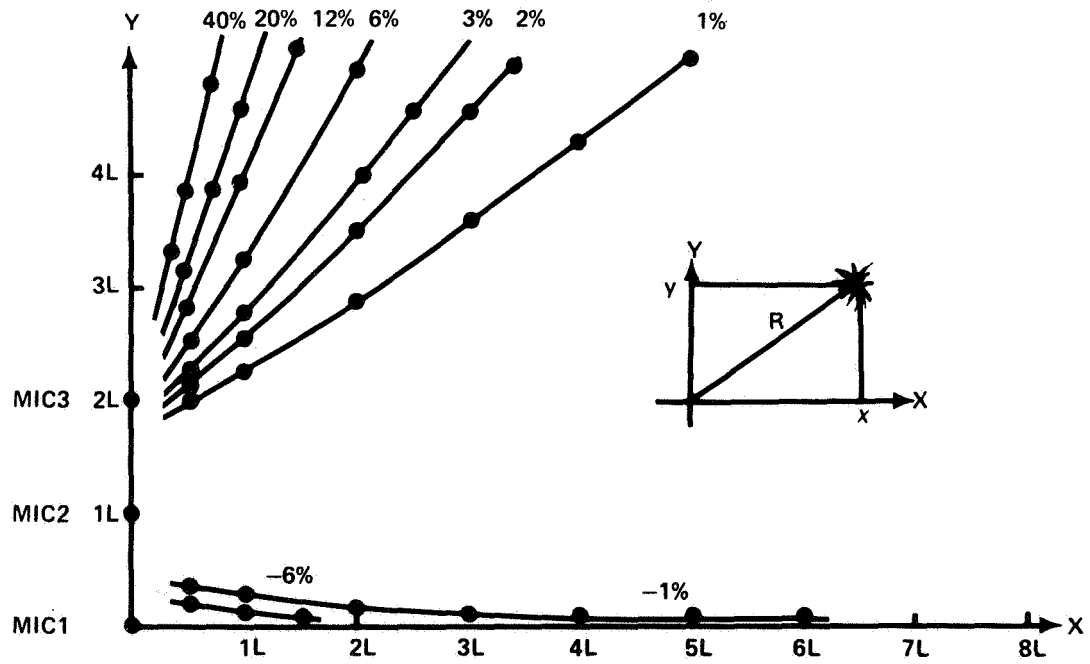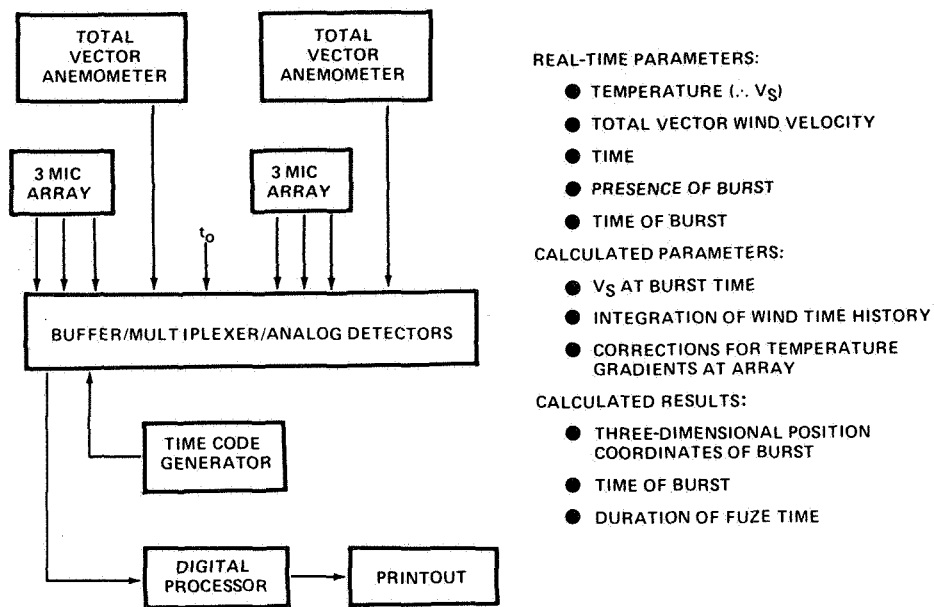

Figure 4.- Error in y caused by 1% error in V_s.

542

REAL-TIME PARAMETERS:
- TEMPERATURE $(\therefore V_S)$
- TOTAL VECTOR WIND VELOCITY
- TIME
- PRESENCE OF BURST
- TIME OF BURST

CALCULATED PARAMETERS:
- V_S AT BURST TIME
- INTEGRATION OF WIND TIME HISTORY
- CORRECTIONS FOR TEMPERATURE GRADIENTS AT ARRAY

CALCULATED RESULTS:
- THREE-DIMENSIONAL POSITION COORDINATES OF BURST
- TIME OF BURST
- DURATION OF FUZE TIME

Figure 5.- Real-time sound ranging block diagram.
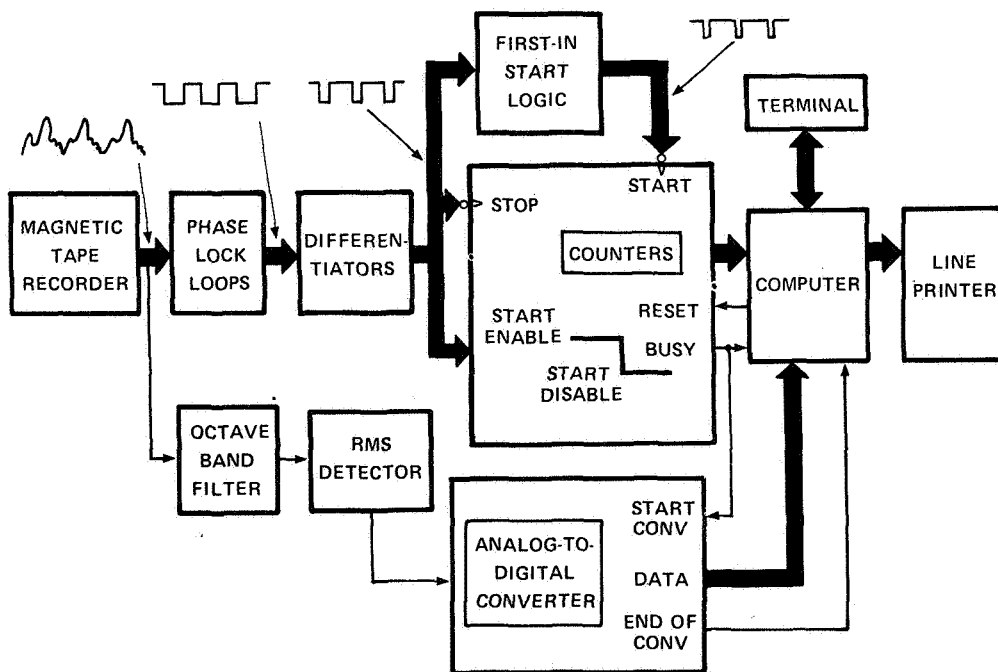
Figure 6.- Data processing system block diagram.

| AMBIENT NOISE LEVEL	53.80 dB		RUN NUMBER 1	
THETA	SPLC	SPI.R	SPLATT	SPLU
14.84	81.37	20.86	0.0	£0.51
20.08	78.28	18.32	0.0	59.97
25.32	79.01	16.41	0.0	62.60
30.38	75.97	14.95	0.0	61.01
39.60	74.72	12.94	0.0	61.77
45.73	77.68	11.93	0.0	65.75
50.12	78.95	11.93	0.0	67.62
59.74	81.54	10.30	0.0	71.24
63.95	79.51	9.96	0.0	69.55
68.37	84.13	9.66	0.0	74.47
75.93	84.10	9.29	0.0	74.81
79.38	85.07	9.18	0.0	75.89
84.94	87.45	9.06	0.0	78.38
90.00	89.40	9.03	0.0	80.37
95.06	88.02	9.06	0.0	78.96
100.62	88.63	9.18	0.0	79.45
104.07	88.04	9.29	0.0	78.74
111.63	87.49	9.66	0.0	77.83
116.05	87.49	9.96	0.0	77.53
120.26	85.28	10.30	0.0	74.98
129.88	83.48	11.33	0.0	72.51
134.27	83.13	11.93	0.0	71.20
140.40	81.69	12.94	0.0	68.75
149.62	78.02	14.95	0.0	63.06
154.68	75.28	16.41	0.0	58.87
159.92	71.41	18.32	0.0	53.09
165.16	72.63	20.86	0.0	51.77

Figure 7.- Typical computer printout.
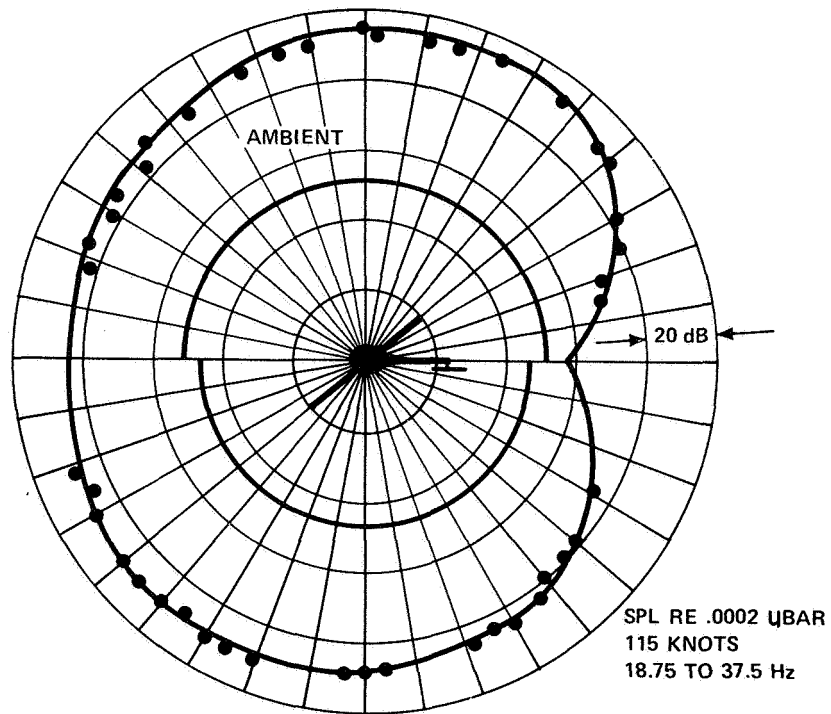
Figure 8.- Typical polar plot.

AN ACTIVE NOISE REDUCTION SYSTEM FOR AIRCREW HELMETS

Peter D. Wheeler and David Rawlinson
Wolfson Unit for Noise and Vibration Control, I.S.V.R.
Southampton University

Stephen F. Pelc and Tony P. Dorey
Department of Electronics, Southampton University

INTRODUCTION

In a high noise environment conventional ear-defenders may be incapable of providing sufficient noise attenuation. An active noise reduction system (ANR) has been developed for use in aircrew flying helmets (ref. 1) in which the acoustic noise field inside the ear defender is detected using a miniature microphone and an antiphase signal is fed back to a communications telephone within the ear defender. The feed-back loop also affects the communications signal which has to be compensated outside the loop in order to retain the original transfer function from telephone amplifier to listeners ear.

The concept was not new at the outset of the work reported. In 1953 Olsen and May (ref. 2) investigated the possibility of creating a noiseless zone in free field conditions, but the technique had not apparently been successfully applied to headsets. However, the Procurement Executive, Ministry of Defence had outlined a method which proved the basis of this present work.

The major engineering development involved in integrating the technique into a conventional aircrew flying helmet was associated with the identification and characterisation of suitable microphones and telephones. At the time of previous publication (ref. 1) the feasibility of active reduction had been demonstrated though tests with random noise had not been undertaken. Some instability problems still existed and the performance with a communications signal had not been assessed.

During the last two years the remaining engineering problems have been overcome and an extensive program of laboratory subjective trials has been completed. In-flight trials of the system are currently underway. Throughout this programme of work there has been active participation by the Royal Aircraft Establishment, Farnborough, and the development has been carried out with the support of the Procurement Executive, Ministry of Defence, U.K.

PRINCIPLES

One channel of the complete system is shown schematically in Figure 1. The design is based upon the existing ear defender shell and seal, and incorporates a high-fidelity type moving-coil telephone and a miniature electret microphone.

A complete analysis of the system shows that the pressure at the ear (P_e) is comprised of two components due to the signal (S_v) and the external noise field without ANR (n_p).

$$P_e = \left[\frac{AT_1}{1 + ABKT_1T_2}\right] S_v + \left[\frac{1}{1 + ABKT_1T_2}\right] n_p \tag{1}$$

where A, B, K, T_1 and T_2 are the transfer functions of the amplifier, feedback loop, acoustic cavity, telephone and microphone, respectively.

It is apparent that the amplification of the two components is different and that if the signal S_v is pre-emphasised, to compensate for its attenuation by the feedback loop, and returned to its original level then an improvement of a factor $(1 + ABKT_1T_2)$ can be achieved.

The product of the terms KT_1T_2 is of fundamental significance as it represents the overall electrical transfer function of the telephone – cavity – microphone system. To provide ANR, the product AB would ideally have a complementary variation with frequency. In practice the frequency response must be tailored to ensure that when the loop gain approaches unity the total loop phase shift does not approach $180°$.

The systems ability to match this transfer function KT_1T_2 will determine the degree of noise reduction which is obtained.

EVALUATION

The ANR system has been comprehensively tested in a series of laboratory trials, prior to flight trials by the Royal Aircraft Establishment.

Two basic methods of measuring ANR have been used throughout the project. These are:

a) An electronic computation method

b) An external broadband noise method

The computer method used a single frequency excitation which was analysed by means of an analogue computer circuit that calculated the value of $1 + ABKT_1T_2$ and continuously plotted its amplitude and phase as a function of frequency.

In the second method, preferred because of its close approximation to the real life situation, subjects wearing the ANR modified flying helmet were

exposed to an external noise field similar to that experienced by pilots in a high performance strike aircraft. Comparisons of attenuation and speech intelligibility scores, with and without the ANR system in operation, were made, and the modified helmet's attenuation was also checked against a standard flying helmet.

Objective measurements of helmet attenuation were made using miniature microphones placed at the subject's pinnae, and outside the helmet.

These two methods of measurement were carefully compared in a structured series of eight experiments to check that the more convenient laboratory computational method gave the same results as the noise excited experiment.

The intelligibility testing was carried out using anglicised modified Rhyme Test material comprising four sets of fifty initial or final consonant words plus twenty five central vowel words. The subject was required to score his reception of a word by marking a score sheet showing all six rhyming alternatives for a given word and, at the end of the experiment, the sheets were marked by the experimenter. For each condition - ANR on or off - two of the four word lists available were presented and the number of subjects was chosen to give a fully balanced experiment with a satisfactory level of statistical significance. The speech signal presented to the ear was matched, for all the helmet configurations tested, to within ± 1 dB(A) overall and ± 1 dB in each ⅓ octave band.

Eighteen subjects were tested twice in each configuration and the mean improvement in attenuation was found to be 12 dB(A) for the noise field used (Figure 2).

Figure 3 shows the ANR performance as a function of frequency, together with a measure of the scatter of results. The comparison between mean helmet attenuation values is shown in Figure 4.

The mean improvement in speech intelligibility with the ANR system in operation was 21% relative to a baseline of 51% when the system was switched off. The individual performances of subjects are shown in Figure 5.

All those tested commented upon the increased comfort provided by the higher attenuation of the ANR system, particularly at lower audio frequencies, where the aircraft's noise energy is concentrated.

CONCLUSIONS

The use of active noise reduction in a laboratory trial simulating flight conditions has been shown to give encouraging objective and subjective results. The system is capable of application to a wide range of situations where high attenuation (with or without voice communications) against low frequency noise is required. The response of the ANR system may be engineered, to an extent, to optimise attenuation for particular noise fields, such as are experienced in rotary wing and fixed wing aircraft, and for certain applications, the system may be fitted into a small, battery operated, electronics package which may be easily worn on the person.

REFERENCES

1. Dorey, A.P., Pelc, S.F., and Watson, P.R. 1975, "An Active Noise Reduction System for use with Ear Defenders". 8th International Aerospace Symposium, Cranfield, 24-27.

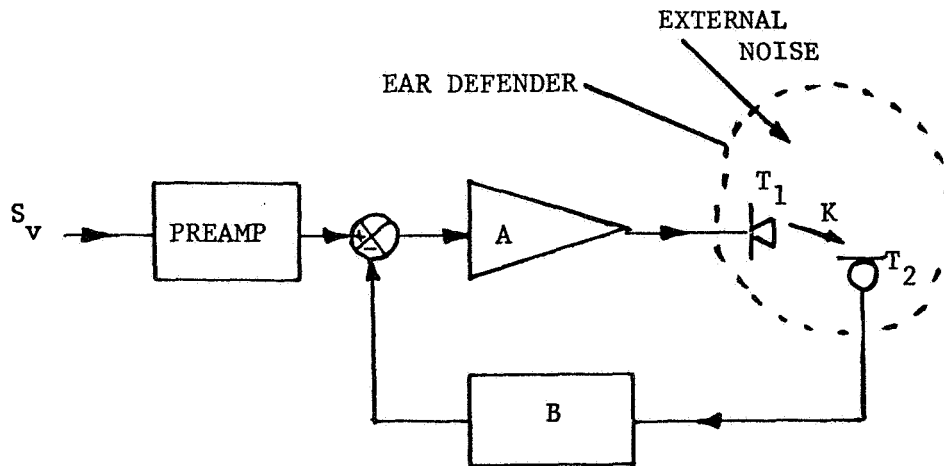2. Olsen, H.F., and May, E.G. 1953, J.A.S.A. 25 , No.6.
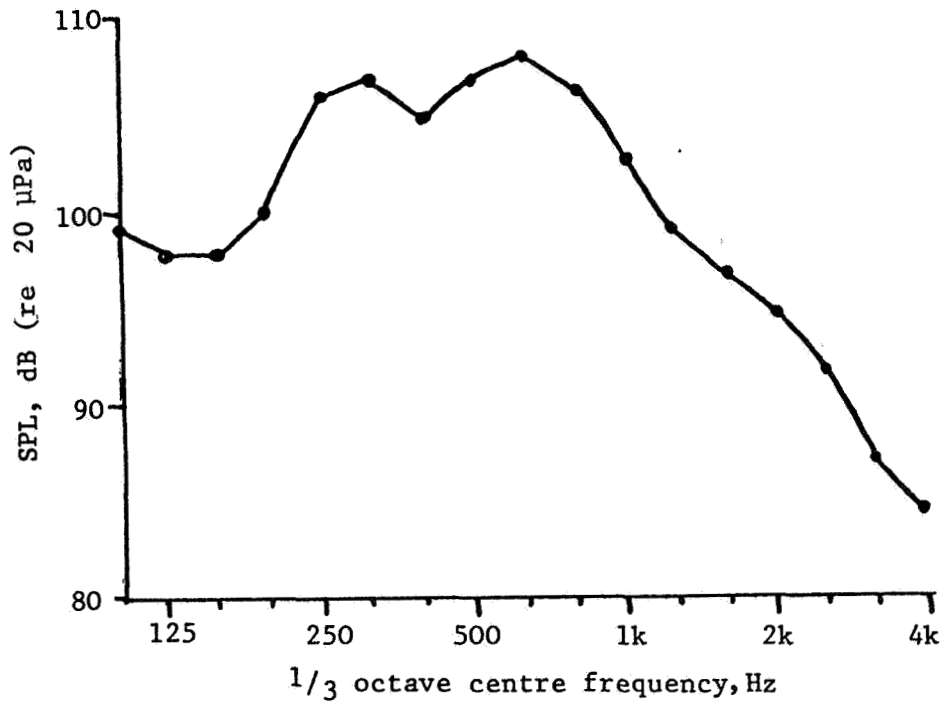

Figure 1.- A system block diagram.
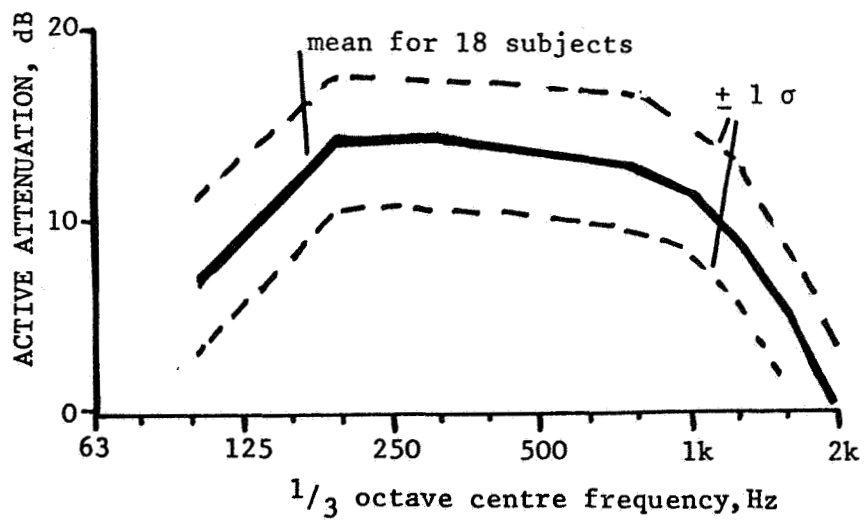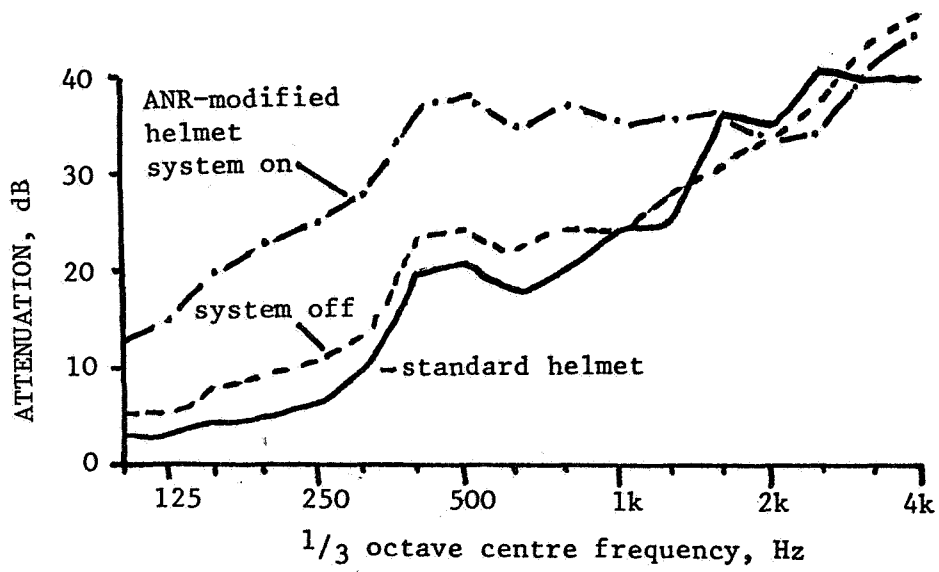
Figure 2.- Simulated aircraft cockpit noise.

Figure 3.- ANR performance.

Figure 4.- Mean helmet attenuation.
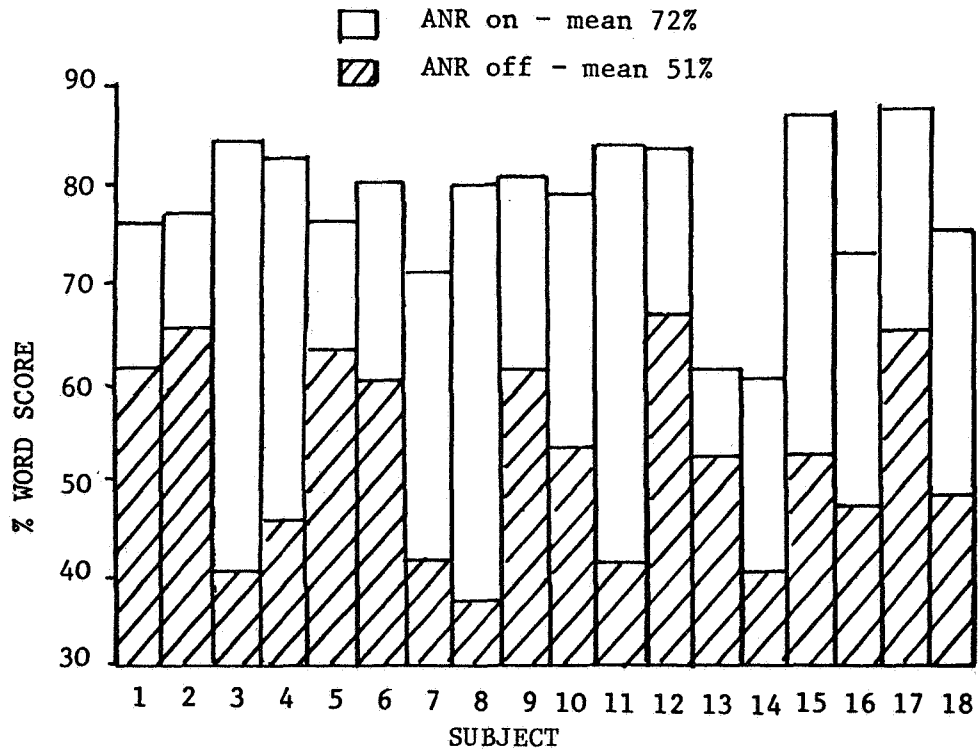
Figure 5.- Word scores for 18 subjects.

DESIGN OF HELICOPTER ROTORS TO NOISE CONSTRAINTS

Edward G. Schaeffer and Harry Sternfeld, Jr.
Boeing Vertol Company

SUMMARY

Results from the initial phase of a research contract, "Study of Design Constraints on Helicopter Noise," NAS1-15226, sponsored by the NASA Langley Research Center are presented. A description of the overall program is included. Basic calculations of nonimpulsive rotor harmonic and broadband hover noise spectra, over a wide range of rotor design variables were accomplished; and the sensitivity of PNL to changes in rotor design parameters are presented. Measured rotor noise data were used to correlate the calculations in verifying the prediction methodology.

INTRODUCTION

Increased emphasis on reducing the noise generated by helicopter rotors to minimize aural detection times in military applications, and increase community acceptance during commercial operations, now require the helicopter manufacturer to consider noise constraints of his product early in the design phase. Impending noise regulations, such as the FAA/ICAO possible noise limits for certification of helicopters, are forcing designers to implement noise control measures during preliminary design performance studies when the sizing of rotors is being determined.

Basic rotor design parameters such as total thrust, blade tip speed, disk loading, number of blades per rotor, and rotor solidity, which invariably affect the noise produced by the rotor, have generally been decided long before noise restrictions are considered. One reason is that most preliminary designers do not have simplified guidelines for predicting rotor noise which can be meaningful during early rotor design decisions stages. Consequently, most designs are semi-finalized, before noise estimates of the configuration can be made. Subsequent changes that may be required in reducing the noise to comply with certain regulations find themselves in conflict with designs that have already been set.

This study, when completed, will result in a general method, and sets of design charts, which will permit evaluations of the noise and performance tradeoffs of single rotors during the early design stage. The measure of performance will be the percentage of available rotor thrust which must be expended in lifting the drive system (rotor blades, hub, and rotor transmission).

Given a desired thrust and noise limit, the charts can be used to define the corresponding radius, chord, and tip speed for 2, 3, 4, 5 or 6 bladed rotors. The rotor which requires the lowest drive system weight is the optimum design. Conversely, given a completely defined rotor the charts can be used to predict the noise.

Results from the completed initial phase of the study, which includes the calculation of both rotor harmonic and broadband, nonimpulsive hover noise and the relative importance of various rotor design parameters that influence changes in Perceived Noise Level (PNL) are discussed in this paper.

SYMBOLS AND ABBREVIATIONS

Values are given in both SI and U.S. Customary Units. The calculations were made in U.S. Customary Units.

T	thrust, N (lb)
V_T	blade tip speed, m/sec (ft/sec)
f_p	peak frequency, Hz
A_b	blade area, m^2 (ft^2)
σ	angle between centerline of rotor shaft and line to observer, deg
S_j	one-third octave frequency band correction
C_L	lift coefficient
r	distance to observer, m (ft)
SPL	Sound Pressure Level, dB (re 2 x 10^{-5} N/m^2)
PNL	Perceived Noise Level, in PNdB
dBA	A-weighted network
dBC	C-weighted network
BB	Broadband noise
PNLT	Tone-corrected Perceived Noise Level
NOY	Unit used in the calculation of Perceived Noise Level. It is the noisiness of a noise for which the Perceived Noise Level is 40 PNdB. The noisiness of a noise that is judged by a subject to be n times that of a 1-NOY noise is n NOYS.

he objective of the program is to provide a "handbook" for helicopter designers
nd configuration managers to evaluate the noise of rotors during the prelim-
nary design phase, and to estimate the effect on rotor payload.

n order to produce an effective designer's tool that can be used during noise
nd performance tradeoff evaluations, the total rotor noise signature has to
e represented accurately. All major sources of rotor noise are included in
eveloping the design charts for the handbook. Figure 1 shows an example of
hese sources and their contribution to the overall noise signature. The sub-
ective weighting of these noise sources; harmonic, broadband (nonharmonic),
nd impulsive, which is the prelude to determining the PNL, are shown in
igure 2 as total NOY values per octave band. The engine noise minor contri-
ution is shown for completeness only. Examination of this figure indicates
hat in terms of annoyance, rotor impulse is the major factor; but if the
otor did not have an impulsive characteristic then broadband noise predomi-
ates the Perceived Noise Level (Figure 2) to a much greater extent than the
ound Pressure Level Spectrum (Figure 1).

he overall study consists of the following phases:

1. Calculating the nonimpulsive rotor harmonic and broadband noise spectra
    using established prediction procedures recognized and used by industry
    and found in open literature. The range of rotor physical parameters
    included in the calculations are: thrust, 44 to 356 kN (10 000 to
    80 000 lb); disk loading, 287 to 575 N/m^2 (6 to 12 lb/ft^2); solidity,
    0.04 to 0.12; number of blades, 2 to 6; and tip speed, 152 to 244 m/sec
    (500 to 800 ft/sec). Calculations are for a sideline distance of
    150 meters from rotor and a height of 150 meters (which corresponds to
    the measurement locations being considered in the regulations). Com-
    bining the noise signatures into one-third octave frequency bands
    calculating PNL, dBA and dBC.

2. Applying impulsive corrections developed by the Boeing Vertol Co. and
    subjective adjustments from Reference 1 to adjust dBA, dBC and PNL values
    to a subjectively equivalent broadband level.

3. Preparing a set of design charts to permit direct determination of values
    of dBA, dBC and PNdB for range of rotor physical parameters. An example
    of a possible design chart format is shown in Figure 3 for determining the
    PNdB in hover and, providing a rationale showing the effects of rotor
    configuration on forward flight noise.

4. Evaluating the performance penalty for each main rotor configuration and
    tip speed combination. The ratio of drive system weight to rotor thrust
    shall be used as an index of the design efficiency.

RESULTS AND DISCUSSION

Prediction of Nonimpulsive Rotor Hover Noise

The harmonic rotation noise calculation was based on the method developed in Reference 2. This widely accepted rotor noise calculation includes the design variables of thrust, disk loading, tip speed, and number of rotor blades. The only change made to the equations of Reference 1 was that an airloads harmonic decay exponent of 1.3 was used instead of 2.0, as specified by the original authors. This modification reflects a more realistic airload harmonic decay of 15 dB per octave which has been measured by other researchers and provides better agreement with measured data in the higher harmonic range.

The broadband, or nonharmonic, rotor noise calculation used was from the unpublished semiempirical prediction made by Robert J. Pegg of the NASA Langley Research Center. The equation from this prediction,

$$f_p = -240 \log T + .746 \, V_T + 786$$

$$SPL = 10 \log A_b + 60 \log V_T + 10 \log (\cos^2 \sigma + .1)$$
$$+ S_j - 20 \log r + f(C_L) - 53.29$$

$$f(C_L) = 10 \log \frac{\overline{CL}}{.4} \quad \text{for } \overline{CL} \leq .48$$

$$f(C_L) = .9 + 80 \log \frac{\overline{CL}}{.48} \quad \text{for } \overline{CL} \geq .48$$

has as its design variables, thrust (T), tip speed (V_T), blade area (A_b) and lift coefficient (C_L).

A computer program was written to include all of the design variables and to provide an automatic calculation of both the harmonic and broadband noise, then combine them into one-third octave frequency bands and print-out the resultant dBA, dBC and PNL. Figure 4 shows a sample of this output. Nine hundred sixty computer cases were run during the initial phase of the program to provide adequate definition of the design variables for preparation of the "handbook" charts.

Prediction-Data Correlation

Measured noise data, shown in Figures 5 and 6, from a nonimpulsive and moderately impulsive rotor were directly compared to the calculated one-third octave SPL using the developed computer program. The agreement between predictions and measurement for the nonimpulsive case (fig. 5) are generally quite good, the discrepancy in the 500 Hz octave band is probably due to destructive interference between the direct and first ground reflected waves which calculates to occur at 556 Hz. In the case of the impulsive rotor (fig. 6) good agreement is attained in the first two harmonics and higher frequency broadband noise since the harmonic noise prediction method does not account for the increase in mid-harmonic loading which typifies impulsive rotor noise.

554

Perceived Noise Level Sensitivity to Rotor Design

To provide an indication of the sensitivity of PNL to changes in design variations, five baseline rotor designs representing different classes of helicopters were investigated. For each baseline configuration the rotor parameters of thrust, disc loading, tip speed and number of blades were varied one at a time (at constant lift coefficient) and the resultant PNdB calculated.

Figure 7 shows an example of the calculated nonimpulsive hover SPL for one particular case (3-bladed, 89-kN (20 000-lb) thrust rotor). Taking this configuration as a baseline design and varying each of the parameters one at a time results in the PNL sensitivity chart shown in figure 8. Similar studies have been done for four other baseline designs which cover a wide range of values and the resultant summary (table I) indicates some rough guidelines which can be used pending release of the final design charts which will result from this study.

CONCLUDING REMARKS

The calculation of the nonimpulsive harmonic and broadband hover noise for a wide range of rotor design variations was accomplished. The prediction methodology used correlated well with measured whirl tower data. Application of the predictions to variations in rotor design (thrust, tip speed, disc loading, and number of blades per rotor) has shown tip speed and thrust as having the most effect on changing the PNL.

REFERENCES

1. Sternfeld, Harry, Jr.; and Doyle, Linda Bukowski: Evaluation of the Annoyance Due to Helicopeter Rotor Noise. NASA CR-3001, 1978.

2. Lowson, M.V.; and Ollerhead, J.B.: Studies of Helicopter Rotor Noise. USAAVLABS Tech. Rep. 68-60, U.S. Army, Jan. 1969.

TABLE I.- INTERIM RESULTS SUMMARY OF SENSITIVITY OF PNL TO DESIGN PARAMETER VARIATION

Parameter	Range	Sensitivity*
Tip speed	137 to 290 m/sec (450 to 950 ft/sec)	2 to 5 PNdB per 30.5 m/sec (100 ft/sec)
Thrust	11 121 to 358 876 N (2 500 to 80 000 lb)	2 PNdB per doubling of thrust
Disk loading	96.1 to 574.6 N/m^2 (2 to 12 lb/ft^2)	0.5 PNdB per 96.1 N/m^2 (2 lb/ft^2)
Number of blades per rotor	2 to 6	<0.5 PNdB per blade addition

*Based on varying parameter under study while holding all others constant.

ALTITUDE 120 m (394 ft)

GROSS WEIGHT 18 140 kg (40,000 lb)

TIP SPEED 234 m/sec (769 ft/sec)

AIRSPEED 111 km/hr (69 mi/hr)
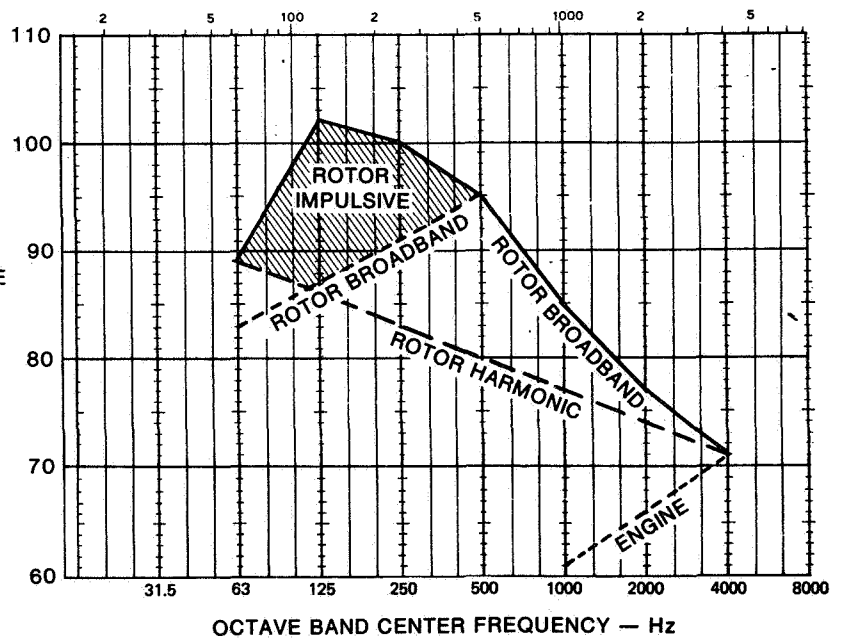
Figure 1.- Helicopter noise source contribution during 6-degree approach.

ALTITUDE 120 m (394 ft)

GROSS WEIGHT 18 140 kg
(40,000 lb)

TIP SPEED 234 m/sec
(769 ft/sec)

AIRSPEED 111 km/hr
(69 mi/hr)

PNL - 107 PNdB
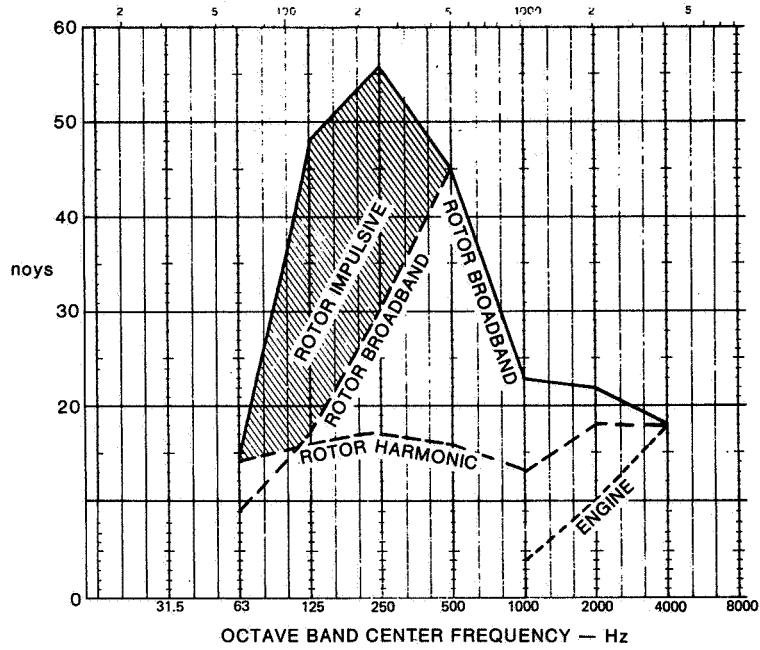
Figure 2.- Subjective weighting of helicopter noise during 6-degree approach.
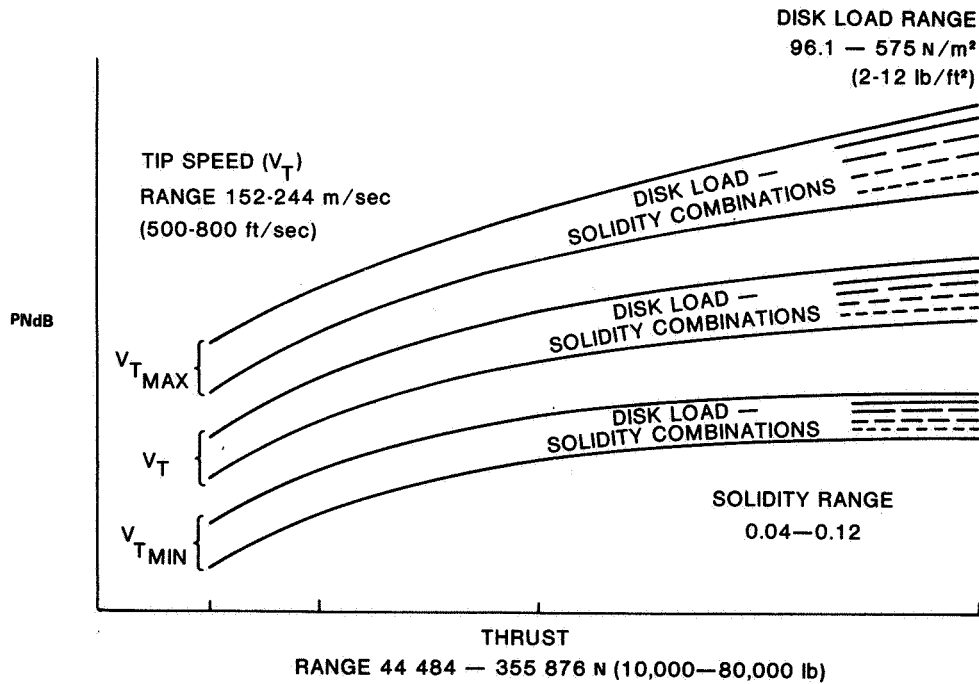
Figure 3.- Possible design chart format for 2-, 3-, 4-, 5-, and 6-bladed rotors.

557

INPUT DATA

KASE 5141

ROTOR THRUST	ROTOR TIP SPEED	ROTOR SOLIDITY	DISC LOAD	NUM BLADES	KNOTS		BB EFFECT. TIP SPEED	HARMONIC FUND.FREQ
15CCC.	750.	.1000	8.00	4	0.		750.	19.54

BLADE RADIUS	ROTOR RPM	TIP MACH NO.	ROTATION MACH NO.	FLIGHT MACH NO.	EFFECT. MACH NO.	LIFT COEF.	PEAK BB FREQ.	PEAK BB SPL
24.4	293.2	.671	.537	.000	.537	.359	343.2	70.4

BB DBA	BB DBC		HARMONIC DBA	HARMONIC DBC		TOTAL DBA	TOTAL DBC
76.7	78.9		70.7	84.9		76.9	85.9

A

****** BROADBAND NOISE ******

FREQ BAND	FREQ	SPL
20	21.5	53.4
25	27.0	55.1
31	34.1	56.7
40	42.9	58.4
50	54.1	59.8
63	68.1	61.2
80	85.8	62.6
100	108.1	63.8
125	136.2	65.5
160	171.6	66.2
200	216.2	67.6
250	272.4	69.0
315	343.2	70.4
400	432.5	69.1
500	544.9	67.7
630	686.5	66.4
800	864.9	66.2
1000	1089.7	66.0
1250	1373.0	65.8
1600	1729.8	64.3
2000	2179.4	62.9
2500	2745.3	61.2
3150	3459.6	61.1
4000	4358.8	60.9
5000	5491.8	59.4
6300	6919.3	57.9
8000	8717.7	56.1
10000	10983.6	54.6

***************** ROTATIONAL NOISE *****************

HARMONIC	FREQ	SPL	FREQ BAND	SPL
1	19.5	87.1	20	87.1
2	39.1	80.7	25	.0
3	58.6	75.6	31	.0
4	78.2	72.7	40	80.7
5	97.7	70.9	50	.0
6	117.3	69.4	63	75.6
7	136.8	68.3	80	72.7
8	156.4	67.3	100	70.9
9	175.9	66.4	125	71.9
10	195.4	65.6	160	69.9
11	215.0	64.9	200	68.3
12	234.5	64.3	250	68.5
13	254.1	63.7	315	68.0
14	273.6	63.2	400	66.7
15	293.2	62.6	500	66.6
16	312.7	62.2	630	66.1
17	332.2	61.7	800	61.9
18	351.8	61.3	1000	.0
19	371.3	60.9	1250	.0
20	390.9	60.6	1600	.0
21	410.4	60.2	2000	.0
22	430.0	59.9	2500	.0
23	449.5	59.5	3150	.0
24	469.1	59.2	4000	.0
25	488.6	58.9	5000	.0
26	508.1	58.7	6300	.0
27	527.7	58.4	8000	.0
28	547.2	58.1	10000	.0
29	566.8	57.9		
30	586.3	57.6		
31	605.9	57.4		
32	625.4	57.2		
33	645.0	56.9		
34	664.5	56.7		
35	684.0	56.5		
36	703.6	56.3		
37	723.1	56.1		
38	742.7	55.9		
39	762.2	55.7		
40	781.8	55.6		

* TOTAL NOISE *

FREQ BAND	SPL
20	87.1
25	55.1
31	56.7
40	80.7
50	59.8
63	75.8
80	73.1
100	71.6
125	72.7
160	71.4
200	70.9
250	71.7
315	72.4
400	71.0
500	70.2
630	69.3
800	67.5
1000	66.0
1250	65.8
1600	64.3
2000	62.9
2500	61.2
3150	61.1
4000	60.9
5000	59.4
6300	57.9
8000	56.1
10000	54.6

B

Figure 4.— Rotor noise calculation – computer program sample output.

558

********** COMBINED BROADBAND AND HARMONIC PERCEIVED NOISE DATA **********

FREQUENCY - HZ	LEVEL - DB	NOYS	CORRECTION
50	59.8	.57	.00
63	75.8	4.36	1.55
80	73.1	4.27	.00
100	71.6	4.86	.00
125	72.7	5.85	.00
160	71.4	6.03	.00
200	70.9	6.79	.00
250	71.7	7.75	.00
315	72.4	8.79	.00
400	71.0	8.55	.00
500	70.2	8.10	.00
630	69.3	7.60	.00
800	67.5	6.74	.00
1000	66.0	6.05	.00
1250	65.8	6.85	.00
1600	64.3	8.06	.00
2000	62.9	8.41	.00
2500	61.2	8.58	.00
3150	61.1	9.13	.00
4000	60.9	9.01	.00
5000	59.4	7.59	.00
6300	57.9	6.38	.00
8000	56.1	4.58	.00
10000	54.6	3.36	.00

PNLT = 91.3
PNL = 89.8
'CORRECTION = 1.55

C

Figure 4.- Concluded.

559

ROTOR THRUST   66,727 N
(15,000 lb)

ROTOR TIP SPEED   229 m/sec
(750 ft/sec)

ROTOR SOLIDITY   0.1

DISK LOAD   303 N/m²
(8 lb/ft²)

BLADE RADIUS   7.5m
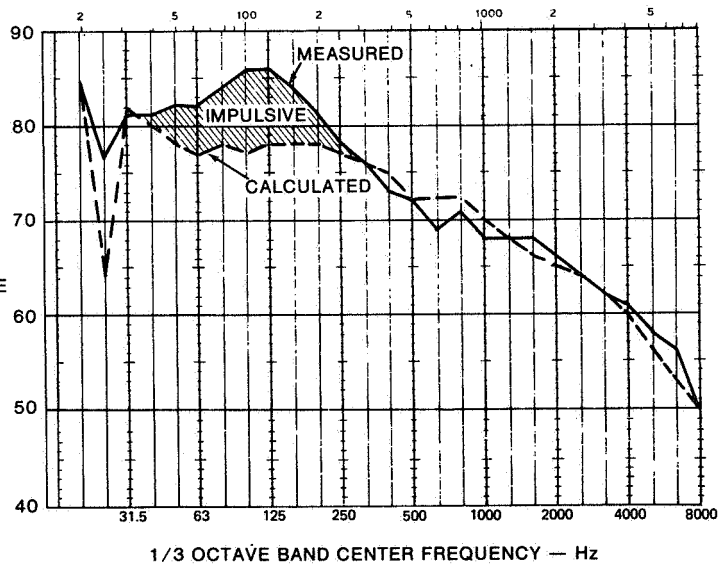(24.5 ft)

SOUND
PRESSURE
LEVEL — dB RE
2 X 10⁻⁵ N/m²
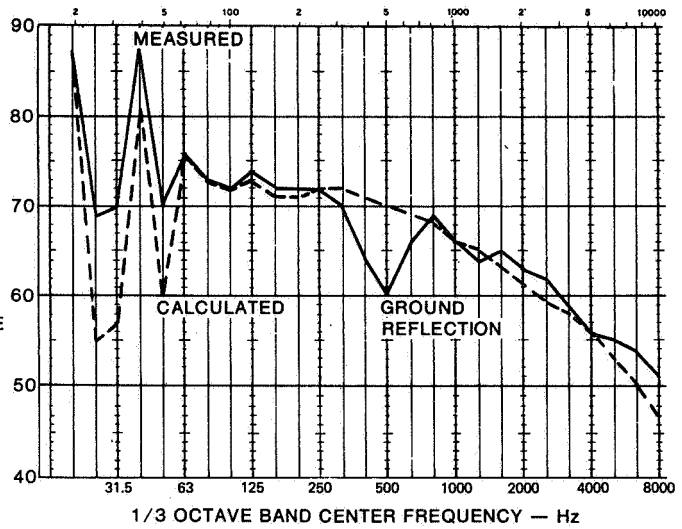
Figure 5.- Correlation of calculations with whirl tower nonimpulsive rotor noise at 152-m (500-ft) distance.

ROTOR THRUST   266,907 N
(60,000 lb)

ROTOR TIP SPEED   229 m/sec
(750 ft/sec)

ROTOR SOLIDITY   0.09

DISK LOAD   430 N/m²
(9 lb/ft²)

BLADE RADIUS   14m (46 ft)

SOUND PRESSURE
LEVEL — dB RE
2 X 10⁻⁵ N/m²

Figure 6.- Correlation of calculations with whirl tower impulsive rotor noise at 152-m (500-ft) distance.

BASE POINT VALUES

THRUST	88,969 N (20,000 lb)
TIP SPEED	229 m/sec (750 ft/sec)
DISK LOADING	287 N/m² (6 lb/ft²)
SOLIDITY	0.06
LIFT COEFF	0.449

SOUND PRESSURE LEVEL — dB RE 2 X 10⁻⁵ N/m²

HARMONIC

BROADBAND

1/3 OCTAVE BAND CENTER FREQUENCY — Hz
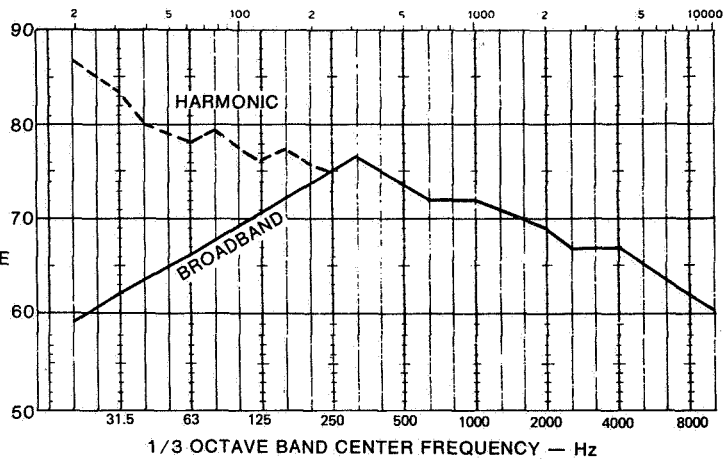
Figure 7.- Calculated - nonimpulsive hover noise 3-bladed rotor at 152-m (500-ft) distance.

APPROXIMATE CHANGE

- 2 PNdB PER 2 X THRUST
- 3 PNdB PER 30.5 m/sec (100 ft/sec)
- 0.5 PNdB PER 96.1 N/m² (2 lb/ft²)
- <0.5 PNdB PER BLADE

CHANGE IN PNdB FROM BASE POINT   (95.6 PNdB)

TIP SPEED
THRUST
DISK LOADING
BLADES

THRUST, N (lb)

DISK LOADING, N/m² (lb/ft²)

TIP SPEED, m/sec (ft/sec)

BLADES PER ROTOR
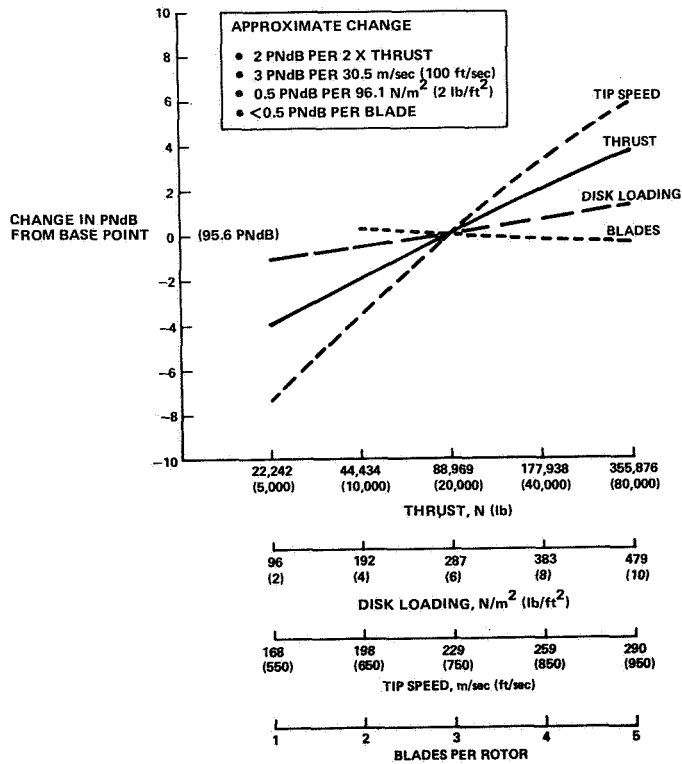
Figure 8.- Relative change in PNdB with design parameter variation.

561

THE COST OF APPLYING CURRENT HELICOPTER EXTERNAL NOISE REDUCTION METHODS WHILE MAINTAINING REALISTIC VEHICLE PERFORMANCE*

MICHAEL A. BOWES
KAMAN AEROSPACE CORPORATION

SUMMARY

Analytical methods were developed and/or adopted for calculating helicopter component noise, and these methods were incorporated into a unified total vehicle noise calculation model. Analytical methods were also developed for calculating the effects of noise reduction methodology on helicopter design, performance and cost.

These methods were used to calculate changes in noise, design, performance and cost due to the incorporation of engine and main rotor noise reduction methods. All noise reduction techniques were evaluated in the context of an established mission performance criterion which included consideration of hover ceiling, forward flight range/speed/payload and rotor stall margin.

INTRODUCTION

The helicopter, which has long been considered an essential military tool, is now enjoying rapidly expanding use in civilian applications. The size of the civil helicopter fleet, which numbered less than 1000 vehicles in 1960, has now grown to over 5000, and continued expansion is anticipated (figure 1). This growth in fleet size, coupled with a corresponding increase in the type and number of civil missions being performed, has caused a heightened awareness of and reaction to helicopter noise in the community. As a consequence of this, the Federal Aviation Administration (FAA) has taken steps to formulate a helicopter noise certification rule, which will limit the allowable noise of future design helicopters in much the same way that the existing Federal Air Regulation (FAR) Part 36 limits jet transport noise.

In establishing such a rule, consideration must be given to the needs of the helicopter operator as well as the desires of the community. Consequently, definition of a reasonable specification requires knowledge of both the communities' subjective acceptance of helicopter noise, and the technological and economic aspects of helicopter noise reduction. The study which forms the basis for this paper (reference 1) was directed towards the technological and economic aspects of the problem. Specifically, the objective of this study was to determine the degree of noise reduction obtainable with current helicopter noise reduction technology, and the cost of applying this technology.

The technical effort included the development of a unified method for predicting helicopter vehicle noise including the noise contributions of the rotors, engines and drive system. Analytical methods were also formulated for determining the impact of noise reduction on vehicle design, performance and cost. These tools were then used to estimate and compare the benefits and costs of alternative noise reduction methods, within the context of established vehicle performance criteria.

STUDY APPROACH

The noise signature of a helicopter is composed of contributions from the rotors, engines and drive train. Well developed technologies exist for reducing the noise generated by each of these components. However, because these contributions combine in a complex, spatially and frequency dependent manner it is not possible to evaluate these noise reduction methods on an isolated component basis. Component noise reduction methods, therefore, must be evaluated within the context of the total helicopter noise signature. This requires the use of a noise calculation method which, although capable of estimating the combined noise contributions of all components, still retains a high degree of detail for estimating the noise output of each individual component. This "systems" approach to helicopter noise modeling was applied in the present study.

The noise calculation approach discussed above provided the means for evaluating the potential for helicopter noise reduction. To apply these approaches realistically, however, it was necessary to determine the nature and extent of changes in vehicle design and performance characteristics which must be made to incorporate noise reduction methodology. This information was also required to assess the economic cost of helicopter noise reduction.

The intent of the overall study effort was to determine how much noise reduction can be achieved in future design civil helicopters using existing noise reduction technology, and what changes in total life cycle cost will result from the achievement of this noise reduction. Since the study concerned itself only with future design civil helicopters, it was necessary to make certain assumptions as to the nature of these vehicles and what their noise and cost characteristics would be if noise reduction was not considered in their design. The effects of noise reduction could then be determined relative to these baseline characteristics. In the study program it was assumed that future design civil helicopters will be required to perform similar missions to those presently being performed. Since vehicle design is principally a function of required mission performance, it was further assumed that future civil helicopters will be similar in design to existing vehicles. These assumptions lead directly to the use of existing civil helicopter characteristics (table 1) as the baseline for determining changes due to the incorporation of noise reduction methodology.

The basic premise of the study was that noise reduction of future civil

564

helicopters will be achieved in addition to, rather than at the expense of, required mission performance. Noise-reduced vehicles will fly as fast, as high, as far and with the same payload, although they may be heavier and more costly to own and operate. This concept of a constant mission performance requirement provided a realistic context within which the effects of helicopter noise reduction could be determined and assessed.

To apply this approach, the following mission performance criteria were established:

1. Constant payload.
2. Constant out-of-ground effect hover ceiling.
3. Constant range (at the best cruise speed of the baseline vehicle).
4. Adequate (equal or greater) stall margin.

In general terms, these criteria were applied in the following manner, as illustrated in figure 2, beginning with a baseline reference vehicle configuration having known performance characteristics. First, the direct effect of the introduction of a noise reduction method was determined in terms of a change in vehicle gross weight at constant payload. This new gross weight was then used to establish a new installed power requirement, and the consequent changes in engine weight and rated fuel consumption rate which result from this change in installed power. Installed power, as well as engine weight and rated fuel consumption, were also changed to reflect any direct effects of noise reduction such as engine silencer losses. Weight and installed power changes were then iterated until a combination was arrived at which satisfied the baseline vehicle out-of-ground effect hover ceiling capability.

The above procedure resulted in a vehicle configuration which could operate at the same altitude with the same payload as the reference configuration. Forward flight performance was then considered in order to satisfy the established range and speed capability criteria. Given the new vehicle gross weight determined by hover performance requirements, rotor stall margin was calculated and compared to that of the baseline vehicle. If insufficient stall margin was indicated, changes in rotor design were effected, which increased stall margin to that of the baseline configuration. Any changes in weight which resulted from these rotor design changes were calculated and accounted for, iteratively, through reconsideration of the hover performance requirement. Once stall margin and hover performance were determined to be consistent with the established criteria, forward flight power required for the new vehicle configuration was calculated.

Forward flight power required was determined for flight at the best cruise speed of the baseline vehicle. This power was then used to determine the need for any change in fuel load required to maintain a maximum range equal to that of the baseline vehicle. If fuel load

was changed, vehicle gross weight was adjusted accordingly and, again, compensated for through consideration of hover performance and stall margin criteria.

The new vehicle configurations resulting from the above procedure were often substantially different in design from the baseline vehicles. In general, these new configuations showed changes in gross weight, airframe weight, installed power, engine weight and fuel load. These changes in vehicle design were in addition to, and were the direct result of, one or more changes in vehicle design associated with the introduction of some noise reduction methodology. Since all of these changes had the potential for affecting the net noise reduction achieved with a given noise reduction methodology all were considered in the subsequent calculation of vehicle noise reduction. These design changes were also used to assess noise reduction cost.

ANALYTICAL METHODS

The analytical methods developed and/or adapted for use in the present program fall into three general categories. These are:

1. Noise calculation.
2. Vehicle design and performance calculation.
3. Cost calculation.

With respect to noise, analytical models were either derived or adapted from existing methods. These enabled calculation of the rotor system, engine (turbine and reciprocating) and transmission noise components. These component models were incorporated in a unified vehicle noise calculation method, which had the capability of generating 1/3 octave sound pressure level spectra as a function of time, at any observer location, for any steady state translational flight condition. This method is illustrated in figure 3. These calculated 1/3 octave spectra are automatically converted to effective perceived noise level (EPNL) and instantaneous A-weighted sound pressure level (dBA), overall sound pressure level (OASPL), perceived noise level (PNdB) and tone corrected perceived noise level (PNLT) units.

A separate analytical method was developed to enable calculation of the changes in helicopter design and performance characteristics which result from the application of noise reduction technology to the various noise producing vehicle components. This method reflects the approach discussed in the preceding section and illustrated in figure 2.

The cost calculation method was developed from historical helicopter cost data, which relate the three elements of life cycle cost to the various vehicle design parameters (table 2). This model considers initial investment cost to be related to vehicle airframe weight and installed engine weight. Indirect operating cost is related to vehicle total empty weight. Direct operating cost is assumed to be a function of both empty weight and installed engine power. The cost calculation

566

method permits determination of both absolute vehicle dollar costs and percentage changes in costs relative to an established baseline helicopter design. Life cycle costs are calculated as a function of both annual usage rate and total useful life.

The preceding analytical methods were used to calculate baseline noise, performance and cost characteristics for several existing helicopter models, with gross weights ranging from 8 kN to 80 kN. Calculated EPNL's for these vehicles are shown in figure 4. Investigation of the results of these calculations revealed that the main rotor and engines contributed most to the vehicle EPNL and, consequently, subsequent noise reduction evaluations were directed at these sources.

TURBINE ENGINE NOISE REDUCTION

Helicopter turboshaft engine noise was found to be dominated by exhaust radiated components. Since these noise components may be effectively reduced through exhaust duct treatment, a study was performed to evaluate the effect of such treatment on the total vehicle noise signature.

Three representative present generation helicopters were chosen for this study (table 1). A generalized exhaust silencer configuration, illustrated in figure 5, was established, and the normalized acoustic and aerodynamic performance characteristics of this duct treatment were derived (figures 6 and 7). Various levels of duct treatment were simulated, for each study vehicle, and estimates of the total vehicle noise reduction were made.

The average of fly-over and fly-by vehicle EPNL reductions achieved with engine silencing is shown in figure 8 as a function of silencer weight, for each study vehicle. To provide a meaningful comparison, silencer weight is expressed as a percentage of vehicle gross weight. On this basis, achieved noise reductions are roughly comparable, for comparable weight penalties, for the three vehicles.

The additions to vehicle gross weight and reductions in engine performance indicated in figures 7 and 8 do not reflect the total impact of engine silencing, and these changes alone do not represent an adequate basis for estimating changes in vehicle cost due to silencer use. To provide this basis, the changes in vehicle design necessary to accommodate these direct penalties were determined.

Incorporation of an engine silencer increases vehicle gross weight by an amount equal to the silencer weight. Vehicle airframe weight, however, must also increase, to carry the added silencer weight. This change in airframe weight further increases gross weight, requiring additional engine power and, consequently, increased engine weight. These three weight changes increase the fuel load required to maintain constant range capability. Additions to fuel load and engine weight further increase airframe weight, gross weight and power required. The ultimate gross weight, airframe weight, engine power and weight and fuel load can be calculated

through an iterative solution of the individual weight and power relationships involved in the analytical method. Additional effects of engine silencing are decreased available power and increased specific fuel consumption. These direct penalties result in the need for increased installed power and added fuel load, and these factors were also taken into account in redesigning the vehicle.

The net effects of incorporating exhaust duct treatment are illustrated in figure 5, which compares induced vehicle design changes to vehicle EPNL reductions. Significant changes are shown in all the design parameters considered, with the magnitude of change increasing sharply with noise reduction. As might be expected, installed engine power is most greatly affected, with a 6% to 10% engine power growth shown for a 3-3.5 EPNdB reduction in EPNL.

The changes in vehicle design shown in figure 9 have been interpreted in terms of changes in vehicle costs. Cost changes have been calculated in terms of percentage changes in the basic cost elements of initial investment cost, indirect operating cost and direct operating cost, as well as total life cycle cost. These calculations have been made using the parametric helicopter cost model discussed previously, with the direct silencer cost added to initial investment cost.

Change in investment and indirect operating costs due to engine exhaust silencing are given in figure 10, with direct operating cost and life cycle cost changes shown in figure 11. The life cycle cost data shown refer to a useful life of 15 years, with an annual usage of 1500 hours.

The magnitudes of the cost increases shown are best illustrated by considering these changes in absolute terms. Considering an S-61 vehicle, for example, a 3 EPNdB noise reduction obtained through engine silencing would raise initial investment cost from $1.779 million per aircraft to $1.846 million per aircraft, an increase of $67,000. Indirect costs, on a yearly basis, would rise by over $5000 per year, from $147,000/year to $152,000/year. Direct operating cost, initially at $272 per hour would go up to $281 per hour, an increase of over $8 per hour. Taken together, and assuming a useful life of 15 years with a usage rate of 1500 hours/year, total cost to own and operate this aircraft would increase by $293,000, from a baseline of $10.111 million to $10.404 million. This represents an annual cost increase of nearly $20,000.

MAIN ROTOR NOISE REDUCTION

Evaluation of the significance of the various helicopter noise components indicated that the main rotor contributes substantially to the total vehicle noise signature. Consequently, analyses were performed to determine the extent of vehicle noise reduction obtainable through the application of rotor noise reduction methodology. Methods considered in these analyses consisted of changes in gross rotor design parameters only, including increased rotor radius, blade chord and blade number and reduced

rotor speed. The effects of these changes were evaluated in terms of the net vehicle noise reduction obtainable, considering potentially offsetting induced changes in vehicle design, for constant performance. These induced design changes were also interpreted in terms of changes in vehicle cost, which were then compared to anticipated vehicle noise reductions. The baseline vehicles used for the preceding engine noise reduction study, the Hughes 500, Bell 205 and Sikorsky S-61, were also used in the performance of the main rotor noise reduction study.

Performance of the main rotor noise reduction evaluation was predicated on the same performance criteria used in evaluating turbine engine noise reduction. In this regard the geometric rotor design parameters, including rotor radius, blade chord and number of blades, were treated as independent variables, and the effects of increasing each of these relative to baseline vehicle values was evaluated separately. This could be done because changes in these parameters could be compensated for by iterating the vehicle design without violating the basic performance criteria. The remaining rotor design parameter, rotor tip speed, was not evaluated independently since a reduction in rotor speed leads directly to a reduced rotor stall margin, and this cannot be compensated for through the type of vehicle reconfiguration considered in the design analyses. Reduced speed can, however, be achieved without sacrificing stall margin, if a compensating increase in blade or disk area is affected, since these area changes tend to increase stall margin. Consequently, in the present study, rotor speed variation has been considered only in conjunction with appropriate blade or disk area changes.

The design implications of changes in rotor radius, blade chord and number of blades are illustrated in figures 12 and 13. These curves show the changes in gross weight and installed power which result from increasing rotor radius, blade chord and number of blades. Data are included for both constant and reduced rotor speed, with rotor speed changes in accordance with the constant stall margin curve of figure 14. While the data of figures 12 and 13 pertain to the S-61 baseline vehicle only, similar results were obtained for the other study vehicles.

In figure 12, gross weight is seen to increase with rotor radius, blade chord and blade number, with identical trends shown for chord and blade number. Rotor radius increases gross weight most quickly and the trend indicated is nonlinear, with increasing slope. This is due to the fact that rotor radius growth necessitates an increased fuselage size, in addition to increased structural weight due to load requirements. The maximum 25% increase in S-61 rotor radius results in a 6.6% increase in vehicle gross weight.

The trend of gross weight with either chord or blade number is linear and less steep than the trend with rotor radius. In this case, airframe weight only increases due to the added rotor system weight and the added structural weight needed to support the heavier rotor. Only a 4.1% gross weight increase is indicated for a 25% blade area change,

whether due to chord or blade number increase. Doubling the chord or number of blades causes a 16.4% increase in gross weight.

The trends of installed power with chord, blade number, and rotor radius are given in figure 13. Installed power is shown to increase linearly with both chord and blade number, but to decrease nonlinearly with rotor radius, in this case with decreasing (absolute) slope. A 9.1% installed power reduction is indicated for the maximum 25% rotor radius increase. Installed power increases 6.3% for a 25% increase in blade area, whether due to blade chord or blade number. Doubling chord or number of blades increases installed power by 24%.

The data of figures 12 and 13 show only an insignificant difference in the effects of rotor geometry changes evaluated alone and evaluated in conjunction with rotor speed reduction. The magnitude of rotor speed reduction considered in these data is, however, relatively small, as indicated in figure 14. This figure relates rotor tip speed to change in blade area, and the curves shown represent lines of constant stall margin. As shown, only a 3.1% reduction in rotor tip speed can be accommodated by a 25% radius increase. A 3.7% reduction in rotor speed is indicated for a similar 25% blade area increase, accomplished by increasing chord or blade number. A 12% tip speed reduction can be obtained by doubling either blade chord or blade number.

The magnitude of vehicle gross weight increase associated with the various rotor system changes strongly suggested that noise reductions anticipated to result from the rotor system changes would tend to be offset by increases in noise due to rotor thrust growth. Based on this indication, it was decided to use a simplified rotor noise calculation method to determine the approximate magnitude of achievable net rotor noise reduction and, based on the results of these calculations, decide whether to proceed with the more involved rotor and total vehicle noise calculations. This approach was arrived at based on the premise that unless significant rotor noise reductions were shown through the simple analysis, no worthwhile reductions would be calculated for the total vehicle using the detailed analysis.

The simplified rotor noise calculation method chosen for use was obtained from reference 2. This method relates the magnitude of the high frequency random component of rotor noise to rotor speed squared, thrust squared and blade area.

This method was used to estimate the maximum possible rotor system noise reduction obtainable with the various rotor system parameter changes considered. The results of these calculations are summarized in table 3 for the three study vehicles. Also given are the changes in cost associated with each of the rotor system variations.

Comparison of the cost and approximate rotor noise reduction data of

Table 3 reveals that the cost of reducing helicopter rotor noise levels is very high. Considering the S-61 study vehicle, for example, increasing rotor size by 25%, raises life cycle cost by over 5.7%, for a 1500 hour per year use rate, and the cost differential is greater for lower annual use rates. In absolute terms, the 25% greater rotor radius increases life cycle cost by almost $.6 million dollars, or more than $38,000/year. This rotor design change reduces rotor noise by less than .5dB which, in all probability, would produce no measurable change in total vehicle noise.

The most beneficial rotor design change, doubling the number of blades and reducing rotor speed by approximately 12%, raises life cycle cost by almost 30%. This translates into a $3.03 million dollar life cycle cost increase, or in yearly terms, over $200,000 added annual cost. In terms of total vehicle noise, as discussed previously, the 2.8dB rotor noise reduction associated with this design change, would probably only result in a 1.6dB reduction in vehicle noise.

Because of the high cost to benefit ratios determined for the selected rotor noise reduction methods, it was concluded that these methods are not practical means for reducing helicopter noise, and that further analyses of these methods was not warranted. Consequently, these methods were not evaluated with the more involved noise calculation techniques originally intended for use. However, a small number of rotor noise reduction design changes were subjected to further evaluation in order to verify the appropriateness of the approximate noise calculation method. In all cases studied, the involved noise calculation technique indicated noise reductions similar in magnitude to those obtained with the approximate method.

CONCLUSIONS

The results of the present study indicate that small, but meaningful, reductions in helicopter noise can be obtained by treating the turbine engine exhaust duct. Furthermore, these reductions do not result in excessive life cycle cost penalties. Currently available main rotor noise reduction methodology, however, was shown to be inadequate and excessively costly. This result strongly suggests the need for additional helicopter rotor noise research, which should be directed at developing more efficient methods for reducing rotor noise.

As with any study of this nature, the results of the present effort should be interpreted only within the context of the study groundrules. In this regard, two such groundrules are particularly important. First, the vehicle design analysis used in this study considered only current helicopter design and fabrication technology. Improvements in these technologies, particularly those which result in better structural efficiency, rotor performance and engine efficiency, could improve the effectiveness of current noise reduction methods, by minimizing the extent of offsetting vehicle design changes.

The second study groundrule which must be considered in evaluating the study results relates to the use of the constant performance concept. While this approach provides a realistic framework for evaluating the cost of noise reduction, other approaches might also be equally valid. One such alternative approach would be the specification of minimum induced design change, with variable performance capability. In this context, the major impact of noise reduction would be interpreted in terms of performance penalties, which would then be related to cost differentials. This approach is equally valid, although it is somewhat more difficult to apply and interpret than the constant performance method.

REFERENCES

1. Bowes, M. A.: Helicopter Noise Reduction Design Trade-off Study. DOT/FAA Report FAA-AEQ-77-4, January 1977.

2. King, R. J. and R. G. Schlegel: Prediction Methods and Trends for Helicopter Rotor Noise. CAC/AVLABS Symposium Procedings, June 1969.

| | | Gross | Installed | |
Study Vehicle	Manufacturer	Weight (kN)	Power (kW)	Fly-Away Cost ($)
S-61	Sikorsky	86.3	2237	1.8m
B-205	Bell	42.2	1043	.6m
H-500	Hughes	10.7	236	.12m

TABLE 1. STUDY VEHICLE CHARACTERISTICS

TABLE 2. COST MODEL

● <u>INITIAL INVESTMENT COST</u> - C_I

   o Airframe = f (Airframe Weight)

   o Engine = f (Installed Power)

   o Initial Spares = f (Empty Weight)

   o Avionics = f (Empty Weight)

● <u>INDIRECT OPERATING COST - IOC</u>

   o Insurance = f (Empty Weight)

● <u>DIRECT OPERATING COST - DOC</u>

   o Maintenance and spares =

       f (Empty Weight)

   o Fuel and Oil =

       f (Installed Power)

   o Crew = f (Empty Weight)

● <u>LIFE CYCLE COST - LCC</u>

$$LCC = C_I + DOC(N_A \; L_U)$$
$$+ \; IOC(L_U)$$

   o N_A = Annual Usage

   o L_U = Useful Life

574

TABLE 3. VEHICLE COST AND NOISE CHANGES FOR
MAXIMUM NOISE REDUCTION CONFIGURATIONS -
S-61

Parameter Varied	Δ Investment Cost (%)	Δ IOC-%	Δ DOC-%	Δ LCC - % (15 Yr Life)		Δ EPNL (EPNdB)
				300 Hr/Yr	1500 Hr/Yr	
+25% Radius	13.66	13.65	.58	10.58	5.73	- .4
+50% Chord	25.0	23.66	9.0	20.44	14.86	-1.08
+5 Blades	51.83	49.82	18.15	43.06	30.99	-1.67
+25% Radius -3% Ω R	14.02	13.98	.73	10.88	5.96	- .68
+50% Chord -7.2% Ω R	24.04	23.30	8.81	20.15	14.65	-1.74
+5 Blades -11.9% Ω R	50.05	48.12	17.61	41.6	29.98	-2.82
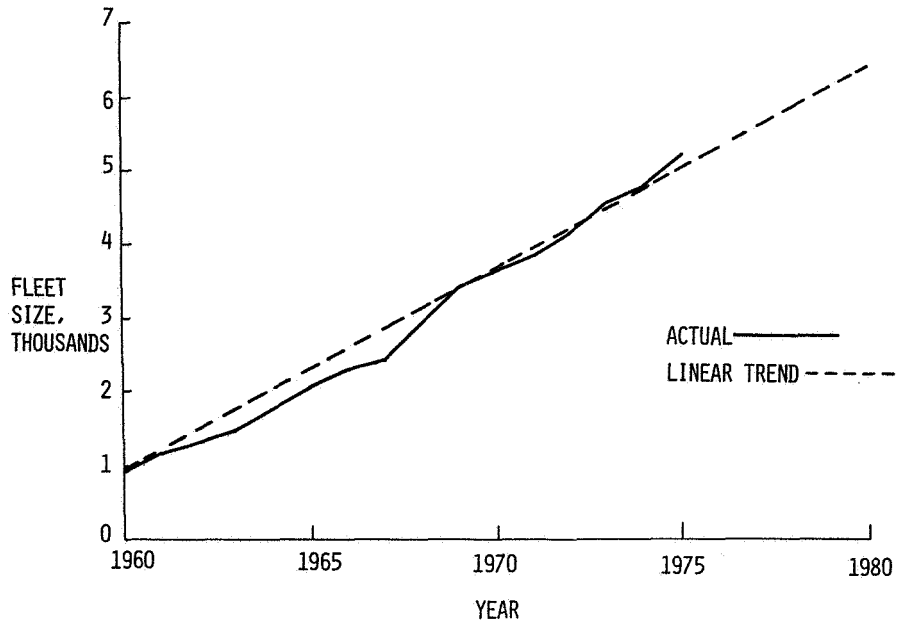
Figure 1.- Domestic civil helicopter fleet growth.
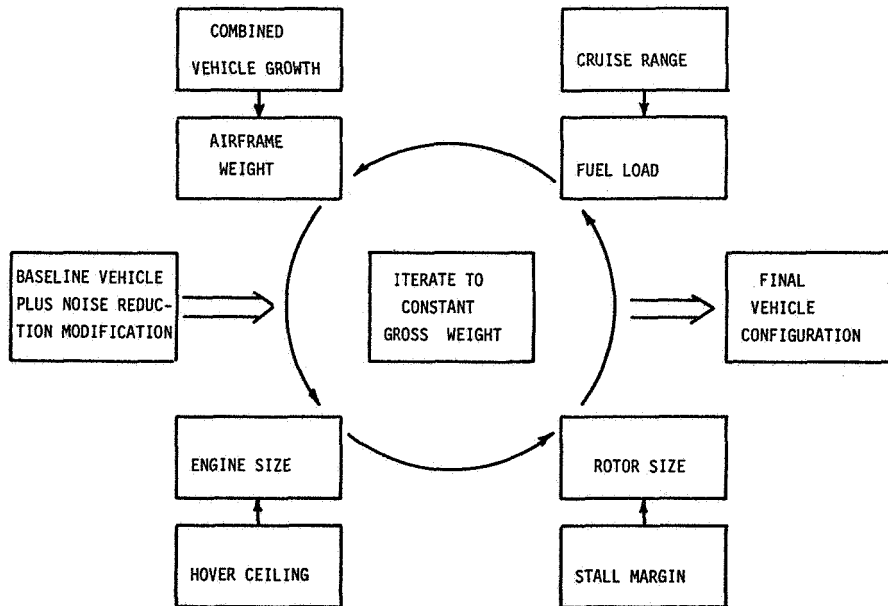
Figure 2.- Vehicle design methodology.

576
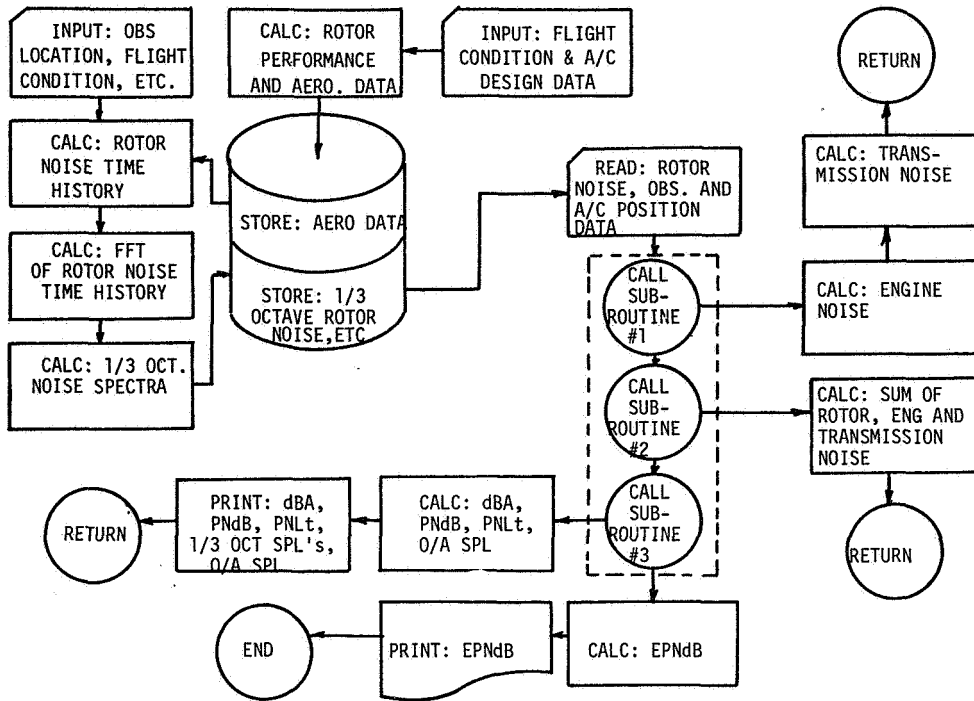
Figure 3.- Noise calculation methodology.
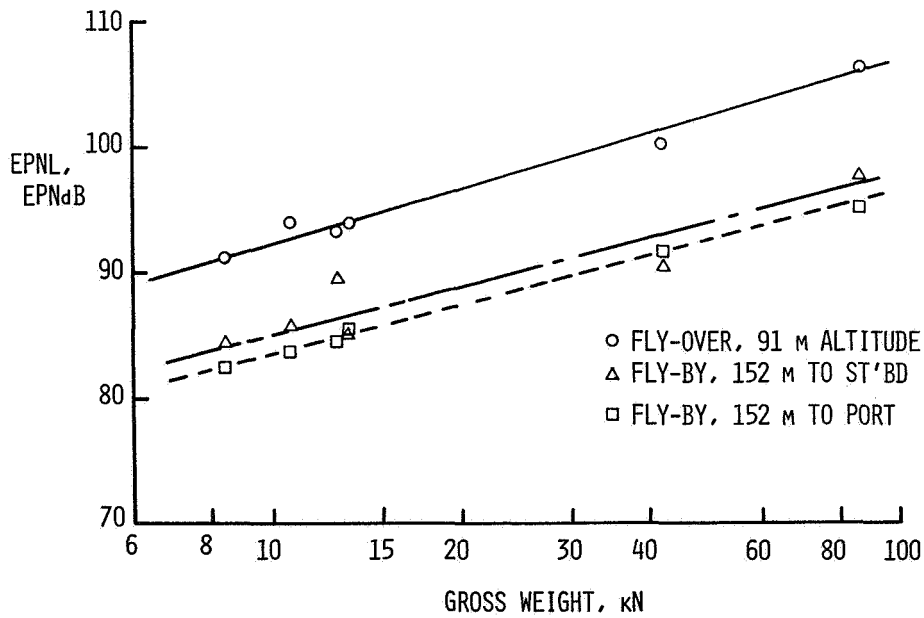
Figure 4.- Calculated vehicle noise.
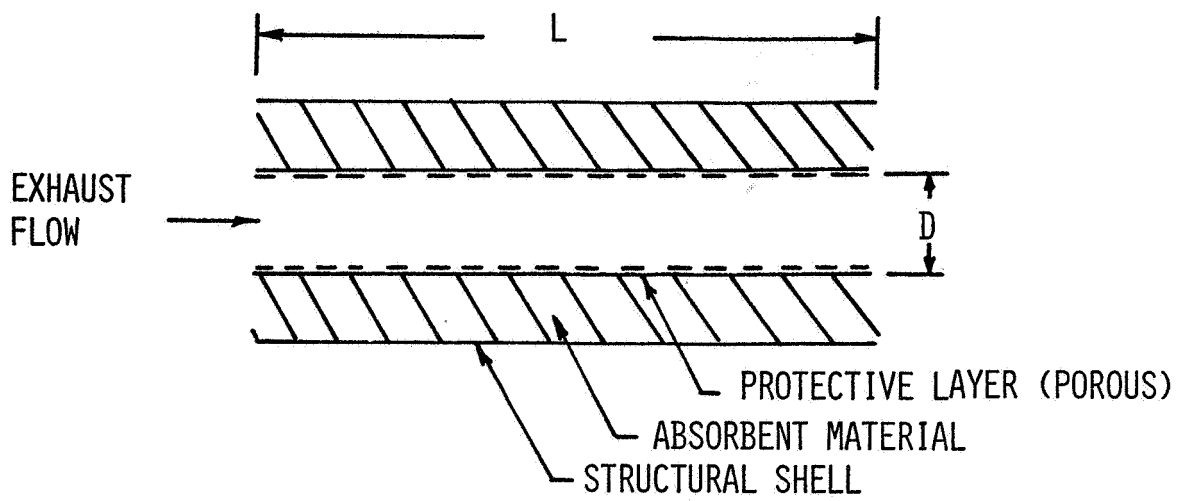
Figure 5.- Exhaust silencer configuration.
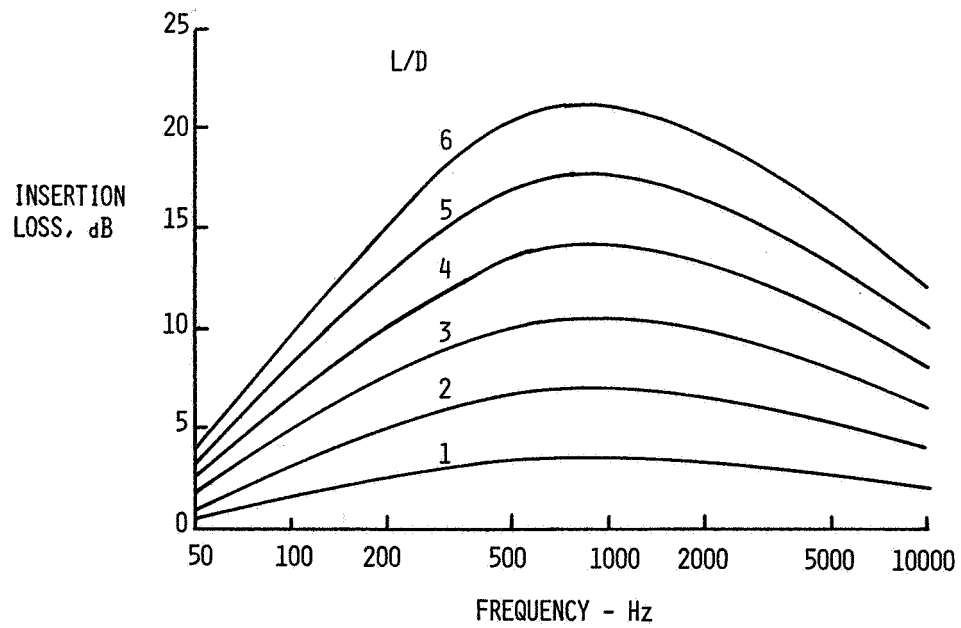
Figure 6.- Exhaust silencer acoustic performance.
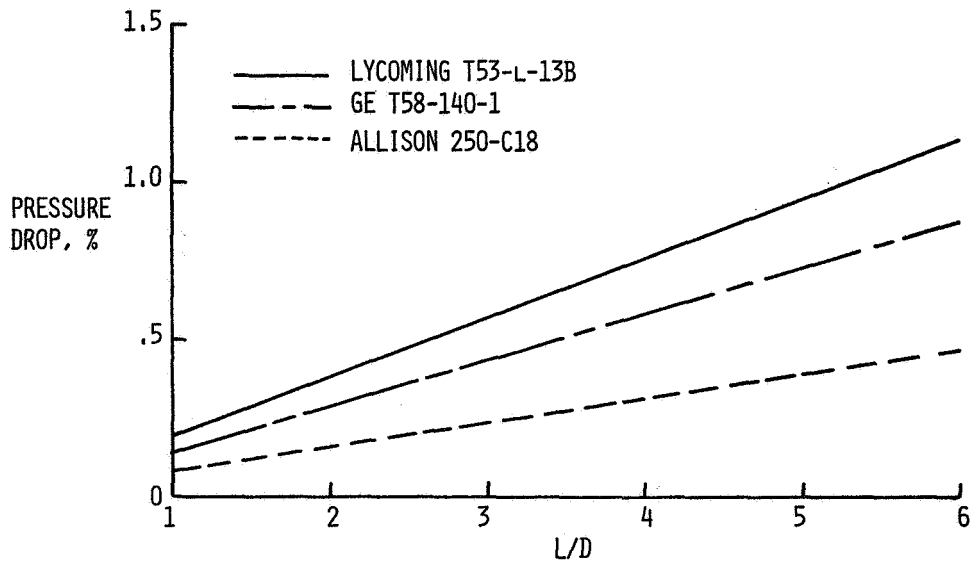
Figure 7.- Exhaust silencer aerodynamic performance.
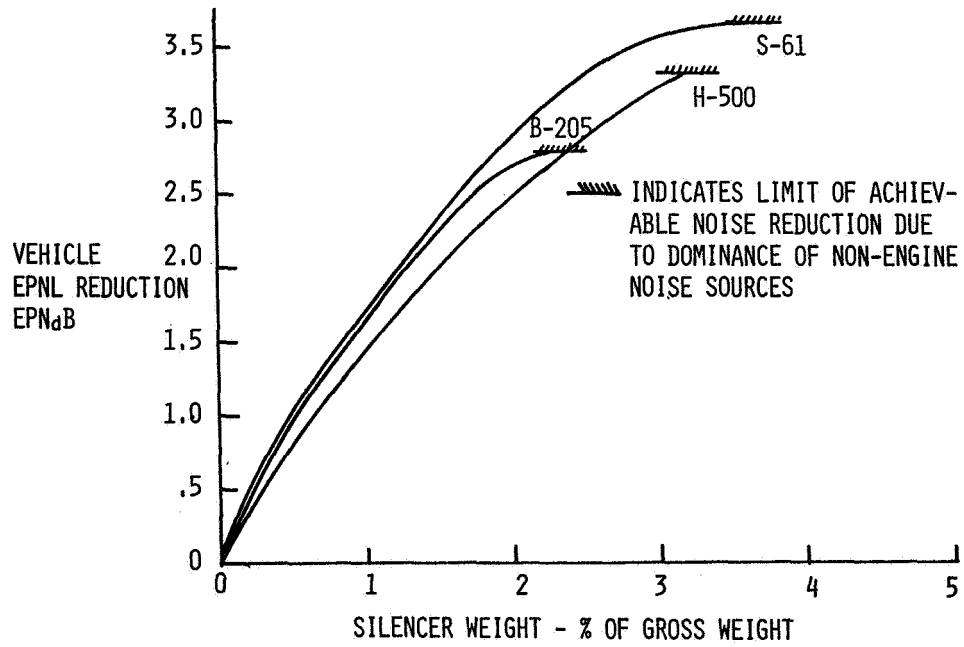
Figure 8.- Exhaust silencer weight.
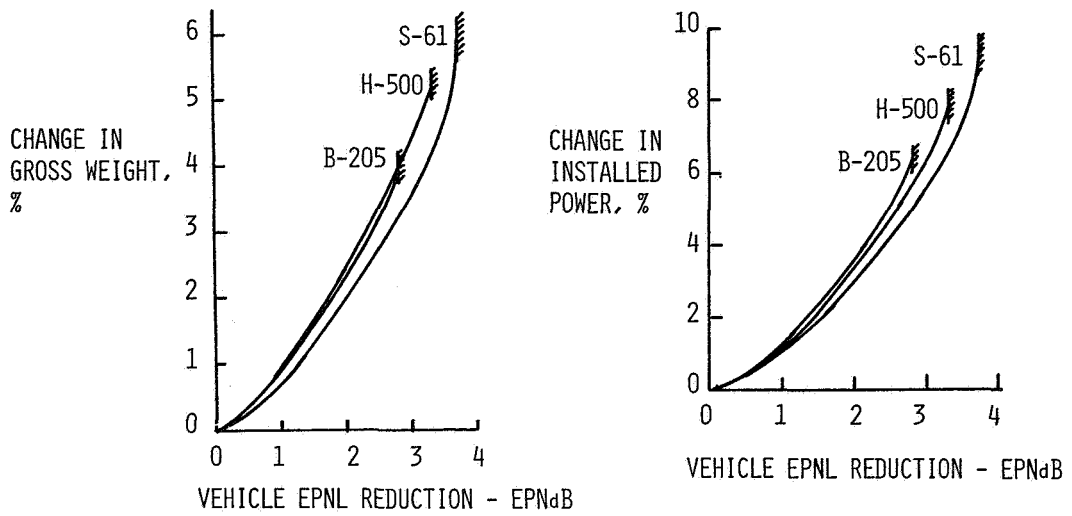
Figure 9.- Design changes due to exhaust silencing.
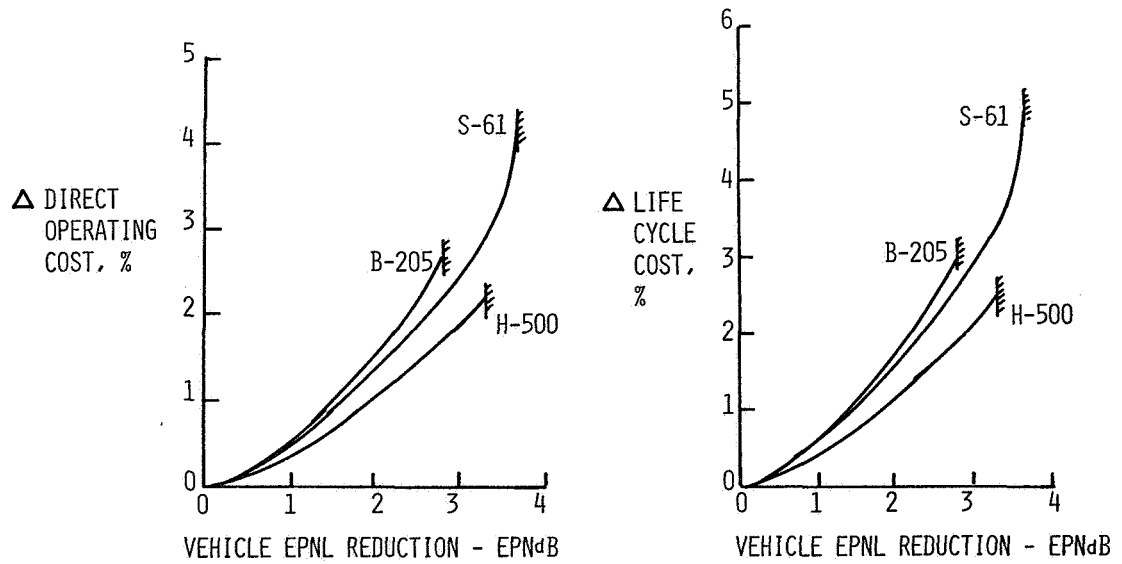
Figure 10.- Direct operating cost and life cycle cost of exhaust silencing.
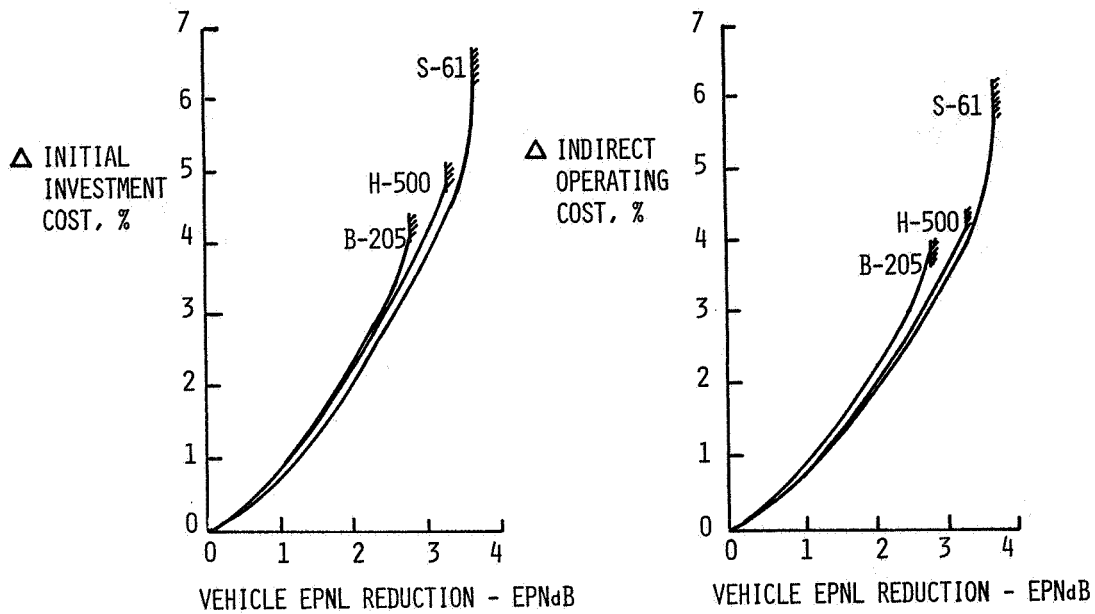
Figure 11.- Initial investment cost and indirect operating cost of exhaust silencing.
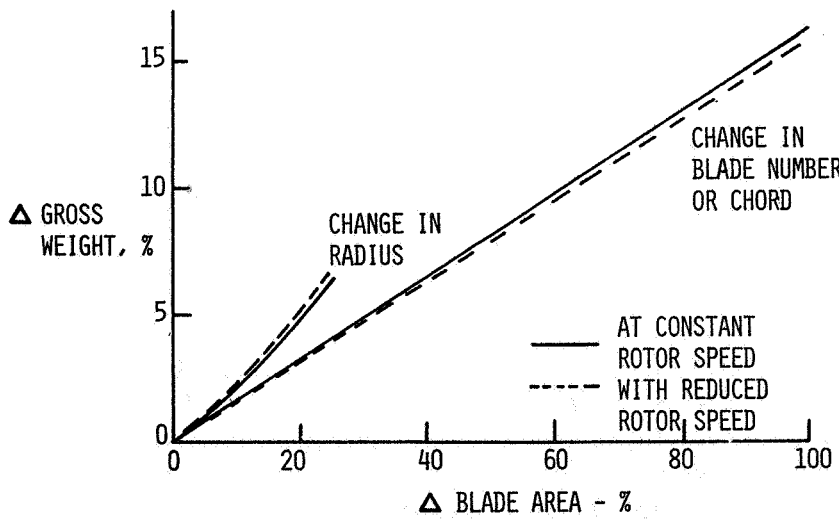
Figure 12.- Gross weight with blade area.
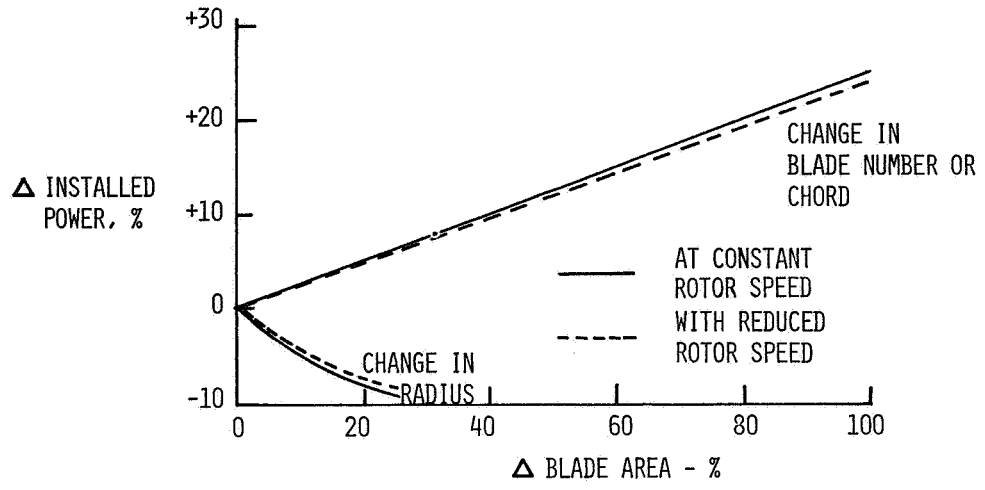
Figure 13.- Installed power with blade area.
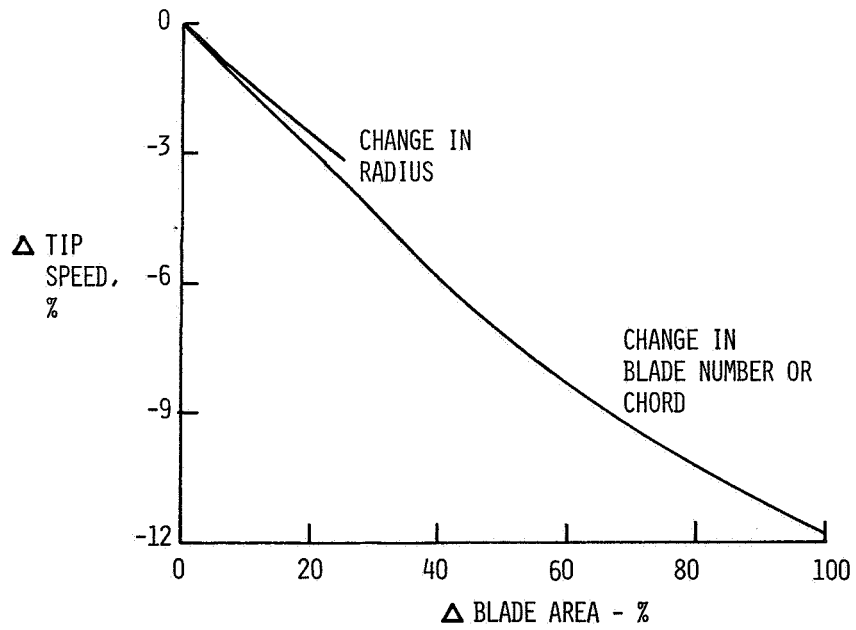
Figure 14.- Constant stall margin.

582

HELICOPTER CABIN NOISE - METHODS OF SOURCE AND PATH

IDENTIFICATION AND CHARACTERIZATION

Bruce S. Murray and John F. Wilby
Bolt Beranek and Newman Inc.

SUMMARY

The effective quieting of helicopter cabins requires that the weight and space of the treatments be minimized. The application of these treatments therefore requires that the paths by which the noise arrives at the cabin, coupled with the radiating surfaces and the sources of origin be identified as clearly as possible. The techniques described in this paper have been employed as part of comprehensive helicopter quieting programs which have achieved notable reduction of cabin noise on several existing helicopter designs.

INTRODUCTION

The continued expansion of and competition for the helicopter market, particularly in the 8-20 seat capacity range, has led to much attention being given to the provision of quiet and comfortable passenger accommodation. The helicopter in this size range when fitted with the best "standard" interior will typically exhibit a cabin noise level of 93-95 dBA when flying at its design speed, whereas a commercial transport will have a typical noise level ranging from 75 to 82 dBA at its cruise speed. Figure 1 summarizes the typical noise levels that can be expected with various interior configurations and shows that, even with the best available treatment, the noise levels are above those for a commercial transport. Of particular note are the tone levels which control the levels in many portions of the spectrum and are of course more annoying than the same levels of random noise which tend to predominate in commercial aircraft. The selection of noise control treatments to reach the lowest helicopter level in Figure 1 requires that the noise sources and their paths to the cabin be carefully measured so that minimal additional mass is applied and that the space occupancy is not affected. In this latter regard the passenger headroom is often critical as the cabin roof may well be a major radiating area.

The mechanical design of a helicopter presents a particular challenge to noise control engineers in that it is usually a tightly coupled structure encased with light rigid panels, which radiate sound efficiently, plus relatively thin side walls and windows, which have a poor transmission loss. The presence of machinery located on the structure plus the location of the passengers within the main structure further compound the difficulty.

The magnitude of the noise control task can be appreciated by reference to Figure 1 which shows that even an engineering program which produces 20-30 dB

reduction in cabin noise levels above 500 Hz from the bare interior is insufficient to meet commercial fixed wing jet aircraft levels. This is a formidable challenge for any noise control project even without the constraint of minimum weight. This unusually high target must therefore be met with the best possible understanding of the details of the noise mechanisms and transmission paths pertaining to the particular aircraft in question.

Cabin noise reduction may be achieved by modification to the source levels, the sound path, and the receiver environment. It is not often possible to reduce the source levels in helicopters as, for example, the impact of reducing the gear noise by altering the mesh forces has wide implications in terms of reliability and load carrying capability. It is thus a matter not lightly undertaken. Accordingly the reduction of cabin noise on existing helicopters is concentrated on modification of the paths between source and receiver.

For the purposes of further discussion it is convenient to consider separately the major groups of internal noise sources in a helicopter. These may be classified as propulsion machinery comprising engine and transmission, and turbulent boundary layer effects.

The intrusion of main and tail rotor noise into the cabin we have not found to be significant. Although some tail rotor blade rate harmonics may appear in a narrow band spectrum taken in the cabin, the treatment applied to the interior to correct other source levels also leads to reduction of these harmonics. The broadband turbulent boundary layer blade noise may be considered as a series of distributed dipoles which do not radiate effectively in the direction from blade to cabin.

PROPULSION MACHINERY NOISE - STRUCTUREBORNE

The tight structural coupling and proximity of the main gearbox and engine(s) to the cabin usually leads to the dominance of machinery noise in the cabin. Indeed, the main reduction gear mesh tone is usually a predominant sensation in the cabin. It should be noted that work is being performed on the feasibility and techniques for mesh noise reduction at the source; however this is beyond the scope of this paper. Figure 2 is a representation of the ways in which machinery noise arrives at the cabin - other paths are possible but in our experience, the identification of the paths outlined is sufficient for all practical purposes.

In an overall sense, we attempt to measure directly the individual contribution of the machinery vibration and its case-radiated noise to the sound field in the cabin. We then analyze individually the paths for the vibrations and noise. Consider as an example the methods used in analyzing the structureborne noise from a main rotor gearbox. A very simplified diagram of the helicopter as it relates to the structureborne noise from the gearbox is shown in Figure 3. There are always more than two mounts. The flexibility and damping of each is taken as the total that exists between the transmission attachment and the structural frame attachment. Also shown is the usual honeycomb overhead panel

hich forms an integral part of the structure and, at the same time, presents a
arge noise radiating area into the cabin. The walls of the structural frame
ill also usually form part of the cabin and may be significant radiators.

The measurement program typically includes the installation of accelerome-
ers at the points located by A in Figure 3 which are chosen to track the vi-
ration from source to receiver (passenger). Flight tests are then performed
ver the required operating range to obtain the magnitude of these vibration
evels which are recorded on seven or fourteen track tape machines. In this
egard it is important to obtain as much coincident time history of the accel-
ration levels as possible to allow the use of correlation analysis later on.
he actual direction and precise location of the accelerometers is a matter for
he experienced judgement of the experimenter as it is simply not feasible to
over all the possibly relevant vibration locations. The locations selected
re clearly influenced by his appreciation of the most likely structural paths,
nd will preferably involve the contribution of the structural designer.

In the flight tests, several cabin microphones will be employed to monitor
he total noise as well as to located obvious acoustic 'hot spots'.

A series of ground vibration tests are conducted with all aircraft systems
hut down in which vibration is applied to the transmission case from a shaker
ystem. The object here is to reproduce only that phenomenon which one wishes
o study without any other acoustic interference. Notwithstanding the tightly
oupled structure of the helicopter it is most desirable to attempt to shake
he gearbox in such a way that the correct distribution of vibration levels is
een in the mounts as occurs in flight. If the noise control program is being
erformed on just one helicopter then it may be necessary to adjust the shaker
ocation and direction to obtain the desired mount vibration distribution. If
owever, it is possible to perform the static tests on another sample then an
lternative method is to provide localized excitation at each mount pad. This
pportunity will also allow the measurement of mount impedance looking into the
tructure. This information, in conjunction with the measured vibration in
light, allows determination of the vibratory power flow into the structure.

Given that one can achieve the correct distribution of vibration on the
static test at the mount pads, we then take readings of the induced noise in
he cabin at the selected locations. This allows us to establish the transfer
function: "Transmission Vibration-Cabin Noise". During this test measurements
re made at the selected structural frame and honeycomb panel locations to
arrive at the proportion of total vibration at these points to that induced by
he transmission vibration alone.

The final step in the procedure is to apply the derived transfer function
to the actual measured inflight vibration levels to arrive at the contribution
to cabin noise levels from the transmission vibration alone.

Figure 4 represents a typical result obtained on a light helicopter and
illustrates the methodology. In the example shown in Figure 4, the transfer
function was based on average mount acceleration versus cabin noise and not on
the actual transmission acceleration. The resultant computed cabin SPL due

to the structureborne transmission noise agrees creditably with the overall result as will be seen later. There is however some discrepancy in the high frequency range which indicates that a more searching analysis could be worthwhile depending on the methods of noise control being contemplated. There are a number of traps for the unwary in this approach of which probably the most significant is the implied assumption of linearity. As most shakers are unable to drive the mechanical elements at frequencies and levels indentical to full-scale conditions, one must resort to testing at lower vibration and acoustic levels and applying linear scaling. This method is usually satis-factory for metallically mounted machinery components, but may be unsuitable for elastomeric mountings which exhibit a nonlinear load deflection curve, hence changes in isolation performance, particularly rear mount resonance may occur unless correct loading of the mounts is achieved. Depending on the particular helicopter design, it may be desirable to measure the isolation provided by the mounts during flight and compare this to the ground test runs with a view to verification of the mount performance.

Although constant bandwidth analysis is useful in determining the major contributors to the cabin noise spectrum, we find that the line density is nor mally so high that it is easier to analyze in 1/3 octave bands, rather than tr; to account for each individual discrete frequency. The use of correlation techniques has been used in some of the analyses, but in view of the highly correlated vibration signatures which appear at the mounts its success has bee: limited to a general overview of the contributions of transmission vibration t cabin noise. We find that the method presented here yields adequate accuracy and allows us to determine the most appropriate methods of noise control which may consist of mount modification, isolated interior panels, or a combination of these.

PROPULSION MACHINERY NOISE - AIRBORNE

The methods we employ to determine the contribution of case radiated nois to the cabin noise levels are similar in principle to those described above. Reference again to Figure 4 will show our assumed acoustic paths for airborne noise which may be grouped as either direct acoustic leaks through holes between the machinery and passenger compartments or as the transmission loss of the walls separating these compartments. The former case is usually easily spotted by visual inspection as well as by localizing hot spots with a roving microphone in the cabin. The latter case is investigated by measuring the acoustic levels in the machinery compartment at a number of locations during flight operations.

Static ground tests are then conducted to evaluate the transfer function between the noise in the machinery compartment and the cabin SPL. Single or multiple loudspeakers are placed in the machinery compartment to generate a acoustic field distribution similar to that observed during flight and simultaneous recordings are made of machinery and cabin noise from which the transfer function is derived.

586

Figure 5 demonstrates a typical result of such a test and this may be compared with the total noise in the cabin shown in a subsequent figure.

TURBULENT BOUNDARY LAYER NOISE

One source of broadband noise in the cabin is the turbulent boundary layer which is present over the exterior of the helicopter. At low forward velocities boundary layer noise will be negligible compared to other sources, but as helicopter speeds increase there is a likelihood that such noise will become important.

The turbulent boundary layer will excite the cabin structure and the windows. However, since the structure will be covered by insulation material and interior trim, the windows will be the important surfaces radiating boundary layer noise into the cabin. In order to estimate this contribution to cabin noise levels, it is necessary first to estimate the vibration of the window and then the acoustic radiation.

For typical helicopter speeds and window thicknesses, the acceleration power spectral density $S_a(f)$ of a window pane can be estimated using statistical energy analysis, under the assumption that resonant response is dominant. The window vibration can be estimated using

$$S_a(f) = \frac{0.143U_c^2}{2\eta C_L KM_s^2} \frac{S_p(f)}{f}$$

where $S_p(f)$ is the boundary layer pressure excitation at frequency f, U_c is the pressure convection velocity, η the panel loss factor, C_L the longitudinal wave velocity in the panel, M_s the panel surface mass density and K the radius of gyration. Acceleration spectra have been estimated for the cabin windows assuming $\eta = .01$ and $U_c = 0.8 \, U_o$ (U_o is the forward flight speed).

The above equation has been used to estimate one-third octave band levels for windows, on a helicopter flying at its normal cruise condition. The resulting spectrum is shown in Figure 6 where it is compared with levels measured on three window panels. The agreement is quite good. The forward door windows show higher levels than predicted, which are probably due to increased turbulence, as these windows are just downstream of the most extreme bends of the fuselage contour and also may be affected by increased turbulence due to rotor downwash. The passenger door window vibration is considerably greater than predicted at frequencies below 400 Hz as this panel responds in a resonant fashion to the rotor pressure field.

The radiated sound pressure levels can be estimated using an equation of the form

$$S_i(f) = \frac{\rho_o^2 c_o^2 \sigma}{\pi^2 \alpha} \cdot \frac{A_T}{A_\alpha} \cdot \frac{S_a(f)}{f^2}$$

where $S_i(f)$ is the power spectral density of the interior sound field, A_T is the transmitting area, A_α is the absorbing area with average absorption coefficient α, ρ_o is the air density, c_o is the speed of sound, and σ is the acoustic radiation efficiency of the transmitting structure. As an upper limit, σ can be assumed to be unity.

The value of $S_a(f)$ can be calculated, as indicated above, or obtained from measured vibration levels. An example of the latter case is shown in Figure 7, where the spectrum represents the acoustic power radiated by all windows of the helicopter cabin. In this particular case, the predicted sound levels resulting from turbulent boundary layer excitation were below those predicted for other sources. However the boundary layer contribution will become more important as helicopter speeds increase and noise control techniques are applied to other sources.

OVERALL RESULTS

Summation of the individual contributors calculated from the noise source diagnosis results should yield a value close to that measured in flight. Figure 8 shows the individual contributors determined for one model of helicopter and is a summary of data presented earlier with the addition of engine structureborne noise. Addition of these contributors yields the solid line shown in Figure 9 and by contrast the directly measured level in the cabin is shown dashed.

The general agreement is quite good considering certain simplifying assumptions such as averaging of the gearbox mount vibration levels. It is certainly adequate for the design of interior noise treatments although further refinements are necessary if it is desired to change the machinery mounting arrangements so as to modify the vibratory power flow or its distribution into the structure.

The estimated level above 2000 Hz in Figure 9 is about 2 dB below that measured and may indicate that an important contributor has been missed. However, given that the spectrum shapes are similar, it is more likely that there is an error in the transfer function determination. A more searching analysis is expected to resolve discrepancies of this order. A similar situation, although reversed, exists below 1200 Hz and may be caused by errors in the experiment where the same path contributes to two source mechanisms. As an example, when performing structureborne noise tests on the machinery, the casing will

588

radiate noise which can also arrive at the cabin via the acoustic path as well as the structural path under study. Experimental care and anticipation of this effect will ensure that nasty surprises are avoided.

CONCLUDING REMARKS

We have shown that by using relatively simple concepts together with careful experimental work it is possible to generate reliable data on which to base the design of high performance noise control treatments.

As an indication of the weight penalties associated with the noise control treatments derived from a thorough study of the source paths we have been able to achieve the best levels shown in Figure 1 for an added weight of some about 40 kg (100 lb) over that for the unfurnished interior. From this can be subtracted the weight of a normally furnished interior which would produce the levels shown in Figure 1. It has also been our experience that it is possible to redefine some interior furnishing arrangements, which have noise control built in, so that no weight penalty is incurred. This is achieved by removing and relocating or redesigning the noise control treatments to obtain the best efficiency.

REFERENCE

1. Wilby, John F. and Smullin, Joseph I.: Interior Acoustic Environment of STOL Vehicles and Helicopters. Presented at NOISE-CON 77, 17-19 October, 1977, Hampton, Virginia.
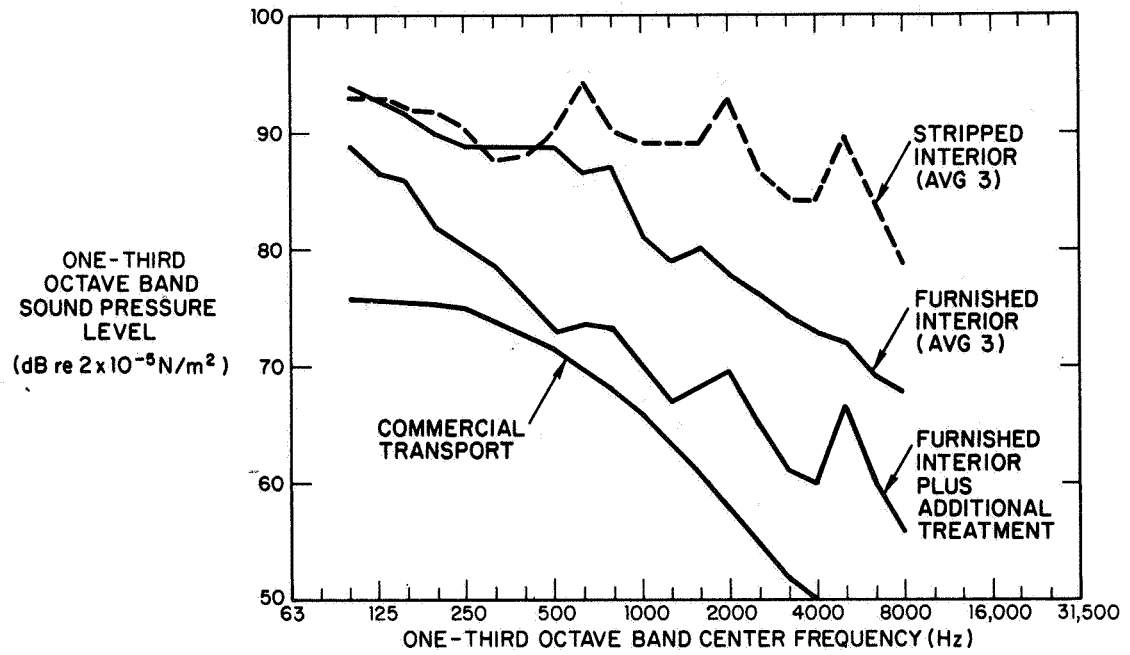
Figure 1.- Typical helicopter interior noise.
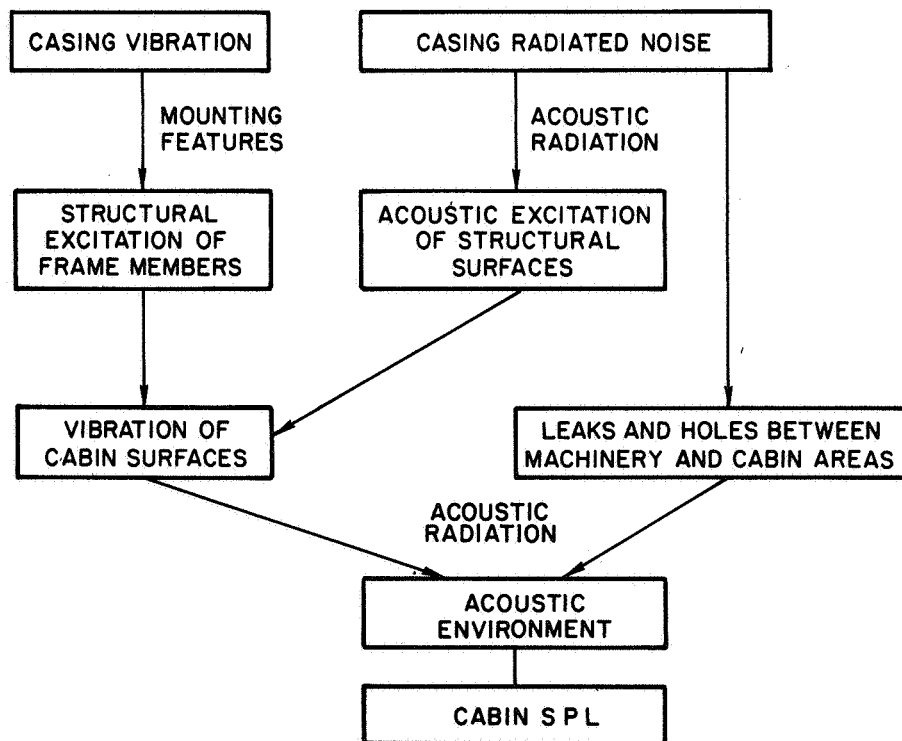
Figure 2.- Paths of engine and gearbox noise to the cabin.

590

MAIN ROTOR
TRANSMISSION

MOUNT

MOUNT

STRUCTURAL
FRAME

CABIN OVERHEAD
HONEYCOMB PANEL
(RIGIDLY ATTACHED
TO THE FRAME)
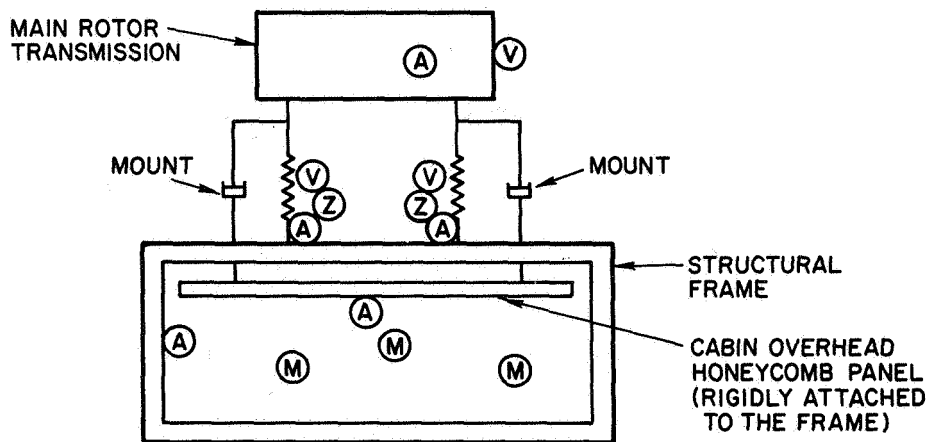
(A) DENOTES ACCELEROMETER LOCATIONS

(M) DENOTES MICROPHONE LOCATIONS

(V) DENOTES SHAKER LOCATIONS

(Z) DENOTES IMPEDANCE MEASUREMENT LOCATIONS

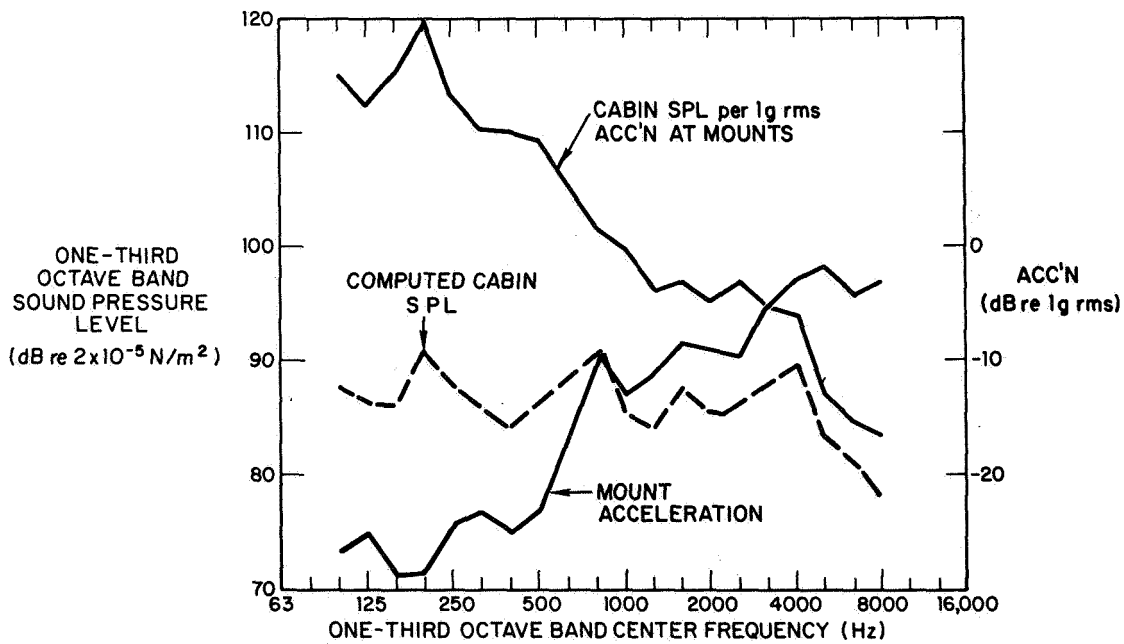Figure 3.- Simplified diagram for transmission noise structureborne into cabin.

ONE-THIRD
OCTAVE BAND
SOUND PRESSURE
LEVEL

$(dB \ re \ 2 \times 10^{-5} \ N/m^2)$

CABIN SPL per lg rms
ACC'N AT MOUNTS

COMPUTED CABIN
S PL

MOUNT
ACCELERATION

ACC'N
(dB re lg rms)

ONE-THIRD OCTAVE BAND CENTER FREQUENCY (Hz)

Figure 4.- Typical result of structureborne transmission noise test.
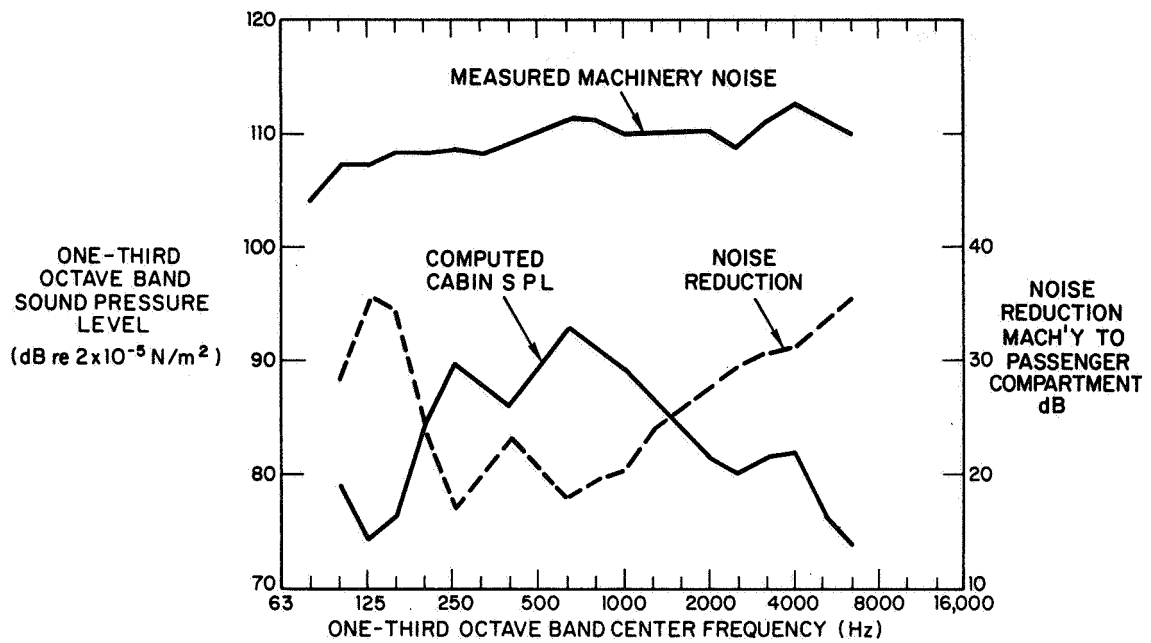
Figure 5.- Computation of cabin noise due to airborne machinery noise.
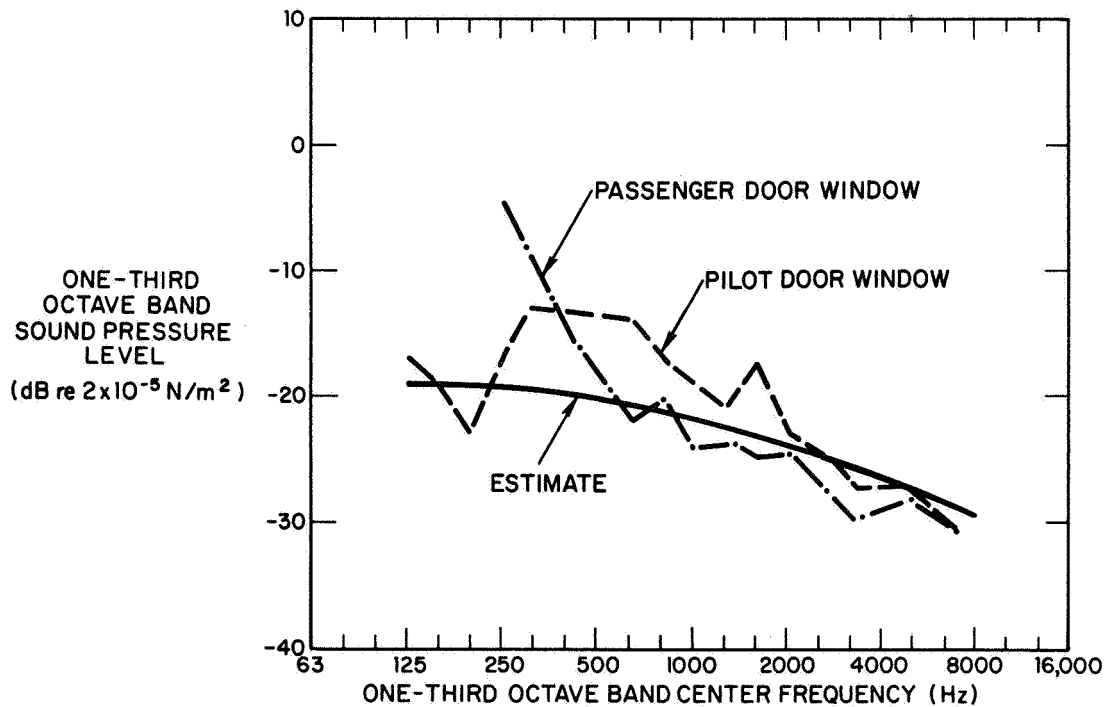
Figure 6.- Cabin window vibration levels - computed contribution of turbulent boundary layer.

592
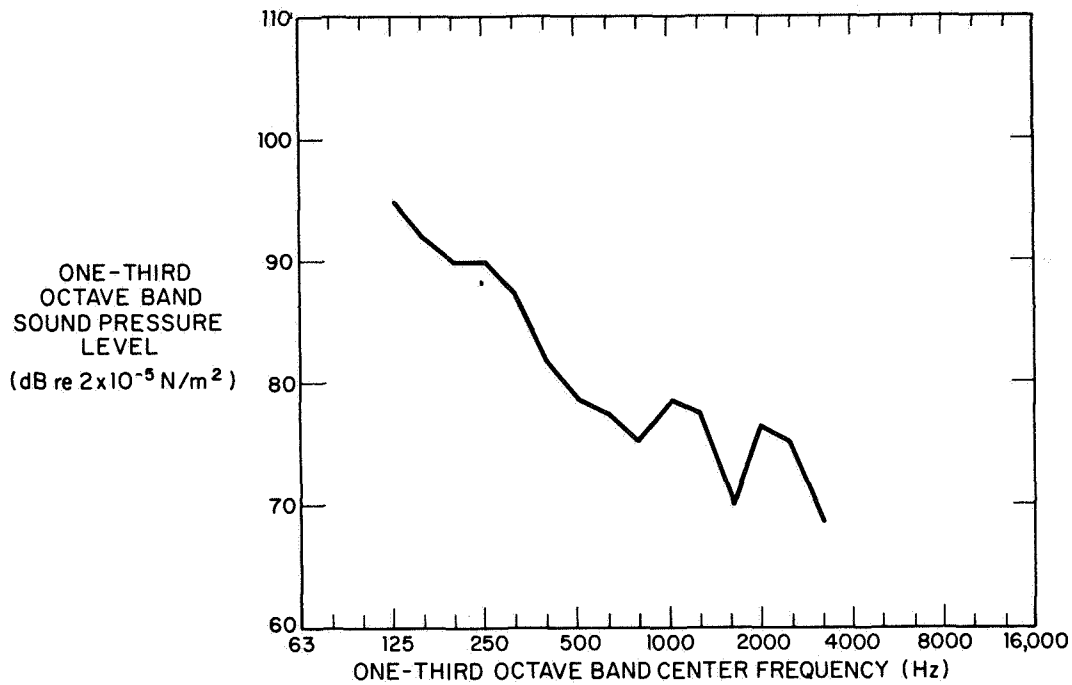
Figure 7.- Predicted cabin noise level induced by turbulent boundary excitation of cabin windows.
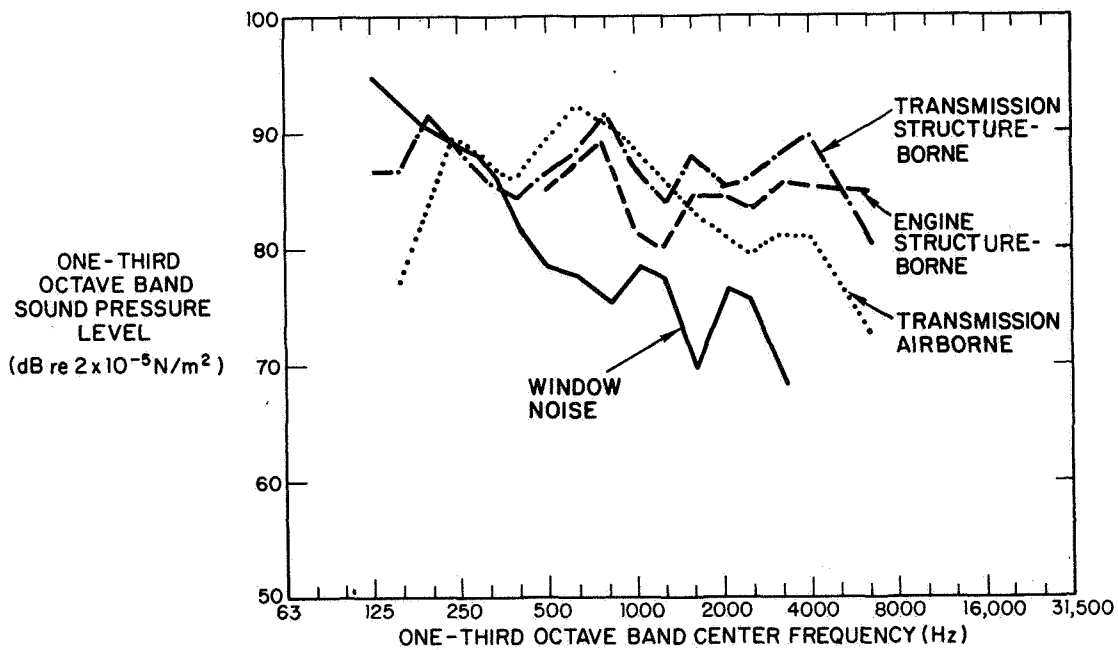
Figure 8.- Composite of noise spectra in cabin unfurnished interior.

ONE-THIRD
OCTAVE BAND
SOUND PRESSURE
LEVEL

$(dB\ re\ 2 \times 10^{-5}\ N/m^2)$

MEASURED LEVEL

SUM OF CONTRIBUTORS
ON FIG 8

ONE-THIRD OCTAVE BAND CENTER FREQUENCY (Hz)
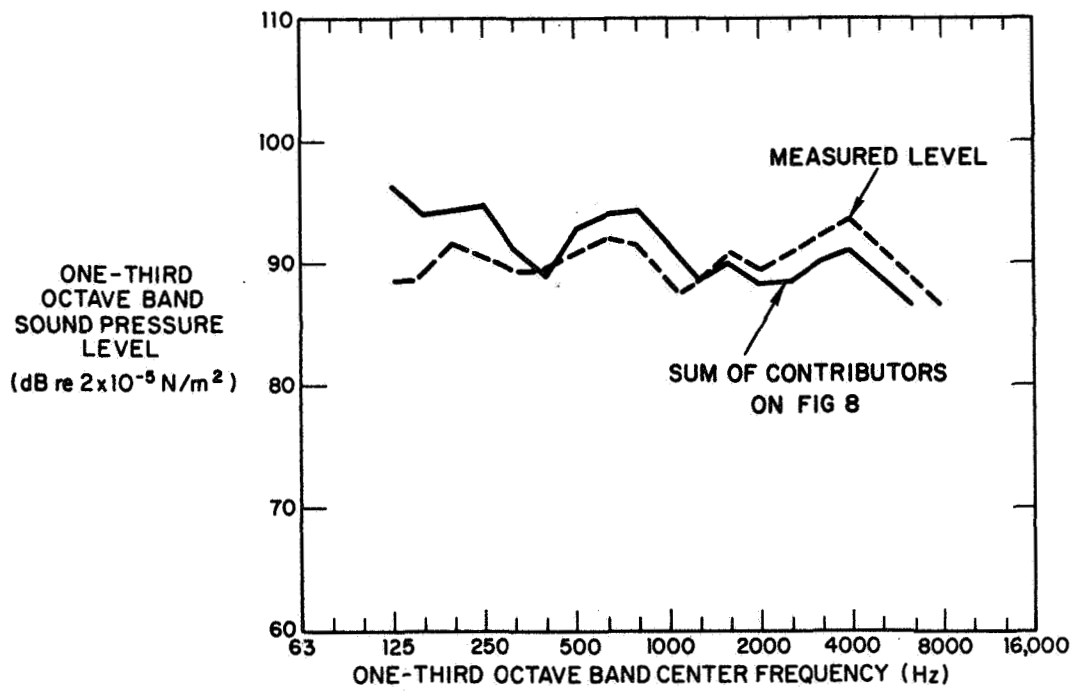
Figure 9.- Comparison of measured and computed cabin noise.

594

A PRACTICAL APPROACH TO HELICOPTER INTERNAL NOISE PREDICTION

Larry S. Levine and Jon J. DeFelice
Sikorsky Aircraft Division
United Technologies Corporation

SUMMARY

A practical and well correlated procedure for predicting helicopter internal noise is presented. The development of the method was supported by NASA Contract NAS1-14446. It accounts for the propagation of noise along multiple paths on an octave-by-octave basis. The method is sufficiently general to be applicable to conventional helicopters as well as other aircraft types, when the appropriate structural geometry, noise source strengths, and material acoustic properties are defined. A guide is provided for the prediction of various helicopter noise sources over a wide range of horsepowers for use when measured data are not available.

The method is applied to the prediction of the interior levels of the NASA/Sikorsky Civil Helicopter Research Aircraft (CHRA), both with and without soundproofing installed. Correlation with measured levels was very good. Speech Interference Level (SIL) was predicted within 1.5 dB at all conditions. A sample problem is also shown illustrating the use of the procedure. This example calculates the engine casing noise observed in the passenger cabin of the CHRA.

INTRODUCTION

Design efficiency has become an increasingly important characteristic in the helicopter industry as manufacturers strive to improve aircraft performance and operators strive to hold operating costs down. As cabin internal noise requirements become more stringent for increased passenger comfort, soundproofing weight becomes an important issue. A designer needs to know the acoustic environment in a bare aircraft cabin to be able to define an effective soundproofing configuration. It would be a waste of valuable aircraft weight-empty to carry many pounds of soundproofing in areas where they are not needed. But it would also be a serious error if an interior failed to meet the design requirement because not enough soundproofing was used. What is needed is a practical, internal noise prediction method that can provide the distribution and spectral content of the cabin noise signature. The goal is to substitute an analytic evaluation of an interior configuration into the noise model to determine the most efficient placement of treatment weight.

· There are many challenges in attempting to formulate and predict helicopter internal noise. The noise observed in a helicopter cabin is produced by several, widely varying source types. For example, rotor noise is generated by the aerodynamic forces of lift and drag. Trans-

mission noise is generated by the mechanical forces transmitted in gear tooth contact. Further complicating the formulation, a given source's noise may be propagated via different means: airborne, structure-borne, or both.

The noise sources that, in general, make a significant contribution to cabin levels are the main transmission, engines, rotors, and boundary layer. Transmission noise is composed of discrete tones at gear clash frequencies and their harmonics and is propagated as both airborne and structure-borne noise. It dominates cabin noise for several reasons. First, the transmission is coupled to the lightly damped airframe which acts as an efficient radiator. Second, primary clash frequencies are high and often fall within the ear's range of peak sensitivity: 500-2000 Hz. Finally, discrete tones are more annoying than broadband noise of the same level. Engine noise is broadband, peaking at 250-500 Hz, except for the compressor shaft rotational and inlet vane passage tones. Its propagation is both airborne and structure-borne and it contributes to the cabin noise spectrum in practically every octave. Rotor noise harmonics are found at the lowest octaves. Their propagation is airborne, but because soundproofing is not very effective at these frequencies, rotor harmonics are difficult to keep out of the cabin. Boundary layer noise is broadband and high in frequency. For this reason it is relatively easy to treat.

An internal noise prediction method must, therefore, be many-faceted. It must integrate ideas from such diverse areas as aerodynamic and structure-borne noise, radiation and propagation effects, material transmission loss and absorption, and rotor, engine, and gear noise source strength prediction. Even though the method must represent a complex physical system, it must also be simple enough to apply within realistic constraints of time and effort. Ideally, it should be sufficiently flexible to be useful in preliminary design as well as in the detail design stage with specific (possible measured) data.

The method discussed in this paper has those capabilities. While a more detailed development and exercise of this method is presented in Reference 1, this paper will serve as a guide to its development and use. The user can assemble the noise model in whatever detail desired. When specific test data is not available for individual noise sources, the generalized prediction methods will provide a reasonable guide. These methods predict rotor, engine, gear, and boundary layer noise source strengths over a wide range of helicopter operating parameters. A means of estimating panel transmission loss based on the barrier's mass, stiffness, and physical dimensions is also included to supplement the user's data base.

The approach of the method is to follow the propagation of each noise source to the observer's location. This may occur via more than one path so each must be dealt with separately. The properties of all intervening barriers and cavities are considered and applied to the sound transmitted through each. This allows one to account for the room acoustics and to show the relative importance of the direct radiated

596

versus the reverberant fields. The frequency breakdown uses the nine preferred octave bands from 31.5 Hz to 8000 Hz (Reference 2). Most aircraft noise specifications are in octave format. Of prime importance are the three SIL or Speech Interference Level octaves: 500, 1000, and 2000 Hz. These frequencies tend to govern an observer's judgment of a noise environment. Not only is human hearing most acute in this range, but the voice also appears primarily within these three octaves.

The method considers two forms of sound propagation, airborne and structure-borne. Conventional room acoustics is used to represent airborne propagation. For the frequencies and cabin dimensions involved, this approach is reasonable. While cabin standing waves cannot be predicted with this technique, it is assumed that noise measurements are spacially averaged. Only at the lower frequencies, where wavelength and cabin dimensions are of the same order, do the assumptions begin to break down. The propagation and radiation of structure-borne noise is a difficult process to analyze in an exact form. So many unknowns exist in describing the properties (mass, stiffness, and damping) of complex structures that a very simplified approach has to be employed to obtain a workable solution. Some gross assumptions are made concerning the blockage of structure-borne noise at turns, structural breaks, and at heavy frames. These assumptions serve to define the extent and shape of the radiating areas. Skin panels and frames are assumed to radiate uniformly within the areas bounded by structural breaks and equally well at all frequencies. While this is not entirely accurate, present knowledge of the subject is insufficient to permit a more specific analysis. It will remain for further work in the areas of structural impedance and radiation efficiency to formulate an exact solution of the program for arbitrary structures.

SYMBOLS

A_b	rotor total blade area, ft^2
$C, C_0, C_1, \ldots$	directivity/distance factor
C_{avg}	average directivity/distance factor
c	speed of sound (sea level std), 340 m/sec (1116 ft/sec); blade chord, ft
f_s	rotor broadband noise peak frequency, Hertz
f_o	boundary layer peak frequency
h	projected blade thickness, ft
I, I_{obs}	acoustic intensity, watts/m^2
I_o	reference intensity, 10^{-13} watts/m^2

L	radiating surface dimension, ft
m	harmonic number
N	number of cavities
q	dynamic pressure
$R, R_0, R_1, \ldots$	room constant; distance to observer, ft
r_1	near-field distance
r_2	far-field distance
S_T	total area
S_s	source area
$S, S_0, S_1, \ldots$	barrier area
T	thrust, pounds
t	blade thickness, ft
U_∞	free stream velocity
V_t	rotor tip speed, ft/sec
W, W_i	acoustic power, watts
W_T	total acoustic power, watts
X	distance from leading edge
α	absorption coefficient
$\bar{\alpha}$	average room absorption coefficient
Δ	non-dimensional fluctuating pressure levels
δ	boundary layer momentum thickness
δ^*	boundary layer displacement thickness
ε	% leakage
θ	blade linear equivalent twist; degrees
ρ, ρ_i	density of air, intensity ratio
Σ	sum

598

σ_i	radiating surface area ratio
τ	transmission coefficient
τ_{eff}	effective transmission coefficient
ω_i	radiating surface power ratio

CONVERSION FACTORS

To convert from	To	Multiply by
ft	m	0.3048
ft^2	m^2	0.0929
horsepower	kW	0.7457
lbm	kg	0.4536
lbf	N	4.448
lbf/ft^2	N/m^2	47.88
$slugs/ft^3$	kg/m^3	515.4

FORMULATION OF THE MODEL

Approach

There are two types of acoustic processes that must be expressed mathematically to predict the internal noise environment. They include the airborne propagation of sound through several cavities and structure-borne propagation over large radiating surfaces, shown in Figure 1. These two propagation modes are the paths by which sound energy reaches the cabin.

It is convenient to break the cabin down into elementary radiating surfaces. The directivity characteristics of these simple radiators determine the direct sound field for a given observer position. The standard equations of room acoustics are used to establish the reverberant field. The two fields are combined to form the complete internal noise environment.

Consider an arbitrary surface of some area S to be radiating noise (Figure 2). The total energy emitted by the plate is W (watts). The sound power level (PWL) of this radiating plate relative to a standard source radiating 10^{-12} watts (W_0) is

$$(1) \quad PWL = 10 \log W/(W_0)$$

The intensity I (watts/m^2) on the surface of this plate (outgoing energy per unit area) is related to the plate's area, S. Since

$$W = I \cdot S \qquad or \qquad I = W/S$$

then the Intensity Level (IL) is

$$IL = 10 \log \frac{W}{W_0} \frac{1}{S} = 10 \log W/W_0 - 10 \log S$$

or

$$(2) \quad IL = PWL - 10 \log S$$

The sound pressure level (SPL) actually observed at an arbitrary point in a room is given by the sum of both the reverberant and direct radiated components. Different types of acoustic sources radiate differently depending on the source type and its extent in space. The point source radiates its power symmetrically about any sphere with that source at its center. Because of spherical spreading, the SPL observed drops off 6 dB per doubling of distance from the source. However, for finite line or surface sources this decay with distance is not the same. The works of E. J. Rathe (Reference 3) and R. B. Tatge (Reference 4) deal explicitly with this subject. Close to a line source, SPL drops off at a slow rate, -3dB/doubling. As the distance to the observer becomes much greater than the source length the roll-off increases to the rate of a point source, -6dB/doubling. Tatge developed several curves which plot the roll-off in observed sound pressure level with distance for one circular and several rectangular sources of different aspect ratios. They are non-dimensionalized with respect to distance in terms of the source dimensions and assume that the observer is either over the center of the source or in its plane.

Recalling equation (2), it would be convenient to determine the observed SPL just by adding a correction factor. This factor would account for source shape and the distance and orientation of the observer to it. Rewriting (2):

$$(3) \quad SPL = PWL - 10 \log S + Correction$$

On the radiating surface, the term would account for pressure doubling. Far away from the source it would show a 6 dB reduction with each doubling

600

of distance. This is exactly what Tatge does in his work. The curves
are derived for radiation normal to a surface's center or in-plane from
the mid-point of one edge (See Figure 3). Tatge's curves are in terms of
dB. These curves were replotted in terms of their antilogs:

$$C = 10^{Corr./10}$$

Equation (3) is then redefined as

$$(3A) \quad SPL = PWL - 10 \text{ Log } S + 10 \text{ Log } C$$

Figures 3-7 plot C for rectangles of 1:1, 2:1, 4:1 and 8:1 aspect ratios
and for a circular disk, respectively. Distance is non-dimensionalized
in terms of the source's long dimension. One may interpolate between
curves to find values of C for intermediate aspect ratios. When the
observer point is not directly over the center of the radiating surface,
the distance from the point to the source center may be used as an approx-
imation. Equation 3A formulates the direct field due to elementary
radiating surfaces and may be used with Figures 3-7 for a given source
type and observer location.

When describing how sound is attenuated in passing through a barrier,
we speak of the barrier's transmission loss (TL). Transmission loss
refers to that portion of the incident pressure that is dissipated or
reflected. The wall's sound transmission loss (STL) can be expressed in
terms of a transmission coefficient τ:

$$(4) \quad STL = 10 \text{ Log } \frac{1}{\tau}$$

The transmission coefficient τ is really the fraction of the incident
pressure that is transmitted through the barrier:

$$(5) \quad \tau = 10^{-(STL/10)}$$

As τ goes to 1, all of the pressure is transmitted and STL goes to 0.

The effective transmission loss (or the effective transmissibility τ_{eff})
of a barrier made up of more than one section lies somewhere between the TL of
each individual section. For a barrier of total area S, composed of N sections
whose τ's are given by τ_1, τ_2... τ_N, the net ETL is given by

$$ETL = 10 \text{ Log } \frac{S}{S_1\tau_1 + S_2\tau_2 + \ldots S_N\tau_N} = 10 \text{ Log } 1/\tau_{eff}$$

This relation can be used to model the presence of an acoustic leak in
the panel. Consider a hole (where $\tau = 1$) of some fraction ϵ of a panel's
total area. Assume a uniform transmission loss over the rest of the area
(τ_1). Then the effective transmission loss of the entire panel is given
by

$$\tau_{eff} = (1-\epsilon)\tau_1 + \epsilon$$

601

Take ε = .01 (1% leakage) as an example. The quantity 1-ε is .99 $\simeq$ 1.0; then

$$\tau_{eff} = \tau_1 + .01$$

Note that for a high transmission loss panel, τ is very small. The limiting value of τ_{eff} is .01, meaning that the maximum ETL possible is 20 dB. Should the area of the acoustic leak be anything larger than .1% of the total area, the net ETL of the panel will be dramatically reduced. Figure 8 illustrates the importance of leakage to panel transmission loss performance. It plots the actual TL obtained from a panel designed for a specific value but suffering from leakage effects. From the figure, it is seen that a panel designed for 40 dB attenuation at a specific octave will yield only 20 dB in the presence of 1% leakage. An efficient interior is usually designed for 0.1% leakage.

The sound field inside an aircraft cabin or any other cavity is composed of both direct radiated and reverberant components. Direct radiation, as the name implies, involves only one path between the source and receiver. Reverberation, on the other hand, involves multiple paths because of reflections from the cavity walls. The ability of a wall to absorb sound is the same quality that distinguishes an acoustically "live" (reverberant) room from an acoustically "dead" one. The absorption coefficient α represents that fraction of the incident pressure that is dissipated when the wall would otherwise be a perfect reflector. When very little energy is dissipated at each reflection, the sound pressure in the cavity due to a source can build up to many times the corresponding free-field value. In a highly reflective room, these levels can grow by 10 dB or more. In this case, it is highly advantageous to add absorption. To reduce the internal levels by 10 dB through blockage (transmission loss) might require adding several hundred pounds of interior weight. The addition of absorptive material into the cabin will reduce the reverberant sound field by dissipation at each reflection. To achieve the same reduction using absorption, only a small weight penalty is required since acoustically absorbant materials such as fiberglass batting and polyurethane foams are extremely light.

The acoustic liveness of a room depends upon the room constant R. It is in units of length^2 and represents the area of perfectly absorbent material present in the room. Embelton (Reference 5 - Chapter 9) derives R as follows: The absorption coefficient of a wall at one octave is given by α. If the total surface area of a cavity is given by

$$(6) \quad S_T = \sum_{i=1}^{N} S_i$$

1en the cavity's average absorption coefficient is defined as

$$(7) \quad \bar{\alpha} = \frac{\sum\limits_{i=1}^{N} S_i(\tau_i + \alpha_i)}{S_T}$$

nd, subsequently, the room constant becomes

$$(8) \quad R = \frac{S_T \bar{\alpha}}{1 - \bar{\alpha}}$$

The Equations of Multibarrier Acoustics

We now have all the tools required to derive the equations governing he propagation of sound through an arbitrary number of cavities. Figure shows a source cavity (0) and an observer cavity (1). The formula that xpresses the impinging sound pressure level SPL_0 on the outlet wall in erms of the source power level PWL_s, source area S_s, room constant R_0, nd directivity/ distance term C_0 is given by

$$(9) \quad SPL_0 = PWL_s - 10 \, Log \, S_s + 10 \, Log \, (C_0 + 4/R_0)$$

quation (9) repeats quantitatively that the SPL observed at an arbitrary oint in a cavity is the sum of both the directly radiated and reverberant components.

The sound pressure level transferred through barrier 0 into cavity 1 SPL_{01} is given by the impinging sound pressure level SPL_0 minus the arrier's sound transmission loss STL_0, or

$$(10) \quad SPL_{01} = SPL_0 - STL_0$$

$$= PWL_s - 10 \, Log \, S_s + 10 \, Log \, (C_0 + 4/R_0) - STL_0$$

Recall STL_0 is given by $10 \, Log \, 1/\tau_0$ in equation (4). The power level entering cavity 1 (PWL_{01}) is the intensity times the barrier area, or

$$(11) \quad PWL_{01} = SPL_{01} + 10 \, Log \, S_0$$

$$(11A) \quad PWL_{01} = PWL_s - 10 \, Log \, S_s + 10 \, Log \, (C_0 + 4/R_0) - 10 \, Log \, 1/\tau_0$$
$$+ 10 \, Log \, S_0$$

PWL_{01} is now the sound power source in cavity 1. Again applying Equation (9), the SPL impinging on the observer in cavity 1 (SPL_1) is given by

$$(12) \quad \text{SPL}_1 = \text{PWL}_{01} - 10 \text{ Log } S_0 + 10 \text{ Log } (C_1 + 4/R_1)$$

By substituting equation (11A) SPL_1 may be expressed in terms of the original source power level

$$(13) \quad \text{SPL}_1 = \text{PWL}_s - 10 \text{ Log } S_s + 10 \text{ Log } (C_0 + 4/R_0)$$

$$+ 10 \text{ Log } \tau_0 + 10 \text{ Log } (C_1 + 4/R_1)$$

As more cavities are added, the terms can be grouped together. For N cavities, the sound pressure level in cavity N is given by

$$(14) \quad \text{SPL}_N = \text{PWL}_s - 10 \text{ Log } S_s + 10 \text{ Log } \Big[(C_0 + 4/R_0)(C_1 + 4/R_1)$$

$$\ldots (C_N + 4/R_N) \Big]$$

$$+ 10 \text{ Log } \Big[(\tau_0)(\tau_1)(\tau_2) \ldots (\tau_{N-1}) \Big]$$

It is interesting to consider some limiting cases. As STL→0, τ→1. If there were no barriers, the product of all the τ's would be 1. Since Log(1) = 0, there would be zero barrier attenuation. As the walls become either more transparent or absorptive, R grows larger and the component due to reverberant build-up disappears. Comparing the relative magnitude of the terms C and 4/R will show whether direct radiation or reverberation dominates the sound field. The proper treatment for noise reduction becomes apparent. Adding absorption will reduce the reverberant component only, while adding transmission loss will reduce the direct radiation. This points out the need for a balanced treatment, in that over-treating one component does nothing for the other. Should the source impinging on S_0 be in the open air, such as with rotor noise, SPL_0 reduces to

$$(15) \quad \text{SPL}_0 = \text{PWL}_s - 10 \text{ Log } S_s + 10 \text{ Log } C_0$$

Hence, when there is no source cavity and the sound pressure level impinging on wall S_0 is already known, the terms in equation (14) that are on the right hand side of equation (15) can be replaced simply with SPL_0.

Structural Radiation

Radiation by structural members is difficult to predict without measured values of structural impedance or mobility. Point (attachments), line (frames, stringers), and surface (skin) sources contribute to the total picture of structural radiation. Rather than attempt to identify each component, a more statistical approach should be used. Whole surfaces are assumed to radiate instead of discrete parts. The power fed

ito the cabin by the source is distributed among the individual radiating
irfaces. The resulting intensity distribution on each surface (power/unit
·ea) is assumed to be uniform.

When more than one surface within a cavity radiates, the expression
Jr the SPL at the observer can become very complex. Some simplification
an be accomplished by expressing the radiation intensity of the surfaces
1 terms of that of one surface. The total intensity observed at one
Jsition is the sum of the intensities propagated from each surface. If
1ere are N surfaces of area S_1, S_2, ... S_N radiating power W_1, W_2, ...
$_N$ then the total intensity observed is

$$(16) \quad I_{obs} = \frac{W_1}{S_1} \cdot C_1 + \frac{W_2}{S_2} \cdot C_2 + \ldots + \frac{W_N}{S_N} \cdot C_N$$

here C_1, C_2, ... C_N represent the directivity factors for the radiating

urfaces. Define a radiation intensity ratio $\rho_i = \frac{W_1/S_1}{W_i/S_i}$. Equation (16)
an be rewritten

$$(17) \quad I_{obs} = \frac{W_1}{S_1} \left[C_1 + C_2/\rho_2 + \ldots + C_N/\rho_N \right]$$

'hen the level is given by

$$(18) \quad SPL_{obs} = PWL_1 - 10 \, Log \, S_1 + 10 \, Log \left[C_1 + C_2/\rho_2 + \ldots + C_N/\rho_N \right]$$

The ratio ρ_i is really the ratio of the intensity of wall 1 to the
.ntensity of wall i. If we assume that the intensity level drops 6 dB at
ι corner or intersection with a heavy frame, as illustrated in Reference
>, Chapter 11, we are saying that the intensity is cut in half. In other
rords, the radiation ratio $1/\rho_i$ equals 1/2. This greatly simplifies the
:quation for the total intensity observed. A generalized expression for
3tructural radiation that includes panel transmission loss and room
ιcoustics follows:

$$(19) \quad SPL_{obs} = PWL_1 - 10 \, Log \, S_1$$

$$+ 10 \, Log \left[\tau_1(C_1 + 4/R) + \frac{\tau_2(C_2 + 4/R)}{\rho_2} + \ldots + \frac{\tau_N(C_N + 4/R)}{\rho_N} \right]$$

SOURCE STRENGTH PREDICTION OF MAJOR COMPONENTS

A guide to the prediction of noise generated by the major helicopter noise sources is presented. Trends are shown over a wide range of operating parameters. Specific examples are given based on the prediction of noise in the NASA/Sikorsky Civil Helicopter Research Aircraft (CHRA), a modified CH-53 A/D. The CHRA is a six bladed, single main rotor helicopter in the 15 900 kg (35,000 lb) weight class, powered by two G.E. T-64 engines.

Transmission Noise

The prediction of gear noise remains the most challenging of all the aspects of helicopter internal noise. Recent work by Grande et al (Reference 6) has demonstrated consistent trends with such variables as horsepower, specific tooth load, pitch-line velocity, manufacturing tolerances, and gear type. Other studies (Reference 7) attempt to correlate with the noise field surrounding the gearbox casing. NASTRAN® and other finite element models are just now being used at acoustic frequencies to analytically predict frequency response and acoustic radiation (Reference 8). It would be a difficult enough problem if the noise radiation stopped at the gearbox casing feet: a problem in direct radiation. However, the casing is mounted to an arbitrary airframe which is driven by the casing's foot motions: a problem in structure-borne noise. Differing airframe geometries, casing designs, and gearbox mounting techniques add a new set of variables to the noise problem. Figure 10 shows the trend in bare cabin gear clash tones with a variety of gearbox mounting types. The curves show the influence of the propagation path from the primary gear clash source to the radiating airframe. Scatter in the data can be attributed to local (but significant) frame resonances.

How, then, can the designer determine the cabin noise levels generated by the main transmission in an arbitrary helicopter? Some assumptions must be made about the propagation of structure-borne noise along the airframe. When driven by a gearbox foot, a heavy structure such as a forging will tend to radiate along its entire length. Intersections between heavy structure and light structure (skins and stringers) tend to reject structure-borne noise because of the impedance mis-match.

Beraneck considers the problem of the attenuation of structure-borne noise at corners and intersections (Reference 5, Chapter 11). He assumes that, with the same structural properties on either side of a 90° turn, a 3 dB attenuation in power will be observed. Similarly, crossing over a heavy frame is assumed to give a 3 dB reduction. On this basis, the analyst can examine the aircraft structure and establish the radiating areas.

As an example, figure 11 illustrates the radiating areas used to model the CHRA structure-borne noise induced by the main transmission. The model resulted from a review of the CHRA NASTRAN work performed by M. W. Dean (Reference 9). The primary area of radiation is the ceiling from

606

tation 282 to station 442. The frame at STA 442 is a major forging and
erves to carry the landing gear loads. The frame at STA 282 is also a
ajor structure and carries the engine support loads. Beyond these
tations, a 3 dB reduction in intensity is assumed. These areas are
ounded forward by the cockpit bulkhead (STA 162) and aft by the tailcone
ntersection (STA 522). Radiation from the sidewalls is assumed to
xtend from the ceiling (waterline 191) down to the sponson intersection
t waterline 132. The presence of the full cell and additional supporting
tructure within the sponson is assumed to stiffen the lower sidewall
ufficiently to eliminate its radiation of structure-borne noise.

In the absence of a detailed prediction scheme, some trends can be
eveloped based on measurements taken in untreated CH-53 aircraft.
igure 12 plots the observed relation between the total radiated acoustic
ower within the cabin at each gear clash fundamental and the consumed
P. This plot was derived from typical CH-53 data measured at Sikorsky.
here are separate lines for the three major gear types in the main
ransmission. For the CH-53D, the phased 2nd stage planetary gears
enerate nearly 15 dB less acoustic power than the unphased first stage
lanetaries. The main bevel is another 5 dB down from the second stage
lanetary level.

As discussed in the section on structural radiation, the observed
ound pressure levels can be determined from the radiation intensity of
he dominant surface ($PWL_1 - 10 \, Log \, S_1$), the room constant R_1, and
lirectivity/distance factors C_i (equation 22). The value of the sound
ower level radiated by the dominant overhead region can be expressed in
erms of the total power (From Figure 11) and the area ratios of the
econdary regions. If the total power radiated by the structure is given
y

$$(20) \quad W_T = W_1 + W_2 + \ldots + W_N$$

nd if the intensity ratio between the dominant (1) and secondary surfaces
(i) is assumed to be

$$(W_i/S_i)/(W_1/S_1) = 1/2$$

or

$$\frac{W_i}{W_1} = \frac{S_i}{S_1} \frac{1}{2} = \frac{\sigma_i}{2}$$

hen the total power radiated into the cabin by N surfaces can be expressed
s

$$(21) \quad W_T = W_1 \, (1 + \sigma_2/2 + \ldots + \sigma_N/2)$$

and

$$(22) \quad PWL_T = PWL_1 + 10 \, Log \, (1 + \frac{\sigma_2}{2} + \ldots + \frac{\sigma_N}{2})$$

607

Finally, the sound power level radiated by the dominant area (PWL_1) in terms of the total power from Figure 12 (PWL_T) is

$$(23) \quad PWL_1 = PWL_T - 10 \text{ Log } (1 + \frac{\sigma_2}{2} + \ldots + \frac{\sigma_N}{2})$$

This equation expresses the acoustic power radiated by the dominant ceiling area in terms of the total acoustic power associated with the gearbox. The gear noise octave spectrum can be generated by calculating the harmonic frequencies of each gear and applying the generalized harmonic spectrum of Figure 13. This spectrum was developed from the findings of Grande, et al. in Reference 6 and agrees well with observed CH-53D data. Once the harmonic frequencies and levels are determined, the total octave levels can be summed according to the bands into which the harmonics fall.

For example, the CH-53D consumes 3.7 MW (5000 HP) (approximately) in both 150 knot cruise and hover at sea level, operating near 15 900 kg (35 000 lb) gross weight. Figure 12 indicates that the acoustic power radiated at the fundamental gear clash frequencies are 134, 118.5, and 115 dB for the first stage planetaries, second stage planetaries, and main bevel gear, respectively. Gear noise harmonics occur at multiples of the first stage gear clash frequency of 527 Hz, and bevel clash frequency of 2710 Hz.

The following table of power levels summarizes the construction of the octave spectrum:

TOTAL ACOUSTIC POWER - PWL_T

Octave Level - dB

Gear	500 Hz	1000 Hz	2000 Hz	4000 Hz	8000 Hz
2nd Pl.	118.5	118.5	103.5	103.5	93.5
1st Pl.	--	134.5	134.5	119.5 119.5	109.5 109.5
Bevel	--	--	115.5	115.5	100.5 100.5
Sum	118.5	134.5	134.5	123.3	113.0

The above table refers to the total structure-borne acoustic power radiated in each octave because of the main transmission. Only a small percentage of this total power is radiated by the transmission casing

608

tself due to its relatively small exposed area and the fact that it is
overed by a rubber drip pan. Most of it is radiated by the cabin ceiling,
idewalls, and frame members. Substitute PWL_T into equation (23) to
etermine PWL_1. Substitute PWL_1 into equation (19) to determine cabin
oise levels.

Engine Noise

A review of turboshaft engine noise radiated by inlet, casing, and
xhaust reveals consistent trends with horsepower. Figure 14 shows the
ound power level radiated by several types of turboshaft engines over a
ide range of horsepower. This chart, derived from Reference 6 and
dditional Sikorsky data, follows the relation $PWL = 10 \ Log(HP) + 108$ dB.
ost of the noise is radiated by the casing and exhaust except when the
ngine blade passage frequency falls within the 8000 Hz octave. Then
nlet noise will dominate the uppermost octave. With the current CH-
3A/D engine installation, inlet noise is not heard in the passenger
abin. Therefore, inlet noise was not considered a major source in the
HRA cabin. By overlaying the spectra of the engines onto one plot
ormalized by HP, a close correspondence in shape was noted. A conserva-
ive, generalized spectral shape was averaged through the upper limit of
he data for casing, exhaust, and inlet power levels. These are plotted
n Figures 15, 16, and 17. By adding $10 \ Log \ (HP)$ to these non-dimension-
.lized spectra, a close estimate of the engine octave power levels can be
btained. Note that the T-64 is quieter in the lower octaves than the
;eneralized spectrum. To calculate the engine noise radiated into the
.ircraft cabin, the radiating areas must be determined. The firewall
.ransmits the casing noise while the aircraft skin aft of the engine
.acelle transmits the exhaust noise. The calculation procedure for
:ngine casing noise is demonstrated in the sample problem later in the
)aper. Exhaust noise contours are plotted in Figure 18. Note that the
.evels fall off sharply in the near-field: 15 dB down at a distance of
;wo exhaust diameters.

Rotor Noise

Few methods exist for the prediction of near-field rotor noise.
;utherland and Brown (Reference 10) provide an excellent technique for
letermining blade passage harmonic levels within a radius of one rotor
liameter. It has been applied successfully to the prediction of both
aain and tail rotor noise. The method is adequately explained in Reference
LO and will not be reproduced here. What is required is a means of
predicting near-field rotor broadband noise in terms of octave bands. Many
:omputer programs exist for the prediction of rotor noise in the far-
field. The method employed at Sikorsky Aircraft is based on the Lowson
and Ollerhead rotor rotational noise program (Reference 11) modified by
3. L. Munch to also predict rotor broadband noise (Reference 12). The
nethod has since been updated to include the effects of blade twist based
on extensive whirlstand testing. A graphical representation of this
nethod was prepared by W. Bausch of Sikorsky Aircraft and was included
in a comprehensive V/STOL noise prediction report authored by B. Magliozzi

(Reference 13). The approach taken will be to use this method to calculate both rotor rotational and broadband noise in the far-field and correct it back to near-field levels. The observer position will be on-axis to further simplify the equations.

Broadband Noise

Rotor broadband noise is a function of tip speed (V_t), thrust (T), total blade area (A_b), blade linear equivalent twist (θ), and distance to the observer (R). On the rotor axis, this relation is given by

$$SPL_{bb} = 20 \text{ Log } V_t + 20 \text{ Log } T - 10 \text{ Log } A_b - .56 \ (\theta)$$

$$- 20 \text{ Log } R + 21.9$$

This represents the overall rotor broadband noise level. To obtain the octave levels, a generalized spectrum shape based on the rotor Strouhal frequency is used. Rotor broadband noise has long been associated with the unsteady vortex shedding at the airfoil trailing edge. The exact mechanism is not clear but a scaling with Reynolds number is observed, hence the association with vortex shedding. The frequency of peak broadband noise (f_s) is well predicted in terms of blade chord (c), thickness (t) and velocity

$$f_s = .28 \ \frac{V_{.7}}{h_1}$$

where $\quad h_1 \ = \ c \sin \theta_{.7} + t \cos \theta_{.7}$

and $V_{.7}$ and $\theta_{.7}$ represent the velocity and blade angle of attack at the 70% radius, respectively.

It is convenient to set the peak frequency to the closest octave center frequency. For example, if f_s is found to be 225 Hz, set it equal to 250 Hz. Using the generalized octave spectrum of Figure 19, the individual octave levels, SPL_{OCT}, are determined by adding the corresponding band level SPL_{BL} to the overall broadband level, SPL_{OA}

$$SPL_{OCT} = SPL_{OA} + SPL_{BL}$$

Rotational Noise

The harmonics of blade passage for a hovering rotor can be determined from thrust, torque, tip speed, and twist. Because the thrust term dominates on-axis, the torque component will be neglected. Obtain the partial level SPL_T from Figure 20 corresponding to the rotor thrust (T). For each harmonic, m, calculate mB and find the corresponding partial level SPL_m from Figure 21. Find the correction for blade twist, SPL_θ from Figure 22. The sum of these partial levels for one harmonic, SPL_{mB},

610

epresents the total on-axis level for a hovering rotor at a distance of
00 ft. At any distance, R

$$SPL_{mB} = SPL_{T} + SPL_{m} + SPL_{\Theta} + 20 \ Log \ (\frac{R}{200})$$

The total rotor noise octave spectrum is obtained by adding the
otor harmonics in each octave, logarithmically, and combining these with
he respective broadband levels. In general, rotor noise dominates only
he lowest octaves. This is because of the rapid roll-off of rotor
armonics and the small amount of transmission loss provided by structural
laterials at low frequencies.

The problem now is to translate far-field octave band data into the
.ear-field. This can be accomplished by using the distance/directivity
:urve for a circular source from Figure 7. By taking the noise measured
or predicted) on the rotor centerline at 10 rotor diameters, and then
loving the levels in on the curve to the desired distance below the rotor
lead, an approximation to the near-field rotor spectrum is obtained. One
.mportant assumption is made for rotor noise very close to the rotor disk.
}ecause a rotor is not a solid surface radiator, it is assumed that C can
)e no larger than 1.0. Realistically, there is no pressure doubling in
;pace as there is near a wall. In equation form,

$$(24) \ SPL_{near} = SPL_{far} + 10 \ Log \ \frac{C(r_1/L)}{C(r_2/L)}$$

where r_2 is the far-field distance, r_1 is the near-field distance, and L
ls the rotor diameter. As an example, let L = 72 ft. If the octave
level measured at 720 ft is 100 dB and the level 7.2 ft under the rotor
ls desired, then

$$SPL_{near} = 100 + 10 \ Log \ \frac{C(7.2/72)}{C(720/72)}$$

}oing to curve 1 of Figure 7, C(.1) = 1.8 and C(10) = .001. However, C
:annot be greater than 1.0, so take C(.1) = 1.0. Then 10 Log (1.0/.001)
▪ 30 and

$$SPL_{near} = 100 + 30 = 130$$

Note that using a simple 6 dB/doubling of distance relation would have
given 140 dB for the near-field level. This technique can also be used
for tail rotors when in-plane levels are required by obtaining C from
curve 2 of Figure 7.

Boundary Layer Noise

In high speed flight, boundary layer noise can be a significant part
of the noise observed in the aircraft cabin. Airframe noise is generated
by any part of the aircraft structure protruding into the flow. It can

be especially intense when generated by struts, flaps, doors, or open cavities. However, the detailed prediction of airframe noise is beyond the scope of this report and will not be dealt with. The CH-53D aircraft is relatively clean in the airframe sense, with no major sources. Only the noise generated by the turbulent boundary layer will be considered. The method used for calculating boundary layer noise is due to Bies (Reference 14). His work is a summary of wind tunnel and aircraft measurements made of turbulent boundary layer pressure fluctuations over a wide range of Reynolds and Mach numbers.

The procedure is summarized as follows. Calculate the overall fluctuating pressure levels from the equation

$$(25) \qquad FPL_{overall} = 20 \ Log \ q + 84 \qquad dB$$

where q is the free stream dynamic pressure $1/2 \rho U_\infty^2$. The boundary layer displacement thickness is approximated by

$$(26) \qquad \delta^* = 0.0016 \ X$$

where X is the distance from the leading edge (assumed greater than 10 ft). The characteristic frequency is determined from

$$(27) \qquad f_o = 0.1 \ U_\infty / \delta^*$$

Figure 23 plots the non-dimensionalized fluctuating pressure levels Δ in 1 Hz octave bands. To determine the dimensional octave levels, use the following equations:

$$(28) \qquad SPL_{1Hz} = FPL_{overall} - 10 \ Log \ f_o + \Delta$$

$$(29) \qquad SPL_{octave} = SPL_{1Hz} + 10 \ Log \ (bw)_{octave}$$

where the octave bandwidth (bw) is given by $\dfrac{\sqrt{2}}{2}$ times the octave center frequency.

The following example calculated the boundary layer noise at station 342 on the CHRA fuselage at 150 knots (253.5 ft/sec). The dynamic pressure q is

$$q = 1/2 \ (.00238) \ (253.5)^2 = 76.5 \ lb/ft^2$$

$$FPL_{overall} = 20 \ Log \ (76.5) + 84 = 121.7 \ dB$$

The boundary layer momentum thickness is

$$\delta = 0.0016 \ (21) = 0.0336 \ ft$$

612

$_o$ is then given by

$$f_o = 0.1 \ (253.5/0.0336) = 754.5 \text{ Hz}$$

he following table lists the values of Δ obtained from Figure 23, the alues of SPL_{1Hz}, and the octave levels:

Octave frequency	$\%f_o$	Δ	SPL_{1Hz}	10 Log(bw)	SPL_{octave}
31.5	.04	-3	90	15	105
63	.08	-3	90	18	108
125	.17	-3	90	21	111
250	.33	-4	89	24	113
500	.67	-5	88	27	115
1000	1.34	-7	86	30	116
2000	1.67	-10	80	33	113
4000	5.30	-14	76	36	112
8000	10.60	-20	70	39	109

The SPL's of the above table indicate the fluctuating pressure levels on the outside skin induced by the turbulent boundary layer.

INTEGRATED METHOD

Checklist

A step-by-step checklist is presented below to summarize the process of translating an external source strength into an internal noise level.

1. Define aircraft structure and geometry.

2. Identify the major sources and paths.

3. Define the source strengths at the required operating parameters.

    a. Engine noise from Figures 14-18 and Equation (14).

    b. Gearbox noise from Figure 12 and Equations (23) and (19).

    c. Rotor noise from near-field data and Figure 7.

    d. Boundary layer noise from Equations (25)-(29).

4. Translate the source strengths into the cabin using Equation (14) or (19) as required:

    a. Determine C_i's from radiating surface size and distance to the observer via Figures 3-7.

    b. Obtain transmission loss data from a data base.

    c. Calculate room constant data from cabin dimensions and Equations (6) - (8).

    d. Apply Equation (14) or (19) octave by octave.

5. Tabulate and sum the octave data from each source and path to obtain total observed sound pressure level.

Application to Engine Casing Noise

The use of the equations of multibarrier acoustics will be demonstrated by working through the calculation of engine casing noise in the bare aircraft cabin (Figure 24). Figure 25 presents an idealization of the engine/nacelle arrangement. Having engineering drawings of the installation is essential in determining the physical dimensions required for the calculations. The complicated arrangement can be simplified by making a few assumptions. First, let the nacelle be a rectangular structure with the firewall corresponding to the outlet wall b_0. Next, let the source be a flat surface with dimensions equal to the engine's average cross-section. Faces a_0, e_0, and f_0 can be combined since they represent the cylindrical nacelle fairing. Face d_0 reduces to an open annulus around the tail pipe extension that serves as the engine cooling air exit. Face c_0 includes the surface area of the engine (which acts as an inner wall) as well as the fiberglass engine intake duct.

The nacelle fairing is made of reinforced fiberglass approximately 0.838 mm (0.033 in.) thick. There is one fire-fighting access hole in the fairing. The firewall, integral with the aircraft skin, is made of titanium. The presence of numerous stiffeners and doublers makes it necessary to use two average values of firewall thickness. Engineering prints indicate that 0.457 and 1.09 mm (0.018 and 0.043 in.) are appropriate values. The proportions are 59% and 41%, respectively. Geometric parameters come from the engineering drawings. Some allowances must also be made for leakage through access holes and joints. One percent has been found to be a good approximation.

Consider the nacelle cavity at the 31.5 Hz octave. Table I summarizes the data and shows how the room constant is calculated for that octave. Most of the walls are made up of two different materials. Wall a_0 (nacelle fairing) is built of .033 fiberglass (69.8 ft^2 area) but also has a fire-fighting access hole (.34 ft^2) in it. This serves to reduce the net trans-

ission loss of the wall. To calculate the effective transmission loss (ETL)
f a composite panel, use the relation

$$\frac{1}{\tau} = \frac{S_T}{S_1\tau_1 + S_2\tau_2}$$

id

$$ETL = 10 \, Log \, \frac{1}{\tau}$$

The absorption coefficient α for fiberglass at 31.5 Hz is .02. Then
+ α is 0.72. Multiplying by the fairing area (70.1 ft^2) then $S(\tau + \alpha)$
s 50.4 ft^2. Repeating the process for the other walls, the room constant R
t 31.5 Hz is calculated to be 101 ft^2.

Following the path of transmission into cavity 1, the directivity/
istance function C_0 must be determined to find the level impinging on
utlet wall b_0. The engine is approximately a 3 x 1 rectangle with long
ide dimension 6.7 ft. The distance r/L is $1.9/6.7 = 0.28$. There is
o chart for C for a 3/1 rectangle, so the average of the 2/1 and 4/1
alues must be taken. C_{avg} is 0.37. Table I shows that the ETL of the
irewall (b_0) is 9.7 dB and τ = .108 at 31.5 Hz. All that remains is to
ind the distance/directivity factor C_1 to account for the propogation
f the casing noise from the firewall to the cabin center. Figure 25 shows
hat the firewall is a 6 x 1 rectangle with long dimension 8.3 ft.
etting the observer be positioned under the main transmission, r/L
ecomes $4.4/8.3 = 0.53$. Taking the average between the 4/1 and 8/1
ectangular source curves, C_1 is 0.085. The work sheet of table II
ummarizes all of the data for each octave including the casing power
evel from the source strength data base. Source 0 on the work sheet is
he engine itself, while Source 1 is the firewall. All of the required
information is known and can now be entered into Equation (14). The
resulting SPL's are listed in the last column.

CORRELATION

The method was applied to the prediction of CHRA internal noise for
ooth the treated and untreated cases. The model included main rotor,
tail rotor, engine, main transmission and boundary layer noise.

The noise levels predicted in the bare cabin agree very well with
the measured data as shown in Figures 26-27. The best correlation
exists in the middle octaves which are dominated by gear noise. The SIL
is predicted within 1.2 dB. The lower octaves are high by 2-4 dB in
hover. This is due to an overprediction of main rotor noise which controls
the level of these octaves. This points out the shortcomings of using a
uniform, circular source to approximate a rotor disc. The correlation
improves in cruise. The upper octaves are underpredicted by as much as 10
dB in both hover and cruise. A review of the narrow-band spectra at these

615

flight conditions confirmed the existence of these high broadband levels over the gear clash harmonic tones. It is significant that this occurs at such high frequencies. Because of the large amount of transmission loss associated with most materials at the upper octaves, these upper octave levels should be very low. This implies that there is some direct radiatio from the skin surface or through a leak. The one source that could provide the necessary levels at the upper octaves is the engine. It is likely that engine-induced vibration was being fed to the firewall and surrounding frames via the engine mounts and forced structural radiation in this area. Engine-induced structure-borne noise was not considered in the calculations because of a lack of the appropriate data.

Correlation of the treated cabin levels shows some interesting effects (Figures 28 and 29). Predicted and measured levels agree very well in the upper octaves, unlike the bare aircraft case. This tends to confirm the contention that engine-induced vibration is being radiated by the skins or frames. The 500 Hz octave is underpredicted by 6 dB. This is due to the fact that the aft bulkhead was radiating a significant amount of structure-borne noise. This was confirmed during flight tests of the treated CHRA when a lead-vinyl curtain was placed over the bulkhead. The levels observed in the gear noise-dominated octaves dropped 2-6 dB. The levels in the 125-500 Hz octaves are underpredicted. This frequency region is dominated by main rotor and engine casing noise implying that there was some sort of leakage or panel resonance. It is probable that these sources entered the ECU ducting behind the valances. The treatment is not continuous over the frames where the valances are attached. Since there is not treatment within the ECU ducts, any noise entering would be free to propagate along the length of the ducting. The contribution of the ECU system was not included in the noise prediction method because an adequate model was not yet available.

Overall, the correlation of predicted levels with measured data is excellent. Comparisons indicate that the method could be improved by adding the effects of engine-induced structure-borne noise and developing a procedure that would account for the ECU ducting.

CONCLUSIONS

1. The integrated method presented provides an easily workable and correlated procedure for the prediction of helicopter internal noise. The method is sufficiently general to be applicable to helicopters and other aircraft types when the appropriate structural geometry, noise source strengths, and material acoustic properties are defined.

2. The levels predicted by the method for the CHRA correlate well with measured data in both hover and cruise. The hover SIL was predicted within 1.2 dB for the bare aircraft and 0.1 dB for the treated aircraft. In cruise, the SIL correlated within 0.2 dB for the bare aircraft and within 1.2 dB for the treated case.

616

3. An accurate definition of the problem is essential for good correlation between measured and predicted levels. This includes the definition of structural geometry, a proper identification of the paths of propagation, a correct estimate of source strengths, and an accurate data base of material acoustic properties (transmission loss and absorption).

4. The approximation of a uniform circular source distribution for near-field rotor noise used in this procedure was shown to slightly over-predict the levels very close to the rotor disc. A more exact model is required that accounts for the fact that most of the acoustic energy is generated by the outboard sections of the rotor disc and is not uniformly distributed.

REFERENCES

1. Levine, L. S. and DeFelice, J. J., "Civil Helicopter Research Aircraft Internal Noise Prediction", NASA Contractor Report, NASA CR-145146, April 1977.

2. USA Standards Institute: USAS-S1.6-1967 Preferred Frequencies and Band Numbers for Acoustical Measurement, 1967

3. Rathe, E. J., "Note on Two Common Problems of Sound Propagation," Journal of Sound and Vibration, 10(3), 472-479, 1969

4. Tatge, R. B., "Noise Radiation by Plane Arrays of Incoherant Sources, JASA Volume 52, Number 3 (Part I), 1972

5. Beranek, L. L., "Noise and Vibration Control", McGraw-Hill Book Company, 1971.

6. Grande, E. and Brown, D., "Small Engine Noise Prediction," Technical Report AFAPL-TR-73-79, Volume II, December 1973

7. Bowes, M. A., Giansante, N; "Helicopter Transmission Vibration and Noise Reduction Program", USAAMRDL-TR-77.14, June 1977.

8. Howells, R. W. and Sciarra, J. J., "Finite Element Analysis Using NASTRAN Applied to Transmission Vibration/Noise Reduction", Paper presented at Fourth NASTRAN Users' Colloquium at NASA-Langley Researc Center (NASA-TMX-3278), September 1975.

9. Dean, M. W., "Correlation of an Extended CH-53 Helicopter Nastran Model with Full Scale Aircraft Shake Test Data," NASA Contractor Report, NASA CR-145012, July 1976

10. Sutherland, L. C. and Brown, D., "Prediction Methods for Near Field Noise Environments of VTOL Aircraft," AFFDL-TR-71-180, May 1972

11. Lowson, M. V. and Ollerhead, J. B., "Studies of Helicopter Rotor Noise," USAAVLABS Technical Report 68-60, January 1969

12. Munch, C. L., "Prediction of V/STOL Noise for Application to Communit Noise Exposure," Dept. of Transportation Report DOT-TSC-OST-73-19, May 1973

13. Magliozzi, B., "V/STOL Rotary Propulsion Systems Noise Prediction and Reduction," Dept. of Transportation, FAA Systems Research and Development Service Report FAA-RD-76-49, May 1976

14. Bies, D. A., "A Review of Flight and Wind Tunnel Measurements of Boundary Layer Pressure Fluctuations and Induced Structural Response, NASA Contractor Report, NASA CR-626, October 1966

TABLE I.- CAVITY AND WALL NOMENCLATURE

WALL	A	B	C	D	E	F
$S(ft^2)$	70.1	11	73	.62		
S_1	69.8	4.5	10	.62		
ETL_1	1.5	14.5	1.5	0		
τ_1	.7	.035	.7	1		
S_2	.34	6.5	63			
ETL_2	0	8	27			
$\overline{\tau}_2$	1	.158	.0012			
ETL	1.5	9.7	10.1	0		
τ_{eff}	.7	.108	.097	1		
α	.02	.02	.02	0		
$\tau_{eff}+\alpha$	.72	.128	.117	1		
$S(\tau_{eff}+\alpha)$	50.4	1.41	8.5	.62		

	ft^2
$S_T = \sum\limits_{i=a}^{f} S_i$	154
$S\bar{a} = \sum\limits_{i=a}^{f} S_i (\tau_i + a_i)$	61
$\bar{a} = \dfrac{\sum\limits_{i=a}^{f} S_i (\tau_i + a_i)}{S_T}$	0.396
$R = \dfrac{S\bar{a}}{1-\bar{a}}$ ft^2	101
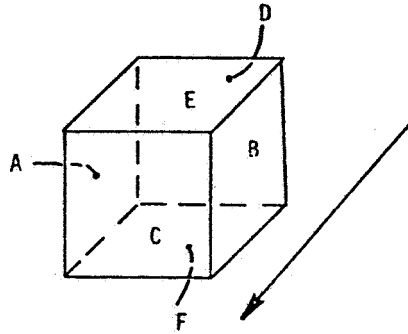
A - OUTBOARD
B - INBOARD
C - FORWARD
D - AFT
E - UPPER
F - LOWER

NOTE: For tone dominance use
transmission loss at
tone frequency.

$I\ ft^2 = .093\ m^2$

DIMENSIONS LISTED IN FEET
FOR COMPATIBILITY WITH
BARRIER EQUATIONS

TABLE II.- ENGINE CASING NOISE - BARE AIRCRAFT

SOURCE	AREA ft^2	TYPE	C
0	10.2	RECT.	.37
1	10.2	RECT.	.085
2			

* REFERENCE EQUATION (14)

1 ft^2 = .093 m^2

DIMENSIONS LISTED IN FEET FOR COMPATIBILITY WITH BARRIER EQUATIONS

BASIC DATA

OCTAVE	R_0	R_1	R_2	C_0+4/R_0	C_1+4/R_1	C_2+4/R_2	τ_1	τ_2
31.5	101	95		.41	.13		.108	
63	86.5	95		.41	.13		.11	
125	56.9	78		.44	.14		.068	
250	18	54		.59	.15		.022	
500	7.2	50		.93	.17		.011	
1K	5.29	53		1.1	.16		.007	
2K	4.41	54		1.3	.16		.0021	
4K	5.9	68		1.0	.14		.0018	
8K	7.49	70		.9	.14		.0007	

SUMMARY CALCULATION*

OCTAVE	SPL or PWL	PWL - 10 Log S	10 Log $(C_0+4/R_0)(C_1+4/R_1)(C_2+4/R_2)$	10 Log $\tau_1 \cdot \tau_2$	SPL_{obs}
31.5	118.8	108.7	-12.7	-9.7	86.3
63	126.8	116.7	-12.7	-9.6	94.3
125	129.8	119.7	-12.1	-11.7	95.9
250	130.3	120.2	-10.5	-16.5	93.1
500	130.8	120.7	-8	-19.6	93.1
1K	127.8	117.7	-7.5	-21.5	88.7
2K	128.8	118.7	-6.8	-26.8	85.1
4K	127.8	117.7	-8.5	-27.4	81.8
8K	132.3	122.1	-9	-31.5	81.8
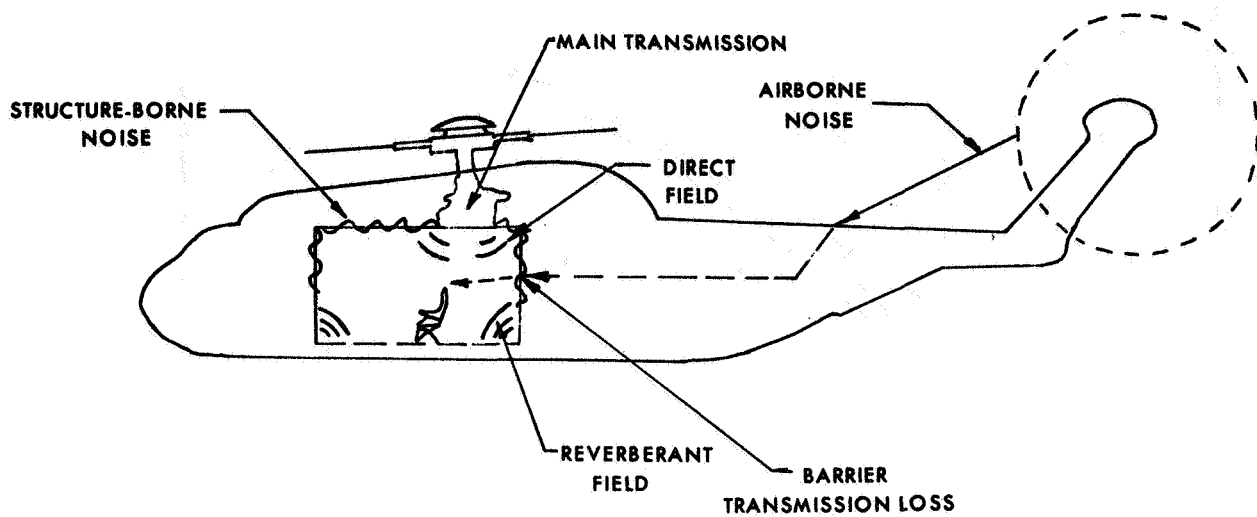
Figure 1.- Modes of propagation for cabin noise.

$$IL = 10 \, LOG \, \frac{I}{I_0}$$

$$PWL = IL + 10 \, LOG \, S$$
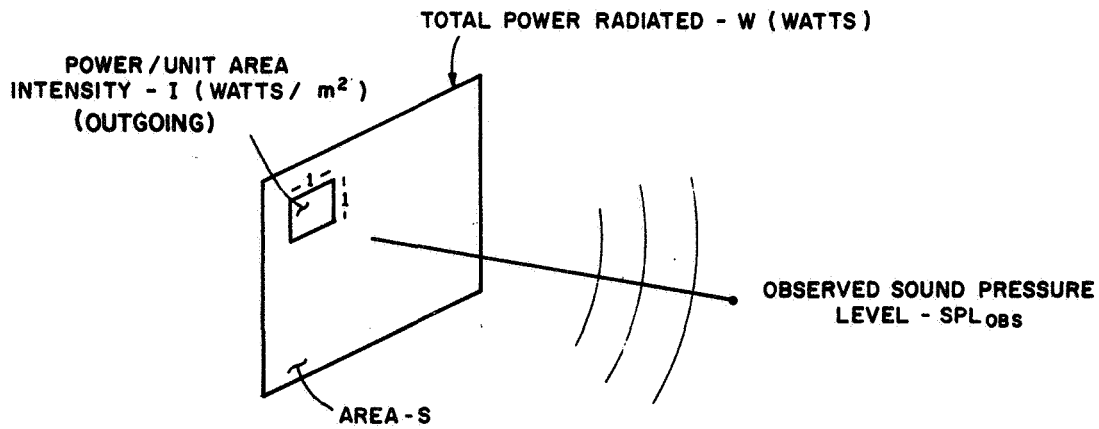
$$SPL = PWL - 10 \, LOG \, S + 10 \, LOG \, C$$

Figure 2.- The relation of PWL, IL, and SPL for a plane source.

621

Figure 4.- Directivity factor for a rectangular plate (2/1).

Figure 3.- Directivity factor for a square plate.

622
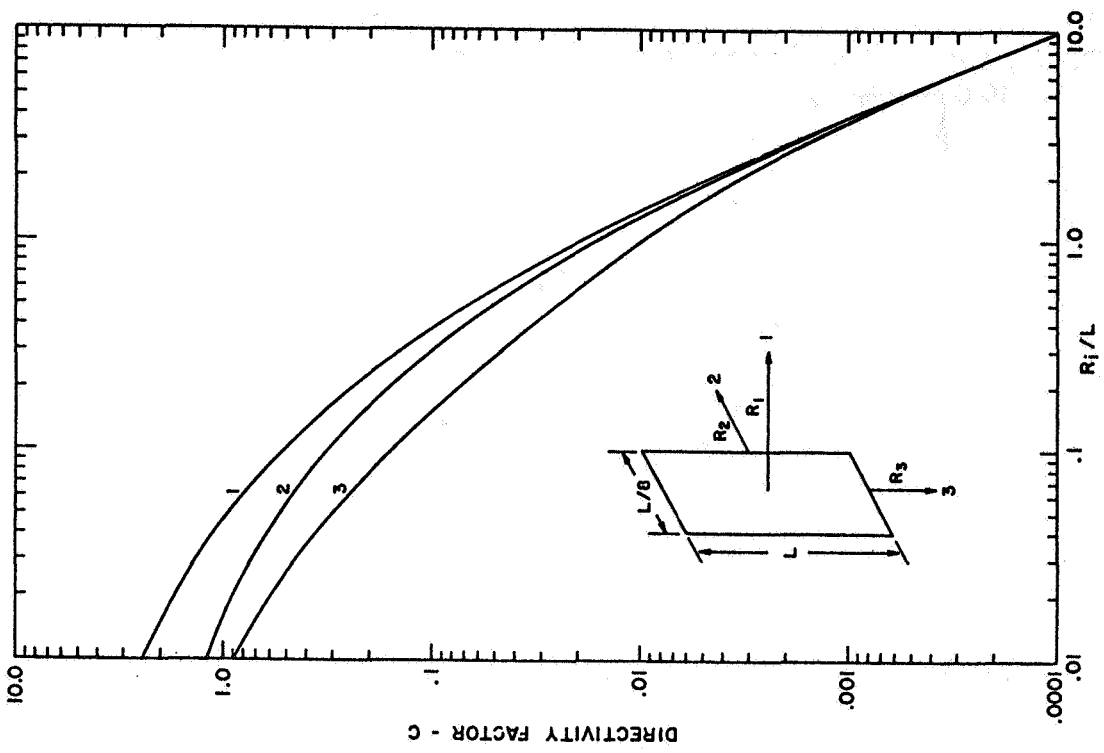
Figure 6.- Directivity factor for a rectangular plate (8/1).
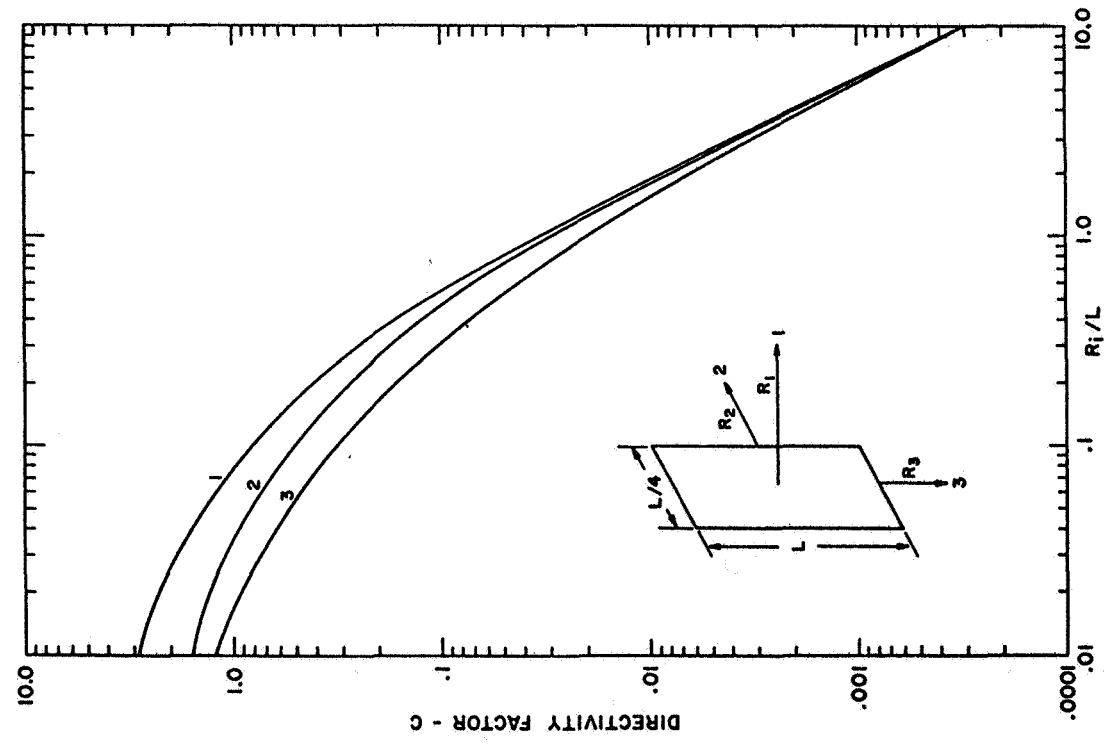
Figure 5.- Directivity factor for a rectangular plate (4/1).

623
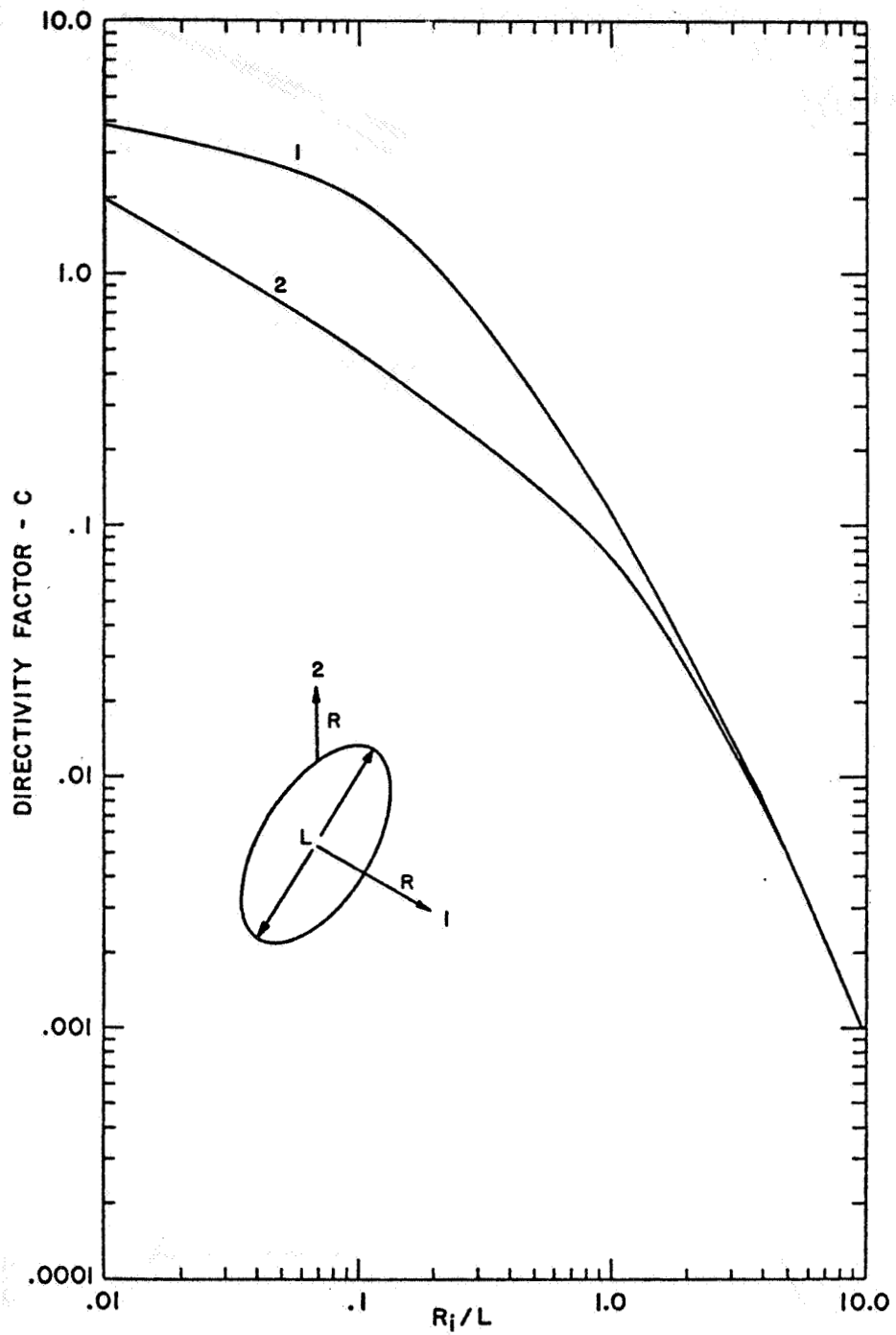
Figure 7.- Directivity factor for a circular disk.
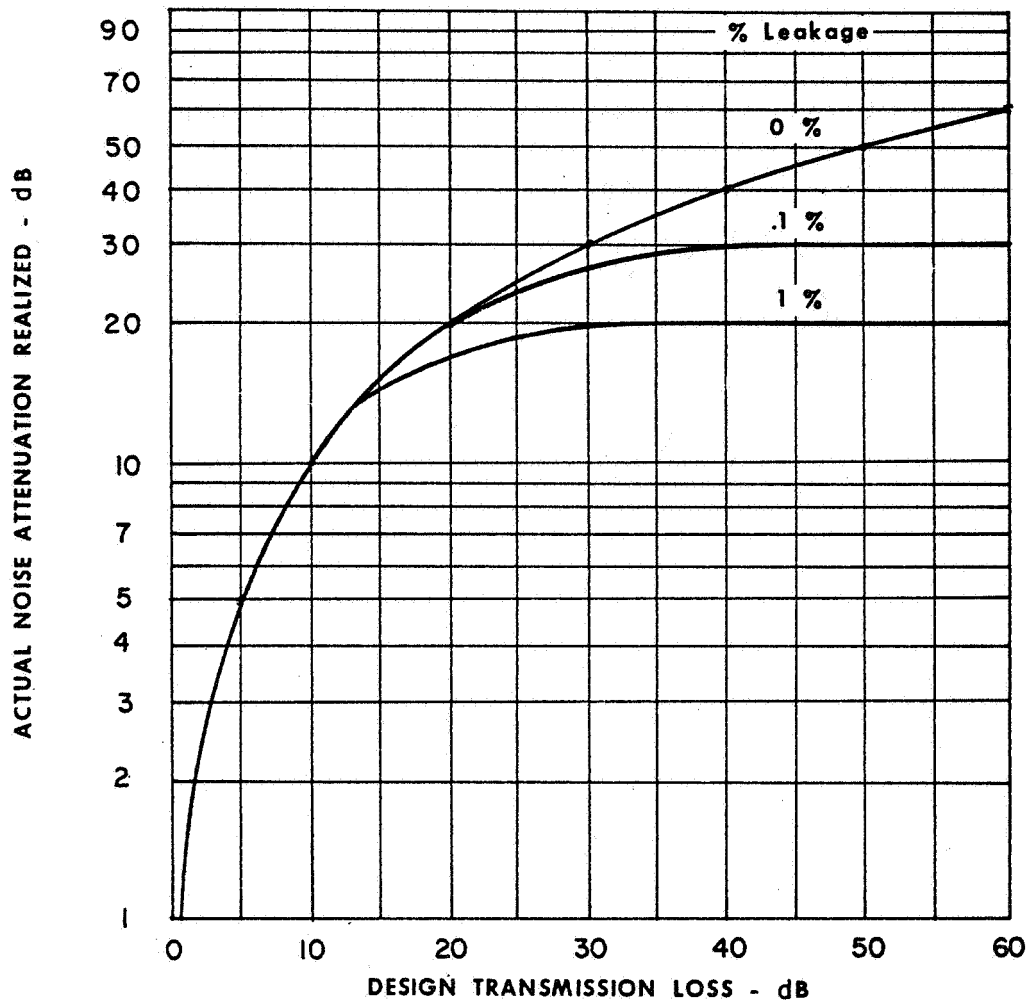
Figure 8.- Effect of leakage on panel transmission loss.
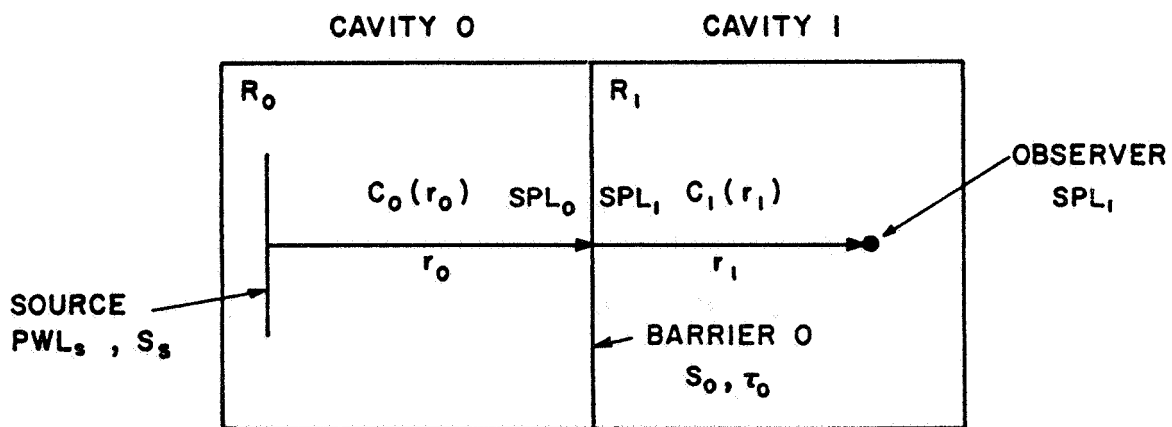
Figure 9.- Two-cavity problem.

NORMALIZED GEAR CLASH PWL* Ref. 10^{-13} WATTS

SHAFT HP, THOUSANDS   I HORSEPOWER = 0.7457 KILOWATTS
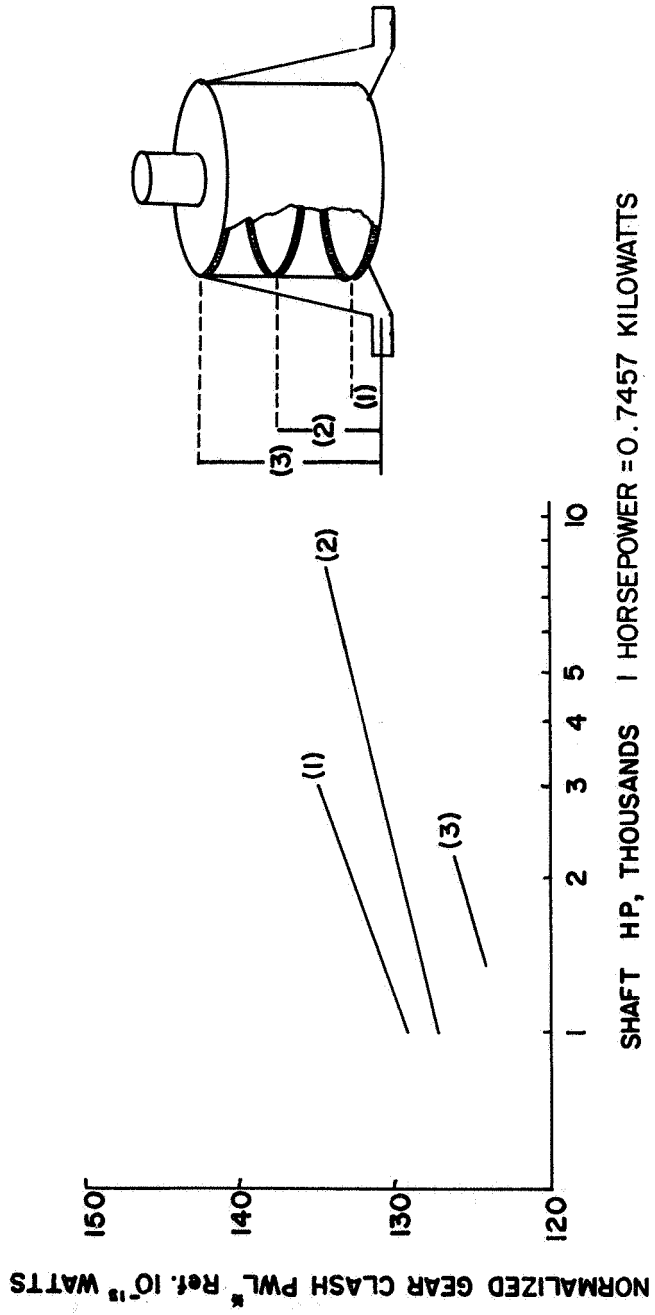
*LEVELS NORMALIZED TO PITCH LINE VELOCITY (plv) AND SPECIFIC TOOTH LOAD (stl) OF GEAR TRAIN IN CURVE (2)

NORMALIZED PWL = PWL − 20 LOG(plv/plv_2) − 20 LOG(stl/stl_2)

Figure 10. The effect of gearbox type on radiated PWL.
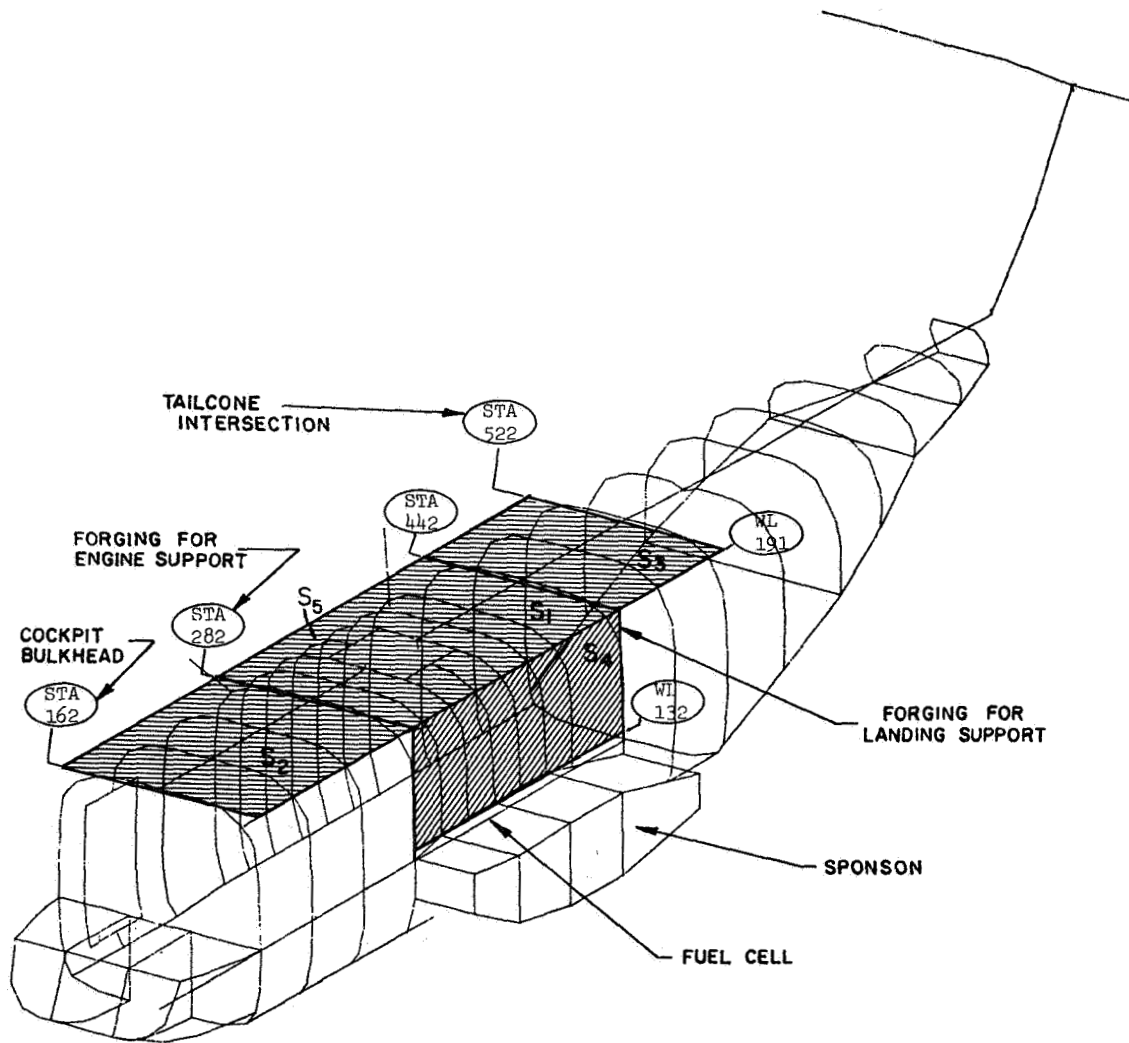
Figure 11.- Radiating surfaces for transmission noise based on the CHRA NASTRAN model.
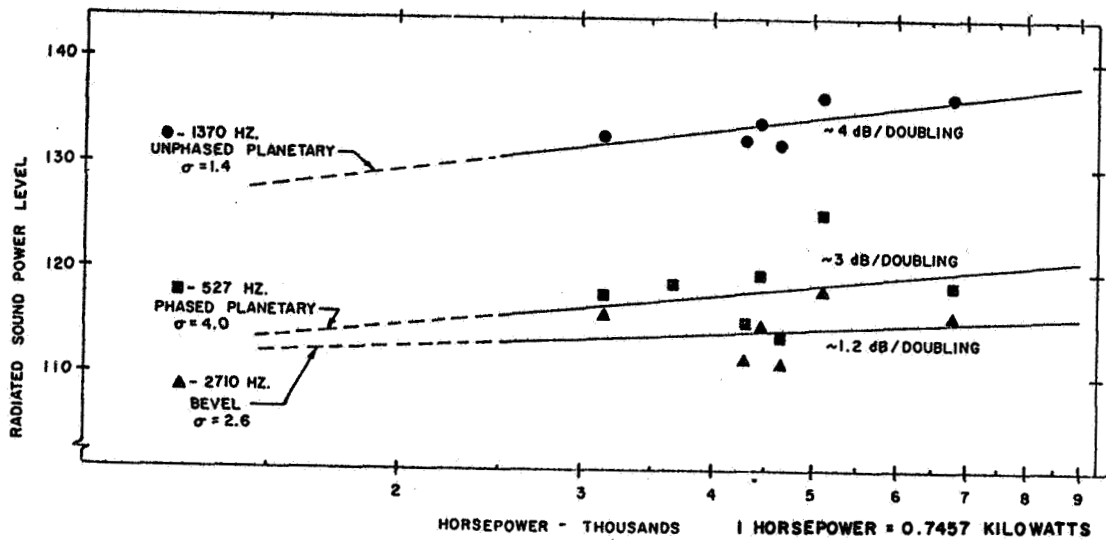
Figure 12.- Total radiated sound power levels versus consumed horsepower for CH-53 A/D aircraft.
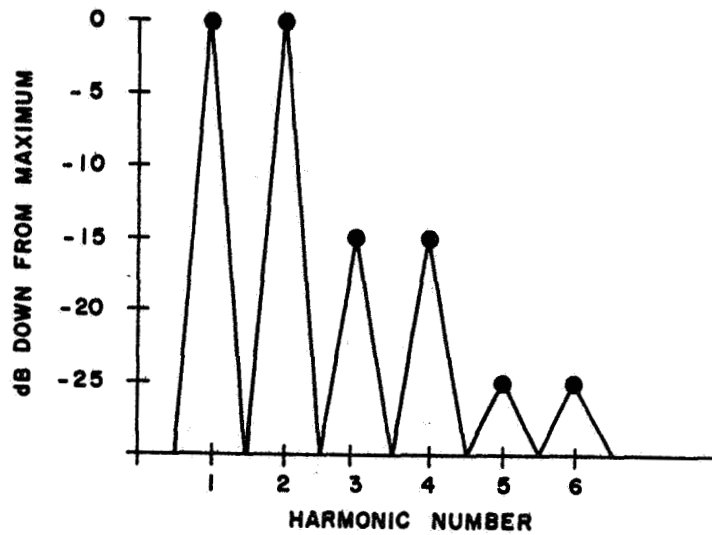
Figure 13.- Generalized gear noise harmonic spectrum.

628
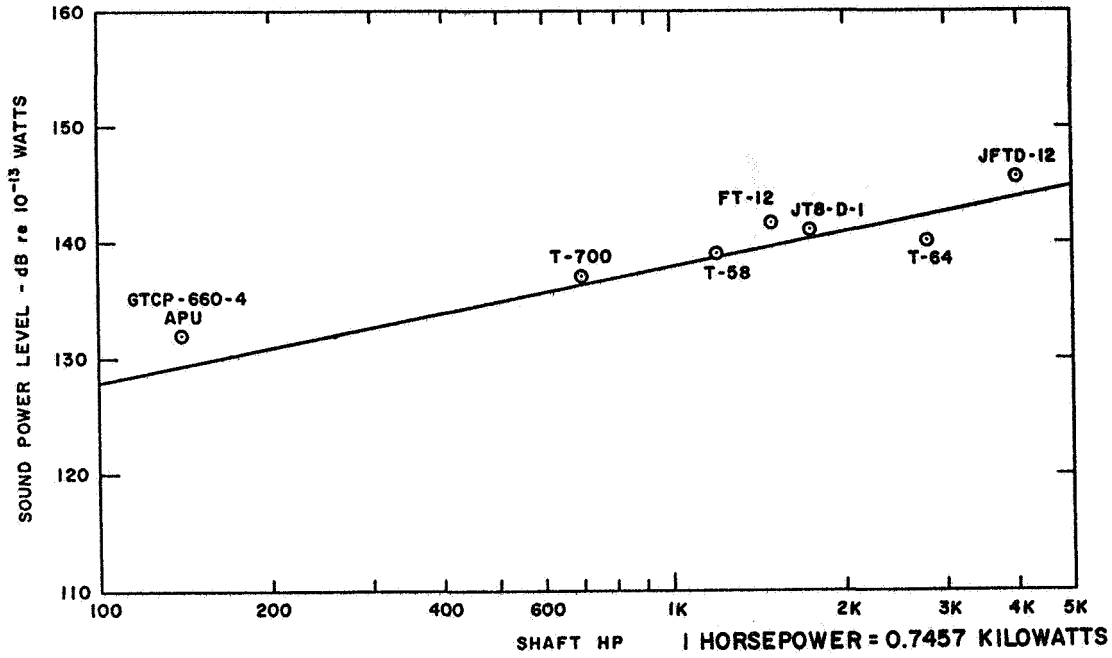
Figure 14.- Overall sound power level vs. horsepower for several engine types.
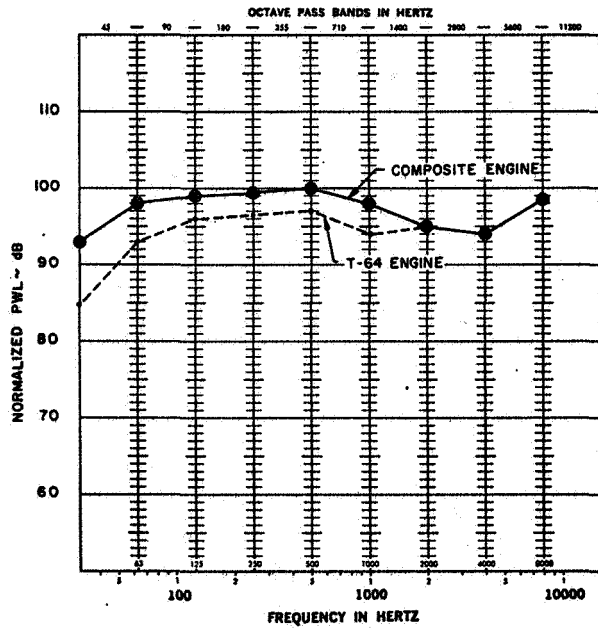
Figure 15.- Composite engine casing noise.

629
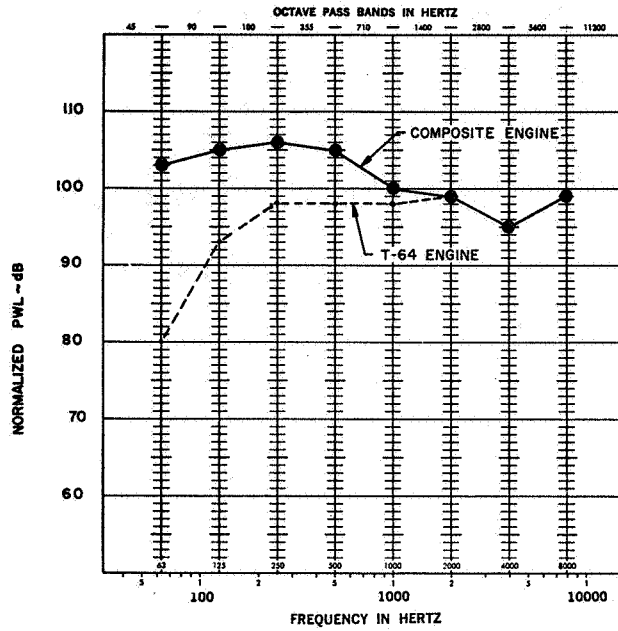
Figure 16.- Composite engine exhaust noise.

ACOUSTIC DATA - OCTAVE SPECTRUM
REDUCED INLET NOISE SPECTRUM

① BLADE/VANE PASSING TONE FALLS WITHIN 8K Hz OCTAVE
② NO TONES IN 8K Hz OCTAVE
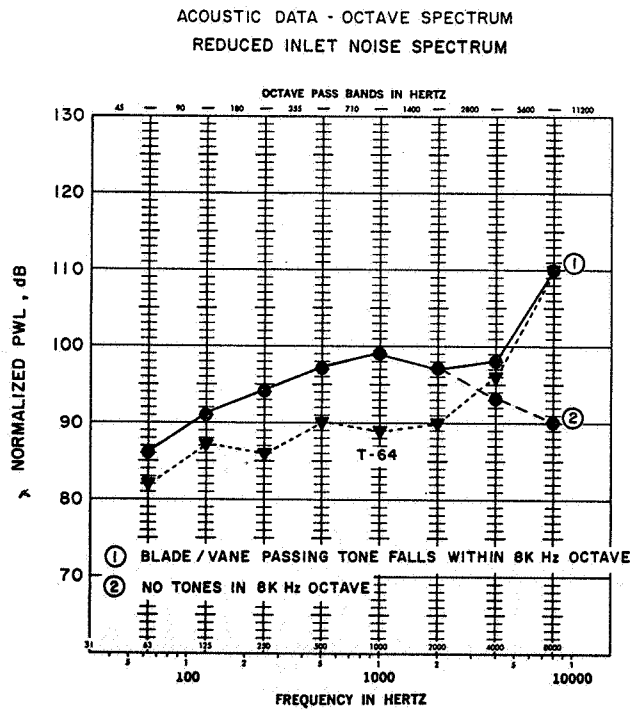
Figure 17.- Composite engine inlet noise.

630
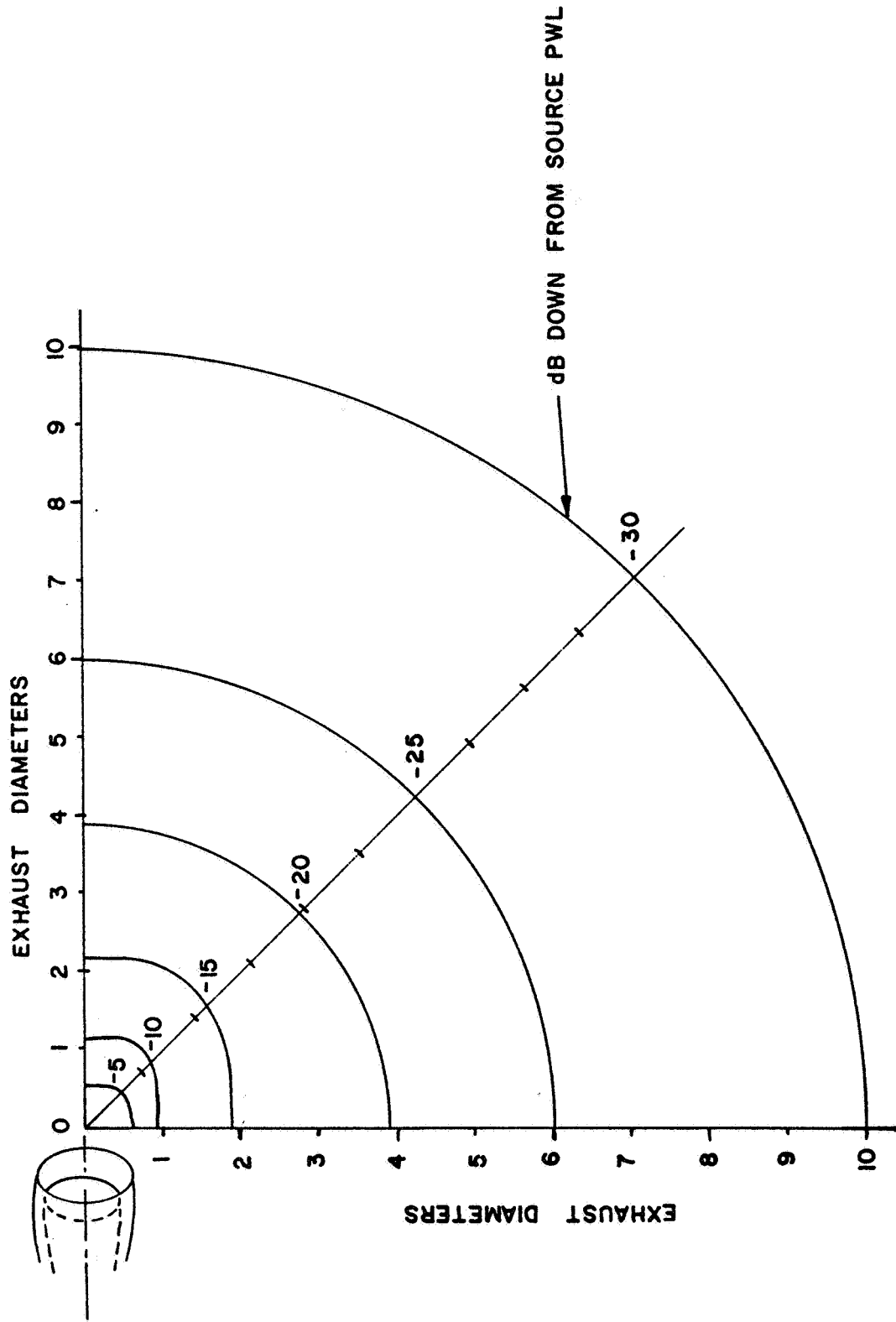
Figure 18.- Engine exhaust noise decay from source.

631
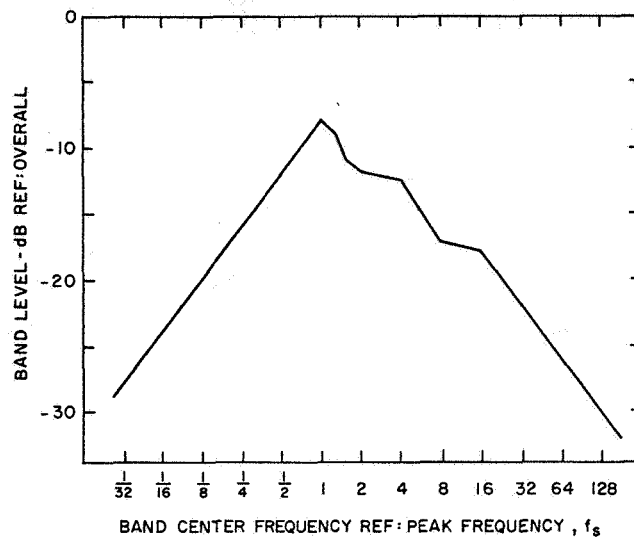
Figure 19.- Rotor broadband noise octave spectrum shape.
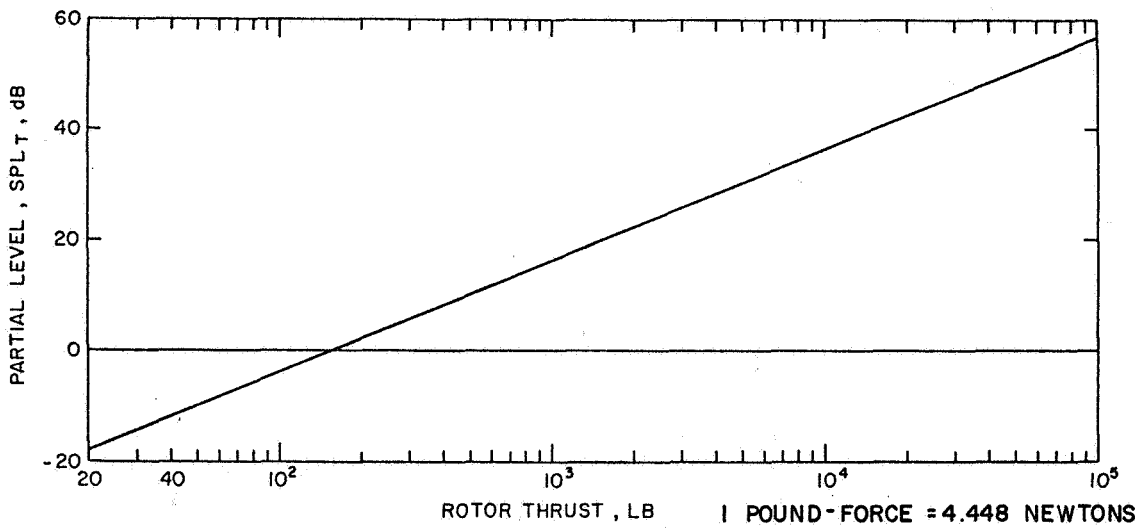
Figure 20.- Helicopter rotational noise partial level based on thrust.
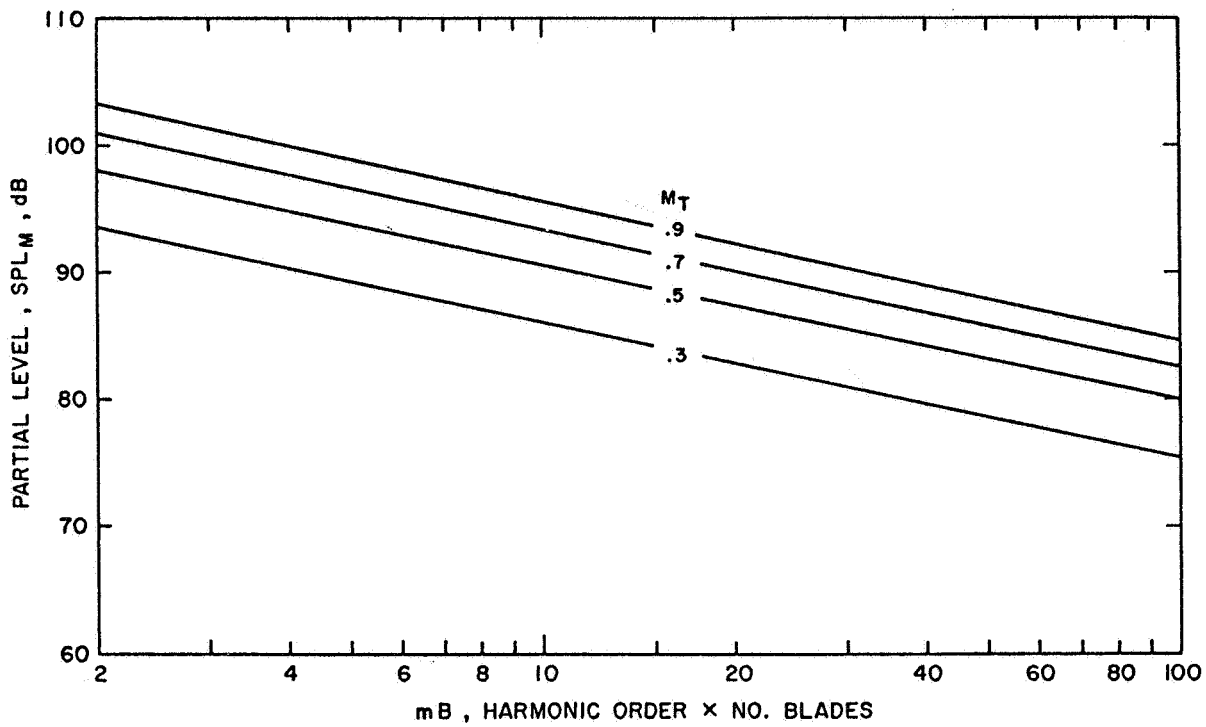
Figure 21.- On-axis thrust component SPL vs. harmonic order as a
function of rotor tip Mach number M_T.
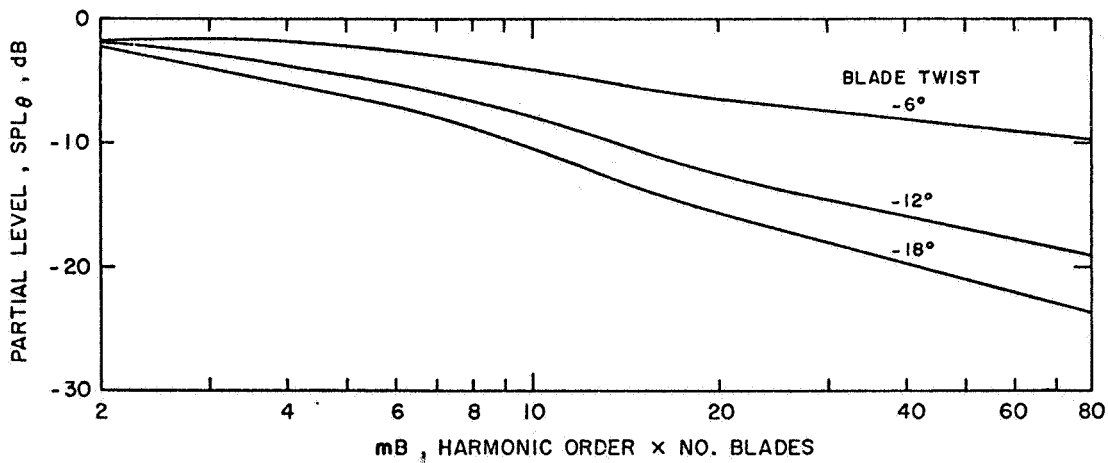
Figure 22.- Effect of twist on rotational noise harmonic thrust component.

633
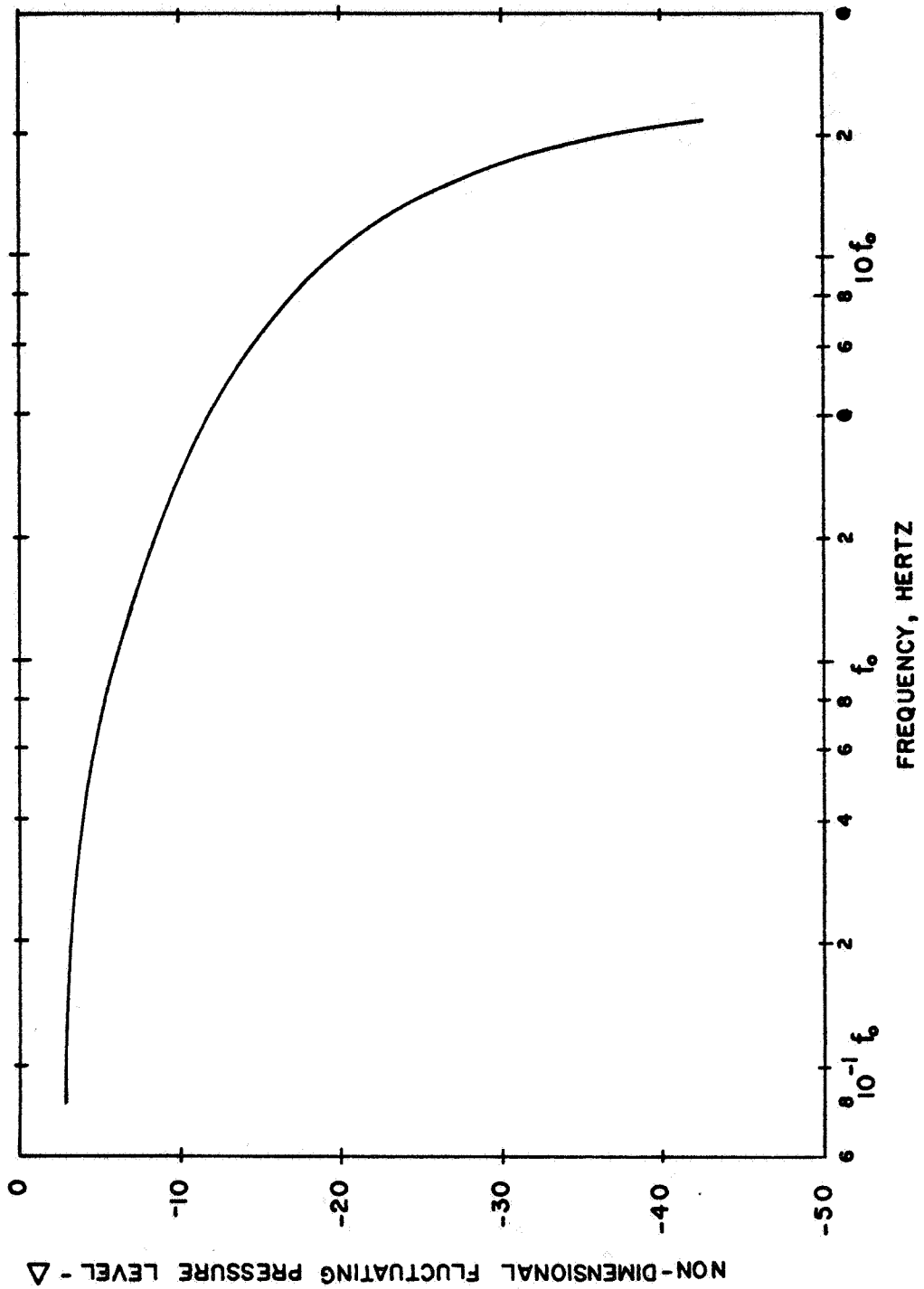
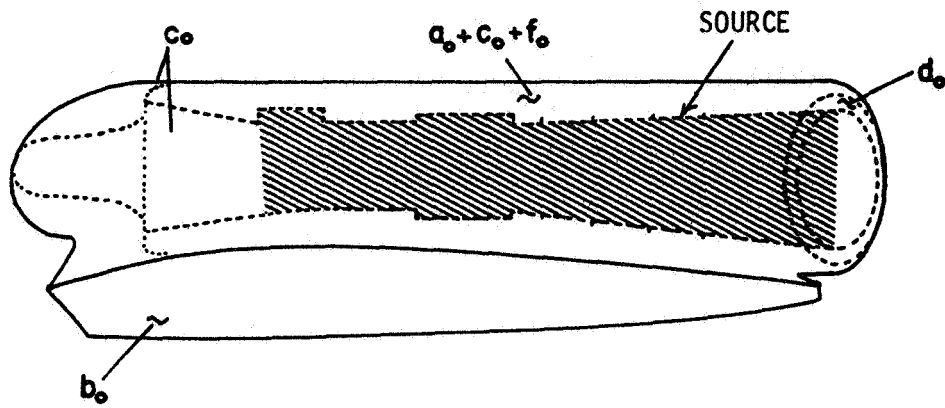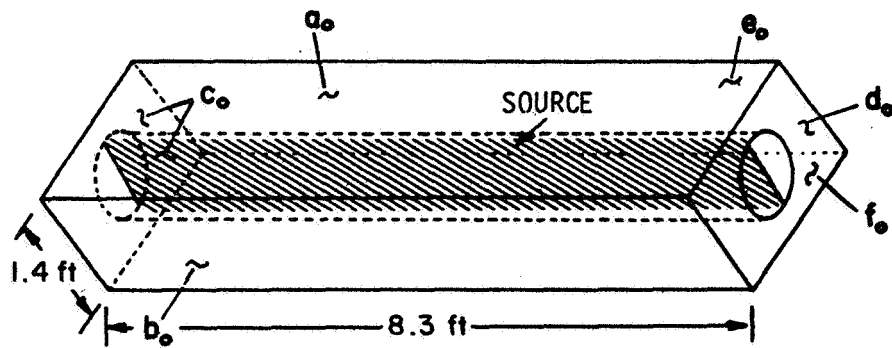Figure 23.- Chart for estimating boundary layer pressure spectra.
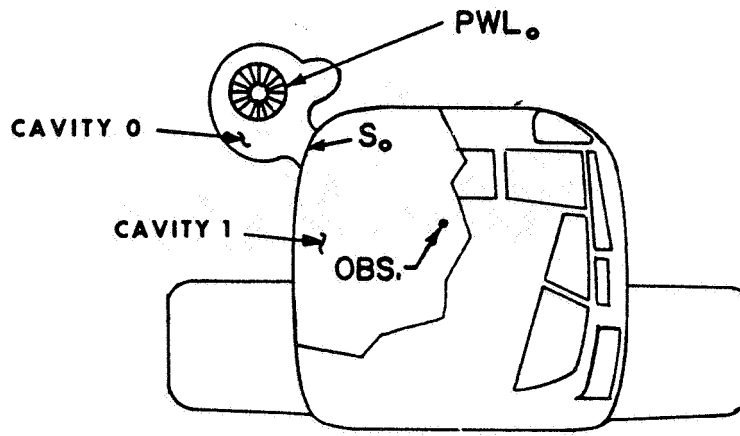
PHYSICAL PROBLEM
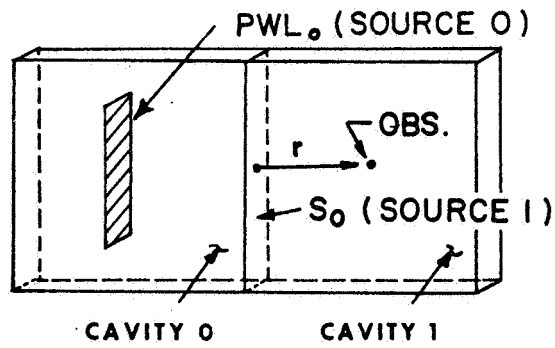
IDEALIZED PROBLEM

Figure 24.- Engine casing noise in bare cabin.

ENGINE/NACELLE ARRANGEMENT

SIMPLIFIED ARRANGEMENT

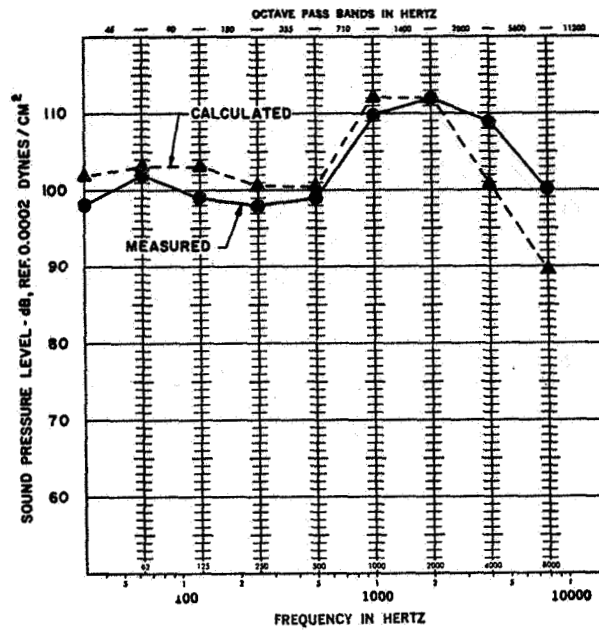Figure 25.- Source cavity representation.

636

Figure 26.- Correlation of measured and predicted bare aircraft noise
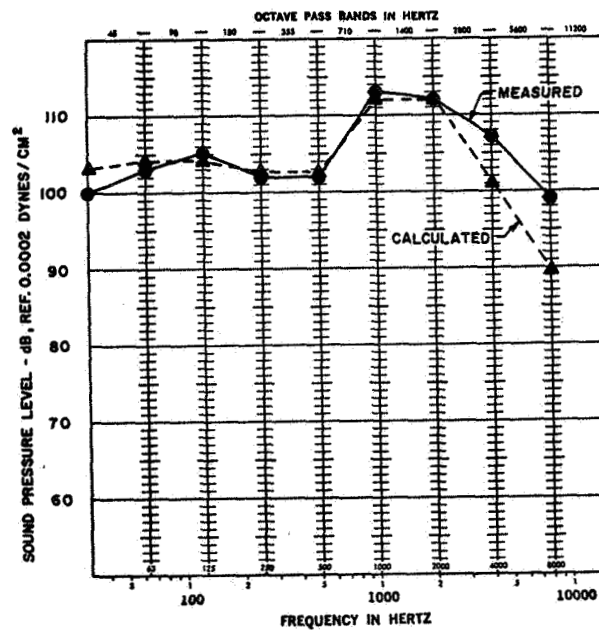levels. Middle cabin; OGE hover.

Figure 27.- Correlation of measured and predicted bare aircraft noise
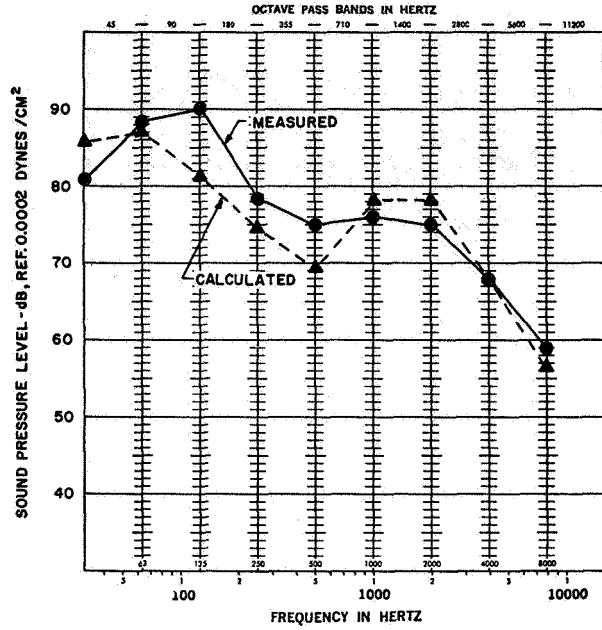levels. Middle cabin; 150 knots indicated air speed.

637

Figure 28.- Correlation of measured and predicted treated aircraft
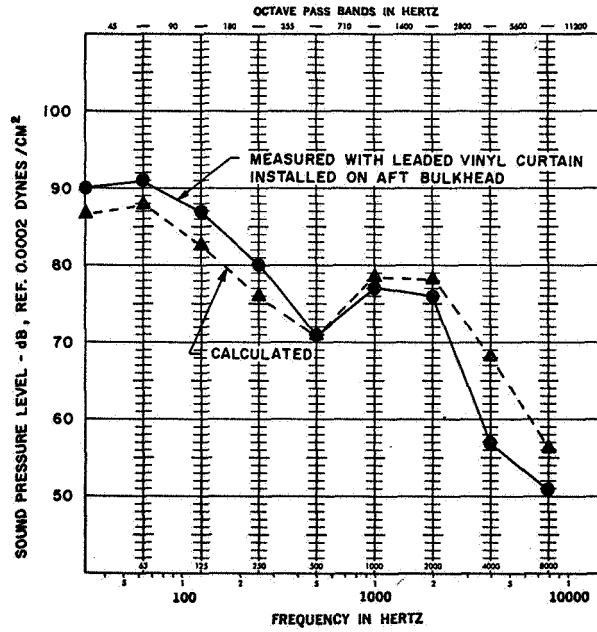noise levels. Middle cabin; OGE hover.

Figure 29.- Correlation of measured and predicted treated aircraft
noise levels. Middle cabin; 150 knots indicated air speed.

HELICOPTER INTERNAL NOISE CONTROL - THREE CASE HISTORIES

Bryan D. Edwards and Charlie R. Cox

BELL HELICOPTER TEXTRON

SUMMARY

Three case histories are described in which measurable improvements in the cabin noise environments of the Bell 214B, 206B, and 222 have been realized. These case histories trace the noise control efforts followed in each vehicle. Among the design approaches considered, the addition of a fluid pulsation damper in a hydraulic system and the installation of elastomeric engine mounts are highlighted. It is concluded that substantial weight savings result when the major interior noise sources are controlled by design, both in altering the noise producing mechanism and interrupting the sound-transmission paths.

INTRODUCTION

Owners and operators of helicopters today expect comfort levels comparable to those of other transportation vehicles in which they travel. The emphasis on passenger comfort reflects recent market trends. For the third consecutive year, business use of helicopters reached a record high in 1977 with 1219 corporations/executives operating helicopters. This is an increase of 12.7 percent more firms using helicopters than during 1976. Additionally, the number of civil government agencies operating helicopters increased by 9.5 percent over the previous year. The helicopter manufacturer has responded to these trends by quieting derived versions and incorporating noise source control in new designs.

The noise environment within a helicopter cabin is made up of contributions from many sources including the rotors, engine(s), gearing, accessories, and aerodynamic turbulence. The relative amplitude of each of these sources may be, and often is, different for each helicopter type. As a general rule, the high frequency sound components of the engine(s), gearing and accessories are the most disturbing.

For existing helicopter designs and their derivatives, the means used to identify the dominant sources include narrowband spectral analysis of noise and vibration data, detailed mapping of sound transmission paths, and sampling of production vehicles. Peaks in the spectral analyses are related to the physical properties (rotational speed, number of gear teeth, number of blades, etc.) of each potential noise source.

Determining the path by which the sound enters the cabin is often difficult. Airborne sound can enter the cabin through the basic structure, around poorly sealed doors and windows, and through openings, cutouts and ducts. Conventional soundproofing treatment is usually effective in the control of airborne sound, and its benefits vary as a function of the mass or density and thickness of the treatment. On the other hand, sound transmitted to the cabin via the structure often bypasses or flanks the soundproofing. The structure-borne path may also amplify the original sound and create'resonances in panels, air cavities and furnishings.

If a resonant or near-resonant condition exists, either at the source or in the structural path, large variations in cabin noise levels can be experienced. In fact, such a variation indicates the probability of resonance. Sampling of a number of production vehicles identifies the magnitude and extent of this problem. The need for corrective action then has justification, particularly if the action necessitates a production change and/or a retrofit.

For new designs, experience gained in previous helicopters can be of significant benefit particularly if the general layout, structure and sound sources are similar. Acoustically weak spots and flanking paths can be designed out and modifications made to the major sources and paths. For designs significantly different from current experience, the manufacturer must rely on in-house developed prediction methods and estimating techniques. An industry-wide need exists for reliable, generally accepted noise prediction methods.

This paper describes three case histories in which the techniques discussed above have been applied to the Bell 214B, 206B and 222 helicopters. Figure 1 illustrates the general configuration and identifies the dominant internal noise source of each helicopter prior to treatment. As can be seen, the offending noise source is different in each of the three designs. For the two derived versions, noise from the hydraulic systems dominates in the 214B, whereas the 206B interior is predominantly influenced by engine gearbox noise. In the newly-designed 222, noise of the hydraulic system and engine is minimal and the level is controlled almost solely by the main transmission.

CASE HISTORY #1: 214B HELICOPTER

Configuration

The Bell 214B is a 15-place single-turbine transport helicopter of 6260 kilograms gross weight. It is derived from the 214A helicopter and received FAA certification in January 1976.

Initial Noise Control

The initial noise control effort involved evaluation of three prototype soundproofing configurations. These treatments consisted of conventional blankets of different thickness and density attached to the cabin roof, aft bulkheads, and side doorposts. Details of the three configurations are

illustrated in Table 1.

Figure 2 shows typical octave band spectra in the aft cabin for the three configurations. In comparison to the austere treatment, the utility interior reduces high frequency noise 10 to 15 decibels, for doubling of the treatment weight. In the VIP interior, additional thicknesses of material are used, increasing treatment weight by 40 percent. This interior provides additional reduction in the very high frequencies, but has little effect on sound below about 2000 Hertz.

This illustrates a practical limit often encountered when using conventional blanket soundproofing - a point is reached where additional treatment weight no longer yields corresponding noise reduction. Another limiting factor is the difficulty in stitching together the large number of layers.

Sound Sources

Concurrent with the evaluation of various interior treatments, a program was initiated to control the noise at the source. The primary sound sources inside the 214B are identified in the narrowband spectral analysis of Figure 3. Main and tail rotor noise typically dominates the frequency range below about 500 Hertz. Above 500 Hertz, the spectrum contains a number of pure tones related to gear meshes within the main transmission and drivetrain, and to the dual hydraulic system.

Hydraulic System Noise Reduction

Because of the amplitude and number of high-frequency tones produced by the hydraulic system, means to reduce this source were investigated. The pump of hydraulic system #1 is driven by an accessory gear on the lower transmission case and generates noise at a fundamental frequency of 787 Hertz. In a similar fashion, the pump of system #2 is driven from the upper case and has a fundamental frequency of 832 Hertz. Both pumps generate a number of harmonic tones related to these fundamental frequencies.

Noise from each pump is transmitted to the cabin by fluid pressure oscillations, referred to as pressure ripple, in the hydraulic lines. Pressure ripple is set up as each piston in the hydraulic pump passes the pressure port. Its magnitude is on the order of 20 kilograms per square centimeter, approximately 1 percent of the steady hydraulic pressure of 210 kilograms per square centimeter. The pressure ripple transmits high-frequency vibratory energy into the structure via the flexible hoses, bypass valves, and hard lines clamped to the aft cabin bulkheads and roof. This structure-borne vibration, in turn, generates sound.

To reduce hydraulic system noise, several approaches were considered. These included vibration isolation of all hydraulic system attachment points, pump modification, and the addition of flow-smoothing devices in the fluid lines to reduce the pressure ripple. Of the three approaches, reduction of the pressure ripple proved to require the least design effort and development.

Vibration isolation would have required replacing all the existing line and hose clamps, and developing elastomeric mounts for bypass valves and possibly the reservoirs. Modification of a pump with variable-spaced piston cylinders, to distribute the fluid oscillations over a random frequency range, would have necessitated extensive prototype design and testing. Reduction of the pressure ripple was the most promising approach.

Laboratory Tests

Laboratory tests were conducted to evaluate the flow-smoothing capability of five devices, each of which was installed in the flex line immediately downstream of the hydraulic pump outlet. The following devices were evaluated:

1) a pulsation damper consisting of a 300 cubic centimeter spherical volume,

2) a pneumatically charged accumulator,

3) a fluid filter normally used for particle filtration,

4) an "acoustic filter" which provides a dual path for fluid flow, introducing interference effects, and

5) a variable length hose.

Of the devices tested, the pneumatically charged accumulator and the pulsation damper were the most effective. The accumulator reduced pressure ripple by a factor of six. However, its installation in a helicopter would have required a maintenance item to periodically check the pneumatic pressure. The pulsation damper, which reduced pressure ripple by a factor of five, required no such maintenance and was selected as the most practical flow-smoothing device. The relative amplitude of the pressure ripple before and after installation of the pulsation damper can be seen in Figure 4. Also schematically illustrated is the effect of this pressure ripple reduction on noise inside a simulated passenger cabin.

Flight Test

The pulsation dampers were then installed in the dual hydraulic system of the 214B and evaluated in flight. The installation is illustrated in Figure 5. In system #1, the pulsation damper is mounted to a transmission support member and connected to the pump and hard lines by means of flexible hoses. In system #2, the unit is installed directly at the pump outlet. In both cases, only minor changes are required in the hydraulic hoses and fittings. The entire installation weighs approximately 2.2 kilograms.

Figure 6 depicts the noise reduction realized with the pulsation damper. Sound levels measured with and without the damper are compared. In system #1, the pump fundamental is reduced by about 13 decibels. The first, second and third harmonics are correspondingly lowered by 3 to 6 decibels. In system #2, the quieter of the two systems, the pump fundamental is reduced by approximately

9 decibels and the first and second harmonics are lowered by 3 to 6 decibels.

Reduction of the hydraulic system noise measureably improves the cabin noise environment. The dominance of a number of pure tones is removed, reducing the objectionability and improving speech intelligibility. The A-weighted sound pressure level in the cabin is reduced by an average of 4 dBA. A maximum reduction of 6 dBA is realized in the aft passenger seat locations. Speech Interference Levels are decreased by an average of 6 decibels.

Based on the above improvements, the pulsation dampers are currently being installed on all production 214B's. Additionally, the damper concept has been successfully applied to the Bell 212. Due to differences in routing of hydraulic lines in the 212, the damper is required in only one of the two hydraulic systems. Flight tests have confirmed this and a reduction of about 14 decibels in the pump fundamental has been measured. Modest reductions, an average of 2 decibels, in the A-weighted noise levels and the speech interference levels were also realized.

CASE HISTORY #2:   206B HELICOPTER

Configuration

The 206B is a five-place single-turbine corporate, business and utility helicopter with a design gross weight of 1451 kilograms. It is derived from the 206A helicopter and received FAA certification in August 1971.

Sound Sources

The 206 series helicopters have a history of high-frequency cabin noise originating from the engine gearbox. One unusual characteristic of this noise is that it varies considerably from one vehicle to another. Figure 7 illustrates this variation. Cabin noise levels sampled inside 167 production vehicles are shown. Levels in the 4000-Hertz octave vary from 84 to 95 decibels for the majority of the sample. At the extremes, however, levels as low as 77 decibels are possible and as high as 101 decibels.

Cabin noise sources of the 206B are identified in Figure 8. The 5000-Hz tone which dominates the audible spectrum is traced to the mesh frequency of the power takeoff (PTO) gear and torquemeter (TM) gear inside the engine output gearbox. Other sources that can be traced include the main transmission input pinion gear mesh at 1900 Hertz and the planetary stage gear mesh at 1300 Hertz.

The engine and integral gearbox are located above and behind the passenger cabin, supported by three sets of bipod legs rigidly attached to the gearbox and airframe as shown in Figure 9. The three engine mounting points are on the engine gearbox housing. Gear mesh vibrations propagate down the support legs directly into a bulkhead aft of the passenger seats. Once into the structure, the vibratory energy radiates as noise inside the cabin.

Engine Gearbox Noise Reduction

Two approaches have been taken to reduce engine gearbox noise. The first involves means of isolating the engine from the airframe. The second approach consists of an investigation by the engine manufacturer aimed at reducing the gearbox vibration at the mounting points.

Engine Mount Isolation

Three engine mount isolation concepts were investigated. The first involves replacing each of the six engine support legs with a new leg made up of concentric metal tubes separated by an elastomer. The second consists of a circular steel/elastomer washer assembly placed at each of the three engine mounting points. The third concept also uses a washer assembly, but with a rectangular flange which provides greater elastomer area.

Hardware for each mount configuration was fabricated, installed in a test helicopter, and evaluated in flight. The concentric metal tubes proved unsuccessful. During ground run, engine motion was excessive and further evaluation was aborted. However, tests of both the circular and the rectangular washer assemblies were successful. Both concepts measurably reduced the 5000-Hertz gearbox tone and caused no excessive engine motion. Two types of elastomer were evaluated: neoprene rubber and silicon. The rectangular washer assembly with silicon elastomer provided the maximum attenuation.

The internal structure and installation details of the rectangular washer assemblies are shown in Figure 10. Vibrations introduced at the engine pad transmit through a 2 millimeter thickness of elastomer before reaching the metal of the bipod legs. Since the engine must be somewhat rigidly retained, the elastomer thickness is kept to a minimum. However, the frequency of interest is sufficiently high (5000 Hertz) that this relatively thin elastomer provides significant isolation. The flanges of the washer assembly are elongated into a rectangular shape to provide as much elastomer shear area as possible within the physical constraints of the existing mount struts.

Cabin noise measurements with the elastomeric washers installed show 7-10 decibel reduction of the 5000-Hertz tone in the aft cabin area. The noise measured at each passenger location before and after installation is shown in Figure 11. At the left passenger location, which has the highest amplitude before installation of the improved mounts, the tone is reduced by 10 decibels. Levels in the center and right hand seat location are lowered by 9 and 7 decibels, respectively. With the improved mounts the noise is fairly constant across the aft cabin.

Installation of the elastomeric washers is relatively simple, requiring enlargement of the bolt hole in each support leg, and machining down the shoulder of the trunnion. The washer design is such that the engine is well supported even in the event of elastomer failure or burnout, and no critical misalignment of the engine and driveshafts is possible. Flight tests have shown that engine motion is well within the design limits and the silicon elastomer is

not susceptible to chemical or environmental erosion. A ship set of the mounts weighs less than 0.5 kilograms. Laboratory tests are now being conducted to determine the service life of the improved mounts. They are expected to be fully qualified by July 1978.

Gearbox Vibration Reduction

The second approach involves studies and tests of gearbox vibration reduction being conducted by Detroit Diesel Allison, manufacturer of the engine. Figure 12 is a schematic of the gas producer and power turbine gear trains, showing the relative positions of the torquemeter (TM) and the power takeoff (PTO) gears. This gear train provides a two-stage speed reduction, converting the 33,290 RPM of the power turbine to 6016 RPM at the power output shaft. The TM and PTO gears are the primary load carrying gears in the output drive train. The 5000-Hertz excitation is generated at the mesh of these two gears.

Analytical studies indicate that both the PTO and TM gears have modes of vibration close to the 5000-Hertz meshing frequency. This possible resonant condition would increase the vibratory energy transmitted to the bearings, to the gearbox housing, and finally through the mounting system.

Hardware changes to the existing gear train are being evaluated on an experimental basis. The modifications and changes under consideration are listed in Table 2. Gear tooth profile modification offers the possibility of reducing the excitation by providing a smoother loading/unloading of each tooth. The damper ring and the spray applied to the gear web are intended to damp out the vibrations transmitted from the gear teeth to the shaft. Changes in the gear resonant frequency by adding mass, the mesh frequency by adding gear teeth, and the gear support stiffness are all designed to reduce any coincidence effects between excitation and resonant frequencies.

This experimental program is currently in progress and final results are not available. It is anticipated that one or more of the above modifications to the engine will lower the high-frequency vibration induced in the engine gearbox. An 8 to 10 decibel noise reduction is expected. Coupled with the improved engine mount, a cumulative reduction of 16 to 20 decibels is possible. This will remove the engine gearing as a dominant noise source in the 206B helicopter and will reduce the wide variation in noise level from one vehicle to another.

CASE HISTORY #3: 222 HELICOPTER

The two previous case histories pertain to derived versions and deal with solutions to existing noise problems, identified after the helicopter is in production. In a new design, many of these problems can be avoided if attention is paid to noise control throughout the concept, preliminary design and development stages. Such is the case for the Bell Model 222.

Configuration

The 222 is a 6-8 passenger, twin-turbine helicopter designed specifically for the civil market. It is powered by two AVCO/Lycoming turboshaft engines driving a two-stage spiral bevel, single stage planetary main transmission.

Design Features

A number of design features are incorporated to reduce cabin noise levels. Double roof construction separates the primary drivetrain noise sources and the cabin area. Provisions are made for a continuous layer of soundproofing below the lower roof. This treatment has a minimum of constrictions or openings. In the hydraulic system, a low-noise pump is specified. All hydraulic lines are kept as short as possible and clamping of lines to panels is avoided. As part of the basic suspension system, the nodalized pylon incorporates elastomeric bearings. These bearings prevent transfer of structure-borne sound from the main power train to the cabin roof. High contact ratio tooth profiles are used extensively in the main transmission. Finally, vendor-purchased accessories such as oil cooler fans, vent/defog blowers and the ECU meet stringent noise specifications or are designed to the lowest practical. noise levels.

These design features result in a well-balanced cabin noise environment requiring only minimal conventional soundproofing. The prototype soundproofing treatment weighs only 10 kilograms. It consists of foam/lead foil/foam sheets attached to the inner roof and aft bulkhead. Roof trim panels of 4 centimeters aluminum sheet extend from the aft bulkhead forward and provide a continuous closure over the soundproofing treatment. The treatment density varies along the roof. Densities of 4.88 kilograms per square meter are used in the aft portion directly beneath the main transmission. A lighter density, 2.9 kilograms per square meter, is used in the forward roof.

Figure 13 is a narrowband frequency spectra of the noise in the aft passenger cabin of the 222. In the frequency range above 500 Hertz, the major sound components emanate from the main transmission. The two input pinions' gear mesh is 3200 Hertz. Gear mesh of the planetary stage's spur gears is 1050 Hertz. Harmonics of these gear meshes, lower in amplitude, are also present. Other secondary sources include the hydraulic system and other tones not identifiable at this time.

The forward passenger seats are slightly quieter than the aft ones, but in general the noise field is uniform throughout the cabin. Table 3 compares the A-weighted sound level and the Speech Interference Level (SIL) for each seat location. The sound level in the forward row of passengers averages 85 dBA; 87 dBA in the middle row, and 86 dBA in the aft row. SILs are 76, 77, and 78 db, respectively. These levels vary little with airspeed and gross weight. Speech intelligibility is excellent and passengers can easily converse with each other.

646

CONCLUDING REMARKS

The above case histories illustrate use of available techniques to control helicopter interior noise levels. Different techniques, it is shown, are required for each type design. Existing or derived designs with noise problems can often be improved and require detailed knowledge of the source characteristics and sound paths. New designs can often benefit from these experiences, particularly in savings of weight required for soundproofing treatments.

Figure 14 illustrates the weight savings benefit. Cabin noise levels of the 214B, 206B, and 222 with different interiors are compared. Maximum levels of the three designs with no soundproofing are approximately the same. The "best seat" levels, however, are lower in the 222 by 6-8 dBA. Less soundproofing weight (10 kilograms) is required in the 222 to reach A-weighted levels of 84 to 89 dBA and SILs of 75 to 81 dB. The percentages of useful load required for soundproofing to reach equivalent cabin noise inside the 214B, 206B and 222 are 1.6%, 3%, and 0.7%, respectively.

The low soundproofing weight penalty of the 222 reflects the early application of noise control in the design. Another important benefit is that future improvements in noise level appear to be possible for modest increases in the interior weight.

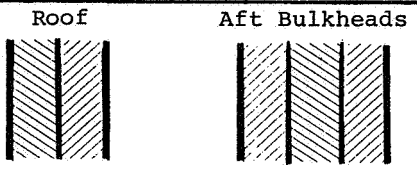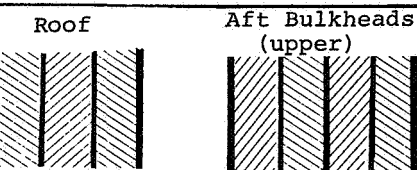TABLE I. 214B PROTOTYPE INTERIOR TREATMENTS
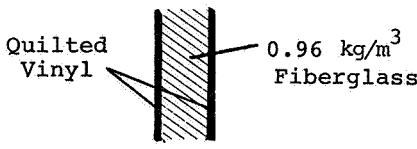
Interior Treatment	Treatment Weight	Blanket Composition
Austere	17 kg	Quilted Vinyl — 0.96 kg/m³ Fiberglass
Utility	31 kg	Roof / Aft Bulkheads
VIP	43 kg	Roof / Aft Bulkheads (upper)

TABLE II. 206B ENGINE GEARBOX EXPERIMENTAL MODIFICATIONS

Design Approach	Modification
Reduce Excitation	. Modify gear tooth profile (increase crown) on TM and PTO gears
Damping	. Attach damper rings to gear webs . Apply damping compound to gear webs
Change Resonant Frequency	. Add mass to TM and PTO gears . Change mesh frequency by increasing number of teeth on both gears . Increase stiffness of gear case

TABLE III. PROTOTYPE 222 CABIN NOISE AND SPEECH
INTERFERENCE LEVELS

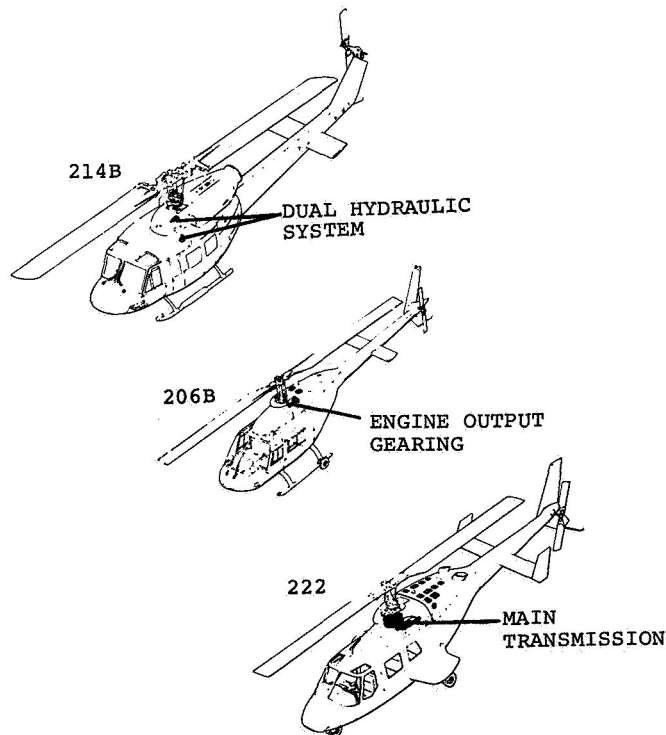|	Left Side		Center		Right Side		Average	
	dBA	SIL	dBA	SIL	dBA	SIL	dBA	SIL
Forward Row	85	77	82	75	87	77	85	76
Center Row	87	77	86	77	87	79	87	77
Aft Row	84	77	86	77	89	81	86	78

214B — DUAL HYDRAULIC SYSTEM

206B — ENGINE OUTPUT GEARING

222 — MAIN TRANSMISSION

Figure 1.- Dominant internal noise sources of the
Bell 214B, 206B and 222 helicopters.
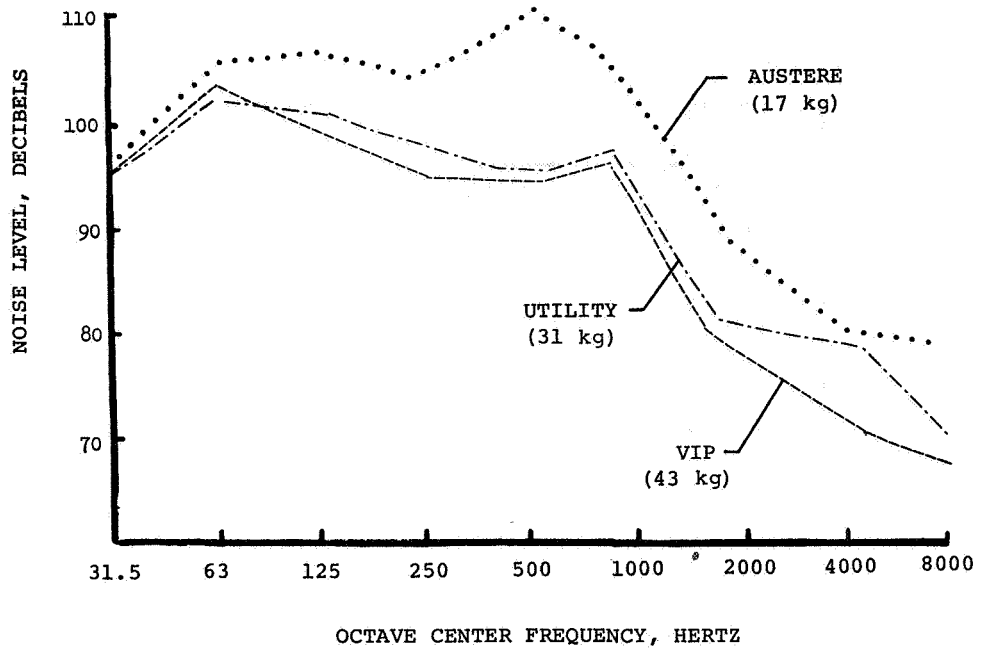
Figure 2.- Effect of 214B prototype interior treatments.

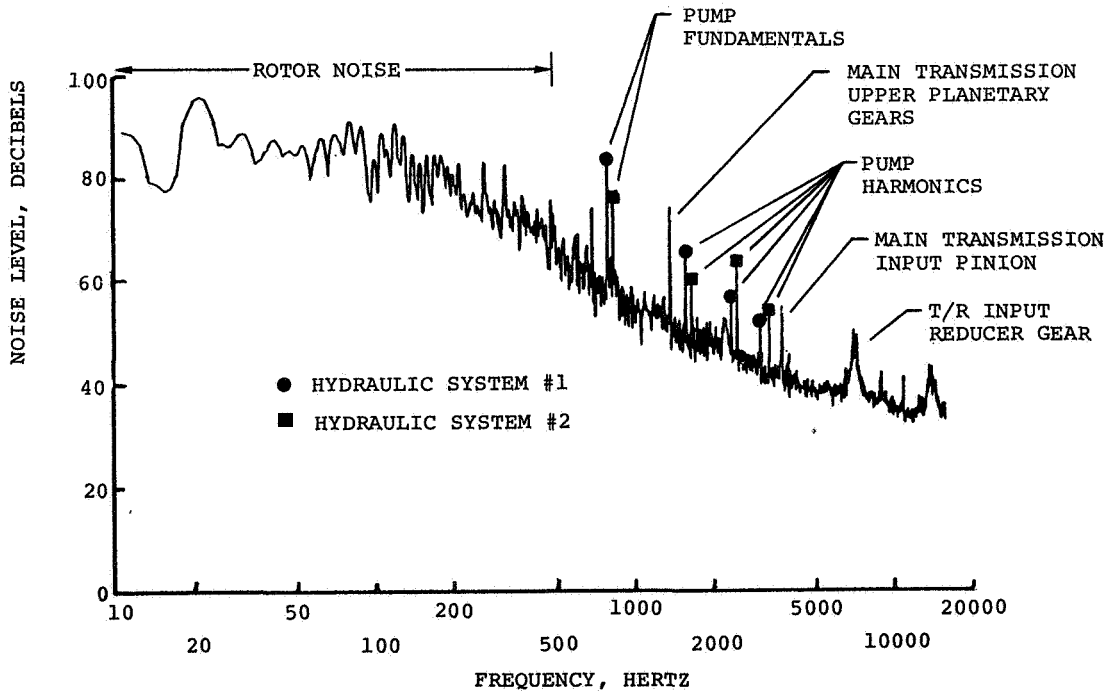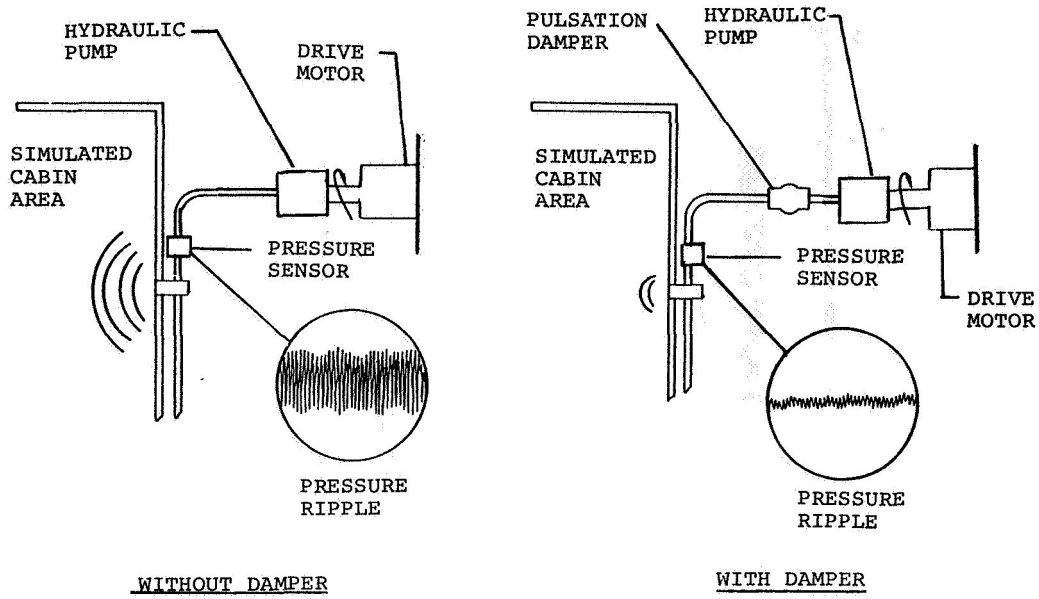Figure 3.- Frequency spectra of 214B cabin noise.

650

WITHOUT DAMPER   WITH DAMPER

Figure 4.- Laboratory setup and effect of pulsation damper
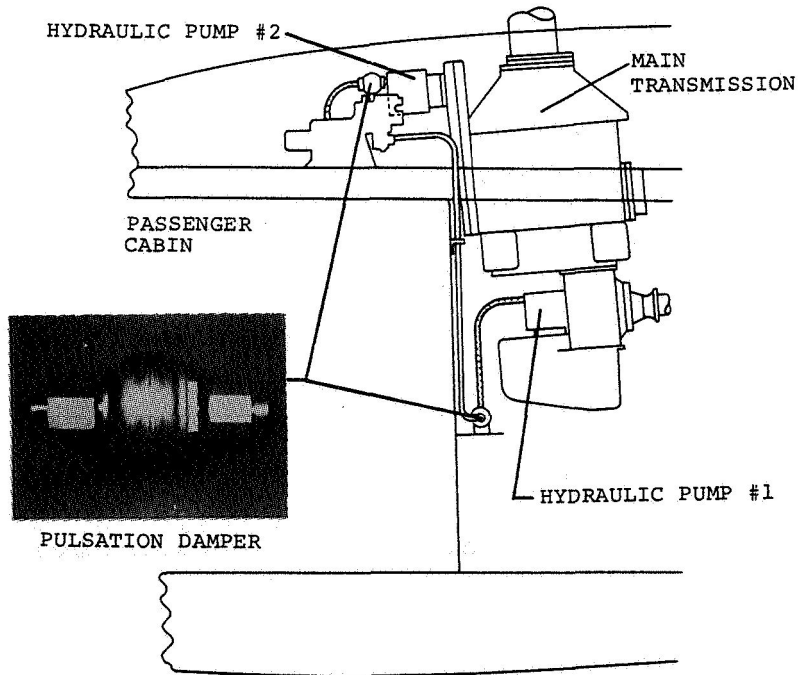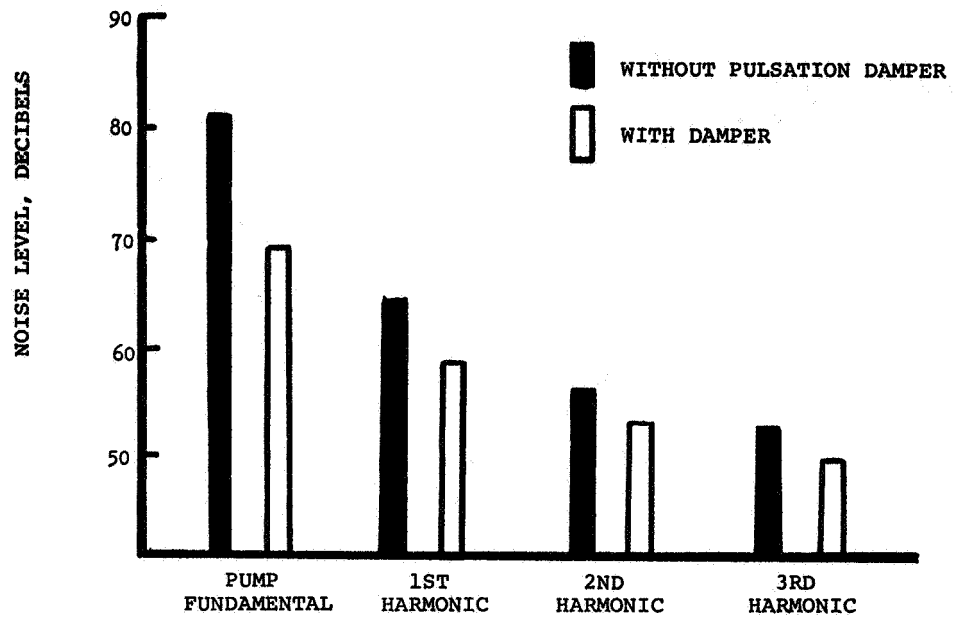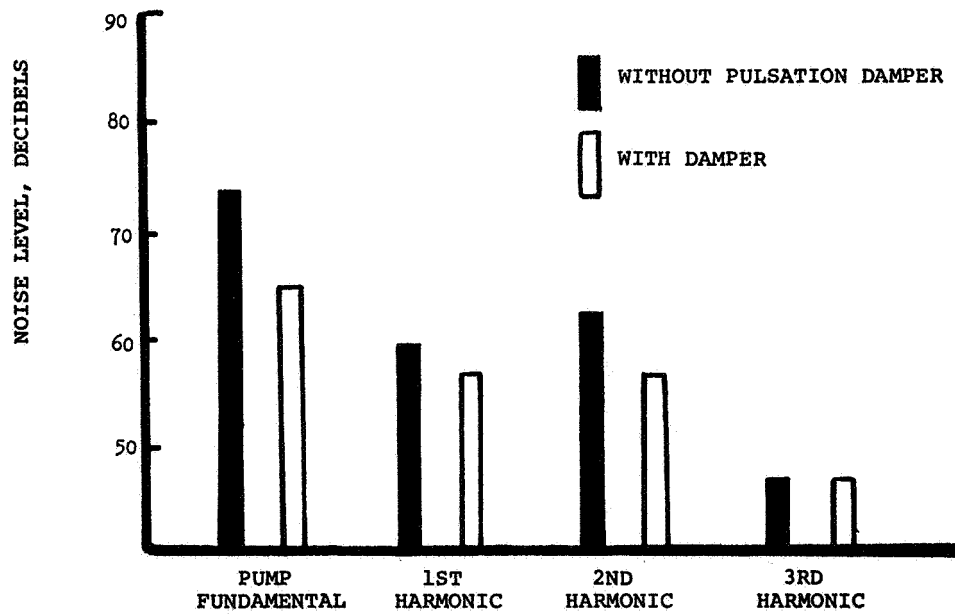on hydraulic system pressure ripple.

Figure 5.- Pulsation damper and installation schematic.

651

(a) System #1.

(b) System #2.

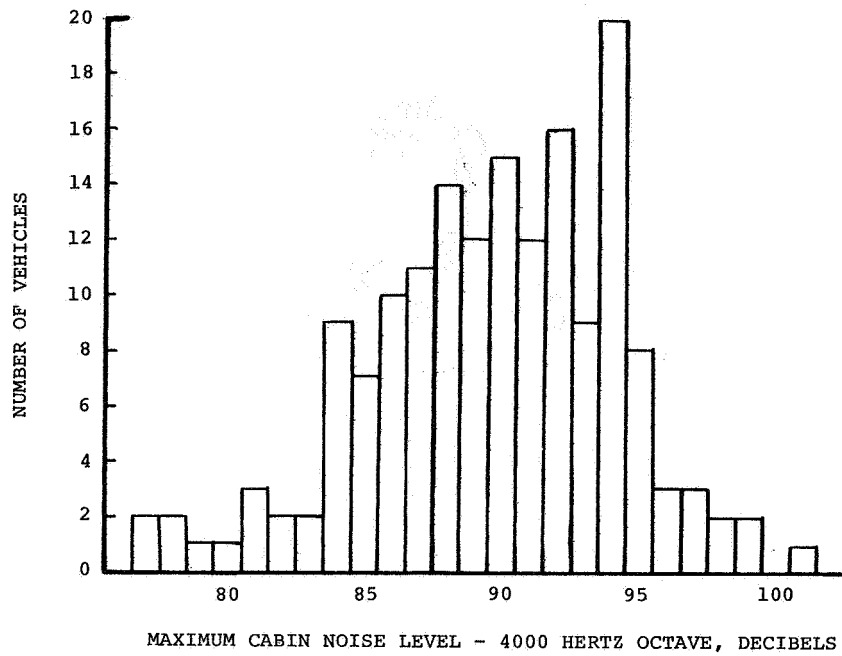Figure 6.- Effect of pulsation damper on hydraulic system noise sources.

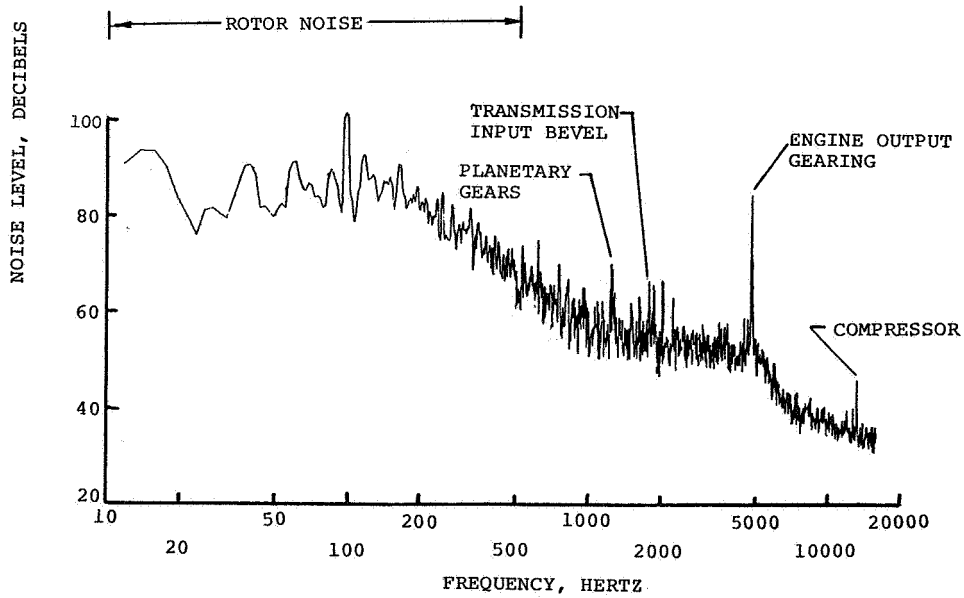Figure 7.- Noise sampling of 206 series helicopters.

Figure 8.- Frequency spectra of 206B cabin noise.

Figure 9.- 206B engine mount assembly.

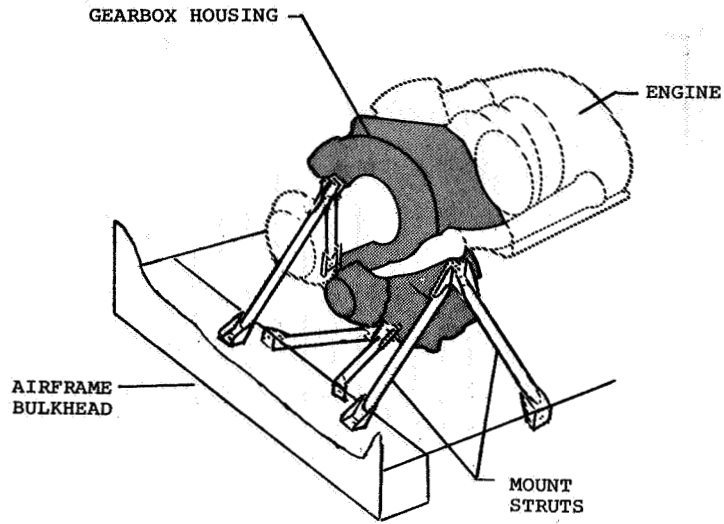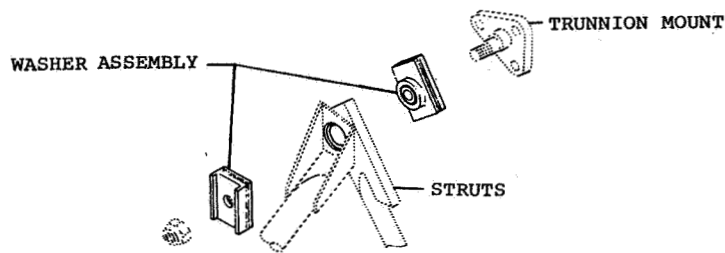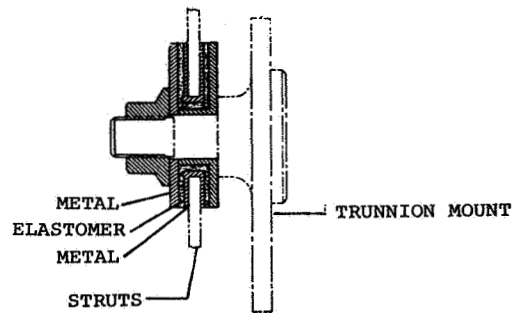(a) Exploded view of mount assembly.

(b) Cross section of installed mounts.

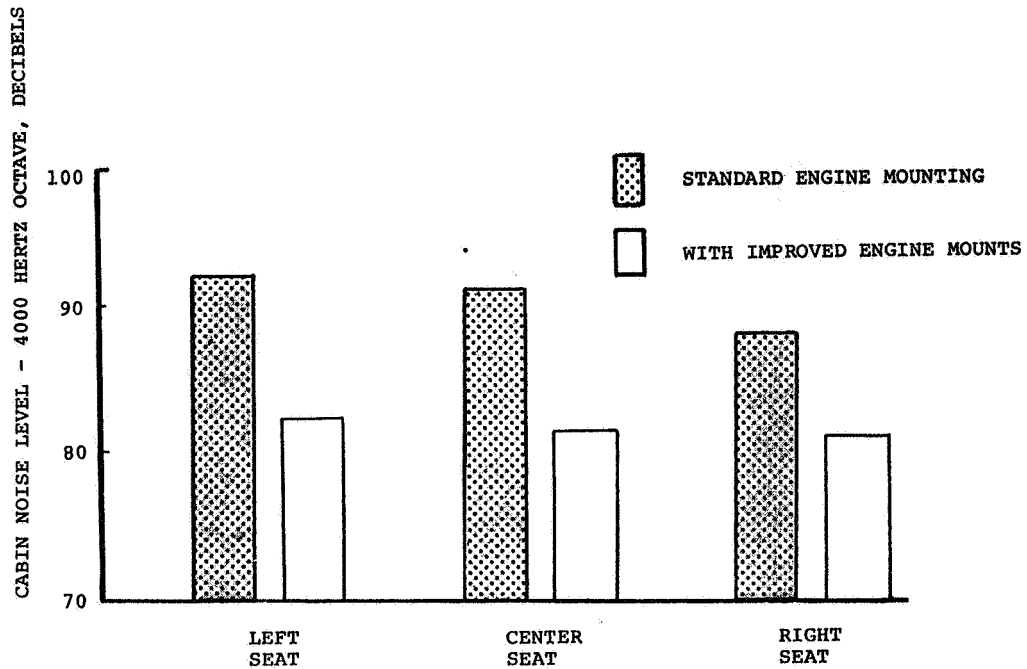Figure 10.- 206B improved engine mounts.

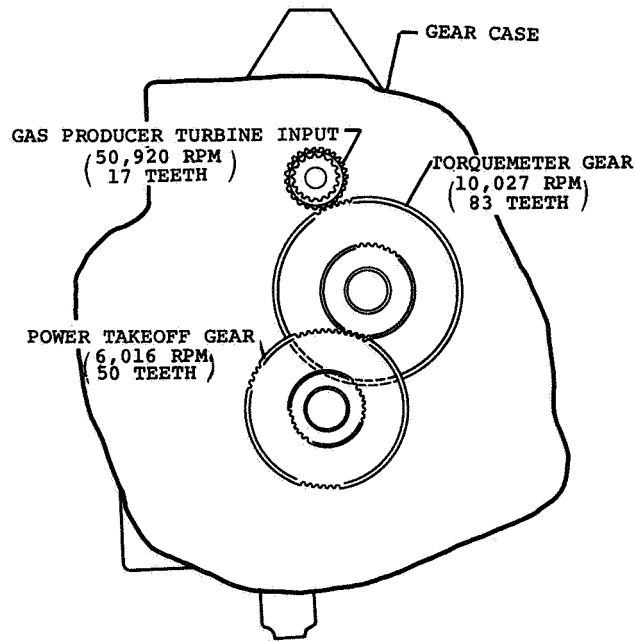Figure 11.- Effect of engine mounting on 206B cabin noise levels.

Figure 12.- Relative positions of engine torquemeter (TM) and power takeoff (PTO) gears.
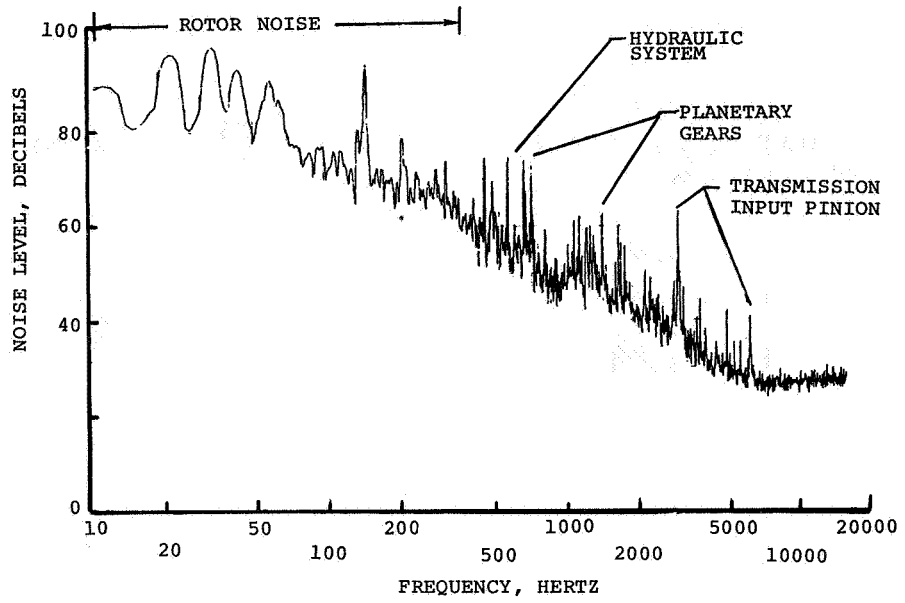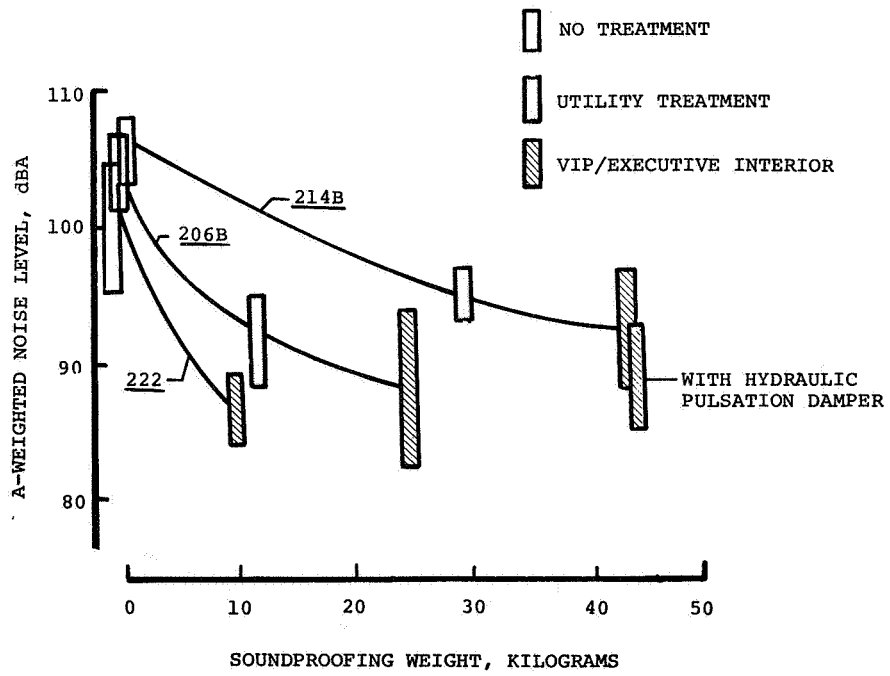
Figure 13.- Frequency spectra of 222 cabin noise.

Figure 14.- Cabin noise levels versus soundproofing weight.

656

AN ANALYTICAL METHOD FOR DESIGNING LOW NOISE

HELICOPTER TRANSMISSIONS*

Robert B. Bossler, Jr., and Michael A. Bowes
Kaman Aerospace Corporation

Allen C. Royal
Applied Technology Laboratory
U.S. Army Research and Technology Laboratories (AVRADCOM)

SUMMARY

The internal noise levels in most civil and military helicopters are excessive. In general, the dominant source of noise is the geared power transmission system which operates at a high power level and is in proximity to the cabin. Within this system, vibratory excitations are produced as a by-product of the gear meshing process. These excitations result in vibration of the transmission housing and airframe which ultimately radiate noise into the cabin. This paper discusses the development and experimental validation of a method for analytically modeling this noise mechanism. This method can be used within the design process to predict interior noise levels and to investigate the noise reducing potential of alternative transmission design details. Examples are discussed.

INTRODUCTION

The nature and extent of the internal noise problem in Army helicopters will be illustrated first. In present day civil and military helicopters, the transmission is mounted in a position close to the cockpit. As the single most dominant source of internal noise, it is imperative that the noise producing characteristics of this component be understood. A hypothesis that was investigated and verified under Army-sponsored efforts is that noise is generated by the transmission case as a result of nonuniform transfer of torque from pinion to gear due to tooth profile errors or to the elastic deformation of gear teeth under load. This nonuniform transfer of torque produces a dynamic force at the gear mesh frequency and its multiples, resulting in a coupled torsional/lateral vibration response of the gear shaft. The lateral vibration (bending) produces displacements at the bearings which in turn cause the case to vibrate, thus producing noise. Figure 1 presents allowable and predicted noise levels for the Army Heavy-Lift Helicopter. It is clear that the noise levels will be unacceptable if a means of controlling the acoustic energy at its source is not found.

---

* Performed under Contract DAAJ02-74-C-0039 to the Applied Technology Laboratory, U. S. Army Research and Technology Laboratories (AVRADCOM)

In order to meet MIL-A-8806, helicopter manufacturers have been using increasing amounts of noise attenuation blanketing with little success and with the penalty of extra weight offsetting the technology advances in light weight gearboxes. See figure 2.

This paper presents the results of a program (reference 1) that is part of 16 years of Army-sponsored programs aimed at understanding and controlling helicopter internal noise and vibration and their effects on personnel and system components.

MODELING METHOD

Problem

A helicopter transmission such as the SH-2D transmission of figure 3 is a complex dynamic system comprised of many interconnected mechanical elements. This system responds, under the influence of periodic forces produced at the various gear meshes, causing vibration of all of the individual elements and noise radiation from the transmission housing. The mechanical elements involved in this response include all of the gears/gearshafts, their support bearings, and the transmission housing. Analytical prediction of the transmission response, and consequently its vibration and noise generation characteristics, requires knowledge of the dynamics of each mechanical element, the nature and extent of coupling among these elements, and the characteristics of the gear mesh induced forcing functions.

The problem of transmission response prediction is compounded by the fact that the gear meshing forces involved occur at high frequency, typically in the hundreds and thousands of Hertz. Since the frequency for which accurate response prediction can be made is a direct function of the degree of detail in which the individual mechanical elements are modeled, very detailed elemental models are required. If the direct approach is taken and the total system is modeled as a whole, such as with finite element modeling methods, the requirement to model in great detail quickly results in an excessively large, complex model which is not amenable to ease of manipulation and use.

Approach

With the method described herein, the transmission is modeled as a fully coupled dynamic system consisting of all rotating gearshafts, the shaft support bearings, and the housing (fig. 4). Individual mechanical elements are modeled separately, in detail, then combined to produce the complete system model. The concept of component synthesis is used to simplify the dynamic modeling task and to reduce the size and complexity of the ultimate system model. Gear mesh vibratory excitations, in terms of relative deflections between mating gear teeth, are calculated independently through consideration of appropriate time-dependent tooth compliances and gear errors. These excitations are introduced in the system model at the proper gear mesh coordinates, and responses are calculated in terms of shaft and housing displacements and radiated sound power level.

Component Synthesis

The technique of component synthesis may be used to calculate the dynamic response of a linear complex structure and modification of it at a relatively small number of discrete frequencies (ref. 2). The component synthesis technique we use has two important features. The first of these relates to the reduction in degrees of freedom. The analysis of each basic component is carried out with as many degrees of freedom as is necessary for a valid analysis. When the resulting analytical model is used, however, the number of degrees of freedom may be drastically reduced and must include only:

(1) Those which interface other components
(2) Those which are to be affected by changes
(3) Those at which a force is applied or dynamic response
     is specifically desired

This reduction in the number of coordinates is performed only once at each frequency of interest with no loss in the validity of the analytical model, regardless of the extent of this reduction.

The other important feature relates to the ease with which changes may be studied. Structural modifications such as local mass or stiffness changes, the addition of springs or dampers between components, addition of vibration absorbers, and changes in boundary conditions may be exactly modeled at virtually no computer cost and without performing a new modal analysis for each change.

A linear structure is often represented in the frequency domain as an impedance matrix. The starting point for the analysis requires a valid impedance matrix for each substructure for each frequency of interest. The criterion for a valid impedance matrix is that it correctly predict the motion at the coordinates of interest at each frequency of interest. It can be shown that the criterion for a valid impedance matrix is that the elements of its inverse correctly represent the true response characteristics of the structure. This argument leads to a direct method of obtaining a valid reduced impedance matrix as follows:

(1) Perform a structural analysis using conventional methods to
     obtain a valid, full size, impedance matrix at each frequency
     of interest, $Z(\omega)$.

(2) Invert Z at each ω to obtain valid, full size mobility matrices $Y(\omega)$.
     Alternately, a modal approach or a direct integration technique
     may be used to obtain $Y(\omega)$.

(3) Select elements from Y at each ω corresponding to the coordinates
     to be retained. These elements are then formed into a new reduced
     mobility matrix, $Y_R(\omega)$.

659

(4) The reduced impedance matrix is then formed by inversion of Y_R:

$$Z_R(\omega) = Y_R^{-1}(\omega)$$

It is to be noted that Z_R is valid only at the frequency at which it has been computed. However, Z_R represents a physical system which, at the frequency ω behaves precisely as the system under study.

The reason for specifically obtaining the impedance matrix of the reduced system is that the impedance of a complex structure is obtained by simply adding the impedance matrices of the separate components at coordinates where the deflections are common. The substructures must be modeled as if they were unrestrained at the interface coordinates.

There are several considerations involved in applying this technique to practical analyses:

(1) It is not important how the reduced mobilities are computed as long as they are valid.

(2) For the method to be practical, the number of reduced coordinates must not be so large that matrix inversions become prohibitive.

(3) Local impedance changes due to addition of spring-mass systems or boundary condition changes are simply added to the reduced component impedances.

(4) When adding impedance matrices, the corresponding elements must represent deflections in the same direction.

(5) The impedance elements add when their deflections are equal; thus, when components are separated by spring-damper devices, the impedance of this device must be added to one of the substructures prior to synthesis.

The ability to accommodate structural modifications including local mass or stiffness changes, the addition of springs or dampers between components, addition of vibration absorbers or changes in boundary conditions is a valuable feature of a structural dynamics program. With the impedances of each element at frequencies of interest stored in a data bank, variation in structural parameters of the individual components can be readily made. The technique is described in reference 2.

Application of component synthesis methods resulted in substantial reduction in the size of the impedance matrix ultimately used to represent the transmission system. The SH-2 transmission system consists of four gearshafts and a planetary system. The total number of degrees of freedom used to model these shafts was 445. The case was modeled with 44 degrees of freedom, for a total of 489 individual element degrees of freedom. The synthesized

660

system impedance model for these combined elements would have been a 473 x 473 term matrix, considering elimination of duplicated interconnection points for the gear meshes and bearings. Reduction of many extraneous degrees of freedom from this impedance model reduced it to a 48 x 48 matrix. Although further reduction could have been achieved, this matrix size was compatible with the available computer capability, and no additional reduction was performed. It is interesting to note, however, that the most commonly performed response calculation, prediction of case surface response to a single gear clash force, could have been accomplished with a 14 x 14 impedance matrix, which represents a 34/1 reduction in size from the unreduced system impedance matrix.

Transmission Case Modeling

Modeling of the transmission housing is accomplished in four steps. First, an approximate, physically valid mass representation of the housing is intuitively derived. Next, the actual housing is shake tested with modal responses measured at all physical coordinates considered in the intuitive mass model. The measured modal data are then used to adjust the approximate mass representation, consistent with the restraints imposed by the orthogonality relationships. Finally, the adjusted or "identified" mass representation and modal data are used to derive the housing impedance, stiffness, and damping matrices. The method is described in reference 3.

In the present program, modal responses of the SH-2D main transmission housing were measured at 44 locations. The transmission case shake test set up is shown in figure 5. Prior to testing, an approximate mass matrix was established, consisting of 44 diagonal and 206 off-diagonal terms. Both real and imaginary case mobilities were measured, with the imaginary mobilities used as an approximation of the normal mode responses. Use of these data with the orthogonality relationships produced only small changes in the approximate mass matrix, typically less than five percent, indicating a high degree of physical as well as mathematical model validity.

Comparisons of measured and calculated real case mobility were made in order to verify the accuracy of the resulting case dynamic model. This represents an independent check of model validity since real data were not used in the derivation. These comparisons showed good correlation, as indicated in figure 6.

Shaft and Bearing Modeling

As for the case modeling, the objective of gearshaft modeling was to obtain valid mechanical impedance representations of each shaft, which could then be joined with the case impedance matrix using component synthesis methods, to form a dynamic response model of the total transmission system. In contrast to the case modeling approach, which is based on physical test data, gearshaft modeling was accomplished by purely analytical methods. An extension of the Holzer-Myklested technique for dynamic modeling of slender shafts was used with local non-slender shaft elements, such as the gears themselves, treated

as lumped masses and inertias (ref. 4). Both shaft flexure (bending) and torsion were considered with a typical shaft consisting of 100 degrees of freedom. All shaft support bearings were modeled as nonlinear orthogonal springs using the method of reference 5.

Excitation Mechanism

The basic mechanism for gear mesh excitation has been incorporated in an analytical calculation technique which permits the determination of local tooth deflections, including fundamental and harmonic components, based on known tooth geometry and loading conditions. This technique was developed through previous Army research efforts and is described in detail in reference 6. Within the present effort, this method has been improved to the extent of incorporating an equivalent spur gear approximation technique for representing helical and spiral bevel gearing. This improvement permits calculation of helical and spiral bevel gear mesh excitations directly from gear data available on gear design drawings. The equivalent spur gear approximation is that described in Appendix III of reference 7.

Acoustic Source Representation

In the present analysis, the transmission case is assumed to consist of a relatively small number of simple, baffled, hemispherical acoustic sources. These sources, which are distributed over the case surface, are assumed to act independently, with the sum of their acoustic outputs equal to the total transmission radiated noise. The output from each source is computed directly in terms of sound power level. Use of this source representation requires only knowledge of case surface motions, amplitude and frequency, and an estimation of the individual source sizes. The total housing radiated sound power is then calculated as the sum of the contribution from each individual source.

TRANSMISSION TESTING

Testing was performed to determine the actual vibration and noise characteristics of an operating helicopter transmission. These data were needed, for comparison with analytically calculated transmission noise and vibration characteristics, to validate the analytical methods used. The test article used in this effort was the SH-2D helicopter main transmission shown in figure 3. Gearbox identities are given in table I. This gearbox is rated at 1695 newton meters (15000 pound inches) of torque (continuous), at an output (main rotor) speed of 287 rpm. Speed reduction through the transmission is 21.3/1. This test article was subjected to simulated operational testing using a regenerative test stand. Measurements were made of all significant dynamic response characteristics including:

   o Shaft bending strain
   o Shaft torsional strain
   o Lateral shaft displacement
   o Housing surface acceleration
   o Radiated sound pressure level

662

esting consisted of recording data signals corresponding to each of the dynamic parameters at discrete points over a range of transmission torque and rpm settings. All test data were recorded on analog tape and reduced off-line using a real time frequency analyzer.

METHOD CORRELATION

Analytical predictions of the dynamic responses of the SH-2D main transmission were made for comparison with the measured test data. While predictions of all relevant transmission responses were made, only case acceleration and radiated noise proved to be of value in correlating the analytical method. Since the accuracy of the vibration and noise radiation predictions is very much dependent on the accuracy of the shaft response predictions, good agreement between measured and predicted acceleration and noise radiation characteristics provides tacit correlation of the shaft response prediction method.

Case Acceleration

Predictions of case surface acceleration at fourteen locations were made and compared to accelerations measured at these same points. Comparisons were made at each gear mesh related frequency of interest, including:

o Planetary system fundamental and second harmonic

o Spur gear mesh fundamental and second harmonic

o Spiral bevel gear mesh fundamental

Since two transmission speeds were considered in both the analytical and test efforts, a total of ten discrete frequency acceleration components were available for comparison, covering the frequency range of 348 Hz to 3060 Hz.

Examples of comparisons of measured and calculated case accelerations are shown in figures 7 and 8. The data of figure 7 show the responses to the planetary system fundamental gear mesh frequency at 80% transmission speed for 60% torque conditions. Figure 8 illustrates similar data for the second harmonic of the spur gear mesh frequency at 100% rpm at 80% torque. The high degree of correlation indicated by these data is similar to that obtained at the other excitation frequencies considered.

Radiated Noise

Analytical predictions were made for the housing radiated sound power levels associated with each of the gear mesh excitation frequencies considered for both conditions of torque. Sound power levels were also calculated from the measured sound pressure levels. Sound power is not a directly measurable parameter but must be calculated from sound pressure. Comparisons of measured and predicted sound power levels are shown in figure 9 at the 80% rpm test condition. Excellent correlation is shown with the average deviation between measured and predicted sound power levels less than 2 dB.

METHOD APPLICATION

The transmission dynamic modeling technique developed in the present program permits the rapid and economical evaluation of transmission design changes. Once the individual mechanical element models have been derived, they can be manipulated in various ways without the need for rederivation. This is accomplished through the use of a computer routine, which is an inherent part of the system modeling method and which can be used to perform the following functions:

o Add (or subtract) structural damping to any element or any part of an element

o Add vibration absorbers at any location of an element

o Add (or delete) lumped masses at any location

o Add spring/damper systems between any two elements or from an element to ground

o Change system geometry

The performance of system design studies is further promoted by the fact that changes in individual elements may be made separately. For example, if a change in shaft stiffness or mass distribution is desired, only the shaft model in question need be changed. The remaining shaft and housing models are left alone, and a new system model is synthesized using the new shaft model with these unchanged models.

An applications study was performed using the analytical method. The purpose of this study was to demonstrate the range of transmission design changes which may be investigated with the method. Design changes which were considered in this study effort are given in table II. While a considerable range of design changes was investigated, none of these individual changes were studied in sufficient depth to establish their ultimate practical value or noise reduction potential. The study results do, however, serve as an indication of the relative sensitivity of transmission response to the various design changes which were considered, at least with regard to the particular transmission studied.

Shaft Stiffness Distribution

Stiffness distributions of the input, spur/bevel, and output shafts were analytically simulated by changing the stiffness cross section of the respective shaft models over a limited segment of each shaft. In each case, shaft stiffness cross section was increased by approximately 10% over one-third of the shaft length. Only the central section of the shaft was stiffened, and no mass was added to the shaft.

The effect of increasing input shaft stiffness is shown in figure 10, in

erms of changes in radiated sound power level for each mesh excitation fre-
uency. The changes given are relative to sound power levels calculated for
he baseline transmission. As indicated, increasing the input shaft stiff-
ess caused significant changes in radiated sound power level at several mesh
requencies and not merely at the spiral bevel gear mesh frequencies of 2448
Iz and 3060 Hz which are most directly associated with the input shaft.
lthough the greatest change, an 11 dB reduction, did occur at the 100% rpm
piral bevel gear mesh frequency of 3060 Hz, a comparable magnitude change
in this case a 10 dB increase) is shown for the 80% rpm, spur gear mesh
econd harmonic frequency, at 2396 Hz. Furthermore, no change in sound power
evel was obtained at the 80% rpm spiral bevel gear mesh frequency of 2448 Hz.

he data of figure 10 provide a graphical illustration of the fact that the
nalytical model considers the transmission as a coupled dynamic system with
esponses determined by all the mechanical elements acting as a unit. This
act must always be considered in applying this method, particularly when it
s used to evaluate potentially beneficial design changes. Such changes,
lthough usually predicated on the basis of reducing the response to only
ne gear mesh excitation, will normally have an effect on all mesh induced
esponses, and furthermore, these effects will be a function of transmission
peed. While a given design change may produce a reduction in response
t the principal mesh frequency of interest, this same change may very well
aise the responses at other mesh frequencies, thus curing one problem and
reating others. In addition, a reduction obtained at one transmission speed
lay not prevail at another speed, even if these two speeds are reasonably
lose. Because of these considerations, transmission design changes should
lways be evaluated with regard to their effect on all gear mesh induced
esponses and for pertinent transmission speeds. Although this approach
loes require extensive evaluation of each design change, the analytical
lethod has been set up to perform the required analyses in an economical,
fficient manner requiring a minimum effort on the part of the analyst.

Planetary System Carrier Stiffness

ince, in many cases, helicopter transmissions exhibit their highest responses
lue to planetary system excitations, an attempt was made to develop and
valuate a method for changing these responses. These efforts concentrated
n the effects of planetary system carrier stiffness modification, and an
xample of the results of these investigations is shown in figure 11.

he data of figure 11 illustrate the effects of reducing the radial stiffness
f the planet carrier by 50%. This change was considered practical because
nly radial stiffness was changed with torsional stiffness held constant.
ince system torque is reacted by the carrier in torsion with little or no
tatic load reacted in the radial direction, the carrier radial stiffness is
lot a primary static design factor and can be changed based on dynamic
equirements. As shown, reducing planet carrier stiffness causes significant
hanges in the planetary system responses at 348 Hz, 435 Hz, and 696 Hz.
urther, the effects are isolated to the planetary system excitations with
ittle or no response change shown for the remaining gear mesh excitations.

665

While further analytical work is required, it is felt that the beneficial effects of this concept could be readily applied in future helicopter transmission designs.

Transmission Housing Modification

One of the major advantages of the present analytical approach is the ability to model the transmission housing. While a prototype housing is required to develop this model, changes in the housing can be simulated by purely analytical means. In this way, changes in mass and stiffness distributions and housing damping can be considered.

The addition of external damping treatments to transmission housings has often been suggested as a means to reduce housing response and radiated noise. With the present program, this approach has been evaluated analytically by simulating surface damping through increasing the housing structural damping coefficient. Three levels of damping increase were considered, with structural damping coefficient (g) of 0.05, 0.1, and 0.2. The structural damping of the housing itself was determined to be very low, with modal damping coefficients ranging from 0.0015 to 0.03. Increasing damping to the degree considered, then, represents a substantial increase, but one which can readily be obtained with commercial materials.

The effects of increased housing damping are indicated in figure 12. As shown, appreciable sound power level reductions were obtained at several gear mesh excitation frequencies, but the reductions were by no means universal. This is to be expected since the effects of damping are dependent upon the proximity of excitation frequencies and system natural response frequencies. For excitations close to natural frequencies, damping can be effective; while, if excitations are substantially removed from the natural frequencies, damping will have no effect. As shown, damping can also produce an adverse effect since added damping may increase response to excitations which are close to system antiresonant frequencies.

Given the data of figure 12 it is apparent that housing damping is a sensitive parameter which can be adjusted to reduce transmission response. Proper application of this approach, however, requires knowledge of system dynamic response characteristics, most importantly the proximity of gear mesh excitation frequencies and system resonant and antiresonant frequencies.

FUTURE USE

The noise modeling method can be applied in various ways depending upon the development status of the subject transmission. During preliminary design, rough estimates of transmission noise can be made using a simplified noise model which has been derived from the more complex method (fig. 13). The simplified noise prediction method is given in equation form in reference 8. The accuracy of the simplified noise prediction method has been subjected to limited evaluation through comparison of predicted and measured UH-1 internal noise levels, obtained from reference 6. As illustrated in figure 14 the

666

calculated UH-1 internal noise spectrum agrees well with the measured data. The noise prediction method is presented in equation form in the appendix. When detail design data become available, the complete system modeling method can be applied using a housing model based on finite element methods. At this stage, significant efficiencies can be achieved using a substructure approach with component synthesis. Finally, during hardware development, improved elemental models may be obtained through the use of mobility test data.

CONCLUSION AND RECOMMENDATIONS

The analytical methods developed in this study represent a significant advancement in the state of the art of helicopter internal noise prediction. These methods are limited, however, to the prediction of the airborne component of transmission noise, although the approach used is compatible with the incorporation of a structure borne noise prediction capability. Extension of the methodology to include structure borne noise prediction capability is considered both feasible and appropriate.

APPENDIX

HELICOPTER TRANSMISSION NOISE PREDICTION METHOD

MICHAEL A. BOWES

It is often desirable to have reasonable, though approximate, estimates of transmission noise characteristics. To answer this need, a simplified transmission noise prediction technique has been developed using parametric trending data generated with the SH-2D transmission analytical model. The validity of this simplified method is predicated on the assumption that the SH-2D transmission has dynamic response and noise radiation characteristics which are representative of helicopter transmissions. This assumption is believed to be appropriate, since the SH-2D transmission is similar in design to most existing helicopter transmissions and its operating torque and rpm conditions are near median values for current and planned vehicles.

The simplified transmission noise prediction method is based on a simple parametric relationship between the physical variables of a given gear mesh and the sound power level of the discrete frequency component due to that mesh. The general form of this relationship is:

$$PWL_G = A \, Log_{10}(\tau) + B \, Log_{10}(f) + C + D \quad (1)$$

where:
PWL_G = sound power level - dB re. 10^{-12} watts

A = a constant indicative of the relationship between torque and sound power level

τ = transmitted torque (in-lb)

B = a constant indicative of the relationship between gear clash frequency and sound power level

f = gear clash frequency - Hz

C = a constant indicative of the type of gear mesh

D = a constant indicative of the gear clash harmonic number

A parametric study was performed, using the available SH-2D transmission analytical model, considering three types of gear meshes, all of which were represented in the SH-2D model. Gear mesh types considered were: spur gear, spiral bevel gear and planetary system. Based on this study, three equations of the form of Equation (1) were derived for the three gear mesh types considered. These are:

$$PWL_{SG} = 20 \, Log(\tau) + 37.8 \, Log(f) - 91 + D_{SG}$$

$$PWL_{SBG} = 20 \, Log(\tau) + 37.8 \, Log(f) - 100 + D_{SBG}$$

$$PWL_{PS} = 12.8 \, Log(\tau) + 37.8 \, Log(f) - 59 + D_{PS} \quad (2)$$

where: PWL_{SG} = sound power level of spur gear mesh

PWL_{SBG} = sound power level of spiral bevel gear mesh

PWL_{PS} = sound power level of planet system

The constants D_{SG}, D_{SBG}, and D_{PS} in Equation (2) are indicative of the relationship between sound power level and gear mesh harmonic number, which was found to be specific to a particular gear mesh type. Values of these constants were defined to be equal to zero for the gear clash fundamental frequency. Finite values were established for these constants for the second and third harmonics of gear clash frequency, and these are given in Table 1.

Table 1. Values of the Constants D_{SG}, D_{SBG}, and D_{PS} in Equation (2)

Gear Clash Type	Harmonic No.	
	2	3
Spur Gear	-5	-22
Spiral Bevel Gear	+7	+6
Planet System	-10.5	-23

REFERENCES

.   Bowes, M. A., et al, Helicopter Transmission Vibration and Noise
     Reduction Program, Eustis Directorate, USAAMRDL TR 77-14, February
     1977.

2.   Berman, A. and Giansante, N., CHIANTI - Computer Programs for Parametric
     Variations in Dynamic Substructure Analysis, Presented at the Shock and
     Vibration Symposium, Albuquerque, N.M., October 1975.

3.   Berman, A., System Identification of a Complex Structure, AIAA Paper No.
     75-809, Presented at AIAA/ASME/SAE 16th SDM Conference, Denver, CO.
     May 1975.

4.   Pan, C. H. T., Vibration Analysis for Shafting of Power Transmissions,
     Report No. SRC 76-TR-20, Shaker Research Corporation, Ballston Lake,
     N.Y., November 1976.

5.   Jones, A. B., A General Theory for Elastically Constrained Ball and
     Radial Roller Bearings Under Arbitrary Load and Speed Conditions,
     Journal of Basic Engineering, ASME Transactions, June 1960.

6.   Laskin, I., Orcutt, F. K. and Shipley, E. E., Analysis of Noise Generated
     by UH-1 Helicopter Transmission, USAAVLABS TR 68-41, Mechanical Technol-
     ogy, Inc., June 1968.

7.   Badgley, R. H. and Laskin, I., Program for Helicopter Gearbox Noise Pre-
     diction and Reduction, USAAVLABS TR 70-12, Mechanical Technology, Inc.,
     March 1970.

8.   Bowes, M. A., Development and Evaluation of a Method for Predicting the
     Vibration and Noise Characteristics of Helicopter Transmissions, AHS
     Preprint No. 77.36-76, Presented at the 33rd Annual National Forum
     of the American Helicopter Society, May 1977.

TABLE I. SH-2 MAIN GEARBOX IDENTITIES

Part	No. of Teeth	Speed - rpm	Excitation Frequency - Hertz
Input Shaft	-	6120	-
Spiral Bevel Pinion	30	6120	3060
Spiral Bevel Gear	47	3906	3060
Spur Gear Pinion	23	3906	1497
Spur Gear	87	1033	1497
Sun Gear	35	1033	-
Planet Gear (6)	28	-	435
Ring Gear	91	-	-
Planet Carrier	-	287	-
Output Shaft	-	287	-

TABLE II. SUMMARY OF DESIGN CHANGES ANALYZED

REDUCED BEARING STIFFNESS
    ALL SHAFTS
      INPUT SHAFT ONLY

INCREASED SHAFT STIFFNESS
    INPUT SHAFT
    OUTPUT SHAFT
    SPUR/BEVEL SHAFT

INCREASED CASE DAMPING

BEARING RELOCATION

SUN GEAR ISOLATION

PLANET CARRIER ISOLATION

INCREASED SHAFT MASS
    INPUT SHAFT
    SPUR/BEVEL SHAFT
    SPUR/SUN SHAFT

INCREASED CASE MASS

670
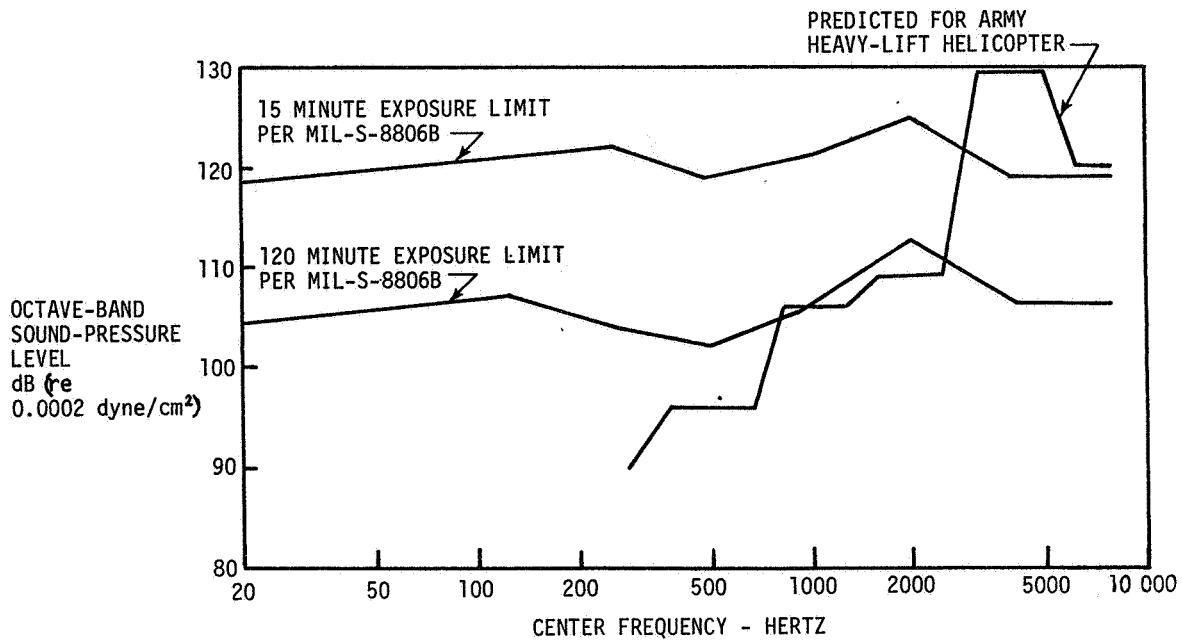
Figure 1.- Allowable and predicted sound pressure levels at
personnel locations for crew members wearing SPH-4 headgear.

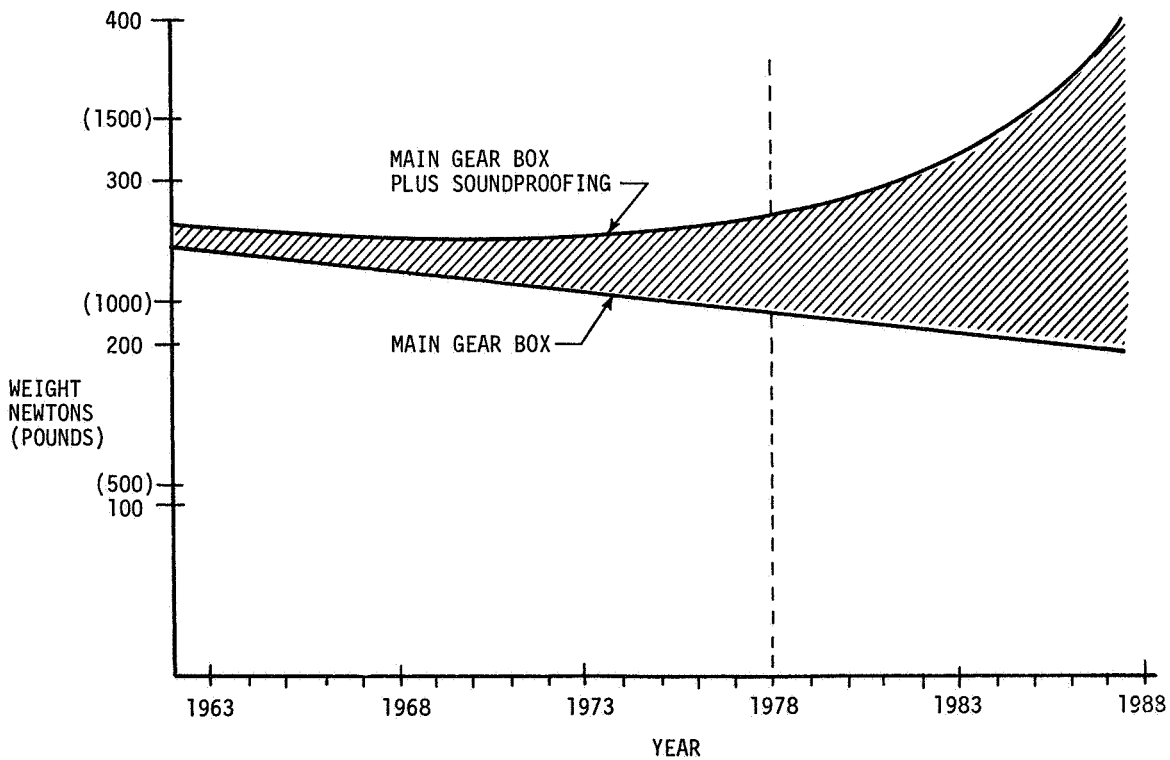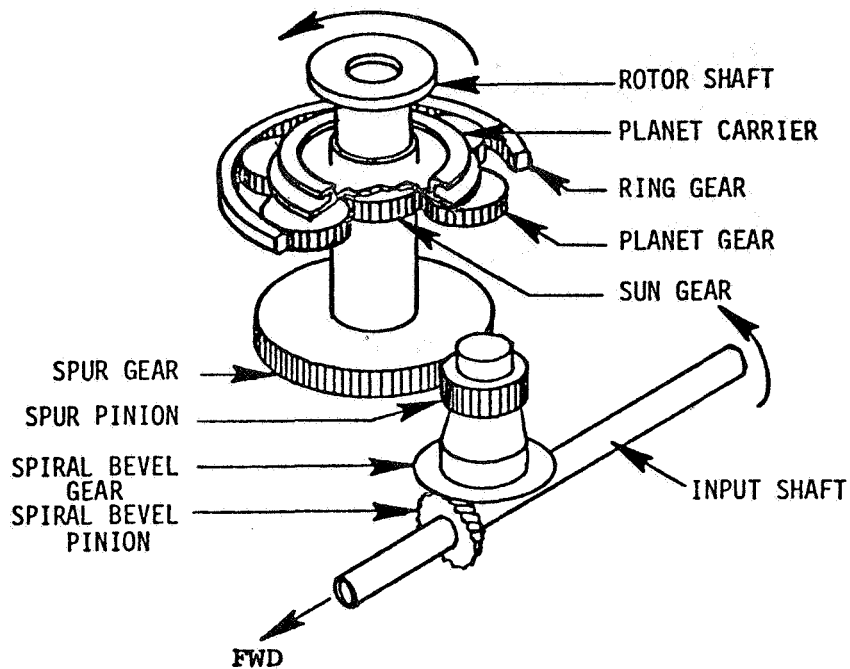Figure 2.- Weight of gearbox and soundproofing as a function of time.

671
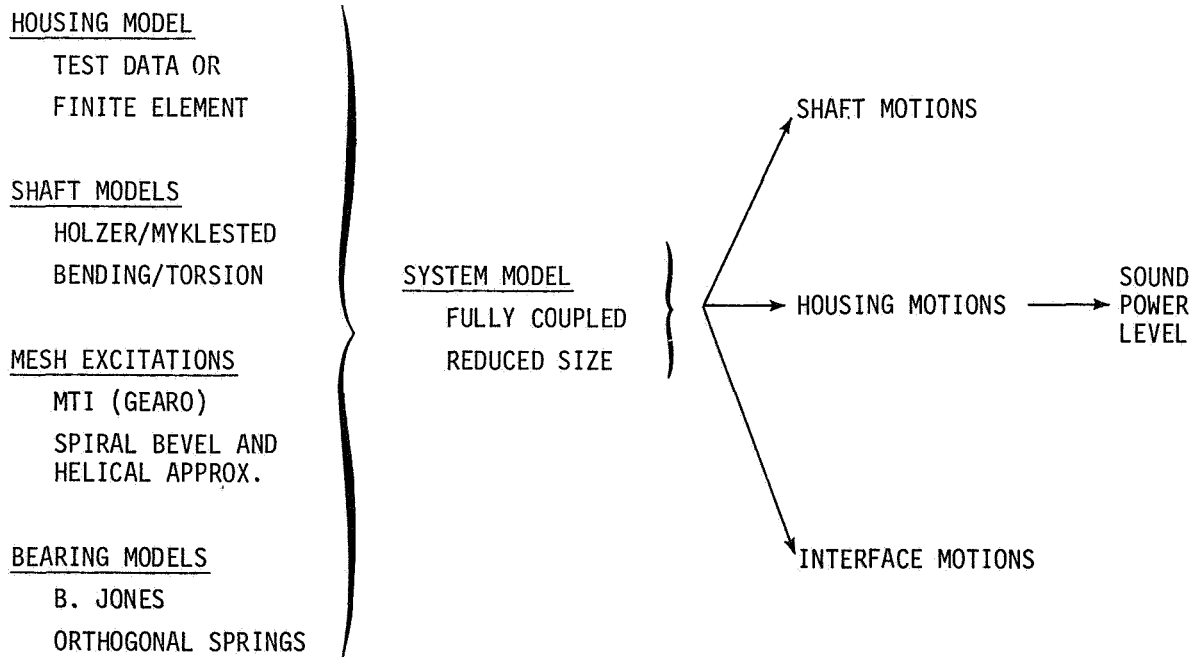
Figure 3.- SH-2 main transmission.

HOUSING MODEL
  TEST DATA OR
  FINITE ELEMENT

SHAFT MODELS
  HOLZER/MYKLESTED
  BENDING/TORSION

MESH EXCITATIONS
  MTI (GEARO)
  SPIRAL BEVEL AND
  HELICAL APPROX.

BEARING MODELS
  B. JONES
  ORTHOGONAL SPRINGS

SYSTEM MODEL
  FULLY COUPLED
  REDUCED SIZE

SHAFT MOTIONS

HOUSING MOTIONS ⟶ SOUND POWER LEVEL

INTERFACE MOTIONS

Figure 4.- Transmission noise modeling approach.

672
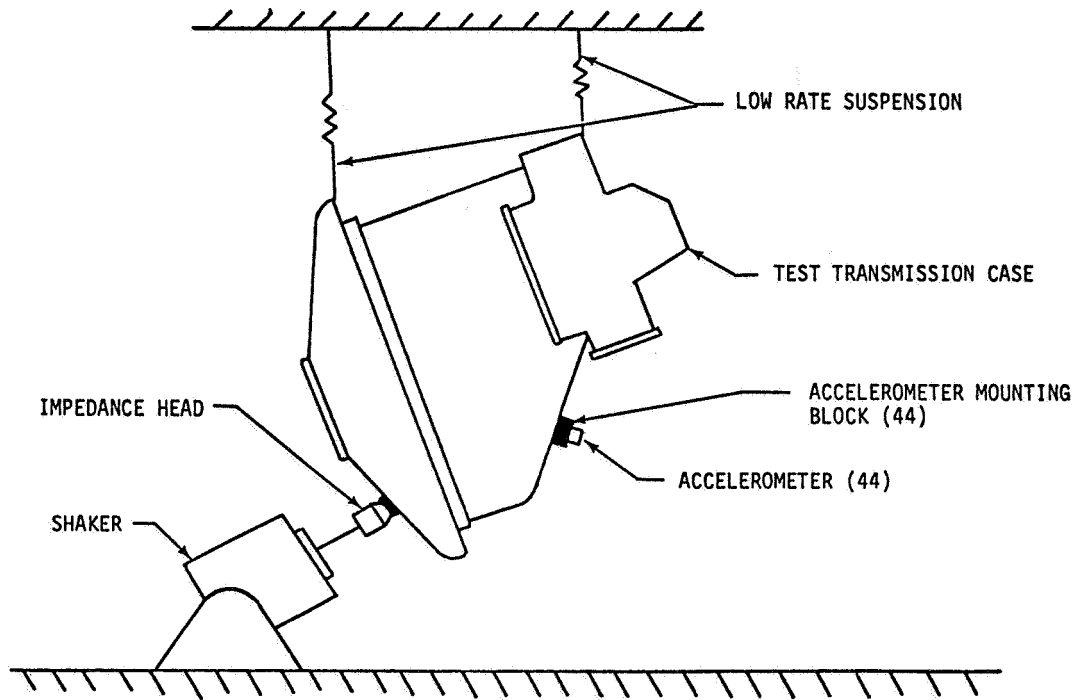
Figure 5.- Transmission case shake-test setup.
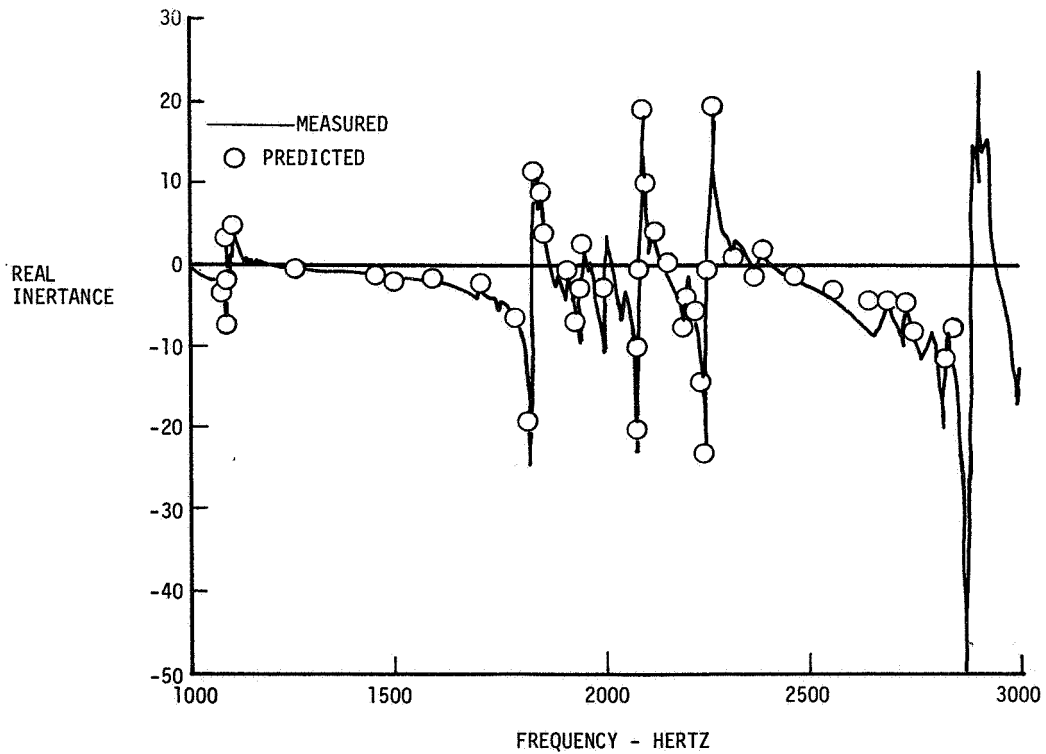
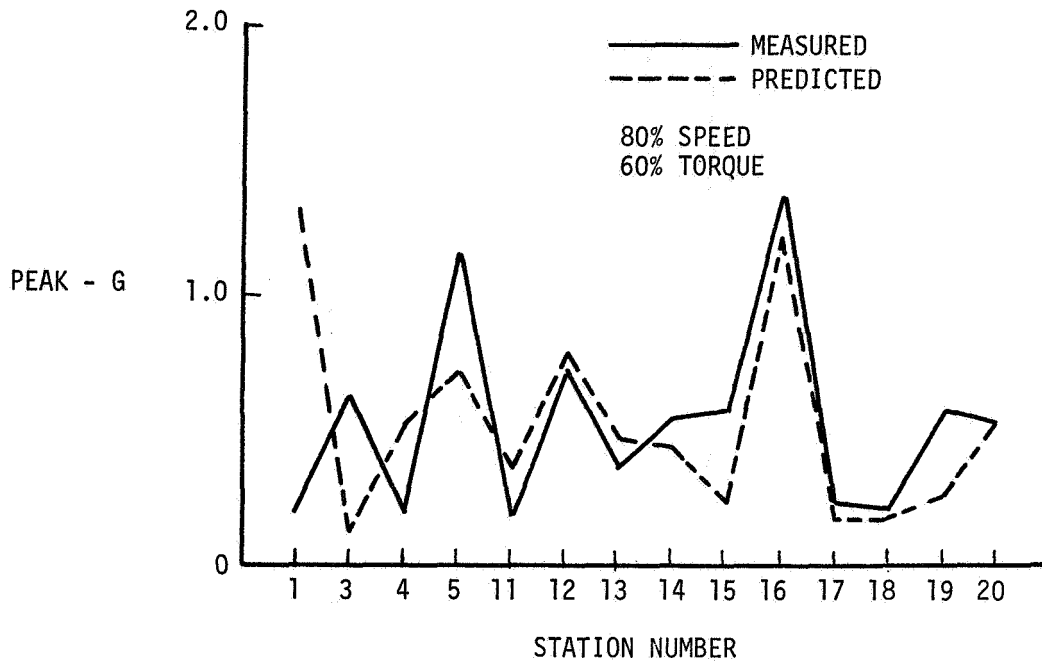Figure 6.- Measured and predicted transmission case inertance.

673

Figure 7.- Measured and predicted case acceleration for planet system excitation (348 Hz).
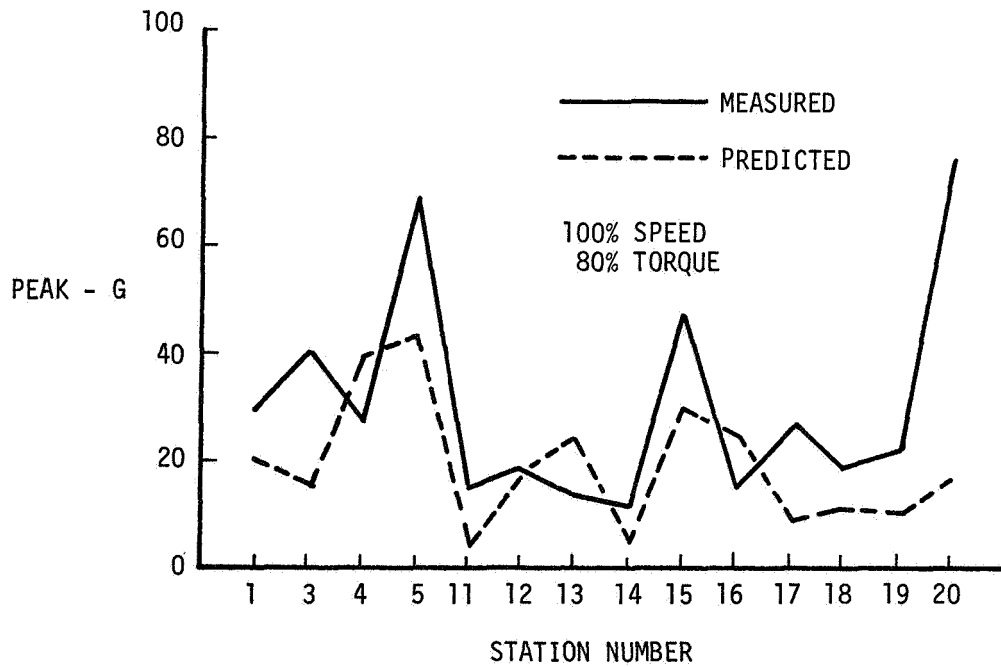

Figure 8.- Measured and predicted case acceleration for spur gear excitation (2994 Hz).
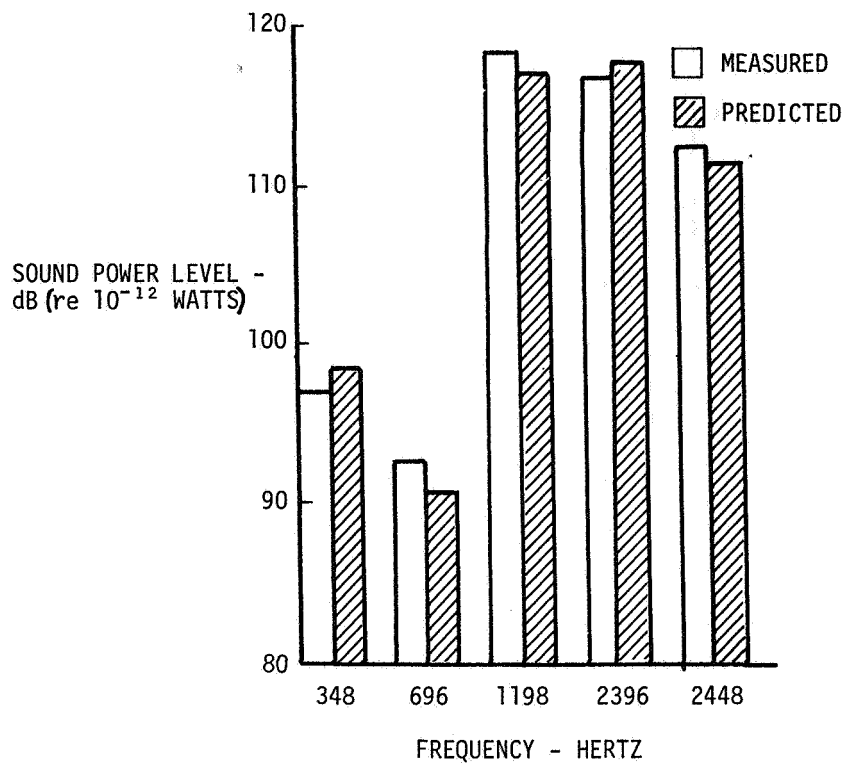
674

Figure 9.- Measured and predicted sound power levels. 80 percent RPM, 80 percent torque.
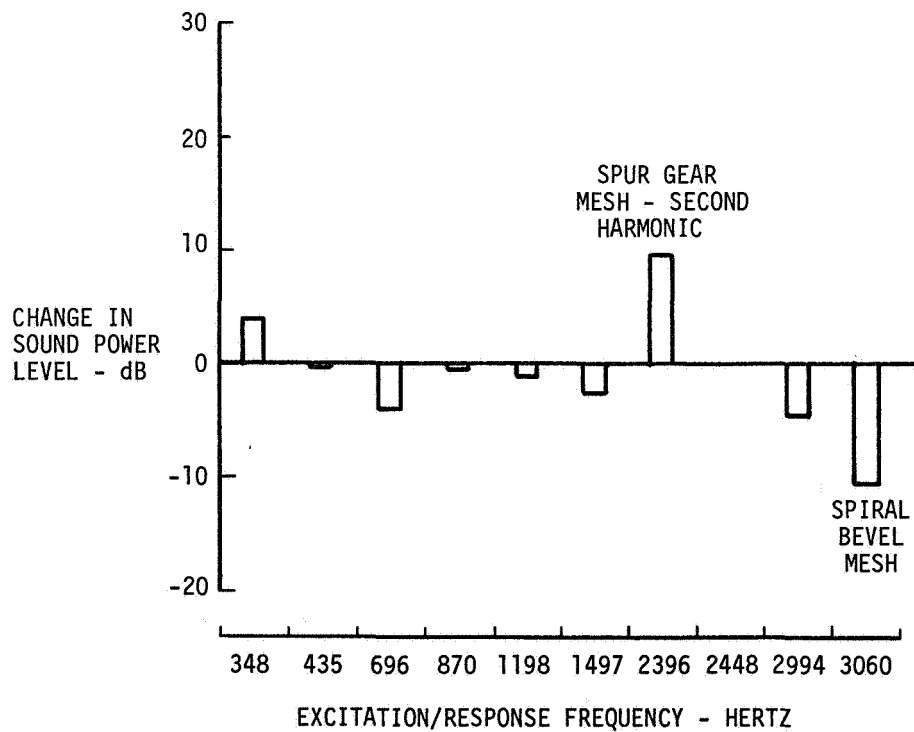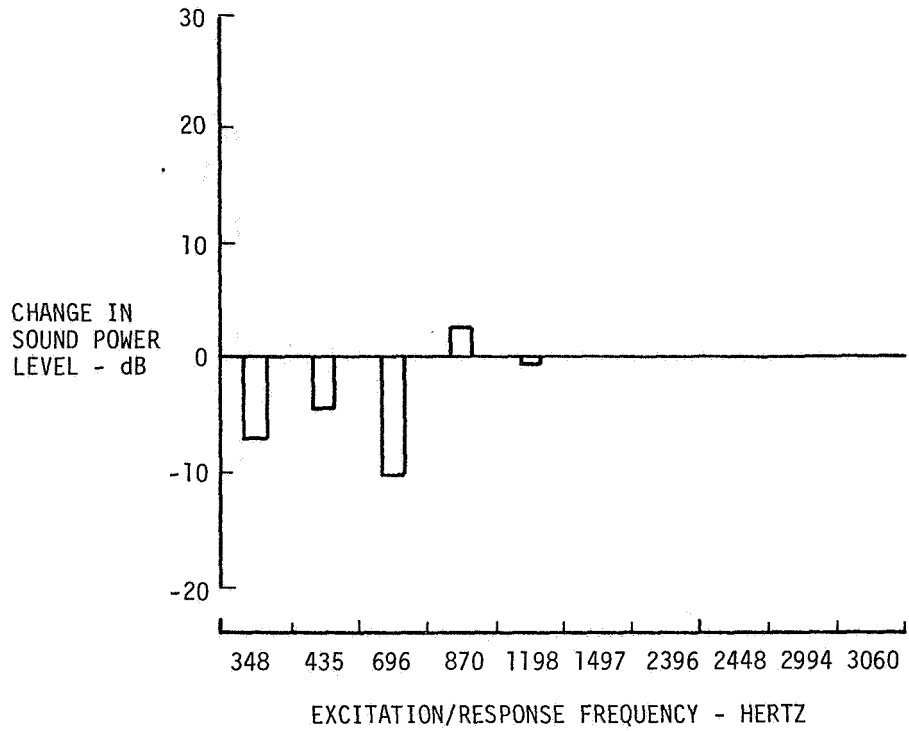

Figure 10.- Effect of increased input shaft stiffness.

Figure 11.- Effect of reduced planet carrier radial stiffness.

Figure 12.- Effect of case damping.

676

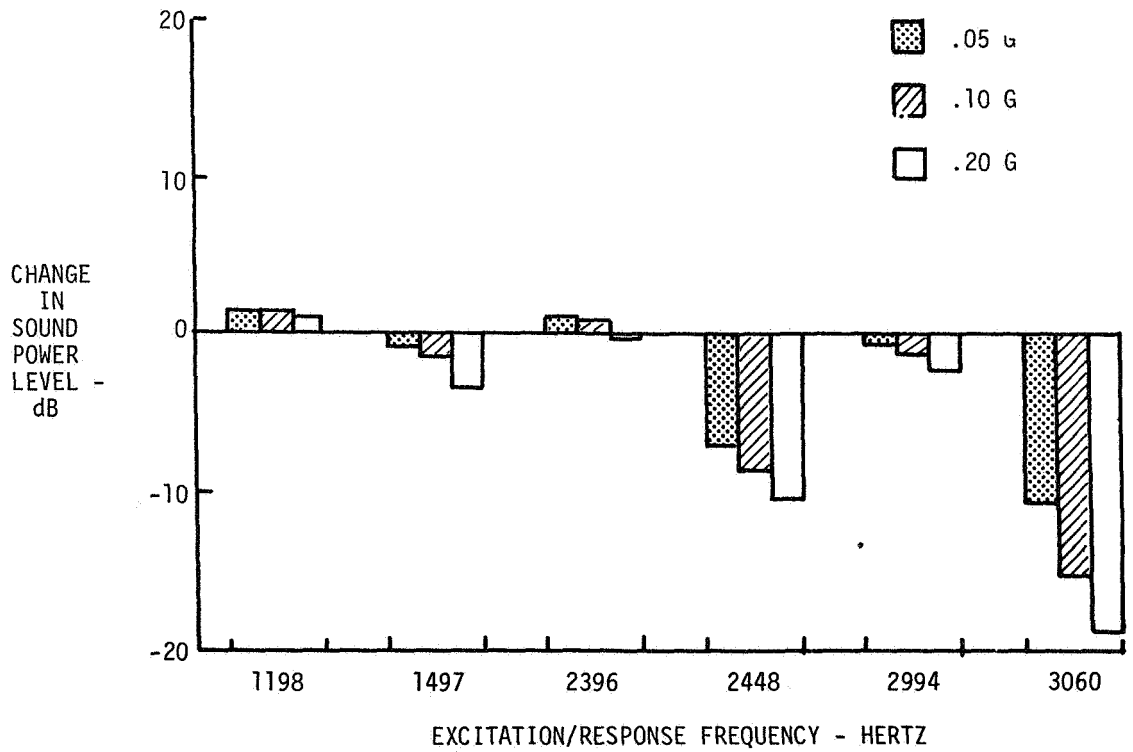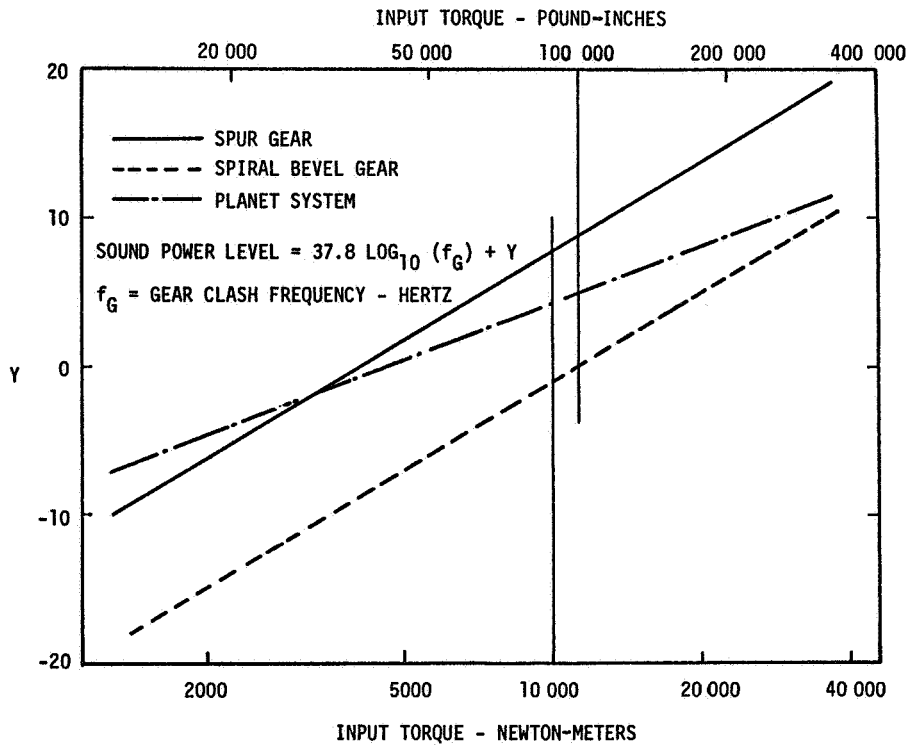INPUT TORQUE - POUND-INCHES

Figure 13.- Simplified transmission noise prediction model for
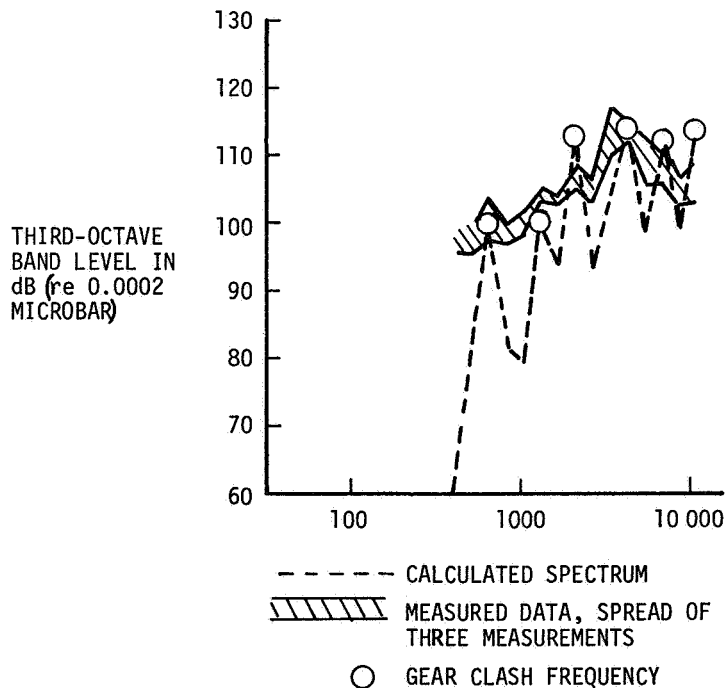fundamental mesh frequency.

Figure 14.- Measured and calculated UH-1 (B-205) internal noise
using simplified transmission noise prediction model.

THE INFLUENCE OF THE NOISE ENVIRONMENT

ON CREW COMMUNICATIONS

John W. Leverton
Westland Helicopters Limited

SUMMARY

A general review is presented on the influence of the noise environment on crew communications in helicopters. The signal-to-noise (S/N) ratio at the microphone and the effect of the attenuation provided by the helmet is discussed. This shows that the most important aspect is the S/N ratio at the microphone, particularly when helmets with improved attenuation characteristics are considered. Evidence is presented which shows that in high noise environments, the system S/N ratio is well below that required and hence there is an urgent need to reduce the cabin noise levels and improve the microphone rejection properties.

In this paper the emphasis is placed on environmental/acoustic considerations and no reference is made to the electrical aspects such as distortion effects or signal "clipping"

INTRODUCTION

The noise levels inside many helicopters are sufficiently high to give rise to severe communication problems as well as causing crew fatigue and general annoyance. The noise levels at the ear are essentially a function of the relative levels of the speech at the microphone, the levels of the cockpit/cabin noise and the amount of attenuation provided by the helmet. This results in a poor signal (speech) to noise ratio (S/N ratio) which cannot be improved by the communications system.

Data are presented in this paper to illustrate these aspects and although the values refer specifically to helicopters, the general trends and implications are equally applicable to the military aircraft (fixed wing) case. Care must be taken, however, in comparing the results, because of the higher speech levels and higher helmet attenuation values, relative to those for the helmet/boom (or throat) microphone combinations used in helicopters, associated with the integral helmet/mask worn by aircraft crew.

SIGNAL-TO-NOISE AT MICROPHONE

The range of noise levels existing in typical helicopter cockpits are indicated in figure 1 together with the corresponding long term rms speech level.

The speech levels quoted are those measured 1 cm from the lips and hence are appropriate to the level experienced by a 'boom microphone' of the type commonly used in helicopters. Also indicated on the figure are the levels appropriate to the Sea King helicopter and a pre-production Lynx helicopter. Fo convenience, the upper limit of the band of noise levels which represents the maximum levels measured in current helicopters - has been termed "noisy" cock- pit and the lower boundary as "quiet" cockpit. In practice, of course, a heli- copter spectrum is 'peaky' in nature and even if some of the octave band levels are near or on the upper limit shown, other octave band levels could be near the lower limit indicated.

The 'boom' microphone used in helicopters has noise cancellation properties which reject certain regions of the ambient noise relative to the speech. The appropriate corrections for a typical boom microphone have been applied to the helicopter data and the results are shown in figure 2. This shows that the S/N ratio in the important 1 kHz/2 kHz regions is extremely poor on the "noisy" heli copter. The helicopter spectrum, however, contains discrete frequency compon- ents and even if the cockpit is relatively quiet, one or two octave bands will be of a high level - this is illustrated for the case of the Lynx and Sea King on figure 1. Thus at one or more octave bands the signal-to-noise ratio on most helicopters is very likely to be near the value shown for the "noisy" cockpit.

Throat microphones are often used in UK helicopters in place of 'boom' microphones. These have better noise-cancelling properties but the speech is generally of inferior quality. Precise figures are not readily available but it has been suggested (ref. 1) that this reduction in voice quality is offset by the improved noise rejection. Thus, it seems reasonable to apply the boom microphone corrections and assume that they are equally applicable to the use of throat microphones; this approach has been adopted in the brief review pre- sented in this paper. Some measurements have been made under operating and laboratory conditions and these suggest that above 1/2 kHz the noise rejection properties are considerably enhanced by use of a throat microphone. This apparent advantage appears, however, to be offset by the lower speech levels and thus, for all practical purposes, the boom and throat microphones can be assumed to give similar results.

HELMET ATTENUATION

The attenuation values for helmets normally quoted by manufacturers and referred to in the general literature are based on results from 'Real Ear at Threshold' (REAT) tests. These tend to give an overoptimistic impression of the noise protection provided by a helmet and from a practical point of view, it is the actual Transmission Loss (TL) results which give a true indication of the attenuation properties of a helmet in a real environment. In the REAT method, the attenuation figures are obtained from the difference of hearing threshold measurements with and without the helmet (refs. 2 and 3), while the TL values are obtained by determining the difference between the noise level at the ear (measured by a microphone inserted inside the ear muff) and the noise

external to the helmet. In this latter test it is usual to make the measurements within a real helicopter or in a test chamber in which the helicopter environment is simulated. It is well known that these methods give very different results, although there appears to be a general confusion in the use of the two forms of results. A typical set of results for the SPH-4 helmet, which is manufact-ured by the Gentex Corporation of Carbondale, Pennsylvania, and used extensively in the U.S.Army,is shown in figure 3. The REAT results are those quoted for the helmet by the U.S. Army[1] and the TL values have been obtained by West-land Helicopters Ltd, (WHL). As can be seen the real attenuation or transmiss-ion loss values are considerably lower than those obtained by using the REAT method. The differences at the low frequencies (250 Hz and below) are of the order expected and of particular importance in the case of a helicopter because of the high levels of low frequency noise present in the cockpit/cabin. The difference between the two methods in the low/mid frequency (500 Hz) range are larger than anticipated and those which occur at high frequency (4 kHz) were not expected. It will also be noted that in the mid/high frequency range (2 kHz) the two methods give, for all practical purposes, identical results. It has also been found that slightly different results are obtained with different types of noise sources; this is, however, of secondary importance when compared to the variation from 'test-to-test'.

It is also clear from the results presented in Figure 3, and other results, that if REAT attenuation values are used to evaluate the protection offered to a pilot/crew member by a helmet, then misleading results can be obtained. In the author's experience, it is not possible to calculate the difference between TL and REAT test results and thus a true evaluation can only be made if TL tests are conducted.

It also follows from such analysis that many of the claims made recently about the dramatic increase in protection provided by the new generation of helmets are incorrect since the comparisons have in the main been made between the known TL values for the existing helmets and REAT results for the new hel-mets. This is illustrated on Figure 3 which shows the TL values for the Mk.3 helmet traditionally used by the UK helicopter pilots/crew members (ref. 1). As can be seen, although the new helmet offers considerable improvement, parti-cularly at the higher frequencies, the gain at the low/mid frequencies are far less than those suggested by incorrectly comparing the REAT results for the SPH-4 and the TL values for the Mk.3 helmet.

A new helmet, the Mk.4, is currently being introduced into service in the UK. This helmet has according to a preliminary evaluation similar or slightly superior attenuation characteristics to the SPH-4. Thus, the observations made in this paper in relation to the SPH-4 helmet, on which a fairly detailed in-vestigation has been conducted, are, in general, equally applicable to the Mk.4 helmet.

---

[1]Communication from Department of Army, U.S. Aeromedical Research Laboratory, Fort Rucker, Alabama, Oct. 1974,

INFLUENCE OF HELMET ATTENUATION

The influence of the helmet attenuation on the S/N at the ear (with intercom off) can be assessed from the TL data. Consider firstly the standard Mk.3 helmet which is used by helicopter crews in the UK Forces. This provides attenuation which increases from practically zero at low frequency (125 Hz) to over 30 dB at 4 kHz. These attenuation values have been applied to the data to give the corresponding levels inside the helmet and these are illustrated in figure 4.

It is generally accepted that the long term speech overall rms level should not exceed 105 dB since, at levels above this, intelligibility is decreased. However, if hearing damage is taken into account, a lower level would seem appropriate. This is, however, a complex subject since factors such as exposure duration, frequency, and rest periods must be taken into account. Within the UK the general consensus is that an appropriate acceptable level would be 90 dB (A) This is in line with the general approach being adopted in a number of fields (including the protection of the industrial worker). It is difficult at the present time to finalize the most desirable limit and for this reason both "speech at the ear" criteria have been added to figure 4. Considering firstly the "105 dB limit" then it will be observed that the S/N on a noisy helicopter is relatively poor. If the "90 dB(A) values" are assumed to apply, then even the quiet helicopter gives rise to a problem in the two lower octave bands considered. If helmets with improved attenuation properties are used, then the overall position is improved. Figure 5 shows the results, corresponding to those presented in figure 4, which would be applicable if a SPH-4 helmet was used. There is typically a 7 dB improvement (relative to the Mk.3 helmet) in attenuation over the complete frequency range (including the low frequency end) and thus the effective S/N ratios are considerably increased.

SYSTEM SIGNAL-TO-NOISE RATIO

Speech signals cover a dynamic range of 30/40 dB with the peaks being typically 12 dB above the long term rms value. For speech to be completely intelligible, it is generally accepted that the ratio of the long term rms to long term rms "noise" level at the ear should be at least 20 dB. Thus, the system should be capable of handling peak levels 32 dB above the basic noise level. According to reference 1, sentences used by aircrew can generally be understood from their context, providing the ear is not overloaded; a long term S/N ratio of 9 dB is just considered acceptable. A review within WHL has suggested, however, that with a more flexible vocabulary, a S/N ratio in the order of 15 dB would be more appropriate.

The communications system essentially covers the frequency range from 250 to 3000 Hz and in deriving the figures quoted above, it is assumed that there are no major bandwidth limitations on the speech transfer. If such reductions in bandwidth occur, then an increase in the signal-to-noise ratio is required to maintain intelligibility.

From the results produced in figures 4 and 5, the effective system signal-to-noise ratios can be derived. These have been determined for the Mk.3 and SPH-4 helmets, respectively, and for the "noisy" and "quiet" cockpit configurations considered. The results are shown in figures 6(a) and 6(b) for the Mk.3 helmet/quiet helicopter and Mk.3 helmet/noisy helicopter, respectively. Figure 7 shows the corresponding result for the SPH-4 helmet, but in this case, the "noisy" helicopter results only have been shown since the system signal-to-noise ratio is largely controlled by the microphone cancellation properties. The summation effect of the two individual noise signals arriving via the microphone and through the helmet has been taken into account and the shaded area represents the system S/N ratio. As can be seen, the "noisy cockpit/Mk.3 helmet" results in an unacceptable S/N ratio (figure 6(b)) and even when the improved helmet is used (figure 7) the S/N ratio is poor. It will also be observed that the S/N ratio is not uniform across the communication band (250 Hz - 3000 Hz). In addition, the helicopter spectrum largely consists of discrete frequencies and thus masking effects and possible distortion in the system has to be taken into account. It is clear, however, from these results that although the improved helmet is required, the ambient (cabin noise) levels must be lowered and/or the microphone cancellation properties improved.

DAMAGE RISK CRITERIA

In the preceding discussion, the problem relating to Damage Risk has been ignored and the assessment was simply based on the signal-to-noise ratio at the microphone and the "speech" level requirement at the ear. The data concerning hearing damage are confusing and often contradictory. It is, however, generally accepted that for an 8 hour/day - 5 days/week exposure, an upper limit of 90 dB(A) is acceptable. The situation in the case of rating helicopter noise is further complicated by the fact that the Damage Risk Criteria commonly quoted refer essentially only to broadband noise. The audio spectrum on a helicopter is, however, dominated by a series of discrete frequencies arising from the gearbox. It is generally accepted that an allowance for such tones can be made by reducing the allowable levels by 5 dB(A). There is also a general feeling that the suggested criteria should be applied to aircrew even though they are not exposed for the full 40 hours per week. Thus, it seems reasonable to assume that the 85 dB(A) criteria should be applied in the helicopter case. This limit (in terms of octave band levels) has been superimposed on the levels "at the ear" for the Mk.3 helmet and SPH-4 helmet, respectively, as shown in figures 8 and 9. For reference, the octave band levels corresponding to an upper limit of 90 dB(A) are also shown. As can be seen the noisy helicopter exceeds the recommended values in several octave bands when the Mk.3 helmet is used and even the quiet helicopter levels are very close to the 85 dB(A) criteria values in the 125 and 250 Hz octave bands. Use of the SPH-4 helmet would improve the situation as illustrated in figure 9 and in this case the noisy helicopter values are below the 90 dB(A) limit. Thus, the use of the SPH-4 helmet (or equivalent) would seem essential.

By using a modified Mk.3 helmet, which has a miniature Knowles microphone mounted in the earpiece to measure the level inside and a microphone attached to measure the ambient noise outside the helmet, a series of measurements have been made on a range of pre-production and "in-service" aircraft. In addition to the noise measurements, the electrical signal on the "tel lines" to the earpiece were measured. These tests have given results which confirm the general trends outlined previously and highlighted a number of points.

In one case the levels at the ear inside the helmet were of the same order as the ambient levels outside the helmet. The results obtained are illustrated in figure 10 which show that in the 1 kHz and 2 kHz bands, the levels are to a first order identical inside and outside the helmet. The aircrew concerned were questioned, but could not give any satisfactory explanation why the amplifier volume control was set so high. Thus, there is no real explanation for these results and so it would appear that they resulted from the crew attempting to raise their speech above the level of the noise in the communication system and/or the annoying high level in the low frequency (125/250 Hz) octave bands. This resulted in high levels inside the helmet without, of course, any real improvement in speech quality.

In an attempt to clarify the position relating to these results, a repeat test was planned but unfortunately, this has to be carried out on a different helicopter. The same intercom system was, however, used and in these tests the system volume control was adjusted to the minimum considered acceptable by the crew. This resulted in the levels measured inside the helmet being considerably lower, as illustrated in figure 11 and although no specific subjective tests were performed, the crew tended to agree that the overall communication was equally as good - or rather equally as bad - as on the previous tests. These observations were also confirmed by a subjective evaluation of the recording taken with "speech".

The increase in noise in the 125 Hz octave band is, incidently, not dependent on the intercom system and appears to be due to a resonance within the Mk.3 helmet. Thus, the published attenuation value at 125 Hz for the Mk.3 helme used in deriving the levels inside the helmet shown on figure 3 would appear to be in error and rather than an attenuation of 1 dB, there appears to be a 5 dB amplification.

It will also be observed on figures 10 and 11 that the rms speech levels are only a few dB above the "noise" on the intercom system and only in the 250 Hz and 1 kHz levels can a clear difference be seen. The corresponding "tel line" recordings are illustrated in figure 12 and as can be seen the S/N ratio in the 500 Hz to 2 kHz band is only 6/8 dB and hence inadequate for good communications.

REVIEW OF TEST RESULTS

One-third octave band analysis has been performed on a number of conditions recorded in the Lynx. Particular interest was placed on the 'high level' recording and a typical one-third octave band spectrum is shown in figure 13. This shows the levels with the intercom disconnected (noise via helmet), levels when the intercom is switched on and the levels which occur during speech. The speech levels shown are the results of conventional rms "slow" analysis and thus neither represent, the true "peak" or the long term rms value. A brief review, however, suggests that the corresponding long term rms values are in the order of 6 dB below the maximum levels shown - this should be taken into account when comparing the results with the idealized values discussed previously. The results in figure 13 show clearly the impact of the combination of the high cockpit levels and the poor throat microphone cancellation properties. It will be noted that the largest S/N ratio occurs in the 250/800 Hz region. If a lower system gain (amplification) is used, then the complete spectrum (i.e. speech and noise) will be lowered. In the region above 800 Hz. the S/N ratio is largely a function of the microphone properties and the speech-noise S/N ratio in the ear piece will remain for all practical purposes unaltered. Between 200 Hz and 800 Hz, the level at the ear is a function of the noise transmitted through the helmet and hence, as the gain of the system is decreased, the effective S/N ratio at the ear will also decrease. Thus, the overall system S/N ratio will decrease and the intelligibility degraded. It follows from this that a subjective assessment of the acoustic acceptability or otherwise, which is often used in rating the cockpit-cabin noise environments, can be very misleading since the apparent absolute level at the ear is simply a function of the gain setting of the communication system. It is also apparent by a comparison of the 1/1 octave band data in figure 10 and the one-third octave band data in figure 13 - that a detailed evaluation cannot be readily made from the conventional octave band analysis.

In addition to the above, the intelligibility is further influenced by the masking effect of the tones, and the nonuniform earpiece cavity response. Masking effects are difficult to quantify, particularly in the case of helicopters where the levels are varying with time by 10 dB and, in some cases, 15 dB. Currently, octave bands are used for assessing cabin noise levels but limited evidence suggests that even if allowances are made according to available methods for discrete frequencies, these methods of rating the noise underestimate the annoyance and influence on intelligibility. In a simple test conducted using Lynx data, it was found that when the noise levels in the 1 kHz and 2 kHz octave bands were decreased by 10 dB from the levels indicated in figure 10 it had no effect on the apprent clarity of speech or the subjective impression. Preliminary evaluation suggested that the signal-to-noise ratio in the individual bands, or in other words the discrete frequency-to-broadband levels, had a marked effect on the subjective impression and can influence the intelligibility. It is also apparent that the nonlinear response of the ear cavity - measurements made by WHL suggest variations (dips and peaks) of ± 10 dB - the spectrum is far from 'flat' as illustrated in figure 14.

CONCLUDING REMARKS

The S/N ratio at the ear is controlled by the cancellation properties of the microphone and the helmet attenuation. When improved helmets are used, the system S/N ratio will become more dependent on the microphone rejection properties in most of the helicopters and will remove the problems associated with hearing damage arising from high levels at the ear.

It follows that either the noise levels in the cockpit have to be lowered or alternatively the noise attenuation properties of the microphone improved. In this context it is of interest to note that the noise rejection characteristics of the boom microphone - and, by implication of the WHL tests, the effective rejection of the throat microphone - decrease with frequency and approach zero at 4 kHz. The mask/mask microphone provides, on the other hand, an effective "shield" whose rejection increases at 1 kHz and above. Unfortunately, at 1 kHz the value is only 5 dB but some general communication noise exclusion microphones provide even better noise rejection with the values reaching typical 20 dB at 1 kHz. Thus, it would seem desirable to attempt to incorporate the advantages of both systems to provide a wide frequency range rejection. Alternatively, concepts of placing the microphone inside the helmet would seem well worth while, particularly when helmets with improved high attenuation at low frequencies are developed. Reduction of the noise at the source must, of course, be pursued with equal vigour but there is a limit, particularly in the cockpit area. Treatments can be readily applied to the cabin area and although these in turn produce some reduction in the cockpit area, it is unlikely that significant gains can be made before radical new fuselage design concepts currentl being considered can be employed.

With the improved helmets, it is worth considering placing more emphasis on the microphone rejection of the noise, since, if this could be achieved, then higher ambient noise levels could be tolerated without infringing Damage Risk Criteria. This solution could be applied to all forms of aircraft/helicopters, whilst noise reduction techniques will, in general, have to be related to specific designs. The overall cost of developing an acceptable microphone system in the long term would, therefore, be most likely to be less than the cost of individual noise control schemes. Even so, it does appear that attempts at obtaining improvements in both aspects must be considered if the communications problems are to be overcome.

REFERENCES

1. On the Specification of Maximum Noise Levels in Aircraft. RAE Technical Report 72089, June 1972.

2. Method for the Measurement of the Real Ear Attenuation of Ear Protectors at Threshold. S3.19, American National Standards Institute, 1974.

3. Method of Measurement of the Attenuation of Hearing Protectors at Threshold. BS5108, British Standards Institute, London, 1974.
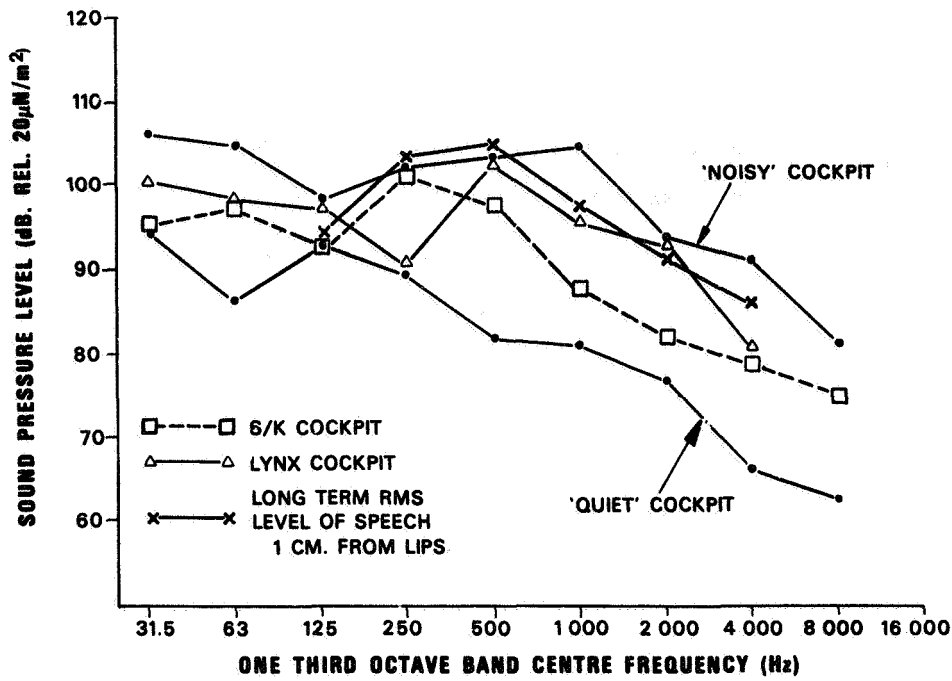
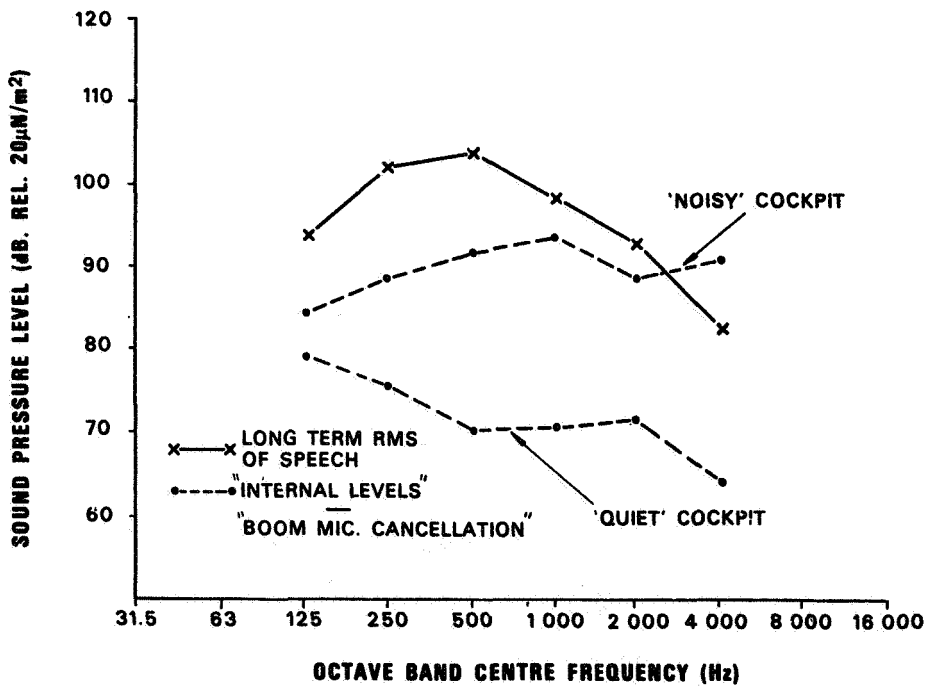Figure 1.- Helicopter internal noise levels compared with
speech levels.

Figure 2.- Ear piece noise levels (boom microphone cancellation
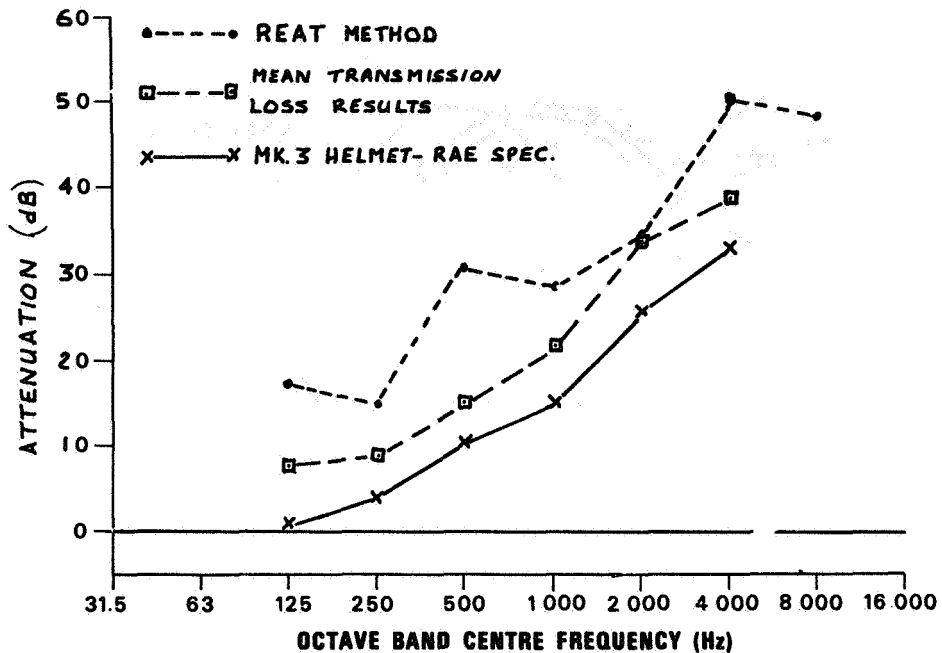corrected) compared with speech levels.

687

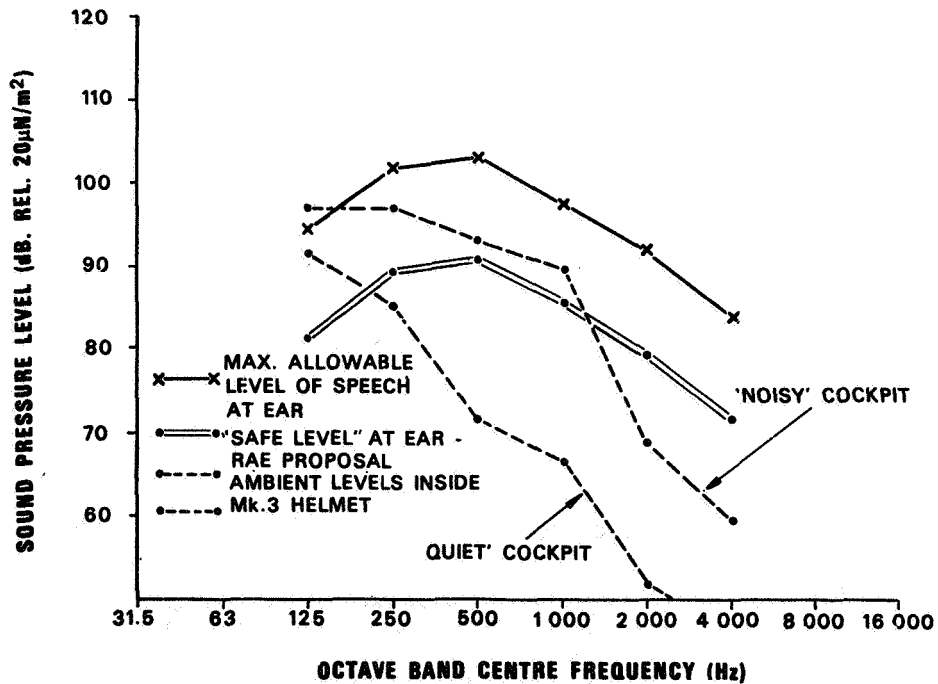Figure 3.- Attenuation of Mk.3 and SPH-4 helmets.
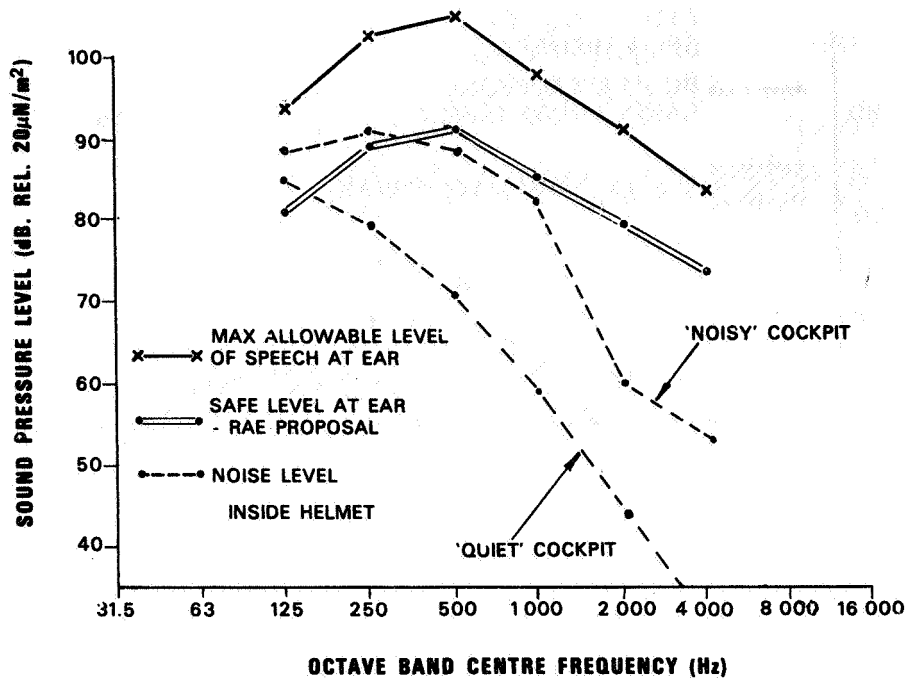

Figure 4.- Noise levels at ear - Mk.3 helmet.

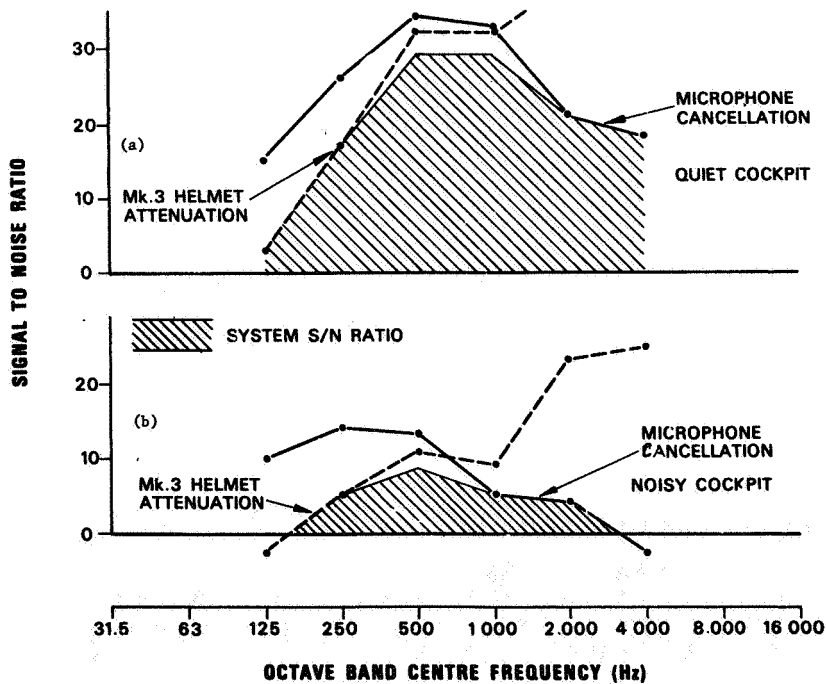Figure 5.- Noise levels at ear - SPH-4 helmet.

Figure 6.- Signal to noise ratios based on a speech level of 105 dB
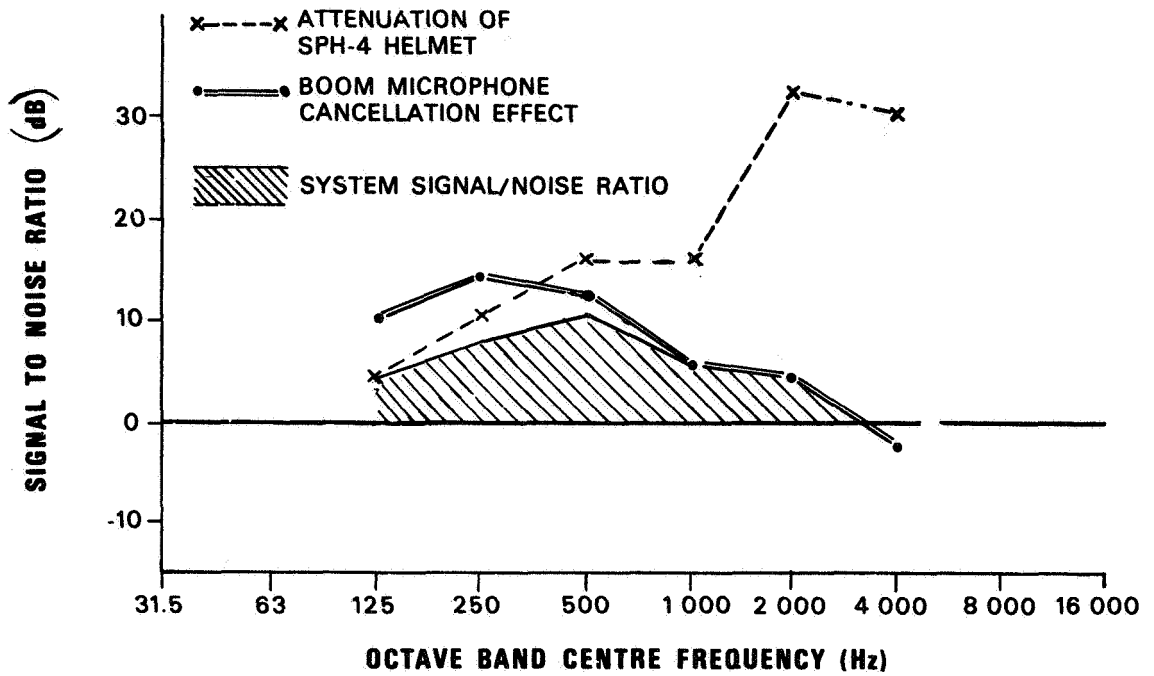- Mk.3 helmet "quiet" and "noisy" cockpits.

Figure 7.- Signal to noise ratios based on a speech level of 105 dB
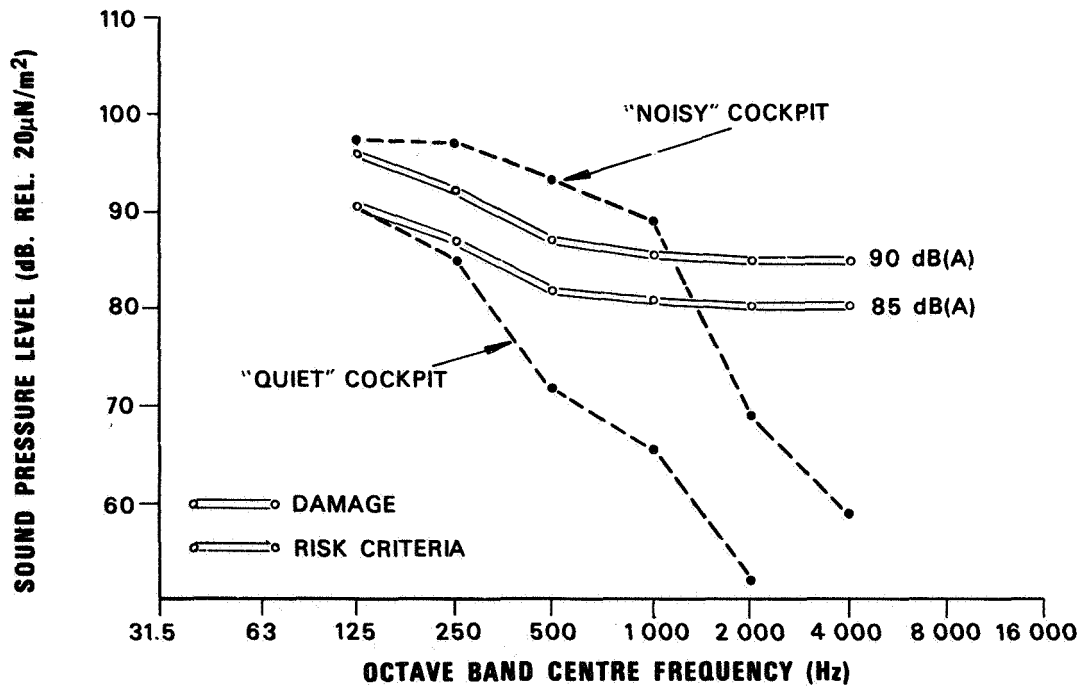- SPH-4 helmet "noisy" cockpit.

Figure 8.- Levels at ear compared with damage risk
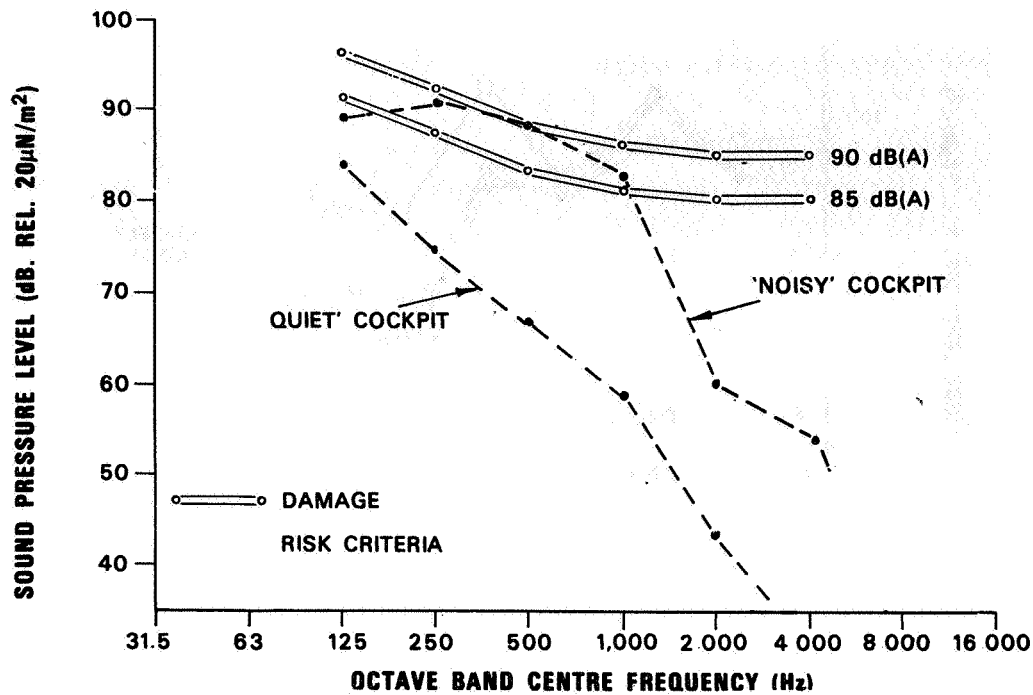criteria - Mk.3 helmet.

Figure 9.- Levels at ear compared with damage risk
criteria - SPH-4 helmet.

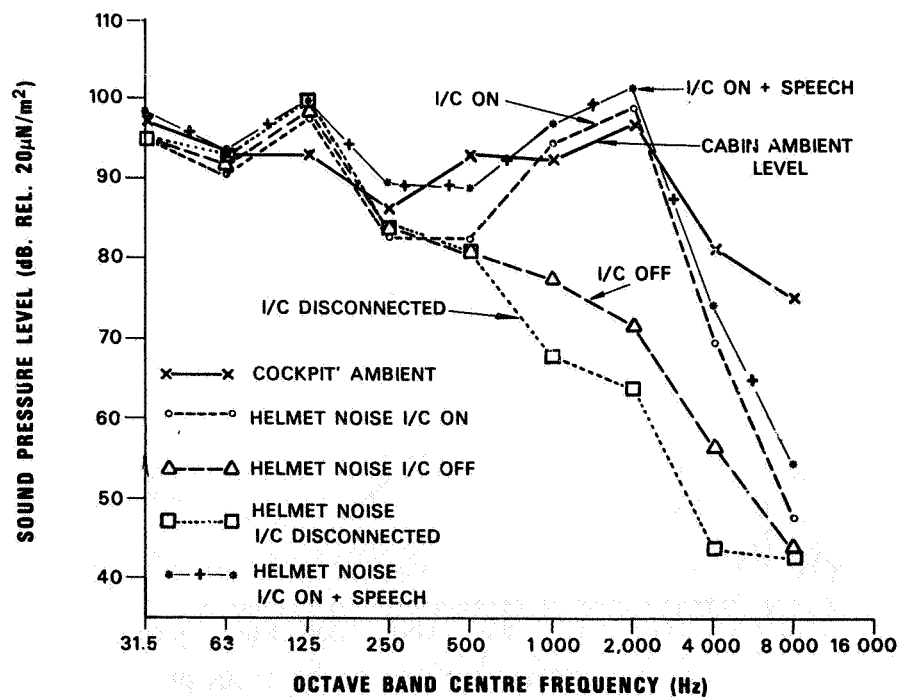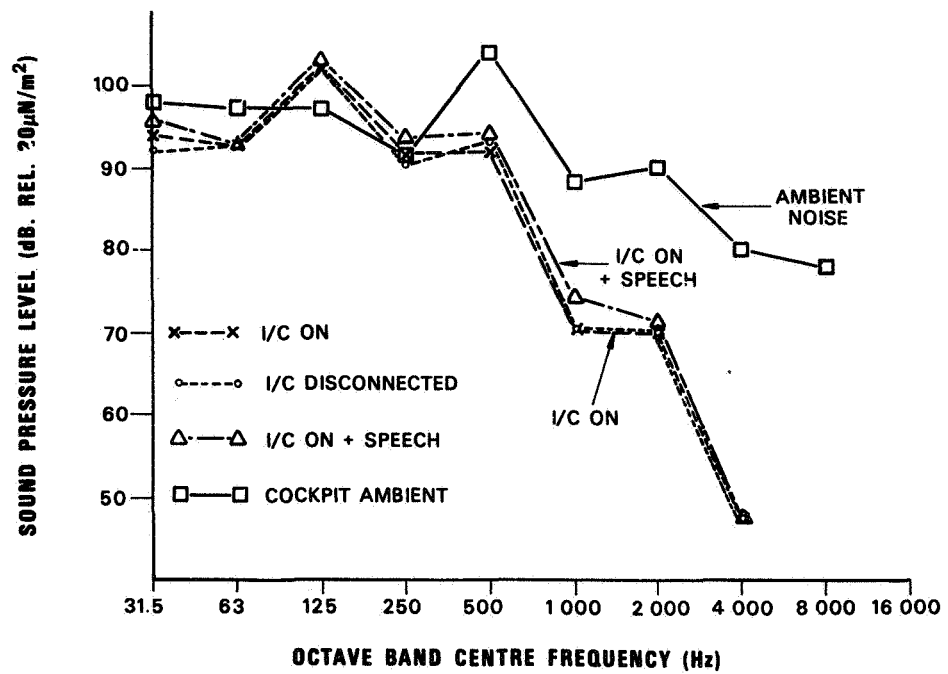Figure 10.- Lynx intercom noise - levels at ear - Mk.3 helmet.

Figure 11.- Lynx intercom noise - levels at ear - effect of reducing intercom system gain setting - Mk.3 helmet.
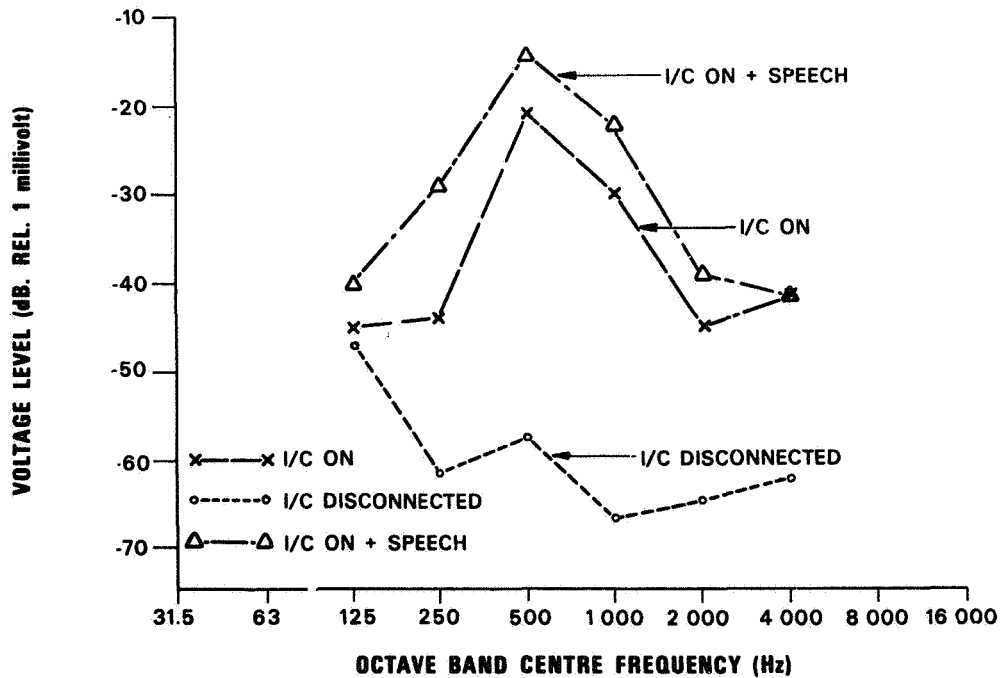

Figure 12.- Lynx intercom noise - electrical signal on headset input.

Figure 13.- Lynx intercom noise - comparison of speech and
background noise levels.

Figure 14.- Frequency response of Mk.3 helmet earpiece.

693

HELICOPTER INTERNAL NOISE REDUCTION RESEARCH AND DEVELOPMENT

APPLICATION TO THE SA 360 AND SA 365 DAUPHIN

H. J. Marze and F. d'Ambra
S.N.I. Aerospatiale

INTRODUCTION

With the extension of the civil commercial market, the noise inside helicopter cabins is becoming one of the foremost problems for the comfort of passengers.

As shown in the statistical study of figure 1, the helicopter is the most noisy vehicle in comparison with other ground or flying vehicles.

QUALIFICATION AND IDENTIFICATION OF ANNOYANCE

We have been concerned for several years by the internal noise problem, and, as a first step, the sources of noise inside cabins have been investigated. As shown in figure 2, there are many possible sources os noise (main rotor, tail rotor, engine(s), gear boxes, or accessories). As each of them has peculiar acoustic noise characteristics (rotational noise, principally), they can be identified by narrow-band analysis of the sound signal.

Analysis of noise recordings taken inside bare cabin helicopters in flight has shown that the most significant source of noise is the main gear box (fig. 3) which gives rise to a large number of pure tones emerging 10 to 30 dB from the broad-band spectrum.

Knowing the source of noise, we have quantified the annoyance by applying the present conventional units (fig. 4):

1) A and D weighted dB

2) Speech interference levels by evaluating the mean level in the voice frequencies

3) Perceived noise level from Noys curves and correction of this level for spectral irregularities

Very soon, we saw from the passengers evaluation that the usual units could be inconsistent with the subjective answers collected and that they were accordingly only imperfectly representative of the annoyance actually felt in helicopter cabins. (See fig. 5.) Such disagreement is bound to the existence of pure tones within the 500 to 5000 Hz range; these frequencies exceed the 20 dB broad-band noise and even sometimes can exceed 30 dB.

In order to quantify the additional annoyance, we have carried out psychoacoustic studies on the effect of the pure tone emergence. (See fig. 6). Wide band type noises actually measured on the helicopter were submitted to a large number of juries for comparison with the same noise to which a pure frequency of 1000, 2000 Hz or 1000 and 2000 Hz had been electrically added. The results of this study have demonstrated that the conventional units, dBA, dBD, PNdB, and even TPNdB, underrated the effect of the emergence of pure tones within the 3 to 9 dB range for dBD and PNdB and within the 1 to 5 dB range for dBA and TPNdB (emergence of 20 dB and 30 dB in narrow-band analysis). This nonexhaustive study of the emergence effect has shown that the significant parameters of the internal noise of helicopters are the pure tones at the meshing frequencies of the main gear box.

MESHING NOISE REDUCTION STUDY OF MAIN GEAR BOX

The purpose of the study undertaken is the acquisition of knowledge on (fig. 7):

(a) mechanisms of vibration generation inside the main gear box - study of meshing

(b) mechanisms of transmission between source and cabin, through the study of dynamic behaviour of main gear box components (pinions, casings, etc.) or those linking the main gear box to the cabin structure

Noise Sources

Gear meshing is a noise generator due to its design and realization; angular meshing errors are generating vibrations which will excite the structure. (See fig. 8). Until the last few years, the compromise made at the design stage between the various gear parameters had for its main objective a minimum weight while ensuring a satisfactory service life. For that purpose, gear toothing was designed to work as closely as possible to the maximum permissible stresses and specific pressures but also to limit axial, radial, and tangential loads on bearings.

This choice is the contrary of the continuous meshing concept; as the tooth bending increases with the load, the low driving and overlap ratios achieved with low spiral angles and diametral pitch or high pressure angle induce sudden load variations during meshing and do not ensure the compensation of machining errors which would require the simultaneous meshing of several teeth.

In a first stage, we have measured the angular meshing error on a pair of pinions under no load by using a "GOULDER MIKRON" type checking machine (fig. 9). The results, recorded on paper in analog form, clearly show the existence of tooth profile errors superimposed on an offset error or distortion of the basic circle. The spectral analysis of these analog signals allows the separation of these phenomena and the quantification of the effect of

696

additional parameters such as backlash.

An example of toothing geometry modification is as follows. On the SA 365 main gear box, the input spiral bevel gear toothing has been redesigned, taking the acoustic aspect into account; the tooth bearing pattern has been optimized to ensure a better meshing continuity. The gain achieved over the original meshing is approximately 15 dB.

Dynamic Behaviour of Detail Parts

If a meshing concept taking the acoustic aspect into account is a necessary condition to achieve a low noise level, it is not sufficient. In fact, in the transfer of vibration energy to the structure, the dynamic behaviour of each of the components constituting the transfer path (pinions, shafts, bearings, casing, and main gear box attachment fittings) has to be considered.

Axisymmetric Part Modes (Pinions, Shafts)

In a first stage, an experimental and theoretical mode determination has been made for the parts constituting the geat train.

Refer to figure 10 for the results of a mode determination made by using a laser holography method and a finite-element mathematical model on a SA 365 spiral bevel and planet gear assembly. The mathematical model established allows the determination of the axisymmetric part modes under load and in rotation. The agreement between modes calculated and those measured in the laboratory using laser holography is excellent up to 7 to 8 kHz.

The search for agreement between the SA 365 main gear box natural and excitation frequencies (fig. 11) shows that it is difficult to design a complete main gear box in which no component natural frequency would be in accordance with a meshing frequency. This difficulty of mastering the full gear train dynamic behaviour has been checked on an actual SA 360 main gear box in which the spiral bevel ring gear rigidity had been modified.

Figure 12 shows the changes in noise levels, measured on the acceptance test bench, for one of the spiral bevel gear meshing frequencies versus rotational speed and in two different configurations, initial ring gear and reinforced ring gear. According to the rotational speed, the modification may be beneficial or not, and for nonnegligible gains achieved at nominal r.p.m. at this frequency, there were appreciable losses at other meshing frequencies.

The introduction of some damping in all the gear train seems to be a useful line to follow in view of reducing the gear train dynamic responses. A calculation model of the forced response for damped axisymmetric parts should be established to allow the design of such assemblies.

Knowing the main gear box casing dynamic behaviour is a very important factor; in fact,

- Due to the vibration of its wall, the casing is a source of noise.

- The vibration energy generated at the source and transmitted to the casing through the bearings will reach the structure through the casing attachment points (main gear box suspension bars and flexible mounting plate).

- Casing supports the shafts and thus ensures proper positioning of meshing gears, hence the risk of coupling between the excitation and casing response.

Modal determination in laboratory.- As for axisymmetric parts, modal determination has been made in the laboratory on SA 330-SA 365 main gear box casings using the laser holography method. Figure 12 shows two examples of mode determination on the SA 360 casing. On the prototype casing, it has been noted that a natural frequency of 1792 Hz was close to the spiral bevel gear meshing frequency of 1850 Hz. A structural change (stiffening of casing through a rib located at midheight) has relocated the natural frequency from 1792 Hz to 1850 Hz and generated a new mode at 1729 Hz. As there is a slippage of natural frequency according to the load (from 1792 Hz to 1850 Hz) and as this has been checked on the prototype casing (fig. 13), the modified casing should not have any longer natural frequencies in accordance with the spiral bevel ring gear meshing frequency. In fact, a gain of some dB's has been noted during the bench testing of this modified casing.

Forced response of complete main gear box on test bench and on aircraft.- To check the results obtained in laboratory tests, a bench accelerometric measurement (see fig. 14 for set-up) has shown there was really a very large response of the main gear box casing at 1770 Hz, and this frequency was moving towards 1850 Hz when torque was getting nearer the nominal load.

A second check on the presence of resonance at 1850 Hz has been obtained in cruising flight by applying a damping product on the main gear box surface. The gain in noise level has been appreciable in the 2 kHz octave (an atten- uation of more than 3 dB for 1 kilogram of damping product) although the attenuation was negligible at the other frequencies.

As for the gear train detail parts, the design of casings using materials that offer a large internal damping seems to be necessary in view of limiting coupling effects between the gear train and casing modes, and also the amplitude of responses at the excitation frequencies. This will be the sub- ject of future research tasks.

Main Gear Box Suspension Bar Dynamic Behaviour

The main purpose of the main gear box suspension bars is to ensure the

ransfer of lift loads to the structure; the attachments on structure and
ain gear box upper section are made through metal hinge fittings. Therefore,
he main gear box casing vibratory motions are transmitted to the structure
ithout possibility of energy dissipation.

For the SA 360 main gear box bars, the first bending modes, in free-free
onfiguration, have been determined in the laboratory (excitation through B
nd K vibrating pot and accelerometric recording). This mode determination
n the laboratory has allowed the validation of the mathematical model used
o calculate the bending modes and the study of the effect on the bars of
he hinges and weight (concentrated or distributed weights).

Figure 15 shows the results of the calculations made on a SA 360 main
ear box bar. We can see the correspondence between the third bending mode
requency (1850 Hz) and the spiral-bevel gear meshing frequency, together
ith the inportant displacement of the resonant frequencies according to
he type of weights added to the bars. The efficiency of these weights has
een verified in flight as, with 1.3 kilogram of lead distributed on the
our bars, the mean noise level dropped by 4.2 dB SIL (Speech Interference
evel).

IMPROVEMENT OF THE INTERNAL NOISE LEVELS BY OPTIMIZING

THE CABIN ACOUSTIC TREATMENT

Although some improvements have been made in the knowledge of means for
oise reduction at the source, these improvements are not sufficient to
nsuré a satisfactory noise level in the cabin, and a sound-proofing treat-
ent isolating the passenger has to be installed and optimized.

The treatments we have optimized associate the three following effects
fig. 16):

(a) An acoustic screen using the weight effect isolates the passenger
rom the noise source. (Item 1 on fig. 16.)

(b) A damping treatment limits the conversion of the vibratory energy
nto acoustic energy. (Item 2 on fig. 16.)

(c) An absorbing treatment achieved either through HELMHOLTZ resonators
r through a glass wool blanket limits the propagation of accoustic waves
nd the wave reflection effects in the cabin. (Item 3 of fig. 16.)

Figure 17, a section of the SA 360-365 cabin structure, shows the
nstallation of the various elements.

Figures 18 and 19 show the efficiency of the various treatments and
heir weight which is to be compared with the maximum weight of aircraft
f about 3000 kg. It can be noted that the conventional sound-proofing

treatments offer the minimum efficiency from the weight penalty aspect.

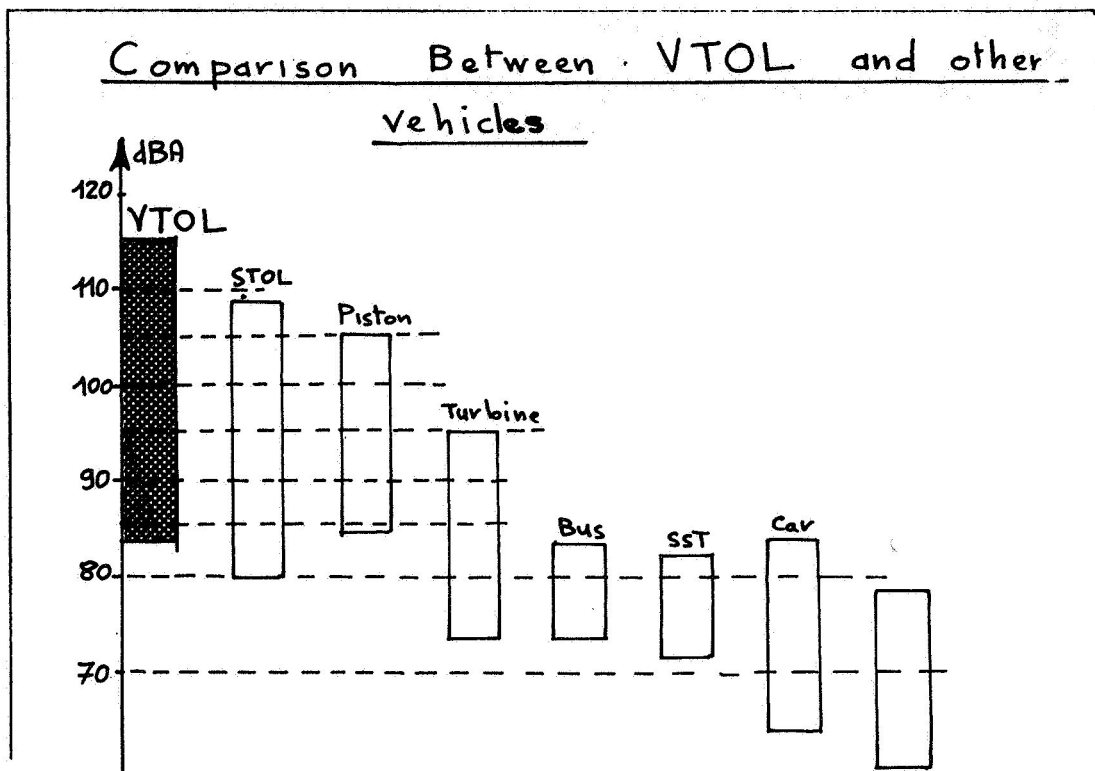| Type of action	Modification	Acoustic gain	Weight penalty
On the source	Modification of teeth geometrical characteristics	6.4 dB SIL	2 kg (approx.)
On the load transfer	(1) Treatment of a housing using a damping material	5 dB SIL	1 kg
	(2) Treatment of attachments by means of lead cloth	4.2 dB SIL	4.2 kg
On passenger's isolation	(1) Damping of cabin structure	6.8 dB SIL	26 kg
	(2) Acoustic screen	13.3 dB SIL	50 kg

CONCLUSIONS

The combined application of treatments at the source in the transfer of vibratory energy level and in the optimization of the sound barriers allowed, at high cost (weight, price), the obtainment of interesting results as shown by the narrow- and octave-band analysis of noise signals recorded in a SA 365 aircraft in flight, both with a prototype main gear box without cabin sound-proofing and with a modified main gear box and sound-proofed cabin. (See fig. 20 and fig. 21.)

A reduction of about 53 dB was optained on a pure tone (1850 Hz) which was at the origin of the main annoyance on the prototype aircraft (fig. 19). The overall noise level expressed in dB SIL and dBA has been improved by about 30 dB (fig.21), which ensures a good comfort in this aircraft.

The comparison with MIL specifications shows that it was dangerous to fly without ear protection device in the prototype aircraft and that it is now possible in the treated aircraft to fly for more than 8 hours per day without ear protection.

The comparison with airliner specifications shows that a great deal remains to be done at the mean octave frequencies of 1 kHz, 2 kHz, and 4 kHz. The possibilities of further improving the conventional acoustic treatments seem to be small.

Only an important research effort to improve the knowledge of the echanisms generating and propagating the noises in helicopter cabins can bring ome additional gains. Results obtained so far represent the maximum of what an be obtained in helicopters where the main gear box is located just above assengers, and at a cost (weight, price) which is the maximum that a elicopter manufacturer can tolerate.
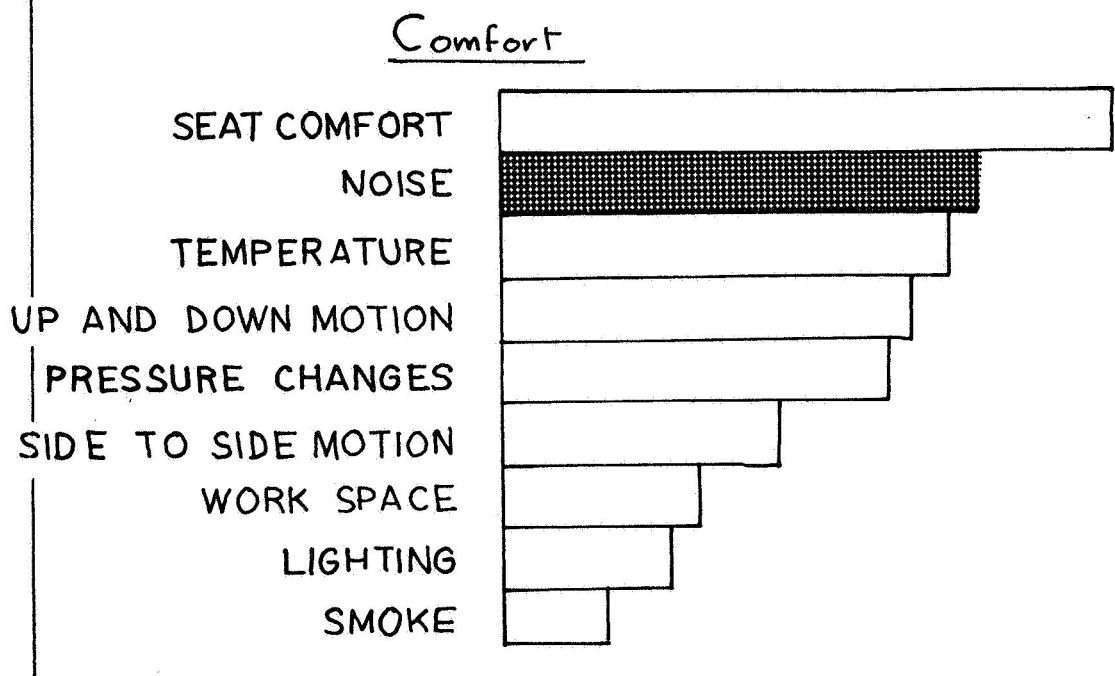
Figure 1.- Interior noise considerations for various transportation vehicles.

SA 360 DAUPHIN

main rotor
20 Hz
500 Hz
+ broad band

M.G.B. 500 Hz
5000 Hz

2000 Hz
10000 Hz
air intake

fan in fin
1000 Hz
2000 Hz
3000 Hz

AIR INTAKE SOUND PROOFING
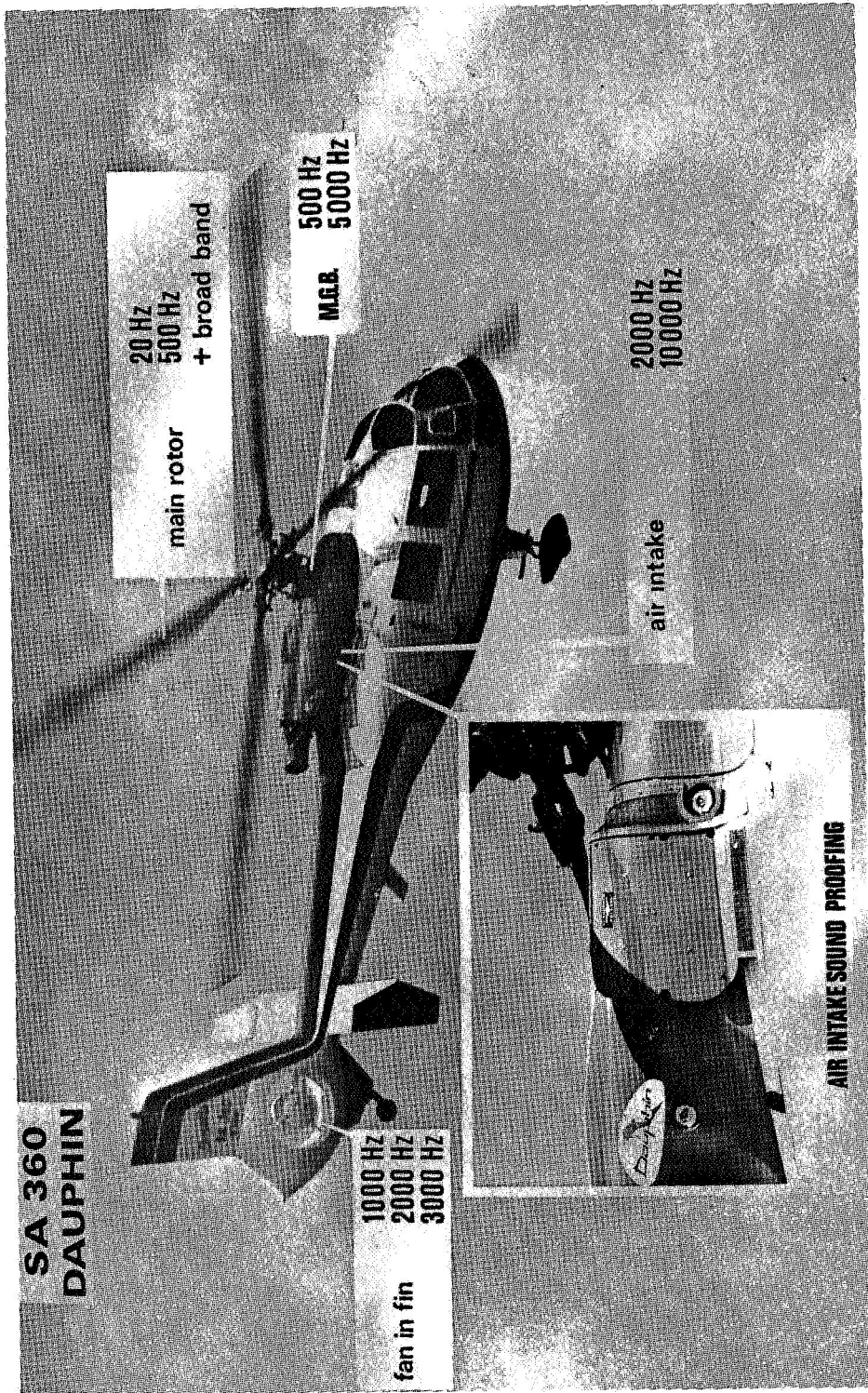
Figure 2.— Helicopter noise sources.
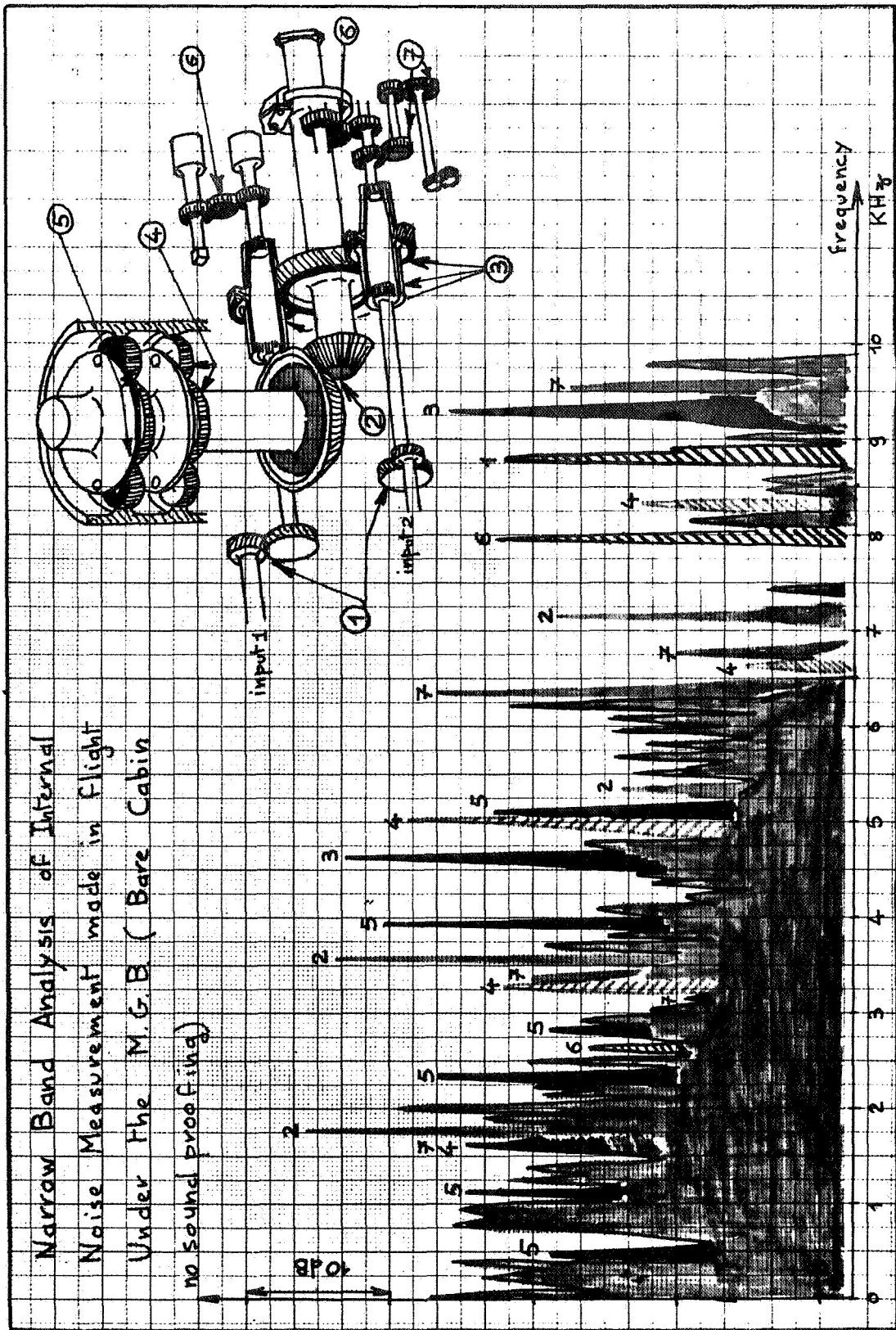
Figure 3.– Example spectrum of main gear box noise.

704

Total Weighted Levels

Attenuation

dBA

dBD

Frequency (Hz)

Average Levels Within Speech Frequencies.

$N \, dB \, SIL = \frac{1}{4}(N1 + N2 + N3 + N4)$

Speech Octaves

Octave Frequency

Perceived noise curves.

NOYS

Frequency (Hz)

Acoustic Pressure Level dB

1_ Calculation of total perceived noisiness N :

Combine the perceived noisiness n_i for the 24 third octave band:

$$N = 0.85 \, n + 0.15 \sum_{i=1}^{24} n_i$$

2_ Calculation of perceived noise level

$$PNL = 40 + 33.3 \log N$$

3_ Correction for spectral irregularities
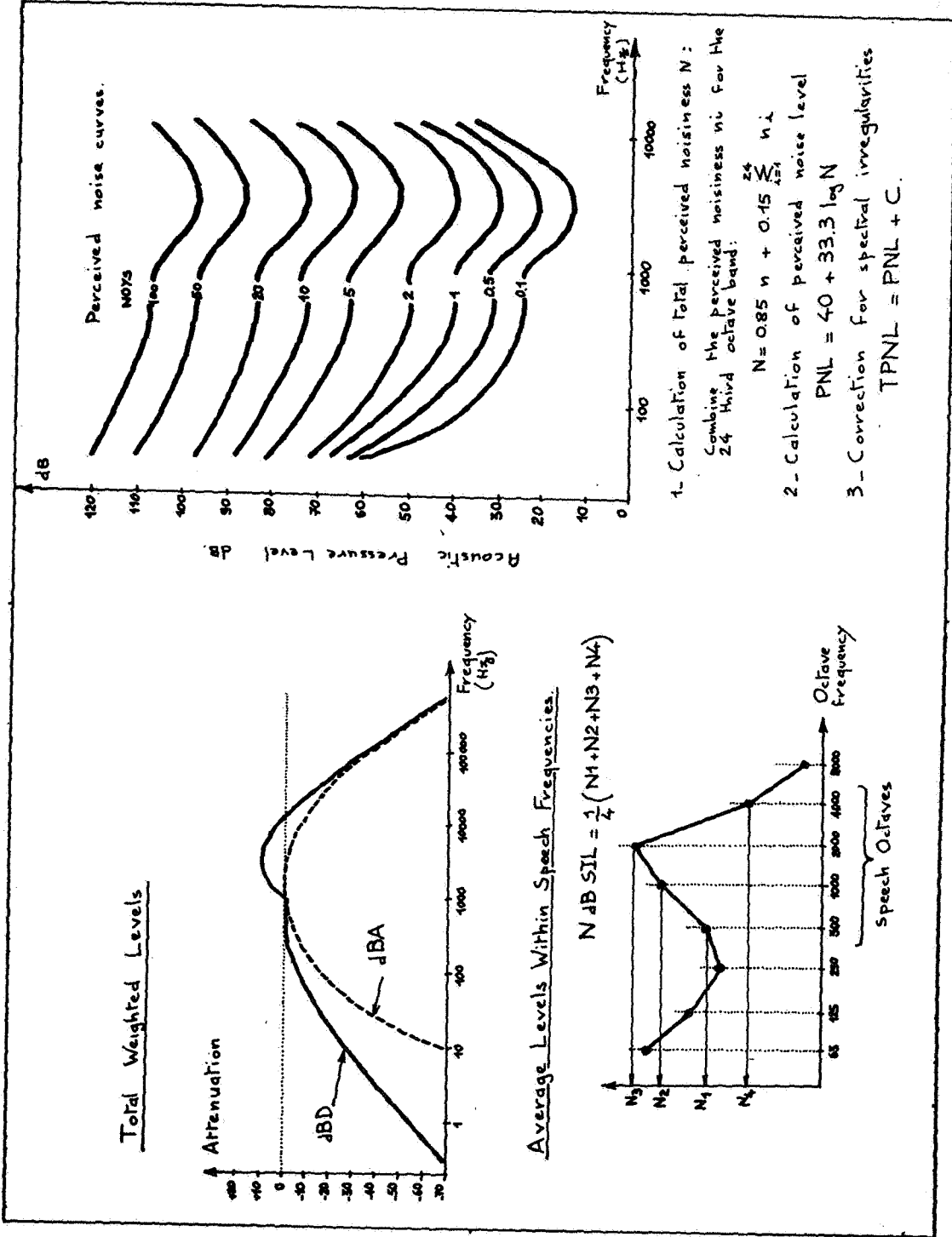
$$TPNL = PNL + C.$$

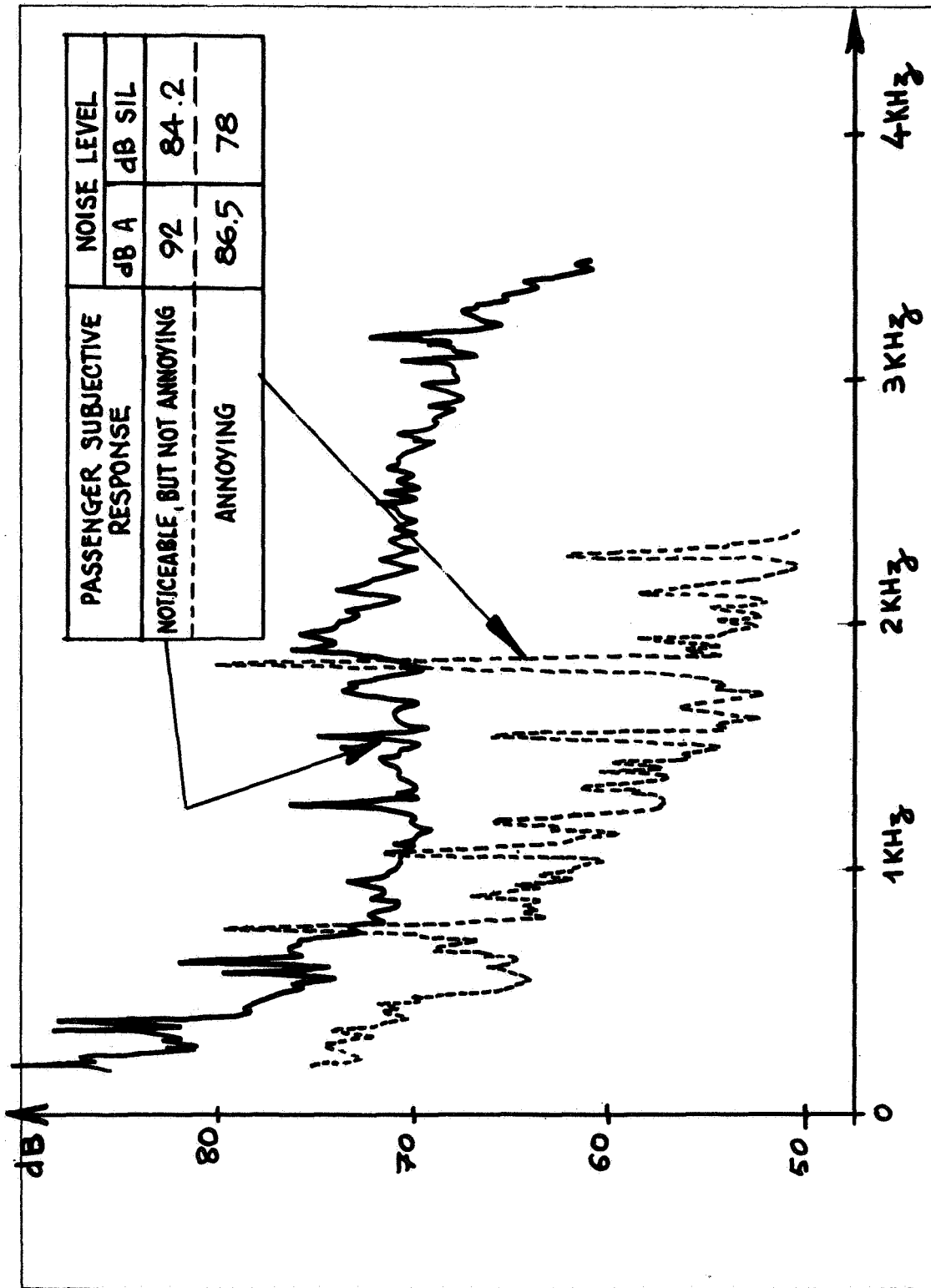Figure 4.- Conventional units for the quantification of annoyance.

Figure 5.— Comparisons of noise level measures and associated passenger
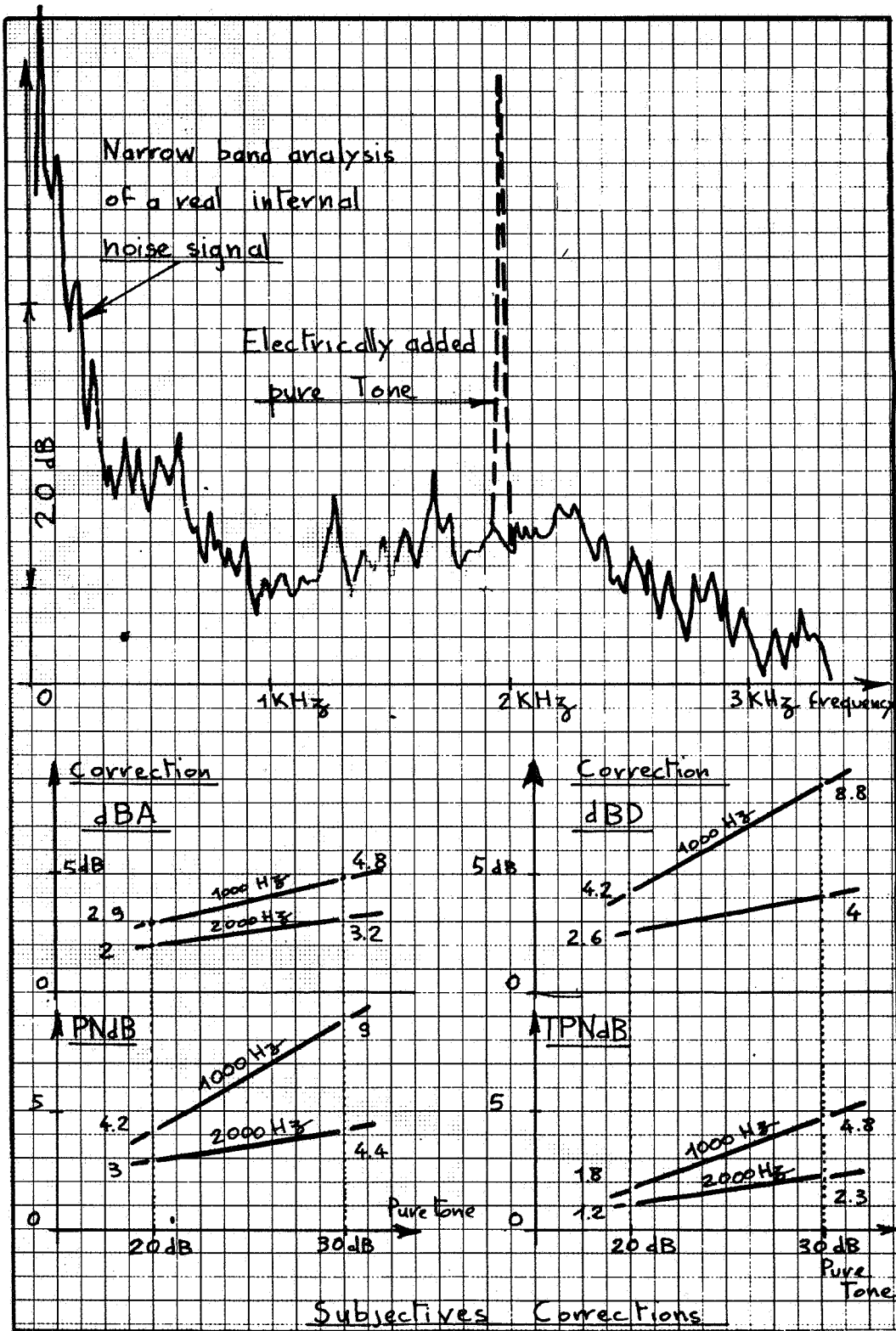subjective responses in two helicopters.

706

Figure 6.- Psychoacoustic study of the noisiness of pure tone internal
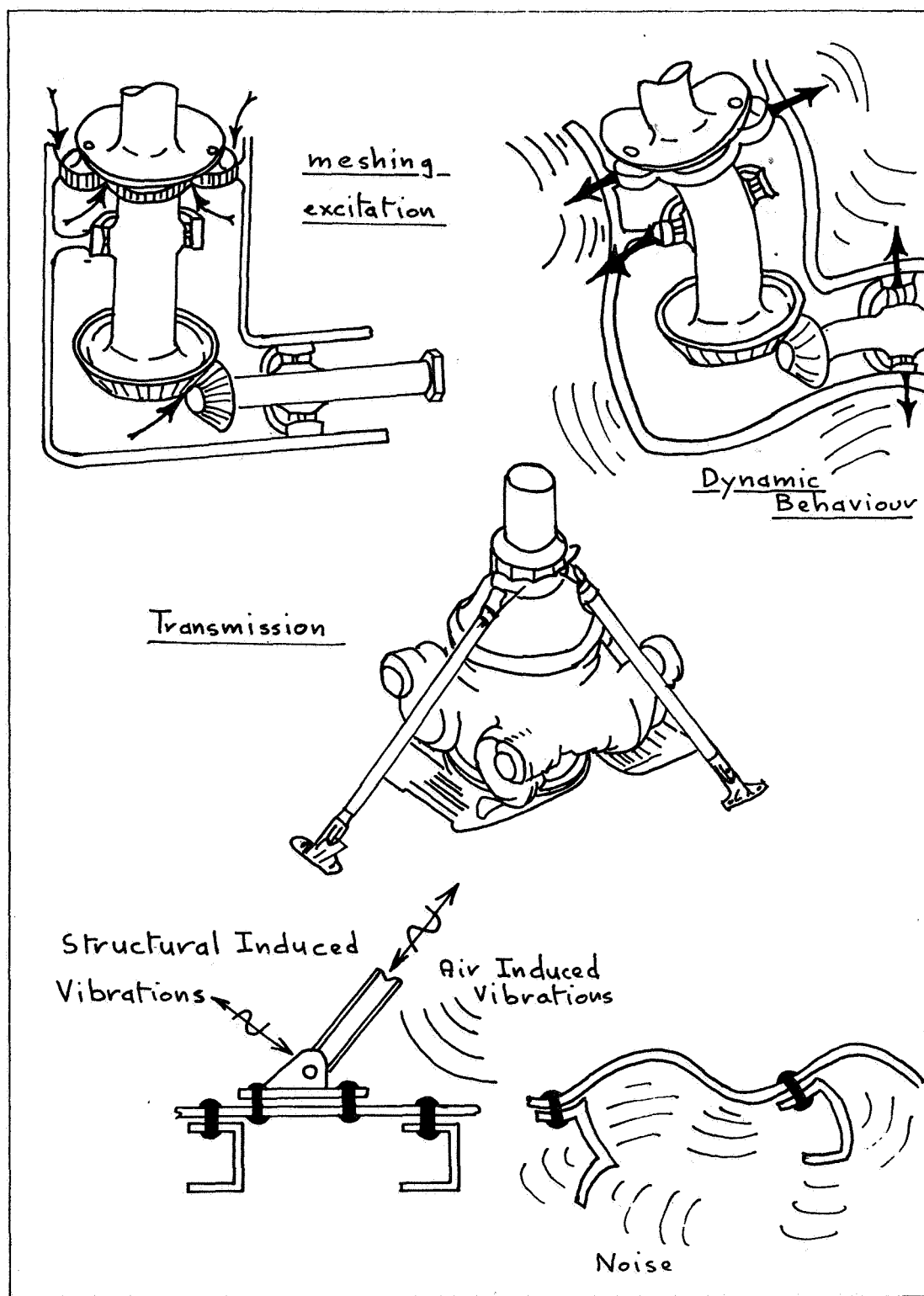noise of helicopters.

Figure 7.- Gear box noise generation and propagation considerations.
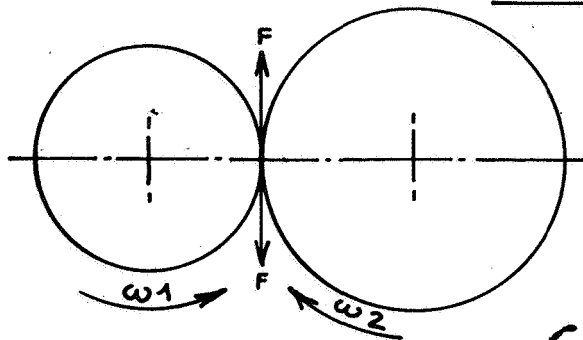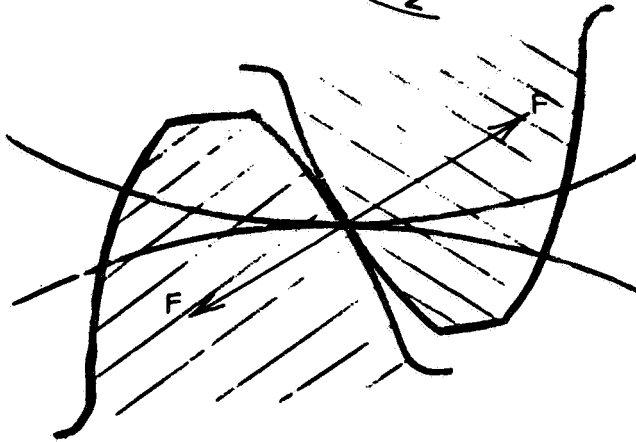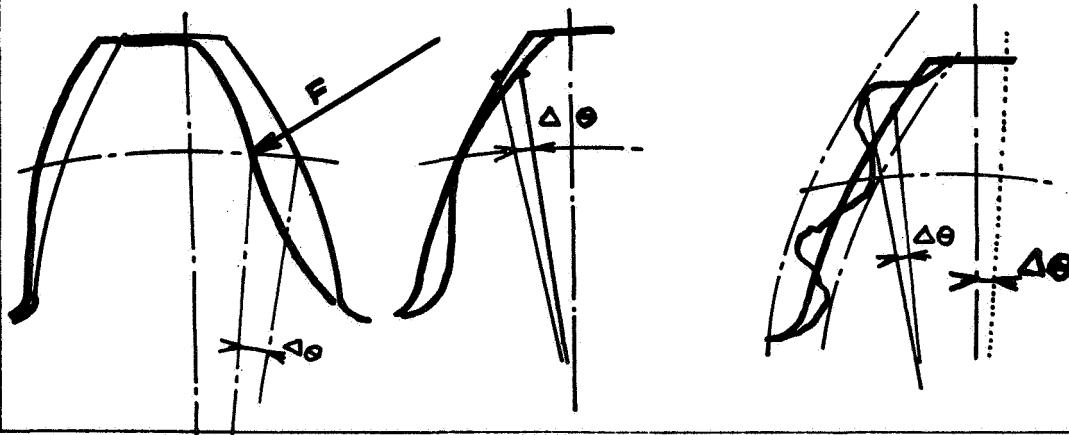
Figure 8.- Gear tooth design factors in the generation of gear meshing noise.
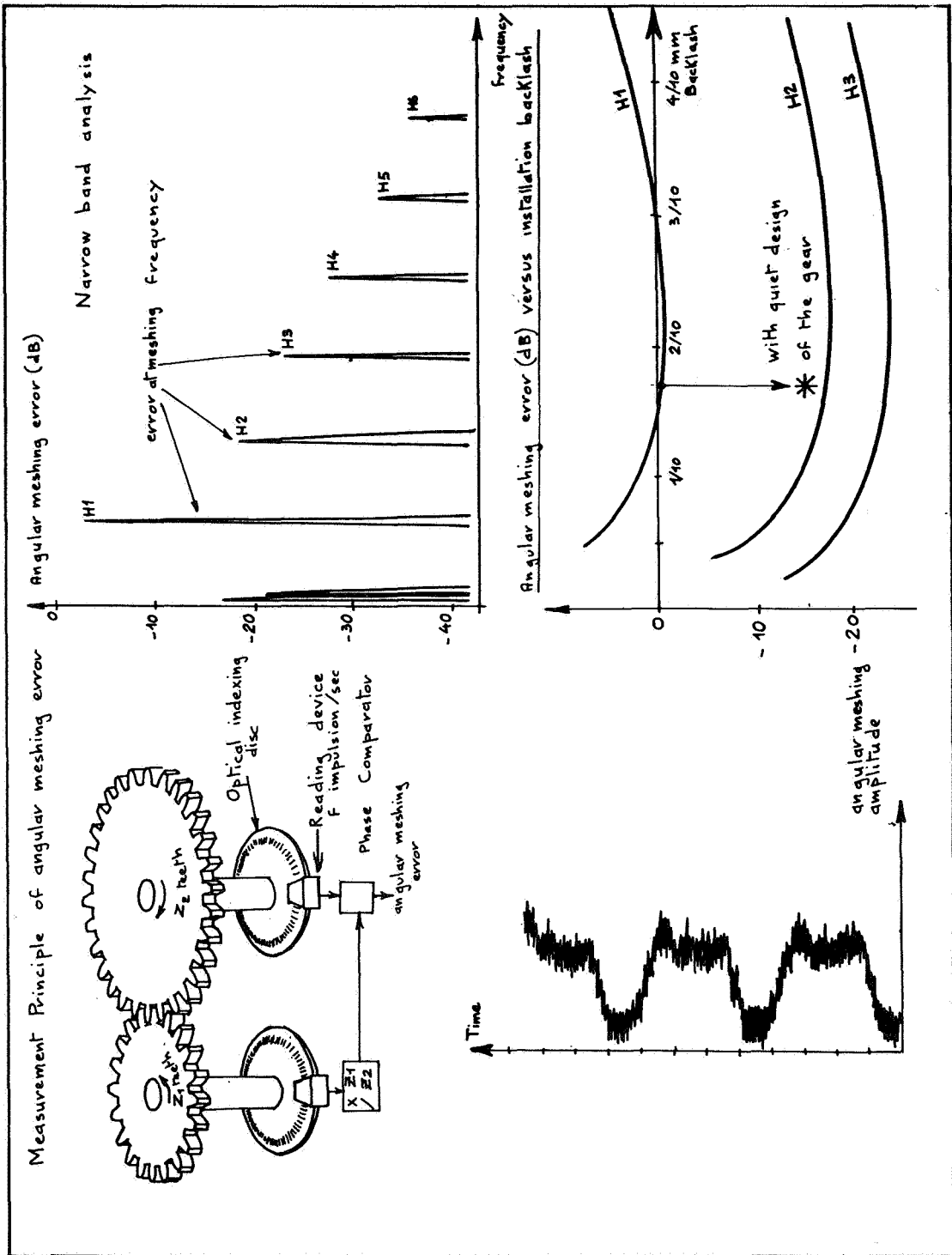
Figure 9.— Angular meshing error measurements on a pair of pinion gears.

710
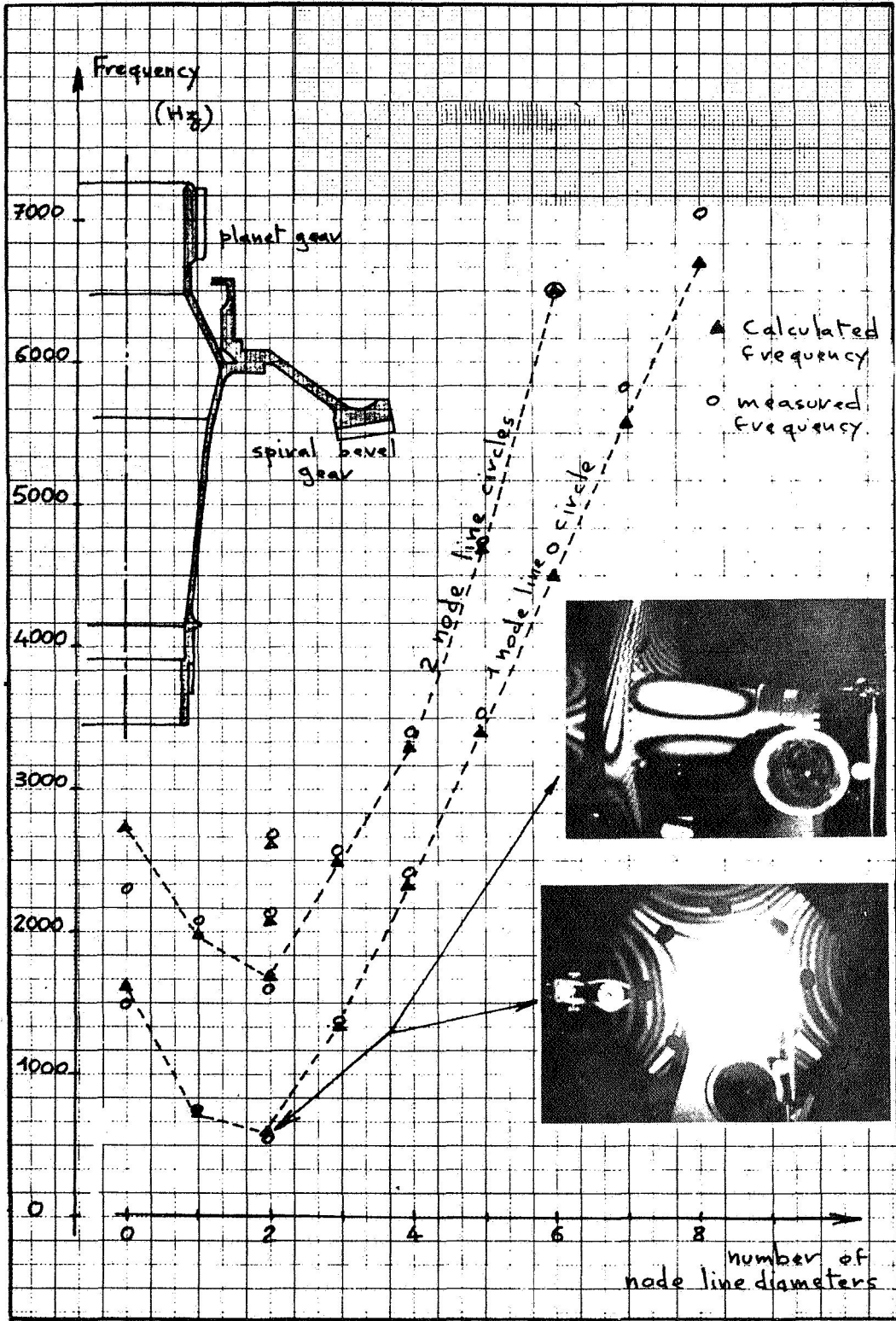
Figure 10.- Comparison between calculated and measured natural frequencies
of a spiral bevel pinion shaft on the SA 365 helicopter main gear box.
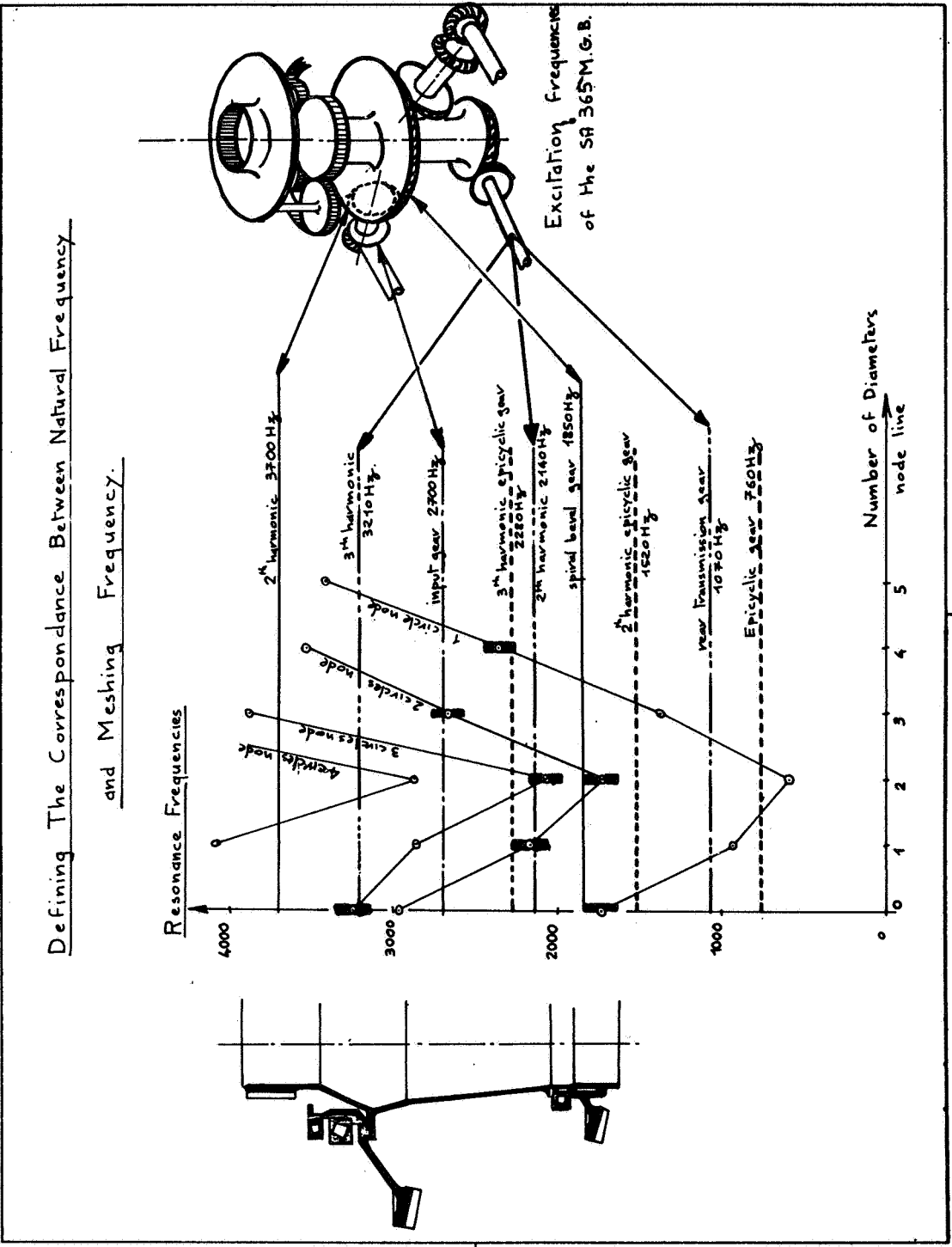
Figure 11.- Comparison of component natural frequencies with gear meshing
frequencies for the SA 365 helicopter main gear box.

712
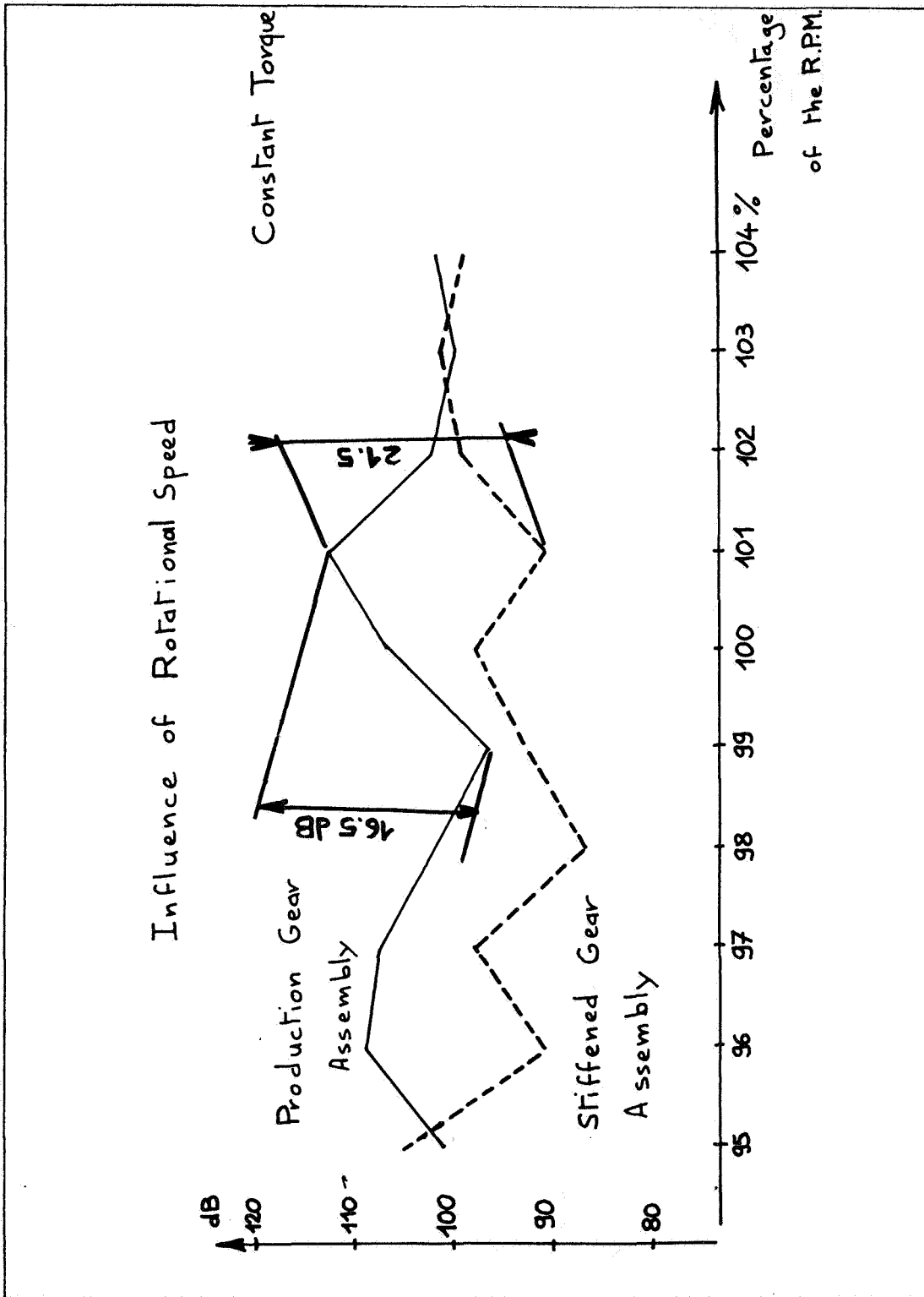
Figure 12.- Influence of stiffening of spiral bevel ring gear on the gear noise (2nd meshing harmonic).

1 - Prototype Gearbox
   Frequency 1792 Hz

2 - Modified Gearbox
   First Frequency 1850 Hz   Second Frequency 1725 Hz
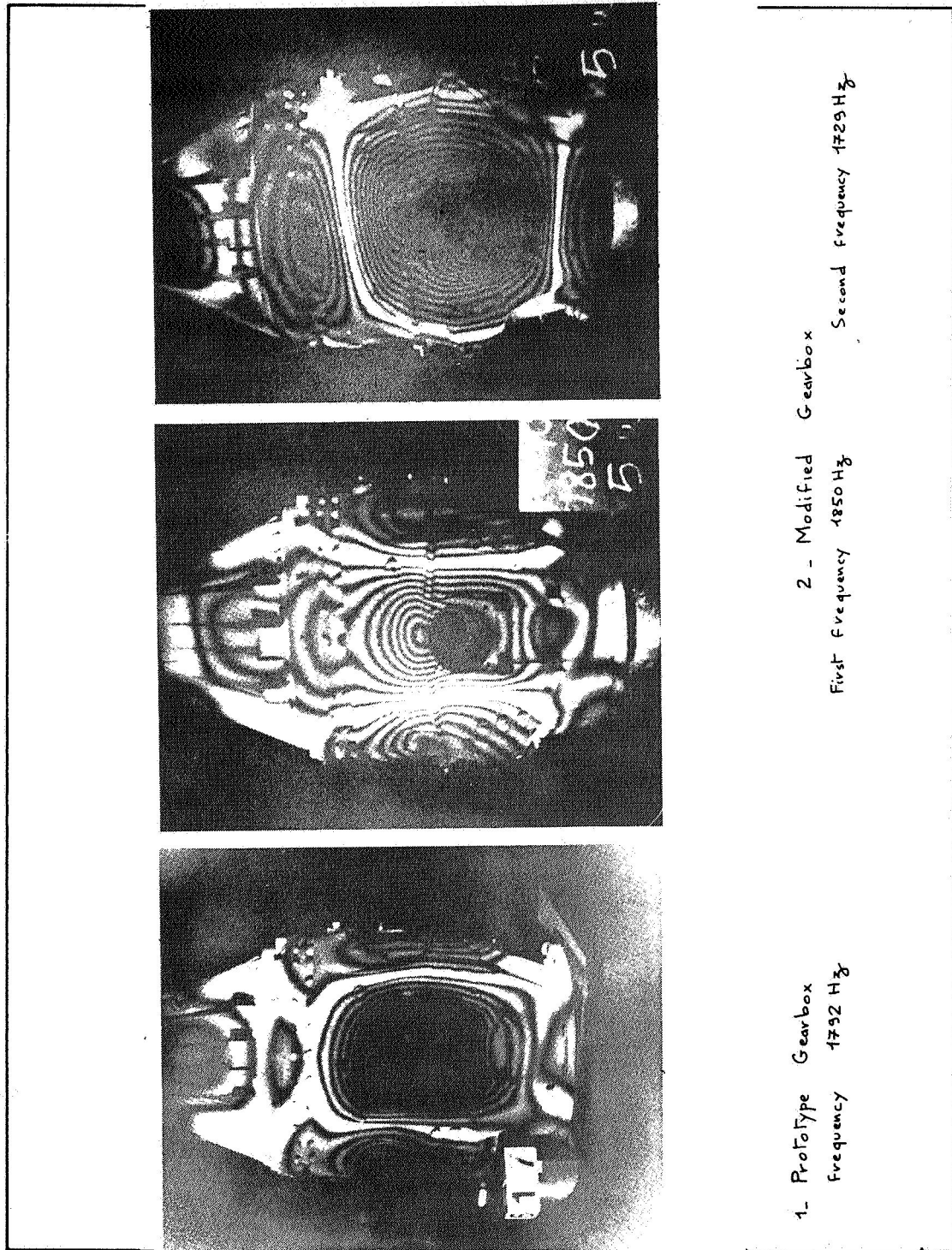
Figure 13.- Gear box housing mode shape representations from holographic measurements.
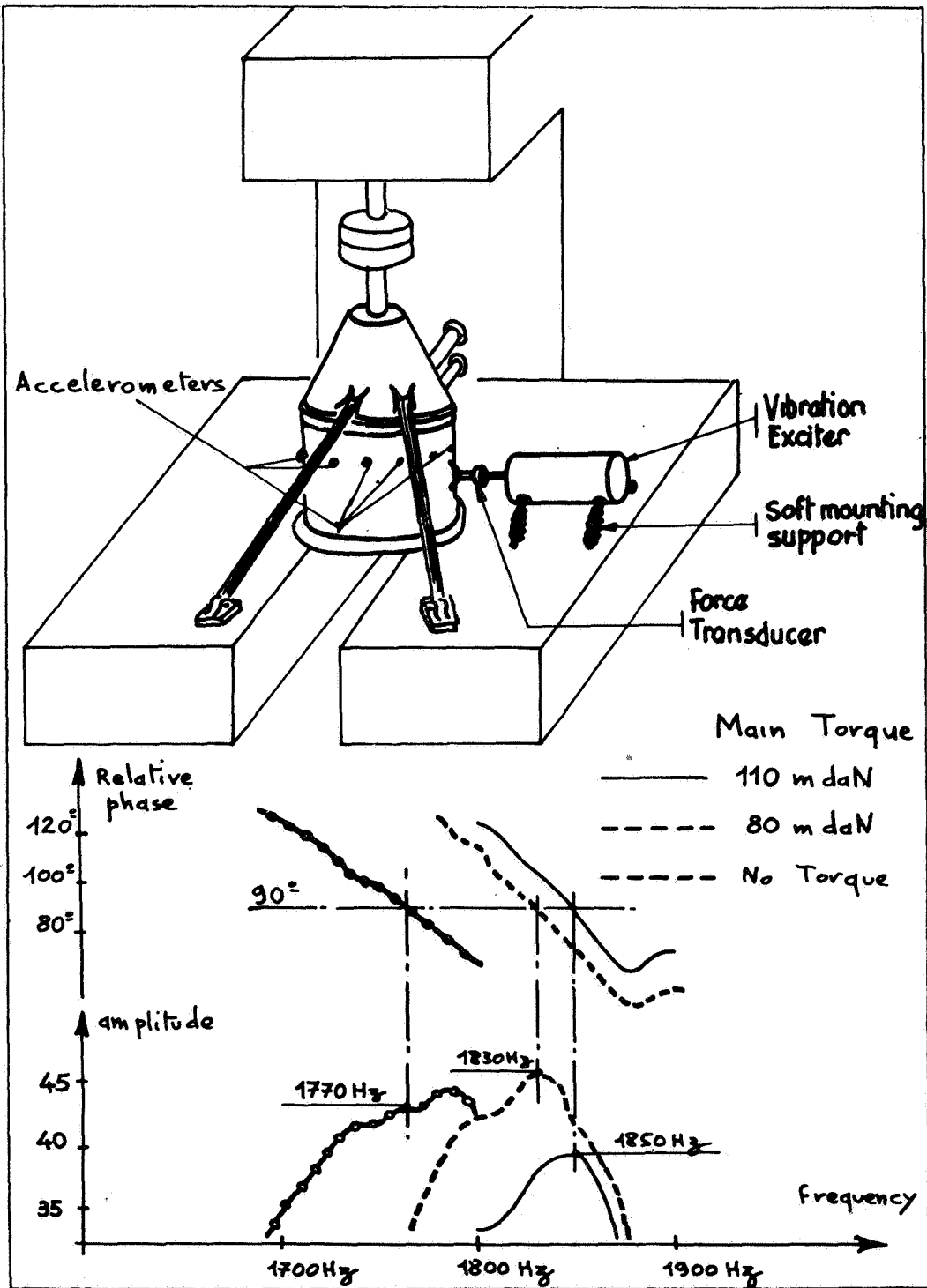
Figure 14.- Effect of torque on the dynamic behaviour of the SA 360 helicopter main gear box housing.
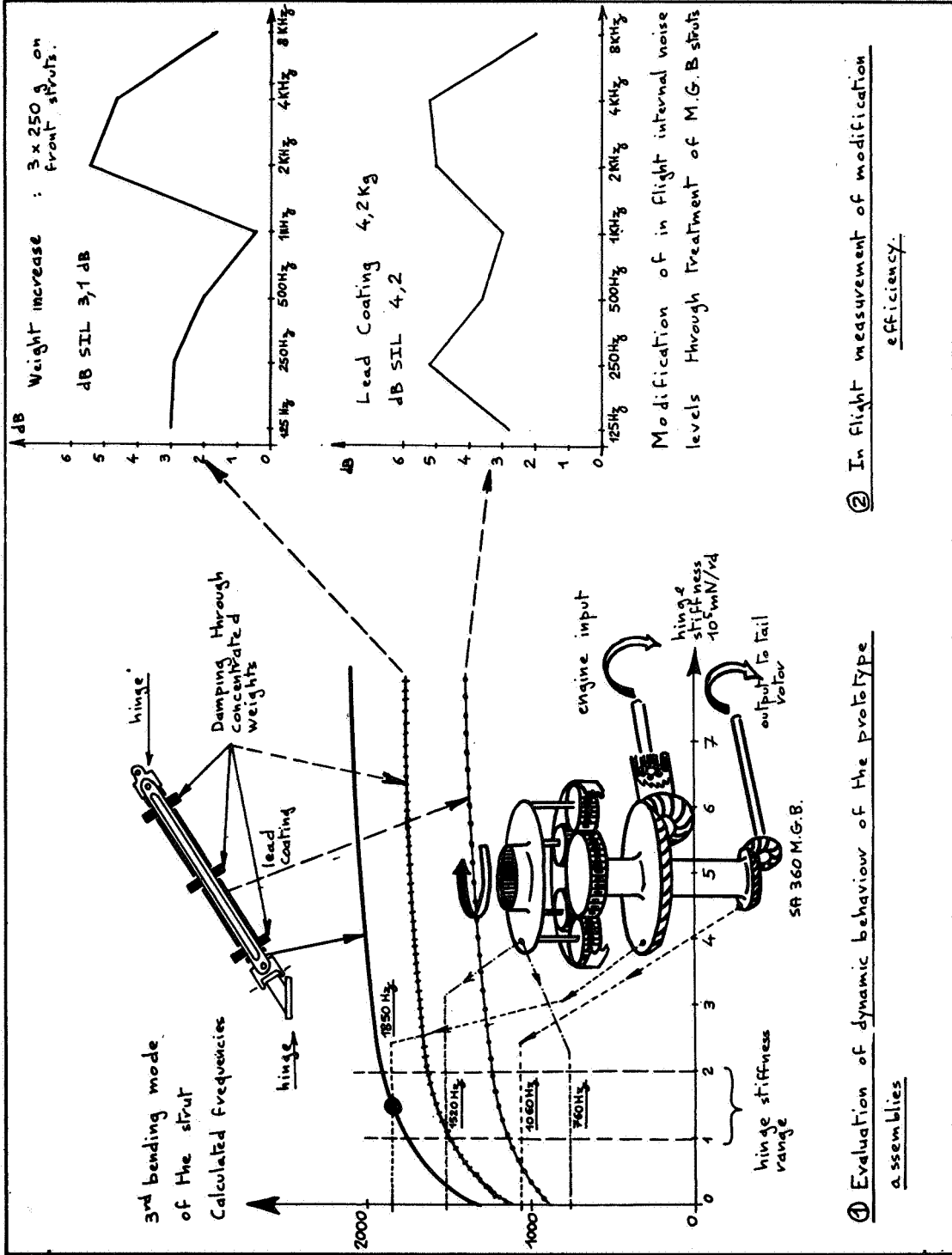
Figure 15.- Effect of dynamic behaviour of the SA 360 helicopter main gear box coupling elements on the internal noise level.

716

1 - Conventional Acoustic Treatment

Weight Law

Acoustic Screen

$$\Delta = 20 \log \dfrac{\omega \beta}{2 \rho c}$$

dB

60
50
40
30
20
10

8000 Hz
4000 Hz
2000 Hz
1000 Hz
500 Hz
250 Hz
125 Hz
63 Hz

ρs   Kg/m²
1 2 3 4 5 6 7 8 9 10

2 Treatment of Structures Through Visco-Elastic Materials.

- Utilisation of damping material

Shear Mode

Reduce vibration level of the structure
through increased damping of bending
motions

Structure
Visco Elastic

3 - Absorbing Panels Resonators.

Perforated material
Glass fiber layer
Glass Wool
Laminated Material

Lead material.
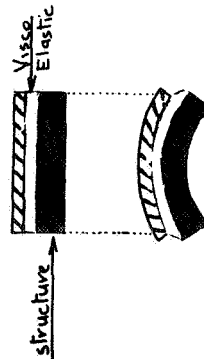
Research on bending Test specimens

Response Curves

before treatment

After treatment

f₂   f₁   Frequency
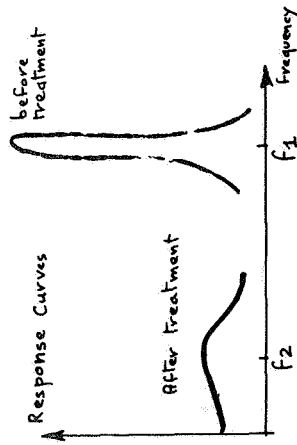
Figure 16.- Sound treatment concepts for the control of internal noise.

717
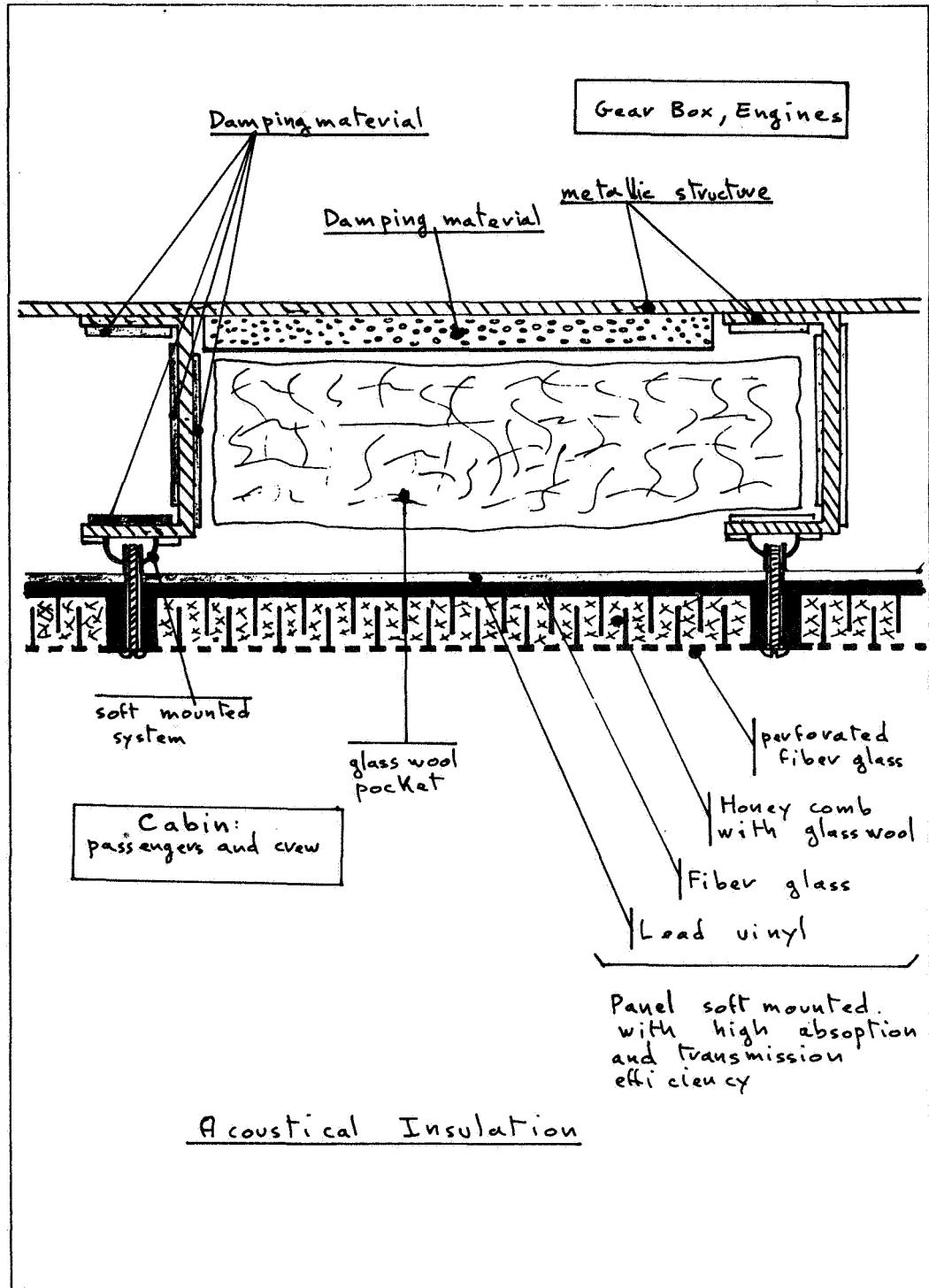
Figure 17.- Sketch showing installation details of acoustic treatments in the SA 360-365 helicopter cabin structure.
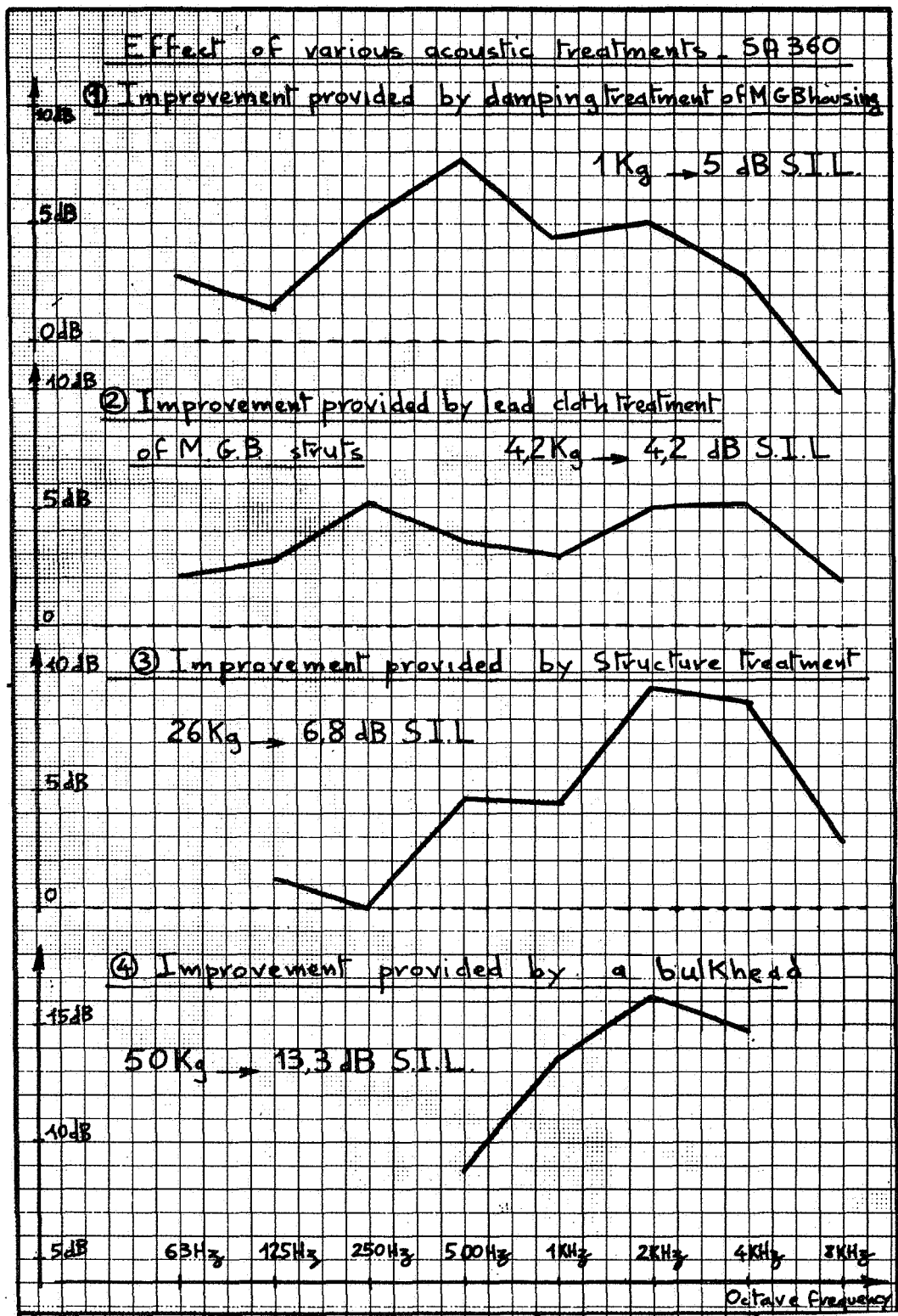
Figure 18.- Acoustic gains and associated weight penalties for various cabin acoustic treatments.
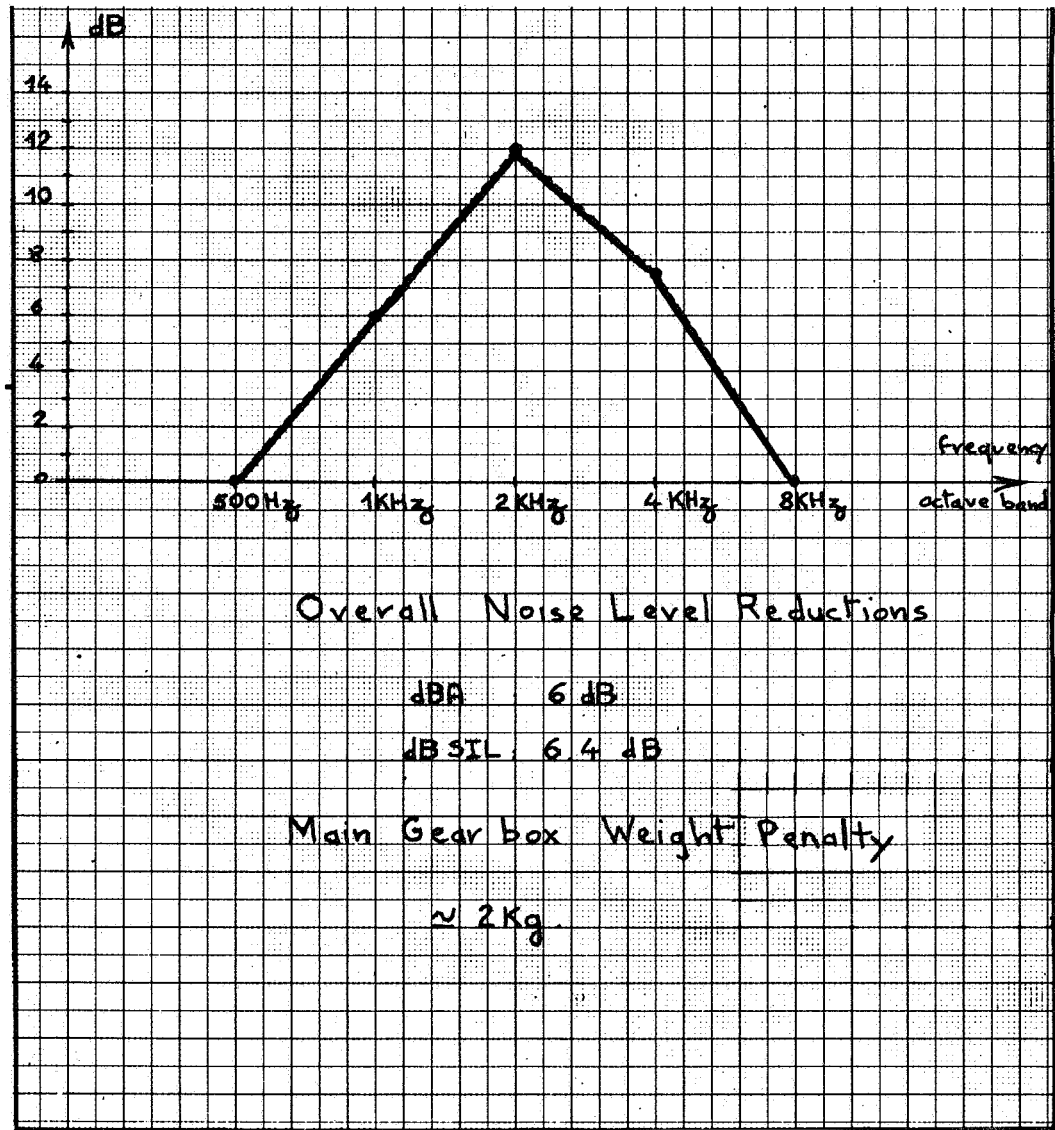
Figure 19.- Influence of spiral bevel gear tooth modifications on the SA 365 internal noise level.
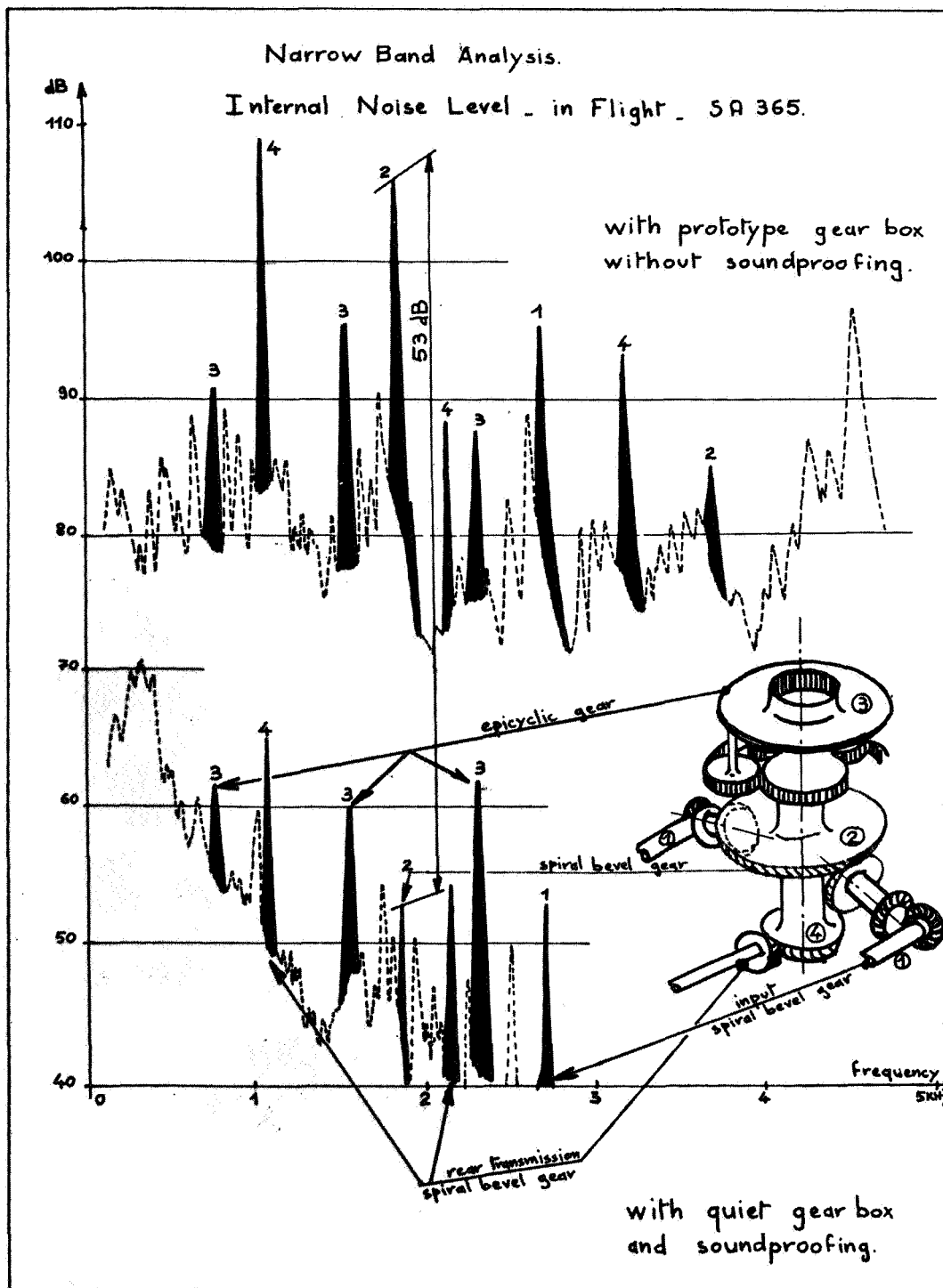
Figure 20.- The effects of main gear box quieting on the measured internal
noise levels of the SA 365 helicopter in flight.
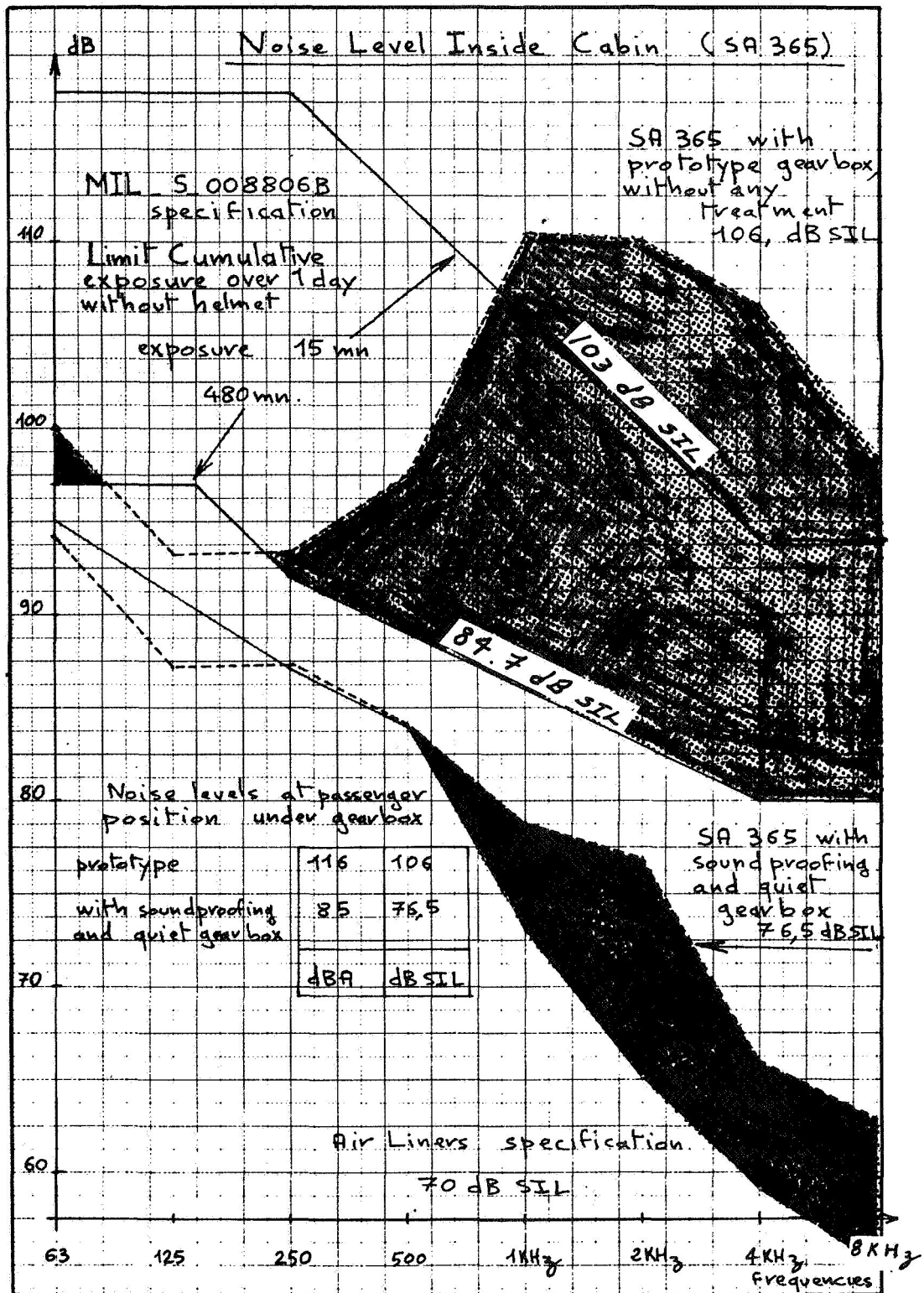
Figure 21.— The effects of main gear box quieting plus cabin sound proofing on the internal noise levels of the SA 365 helicopter in flight.

722

THE STATUS OF ROTOR NOISE TECHNOLOGY

ONE MAN'S OPINION

Richard P. White, Jr.
RASA Division, Systems Research Laboratories, Inc.

SUMMARY

In the last two decades, the somewhat "black art" of rotor noise prediction has grown into a science that might be called Rotor Noise Technology. This transformation has been due to many reasons, not the least of which has been the growing interest of the aerodynamicist in rotor acoustics. This paper will approach the problem of establishing the state of the "technology" by first identifying the various characteristics of rotor noise and then assessing the state of technology in understanding and predicting the most important of these rotor noise characteristics in a real-world environment.

INTRODUCTION

On the basis of experience gained in investigating propeller noise (i.e., refs. 1 to 6), some basic aeroacoustic investigations were conducted on the mechanisms associated with helicopter rotor noise prior to 1960. Most of these investigations, however, were centered around defining the characteristics of helicopter noise and evaluating the effects of basic helicopter parameters on these characteristics (i.e., refs. 7 and 8). These investigations determined the effects of basic rotor parameters such as blade number, disk loading, tip speed, blade chord, and forward flight velocity on the noise output of helicopter rotor systems. The results of these studies illustrated that the best way to reduce rotor noise is to reduce the rotor tip speed and disk loading and increase the number of blades. Many of these early investigations were prompted by the thought that if the other noise sources, such as engine, gear boxes, accessories, etc., could be reduced, then rotor noise would become the primary noise source of helicopters and, therefore, means of controlling rotor noise should be investigated.

As these investigations continued into the sixties, they were expanded such that the origin of the various sources of rotor noise and ways of reducing these sources of noise were considered (i.e., refs. 9 to 12). Although these studies were more directed toward the measurement of the effects of various parameters on the noise being generated by a rotor system, they began to highlight the effects of various aerodynamic parameters as the sources of rotor noise. As it became apparent that, due to the rapid advances being made in the development of new helicopter configurations because of the extensive application of gas turbines, a detailed understanding of the aerodynamic forces associated with the various sources of rotor noise must be obtained if

adequate methods of predicting rotor noise in a variety of flight conditions were to be developed. Because of this need, the aerodynamicist has become increasingly involved in the exciting and challenging research associated with the development of satisfactory rotor noise prediction techniques. The evolution of the understanding and the development of rotor noise prediction technology over the last decade is the subject of the review that is presented herein.

Because this symposium is basically establishing the current "State of Rotor Noise Technology," it would be inappropriate for this review paper to microscopically examine the technology of predicting the noise output of various sources. This task has been relegated to the session reviewers. The review presented herein is much more general in nature and tries to highlight the state of the technology in understanding and predicting the noise characteristics of rotors in the real-world environment of helicopter flight.

SYMBOLS

b	span of reflection plane model, meters
C_T	coefficient of thrust
c	chord of reflection plane model, meters
c_{MR}	chord of main rotor, meters
c_p	coefficient of pressure
Δp	differential pressure, newtons per centimeter^2
q	dynamic pressure, newtons per centimeter^2
R	radius of tail rotor, meters
T_0	disk loading, newtons per meter^2
V	velocity, meters per second
V_D	velocity of descent, meters per minute
V_F	free-stream velocity, meters per second
V_T	velocity of translation, meters per second
x	chordwise location of reference point on reflection plane model, meters
y	spanwise position of reference point on reflection plane model, meters

α   angle of attack, degrees

λ   sweep angle of leading edge with respect to relative airstream,
         degrees

μ   advance ratio

ψ   azimuth angle, degrees

Ω_{MR} rotational speed of main rotor, radians per second

Ω_{TR} rotational speed of tail rotor, radians per second

TECHNICAL DISCUSSION

In considering the noise generated by helicopter rotors operating in a
real-world environment, it is obvious that the helicopter configuration plays
an important role in the rotor noise signature. Even to the casual observer,
it is obvious, for example, that the noise produced by a UH-1, a CH-47, or a
CH-53 is quite different. While these differences can be caused by many con-
figuration parameters, such as disk loading, blade number, number of rotors,
and blade tip speed, the basic sources of noise are all present in varying
amounts for each configuration. The degree to which each noise source con-
tributes to the overall noise signature of a helicopter depends upon the heli-
copter and rotor configuration.

The picture of a CH-53E shown in figure 1 can be utilized to point out
some of the real-world environmental effects that strongly influence the noise
generated by rotors operating in a forward flight on a realistic helicopter.
The CH-53E was not chosen as an example because of its noise characteristics
but because it was a good picture of a helicopter in flight that could be used
to point out the environmental effects of interest that will be discussed in
further detail herein.   .

In viewing the picture of the CH-53E, it can be visualized that there are
many free and self-induced environmental effects that can affect the noise char-
acteristics of the blades in the main rotor. At least the following are of pri-
mary importance:

(a) The aerodynamic turbulence in the free stream through which the rotor
    flies

(b) The aerodynamic compressibility effects below the critical Mach number
    on the advancing blade velocities

(c) Shock waves generated by airflow above the critical Mach number near
    $\psi = 90^\circ$

(d) Separated flows generated by high angles of attack on the retreating
    side of the rotor disk

(e) The concentrated vortex flows generated at the blade tips

(f) The highly turbulent flow field induced by the complete rotor wake

(g) The effects of fuselage blockage and separated flow

The tail rotor has all of these same environmental effects induced by its own blades as well as those which the concentrated and general nonuniform wake of the main rotor induce when it interacts with the fin and blades of the tail rotor. When the noise generated by the rotor blades operating in this type of aerodynamic environment is measured, a spectrum similar to the generalized spectrum shown in figure 2 is obtained. For the sake of discussion, the spectrum has been separated into three different categories of noise:

(a) Noise due to steady loads

(b) Noise due to unsteady loads

(c) Noise due to incoherent or random loads

The noise due to the steady loads are related to the integrated torque and thrust forces developed by the rotor system to maintain flight. The basic characteristics of the noise produced by the steady rotating loads were predicted by Gutin many years ago (ref. 13). References 2, 4, 5, 14, 15, and 16 outline improvements made to Gutin's basic theory to account for noise in the near field, thickness noise, and far-field distortion due to source translational motion. Reference 17 was an early attempt to extend Gutin's basic theory to remove its inherent limitation when applied to helicopter rotors. Since then there have been numerous investigations to improve the prediction of the rotational noise produced by the steady rotating loads which has resulted in theories which can adequately predict the primary characteristics of this type of noise. The noise labeled incoherent noises are nonperiodic noises that are generally related to the viscosity effect of the air and are due to such phenomena as inflow turbulence, boundary-layer effects, separated flows, and vortex shedding. Wright (ref. 18) has aptly referred to this noise as "self-noise." These two noise sources, noise due to the steady loadings and self-noise, are believed to be unavoidable when operating a helicopter and thus may be considered to be the lower limits to which helicopter noise might be lowered. The third source of noise that has been listed in figure 2 is that due to unsteady loads which are generated by the previously noted real-world environmental effect in which helicopter rotors must operate. Since these noise sources do not arise from the loads needed to fly the helicopter, some authors have labeled the category of noise as "excess noise" (ref. 19). Since this type of noise generally is the major contributor to the noise in the frequency spectrum of interest to this symposium, i.e., annoyance, detectability, etc., establishing the status of the technology in understanding, predicting, and modifying this category of noise is the one to which this review will be directed.

The excess noise sources can result from loadings having frequencies in the noted range or from a loading impulse that happens only over a short time interval. The shorter the time period, the greater is the number of harmonics of noise that is produced. While the various types of loadings that result in

726

the excess noise consists of both types of noise sources, the majority of the noise is due to the harmonics of loading impulses which occur one or more times in the azimuth. The major sources of rotor noise which contribute to the excess noise will be discussed in some detail in the following sections of this review in an attempt to establish the state of the technology in understanding, predicting, and modifying these sources of noise.

Blade Stall

Blade stall can occur in hover around the entire azimuth when the blade angle is increased to sufficiently large values or over relatively small portions of the azimuth in forward flight. Since the blade stall angle of attack is strongly affected by the relative Mach number, stalling can occur over the advancing side of the rotor disk for highly loaded rotor system in forward flight as well as over the retreating side of the rotor disk. When stall effects do occur on the advancing blade they produce a greater amount of excess noise than on the retreating side because of the higher dynamic pressure at which it occurs and the smaller increment of azimuth angle over which it occurs.

Hubbard and Maglieri, in 1958, demonstrated the large effect blade stall could have on the noise characteristics of a hovering rotor. Figure 3, taken from reference 7, presents data which show the effect of stall on the overall noise level at different rotor tip speeds as well as the effect of stall on the frequency spectrum for a rotor tip speed of 183 m/sec. In the top half of figure 3, the solid symbols represent the conditions at which the authors indicated that blade stall was present and for which the noise output was considerably greater than the conditions at which stall was not present. The spectrum shown in the bottom half of figure 3 shows how stall affects the frequency content of the noise. The authors reported that the noise presented in the spectrum did not have discrete spikes and correlated well with that which would be calculated based on the experimentally determined Strouhal numbers. The authors suggested, therefore, that the noise due to stall was probably due to vortex shedding from the blades. Schlegel, et al., reported in reference 17 that the noise generated by small pockets of stall on the retreating blade had signature characteristics similar to that of impulsive noise and was believed to be associated with the modulation of high frequency loadings due to discrete vortex shedding. These results indicate that blade stall might produce a significant amount of noise in the higher rotor frequencies, particularly if it occurs over just a small portion of the azimuth. As noted by the authors of the referenced investigations, the noise produced during stall may be associated with discrete vortex shedding on a continuous basis or on a modulated basis during blade vortex interactions on the retreating side.

While the referenced investigations were conducted a number of years ago, it is believed that the understanding of the noise produced by the aerodynamic forces generated during stall has not increased markedly since that time. This lack of an intensive effort to predict stall-induced loadings and associated noise has probably been due to the lack of a suitable theory to realistically predict stall-induced loadings and because of the need to reduce the more dominant excess noise sources caused by blade vortex interactions and unsteady potential airloads. It is believed, however, that because of the potentially

stronger aerodynamic interaction between the rotor and fuselage that is possible with the newer helicopter configurations that stall-induced noise may have more significance in the future, particularly if the noise produced by some of the more dominant excess loading sources is reduced. If this type of noise source does become of more importance in the future, its prediction will be a very difficult undertaking if it is attempted by other than empirical or semi-empirical methods. This is believed to be the state of the technology as the effort that has been directed towards predicting the dynamic stall characteristic of rotor blades in forward flight has not produced a reliable and useful prediction technique. It is reasoned, therefore, that the true prediction of stall-induced noise will be very difficult and will require a reasonable amount of additional research effort.

Compressibility Effects

I have chosen to separate those effects which are due to drag divergence and those which are due to the aerodynamic mass acceleration around a solid airfoil section at higher Mach numbers commonly referred to as thickness noise. The Mach number at which drag divergence occurs is a fairly strong function of angle of attack, i.e., the higher the angle of attack the lower the drag divergence Mach number. For rotors in which there is not a strong blade vortex interaction, the increased noise due to drag divergence effects usually occurs in the rotor azimuth range of 10° to 80°. Since the compressibility effects due to drag divergence are pronounced only over a small azimuth range, it would be expected to produce a significant amount of noise at the higher harmonics of blade passage. Arndt and Borgman tend to confirm this conclusion as they showed in reference 20 that including the effects of drag divergence in the prediction of rotational noise increased the noise significantly in the higher harmonics of blade passage. Comparison of predicted results with experimental data presented by Cox in references 21 and 22 also showed that the inclusion of drag divergence effects significantly improved the correlation between the predicted and experimental results in the frequency range of excess noise.

Figures 4 and 5, taken from reference 23, present the angle of attack and Mach number contours, respectively, determined for a UH-2 flying at an advance ratio of 0.48. It is noted that, in the azimuth range of 10° to 50°, the data indicate that the compressibility boundary moves inward leaving the outer 20 percent of the blade radius operating above the critical Mach number. This inward movement of the compressibility boundary is due to the increase in the angle of attack and relative velocity over the same range of azimuth angles. With 20 percent of the blade radius operating above the critical Mach number it would be expected that the impulsive increase of drag loading would generate a significant pressure wave in the plane of the rotor. Since the movement of the compressibility boundary happens only over a small portion of the azimuth, it would be expected that higher harmonics of rotational noise would be produced. Increasing the rotor speed, flight speed, or the rotor thrust increases the angle of attack and velocity over a larger region of the advancing side of the rotor disk and, therefore, the noise due to drag divergence would increase in intensity and be noticeable over a larger range of frequencies.

With the advances that have been made in airfoil designs for rotor blades, the problem of noise due to compressible drag divergence effects has decreased. In addition, since most modern rotor noise prediction techniques include the effects of Mach number in the definition of the airfoil sectional characteristics, the prediction of the noise due to compressibility effects can be readily handled if the angle of attack and velocity distributions over the disk are known. Unfortunately, this knowledge cannot be gained experimentally and can only be gained by the utilization of predictive free rotor wake flow analyses such as that presented in reference 24 and extensively expanded since that time. While direct correlation between theory and measured angle of attack distribution cannot be made, correlation of harmonic loadings indicates that relatively good predictions of the radial and azimuthal distribution of angle of attack can be obtained using such analyses techniques. It is believed, therefore, that the understanding of the effects of compressibility and the associated noise produced by helicopter rotors in forward flight is on firm ground and that means of predicting the effects of various real-world parameters on this noise source are available if the existing analyses procedures are properly utilized.

Rotor Noise Resulting From Blade Vibration

Prior to discussing other primary sources of excess noise because of pressure pulses at higher harmonics of blade passage frequencies due to discrete happenings in the azimuth, a brief discussion of the noise that can be generated by the structural vibration of rotors will be presented. This type of excess noise occurs at the frequency of the motion and not at higher harmonics of discrete impulsive pulses. It is believed pertinent to discuss this possible problem at this point in the review as much of what will be presented in the following portions of the review is associated with model tests. While some investigators in the past have postulated that higher harmonic blade vibration of full-scale rotor systems could affect the noise signatures in the higher frequency spectrum, no strong evidence of this type of noise source has been found for full-scale rotors. For small scaled models of full-scale systems, however, this source of noise may be of significance due to the higher structural frequencies of the scaled models. A recent experience, during wind-tunnel tests of small remotely piloted vehicle (RPV) propeller blades, reminded me of the possible contamination of rotor noise data due to structural vibration. Figure 6 shows a photograph of an RPV propeller blade that generated a significant noise due to the near coalescence of the third flapwise bending frequency with the 8/rev harmonic of rotational speed. Figure 7 presents the spectrum of the noise measured for this configuration when it was operating near the resonant condition. As can be seen from the data presented in this figure, the noise produced by the blade bending vibration dominated the other sources of aerodynamic noise generated by the propeller. While it was obvious that the noise produced by blade vibration had contaminated the noise signature, it might not be so obvious for model rotor systems that have higher damping in the bending modes and for conditions that are not as close to a resonant condition as they were for the propeller blades. In order to prevent the contamination of the noise signature produced by aerodynamic forces under investigation by that produced by structural vibration, it is suggested that the vibration and stability

characteristics of model rotor systems be determined prior to the collection
of model noise data to insure that no unwanted structural or aeroelastic
motions and the associated noise due to these motions are present at the test
conditions.

Rotor Impulsive Noise

As many investigators have said time and time again "impulsive noise is
one of the most annoying and easily detectable sounds a helicopter can generate
and when it occurs, it is the dominant source of noise." As such, it is also
one of the more challenging and exciting areas of research in helicopter noise
as attested to the large number of research efforts that have been conducted
and reported by investigators in universities, industry, and government research
organizations throughout the world. Impulsive noise can be generated by many
sources and for the purposes of this review the discussion will be divided into
two different general areas of impulsive noise as indicated in figure 8. One
area is high-speed impulsive noise and the other is blade vortex interaction.
While these areas of impulsive noise have been somewhat arbitrarily separated
in this manner for purposes of discussion, it has been shown for some configu-
rations that the two areas of impulsive noise, shown separated in figure 8, are
in fact connected.

High-Speed Impulsive Noise

High-speed impulsive noise has been attributed to intense compressibility
effects on the advancing blade of a helicopter in high-speed forward flight
when the advancing tip Mach number approaches or exceeds unity. In the past,
there have been some differences of opinion as to the major source of this noise.
These differences are the result of the limitations and difficulties of making
suitable acoustic measurements which have restricted the evaluation of the noise
source to qualitative observations. Test data, which are obtained during air-
craft flyovers with ground-based microphones (i.e., refs. 25 and 26), are diffi-
cult to assess on a quantitative basis due to uncertainties in the retarded
time effects, the acoustic transmission path, and ground reflection effects.
Data obtained from tests conducted in conventional wind tunnels may have seri-
ous limitations, as regards its quantitative value, because of reverberation
effects and high ambient operational noise levels. Another approach that has
been utilized to obtain inflight noise data is to place microphones on the
exterior of an aircraft (i.e., refs. 27 to 29). This technique is somewhat
limited in that the microphone placement is, by necessity, limited to the heli-
copter's low to mid frequency acoustic near field and thus, it can be diffi-
cult to quantitatively assess how much of the noise actually radiates to the
far field. In addition, to obtain directivity patterns for noise sources that
radiate in the tip path plane, the use of inflight microphones attached to the
vehicle generating the noise is extremely difficult, if not impossible.

In order to surmount the above noted difficulties and limitations, Schmitz
and Boxwell (ref. 30) developed a rather unique inflight far-field measurement
technique to obtain quantitative data of the effects of various flight param-
eters on the high-speed impulsive noise source. Figure 9 presents a schematic

of the inflight far-field measurement technique. This measurement technique utilizes a quiet fixed-wing aircraft, instrumented with a microphone, and flown to maintain fixed relative positions with a helicopter. Because impulsive noise is thought to have its maximum intensity of radiation in the general direction of forward flight, the microphone was installed on the tail of the monitoring fixed-wing aircraft which is flown in front of the helicopter as illustrated. Estimated values of microphone wind noise and monitoring aircraft noise levels indicated that with the proper choice of a fixed-wing aircraft, the periodic phenomenon of helicopter high-speed impulsive noise could be quantitatively measured. By using this testing procedure, acoustic far-field impulsive noise radiation patterns have been obtained by Schmitz and Boxwell for a wide range of steady operating conditions.

The flight test envelope over which data have been obtained for a UH-1H using this technique is indicated in figure 8 and a sample of the high-speed impulsive noise data obtained is presented in figure 10. The data presented in this figure were averaged 128 times to eliminate the slight variability due to small blade differences as well as to eliminate the random background noise which had an amplitude less than 1/10 of the smallest of the primary pressure pulse.

As can be seen from the data presented in figure 10, the negative pressure spike, due to intense compressibility effects, dominates the noise signature and the amplitude of the spikes is a stronger function of forward speed than it is of descent rate. The authors of reference 30 noted that the noise associated with the large negative pressure peaks shown in figure 10 is rich in low frequency harmonics (10 to 300 Hz) and radiates not only near the tip path plane of the rotor but over wide azimuth angles in the general direction of forward flight. In addition, they noted that the extremely rapid increase in pressure which closely follows the negative pressure disturbance, forming a sawtooth-shaped pressure pulse with some apparent overshoot at high airspeeds (fig. 10), dominates the middle and high frequency harmonics (above 300 Hz) and radiates within narrow azimuth angles in the direction of forward flight near the tip path plane of the rotor. Using the flight test data presented in reference 30 as a basis for evaluation, Schmitz, Boxwell, and Vause (ref. 31) showed that, through careful testing in an acoustically lined wind tunnel, the high-speed impulsive noise characteristics of the full-scale flight vehicle could be duplicated by using appropriately scaled models. Having established the scaling and modeling technique required to duplicate the high-speed impulsive noise developed by full-scale blades with the use of scaled models, it is believed that the more detailed investigation of the source(s) of high-speed impulsive noise using advanced flow measurement techniques, such as schlieren photography and laser velocimeters, can be conducted with confidence.

It is believed that the data obtained by Schmitz and coworkers in their pioneering efforts to quantify the characteristics of high-speed impulsive noise (refs. 30 and 31) show the character and dominance of high-speed impulsive noise and provide an excellent quantitative data base for analyzing this type of noise source being generated by helicopter rotor blades operating in a real-world environment.

Tangler (ref. 32) has presented some interesting insight into the formation of the shock wave associated with high-speed impulsive noise. Through the use of schlieren photograph techniques he has shown that the shock waves formed on the upper and lower surface of the blade in an azimuth angle range 50°
to 90° leave the blade as the relative velocity decreases (ψ = 90° to 150°),
coalesce into a unified shock front, and propagate at an azimuth angle approximately 20° to the flight path. Tangler reasoned that the more rapid compression and apparent overshoot of the pressure wave measured in the far field and noted by Schmitz and Boxwell in reference 30 are due to the strong crescent shock wave that is formed and propagated forward. (See fig. 10.) Tangler also noted, on the basis of data obtained during an extensive wind-tunnel test program, that blade thickness was a significant parameter in high-speed impulsive noise and that blade thrust had a significant effect on the directivity pattern of the noise that is propagated.

On the basis of the measurements that have been taken and analyzed during the above noted investigations, which represent the present state of experimental technology in this area of research, it is believed that considerable knowledge has been obtained as regards an understanding of the physical characteristics of the aerodynamic flows associated with high-speed impulsive noise. It is obvious, however, that, while some effort has been directed towards determining the effect of blade parameters on the shock and noise characteristics of high-speed impulsive noise (refs. 31 and 32), much more needs to be done in this area to further our understanding and to provide quantitative data in support of the development of adequate prediction techniques.

While improvements in experimental and measurement techniques have led to significant advances in the investigation of the flow physics associated with high-speed impulsive noise over the last few years, theoretical means of predicting this dominant source of noise has also recently received much attention. The papers presented at this meeting, if nothing else, attest to the significant effort that is being devoted to this subject area. Although a great deal of theoretical effort is now being directed toward the prediction of high-speed impulsive noise, a considerable amount of theoretical research effort has been conducted over a number of years in this area. As early as 1933, Deming (ref. 33) looked into the effects of blade thickness on radiated noise. Lyon (ref. 34) represented the thickness noise using monopoles and used dipoles to represent the force noise. With these representatives he replaced the blade by a progression of accelerating "torpedoes." Using this rather unique approach he found that monopole thickness effects may be important at advancing tip Mach numbers near unity. Arndt and Borgman (ref. 20) related the high-speed impulsive noise to the drag divergence phenomenon at high advancing Mach numbers. Although they did indicate that the high-speed impulsive noise could dominate the lower frequency spectrum (up to 300 Hz), their results did not correlate well with experimental data.

It was not until 1969 when Ffowcs Williams and Hawkings rederived the classical acoustic equations for bodies moving at high Mach numbers and emphasized the noncompactness of the problem (ref. 35) that the basic theoretical formulation for studying high-speed impulsive noise was formed. Much of the recent analysis effort has been centered about this basic formulation.

732

Farassat (ref. 36), Hawkings and Lowson (ref. 37), and Isom (ref. 38) applied the Ffowcs Williams and Hawkings formulation to the high tip speed rotor problem using noncompact monopole terms to represent thickness and distributed dipoles to represent the localized pressure. Lowson (ref. 39) working in the frequency domain and comparing results with the data of reference 30 reported agreement with experimental data within 3 to 6 dB for a number of measurement points.

Schmitz and Yu (ref. 40) recently used monopoles to represent thickness effects and dipoles to represent local forces and obtained results similar to Lowson. The authors also included the effect of quadrupole sources as acoustic radiators in an attempt to improve the correlation between theory and experiment. While they showed that quadrupole radiation did improve the correlation with experimental data, it was not the reason for the almost 2/1 discrepancy between the measured and predicted pressures. An important result of the work presented in reference 40 was that a relatively simple and easy to use acoustic model can be utilized to conduct a numerical evaluation of high-speed impulsive noise.

Farassat (ref. 36) and Farassat, Pegg, and Hilton (ref. 41) have compared the results of Farassat's prediction technique with experimental data and some of these results are presented in figure 11. As can be seen from the results presented in figure 11, the predicted results compare rather favorably with the experimental data. It is noted, however, that for this case the experimental data do not exhibit the more rapid rise time of the positive pressure gradient reported in references 30 and 32. Since this disparity in the pressure pulse has been shown to be of importance to high-speed impulsive noise, it would be of interest to determine if Farassat's theory adequately predicts the impulsive noise when these measured characteristics were present. Farassat utilized his prediction technique to investigate the effects of the airfoil profile on the characteristics of high-speed impulsive noise. The results of these predictions which are also presented in reference 41 are shown in figure 12. As can be seen, airfoil profile was shown to have a significant effect on the negative pressure pulse associated with high-speed impulsive noise as the supercritical airfoil had a pressure peak almost twice that of the biconvex airfoil.

On the basis of the review of recent theoretical efforts directed toward the prediction of high-speed impulsive noise due to shock effects, it is concluded that great advances have been made and that the basic characteristics of this noise source are fairly well in hand. Based on the effort being applied in this area, as indicated by the number of papers presented in this meeting, one can probably look forward to reliable prediction techniques in the not too distant future.

Impulsive Noise Due to Blade Vortex Interaction

While impulsive noise due to compressibility and blade thickness effects can result in a discomforting noise in high-speed forward flight, the impulsive noise caused by blade vortex interaction during slow-speed descent into a terminal area can be a more troublesome noise source to the passengers, the surrounding community, and the people in the terminal area. Referring to figure 8, the

flight region in which this noise source is of primary importance, for at least single rotor helicopters, is generally at forward velocities of 20 to 40 m/sec and for descent rates of 50 to 100 m/min. It is in this range of flight velocities and descent rates that the freely deforming rotor wake, containing the concentrated vortices trailed from the blade tips, can induce a strong and rapid pressure fluctuation on the rotating blades. The number of investigators that have undertaken research directed towards an understanding and prediction of the noise generated by blade vortex interactions are too numerous to reference and discuss the results of all their efforts. A cross section of the investigations that have been conducted can be summarized by a few notable references of previous effort. These references are Sternfeld's work in reference 42 on tandum rotors; Leverton and Taylor (ref. 43); Leverton (ref. 44); Schlegel, et al. (ref. 17); Widnall, et al. (ref. 45); White and Balcerak (ref. 46); and more recently, Charles (ref. 29), Tangler (refs. 32, 47, and 48), and Schmitz and Boxwell (ref. 30). On the basis of the efforts that have been undertaken by these and other investigators, the primary parameters associated with the intensity of the impulsive noise due to blade vortex interactions are the orientation of the previously trailed concentrated tip vortex with respect to the interacting blade, the strength of the concentrated tip vortex, and the distance of the concentrated tip vortex from the interacting blade. Sternfeld (ref. 42) showed that the relative location of the two rotor planes of a tandum helicopter was one of the primary parameters controlling whether impulsive noise due to blade vortex interactions was obtained in steady-state level flight. Figure 13 illustrates the type of vortex interaction that is generally obtained with tandum rotor configurations. The results presented in figure 13 were obtained by a rather unique smoke visualization system developed by the Boeing Vertol Company that could be used on a whirl tower or during flight tests of full-scale tandum configurations. The results obtained by Sternfeld indicate that the impulsive noise due to the interaction of a blade with a concentrated vortex was due to the blade of the rear rotor interacting with the trailed tip vortex from the forward rotor. The orientation of the concentrated vortex relative to the interacting blade is shown in the lower left-hand part of figure 13. Once the type and location of the blade vortex interaction was determined, the aft rotor was moved up so that the paths of the aft rotor plane and the concentrated freely deforming vortex from the blade of the forward rotor no longer crossed, thus eliminating the impulsive noise.

Tangler, in reference 32, through the use of schlieren techniques determined at least seven possible locations of blade vortex interaction points for a two-bladed rotor in descending forward flight in the range of 0 to 305 m/min. Figure 14 indicates where these points of interaction are with respect to blade azimuth and descent rate. The two most important of these intersections occur at $\psi = 55°$ and $70°$ as they are heard both in the helicopter cabin and on the ground. On the basis of schlieren pictures, it was determined that the blade vortex interaction at $\psi = 55°$ occurred with a vortex that was 1.5 revolutions old while that which occurred at $\psi = 70°$ was with a vortex generated by the interacting blade during the previous revolution. Since both of these interacting vortices were below the blade chord plane, the velocity induced on the blade by the vortex generated a near sonic velocity on the blade resulting in strong bow shock waves. These shock waves radiated a strong pressure wave much in the same manner as the high-speed impulsive noise generated by compressibility effects as previously discussed. It is noted, however, in reference 49,

734

that a very similar but less intense impulsive noise was also generated at approximately the same azimuth locations during tests of a two-bladed rotor in descending flight having a tip speed of only 152 m/sec. It is concluded, therefore, that while the trailed tip vortex is the basic cause of the impulsive noise due to blade vortex interaction in the first quadrant of the rotor azimuth, the induced effects of the vortex can also generate noise due to compressibility effects if the tip speed of the blade is sufficiently high.

The investigation conducted by Tangler in reference 32 on the character of the vortex interaction and the noise produced by those interactions on the retreating side of the azimuth in the vicinity of $\psi = 270^\circ$ (interactions 6 and 7 of fig. 14) indicated that these interactions induced local stalling on the blades. A similar type of impulsive noise generated on the retreating side of the rotor disk was also noted by Cox and Lynn (ref. 50) many years ago during a 1.5g left turn during a flyby of an HU-1A helicopter. Figure 15 presents a filtered trace of the noise measured during the time of blade slap. The authors of reference 50 reasoned that, on the basis of the characteristics that were measured, the interacting vortex induced stall on the blade which in turn generated high frequency vortex shedding. A similar conclusion was also reached by Schlegel, et al. in reference 17 on the basis of measurements made of the impulsive noise generated on the retreating side of the blade disk. The change in the noise spectrum that was obtained by Schlegel due to vortex shedding induced by stall is shown in figure 16. More noise was obtained in the higher octave bands when stalling, which was induced by an interacting vortex, occurred over a small portion of the azimuth.

On the basis of at least these studies, it might be concluded that the impulsive noise generated by the interaction of a blade and a concentrated vortex can be associated with blade stall and subsequent vortex shedding, impulsive loading of a subsonic blade section, or induced compressibility effects on a high tip speed rotor.

Basic to the prediction of any of these vortex-induced impulsive noises is the prediction of the freely deforming position and strength of the trailed vortices as a function of the azimuth position in which they were originally formed. There have been a few investigators who have conducted extensive investigations into the prediction of the strength and position of the vortices trailed from the tip of rotor blades in hovering and forward flight. Notable among these are Landgrebe (refs. 51 and 52) and the technical staff at the RASA Divison of Systems Research Laboratories, whose initial efforts in the development of the Non-Uniform WAke Induced VElocity (NUWAIVE) prediction technique are reported in references 24 and 53. Since these initial efforts, RASA has extended and refined the force free rotor wake analysis for use in the prediction of the wake geometries and rotor loads developed by advanced and unique rotor systems such as the Advancing Blade Concept (ABC) (ref. 54), the Variable Geometry Rotor system (VGR) (ref. 55), and the "X" Wing configuration (ref. 56) being developed by the Naval Ship Research and Development Center (NSRDC). As an example as to the use of the free wake analysis in conjunction with the time dependent rotor noise prediction technique developed by RASA (refs. 57 and 58) to analyze the noise developed by helicopter rotors, the results of calculations conducted to predict the impulsive noise generated by the HU-1A in a 1.5g climbing left turn (ref. 50) will be given. The results of this

investigation were previously reported in reference 59 and figure 17 shows the location at which the blade intersects the predicted deformed wake. The spectrum of the noise heard by an observer located on the flight path and 305 m downstream of the aircraft is shown on the left side of figure 18. The noise due to the blade slap is rather weak because it occurs on the retreating side of the azimuth and the observer is a long distance from the aircraft. The humping characteristic of the noise spectrum is due to the predicted ground reflection effects at the observer's ear located approximately 1.5 m from the ground. When the effects due to vortex interaction are removed from the problem the spectrum on the right-hand side of figure 18 is obtained. By comparing the two spectrums it can be seen that, even though the blade vortex interaction occurs in a low region of dynamic pressure, a significant amount of impulsive noise is generated. Predicted pressure time histories of the noise during blade vortex interaction are presented in figure 19. The time history at the top of this figure includes both rotational and vortex shedding noise while that at the bottom of the figure presents only the rotational components of the noise. It can be seen, by comparing these two signatures, that during the interaction of the blade and vortex, the vortex shedding noise is significantly greater than it is at other times. This characteristic seems to be in agreement with that reported in references 17, 32, and 50. It is noted that the reason the time history of the blade passage noise is so broad is because of the low relative velocity between the blade and airstream on the retreating side of the azimuth.

The NUWAIVE deformed wake analysis and the rotor noise prediction, coined TRAMP by NASA, are in use by a number of firms, notably Kaman Aerospace and Hughes Helicopters to investigate the noise characteristics of various rotor systems under development. It is believed that these above noted analysis techniques are rather versatile and, if nothing else, provide at least an initial step towards the development of a program to predict the noise characteristics of rotor systems operating in a realistic environment.

Possibly because of the challenge or because of the inquisitive and imaginative character of the helicopter community, the helicopter aerodynamicist has for many years been investigating means of altering the characteristics of the trailed tip vortex to either eliminate or significantly reduce the impulsive noise associated with the interaction of a blade and a concentrated vortex. More recently, because of the vortex hazard created by jumbo jets the fixed-wing aerodynamicist has also been looking extensively into ways of altering the characteristics of concentrated trailed vortices. References 60 through 65 present some results of the investigations that have been conducted and figure 20 presents a pictorial summary of some of the various techniques that have been investigated. Tangler, in reference 48, also presented the results of an investigation using differential flaps, sub wing tips, and split tip configurations to alter the characteristics of the tip vortex generated by a rotor blade. While some of the configurations shown in figure 20 had some apparent beneficial effects on modifying the characteristics of the trailed tip vortex, it was found that the performance penalties negated the practical application of most of the techniques. Two techniques that have shown promise, however, are the Tip Air Mass Injection (TAMI) system illustrated in figure 20 and a passive system called the Ogee tip. Since both of these approaches, one active and one passive, have been rather thoroughly investigated and have shown a

736

reasonable degree of success in reducing the impulsive noise due to blade vortex interaction, the approaches being utilized and the success that has been achieved with both systems will be reviewed briefly.

The TAMI system has been developed over a number of years by the RASA Division. References 49 and 66 through 73 present the results of some of these studies. The principle behind the TAMI approach is to inject a high pressure jet of air along the axis of the core of the vortex as it leaves the lifting surface. The mass flow and pressure injected into the core of the vortex causes an instant aging of the vortex (rapid radial redistribution of the vorticity) as well as causing a more rapid dissipation of the vorticity because of the higher level of turbulence induced by the jet stream within the vortex core (ref. 69). Reference 49 presents the results of tests of the system conducted in a wind tunnel using a model rotor system. Figure 21 shows a photograph of the two-bladed 2.13-m-diameter model rotor system mounted in the University of Maryland wind tunnel. The model, during this test series, had a tip speed of 152 m/sec and was operated over a large range of simulated descent rates at an advance ratio of 0.14 for a thrust coefficient C_T = 0.00455. This advance ratio was chosen as it was the one that full-scale flight tests indicated passes through the center of the most intense blade-slap noise as the descent velocity is increased (fig. 8). The model tests also confirmed that at an advance ratio of μ = 0.14 the rotor descends through the center of the most intense noise. Figure 22 presents some of the results obtained during the model test. It is noted that the data presented in this figure have been scaled up to full-scale frequencies and descent rates. The results, presented on a dB(A) basis, show that in the continuous-loud banging area (V_D = 183 m/min) the overall dB(A) was reduced by 7.5 dB(A); while in the area of most intense noise, the overall dB(A) was reduced by only 4.5 dB(A). It is noted that the primary reduction in the dB(A) was at the higher frequencies and not at the frequency range that controls the overall dB(A) (150 to 300 Hz). This result is consistent with the change in the pressure time histories which showed that the interactive spikes were eliminated with the TAMI system operating but the level of the other rotational noise harmonics was not altered. These results indicate, therefore, that at least for impulsive noise which is not associated with compressibility effects, the acoustic energy of interest is concentrated more in the overall turbulence generated by the entire rotor wake which is close to the rotor plane, than it is with the impulsive noise generated by the discrete interaction of a blade with one or two concentrated vortices. It is believed that this observation has very meaningful implications as regards what can be done to relieve the impulsive noise due to blade vortex interactions. The basic question that must be answered is, During flight condition in which discrete blade vortex interactions occur, is the major acoustic energy associated with the discrete blade vortex interactions or with the induced turbulence generated by all of the concentrated vortex energy in the rotor wake? It is this "one man's opinion" that it is the latter. It is believed that an answer to this question can be obtained by present technology, if it is properly applied to the problem.

If the primary source of excess noise during descent is associated with the entire field of concentrated vortex energy distributed below the rotor, then there may be a limit to the reduction of blade-slap noise that can be obtained in this mode of operation. If so, then a review of the techniques

being utilized to reduce blade impulsive noise during descent should be conducted in order to evaluate whether the approaches being utilized presently have the capability of reducing the impulsive noise to the degree that is desired.

As previously noted, another technique of reducing the impulsive noise due to blade vortex interaction that has been extensively investigated and which has been shown to have beneficial effects is a passive tip modification known as the Ogee tip. A strikingly similar tip shape was utilized on a helicopter rotor approximately 50 years ago. Figure 23 presents a 1930 photograph of the Curtiss-Bleeker helicopter which had low-aspect-ratio blades and a planform similar to the planform of just the Ogee tips. The reason the Curtiss-Bleeker helicopter utilized such a unique blade planform is not known, but I venture to suggest it was not to reduce the impulsive noise due to blade vortex interaction during descent or to reduce high-speed impulsive noise.

Research into the use of the Ogee tip on rotor blades to reduce the impulsive noise and dynamic loads due to blade vortex interactions in recent years is pretty well summarized by the investigations reported in references 74 through 76. The purpose of the Ogee tip is to distribute the aerodynamic loading in the tip region in a manner such that the vorticity shed at the blade tip is more like a vortex sheet than a concentrated line vortex which concentrates the vortex energy in a small compact volume. The effectiveness of the Ogee tip planform in redistributing the vortex energy is demonstrated by the data presented in figures 24 through 26. Figure 24 shows pressure isobars that were measured over a rectangular tip of an untapered rotor blade at an angle of attack of 12°. The data presented in this figure were obtained from reference 62. As can be seen from the data presented in figure 24, the formation of the concentrated vortex in the tip region generates a strong three-dimensional loading distribution having strong pressure gradients. In figure 25, pressure distributions that were measured over the Ogee tip show that approximately a two-dimensional pressure distribution is maintained over the entire tip region. This type of smooth pressure distribution (ref. 76) is also maintained over the Ogee tip when the blade is swept forward (fig. 26) as it would be in the second quadrant of the rotor azimuth. This is the rotor quadrant where the vortex is formed that intersects a following blade to generate the impulsive noise. Since the spanwise loading gradients are gradual in the region of the Ogee tip, the vorticity in the tip region would tend to be trailed as a weak unstable sheet and thus a large diameter diffuse trailed vortex would be formed.

Some preliminary results of flight tests of the Ogee concept were presented by Mantay in reference 77. Since he is presenting more detailed results of the flight test investigation in this symposium (ref. 78), I will just briefly discuss what I feel are the primary results that have been reported previously. Figure 27 presents the pertinent details of the aircraft that was used during the flight test. The aircraft was a UH-1H and the noise generated by the standard and Ogee tip blades having the same overall radius was compared over a range of flight velocities and descent rates. A brief composite summary of the data presented in reference 77, which I feel summarizes the results obtained as regards impulsive noise, is presented in figure 28. As can be seen from the results presented in this figure, which shows the acoustic signature for comparable locations within the respective impulsive noise boundaries, the

738

pressure time histories are very similar although the peak pressures are some-
what lower for the Ogee tip than they are for the standard tip. It is suspected
that, since the acoustic energy not associated with the interaction "spikes"
has not been altered significantly, a dB(A) weighed spectrum might be similar
to that obtained with the TAMI system (fig. 22).

It is believed that a major result of the tests discussed in reference 77
is the change in the location of the impulsive noise area as shown in fig-
ure 28. The significant increase in the descent rate at which the Ogee tip
intersects the impulsive noise boundary significantly opens up the "noise-free" ,
descent-approach corridor available to the pilot. Even if the noise within the
impulsive noise boundary is not altered, the significant movement of the bound-
ary within the flight envelope may be sufficient for commercial aircraft to
make a quiet descent into a terminal area. It is believed that the large move-
ment of the impulsive noise boundary might be related to the differences in the
Mach number, loading distribution, and radial location of the formation of the
tip vortex between the Ogee and standard blades. A series of wind-tunnel tests
will be conducted to determine whether, in fact, this is the reason for the
significant change in the impulsive noise boundary.

While the effort to date on ways to modify the impulsive noise due to
blade vortex interaction has been largely experimentally oriented, it is
believed that the state of the technology is such that theoretical investiga-
tions to evaluate the benefits that can be derived by various approaches can
be undertaken to provide at least guidelines as to what might be expected by
various vortex or blade modifications. For example, various new lifting line
or lifting surface theories for helicopter rotor blades can predict the required
detailed chordwise-spanwise loading distributions if the induced velocity dis-
tributions associated with the nonuniform wake and concentrated vortices are
known. It is believed that the available freely deforming wake analysis, such
as NUWAIVE (refs. 24 and 53), can provide these needed induced velocity distri-
butions. Investigations are currently being conducted at RASA using the NUWAIVE
program to determine the effects of various modifications to the vortex wake
structure on the detailed loading distributions of highly elastic compliant
rotor blades. The results obtained using the NUWAIVE program in conjunction
with the Rotor Aeroelastic Response Analysis (RARA), which is an extension to
the analysis procedure presented in reference 79, indicate that the analysis
procedures predict the changes in loading one might expect due to changes in
the vortex structure. It is believed that these or similar analysis procedures
used in conjunction with a suitable rotor acoustic prediction program such as
TRAMP (refs. 57 and 58) could be utilized to answer the question as to the
division of acoustic energy between the discrete blade vortex interaction and
that which is due to the concentrated vortex field in close proximity to the
rotor during flight. It is also believed that these same or similar analyses
could be utilized to establish the reason the impulsive noise boundaries for
the Ogee tip are significantly different from those for the standard blade.

It is concluded, therefore, that analysis procedures which represent the
state of the technology, or with slight extensions thereof, can and should be
utilized to investigate various aspects of the impulsive noise due to blade
vortex interactions. If this effort is undertaken, it is believed that a much

more rapid advance in means of improving the noise characteristics of heli-
copters during descent could be accomplished.

Noise Due to Tail Rotors

Tail rotor noise, because of its higher blade passage frequency, can be a
dominant source of noise in the frequency range of the so-called excess noise.
On many helicopters in which the main rotor impulsive noise is not present, the
noise source that draws attention to the helicopter as it is approaching is
that developed by the tail rotor. It is a noise source, however, that has not
received much attention in the past, particularly as regards noise reduction.

Pegg in reference 80 noted that the tail rotor developed acoustic signa-
tures having significant high harmonic content along the flight path at fre-
quencies of up to five times that at which the main rotor signature is lost in
the background noise. A reason for the strong propagation of the tail rotor
noise during these flight tests was not determined. However, acoustic data
taken during flight tests of many helicopters show the same type of propagation
characteristics of the tail rotor along the flight path although they may not
be as severe as that reported in reference 80.

Hughes Helicopters, during the full-scale research program to develop a
quiet helicopter (ref. 81), recognized the importance of the tail rotor to the
overall noise signature of a helicopter and investigated the effects of various
parameters on the noise characteristics of the tail rotor. It was found that
by increasing the blade number from 2 to 4, reducing the rotational speed, and
phasing the tail rotor blades in azimuth at 75° by 105°, a significant reduc-
tion in the noise developed by the tail rotor could be realized. This investi-
gation was rather unique in that it was the only one, as far as is known, which
had directed a significant effort towards reducing the noise output and propa-
gation characteristics of tail rotors.

A reasonable question that might be asked at this point is, If tail rotor
noise is a significant contributor to the excess noise that provides early
detection and contributes to the annoyance characteristics of helicopters, why
hasn't more effort been directed towards understanding and reducing this source
of rotor noise? I do not think a unique answer to this question can be given,
but it is suggested that the answer might lie somewhere between the following
two answers:

(1) Until a solution is found to significantly reduce main rotor impulsive
and rotational noise, the reduction of tail rotor noise is not going to sig-
nificantly improve the noise characteristics of the helicopter.

(2) The noise associated with tail rotors is so much more difficult to
analyze and understand than the noise due to main rotors because of the environ-
ment in which it is operating, it is not yet a trackable problem.

Since it is possible that answer (1) may be invalid in the near future, I would
like to address my comments to the latter answer.

Is the aerodynamic environment in which the tail rotor operates complicated
and basically a real mess? Yes, without a doubt, it is one of the most, if not
the most, difficult aerodynamic environment in which a lifting surface is required
to perform. Figure 29 is a sketch of "simplified" representation of the velocity
components to which a tail rotor is subjected. As is indicated in this figure, in
addition to all of the complicated aerodynamic effects to which a main rotor is sub-
jected, the tail rotor also is subjected to the periodic induced effects of the con-
centrated vortex wake from the main rotor. If the advance ratio is such that the
concentrated vortices from the forward and aft portions of the main rotor disk have
paths such as shown in the top of figure 29, the relative velocity the tail rotor
would experience at the top of the disk would be somewhat as shown. As can be seen,
the induced effect of the main rotor vortices is such that it causes a rapid varia-
tion in the spanwise loading which can create a significant source of noise. Since
the tail rotor does not operate at the same rotational speed as the main rotor, the
impulse frequency generated by these interactions would occur as the sum of the
harmonics of the blade passage frequencies of the main and tail rotors as on the
figure. While theoretically, for every value of N, M can have values of 0 to ∞,
the practical value of M generally never exceeds 3. The difference in the operat-
ing speed of the two rotor systems, $\Omega_{TR}/\Omega_{MR} \approx 5$, allows the tail rotor blade to
interact a number of times with the same group of main rotor vortices during the
time interval it takes the vortices to cross the tail rotor disk. Because of the
difference in the orientation of the blades with respect to the vortices during
each intersection, the directivity pattern of the impulsive signature would be
different for each intersection.

At a lower advance ratio, when the main rotor vortices interact with the
retreating blade of the tail rotor, the relative velocity the tail rotor blade
might see at the bottom of the disk is shown at the bottom of figure 29. As can
be seen, the velocity gradients and, thus, the loading gradients can be larger
due to the induced effects of the main rotor vortices than they were for the
advancing blade. Since the directivity pattern of the impulsive noise would
be directed aft, it would not create the annoyance or detection problems that
are caused by the blade vortex interactions with the advancing blade. Since
the vortices are traveling in the same direction as the retreating blade of the
tail rotor, the impulsive frequency due to the interactions of the main rotor
vortices with the tail rotor blade would be at lower frequencies than they were
for the advancing blade and would be defined by the relationship at the bottom
of figure 29.

If the direction of the tail rotor was reversed, the advancing blade and
retreating blades would have approximately the same perturbed velocity distri-
butions as indicated in figure 29 but would be reversed in their azimuth loca-
tion in the tail rotor disk. With the direction of rotation now clockwise, the
main impulsive noise on the advancing blade due to the tail rotor/main rotor
wake interaction would occur at low advance ratios when the rotor wake passed
over the lower part of the tail rotor disk instead of at high advance ratios
with the tail rotor operating in the counterclockwise direction. At high
advance ratios, however, when the strength of the main rotor vortices is higher
and the main rotor wake is intersecting the top portion of the tail rotor disk,
the tail rotor with the reversed direction would direct the impulsive noise aft
and the tail rotor noise to an observer of an approaching helicopter would
appear less than that of a helicopter having a tail rotor operating in the

counterclockwise direction. On a subjective basis, therefore, a clockwise rotation of the tail rotor would seem to be advantageous.

In actuality, the problems associated with understanding and predicting the noise developed by tail rotors are much more complicated than just indicated. When the effects of the turbulence generated by the complete main rotor wake, the interaction of the main rotor and tail rotor wake flows, the interaction of the tail rotor wake (tractor configuration) or inflow (pusher configuration) with a lifting vertical fin, and the non-integer rotational speed ratio between the main rotor and tail rotor are considered, a more complete understanding of the complicated flow field at the tail rotor is obtained. References 82 and 83 present an excellent discussion on the effects of these various parameters on the aerodynamic characteristics of tail rotors and are recommended reading for anyone interested in understanding or predicting the noise characteristics of tail rotors.

Recently Leverton, et al., references 84 through 87, reported the results of a noise investigation conducted on the tail rotor of the Lynx helicopter at Westland Helicopters Ltd. This very interesting and intriguing study investigated the modulated noise developed by a four bladed tail rotor intersecting the main rotor concentrated vortex flow. This modulated noise, labeled a "Burbling Sound" by Leverton, was determined to be caused by a main rotor vortex being intersected four or five times by the tail rotor blades as it passed through the tail rotor disk, thus giving rise to groups of impulses as each tip vortex of the main rotor passed through the tail rotor disk. Due to this grouping effect and the variation in the amplitude of the pressure pulse, the chain of impulses is effectively modulated and the interaction noise is heard as a deep throated burbling sound. Figure 30 presents a spectrum of the noise measured by Leverton as the helicopter approached (ref. 84). The tail rotor peaks as well as the blade passage peaks developed by the main rotor vortices are clearly evident in this spectrum. Figure 31 shows the effect Leverton measured for a 130-knot flyby of the Lynx helicopter when the tail rotor direction of rotation was changed from counterclockwise to clockwise. Since, at this speed, the main rotor wake is interacting with the top portion of the tail rotor disk (fig. 29), the significant difference in the noise level during approach is explainable as the tail rotor blades are in the retreating side of the disk when they intersect the main rotor vortices. The work Leverton presented in reference 84, and the associated references, is well worth studying as it presents a great deal of information regarding an understanding of the tail rotor noise produced by the interaction of the blades of the tail rotor with the concentrated vortices of the main rotor wake.

Recently an exploratory investigation of the effects of a number of configuration parameters on the noise produced by tail rotors operating in a realistic aircraft environment was conducted by the RASA Division for the NASA Langley Research Center (refs. 89 and 90). Figure 32 shows a picture of the model that was constructed specifically for these investigations. The model was approximately a 1/16-scale version of a UH-1 series helicopter. The main rotor blades had a diameter of 91.4 cm, had a chord of 4.45 cm, had a twist of -8° from the blade root to blade tip, and were hinged at the 4.2 percent blade radius. The tail rotor blades were 19.1 cm in diameter and had a chord

ɔf 1.14 cm. The tail rotor blades had an NACA 0015 airfoil section, were untwisted, and were mounted as cantilever beams to the tail rotor hub.

The helicopter model was designed to duplicate the thrust coefficient, solidity, and advance ratio of a full-scale UH-1 series helicopter. With this scaling the main and tail rotor wake flows for the model and the full-scale helicopter would retain the same location in space relative to each other and to the rotor blades. However, because of the requirement for an advance ratio ɔf 0.30 at a tunnel velocity of 30 m/sec, the scaled rotor was designed to operate at a lower tip speed than the full-scale rotor. Because of this scaling the effects of compressibility could not be tested with the model in its present form. The manner in which the model was designed and constructed provided the capability for variations in many of the main rotor wake/tail rotor parameters of primary importance. The following table lists these parameters and the range over which they could be varied:

Main rotor collective pitch angle	0° to 20°
Tail rotor collective pitch angle	0° to 8°
Tail rotor/fin offset spacing	0.20R to 0.31R
Shaft tilt angle	0° to 15° nose down
Tail rotor/main rotor disk longitudinal spacing	$0.50c_{MR}$ to $4.05c_{MR}$
Tail rotor/main rotor hub vertical spacing	-1.85R to 1.62R
Main rotor rotational speed	0 to 4100 rpm
Tail rotor rotational speed	0 to 13,000 rpm
Tail rotor direction of rotation	Clockwise or counterclockwise
Tail rotor thrust mode	Tractor or pusher
Fin blockage area	12% to 25% tail rotor disk area

Figure 33 presents a typical spectrum of the noise measured for the helicopter model at an advance ratio of 0.09. The similarity between the characteristics of the model and full-scale spectrum presented in figure 30 are apparent and although not marked in figure 30, the peaks at $2N\Omega_{TR} \pm 2M\Omega_{MR}$ due to the main rotor wake are very pronounced.

The following table presents the general effect of various parameters on the noise produced by the tail rotors that were noted during the brief exploratory investigation that was conducted:

Parameter	Effect		
	Large	Moderate	Slight
Advance ratio	X		
Longitudinal spacing			X
Lateral spacing	X		
Fin blockage area		X	
Operating mode (pusher, tractor)	X		
Direction of rotation*	X		
Tip speed		X	
Tail rotor/main rotor speed ratio			X
Main rotor thrust			X

*Since the investigation did not extensively investigate the effects of directivity, the effect of the direction of rotation may be somewhat overstated.

Pegg, et al. (ref. 88) have reported during this symposium, the results of an additional research investigation that NASA has recently conducted with the same model. These results tend to confirm and expand upon the results obtained during the brief exploratory investigation reported in references 89 and 90.

Since a rather systematic set of acoustic data on the effects of various parameters on the noise produced by a tail rotor operating in a realistic environment had been obtained (refs. 89 and 90), an effort was undertaken by the RASA Division to determine whether, by utilizing existing theoretical programs, the tail rotor noise characteristics measured for the model could be predicted. The analyses that were used in this investigation were the advance version of NUWAIVE free wake analysis developed from the analysis presented in reference 53 and the rotor noise prediction program discussed in reference 58. The relative paths of the main rotor concentrated vortices as they pass through the tail rotor disk, as predicted by the NUWAIVE program at an advance ratio of 0.20, are presented in figure 34.

As can be seen from figure 34 the concentrated vortex generated in the forward portion of the main rotor disk passes through the tail rotor plane clos to the path of the concentrated vortex trailed from the aft portion of the roto disk. While the proximity of the two vortex paths might be surprising, it is as would be expected when the strong upwash induced on the forward vortex filaments by the rotor wake as it passes across the rotor disk is recognized. To obtain a realistic understanding of the real effects of the main rotor wake on the noise produced by a tail rotor, it is believed that knowledge of the force-free wake positions is of paramount importance, particularly in the transition flight regime where the wake induced effects can be dominant. The solid outline is the tail rotor position for which a comparison of experimental and theo retical results will be presented. The dashed outline of the tail rotor disk are positions for which experimental data are also presented in reference 89.

In the following discussion, various degrees of sophistication in the prediction of the aerodynamic flow field will be used in order to demonstrate the characteristics that need to be modeled in order to predict the noise output of a tail rotor operating in a realistic aerodynamic flow field. The first results that will be presented are based on the following assumptions:

(1) The downwash of the tail rotor is represented by a uniform flow field.

(2) The main rotor wake is represented by a uniform downwash containing only the concentrated vortices from the blade tips.

(3) The tail rotor rotational speed is an integral harmonic of the main rotor rotational speed $\Omega_{TR}/\Omega_{MR} = 5$.

The predicted pressure time history of the tail rotor noise at a microphon upstream of the model is presented in figure 35. The intersections of the two blades with the various vortices are indicated and the obvious periodicity of the pressure time history is apparent. As time continues, because of the assumed integral relationship between the rotational speeds of the main and tail rotors, the pressure time history shown in this figure would be repeated.

744

The spectrum of the periodic pressure time history is presented in figure 36. As can be seen, the correlation with the experimental data is very poor. Except for the pressure at the first blade passage frequency, the predicted dB level is almost the same throughout the frequency range. Using the actual value $\Omega_{TR}/\Omega_{MR} = 5.09$ instead of the previous assumption of an integral relationship between the main rotor and the tail rotor rotational speeds, $\Omega_{TR}/\Omega_{MR} = 5$, gives the pressure time history shown in figure 37. A significant difference in the wave form of the primary pressure peaks can be seen when this pressure time history is compared with that presented in figure 35. If time was allowed to continue, each of the following wave forms would be different from its predecessor in the same time interval. The spectrum of this pressure time history (fig. 37) is presented in figure 38. Comparison of this spectrum with that presented in figure 36 shows that, while the pressure peak of the first blade passage frequency is predicted fairly well and a small pressure peak associated with the second blade passage frequency is now apparent, the correlation of the predicted and measured spectrum has not been improved significantly over that which is predicted on the basis of an integral relationship between the rotational speeds of the two rotor systems. The removal of the integral relationship between the rotational speeds does remove the repetitive characteristic of the spectrum in the frequency range of 0.5 to 4.0 Hz. When the complete nonuniform unsteady downwash characteristics of the main rotor wake are considered in addition to the concentrated tip vortices, the spectrum presented in figure 39 is obtained. As can be seen, the correlation between predicted and measured results is rather good with the remaining differences probably due to the nonuniform wake effects of the tail rotor.

On the basis of the results presented in the last series of figures, it is concluded that, while some characteristics of the tail rotor noise may be evaluated considering only the interaction of the concentrated main rotor blade tip vortices with the tail rotor blades, the tail rotor noise is dominated by the total unsteady induced velocity characteristics of the main rotor wake. In addition, it is apparent that the significant aerodynamic parameters which need to be included in an analysis which can be used to predict the noise characteristics of tail rotors must be at the least the following:

(1) Definition of the deformed spatial positions of main rotor wake over the tail rotor disk

(2) The induced velocity of the wake of the main rotor on the tail rotor inflow and downwash

(3) Representation of the nonperiodicity and arbitrary phasing of the interaction phenomenon

(4) Nonuniform wake effects of the tail rotor

(5) The aerodynamic interference effects of the tail fin on the tail rotor inflow and downwash

It is believed that by extending and modifying deformed wake analysis procedures, such as that represented by NUWAIVE (ref. 53), the wake-induced aerodynamic flow field over the tail rotor disk can be predicted to the required

degree of accuracy for inclusion in the rotor noise prediction theory of reference 58 so that the effect of various aerodynamic and geometric parameters on the noise output of tail rotors can be realistically investigated. It is believed that, through the proper application of the above noted predictive techniques, a meaningful investigation of ways of reducing tail rotor noise can be undertaken.

As indicated, while the unsteady loadings developed by a tail rotor operating in a realistic environment are rather complex and result in a rather complex noise signature, it is believed that existing technology, or a relatively minor extension of existing technology, if properly utilized, can form the basis of analyzing means of relieving the tail rotor noise problem.

Another unique rotor system that has demonstrated superior performance dynamic loads and acoustic characteristics is called the VGR. The concept upon which the rotor design is based is to determine the most favorable relationship between the location of the rotor system with respect to the wake it develops. The rotor system parameters that have been utilized to investigate the most beneficial relationship are the relative vertical spacing and the azimuthal spacing of the rotor blades with respect to each other. Some results of a full-scale test of a VGR system on a whirl tower are presented in figure 40. These results were obtained for a six-bladed rotor in which the blades were coplanar and spaced 60° in azimuth and also for a corotating rotor system in which alternate blades were moved 1 chord below the other three blades. In this configuration there are basically two three-bladed rotor systems in which the blade phasing between the blades is 120° while maintaining 60° between the blades of the total rotor system. The significant reduction in the noise output of the rotor system when the separated rotor planes was incorporated is obvious from the data presented. The effects of both rotor separation and blade azimuth phasing on the performance, dynamic loads, and acoustics of the VGR concept were investigated theoretically using the deformed wake, loads analysis, and noise prediction programs (refs. 53 and 58). The investigation (ref. 55) indicated results similar to those obtained in hover as it was shown that, with the proper blade spacing and phasing, the performance and blade dynamic characteristics could be enhanced and the acoustic signature altered significantly.

It is believed that these investigations have shown that although, at first glance, the problems associated with predicting the noise characteristics of rotor systems operating in a complex flow field seem beyond the scope of reality, the proper and knowledgeable application of existing state of the technology techniques can be used successfully to investigate the effects of various rotor and aerodynamic parameters on the noise characteristics of rotors operating in such an environment.

CONCLUDING REMARKS

In reviewing the efforts of many investigators over the last 10 to 15 years, it became obvious that a significant advance has been made in the area of Rotor Noise Technology. This is particularly true as regards the understanding and predictability of the basic aerodynamic mechanisms associated with the generation of rotor noise, i.e., noise due to steady loadings, compressibility,

746

and thickness. However, it also became apparent that the real helicopter environmental effects, such as free-stream turbulence, the induced effects of the rotor wakes, lifting surfaces, and fuselages have not been adequately considered in the development of these techniques. It is these self-induced and configuration effects which can be the primary reason the basic aerodynamic mechanisms result in the undesirable amplification of excess noise. It is important therefore to develop prediction programs to include these environmental effects so that the helicopter rotor noise that must be reduced to acceptable levels can be understood and investigated. The following table sets forth my evaluation of the status of Rotor Noise Technology as regards both the basic mechanisms and the application of the basic mechanisms to the real helicopter environment. It is readily apparent, after studying my evaluation, that

| EXCESS NOISE SOURCE | IMPACT ON NOISE | | | UNDERSTANDING OF BASICS | | | | | | UNDERSTANDING IN REAL ENVIRONMENT | | | | | | HOPE FOR NEEDED CORRECTION | | | | | |
| | | | | EXPERIMENTAL | | | THEORETICAL | | | EXPERIMENTAL | | | THEORETICAL | | | EXPERIMENTAL | | | THEORETICAL | | |
	L	M	H	P	F	G	P	F	G	P	F	G	P	F	G	P	F	G	P	F	G
MAIN ROTORS		X	X			X		X	X	X			X				X	X		X	X	
Structural Vibrations	X	X				X			X	X	X			X	X	X				X	X	
Stall	X	X			X		X	X		X	X		X			X	X		X	X	
Free Stream Turbulence	X	X			X			X		X				X		X	X		X		
Compressibility Effects M<0.85		X	X			X			X	X			X	X		X	X		X	X	
Compressibility Effects M>0.85			X			X		X	X		X	X		X	X	X	X		X	X	
Blade Vortex Interactions		X	X	X	X			X			X		X	X		X	X		X	X	
Wake Turbulence		X			X			X			X		X	X		X			X		
Body-Lifting Surface Interference	X	X		X	X		X	X		X	X		X	X		X	X		X	X	
TAIL ROTORS		X	X		X		X	X		X	X		X	X		X	X		X	X	
Structural Vibrations		X		X	X			X	X	X				X		X	X		X	X	
Stall	X	X			X		X	X		X	X		X			X	X		X	X	
Free Stream Turbulence	X				X			X			X			X		X	X		X		
Compressibility Effects M<0.85		X			X			X	X	X	X		X	X		X	X		X	X	
Compressibility Effects M>0.85		X			X				X	X	X		X	X		X	X		X	X	
Blade Vortex Interactions		X	X	X	X			X		X	X		X	X		X	X		X	X	
Wake Turbulence Main		X	X		X			X						X		X			X	X	
Wake Turbulence Tail	X			X	X			X		X	X		X	X		X			X		
Body-Lifting Surface Interference	X				X			X		X	X		X	X		X			X	X	

I do not believe our understanding and prediction of the helicopter self-induced environmental effects on rotor noise are on as solid a foundation as that which has been developed for the basic noise mechanisms. This is particularly true as regards the environment in which the tail rotor operates. As indicated by my relatively high rating of the possibility of reducing the excess noise to acceptable levels, I believe there should be a reasonable degree of confidence in our ability to analyze and predict the self-induced environmental effects. To either verify or negate these confidence ratings, I would recommend that state-of-the-art predictive techniques (or a minor extension thereof) of the helicopter self-induced environmental characteristics be utilized in conjunction with the basic noise predictive analysis techniques to determine the true State of Rotor Noise Technology. It is believed that such a study is warranted

particularly for tail rotors. The results of such an investigation should bring to light possible deficiencies in either the understanding of or in the parameters required for the prediction of the basic types of noise mechanisms. In addition, the results of such an investigation would also establish limitations in the analyses used for the prediction of the true helicopter rotor environment (i.e., rotor wake analyses, rotor body interference analyses). Since it is the rotor noise produced in the real-world environment that must be reduced and not that produced within the "laboratory" type environment, the initial steps in this direction should be undertaken soon.

One final thought that came to mind during the preparation of this review paper is associated with the validation of theoretical predictive techniques. It is rather universally assumed that, if the results of a predictive analysis do not match a measured result, the theory must be incorrect. I believe that this assumption can be totally inaccurate and it may be responsible for unnecessarily limiting our confidence in the capabilities of various predictive techniques. A simplified analysis can demonstrate that, if the basic parameters which define the equipment and test conditions are not adequately defined, the measured results may be extremely misleading and useless as a correlative data base. It is recommended that state-of-the-art sensitivity analyses be undertaken to evaluate the degree to which the basic system and test parameters must be defined in order that the measured noise data have a confidence level to within ±20 percent. To some, the results of such analyses might be surprising as it was to me when I undertook such a study to evaluate parameter input requirements for establishing a reliable correlative data base for rotor dynamic loads. It is believed important to undertake such an evaluation in order that present "data banks" can be analyzed as to their applicability in assessing the adequacy of predictive techniques. It may be found that there are no adequate data and that a directed effort will be required to develop a suitable data bank.

It is suggested that we can be successful in reducing the excess noise to acceptable levels if we are bold enough to open the laboratory door and accept the challenge to further the development of the capabilities to understand, analyze, and predict the noise developed by rotors in their true operating environment.

748

REFERENCES

1. Hubbard, Harvey H.; and Lassiter, Leslie W.: Some Aspects of the Helicopter Noise Problem. NACA TN 3239, 1954.

2. Garrick, I. E.; and Watkins, Charles E.: A Theoretical Study of the Effect of Forward Speed on the Free-Space Sound-Pressure Field Around Propellers. NACA Rep. 1198, 1954. (Supersedes NACA TN 3018.)

3. Hubbard, Harvey H.; and Regier, Arthur A.: Free-Space Oscillating Pressures Near the Tips of Rotating Propellers. NACA Rep. 996, 1950. (Supersedes NACA TN 1870.)

4. Arnoldi, R. A.: Propeller Noise Caused by Blade Thickness. Rep. R-0896-1, United Aircraft Corp., Jan. 10, 1956.

5. Hubbard, Harvey H.; and Regier, Arthur A.: Propeller Loudness Charts for Light Airplanes. NACA TN 1358, 1947.

6. Oestreicher, Hans L.: Field of a Spatially Extended Moving Sound Source. J. Acoust. Soc. America, vol. 29, no. 11, Nov. 1957, pp. 1223-1232.

7. Hubbard, H. H.: Noise Characteristics of Helicopter Rotors at Tip Speed up to 900 Feet per Second. J. Acoust. Soc. America, vol. 32, no. 9, Sept. 1960, pp. 1105-1107.

8. Hicks, Chester W.; and Hubbard, Harvey H.: Comparison of Sound Emission From Two-Blade, Four-Blade, and Seven-Blade Propeller. NACA TN 1354, 1947.

9. Bell Helicopter Co.: Study of Methods of Reducing Helicopter Noise. Contract DA 44-177-TC-729, U.S. Army Transp. Res. Command, June 1961.

10. Sternfeld, H., Jr.: Spencer, R. H., and Schaeffer, E. G.: Study To Establish Realistic Acoustic Design Criteria for Future Army Aircraft. TREC Tech. Rep. 61-72, U.S. Army, June 1961.

11. Fisher, C. P.: Helicopter Noise Mesurements, General Dynamics/Fort Worth Rep. FZM-2471 (Bell Helicopter Co. Rep. 299-099-192), Apr. 1962.

12. Mull, H. R.: External Noise Characteristics of Two Commercial Transport Helicopters. Rep. R-642 and Addendum, United Acoustic Consultants, Jan. 23, 1964.

13. Gutin, L.: On the Sound Field of a Rotating Propeller. NACA TM 1195, 1948. (Translated from Phys. Zeitcher der Sowjetunion, Ed. 9, Heft 1, 1936.)

14. Ingard, Uno: Sound Radiation From a Propeller in a Nonuniform Medium. Pratt & Whitney Aircraft, Jan. 1964.

15. Van de Vooren, A. I.; and Zandbergen, P. J.: Noise Field of a Rotating Propeller in Forward Flight. AIAA J., vol. 1, no. 7, July 1963, pp. 1518-1526.

16. Zandbergen, P. J.; and Van der Walle, F.: On the Calculation of the Propeller Noise Field Around Aircraft. NLR-TM G-23, Natl. Aero- & Astronaut. Res. Inst. (Amsterdam), 1962.

17. Schlegel, Robert; King, Robert; and Mull, Harold: Helicopter Rotor Noise Generation and Propagation. USAAVLABS Tech. Rep. 66-4, U.S. Army, Oct. 1966.

18. Wright, S. E.: The Acoustic Spectrum of Axial Flow Machines. J. Sound & Vib., vol. 45, no. 2, Mar. 22, 1976, pp. 165-223.

19. Pegg, Robert J.: Insights Into the Nature and Control of Rotor Noise. Aircraft Safety and Operating Problems, NASA SP-416, 1976, pp. 551-562.

20. Arndt, Roger E. A.; and Borgman, Dean C.: Noise Radiation From Helicopter Rotors Operating at High Tip Mach Number. No. 402, 26th Annual National Forum Proceedings, American Helicopter Soc., Inc., June 1970.

21. Cox, C. R.: Rotor Noise Measurements in Wind Tunnels. Proceedings Third CAL/AVLABS Symposium, Volume I, June 1969.

22. Cox, C. R.: Full-Scale Helicopter Rotor Noise Measurements in Ames 40- by 80-Foot Wind Tunnel. Rep. No. 576-099-052, Bell Helicopter Co., Sept. 1967.

23. Blackburn, W. E.; and Whitfield, A. A.: UH-2 Helicopter High-Speed Flight Research Program Utilizing Jet Thrust Augmentation. TRECOM TR-65-14, U.S. Army, Mar. 1965.

24. Sadler, S. Gene: Development and Application of a Method for Predicting Rotor Free Wake Positions and Resulting Rotor Blade Air Loads. NASA CR-1911, 1971.

25. Munch, Charles L.; and King, Robert J.: Community Acceptance of Helicopte Noise: Criteria and Application. NASA CR-132430, [1974].

26. Brown, David: Baseline Noise Measurements of Army Helicopters. USAAMRDL TR-71-36, U.S. Army, Mar. 1972.

27. Halwes, Dennis R.: Flight Operations To Minimize Noise. Verti-Flite, vol. 17, no. 2, Feb. 1971, pp. 4-9.

28. Cox, C. R.: How To Operate the Medium Helicopter More Quietly. U.S. Army Aviation Digest, vol. 19, no. 9, 1973, pp. 25, 33-38.

29. Charles, Bruce D.:   Acoustic Effects of Rotorwake Interaction During Low-Power Descent.   Presented at the United States National Symposium on Helicopter Aerodynamic Efficiency (Hartford, Conn.), Americal Helicopter Soc., Mar. 1975.

30. Schmitz, F. H.; and Boxwell, D. A.:   In-Flight Far Field Measurement of Helicopter Impulsive Noise.   J. American Helicopter Soc., vol. 21, no. 4, Oct. 1976, pp. 2-16.

31. Schmitz, F. H.; Boxwell, D. A.; and Vause, C. R.:   High Speed Helicopter Impulsive Noise.   J. American Helicopter Soc., vol. 22, no. 4, Oct. 1977, pp. 28-36.

32. Tangler, James L.:   Schlieren and Noise Studies of Rotors in Forward Flight.   Preprint AHS-77-33-05, American Helicopter Soc., May 1977.

33. Deming, A. F.:   Noise from Propellers With Symmetrical Sections at Zero Blade Angle.   NACA TN 679, 1938.

34. Lyon, R. H.:   Radiation of Sound by Airfoils That Accelerate Near the Speed of Sound.   J. Acoust. Soc. America, vol. 49, 1971, pp. 894-905.

35. Ffowcs Williams, J. E.; and Hawkings, D. L.:   Sound Generation by Turbulence and Surfaces in Arbitrary Motion.   Philos. Trans. R. Soc. London, ser. A, vol. 264, no. 1151, May 8, 1969, pp. 321-342.

36. Farassat, F.:   Theory of Noise Generation From Moving Bodies With an Application to Helicopter Rotors.   NASA TR R-451, 1975.

37. Hawkings, D. L.; and Lowson, M. V.:   Theory of Open Supersonic Rotor Noise.   J. Sound & Vib., vol. 36, no. 1, 1974, pp. 1-20.

38. Isom, M. P.:   The Theory of Sound Radiated by a Hovering Transonic Helicopter Blade.   POLY-AE/Am Rep. No. 75-4, Polytech. Instit. of New York, May 1975.

39. Lowson, Martin V.:   Research Requirements for the Improvements of Helicopter Operations.   Rotorcraft Design.   AGARD-CP-233, Jan. 1978, pp. 21-1 - 21-13.

40. Schmitz, F. H.; and Yu, Y. H.:   Theoretical Modeling of High-Speed Helicopter Impulsive Noise.   Presented at the Third European Rotorcraft and Powered Lift Aircraft Forum (Marseilles, France), Sept. 1977.

41. Farassat, F.; Pegg, R. J.; and Hilton, D. A.:   Thickness Noise of Helicopter Rotors at High Tip Speeds.   AIAA Paper 75-453, Mar. 1975.

42. Sternfeld, H: Influence of the Tip Vortex on Helicopter Rotor Noise.   AGARD CP No. 22, Sept. 1967.

43. Leverton, J. W.; and Taylor, F. W.:   Helicopter Blade Slap.   J. Sound & Vib., vol. 4, no. 3, 1966, pp. 345-357.

44. Leverton, J. W.: Helicopter Noise - Blade Slap. Part 1: Review and Theoretical Study. NASA CR-1221, 1968.

45. Windall, Sheila; Chu, Sing; and Lee, Albert: Theoretical and Experimental Studies of Helicopter Noise Due to Blade-Vortex Interaction. Helicopter Noise Symposium, U.S. Army Res. Office - Durham and American Helicopter Soc., Inc., Sept. 1971, pp. 25-34.

46. White, Richard P., Jr.: An Investigation of the Vibratory and Acoustic Benefits Obtainable by the Elimination of the Blade Tip Vortex. Paper presented at the 29th Annual National Forum of the American Helicopter Society (Washington, D.C.), May 1973.

47. Tangler, J. L.: Investigation the Stability of the Tip Vortex Generated by Hovering Propellers and Rotors. Paper presented at the AIAA 2nd Atmospheric Flight Mechanics Conference (Palo Alto, Calif.), Sept. 1972.

48. Tangler, James L.: The Design and Testing of a Tip To Reduce Blade Slap. Preprint No. 963, 31st Annual National Forum, American Helicopter Soc., May 1975.

49. White, Richard P., Jr.: Wind Tunnel Tests of a Two Bladed Model Rotor To Evaluate the TAMI System in Descending Forward Flight. NASA CR-145195, 1977.

50. Cox, C. R.; and Lynn, R. R.: A Study of the Origin and Means of Reducing Helicopter Noise. TRECOM Tech. Rep. 62-73, U.S. Army, Nov. 1962.

51. Landgrebe, A. J.: An Analytical Method for Predicting Rotor Wake Geometry. J. American Helicopter Soc., vol. 14, no. 4, Oct. 1969, pp. 20-32.

52. Landgrebe, A. J.: Moffitt, R. C.; and Clark, D. R.: Aerodynamic Technolog for Advanced Rotorcraft. Paper presented at American Helicopter Society Symposium on Rotor Technology (Essington, Pa.), Aug. 11-13, 1976.

53. Sadler, S. G.: Main Rotor Free Wake Geometry Effects on a Blade Air Loads and Response for Helicopters in Steady Maneuvers. Volume I - Theoretical Formulation and Analysis of Results. NASA CR-2110, 1972.

54. Shipman, Keith: Effect of Wake on the Performance and Stability Characteristics of Advanced Rotor Systems. USAAMRDL TR-74-45, U.S. Army, 1974.

55. Gangwani, S.T.: The Effect of Helicopter Main Rotor Blade Phasing and Spacing on Performance, Blade Loads, and Acoustics. NASA CR-2737, 1976.

56. White, Richard P., Jr.; and Gangwani, Santu T.: Application of NUWAIVE to the "X" Wing Configuration for Advance Ratios of Zero to Infinity. RASA/SRL Rep No. 14-78-02, 1978.

57. Johnson, H. K.: Development of a Technique for Realistic Prediction and Electronic Synthesis of Helicopter Rotor Noise. USAAMRDL TR 73-8, U.S. Army, Mar. 1973.

752

48. Johnson, H. K.: Development of an Improved Design Tool for Predicting and Simulating Helicopter Rotor Noise. USAAMRDL TR 74-37, U.S. Army, June 1974.

49. White, Richard P., Jr.: V/STOL Rotor and Propeller Noise: Its Prediction and Analysis of its Aural Characteristics. AIAA Paper 75-452, Mar. 1975.

50. Padakannaya, Raghuveera: Effect of Wing Tip Configuration on the Strength and Position of a Rolled-Up Vortex. NASA CR-66916, 1970.

51. Spencer, R. H.; Sternfeld, H.; and McCormick, B. W.: Tip Vortex Core Thickening for Application to Helicopter Rotor Noise Reduction. R-403-A, U.S. Army Aviation Materiel Lab., Sept. 1966.

52. Chigier, N. A.; and Corsiglia, V. R.: Tip Vortices - Velocity Distributions. American Helicopter Soc. Preprint No. 522, May 1971.

53. Scheiman, James; and Shivers, James P.: Exploratory Investigation of the Structure of the Tip Vortex of a Semispan Wing for Several Wing-Tip Modifications. NASA TN D-6101, 1971.

54. Patterson, James C., Jr.; and Flechner, Stuart G.: An Exploratory Wind-Tunnel Investigation of the Wake Effect of a Panel Tip-Mounted Fan-Jet Engine on the Lift-Induced Vortex. NASA TN D-5729, 1970.

55. Yuan, S. W.: Vortex Pollution, Wing-Tip Vortices: The Hazard and the Remedy. J. Aeronaut. Soc. of India, vol. 23, no. 2, May 1971.

56. Rinehart, Stephen A.: Study of Modification of Rotor Tip Vortex by Aerodynamic Means. RASA Rep.70-02 (ONR Contract No. N00014-69-C-0169), Jan. 1970. (Available from DDC as AD 704 804.)

57. Rinehart, Stephen A.: Effects of Modifying a Rotor Tip Vortex by Injection on Downwash Velocities, Noise and Airloads. Paper presented at AHS/AIAA/UTA Joint Symposium on Environmental Effects on VTOL Designs (Arlington, Texas), Nov. 1970.

58. Rinehart, Stephen A.; Balcerak, John C.; and White, Richard P., Jr.: An Experimental Study of Tip Vortex Modifications by Mass Flow Injection. RASA Rep. 71-01 (ONR Contract No. N00015-690C-0169), Jan. 1971. (Available from DDC as AD 726 736.)

69. White, Richard P., Jr.; and Balcerak, John C.: An Investigation of the Mixing of Linear and Swirling Flows. RASA Rep. 72-04 (ONR Contract No. N00014-71-C-0226), Feb. 1972. (Available from DDC as AD 742 854.)

70. White, Richard P., Jr.; and Balcerak, John C.: Investigation of the Dissipation of the Tip Vortex of a Rotor Blade by Mass Injection. USAAMRDL Tech. Rep. 72-43, U.S. Army, Feb. 1972.

71. White, Richard P., Jr.; and Balcerak, John C.: The Nemesis of the Trailed Tip Vortex - Is It Now Conquered? Preprint No. 624, 28th Annual National Forum of the American Helicopter Society (Washington, D.C.), May 1972.

72. Balcerak, J. C.; and Zalay, A. D.: Investigation of the Effects of Mass Injection to Restructure a Trailing Tip Vortex at Transonic Speeds. RASA Rep. 73-03 (ONR Contract N00014-71-C-0226), Feb. 1973. (Available from DDC as AD 760 363.)

73. Pegg, Robert J.; Hosier, Robert N.; Balcerak, John C.; and Johnson, H. Kevin: Design and Preliminary Tests of a Blade Tip Air Mass Injection for Vortex Modification and Possible Noise Reduction on a Full-Scale Helciopter Rotor. NASA TM X-3314, 1975.

74. Rorke, J. B.; Moffitt, R. C.; and Ward, J. F.: Wind Tunnel Simulation of Full-Scale Vortices. Preprint No. 623, 28th Annual National Forum of the American Helicopter Society (Washington, D.C.), May 1972.

75. Balcerak, John C.; and Feller, Raymond F.: Vortex Modification by Mass Injection and by Tip Geometry Variation. USAAMRDL Tech. Rep. 73-45, U.S. Army, June 1973. (Available from DDC as AD 771 966.)

76. Balcerak, John; and Feller, Raymond F.: Effect of Sweep Angle on the Pressure Distributions and Effectiveness of the Ogee Tip in Diffusing a Line Vortex. NASA CR-132355, 1973.

77. Mantay, Wayne R.; Shidler, Phillip A.; and Campbell, Richard L.: Some Results of the Testing of a Full-Scale Ogee Tip Helicopter Rotor; Acoustics, Loads, and Performance. AIAA Paper 77-1340, Oct. 1977.

78. Mantay, Wayne R.; Campbell, Richard L.; and Shidler, Phillip A.: Full-Scal Testing of an Ogee Tip Rotor. Helicopter Acoustics, NASA CP-2052, Pt. I, 1978. (Paper no. 14 of this compilation.)

79. Sutton, Lawrence R.; and Rinehart, S.: Development of an Analysis for the Determination of Coupled Helicopter Rotor/Control System Dynamic Response Part I - Analysis and Applications. NASA CR-2452, 1975.

80. Pegg, Robert J.: The Effect of Various Operating Parameters on the Noise Radiation Patterns From a Helicopter in Forward Fight. Preprint No. SW-70-5. Joint Symposium on Environmental Effects on VTOL Designs (Arlington, Texas), Nov. 1970.

81. Barlow, W. H.; McCluskey, W. C.; and Ferris, H. W.: OH-6A Phase II Quiet Helicopter Program. USAAMRDL Tech. Rep. 72-29, U.S. Army, Sept. 1972.

82. Lynn, R. R.; Robinson, F. D.; Batra, N. N.; and Duhon, J. M.: Tail Rotor Design. Pt. I: Aerodynamics. J. American Helicopter Soc., vol. 15, no. 4, Oct. 1970, pp. 2-15.

83. Huston, Robert J.; and Morris, Charles E. K., Jr.: A Note on A Phenomenon Affecting Helicopter Directional Control in Rearward Flight. J. American Helicopter Soc., vol. 15, no. 4, Oct. 1970, pp. 38-45.

84. Leverton, J. W.; Pollard, J. S.; and Wills, C. R.: Main Rotor Wake/Tail Interaction. Vertica, vol. 1, no. 3, 1977, pp. 213-222.

85. Pollard, J. S.; and Leverton, J. W.: Lynx External Noise "Burble" Noise Investigation. Applied Acoustics Group Note 1044, Westland Helicopters Ltd., Oct. 1973.

86. Pollard, J. S.: Lynx "Burble" Noise Effect of Forward Speed and Direction of Rotation of Tail Rotor. Applied Acoustics Group Note 1053, Westland Helicopters Ltd., Jan. 1974.

87. Wills, C. R.: Reversed Direction Tail Rotor Lynx "Burble" Noise Investigation - Test Report. Applied Acoustics Group Note 1115, Westland Helicopters Ltd., June 1975.

88. Pegg, Robert J.; and Shidler, Phillip A.,: Exploratory Wind-Tunnel Investigation of the Effect of the Main Rotor Wake on Tail Rotor Noise. Helicopter Acoustics, NASA CP-2052, Pt. I, 1978. (Paper no. 11 of this compilation.)

89. Balcerak, John C.: Parametric Study of the Noise Produced by the Interaction of the Main Rotor Wake With the Tail Rotor. NASA CR-145001, 1976.

90. White, Richard P., Jr.; Balcerak, John C.; and Pegg, Robert J.: A Parametric Model Study of the Noise Generated by the Aerodynamic Interaction of the Tail Rotor With the Wake of the Main Rotor. Paper presented at American Helicopter Society Symposium on Rotor Technology (Essington, Pa.), Aug. 11-13, 1976.

Figure 1.- CH-53E helicopter.
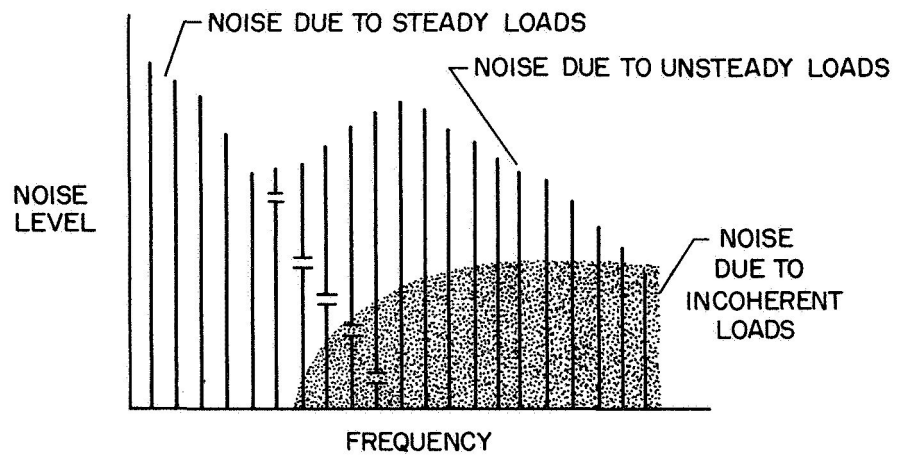
Figure 2.- Generalized acoustic spectrum for rotors.
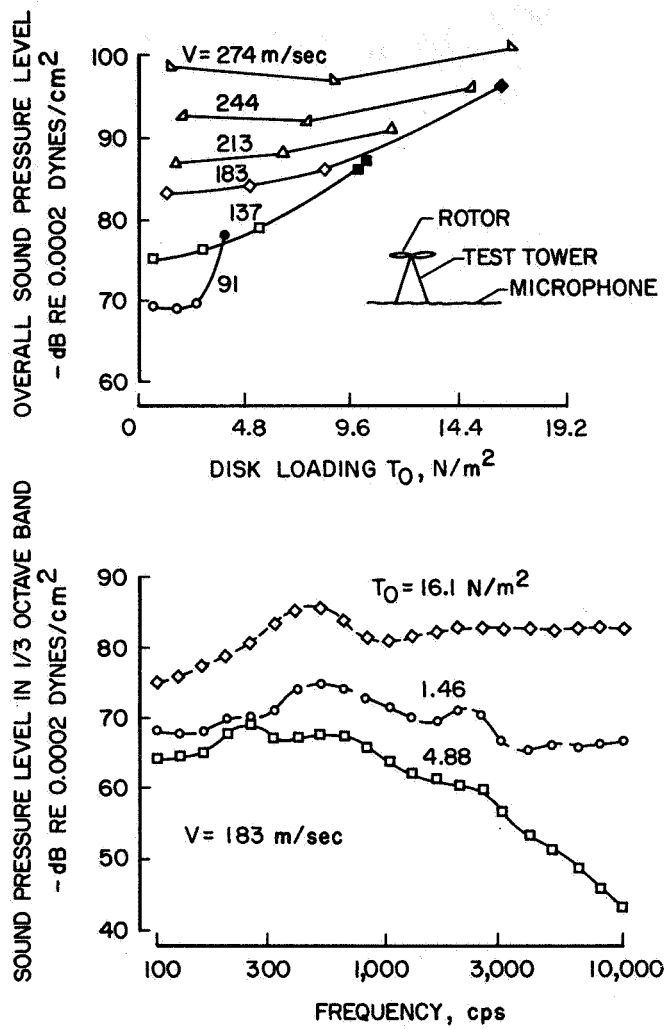
Figure 3.— Effect of stall on rotor noise.
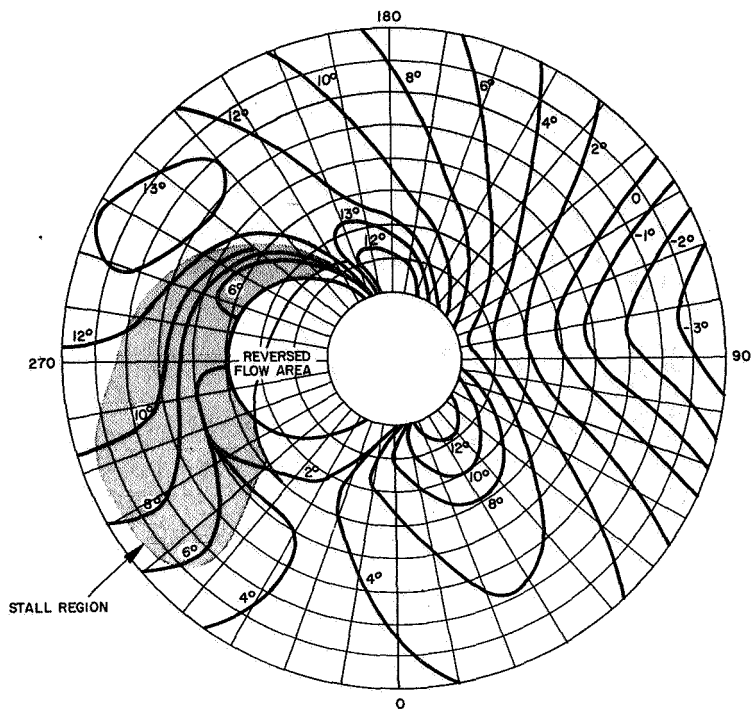
Figure 4.- Angle of attack contours.
UH-2, $\mu \cong 0.48$.
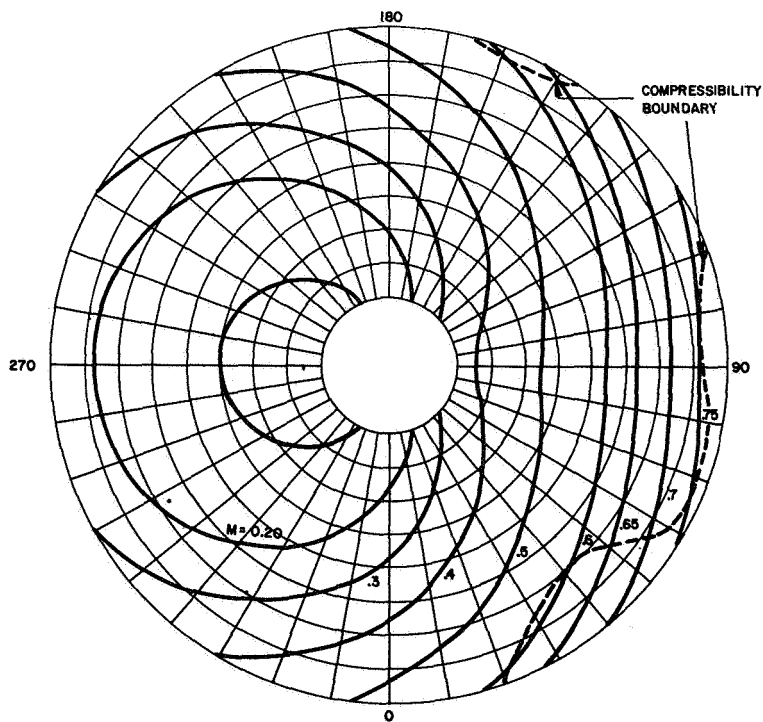
Figure 5.- Mach number contours.
UH-2, $\mu \cong 0.48$.

Figure 6.- RPV propeller in the test facility.
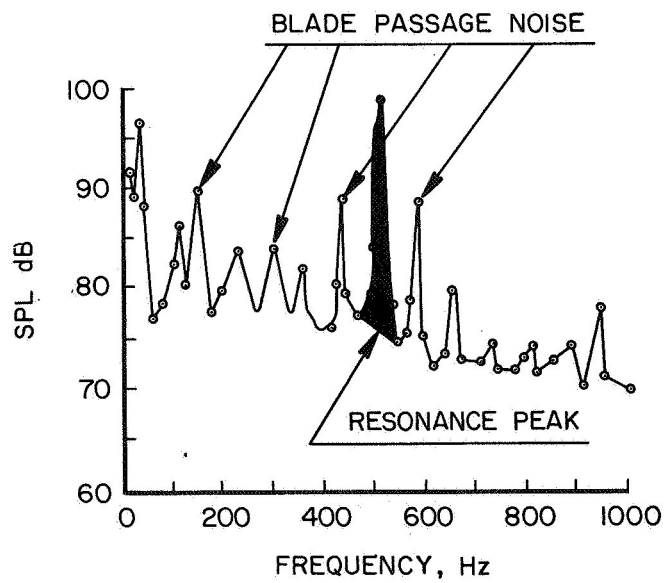
Figure 7.- Noise due to propeller resonance.
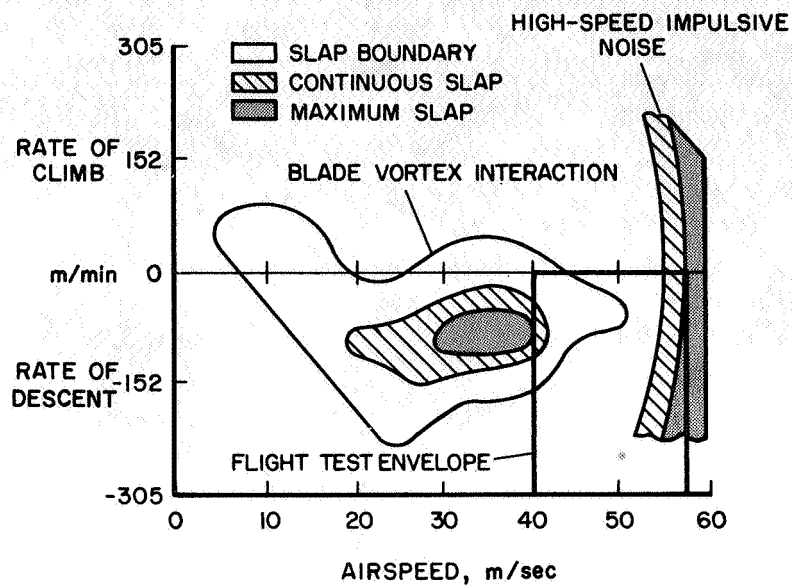
Figure 8.- Impulsive noise boundaries for UH-1
series helicopters.
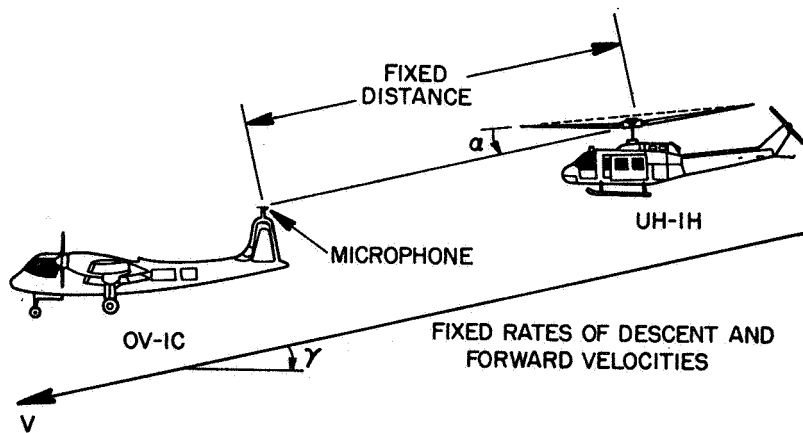
Figure 9.- Schematic of in-flight far field
measurement technique.

760
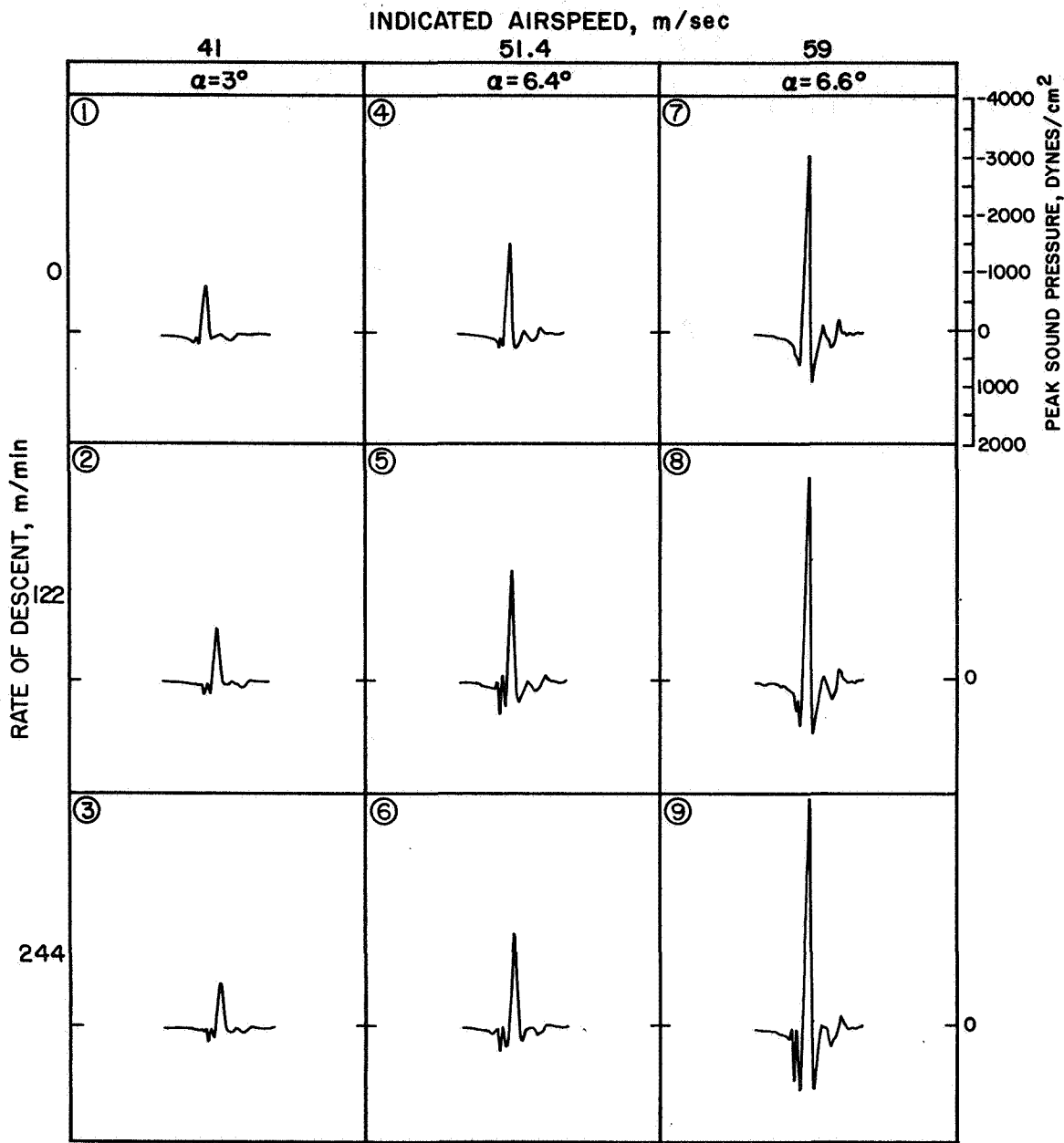
Figure 10.- Averaged acoustic signature of UH-1H impulsive noise versus forward airspeed and rate of descent.
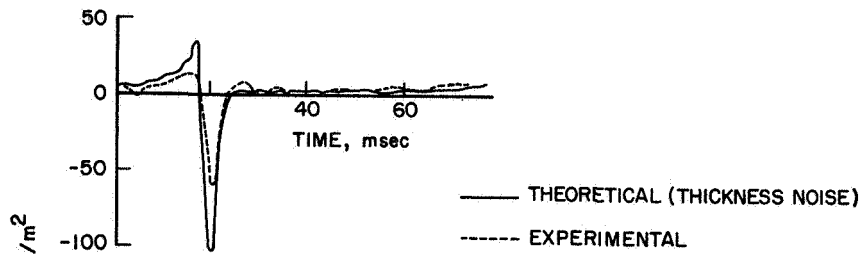
(a) Helicopter speed, 140 knots.
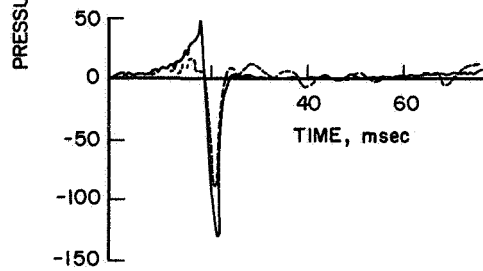
(b) Helicopter speed, 170 knots.

Figure 11.- Comparison of experimental and predicted thickness noise.
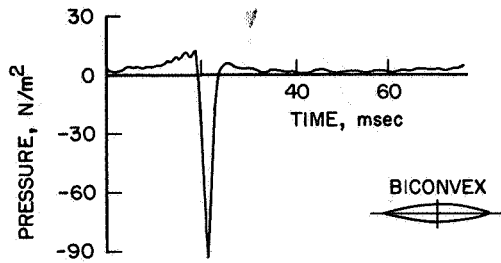
(a) Biconvex airfoil (parabolic arc).
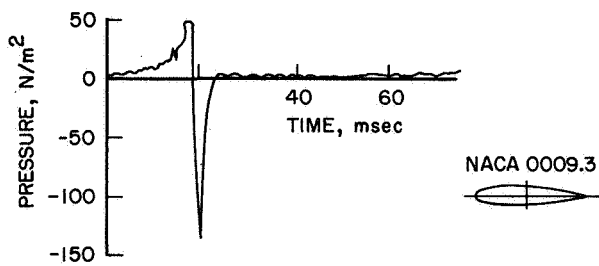
(b) NACA four-digit airfoil.
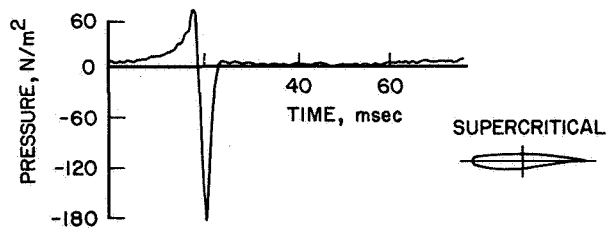
(c) Supercritical airfoil.

Figure 12.- Theoretical effect of change in thickness distribution on acoustic pressure signature. Thickness noise only. (Note change of scale.)
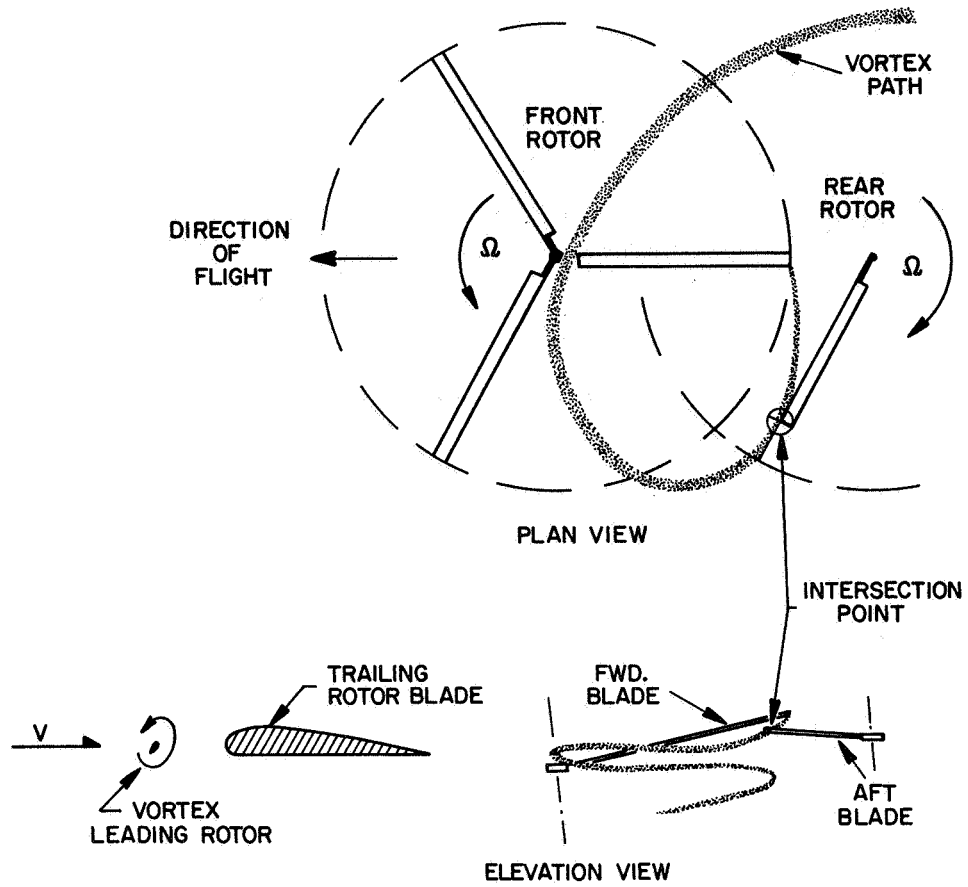
Figure 13.– Diagram of tandem rotor wake geometry in forward flight during impulsive noise.
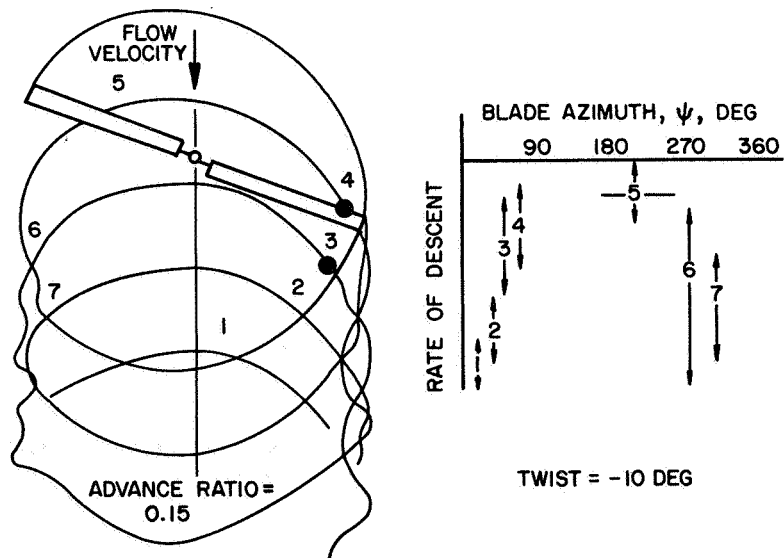
Figure 14.– Blade/vortex intersections during partial power descent.
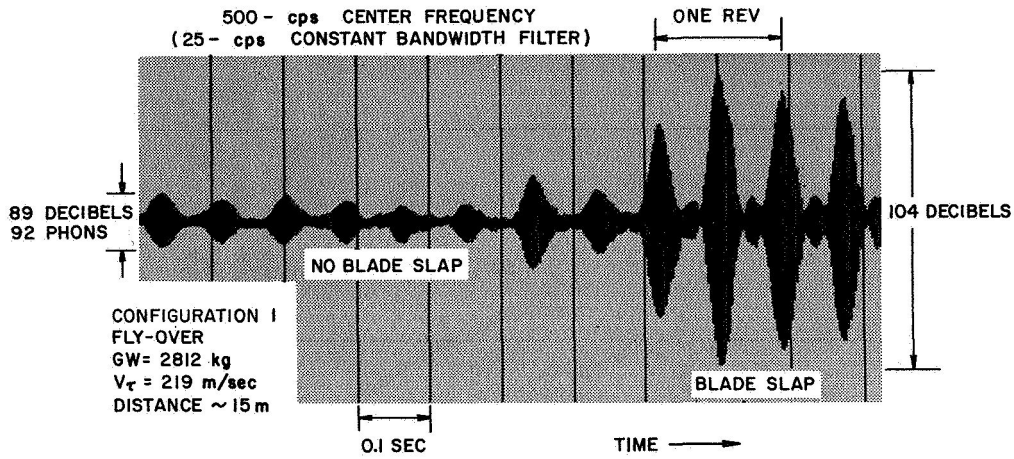
Figure 15.- Single rotor helicopter blade slap during
turn at a frequency of 500 cps.
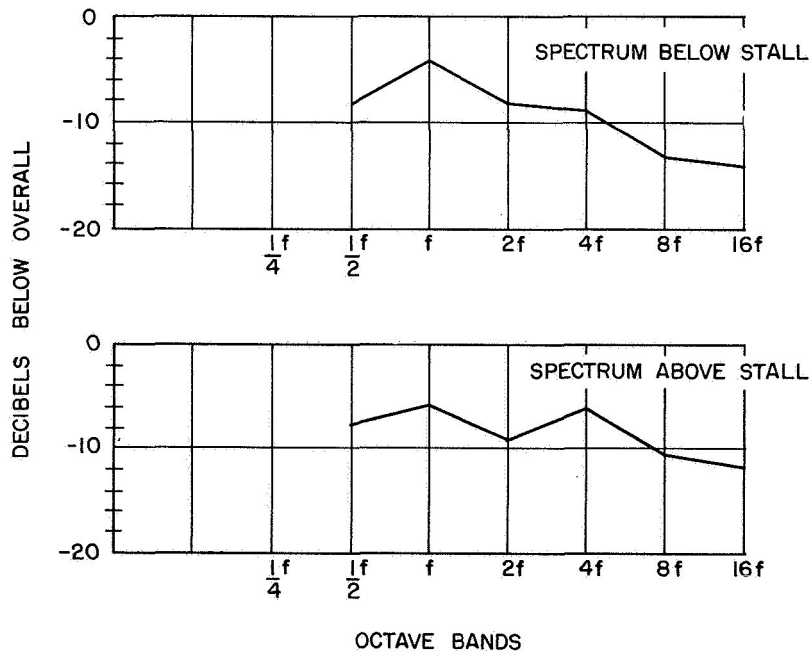
Figure 16.- Changes in spectrum due to retreating
blade slap.

DIRECTION OF FLIGHT

BLADE I

BLADE 2

BLADE VORTEX
INTERACTION AREA
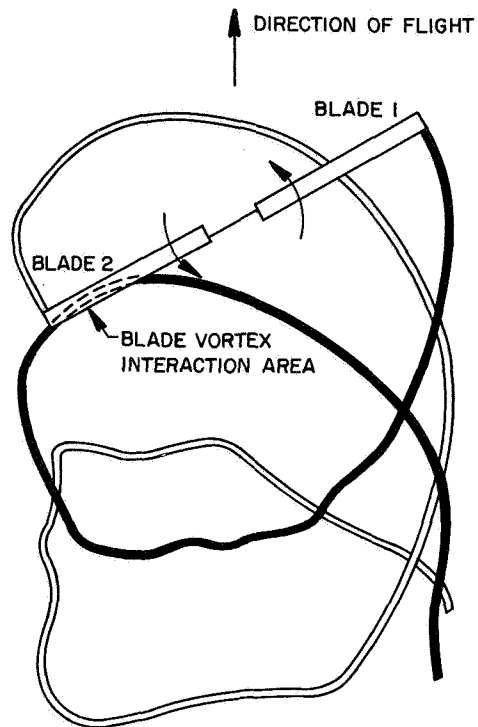
Figure 17.- Predicted deformed wake position of
UH-1 helicopter in a 1.5g climbing left turn.

BLADE SLAP

NO BLADE SLAP

SPL (dB)

90

60

30

90

60

30

MASKED
THRESHOLD OF HEARING

MASKED
THRESHOLD OF HEARING

200 400 600 800

200 400 600 800

FREQUENCY (Hz)
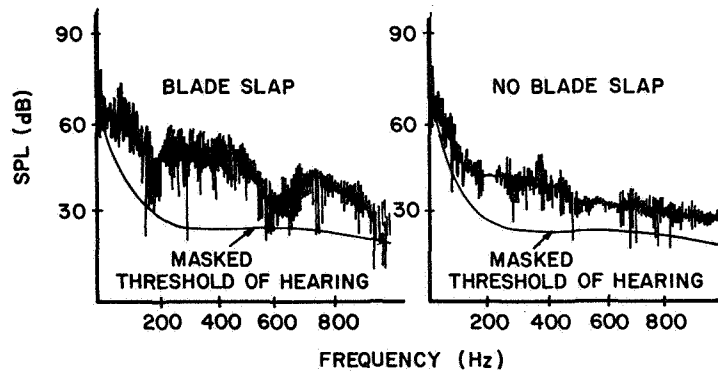
Figure 18.- Spectra of UH-1 in a
1.5g climbing left turn.

766

INTERACTION
PULSE

WITH VORTEX
INTERACTION
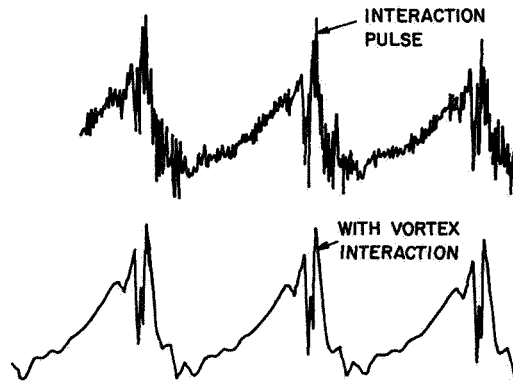
Figure 19.- Pressure time histories
of a UH-1 in a 1.5g climbing left
turn.

SWEPT TIP

TAPERED TIP

RAKED TIP

ELLIPTICAL TIP

POROUS TIP

GULLED OUTER
PANELS

END PLATE

SPANWISE OR ANGLED
BLOWING

LIFTING SURFACE DRAG
SPOILER

REVERSE SWIRL
GENERATOR

JET ENGINE

RASA
LINEAR AIR INJECTION (TAMI)
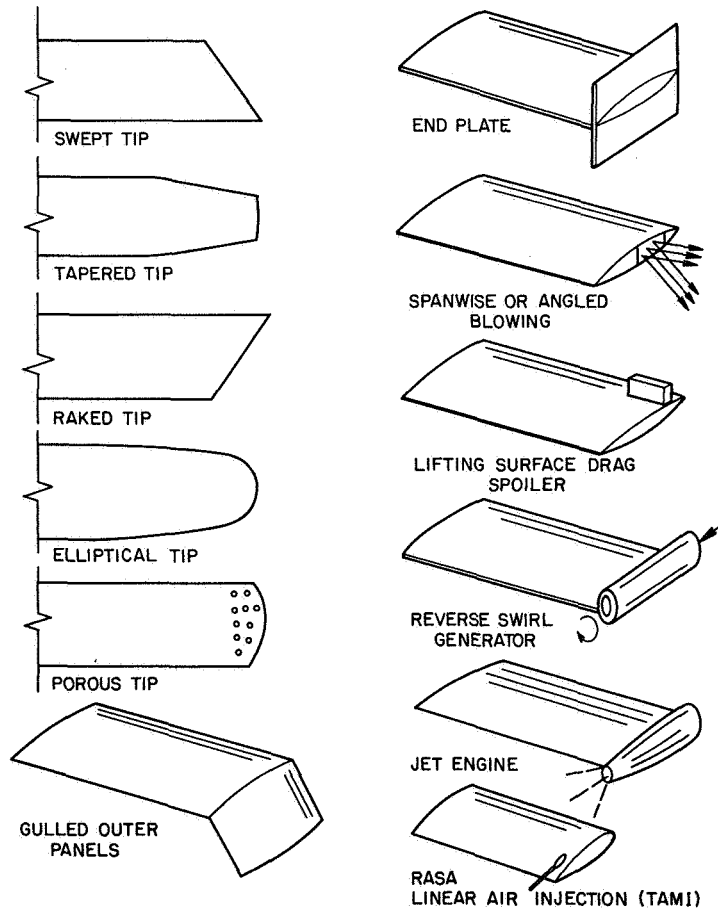
Figure 20.- Configurations for distributing, dissipating,
or relocating tip vortices.
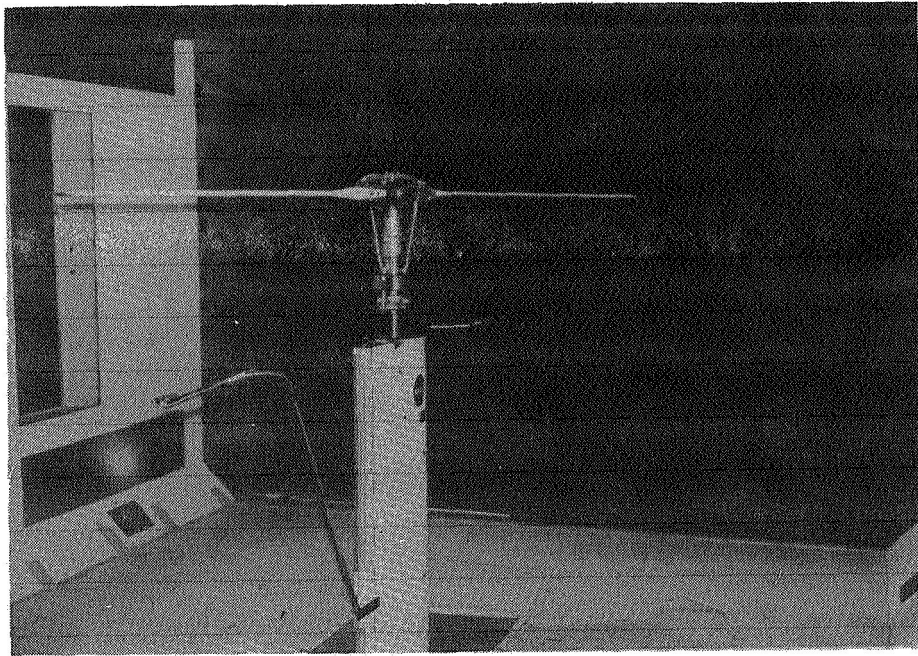
Figure 21.- TAMI model in wind tunnel.
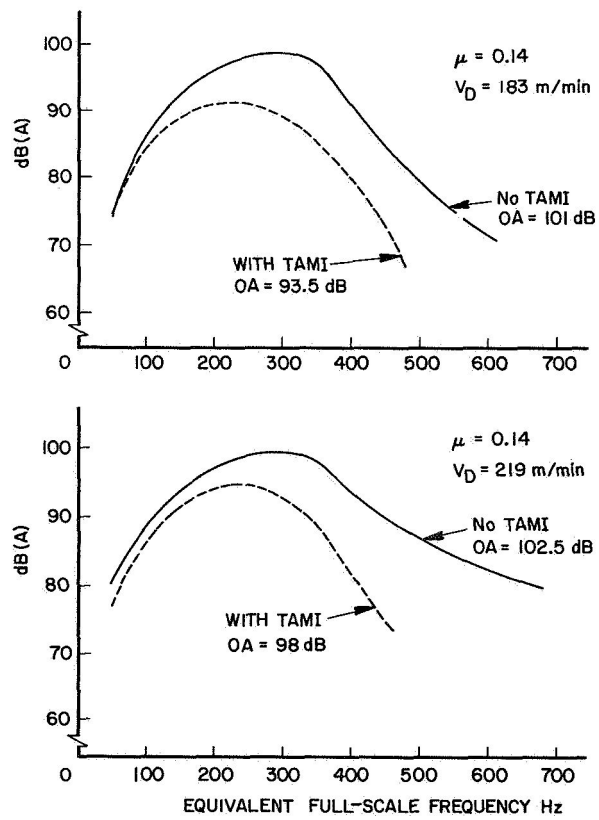
Figure 22.- Effect of TAMI on dB(A) weighted spectrum.
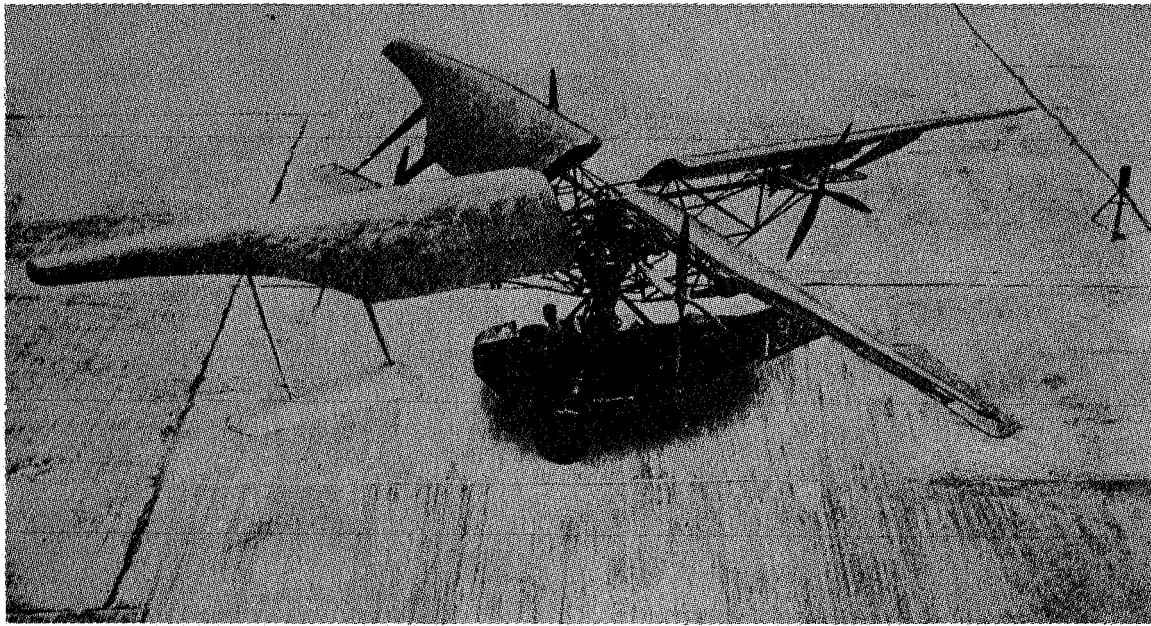
Figure 23.- Curtiss-Bleeker helicopter - 1930.
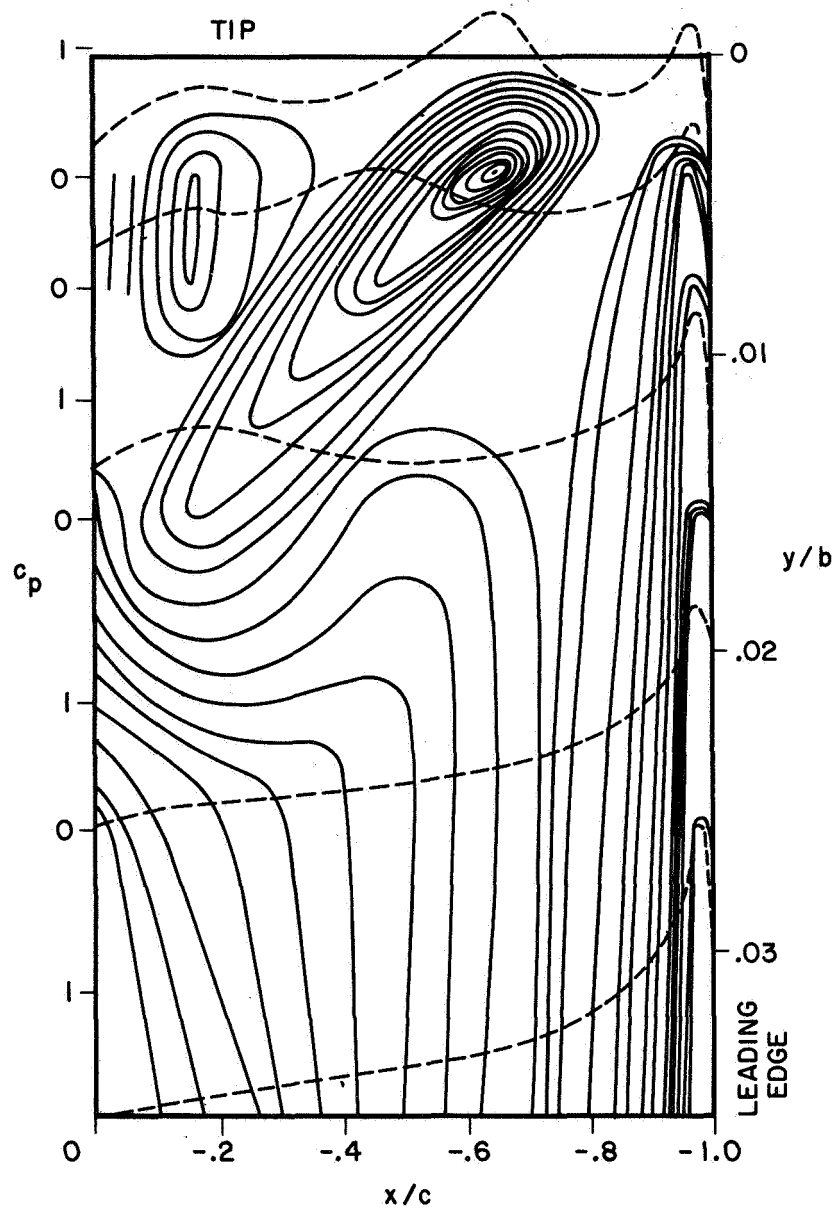
Figure 24.- Pressure isobars on top surface of blade tip at $\alpha = 12°$ and $\lambda = 0$.

LINES OF CONSTANT $\Delta p/q$

$\Delta p/q$

-2.0 -1.5 -1.0 -.75   -.5 -.4 -.3   -.2   -.1   0
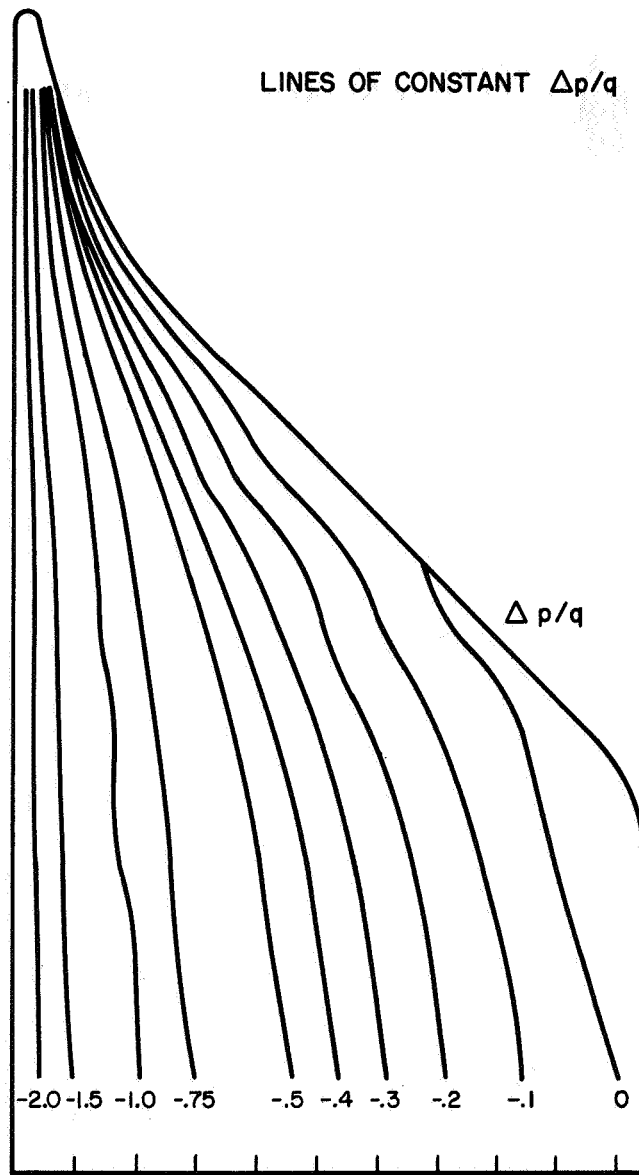
Figure 25.- Contour pressure plot of the Ogee-tip section
at $\alpha = 8^\circ$ and $\lambda = 0^\circ$.

LINES OF CONSTANT $\Delta p/q$

$\Delta p/q$

-2.0 -1.5 -1.0 -.75   -.5 -.4 -.3   -.2   -.1   0
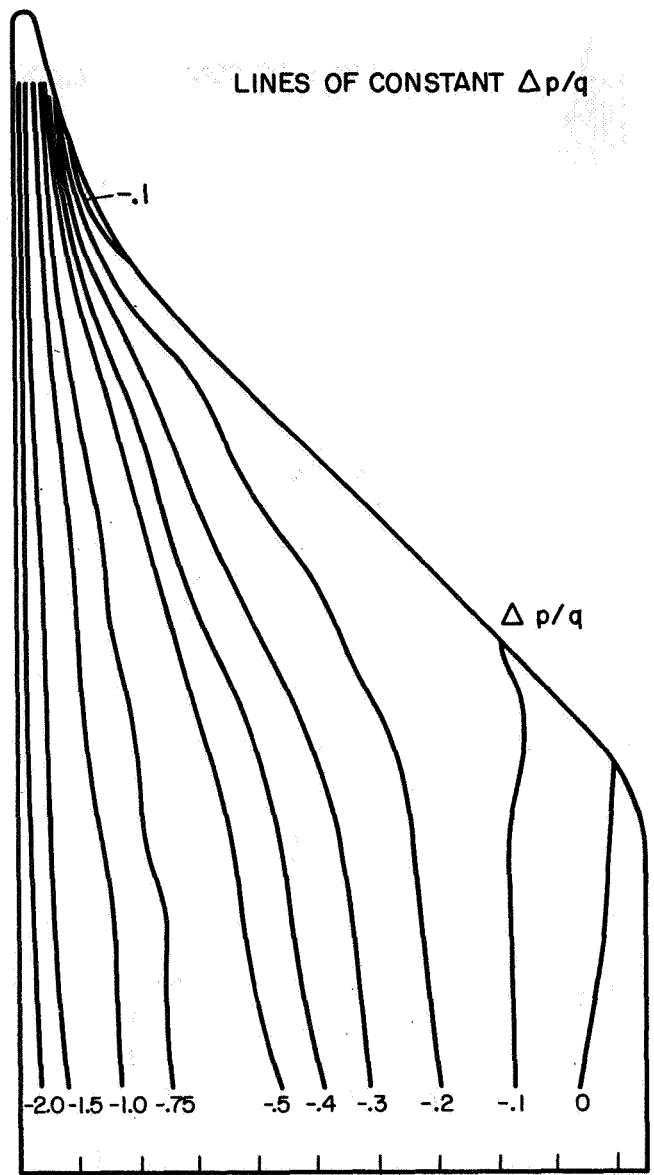
Figure 26.- Contour pressure plot of the Ogee-tip section
at $\alpha = 8^0$ and $\lambda = -20^0$.
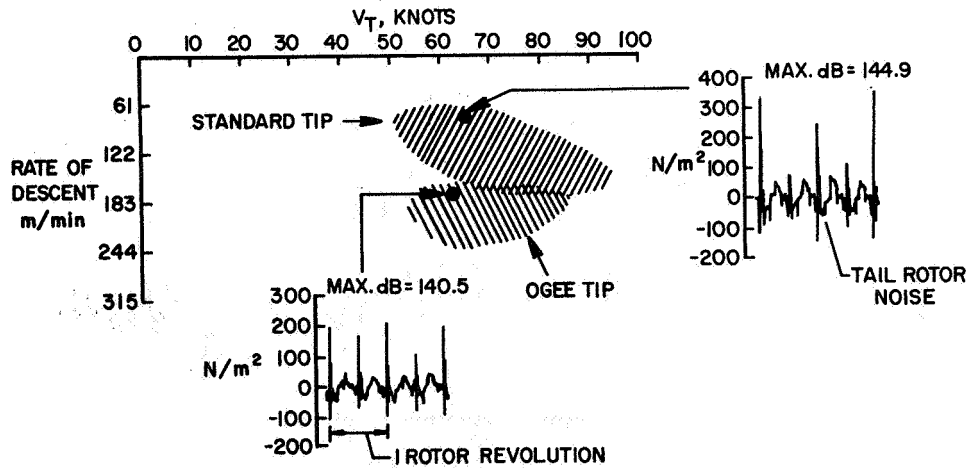
772
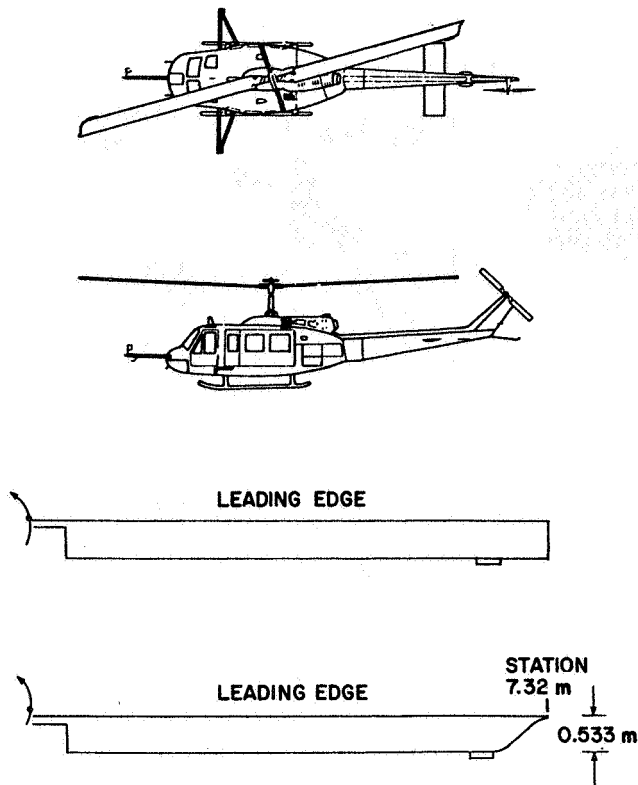
Figure 27.- UH-1H test helicopter.

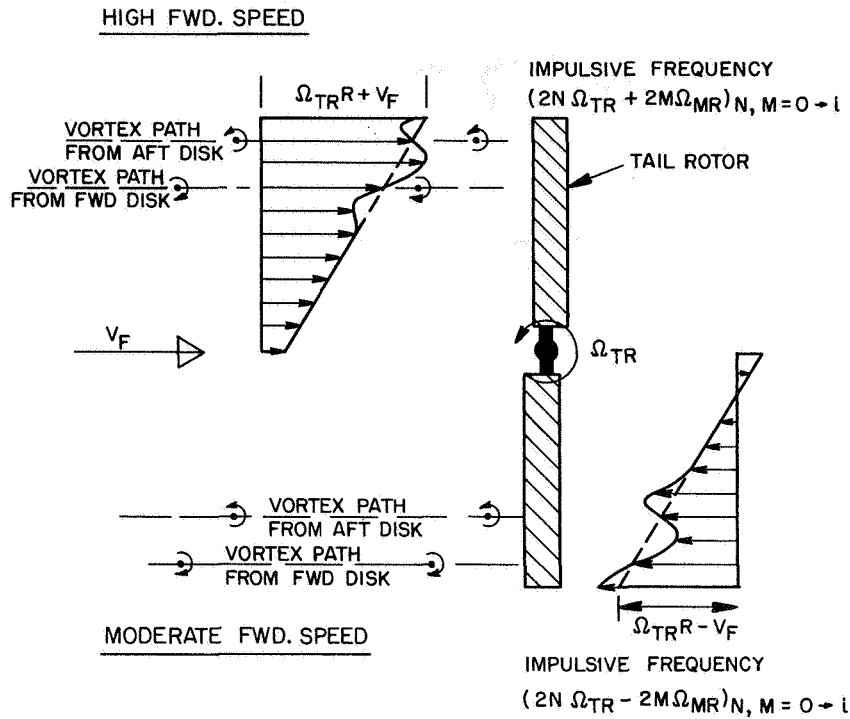Figure 28.- Peak levels of near-field impulsive noise
as measured by IFAMS.

HIGH FWD. SPEED

IMPULSIVE FREQUENCY
$(2N\Omega_{TR} + 2M\Omega_{MR})_{N, M = 0 \to i}$

VORTEX PATH
FROM AFT DISK
VORTEX PATH
FROM FWD DISK

$|\Omega_{TR}R + V_F|$

TAIL ROTOR

V_F

Ω_{TR}

VORTEX PATH
FROM AFT DISK
VORTEX PATH
FROM FWD DISK

MODERATE FWD. SPEED

$\Omega_{TR}R - V_F$

IMPULSIVE FREQUENCY
$(2N\Omega_{TR} - 2M\Omega_{MR})_{N, M = 0 \to i}$

Figure 29.- Schematic diagram of main rotor vortex interactions
with tail rotor.
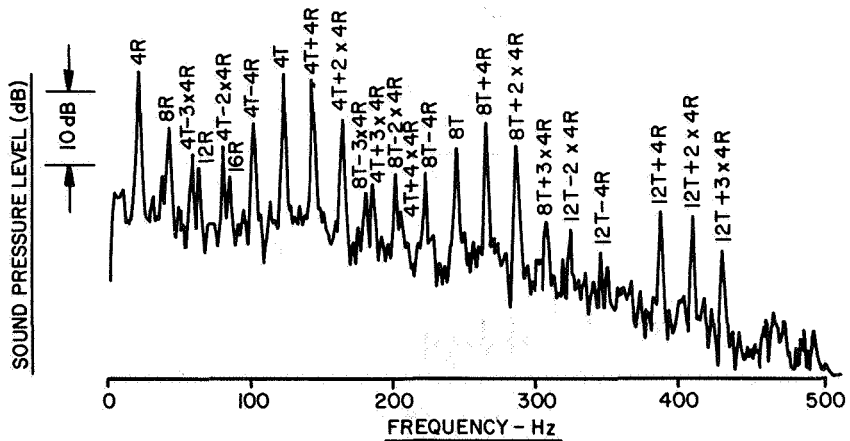
Figure 30.- Tail rotor noise as measured by Westland Helicopters
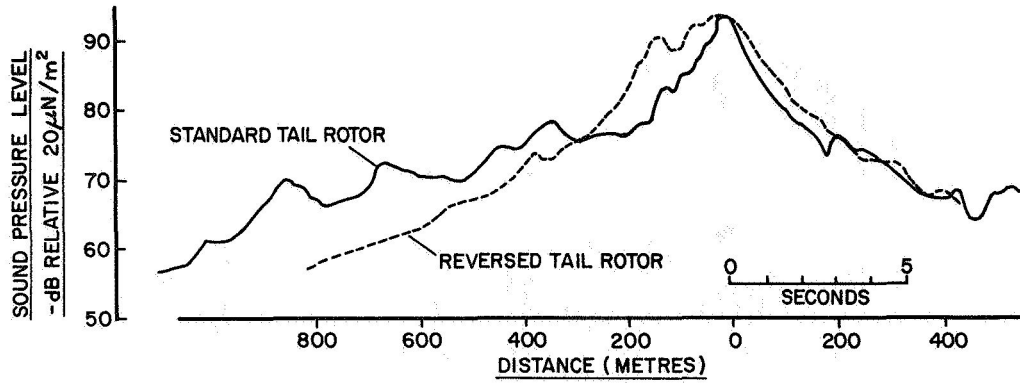Limited for the Lynx.

774

Figure 31.- Comparison of dB(A) time histories for standard and reversed tail rotors at a flyover condition of 50-m altitude and 130 knots.
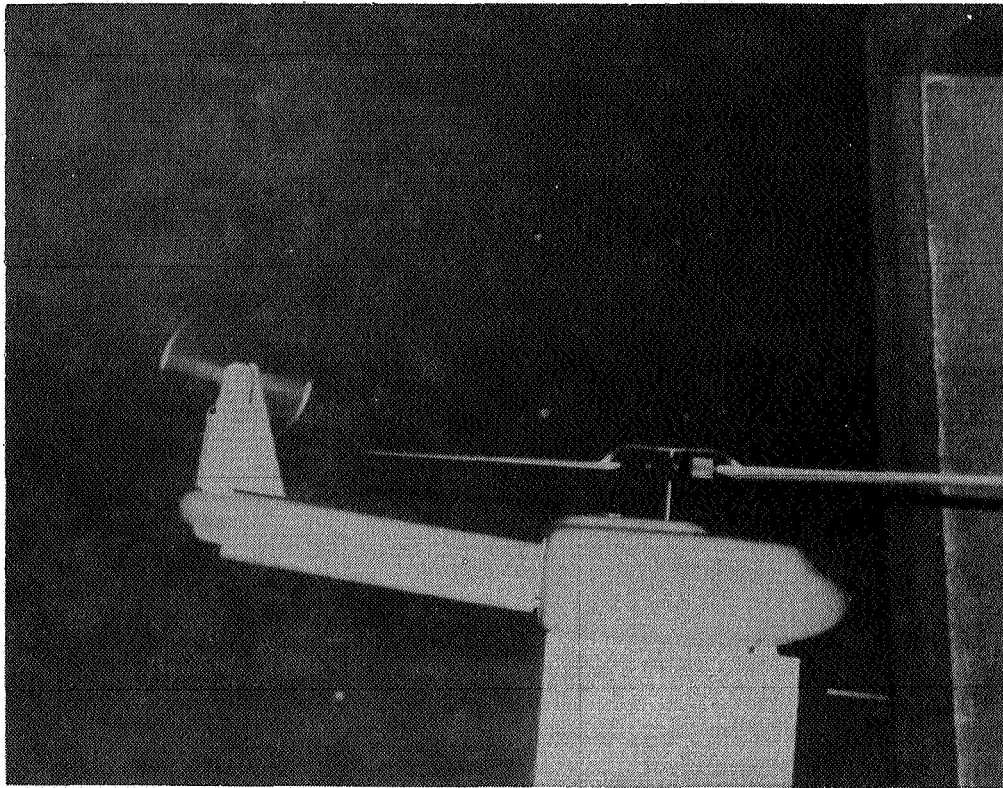
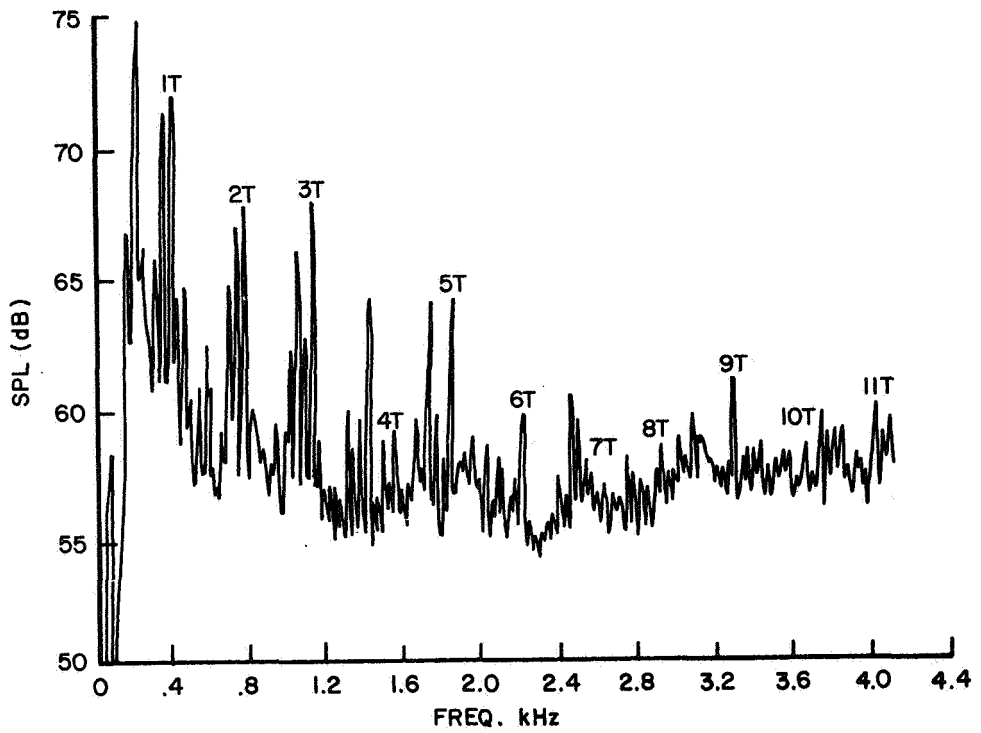

Figure 32.- Main rotor/tail rotor test model.
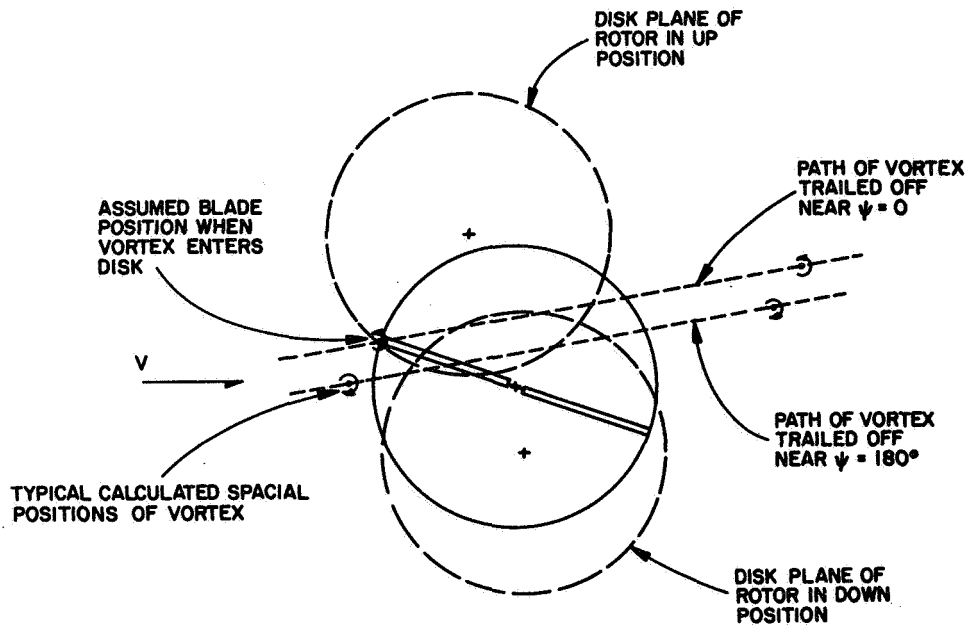
Figure 33.- Noise spectra at $\mu = 0.09$.

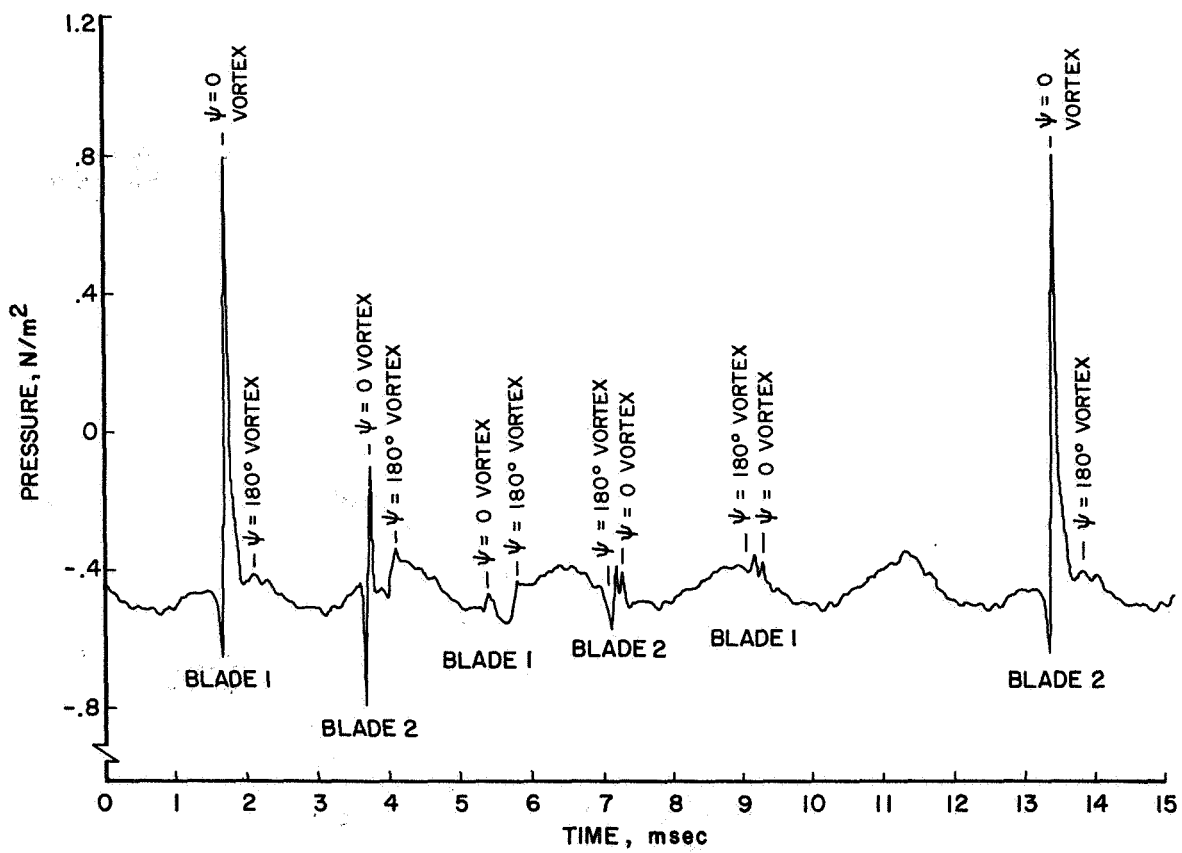Figure 34.- Main rotor wake/tail rotor interaction at $\mu = 0.20$.

PRESSURE, N/m^2

1.2

.8

.4

0

-.4

-.8

$\psi = 0$ VORTEX

$\psi = 180°$ VORTEX

$\psi = 0$ VORTEX

$\psi = 180°$ VORTEX

$\psi = 0$ VORTEX

$\psi = 180°$ VORTEX

$\psi = 180°$ VORTEX

$\psi = 0$ VORTEX

$\psi = 180°$ VORTEX

$\psi = 0$ VORTEX

$\psi = 0$ VORTEX

$\psi = 180°$ VORTEX

BLADE 1

BLADE 2

BLADE 1

BLADE 2

BLADE 1

BLADE 2

0   1   2   3   4   5   6   7   8   9   10   11   12   13   14   15

TIME, msec

Figure 35.- Calculated sound pressure versus time with periodic
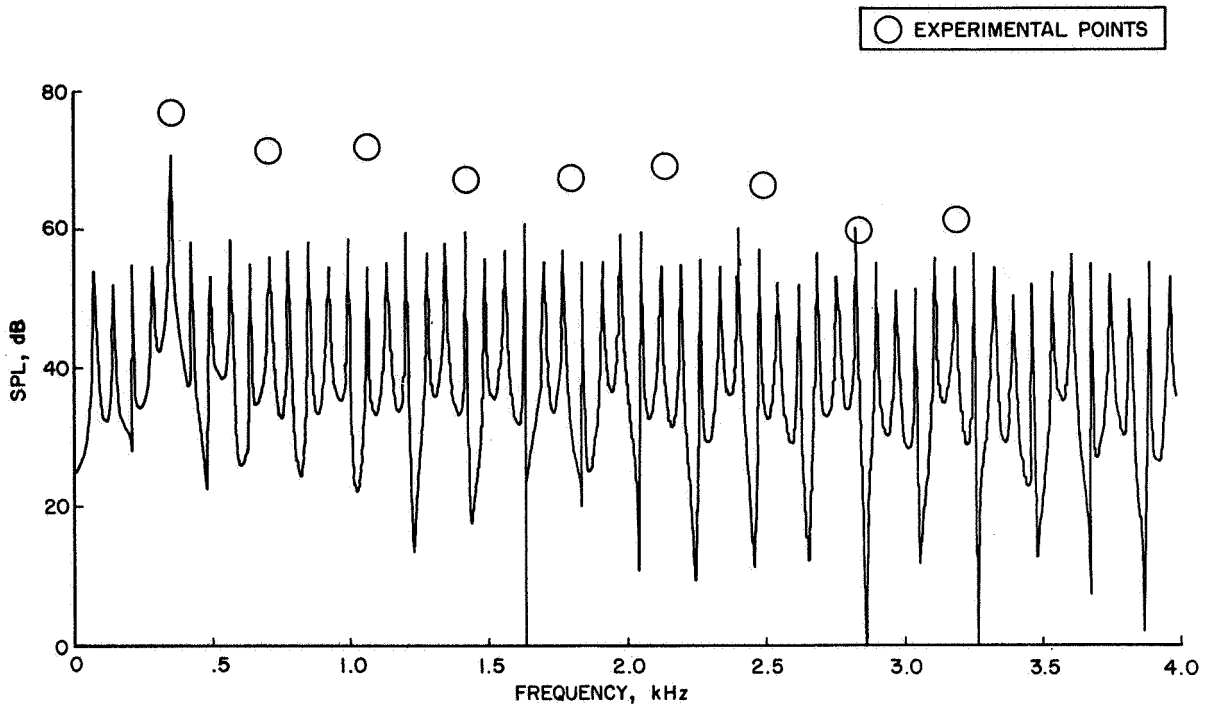main rotor wake interaction at μ = 0.20.

777

Figure 36.- Calculated noise spectrum with periodic main rotor
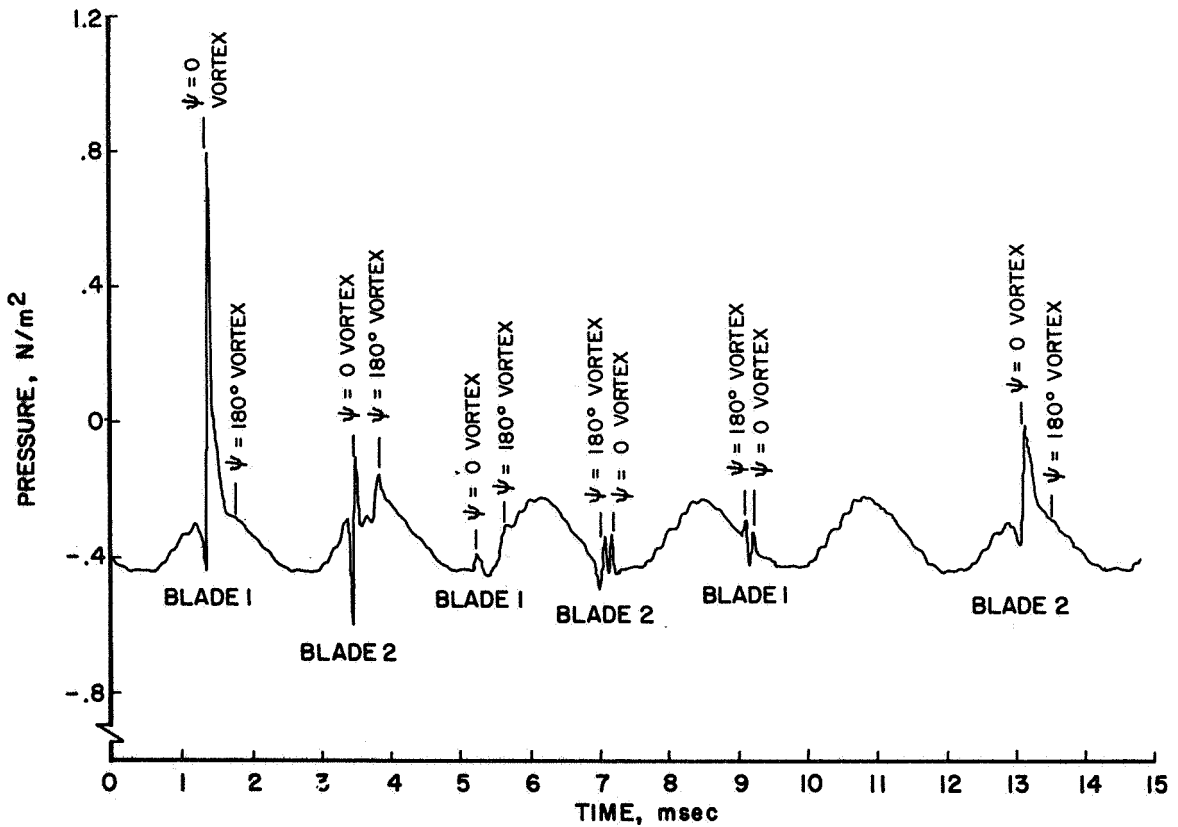wake interaction at μ = 0.02.

Figure 37.- Calculated sound pressure versus time with nonperiodic
main rotor wake interaction at μ = 0.20.
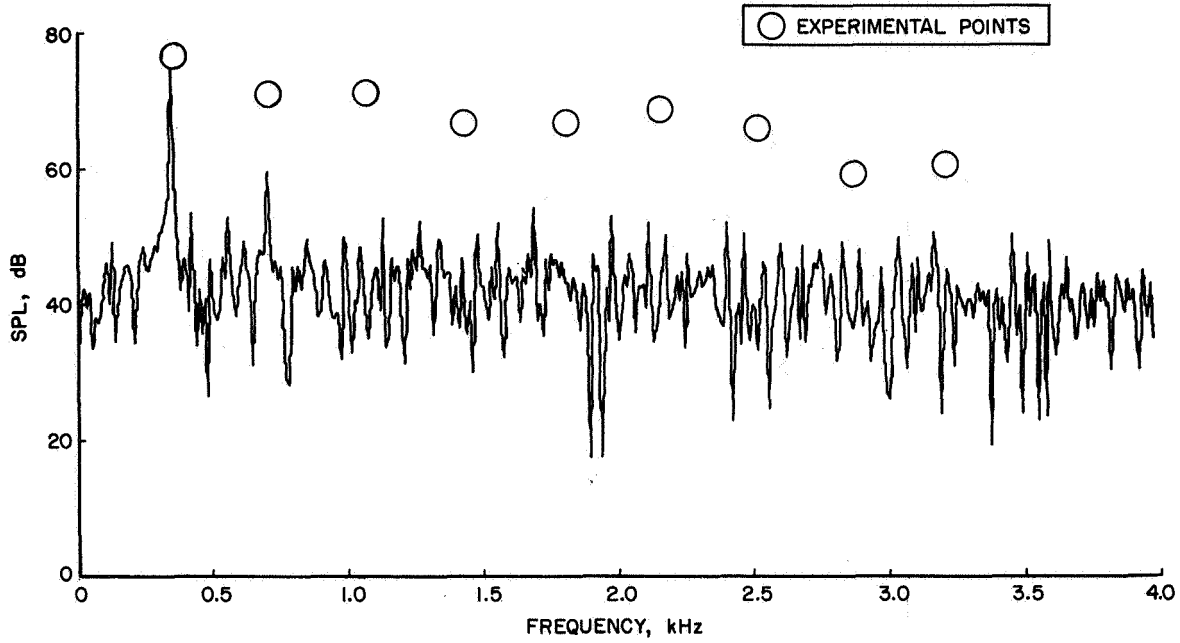
Figure 38.- Calculated noise spectrum with nonperiodic main rotor wake interaction at μ = 0.20.

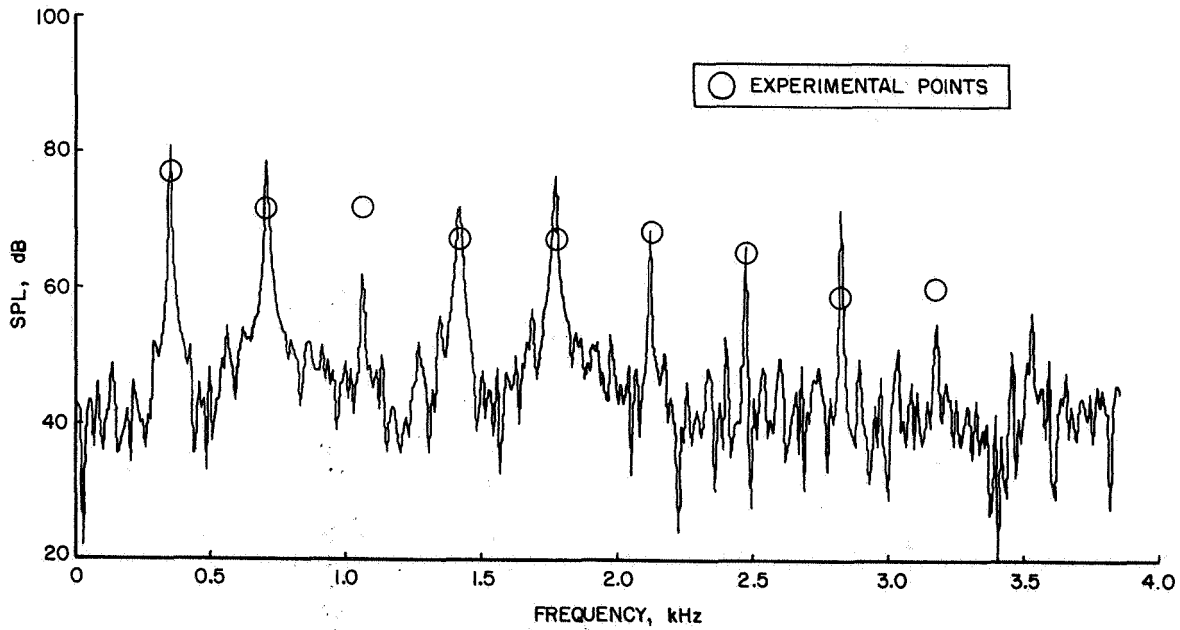Figure 39.- Calculated noise spectrum with nonperiodic main rotor wake interaction and nonuniform tail rotor wake at μ = 0.20.
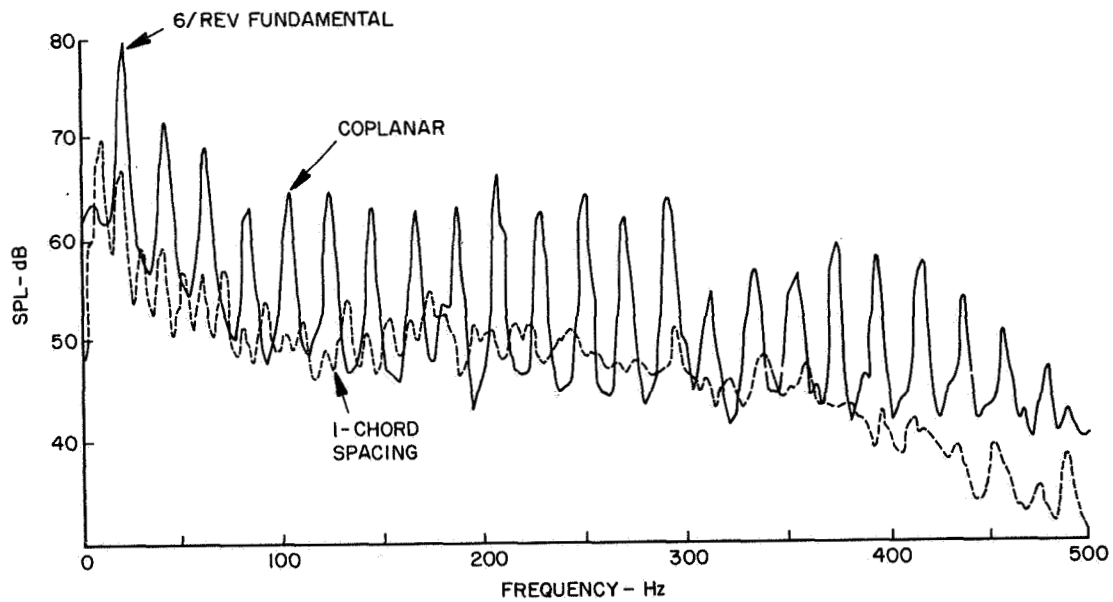
Figure 40.- Effect of rotor dissymmetry on noise spectrum
of a six-bladed rotor in hover.

TRENDS IN LANGLEY HELICOPTER NOISE RESEARCH

Harvey H. Hubbard, Domenic J. Maglieri,
and David G. Stephens
NASA Langley Research Center

INTRODUCTION

This paper presents a broad perspective of needs in helicopter exterior and interior noise control and contains descriptions of the Langley program and facilities in the related technology areas. Emphases are given to those items which support noise certification of civil helicopters and which result in reduced environmental noise impact to community residents as well as to helicopter passengers. The activities described herein are related to the Langley responsibilities for helicopter acoustics as defined by NASA roles and missions.

PROGRAM GOALS

The main goal of the Langley program is to develop a broad base of improved noise and noise-induced vibration control technology. Anticipated outputs from the program are indicated at the bottom of figure 1. They include the ability to design helicopters to comply with noise regulations, as well as the increased passenger and community acceptance.

Parallel thrusts are underway as indicated in figure 2 in the design and operations and the human factors related areas. The so-called physical acoustics portions of the program include the development of various categories of helicopter noise reduction information and also the development and validation of prediction methods. The human factors activities, on the other hand, are aimed at a fuller understanding of the effects of helicopter noise on people. The identification of valid noise quantification units, and the development of acceptance criteria, are included as part of a general understanding of the response of people to combined noise and vibration environments. Also implied is an understanding of the significance of operational procedures as a means for controlling community noise responses and thus minimizing the resulting environmental impacts.

ELEMENTS OF LANGLEY PROGRAM

The main elements of the Langley helicopter acoustics program, in both the physical acoustics and psychoacoustics areas, are listed as follows:

Source noise control
    Farassat theory and refinements
    Parametric sensitivity studies (experimental and theoretical)
    Evaluation of active and passive rotor tips
    Main rotor/tail rotor interactions

Operational factors
  Noise footprint definition

Prediction
  Noise prediction module development
  Flight test validation
  Establishment of data bank

Community acceptance
  Laboratory subjective tests
  Laboratory/field tests (Wallops Flight Center)
    Flyover human jury tests
    Indoor/outdoor effects tests
  Community response tests

Passenger acceptance
  Laboratory simulation
  Field flight tests

A number of specific projects are identified in source noise control, prediction, operational factors, community noise, and interior noise. Although the listing is not necessarily complete, those included are meant to suggest the nature and scope of the current research program. Also included in this material are indications of the research tools and methods to be brought to bear on particular types of problems.

Source Noise Control

The Farassat theory for rotor noise is a potentially powerful tool for basic rotor noise sensitivity studies over a wide range of rotor tip speeds and loading conditions (see ref. 1). The immediate problem is to establish credibility in this and any other similar theoretical methods that may become available. The plan is to make a few critical checks for current helicopters. This involves the ingredients identified in figure 3. The inputs to the computer program include details of the rotor geometry and its flight conditions along with details of its spanwise and chordwise blade loading time history. The above information is needed for cases for which flyover noise information is also available. The output of the computer program is a time history instantaneous pressure p which can in turn be resolved into frequency spectra and noise level time histories. Measured and calculated noise signatures will be compared for one or more helicopter configurations, for which appropriate input data are available. Anticipated results include the identification of operating ranges for which the theory is acceptable along with some indications of the areas in which refinements may be required.

Once the theoretical methods have been validated by wind tunnel and flight test results, the plan is to exercise them in parametric theoretical studies in which the effects of systematic changes in the input variables are evaluated in terms of the rotor noise output. These data will be directly useful in establishing the sensitivity of the rotor noise to any of several possible changes in geometry and operating conditions.

782

One of the demonstrated approaches to control of rotor noise is by means of the alteration of the blade tip vortex structure and the manner in which it subsequently interacts with the aerodynamic flow environments of the following blades. The blade tip flow fields have in the past been helpfully altered by means of blade tip geometry changes and by air mass injection at the tips (see refs. 2 and 3). In order to try to answer some questions about the basic source mechanisms and the relative changes in aeroacoustic performance due to such tip modifications, further experiments are planned in both the University of Maryland (under contract) and the Langley V/STOL wind tunnels (see fig. 4). In the University of Maryland studies, the aeroacoustic performance of both active and passive tips will be compared on blade models of the same diameter and over the same range of operating conditions. The V/STOL tunnel tests will be accomplished with the general research rotor system model (see ref. 4). A standard blade will be run over a range of forward flight and descent conditions to map out the conditions under which banging is encountered. Then subsequent tests will evaluate the effectiveness of the various tip shapes in the figure to alleviate blade banging.

Another well-recognized noise producing phenomenon is the interaction of the tail rotor with the downwash flow field from the main rotor (see ref. 5). As indicated in the sketch of figure 5, the tail rotor may be totally or partially immersed in the main rotor flow field and in some cases may encounter periodic disturbances associated with the tip vortex structure of the main rotor. Further parametric studies in a quiet wind tunnel are planned with a variable geometry main rotor/tail rotor model to evaluate systematically the effects of such variables as main rotor/tail rotor relative position, direction and speed of rotation, number of blades and blade planform (including sweep) on the tail rotor noise. Attempts will also be made to characterize the inflow to the tail rotor for a range of operational conditions as the basis for identification of optimum tail rotor aeroacoustic configurations.

Operational Factors

Recent measurements of helicopter in-flight noise signatures have indicated that the ground exposures are closely related to the manner in which the helicopter is operated (see ref. 6). Figure 6 illustrates the level flight ground noise patterns for two different helicopters one of which operates in a banging mode. The two associated noise contours differ in shape. The nonbanging rotor tends to have a radiation pattern such that the most intense noise is directed downward and the constant noise level contour is essentially symmetrical about the ground track. The banging rotor, on the other hand, apparently has a radiation pattern such that the most intense noise radiates in or near the plane of the rotor disk and is skewed left with respect to the flight direction. For operation in built-up areas a good appreciation of the sizes and shapes of these ground noise contours is essential for minimizing the community noise impacts. Further measurements of the type illustrated in figure 6 are planned for other operating conditions using the ROMAAR facility at NASA Wallops Flight Center.

Noise Prediction

One of the greatest needs of the helicopter designer in order to meet specified noise requirements is the availability of good engineering methods for flyover noise prediction. These are largely empirical at the present time and tend to be configuration sensitive. Consequently, there is an urgent need for analytically based methods valid for a range of configurations and operating conditions.

A proposed approach to an analytical prediction method is illustrated in the schematic diagram of figure 7. The noise critical inputs include detailed information on the configuration, its operating conditions and the rotor load distribution. The prediction program then calculates noise from the rotor system and the other noise generating components of the helicopter and sums them up. The overall noise is then propagated to the ground level observer location through a stratified atmosphere. A series of such calculations will produce a flyover noise time history in arbitrary evaluation units (see ref. 7).

Once a validated procedure is available, two quite different applications are planned. One is a series of sensitivity studies involving theoretical calculations in which the inputs are varied parametrically to evaluate their effects on the noise radiation field. The results of such calculations will form a data bank for evaluating future designs. Another planned application of the prediction methods is illustrated in figure 8.

Assuming that the computerized prediction method properly accounts for the configuration and operating conditions of the particular helicopter in question, it can then be coupled to the input of a noise synthesizer (see ref. 8). The synthesizer translates the computer program into audio signals which represent the noise from a particular helicopter operation. These audio signals can then be used to expose a jury of test subjects to helicopter noises for subjective evaluation. This is a tool for identifying those features of the noise signature which are most annoying and then relating them back to particular features of the helicopter design and/or operations. This offers the possibility of optimizing the acoustic signature of a helicopter in its early design stage.

Community Acceptance

Community response to the unique noise signatures and operating characteristics of helicopters is important to their development and utilization. Closely related to this issue is the development of procedures in support of certification of helicopters with respect to noise, as previously discussed. The Langley approach to research in the area of human response involves controlled laboratory studies, controlled flyover tests, and commmunity repsonse surveys.

Some of the laboratory simulation facilities available for human response studies are shown in the photographs of figure 9(a). They consist of an Exterior Effects Room (EER) and an Interior Effects Room (IER). The EER is an auditoriumlike room having a multichannel audio system capable of reproducing noise signatures which properly represent the direction and movement of the

source. The IER is configured as a living room in a house and is used for obtaining the subjective response to noise signatures as they would be heard indoors. In addition, vibration exciters are available to simulate noise-induced vibrations associated with helicopter overflights.

Examples of helicopter-related experiments which have recently been performed in these simulation facilities are illustrated in figure 9(b). The EER has been used to examine the effects of several characteristics of helicopter blade-slap noise as described in reference 9. Blade-slap noise was simulated by superimposing impulsive noises on broadband background noise. Variables included: the number of sine waves in a single impulse; the frequency of the sine waves; the impulse repetition frequency; the sound pressure level (SPL) of the continuous noise; and the idealized crest factor of the impulses. Analysis of the subjective data indicated that each of the five parameters had a statistically significant effect upon the annoyance judgments. Detailed results are presented in references 9 and 10.

A sketch of the IER test set up to evaluate both flyover noise and noise-induced vibration is illustrated at the bottom of the figure along with an example of expected results. Subjects are simultaneously exposed to noise and various levels of building vibrations. Of particular concern is whether the associated vibrations are detectable and, if so, are they an important consideration in community response to helicopter operations (see ref. 11). The laboratory study is being guided by an analysis of the vibration levels recorded during recent helicopter noise tests conducted at the Wallops facility.

This latter study was conducted at Wallops to provide information on the relative importance of the impulsive characteristics of helicopter noise to human response. The design of the experiment is shown schematically in figure 9(c) and scenes of the test are shown in the photograph of figure 9(d). Subjects were located in each of the three test areas situated in a straight line parallel to the flight paths. The primary subject groups were located out of doors and made judgments of the overflights. A second and third group made judgments, respectively, where both interior noise and house vibrations were recorded. Four level flight paths were used as shown in the figure for the helicopters and a fixed-wing reference aircraft.

The data from this experiment are being analyzed to determine whether an impulsiveness correction to the proposed certification noise measure, EPNdB, is necessary to adequately predict the annoyance of helicopter noise. The necessity for and magnitude of such a correction will be indicated if the results of the experiment are separable in terms of some measures of impulsiveness as indicated in the right-hand sketch of the figure.

A related program has recently been initiated under contract to study the reactions of people in communities highly impacted by helicopter noise. The program is designed to determine whether a significant difference exits in the percent of a population highly annoyed by a noise environment uniformly composed of many sources and one with a noise environment containing a high proportion of helicopter noise. If a significant difference in the percent highly annoyed is detected, a helicopter "penalty factor" will be developed which can be used to adjust aircraft noise metrics upward to account for the increased

attitudinal response to helicopter noise. The program will consist of both a telephone survey of social attitudes and a field noise measurement survey in two communities to be selected - one subjected to high helicopter noise impact, and one similar in all respects except for an absence of helicopter noise. A computerized multivariate regression analysis will combine the social and physical data to distinguish the difference in the proportion highly annoyed that is attributable to helicopter noise, and from this, the "penalty factor" will be determined, based on established relationships between community noise exposure and expected degrees of annoyance.

Passenger Acceptance

The interior environment of current and future helicopters is important to the ride quality and passenger acceptance of these vehicles. To fully evaluate the influence of the interior noise (and vibration) on passenger acceptance, the vehicle noise environment as well as the response of passengers to this type of stimulus must be understood. Such an understanding of the environment and its effects is essential to the development of cost effective interior noise control technology.

Passenger or subjective response to noise and vibration is being studied both in the laboratory and in the field. In general, the laboratory studies examine the details of the environmental stimuli which cause adverse response whereas the field studies concentrate on understanding the integrated effect of noise and other environmental factors on passenger acceptability.

The ongoing ride quality program being conducted at Langley Research Center (ref. 12) utilizes the three-degree-of-freedom motion simulator shown in the photograph of figure 10(a). The simulator is configured to represent the interior of an aircraft and can be fitted with four first-class seats (as illustrated) or with six tourist-class seats. The simulator is driven by hydraulic actuators which provide motion in the vertical, lateral, and roll direction. Single- or multiple-axis inputs can be obtained by oscillators or actual field-recorded tapes over a frequency of 0 to 30 Hz and an amplitude of up to $0.5\ g_{peak}$.

The ongoing studies are directed toward the development of a ride quality model which includes the effects of both multifrequency and multiaxis vibratory inputs, as well as noise. The approach being followed consists of the development of "equal vibration discomfort curves" as a function of level and frequency for each axis of vibration, and determination of within-axis and between-axis masking, and the interaction of vibration and noises.

Example results of this program are summarized in the chart of the figure where successive constant discomfort curves (DISC curves) ranging from 1 to 7 are presented in terms of the A-weighted sound pressure level and the rms vibration acceleration level in g units. A DISC of 1 is approximately the discomfort threshold whereas a DISC of 7 would be relatively uncomfortable. Results suggest that human response is highly dependent upon both noise and vibration, and furthermore, the degree of dependence is related to the level of the stimuli. For example, at high noise levels, the vibration influence

786

.s relatively small in comparison to the influence at low levels of interior
noise. Current studies are being directed toward quantifying the response to
these combined stimuli over a wide range of conditions and incorporating the
results into a user oriented ride quality model.

On a comparative basis, the range of interior noise levels of helicopters
is generally higher than that for conventional aircraft and surface vehicles, as
indicated in the upper chart in figure 10(b). In order to evaluate the environ-
ment and passenger acceptance of large helicopter airliners, a modified version
of the CH-53 military transport helicopter has been flight tested. A photograph
of the helicopter, the modified cabin, and the results of a study to evaluate
the effectiveness of various interior treatments are shown in the figure.

Interior noise levels in the untreated (military) helicopter were approxi-
mately 110 dB(A). The acoustic treatment reduced these levels to 90dB(A) inside
the passenger cabin, but results of questionnaires indicated that this was not
satisfactory. The primary source of interior noise in the treated cabin was
found to be gear clash in the main gearbox. A reduction of this gear clash
noise by 12 dB would result in interior noise levels which are comparable to
current narrow-body jet transports during cruise (ref. 13). Research into the
fundamentals of gear noise control at the source and methods of mechanical
isolation of the gearbox are obviously needed to control gear noise.

CONCLUDING REMARKS

An attempt has been made to characterize the Langley Research Center pro-
gram in helicopter acoustics and to identify future trends wherever possible.
The main thrusts in physical acoustics are noted to be in rotor noise generation
and control and in the development of engineering prediction methods. Emphasis
is on the development of theoretical methods in conjunction with parametric
model tests in quiet wind tunnels.

Community and passenger acceptance studies involve the application of some
unique laboratory facilities as well as field investigations to define and
quantify characteristics of helicopter stimuli affecting human response. The
results provide criteria and design guidelines for reduction of community noise
as well as the noise and vibration transmitted into the passenger cabin.

REFERENCES

1. Farassat, F.; Nystrom, Paul A.; and Brown, Thomas J.: Bounds on Thickness and Loading Noise of Rotating Blades and the Favorable Effect of Blade Sweep on Noise Reduction. Helicopter Acoustics, NASA CP-2052, Pt. I, 1978. (Paper no. 18 of this compilation.)

2. Mantay, Wayne R.; Campbell, Richard L.; and Shidler, Phillip A.: Full-Scale Testing of an Ogee Tip Rotor. Helicopter Acoustics, NASA CP-2052, Pt. I, 1978. (Paper no. 14 of this compilation.)

3. White, Richard P., Jr.: Wind Tunnel Tests of a Two-Bladed Model Rotor To Evaluate the TAMI System in Descending Forward Flight. NASA CR-145195, 1977.

4. Hoad, Danny R.; and Greene, George C.: Helicopter Noise Research at the Langley V/STOL Tunnel. Helicopter Acoustics, NASA CP-2052, Pt. I, 1978. (Paper no. 10 of this compilation.)

5. Pegg, Robert J.; and Shidler, Phillip A.: Exploratory Wind-Tunnel Investigation of the Effect of the Main Rotor Wake on Tail Rotor Noise. Helicopter Acoustics, NASA CP-2052, Pt. I, 1978. (Paper no. 11 of this compilation.)

6. Hilton, David A.; Henderson, Herbert R.; Maglieri, Domenic J.; and Bigler, William B., II: The Effect of Operations on the Ground Noise Footprints Associated With a Large Multibladed Nonbanging Helicopter. Helicopter Acoustics, NASA CP-2052, Pt. II, 1978. (Paper no. 27 of compilation.)

7. Zorumski, William E.: Aircraft Flyover Noise Prediction. NOISE-CON 77 Proceedings, George C. Maling, Jr., ed., Noise Control Found., c.1977, pp. 205-222.

8. Mabry, J. E.; and Sullivan, B. M.: Responses to Actual and Synthesized Recordings of Conventional Takeoff and Landing Jet Aircraft Noise. NASA CR-145318, 1978.

9. Lawton, Ben William: The Noisiness of Low-Frequency One-Third Octave Bands of Noise. NASA TN D-8037, 1975.

10. Powell, Clemans A.: Annoyance Due to Simulated Blade-Slap Noise. Helicopter Acoustics, NASA CP-2052, Pt. II, 1978. (Paper no. 23 of this compilation.)

11. Cawthorn, Jimmy M.; Dempsey, Thomas K.; and DeLoach, Richard: Human Response to Aircraft-Noise-Induced Vibration. Helicopter Acoustics, NASA CP-2052, Pt. II, 1978. (Paper no. 24 of this compilation.)

12. Leatherwood, Jack D.; and Dempsey, Thomas K.: A Model for Prediction of Ride Quality in a Multifactor Environment. NASA TM X-72842, 1976.

13. Howlett, James T.; Clevenson, Sherman A.; Rupf, John A.; and Snyder, William J.: Interior Noise Reduction in a Large Civil Helicopter. NASA TN D-8477, 1977.
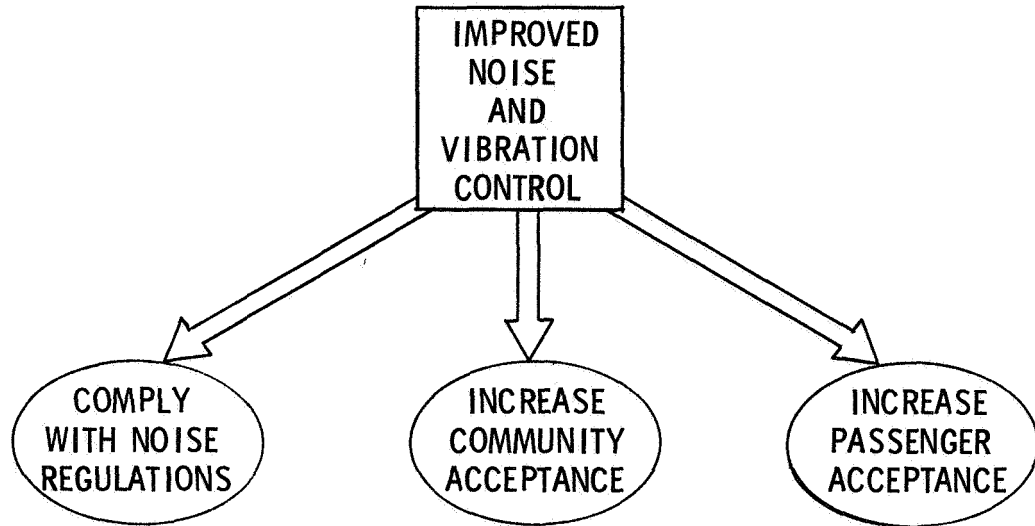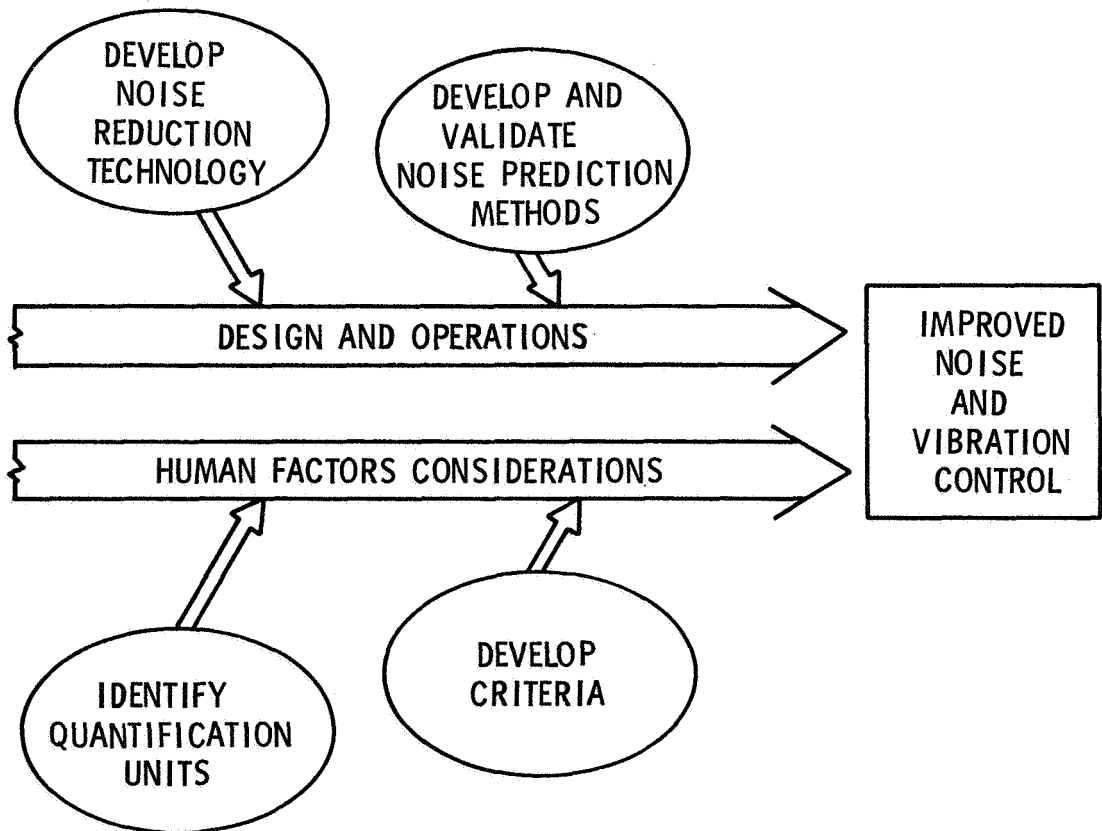
Figure 1.- Goal of Langley programs.
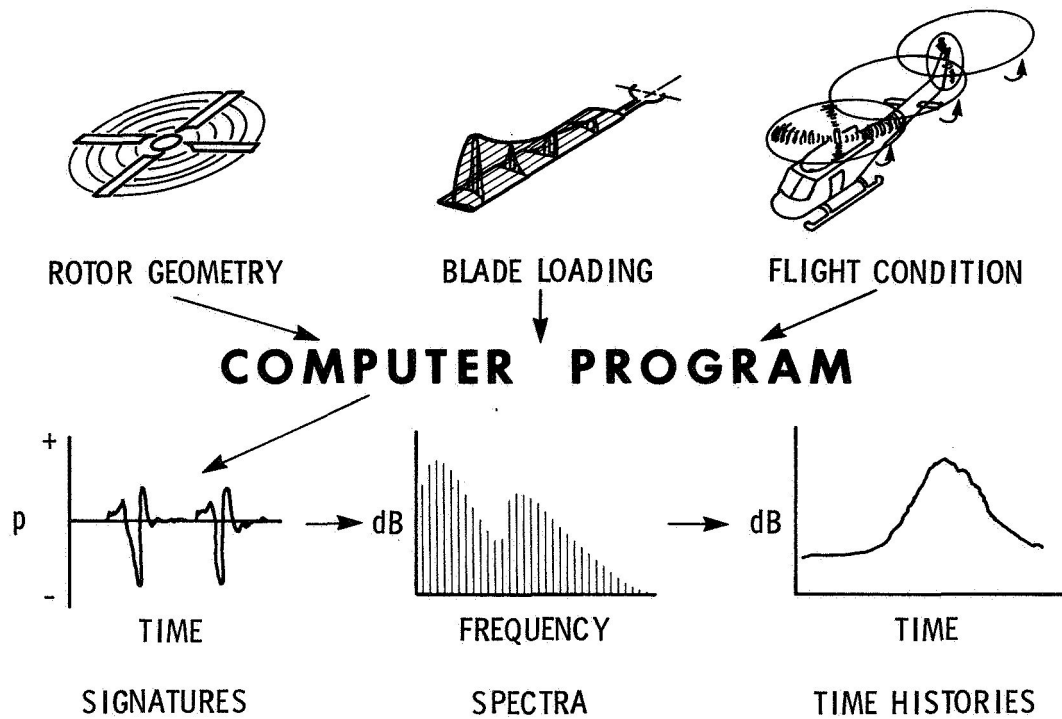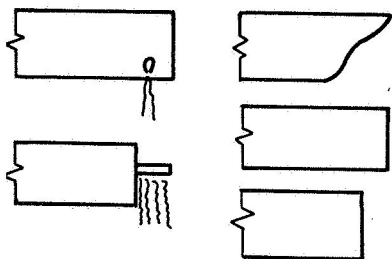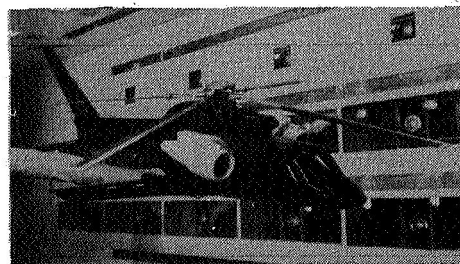

Figure 2.- Thrust of Langley program.

ROTOR GEOMETRY   BLADE LOADING   FLIGHT CONDITION

COMPUTER PROGRAM

p

+

-

TIME

dB

FREQUENCY

dB

TIME

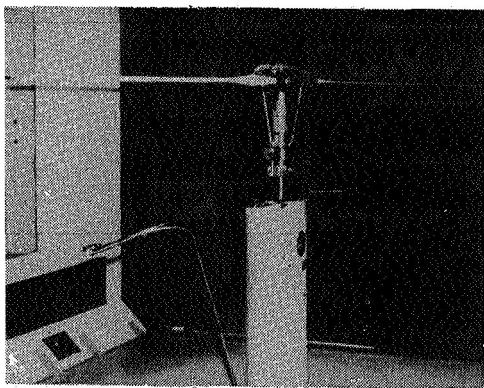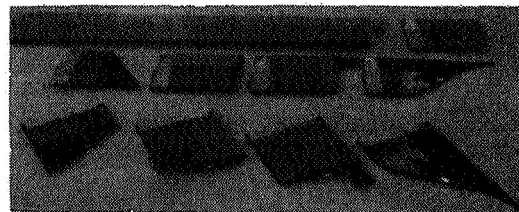SIGNATURES   SPECTRA   TIME HISTORIES

Figure 3.- Farassat rotor noise theory.

UNIV. MARYLAND WIND TUNNEL MODEL TESTS

FLIGHT TESTS

V/STOL TUNNEL TESTS

Figure 4.- Tip vortex modifications.

TAIL ROTOR VARIABLES

- ROTATIONAL SPEED
- DIRECTION OF ROTATION
- BLADE PLANFORM
- LOCATION RELATIVE TO MAIN ROTOR
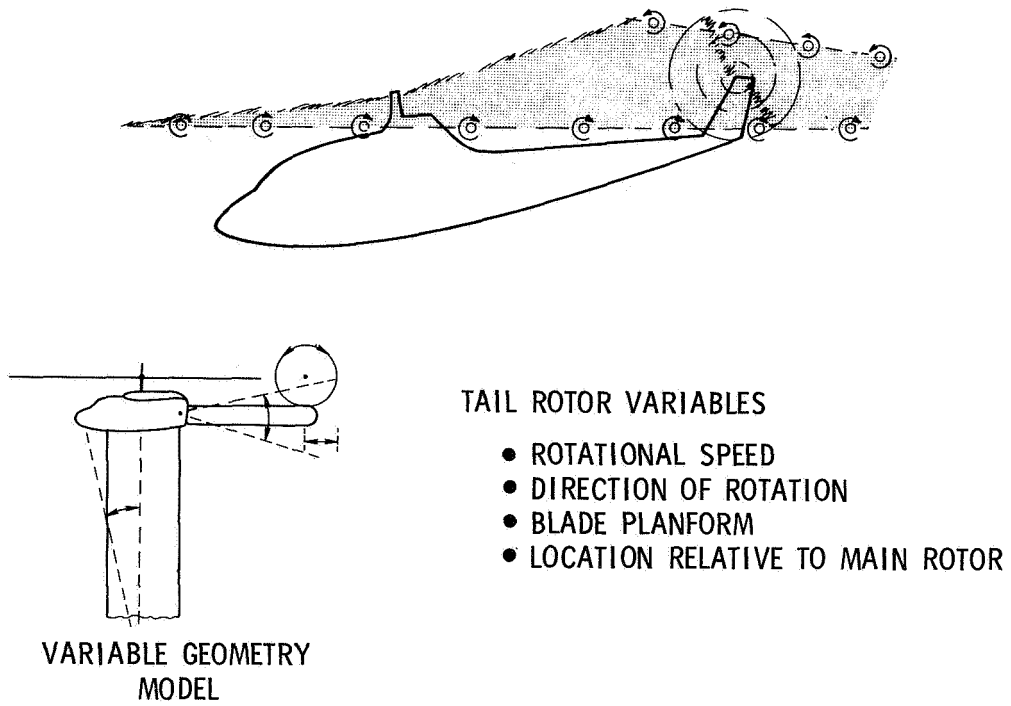
VARIABLE GEOMETRY
MODEL

Figure 5.- Anechoic wind tunnel tests of main
rotor/tail rotor interaction noise.
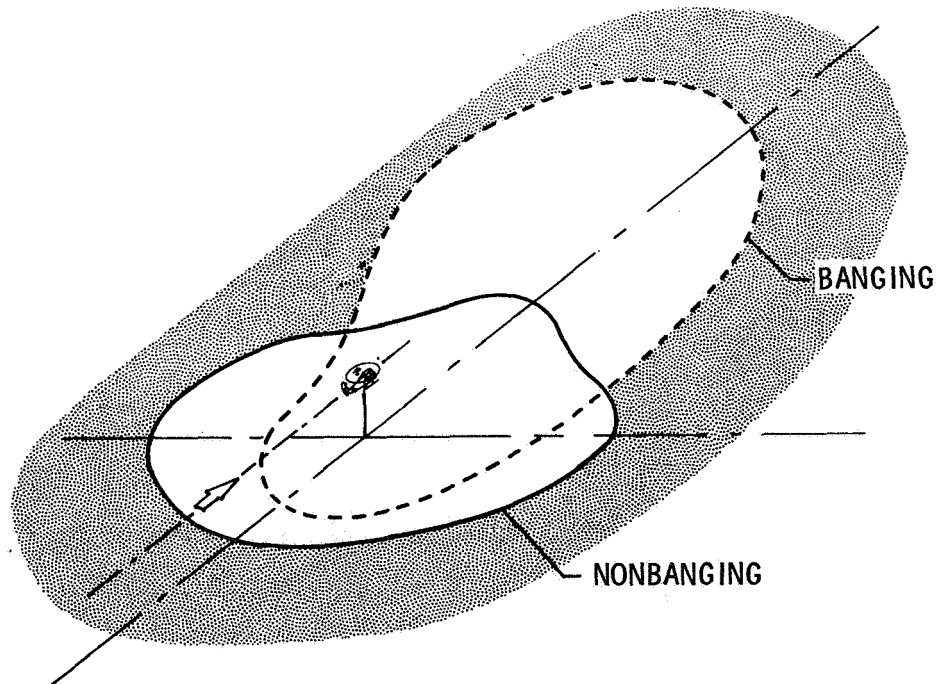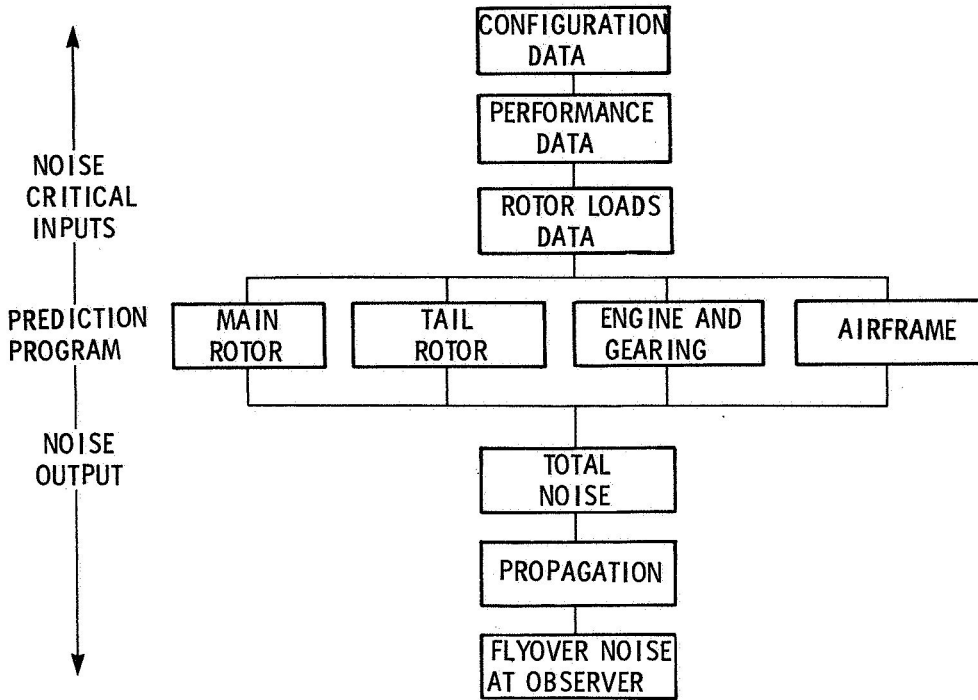

Figure 6.- Level flight dB(A) ground noise patterns.

Figure 7.- Helicopter noise prediction.

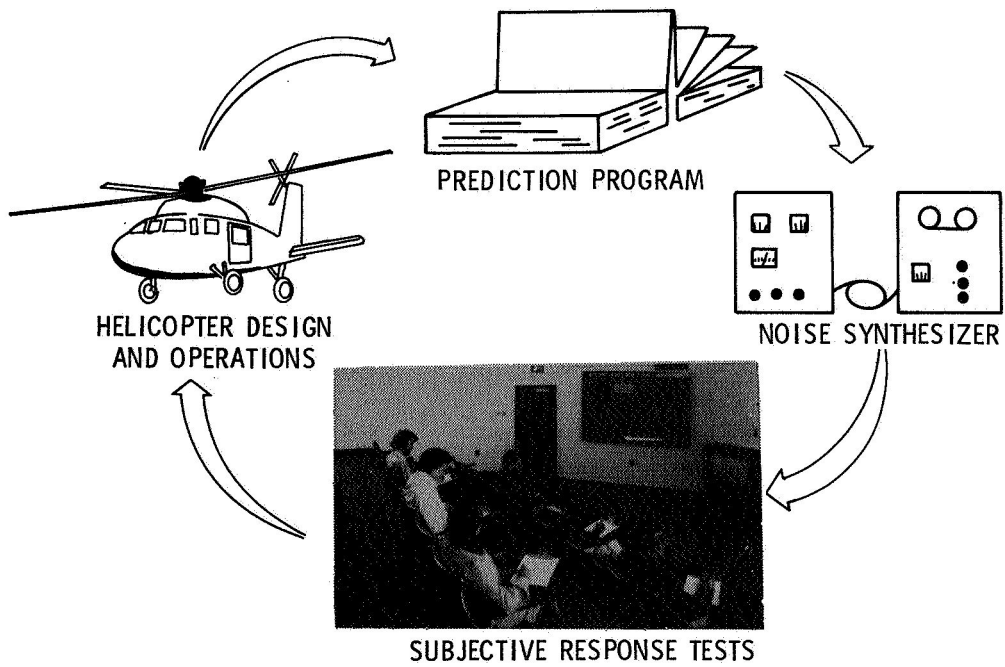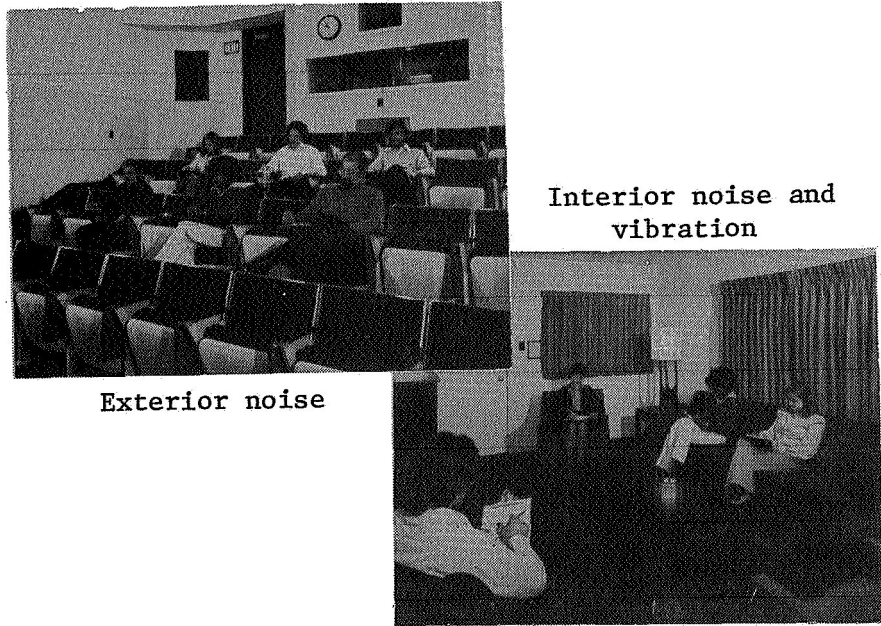Figure 8.- Helicopter noise synthesis.

Interior noise and vibration

Exterior noise

(a) Laboratory simulation facilities.

SPEAKERS

SHAKERS

DETECTION, %

FLOOR ACCELERATION, dB (RE 1 μg)
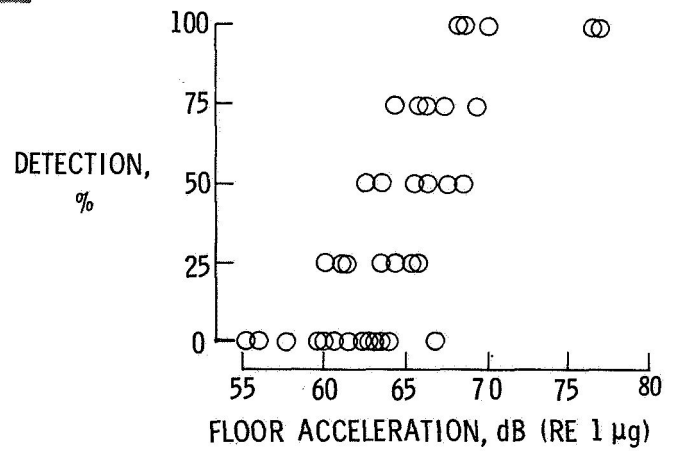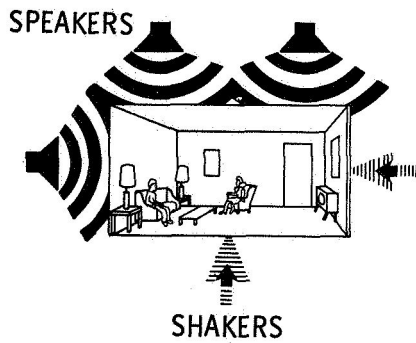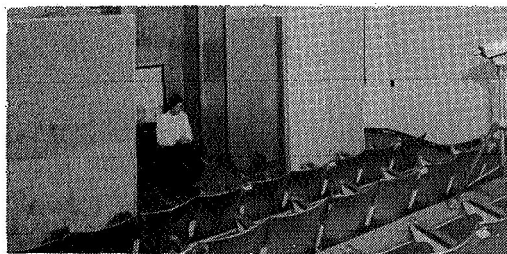
(b) Laboratory research results.

Figure 9.- Community acceptance.

FLIGHT PATHS   ANTICIPATED RESULTS

270 m

360 m

120 m   90 m

SUBJECT
LOCATIONS

LEVEL OF
IMPULSIVENESS
HIGH
MEDIUM
LOW

SUBJECTIVE
ANNOYANCE
RESPONSE

Δ

NOISE LEVEL, EPNdB
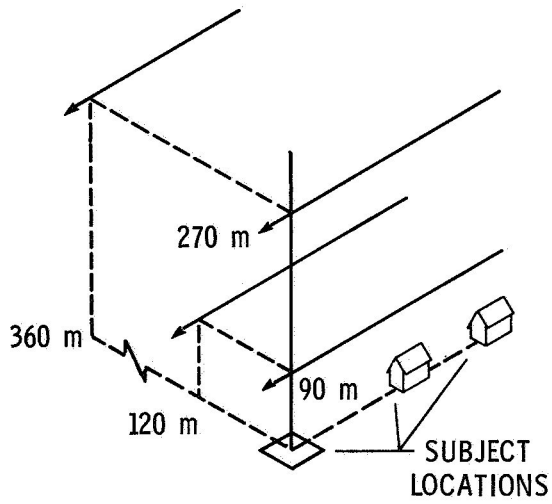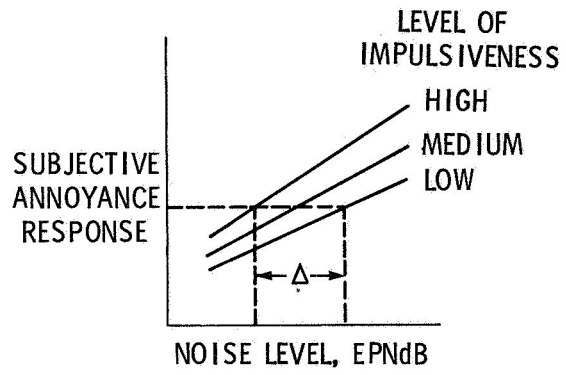
(c) Plan for field test of blade slap.
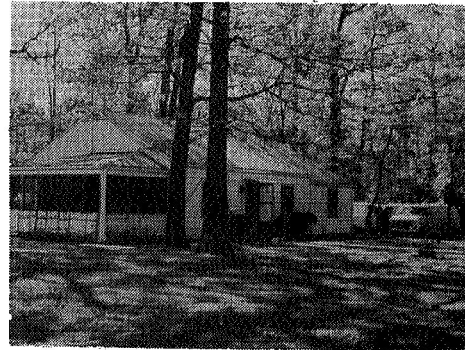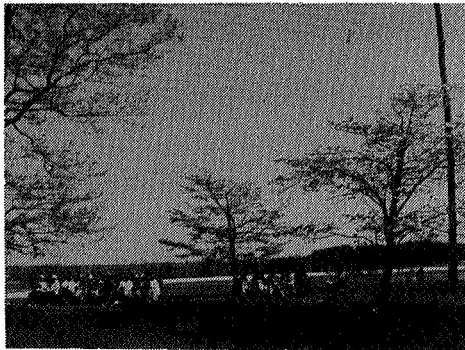
(d) Subject locations for field test of blade slap.

Figure 9.- Concluded.

PASSENGER RIDE
QUALITY APPARATUS

NOISE LEVEL, dB(A)

DISC 1

rms ACCELERATION, g UNITS

NOISE AND VIBRATION
CRITERIA

(a) Laboratory research.

dB(A)

HELICOPTERS

AIRCRAFT

SURFACE
VEHICLES

TREATED

UNTREATED

INTERIOR NOISE, dB(A)
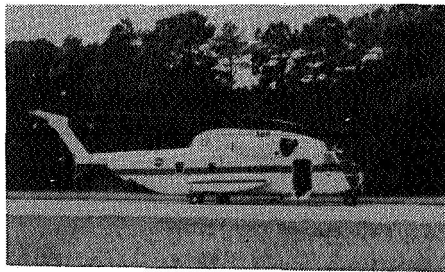
QUESTIONNAIRE

(b) Field research.

Figure 10.- Passenger acceptance.

AEROACOUSTIC RESEARCH — AN ARMY PERSPECTIVE

H. Andrew Morse and Fredric H. Schmitz
Aeromechanics Laboratory
U.S. Army Research and Technology Laboratories (AVRADCOM)
NASA Ames Research Center

SUMMARY

A short perspective of the Army aeroacoustic research program is pre-
sented that emphasizes rotary-wing, aerodynamically generated noise. Exciting
new breakthroughs in experimental techniques and facilities are reviewed which
are helping build a detailed understanding of helicopter external noise. Army
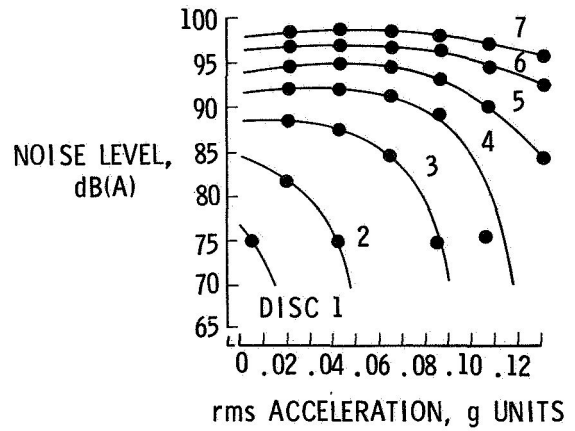and joint Army/NASA supported research programs in acoustics are leading to a
rapidly developing technology which promises to reduce the noise of future
helicopters without severe performance penalties.

INTRODUCTION

The Reforger 76 NATO exercises reinforced the Army's concept of aviation's
role in the combined arms team. The Army has considerably expanded its use of
the helicopter to include the traditional functions of land combat mobility
including intelligence, firepower, combat service support, command control, and
communications. The use of the helicopter by ground forces has added another
battlefield dimension by enhancing the ability to conduct land combat
functions.

The unique maneuvering capability which has made the helicopter so
valuable has also brought with it unique acoustic problems (fig. 1). High tip
speed rotors are one source of aeroacoustic near- and far-field noise which is
unique to rotary-wing vehicles, and this noise has a very distinctive character.
It is responsible for large detection distances, severe community annoyance,
and can significantly influence internal noise levels. High-speed and power
transmissions, shafts, and engines also contribute significantly to both
internal and external noise levels. Although the helicopter has become an
integral part of the Army airmobile concept, its usefulness and acceptance can
be enhanced if detectability, annoyance, and internal noise levels can be
reduced with minimal loss of its desirable performance capabilities.

In response to these problems, the Army has focused its acoustic research
program on those noise sources unique to rotary wing. Initially, the program
attempted to apply existing technology to alleviate the high noise levels.
After determining that the technology was inadequate, the emphasis of the
program shifted. Today, the Army program emphasizes a more fundamental
approach — to isolate the most offending sources, to analytically describe
their dependence, and then to control helicopter noise with a new, more

accurate technology in a cost-effective manner. This research is being per-
formed in-house, in joint participation with NASA and through contracts with
industry and universities.

AEROACOUSTIC RESEARCH

For purposes of this paper, it is convenient to separate the noise sources
into two broad categories: first, noise of aerodynamic origin from main or
tail rotors which will be referred to as rotary-wing aerodynamically generated
noise; and second, the helicopter noise that originates from the generation
and distribution of power or mechanical vibrations which we can call power-
and mechanically generated noise. The Army research programs involve all
noise sources, but the main emphasis of this paper is on the first category.

Some indication of the extent of Army-supported research is indicated in
table 1. Of particular significance are the joint Army/NASA programs which
make available special facilities and/or joint resources to provide a sound
rotary-wing acoustic technology base of mutual benefit to commercial and
military helicopter development. The Army rotary-wing acoustic technology
program is highly dependent on the special skills and capabilities provided by
the universities and industry, largely through the Army Research Office (ARO).

ROTARY-WING AERODYNAMICALLY GENERATED NOISE

Rotary-wing aerodynamically generated noise can be further broken down
into conventional categories of high-speed impulsive, blade vortex inter-
action, broadband, and inflow turbulence noise sources. There have been
several excellent technical summaries over the years which have described what
was known about each source of noise (refs. 1-6). By reading them in the
listed order, one can gain a feeling for the rapid progress being made in the
field of rotary-wing acoustics. Of these sources, one of the most objection-
able is the high-speed impulsive noise source. When rotor tip speeds are high,
whether due to high rotational tip speeds or combinations of rotational and
translational velocities, large pressure waves are propagated out from the
rotor disk plane.

Due to the complexity of the problem, it has been very difficult, if not
impossible, to isolate and identify the contribution of the separate sources
to the total helicopter-generated noise. Isolated tests of rotors in wind
tunnels or fly-by measurements are plagued with additional complications
associated with reverberation, the peculiar rotor noise directivity, and other
complicating factors. A technique was sought which would allow direct
measurement of a helicopter far-field noise radiation pattern without inducing
complications associated with reverberated pressure waves and other con-
ventional constraints. These objectives required noise measurements of a
helicopter when operating in its own environment.

798

An in-flight noise measurement technique was developed that allows the helicopter to operate under desired conditions in free space while the microphones and recording equipment are supported on a quiet fixed-wing aircraft that is capable of maintaining the microphone at the desired position fixed relative to the rotor (fig. 2). (Symbols used in the figures are defined in the appendix.)

The in-flight helicopter noise source calibration experiment was first conducted utilizing an OV-1C as the microphone support and recording station and a UH-1H helicopter as the test aircraft (ref. 7). The aircraft were flown in close formation with the UH-1H helicopter, maintaining position and distance behind the OV-1C aircraft. The free turbine engines allowed the OV-1C propeller speeds to be selected to minimize interference with the rotor fundamental and harmonic frequencies. From this first experimental in-flight helicopter noise measurement test, the first true picture of the high-speed impulsive noise and blade vortex interaction noise radiation patterns was recorded. Some unexpected results were obtained and previous techniques used for UH-1H noise abatement operations had to be abandoned as ineffective.

In addition, the details of the recorded time history of the pressure waves raised questions as to the validity of theoretical predictive techniques and provided a strong emphasis for better data with lower background noise levels. An idealized pressure time history or wave form (fig. 3) shows the large negative pressure wave associated with high-speed impulsive noise. This peak negative pressure increases as the tip Mach number increases. Also shown are several positive pressure pulses which occur just prior to the negative spike: the positive spikes are caused by blade vortex interactions. Recorded in-plane pressure signals of the UH-1H (fig. 4) show how the peak negative pressure increases with forward speed: the negative peak pressure increase with forward velocity from 80 to 100 and to 115 knots is similar in level flight, 122 m/min (400 ft/min) and 244 m/min (800 ft/min) rates of descent.

Note, however, that the positive pressure spikes attributed to blade vortex interaction increase from the top left to bottom right. Intuitively, one would expect blade vortex interaction noise to be maximum at a consistent forward velocity to descent rate ratio which results in the tip vortex remaining in the rotor disk plane where intersections occur with following blades. As would be expected, this noise level also increases as the blade velocity or Mach number increases. The success of the in-flight test technique in producing interference-free time-pressure histories and directivity patterns of different rotor noise sources proved the concept and increased the desire to find an improved microphone platform.

Fortunately, an almost ideal quiet flying platform had been developed in very limited quantities by the U.S. Army for surveillance and target acquisition. The aircraft, designated the YO-3A (fig. 5), was an extensively modified Schweitzer 2-32 sailplane that saw only limited service during the last Asian conflict. They were surplused to other government agencies, and the F.B.I. acquired two of the few remaining "YO-3A quiet aircraft." The Aeromechanics Laboratory borrowed one of the F.B.I. aircraft and instrumented it for acoustic testing (ref. 8) in a similar manner to the OV-1C (fig. 6). In addition to a tail-mounted microphone, wing-tip microphones were used to

gather data for noise source identification. The background noise of the YO-3A is about 15 dB below that of the OV-1C, thus assuring excellent signal-to-noise levels.

A sample of the quality of data obtainable by in-flight measurements with the YO-3A is shown in figure 7 for the UH-1H helicopter. At 80 knots forward speed and 122 m/min (400 ft/min) descent rate, even though the tail rotor is about 13 tail rotor diameters from the microphone, the impulsive pressure wave is discernible. Main rotor positive pressure spikes from blade vortex inter-section and the high-speed impulsive negative pressure pulse can also be clearly seen. Note the symmetry of the high-speed pressure pulse at 80 knots in comparison to the very rapid pressure recovery at 115 knots. The obvious advantages of the in-flight technique utilizing the YO-3A aircraft for acous-tic calibration or rotorcraft led to measurements for the Army SSEB during evaluation of both the UTTAS (fig. 8) and the AAH helicopters (fig. 9). Unfor-tunately, the recorded data cannot be released because of security classifica-tion; however, all four of these helicopters exhibited the same characteristic high-speed impulsive noise and the blade vortex interaction noise. The magni-tude and degree of presence of these characteristic sources differed between the aircraft but were present and detectable in each.

The data collected by in-flight measurement are serving another important purpose. It has demonstrated the validity of using scaled model rotors to experimentally measure, in acoustically treated wind tunnels, high-speed impulsive noise (ref. 9). As shown in figure 10, the wave forms are nearly identical although there is a difference in geometric scale of 7 to 1. Figures 10 and 11 show that the shape of the peak pressure variation with tip Mach number and the peak pressures are also in good agreement. Small-scale wind-tunnel tests provide the opportunity to utilize laser velocimeters, flow visualization techniques, and other specialized instrumentation to investigate this noise source.

The steepening of the high-speed impulsive negative pressure recovery at high forward speeds leads one to speculate as to the cause of this un-expected change. If the same noise source could be studied in the simplest of all rotor operating conditions (hover), additional insight could be obtained. The hovering rotor also affords opportunities to utilize specialized instrumentation.

The U.S. Army, in cooperation with NASA, has developed a very specialized facility capable of testing model rotors (fig. 12). The facility is acousti-cally treated to eliminate acoustic reverberations down to 110 Hz. The flow enters from the roof and passes through acoustically treated passages that attenuate external ambient noise; the flow then passes at very low velocity into the room. The rotor wake is the driving force as the wake passes into the ejector, under the lower floor, and out the end doors; fresh air is drawn in through the top of the building. Both aerodynamic performance and acoustic measurements can be made. Model rotors up to 2.4 m in diameter can be tested on the metric drive system which is capable of providing up to 89.52 kW (120 hp) and over 3000 rpm (fig. 13). This facility

as been used to obtain high-speed impulsive wave forms of the same 1/7-scale H-1H rotor used in previous wind tunnel tests.

A sample is shown in figure 14 (from ref. 10). Note the very rapid pressure recovery which is not predicted by theory. The shapes of the experimental and theoretical curves are totally different and the peak pressure is underpredicted by a factor of 2. The experimental wave form is essentially identical in shape to those obtained at M = 0.9 in both the wind tunnel and on the full-scale UH-1H in flight, free from interference. It must be concluded that the theoretical model is inadequate.

Figure 15 shows that the peak negative pressure is also not predictable nor is the variation of the peak pressure with Mach number. A great deal of progress has been made. Although the theory has been shown to be inadequate, a technique to measure full-scale interference-free helicopter-radiated noise has been developed, and it has been shown that small-scale rotors can be used in hover and wind tunnels to simulate the full-scale, high-speed impulsive rotary-wing noise source.

The wind tunnel also holds promise of providing the necessary tool for experimental investigations of blade vortex interaction noise (fig. 16). The question of how Reynolds number affects this noise source has not yet been adequately answered. Larger scale models or boundary layer transition strips may be required to simulate the full-scale blade vortex interaction effects.

Recent experimental investigations in both model-scale and full-scale flight have shown that rotor blade tip shapes can, in fact, alter the power required and radiated noise of helicopter rotors. These results are in agreement with what many helicopter enthusiasts have believed possible for a long time but had not been proved until recently. The Ogee tip shape flown on a UH-1H helicopter has both increased the aerodynamic efficiency and reduced the total radiated noise (ref. 11).

Further refinements and improvements are sure to follow once the effects of the Ogee tip are fully understood. A great deal of theoretical effort combined with well-conceived experimental programs is required to provide a basic technology from which improved blade geometry will result in reduced blade vortex interaction noise. The detailed problem of vortex formation must be examined and the rotor flow field defined with sufficient accuracy such that the vortex size, strength, and spacial location can be determined.

BROADBAND NOISE

Although on sounder footing, broadband noise is probably a more complex problem because of its sensitivity to both turbulence levels and the rotor wake (ref. 5). Obtaining high quality experimental data is more difficult in that the background noise must be lower, the frequency of broadband noise is higher, and Reynolds number is likely to be a very important parameter. The acoustic rotor hover facility and small-scale rotor tests in wind tunnels may

be beneficial in defining the sensitivity of the broadband noise to the scaling parameters. However, in-flight noise measurements will be required to assess the magnitude of the errors induced by scaling effects, background noise, or wall effects. The theoretical treatment of broadband noise has not yet really withstood the baptism of fire. The low-frequency impulsive noise and blade-vortex interaction noise both induce very rapid time variations in pressure which contribute to the amplitude of the higher harmonic frequencies. It is therefore essential that these contributions be predictable before an adequate assessment of broadband noise theoretical calculations can be obtained.

INTERIOR NOISE

As techniques for alleviation of impulsive, blade-vortex interaction, and broadband noise are implemented, the effects of the aerodynamically generated rotor noise on the cabin interior noise levels will be reduced. The main sources of interior noise are noise transmission from the power generation and drive system and noise generated by sympathetic vibrations of fuselage structures. Techniques must be devised for noise isolation. Insulation of cabin interiors can considerably reduce the internal noise, but only by relatively large infringements on the payload capability.

Noise deadening and noise isolation appear to hold the most promise for reducing cabin interior noise levels with a minimum reduction in payload capability. Considerable effort in both materials and applications is required. Better theoretical models for sound transmission will have to be developed. Refinements are required to accurately calculate the blade passage unsteady pressure environment of the fuselage structure. The Army Aeromedical Research Laboratory is developing improved equipment for better communications in the noisy environment of current helicopter interiors. However, in the longer term, both interior and exterior noise reduction techniques are required that will not severely affect the unique performance capabilities of the helicopter.

CONCLUDING REMARKS

Rotary-wing acoustics is emerging from a complex, confusing, and often contradictory era into a well-founded scientific discipline. We are fortunate to be involved in this exciting emergence of a rapidly evolving technology. We believe that this change is primarily due to recent advancements in experimental techniques and philosophy which are resulting in a wealth of new information that is pressing our theoreticians to face current theoretical limitations and to push forward the frontiers of the theoretical treatment. The experimentalists must coordinate their efforts to avoid unnecessary duplication and to maintain a flexibility to provide verification data for emerging theoretical refinements. The Aeromechanics Laboratory, in co-operation with Ames Research Center, intends to continue refinement of the

full-scale, in-flight noise measurement techniques utilizing the YO-3A aircraft and to further develop the anechoic hover testing facility. The Ames YO-3A aircraft will be maintained as an in-flight acoustic platform facility for future problems in low-speed V/STOL noise research. The Army will continue to utilize its technical expertise to improve the rotary-wing acoustic technology by a systematic approach of reviewing and improving theoretical techniques while utilizing specially developed experimental equipment and facilities made available through the joint agreement with NASA.

APPENDIX

SYMBOLS

A/S   airspeed

C_T rotor thrust coefficient

D   diameter of rotor

M_{AT} Mach number of advancing blade tip

M_T tip Mach number in hover

R/S   rate of descent

r   distance from microphone to rotor center line

V   flight velocity

α angle of tip path plane relative to a line between the tail microphone and the rotor hub

α_{TPP} tip path plane angle

γ rate-of-descent angle

μ advance ratio

σ rotor solidity

804

REFERENCES

1. Sears, W. R.: Aerodynamics, Noise, and the Sonic Boom. 1968 Von Karman Lecture, AIAA Journal, vol. 7, no. 4, Apr. 1969.

2. Ollerhead, J. B.; and Lowson, M. V.: Problems of Helicopter Noise Estimation and Reduction. AIAA Paper 69-195, presented at the AIAA/AHS VTOL Research, Design, and Operations Meeting, Feb. 1969.

3. Cox, C. R.: Subcommittee Chairman's Report to Membership on Aerodynamic Sources of Rotor Noise. Presented at the 28th Annual National Forum of the American Helicopter Society, Washington, D.C., May 1972.

4. Stepniewski, W. Z.; and Schmitz, F. H.: Possibilities and Problems of Achieving Community Noise Acceptance of VTOL. The Aeronautical Journal of Great Britain, vol. 77, no. 750, June 1973.

5. George, A. R.: Helicopter Noise - State of the Art. Presented at the AIAA 4th Aeroacoustics Conference, Atlanta, Ga., Oct. 3-5, 1977.

6. White, Richard P., Jr.: The Status of Rotor Noise Technology - One Man's Opinion. Helicopter Acoustics, NASA CP-2052, Pt. II, 1978. (Paper no. 38 of this compilation.)

7. Schmitz, F. H.; and Boxwell, D. A.: In-Flight Far Field Measurement of Helicopter Impulsive Noise. J. American Helicopter Soc., Oct. 1976.

8. George, R. E.; and Duffy, V.: In-Flight Measurement of Aircraft Acoustic Signals. Presented at the 23rd International Instrumentation Symposium, Las Vegas, Nev., May 1977.

9. Schmitz, F. H.; Boxwell, D. A.; and Vause, C. R.: High-Speed Helicopter Impulsive Noise. J. American Helicopter Soc., Oct. 1977.

10. Boxwell, D. A.; Yu, Y. H.; and Schmitz, F. H.: Hovering Impulsive Noise - Some Measured and Calculated Results. Helicopter Acoustics, NASA CP-2052, Pt. I, 1978. (Paper no. 15 of this compilation.)

11. Mantay, W. R.; Campbell, Richard L.; and Shidler, Phillip A.: Full-Scale Testing of an Ogee Tip Rotor. Helicopter Acoustics, NASA CP-2052, Pt. I, 1978. (Paper no. 14 of this compilation.)

TABLE 1.- HELICOPTER NOISE RESEARCH EFFORTS

Army in-house	AARL ECOM R&T Labs
Joint programs	Army/NASA
Universities	Cornell M.I.T. George Washington U. Poly. U. of New York U. of Mississippi } ARO Stanford U.
Industry	Bell Helicopters Boeing VERTOL ——— ARO UTRL RASA

HIGH SPEED
IMPULSIVE
BLADE VORTEX
INTERACTION
BROADBAND
INFLOW
TURBULENCE

TAIL ROTOR
HIGH SPEED IMPULSIVE
VORTEX INTERACTION
MAIN ROTOR WAKE
TURBULENCE
BROADBAND

ENGINE
TRANSMISSION
FUSELAGE PANEL VIBRATION
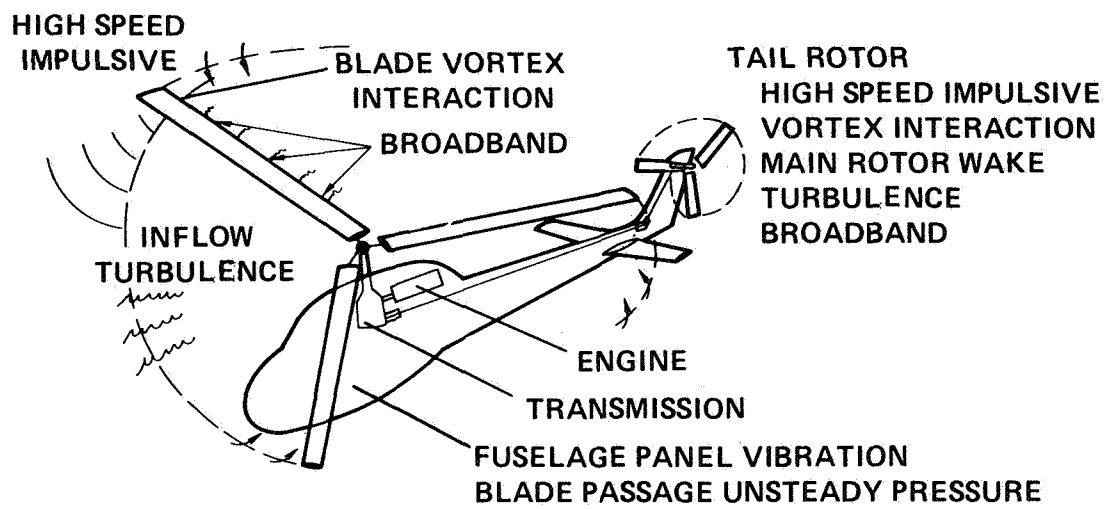BLADE PASSAGE UNSTEADY PRESSURE
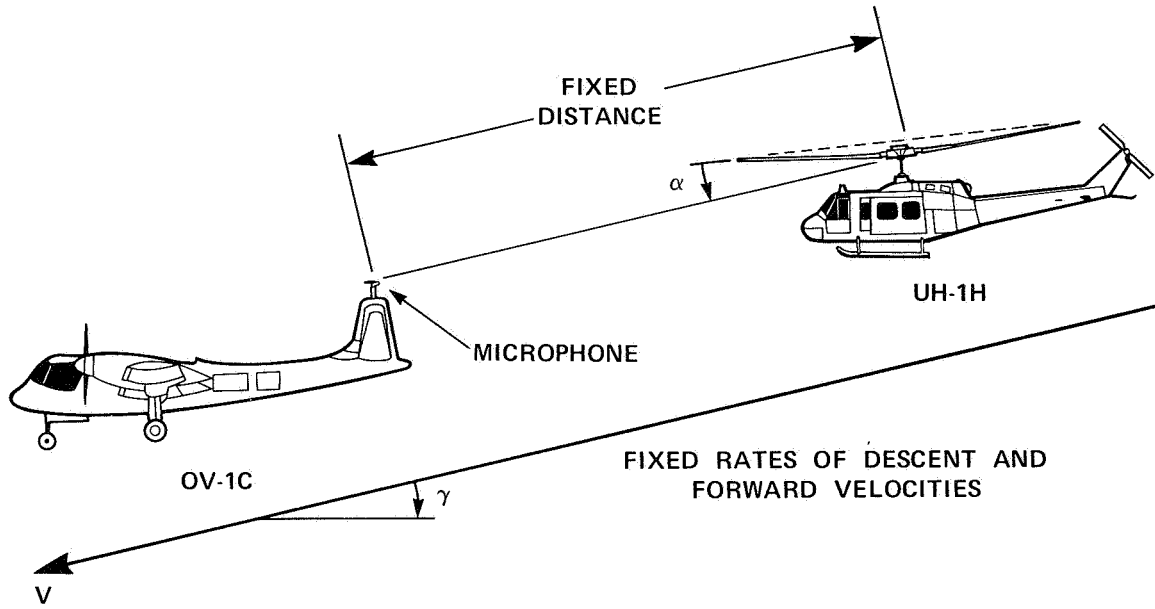
Figure 1.- Helicopter noise sources.

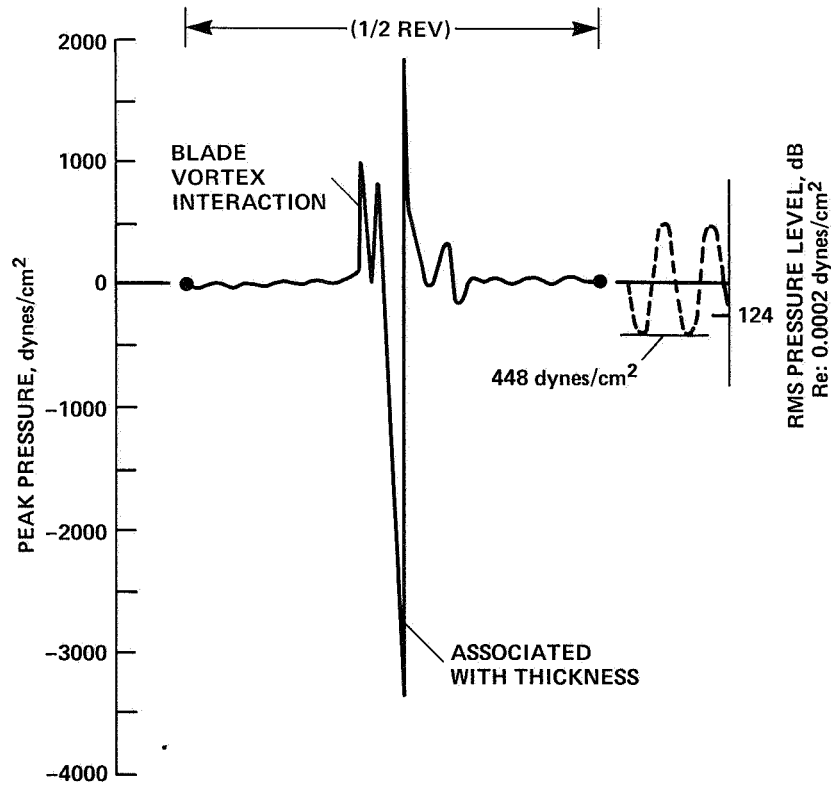Figure 2.- Schematic of in-flight far-field measurement technique.

Figure 3.- Composite illustration showing dominant UH-1H acoustic waveform features.
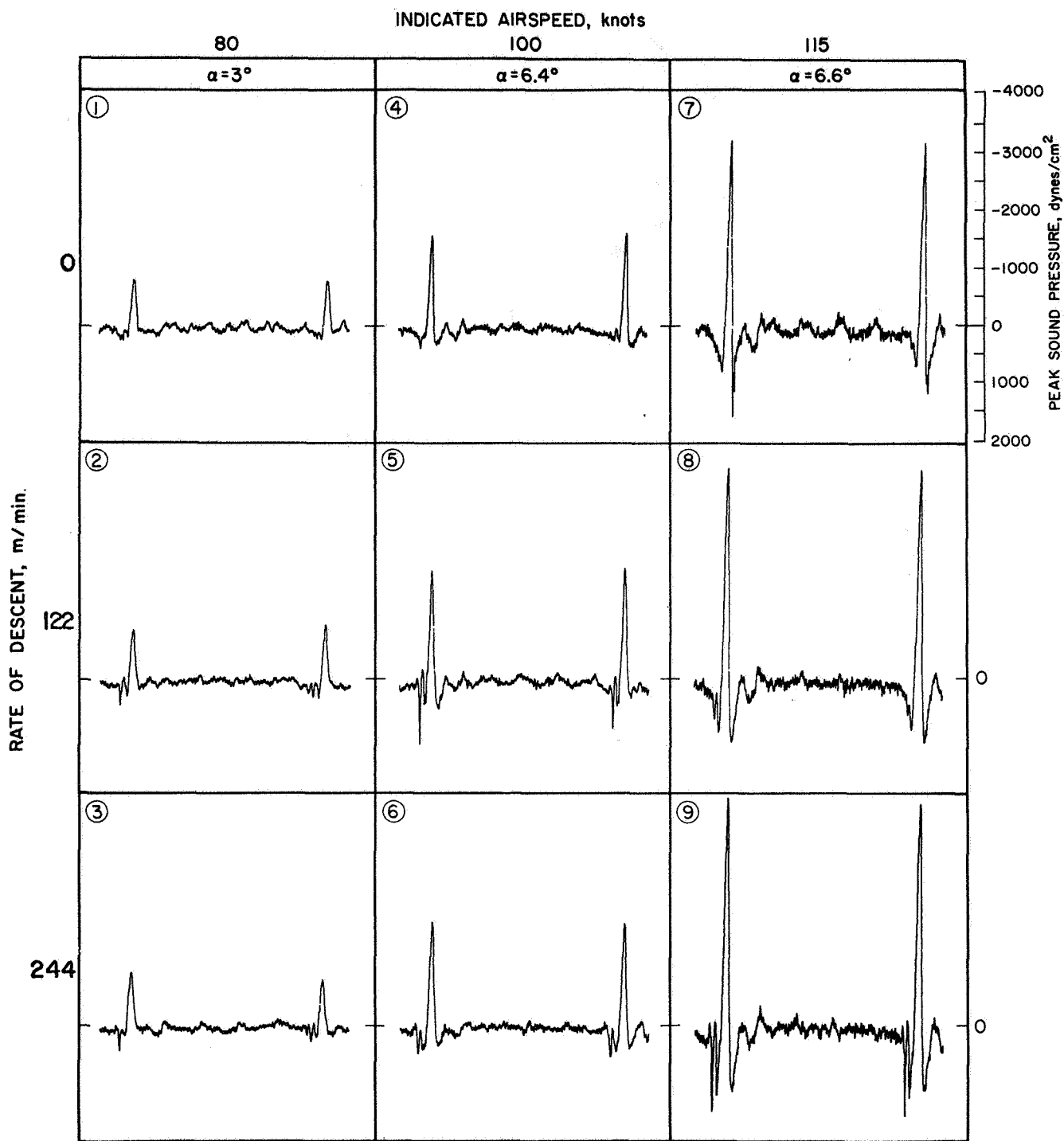
Figure 4.- UH-1H impulsive noise.
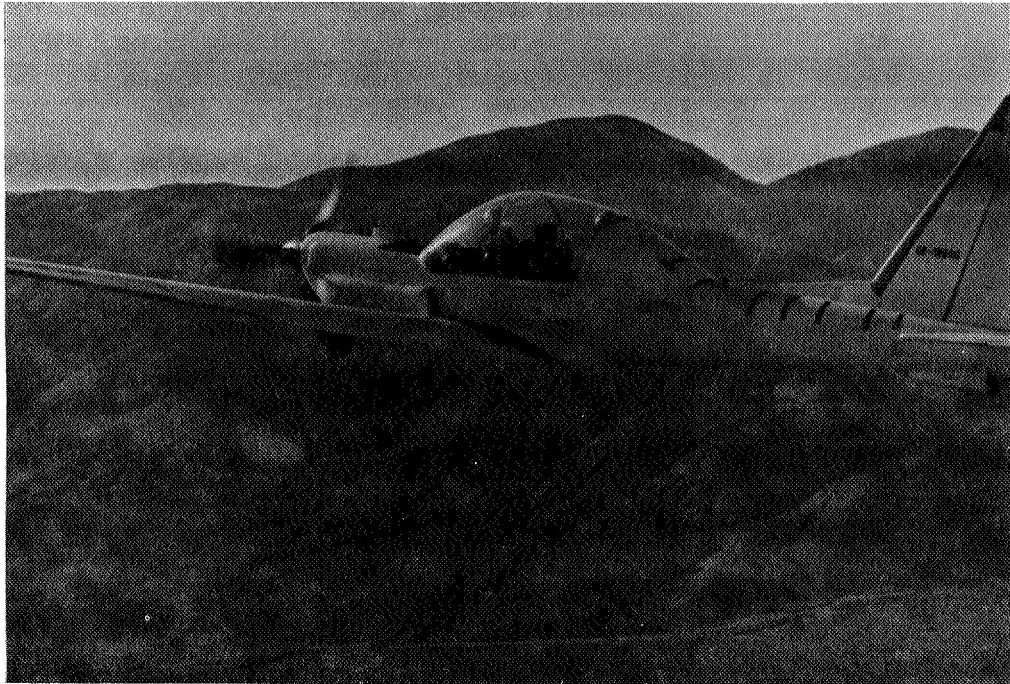
Figure 5.- YO-3A "quiet aircraft."
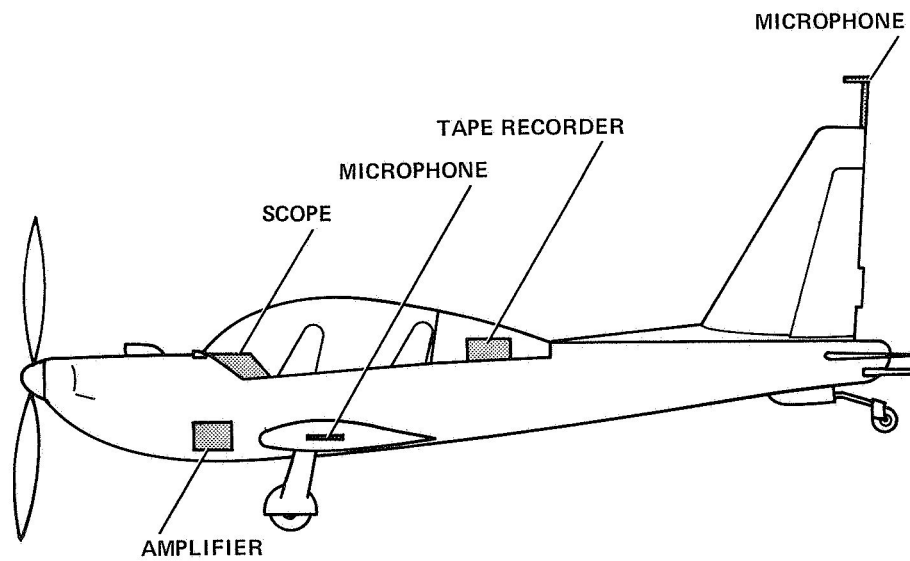
Figure 6.- Instrumentation on YO-3A.
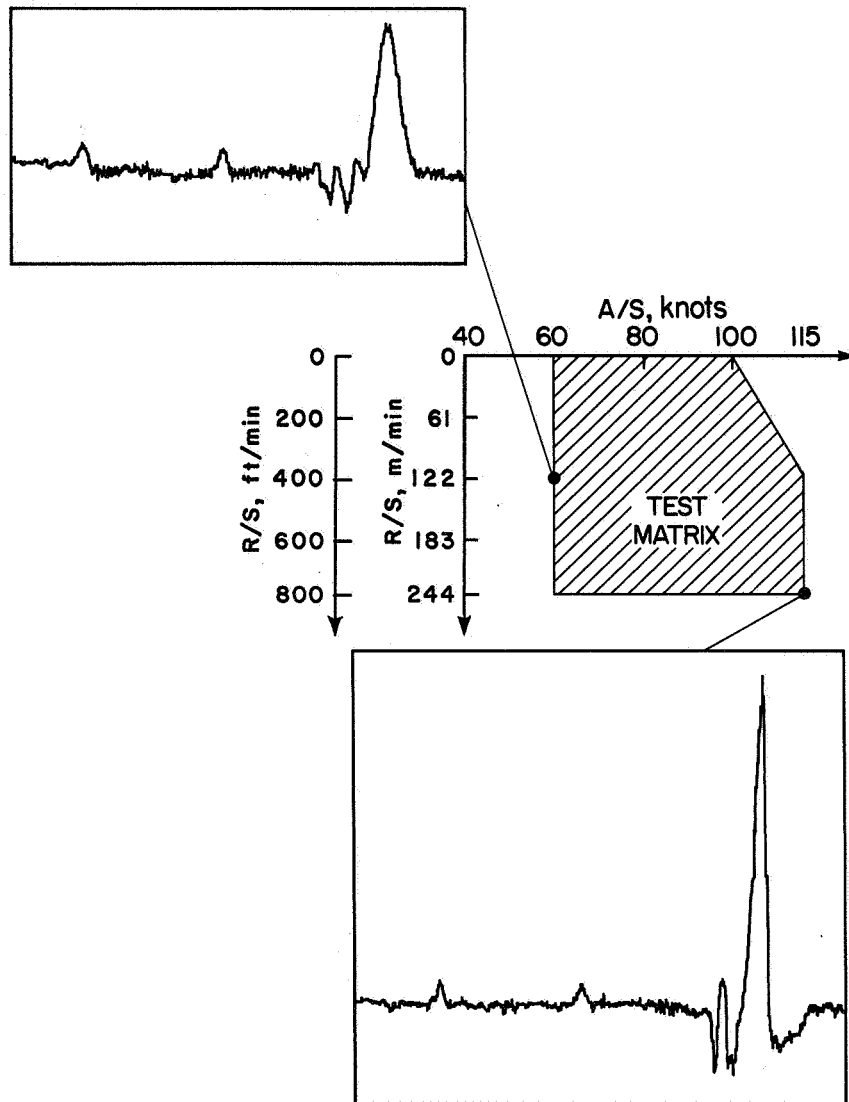
Figure 7.- Waveform shapes from YO-3A flight program — preliminary data.

Figure 8.- YO-3A gathering acoustic data on Sikorsky UTTAS.

Figure 9.- YO-3A gathering acoustic data on Hughes AAH.

812
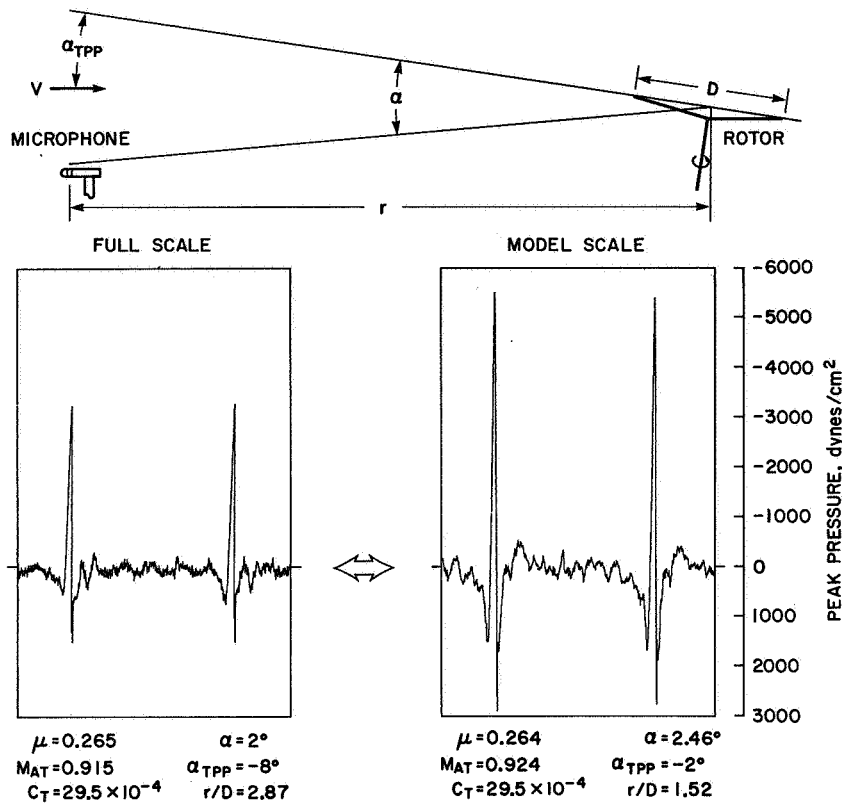
Figure 10.- Waveform comparison — full-scale and model-scale high speed data.
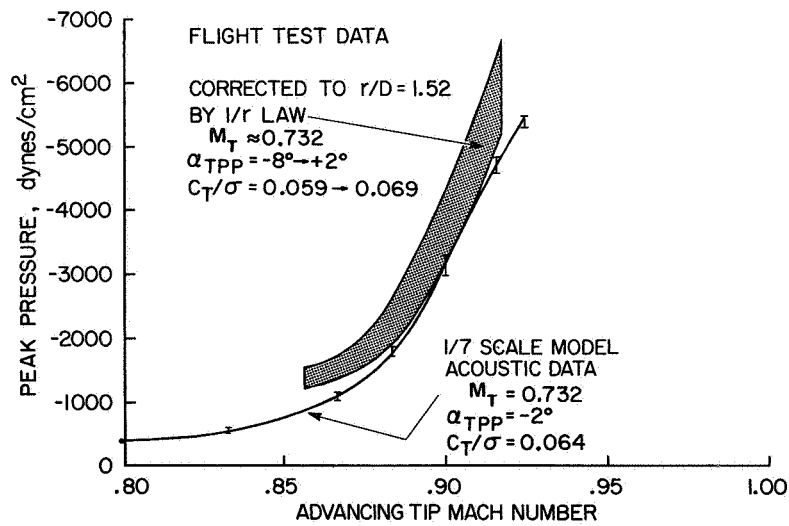
Figure 11.- Peak negative amplitude comparison — full-scale and model-scale high speed data.
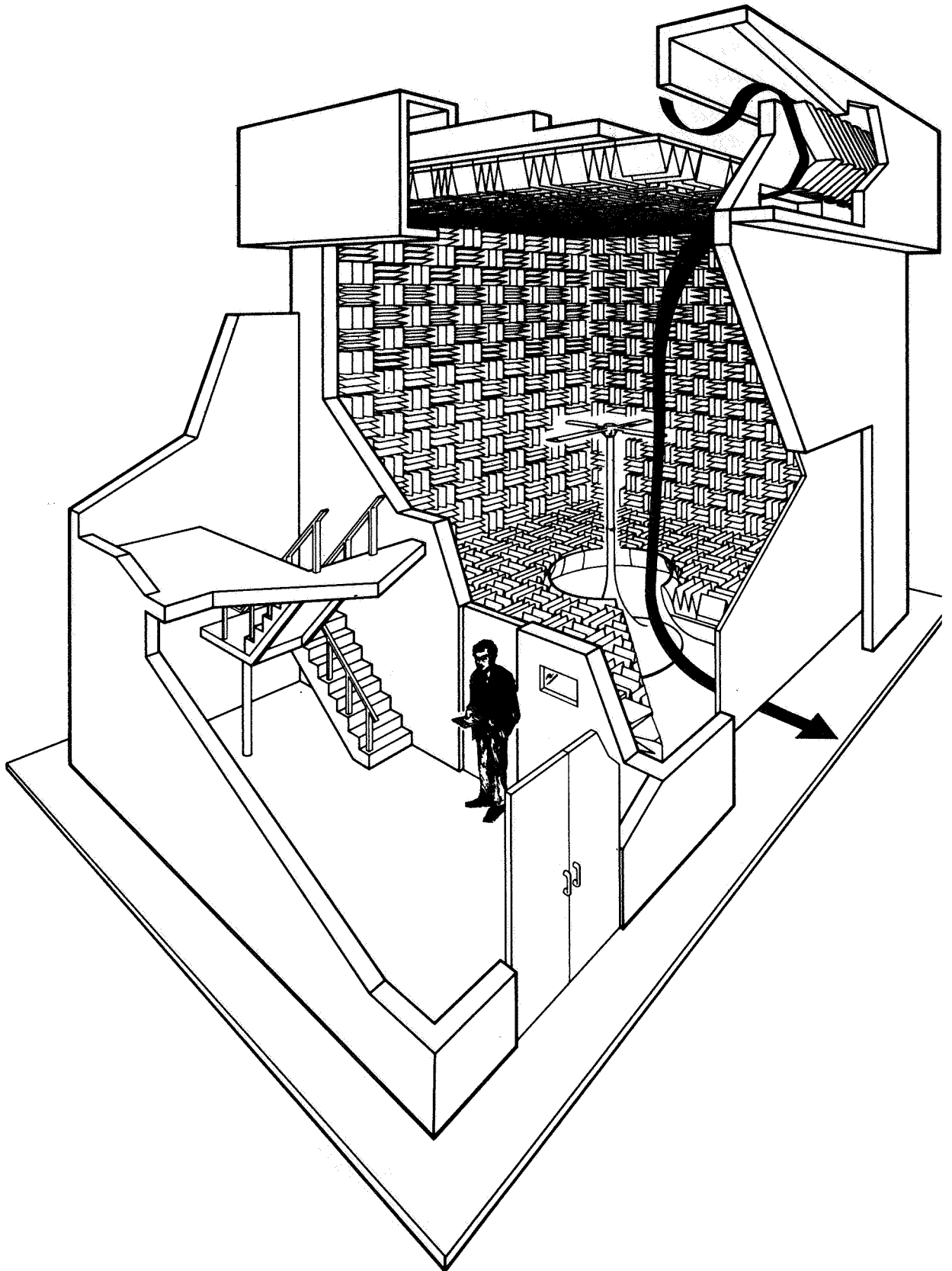
Figure 12.- Schematic of the anechoic rotor hover testing facility.
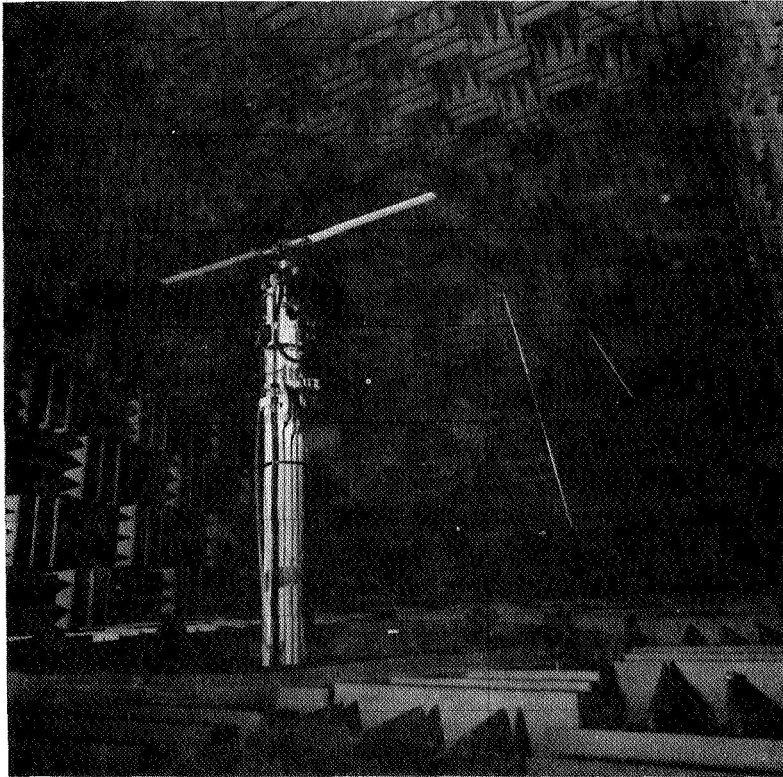
Figure 13.- 1/7-scale UH-1H model rotor in the anechoic rotor hover testing facility.

$M_T = 0.9$
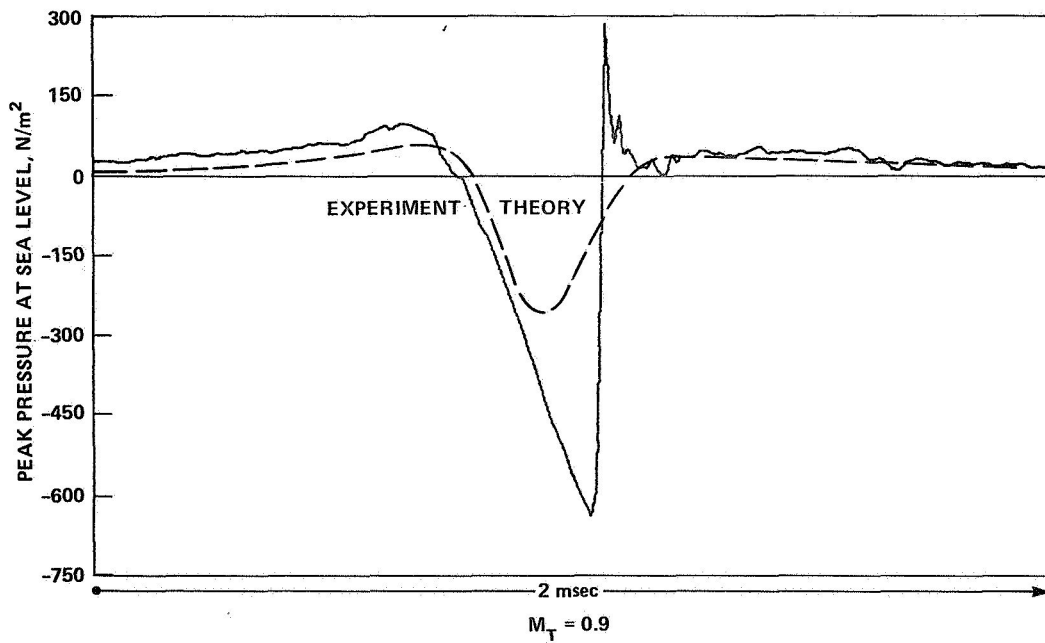
Figure 14.- Hovering model rotor comparison of theory and experimental pressure-time history in-plane.
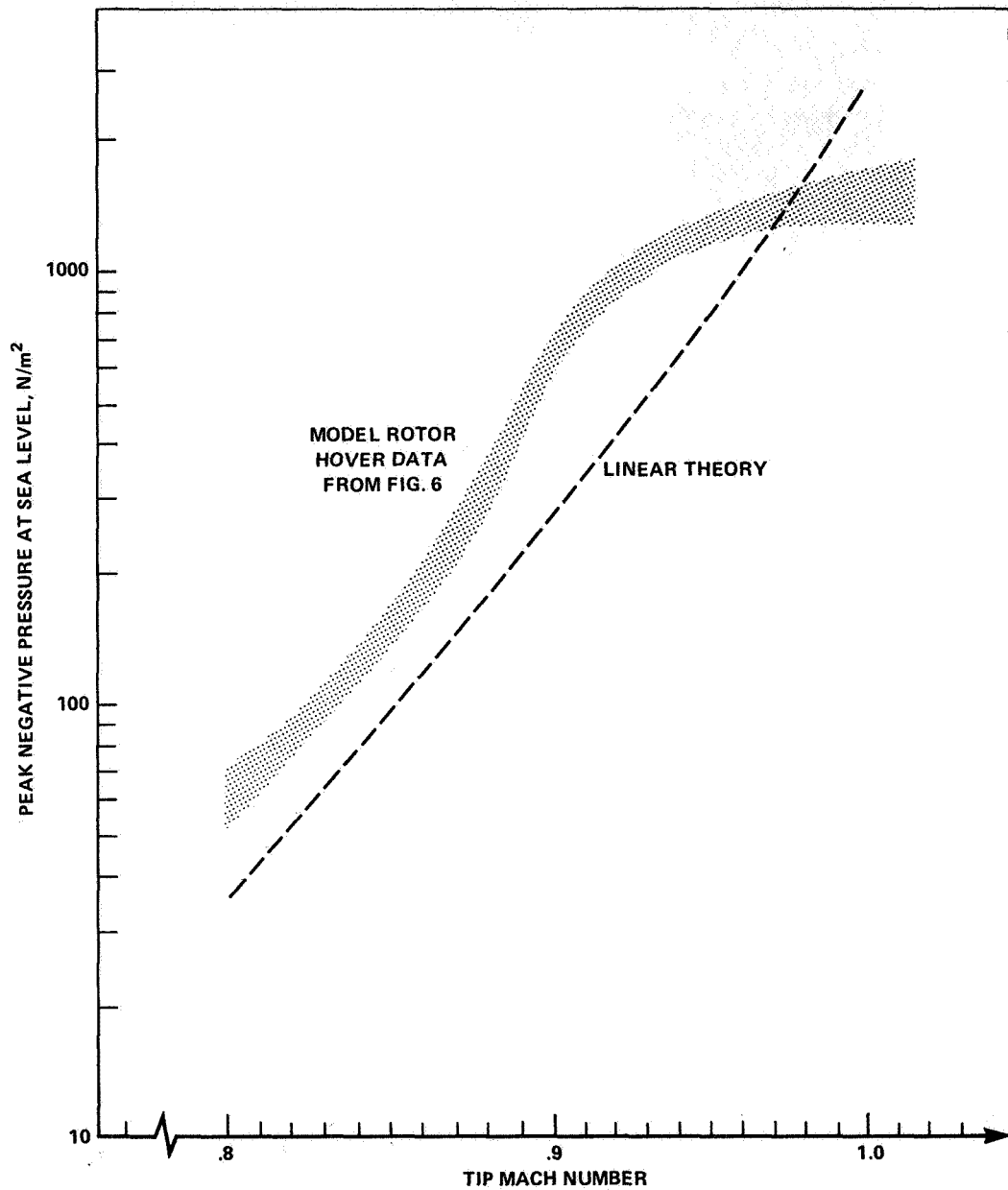
Figure 15.- Hovering model rotor comparison of peak negative pressure — theory and experiment.

Figure 16.- Model UH-1H rotor interacting with previous tip vortices.

REGULATIONS

Charles J. Hoch
Federal Aviation Administration

SUMMARY

The opening plenary session on Regulations included presentations by
Charles R. Foster, Acting Deputy Associate Administrator for Policy Development
and Review, Federal Aviation Administration; R. A. Wagner, Chairman, HAA Com-
mittee on Helicopter Acoustic Certification Standards; Charles R. Crawford,
U.S. Army Aviation Research and Development Command; and Stanley R. Spector,
Assistant to the President, Hughes Helicopters, Division of Summa Corporation.
These gentlemen addressed the helicopter regulatory question from four
different and important perspectives. Mr. Foster provided FAA's status with
regard to future regulatory action and touched upon additional testing activi-
ties to be undertaken in conjunction with that action. Mr. Wagner stated the
HAA's position on the subject and stressed the need for further study on the
cost to the industry of helicopter noise suppression. Mr. Crawford discussed
the military view on the subject and called for a simplification of certifica-
tion procedures. Mr. Spector concluded with an overview of local government
actions impacting the operation of helicopters in urban areas. The discussion
session that followed identified and summarized those outstanding elements to
be undertaken in conjunction with helicopter regulatory action.

INTRODUCTION

The opening plenary session was indeed an informative one and properly
framed subsequent sessions addressing helicopter acoustics. When asked by
Dr. Roberts to summarize that initial gathering within the space of a six-
minute presentation, this reporter did not approach that task with any degree
of certainty. Therefore, what has been attempted here is a rather curt sum-
marization of the major points made in each of the presentations, concluding
with a synopsis of those remaining problem areas as identified by each of the
Regulatory session participants.

Presentation by Charles R. Foster: Mr. Foster first reviewed the opera-
tional growth of helicopters and the implication of that growth for the future.
He then commented on the status of regulatory activity within both FAA and the
International Civil Aviation Organication (ICAO). Specifically, both FAA and
ICAO are developing a complimentary data base and are proceeding along a com-
plimentary certification approach at this point. The legislative background
was then described from which FAA draws its authority and responsibility to
act on this subject, the basis being Public Law 90-411, which added Section
611 to the Federal Aviation Act of 1958.

It was noted that FAA has gathered important data regarding the issues surrounding helicopter regulatory actions by virtue of a December 1973 Advance Notice of Proposed Rule Making (ANPRM). A discussion of the certification procedure issue then followed, including a description of a flyover, approach, and takeoff procedure currently under study by FAA.

The current FAA status on the subject is on track for a possible issuance of a Notice of Proposed Rule Making (NPRM) by the fall of 1978. This may be accomplished at the same time that additional needed information is obtained and consensus achieved on such issues as, for example, the correction to allowable noise levels which accounts for "blade slap."

Concurrent actions will also be taken by FAA to develop further helicopter data in field tests scheduled at Wallops Island and at NAFEC.

Mr. Foster concluded by saying that FAA regulatory actions might consider a less stringent noise standard for "remote use" helicopter activity but that an additional problem arises with this approach. That problem stems from the question of how to ensure the restricted use of these louder helicopters in remote areas.

Presentation by R. A. Wagner: Mr. Wagner urged that each helicopter model be allowed to fly its own "best" flight approach procedure during certification tests. He went on to stress the position that current information on vehicle cost of noise suppression is inadequate and that additional FAA work must be undertaken on this question before regulatory action is concluded.

Mr. Wagner then questioned the vagueness of the regulatory establishment criteria of "economic reasonableness" and "technological practicability" and commented that FAA's contemplated noise levels could not be met by over 70% of the helicopters in operation today. He urged that no retroactive application of helicopter noise standards be attempted by FAA since such activity would surely result in degradation of helicopter performance and possibly safety. Mr. Wagner agreed with Mr. Foster that some accommodation be made to allow "noisy" helicopter operations in remote areas. He concluded with comments to the effect that EPNL should be adopted as the appropriate certification noise descriptor without regard for impulsiveness correction (blade slap).

Presentation by Charles R. Crawford: Mr. Crawford's opening remarks recognized that little military effort had been expended to establish external noise standards for helicopters. He quickly stated, however, that the military is sympathetic to FAA efforts and shares a desire to reduce noise impacts on the public. An additional military need exists to establish internal noise standards to achieve an improved level of intelligibility in communication among flight crews and passengers.

Mr. Crawford pointed towards a deficiency in the current state-of-the-art of noise prediction methodology for new design helicopters. FAA/ICAO were

urged to further simplify certification procedures consisting of "fly-by" and hover procedures at 100% rpm. This, according to Mr. Crawford, would be preferable in comparison to the complicated flyover, approach, and takeoff procedures now being considered.

Presentation by Stanley R. Spector: Mr. Spector brought into the discussion the issue of individual local government actions currently being taken which have already impacted helicopter operations in populated areas. Public concern for safety and noise is the apparent motivating force behind such local actions, and unless that concern is adequately addressed in the future, the helicopter industry will not achieve the growth that is potentially there. According to Mr. Spector, this growth will be caused, in part, as a result of further expansion of the metropolitan growth "rings" emanating outward from the core of the larger cities. This sprawl will increase the need for the kind of transportation which can be provided by helicopters. If public concern about helicopter use can be minimized, a potential three-fold growth will be realized in helicopter operations by 1985. Mr. Spector followed by describing the specific kinds of actions that have been taken in the State of California, along with a case study showing how an operational technique was able to satisfy the local requirements.

The remaining needs highlighted in Mr. Spector's presentation may be met by a joint government/industry effort in the development and implementation of a comprehensive helicopter noise reduction program. Such a program should foster improved piloting techniques, less noise-creating blade design, noise reduction through reduced rotor speeds, and improved engine muffling concepts.

In concluding, Mr. Spector stressed the need to make local governments aware of the potential debilitating impact of unnecessarily stringent regulatory actions on the helicopter industry.

DISCUSSION

In the exchange that followed the first day's plenary session, Mr. E. S. Carter, Jr., Sikorsky Aircraft Division and Chairman of that session, questioned the current capability of technology to bring about helicopter noise reductions in higher gross weight models. Accordingly, Mr. Carter implied that regulating the higher weight versions may be premature until this technology void is filled.

At the conclusion of the session reviews, a panel was formed to address specific questions relevant to the scope of the total symposium. One of those questions, posed by Chairman Leonard Roberts, NASA Ames Research Center, focused upon the regulatory activity. That question was, "Does an adequate understanding exist to allow intelligent formulation of helicopter noise regulations?" In response to that question, the author stated that there are apparently many points of information and data still outstanding on the general subject of

helicopter acoustics. For example, no concensus exists on how to handle the impact of "blade slap" in developing allowable noise levels. Additionally, further testing of helicopter takeoff noise has already been planned by FAA. Of added concern is the need to quantify the benefits of helicopter regulatory action. For example, how many people are today impacted by helicopter operations and what is the extent of those impacts? As a result of alternative regulatory actions, how many people will be removed from noise-impacted areas in the future and what is the value of such actions?

Additionally, the cost of imposing helicopter regulatory action is already recognized as needing further study and FAA is undertaking that work. Finally, the technological capability of the industry to reduce the noise impact of high gross weight models has been raised as an issue.

In summary, there are many points still left outstanding. The FAA does not believe, however, that because of this lack of information or because of disagreement in certain areas that we cannot conscientiously move together towards helicopter regulatory action. If one theme did gain concensus, it was that action is necessary in the best interests of the industry as well as the public. We are optimistic that we can proceed into the rulemaking process while gaining the information we need to satisfactorily address all of these crucial areas. The rulemaking process itself will act as a source of much of this information. Last but not least, the insights and exchange of views made possible through this symposium have allowed us to come away better equipped to accomplish this task.

ROTOR NOISE PREDICTION*

A. R. George
Cornell University

INTRODUCTION

I have been asked to present a brief summary of the highlights and remaining problems of the theoretical and prediction aspects of rotor noise, with particular emphasis on the work presented at this conference. As there were fifteen papers given in the rotor noise sessions as well as several related papers in other sessions, I will not try to review them individually. I will try to give an overall perspective, dividing the subject into the three areas of nonimpulsive, blade-vortex, and high speed noise.

NONIMPULSIVE NOISE

In the area of nonimpulsive noise, the papers of Gupta and Hawkings reviewed present harmonic noise prediction methods which are based upon empirical loading harmonic laws. These methods, while useful in some cases, were shown to typically involve errors of the order of 10 dB in parts of the predicted spectra. This is clearly unsatisfactory for design purposes. However, several papers were presented which gave evidence that the broadband noise and harmonic peaks due to inflow turbulence can be satisfactorily predicted using recently developed analytical methods. These methods use blade loadings fluctuations calculated from the inflow turbulent velocities. The papers of Amiet, of Aravamudan, Lee, and Harris, and of Hayden and Aravamudan all showed good agreement between measured and calculated spectra in cases where the incident turbulence was known. Also, these and other theoretical analyses were used as bases to make scaling and parameter studies of broadband sources.

On the other hand, it is not clear that all of the important broadband and harmonic noise sources are fully understood yet. One notable example is the noise due to the interaction of the main rotor wake with the tail rotor. Experimentally, great progress in this area was reported at the conference by Pegg and Shidler, and hopefully we will learn how to analyze and avoid this extra noise in the future. A new noise mechanism associated with unsteady blade thickness-turbulence interaction was analyzed by Hawkings who showed it can be important for noise near the rotor plane.

Finally, a number of new concepts were presented which hold out some promise for nonimpulsive noise reduction. Williams and Cheeseman showed the noise reduction potential of the circulation control rotor and Hayden and other speakers suggested various promising tip and trailing edge modifications.

The nonimpulsive rotor noise area can be summarized by saying that we seem to understand the primary noise sources but prediction methods still need improvement and that main/tail rotor interaction and some secondary sources such as tip separation and trailing edge noise need further study. Also there is a serious lack of nonimpulsive noise data where inflow velocities and turbulence and other flow properties are simultaneously measured.

BLADE-VORTEX INTERACTION NOISE

Blade-vortex interaction noise is, of course, an "excess" noise which in principle is avoidable. Practically speaking, however, most helicopters' blades do interact with their tip vortices in some important flight regimes such as descent. Among the highlights of the recent meeting were the reports by Mantay, Campbell, and Shidler, and by White on the noise reduction associated with modifications of tip vortices by blade tip changes. In particular, the Ogee tip was shown to decrease noise significantly while increasing performance of a UH-1H. This certainly is a most promising development. It now remains to obtain an understanding of and prediction capability for both the nature of the tip vortex flow modifications and the vortex trajectory changes. We need to know why the Ogee tips are so effective in order to determine if they will be as effective for the full range of helicopter designs, including machines of lower performance than the UH-1H.

HIGH SPEED NOISE

High speed noise is associated with high advancing tip blade Mach numbers and can be reduced by reducing flight speed when flying over sensitive areas. However, this is economically undesirable and other noise reduction methods are needed. A variety of presentations at this conference moved toward better understanding of high speed noise mechanisms and calculation methods.

The state of the art is advancing very rapidly in this area. Several new techniques for thickness noise calculations and a start on the problem of designing blades with maximum or minimum noise were presented. At present there remain some significant differences between theoretical calculations of high speed noise and the excellent available experimental data of Schmitz and Boxwell and of other experimenters. Thus many investigators have been looking at other high speed mechanisms beyond thickness and loading noise. Hanson and Fink presented an analysis of quadrupole effects on radiated noise which seems to explain some of the discrepancies found at transonic tip speeds. However, the high speed hover data of Boxwell, Yu, and Schmitz show other discrepancies which appear to involve strong nonlinear effects probably associated with shock waves.

824

Although there are several important questions remaining which concern high speed noise, there are many excellent researchers working in the area who are making rapid progress. I expect further insights into designing for reduced high speed noise will follow our expanding understanding of these sources.

SUMMARY

In closing, I would like to emphasize the tremendous progress that has been made in the past five to ten years in helicopter noise. We have come from discussing empirical prediction schemes and qualitatively what the mechanisms are to centering on quantitative calculations for many nonimpulsive and high speed noise mechanisms. Although present prediction methods are inadequate for designing to particular specifications, the rate of improvement of knowledge suggests that we may get close to that goal in a few years.

MODEL AND FULL-SCALE TESTING OF ROTOR NOISE

F. H. Schmitz
Aeromechanics Laboratory
U.S. Army Research and Technology Laboratories (AVRADCOM)
NASA Ames Research Center

Model and full-scale acoustic/aerodynamic testing can probably be classified as an "art" that is trying to become a "science" (or an engineering discipline). Not long ago, cause and effect in the field of helicopter acoustics was treated by parameterization. In many cases, some gross aspect of the radiated noise was empirically modeled using as a guide the simple order of magnitude arguments of the theoretical acousticians. While this technique is expedient, it is also quite superficial and yields little quantitative information. Fortunately, as the papers in this conference (ref. 1) have indicated, this generalized approach is giving way to attempts to isolate and quantify the sources of helicopter external noise.

Major aspects of helicopter external noise that are receiving attention are high-speed impulsive noise, blade vortex interaction noise, Ogee tip effects, the relationships between tail rotor placement and noise, and broadband noise. The importance of this good experimental research should be stressed. It will be the carefully completed experimental program, designed to achieve definite goals, that will help the theoretician find his way through a maze of potential acoustic sources and isolate the primary cause of the radiated noise.

In this light, there are at least four developing trends which characterize the model and full-scale acoustic testing reported at the conference. The first is the development and use of more sophisticated experimental techniques to isolate the acoustic or aerodynamic phenomena of interest. In many cases, stationary microphones by themselves are not enough to trace the origins of the radiated noise. Rotor blade pressure instrumentation, Schlieren photographs, "flying" microphones, etc. are but a few of the new techniques that are being developed for acoustic research.

A second notable trend in experimental rotor acoustic testing is the growing use of acoustic treatment for wind-tunnel testing. It is becoming apparent that acoustic treatment of some degree is a tremendous help (if not a necessity) when gathering acoustic data in wind tunnels. For high-speed impulsive noise, limited wall treatments may be adequate. For other noise sources, more extensive treatments will undoubtedly be required.

The third notable trend is really a natural evolution and merging of the disciplines of acoustics and aerodynamics. Because aerodynamic factors are the ultimate cause of all rotor noise as we know it, the importance of the aerodynamicist as an acoustic researcher is growing. It is becoming apparent that the acoustician's task of "summing up" the sources of noise for the

rather complicated rotating-translating source motion of the helicopter blades can now be done on an almost routine basis. It is now up to the aerodynamicist to isolate and quantitatively describe these sources or to improve and refine the theoretical technique for dealing with the radiative properties of the flow field.

The last and most significant trend is the ever increasing use of "scale models" for acoustic testing. The advantages of using scaled rotors for acoustic testing are quite similar to those of aerodynamic model rotor testing. Smaller models require smaller test facilities which in turn are more easily treated acoustically. However, there are some added dangers in model acoustic testing that should be carefully explored. It must be remembered that the primary purpose of model scale testing is to duplicate a particular phenomenon on a full-scale rotor.

Therefore, the model experiment must be scaled in such a way that all influencing parameters are properly simulated, and parameters of unknown influence must be isolated to determine their importance. Improper scaling can result in erroneous data which complicate and impede the development of rotary-wing acoustic technology.

This latter trend in model and full-scale acoustic testing can probably be best illustrated by an example of some unpublished aerodynamic/acoustic data taken on a 1/7-scale UH-1H rotor tested in the Aeromechanics Laboratory's acoustically treated 7- by 10-foot wind tunnel. The purpose of the experiment was to compare model and full-scale in-flight acoustic data (fig. 1) under high-speed blade-vortex interaction impulsive noise conditions. As shown in figures 2 and 3 (from ref. 2), the shape of the pressure time histories and the scaled amplitudes are remarkably similar. For this test, geometry and time were scaled while advance ratio, advancing tip Mach number, thrust coefficient, and tip-path-plane angle were duplicated.

One can see from figure 4 that the tip Reynolds number for this 2.13-m (7 ft) diameter rotor is about 1.2×10^6 based on a chord of 7.6 cm (3 in). The model rotor is operating in the classical transition regime — the local boundary layer could be laminar or turbulent. The full-scale rotor, whose Reynolds number is 7 times as large, operates with a turbulent boundary layer near the tip of the blades. Therefore, to approximate the aerodynamics of a full-scale rotor with a 1/7-scale model, some surface roughness is required to transition the boundary layer from laminar to turbulent. This was confirmed by utilizing a strobed Schlieren to photograph a two-dimensional picture of the three-dimensional shock structure of the local flow on the advancing side of the disc in high-speed flight (azimuth angle $\psi \approx 85°$). Figure 5 shows an almost classic laminary boundary-layer shock interaction on the smooth surface model blades. The attached shock abruptly separates the flow and causes large increases in power.

This same rotor was run again at similar conditions but with some surface roughness (fig. 6). The aerodynamic flow field was significantly changed — now characterized by a turbulent boundary-layer shock interaction. Again, flow separation was present but much different in character than in the preceding case.

828

From figures 5 and 6, one can see that the aerodynamic flow field of this model scale rotor is strongly influenced by surface roughness. If the model rotor had been much smaller, no duplication of full-scale Reynolds numbers and thus full-scale aerodynamics would have been possible.

It is indeed remarkable that the high-speed impulsive model acoustic data taken with smooth rotor blades scaled so well in amplitude and shape. That it did implies that Reynolds number is a secondary factor in that source of noise. However, preliminary findings suggest that blade-vortex interaction high-speed impulsive noise data do not scale as well. It may be that more careful attention must be paid to additional scaling parameters for this source of noise. In particular, local Reynolds number scaling effects may be important.

In summary, model and full-scale acoustic testing is quickly beginning to attain a status on a level with the other rotor disciplines. Further progress in the field of acoustics will depend on experimental guidance of a quantitative nature — to help the aerodynamist/acoustician isolate the sources of the radiated noise.

REFERENCES

1. Rotor Noise. Helicopter Acoustics, NASA CP-2052, Pt. I, 1978. (Paper nos. 5 to 19 of this compilation.)

2. Schmitz, F. H.; Boxwell, D. A.; and Vause, C. R.: High-Speed Helicopter Impulsive Noise. J. American Helicopter Soc., vol. 22, no. 4, Oct. 1977, pp. 28-36.

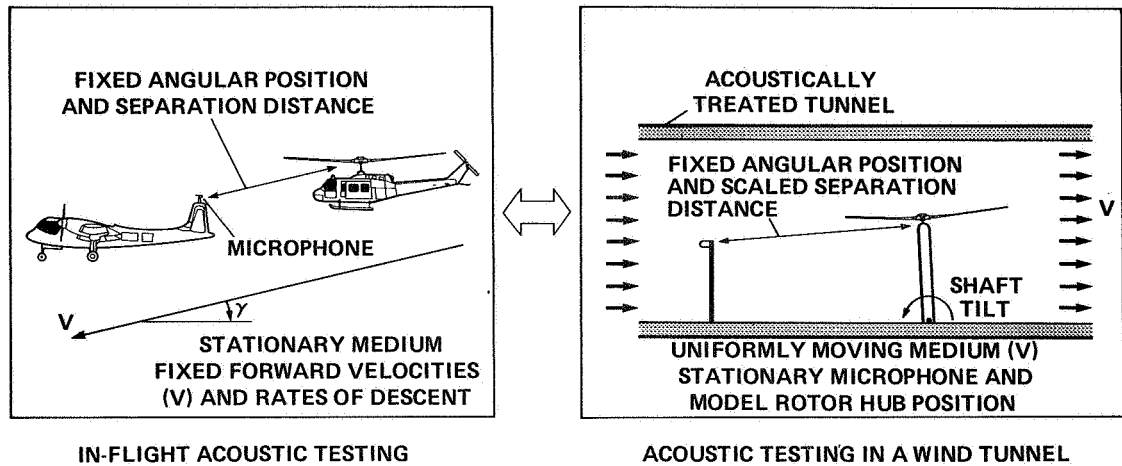Figure 1.- Model and full-scale acoustic testing.
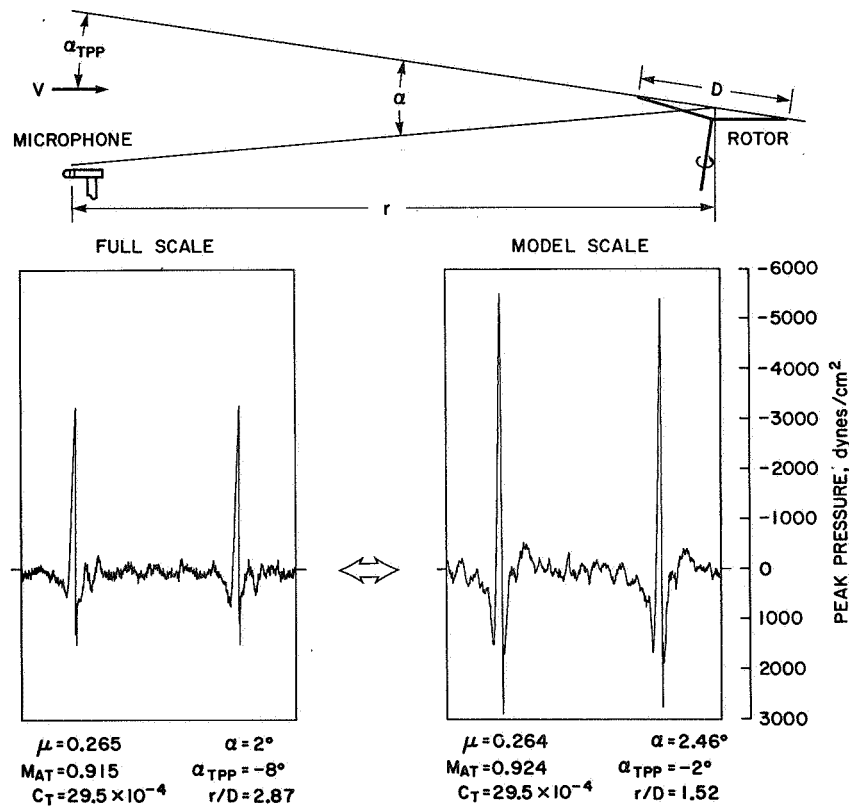

Figure 2.- Waveform comparison - full-scale and model-scale high-speed data. μ denotes advance ratio; M_{AT} denotes Mach number of advancing blade tip; C_T denotes rotor thrust coefficient.
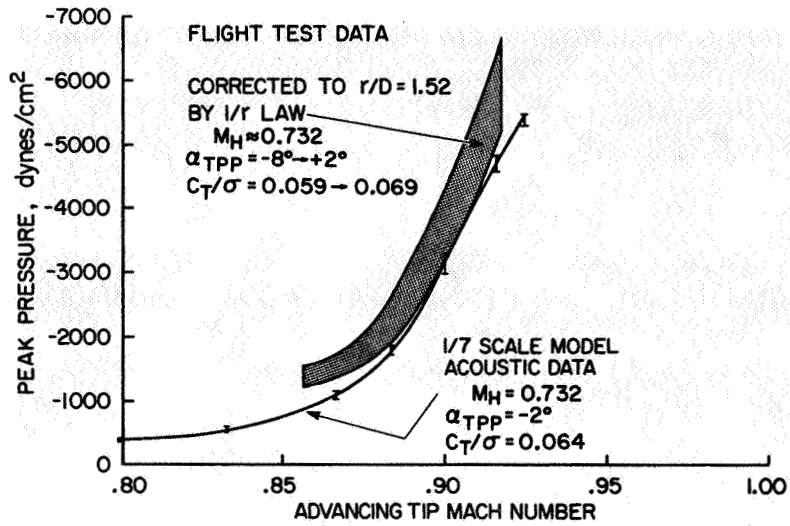
Figure 3.- Peak negative amplitude comparison - full-scale and model-scale high-speed data. M_H denotes hover tip Mach number.

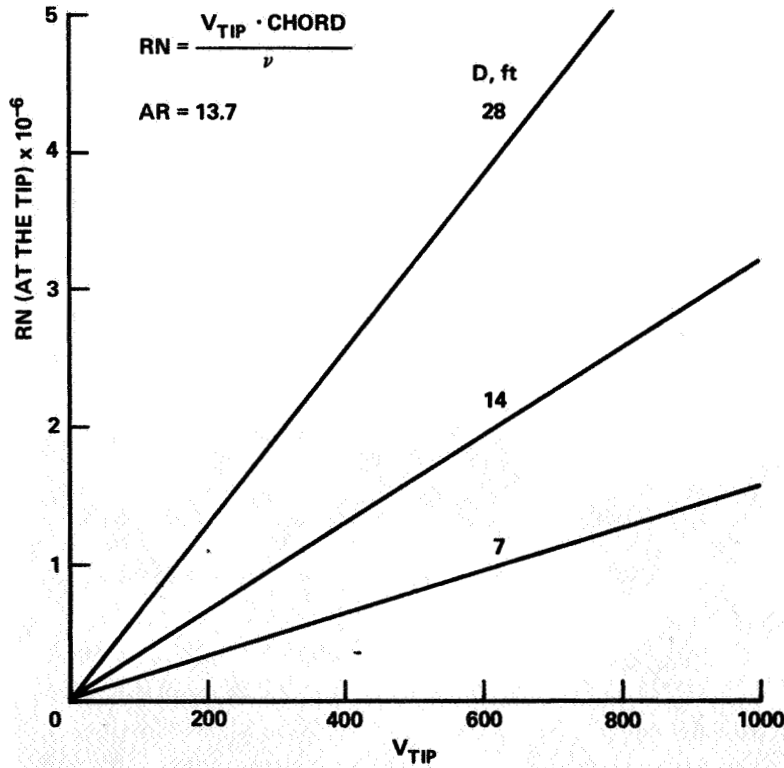
Figure 4.- Reynolds number versus rotor tip velocity.
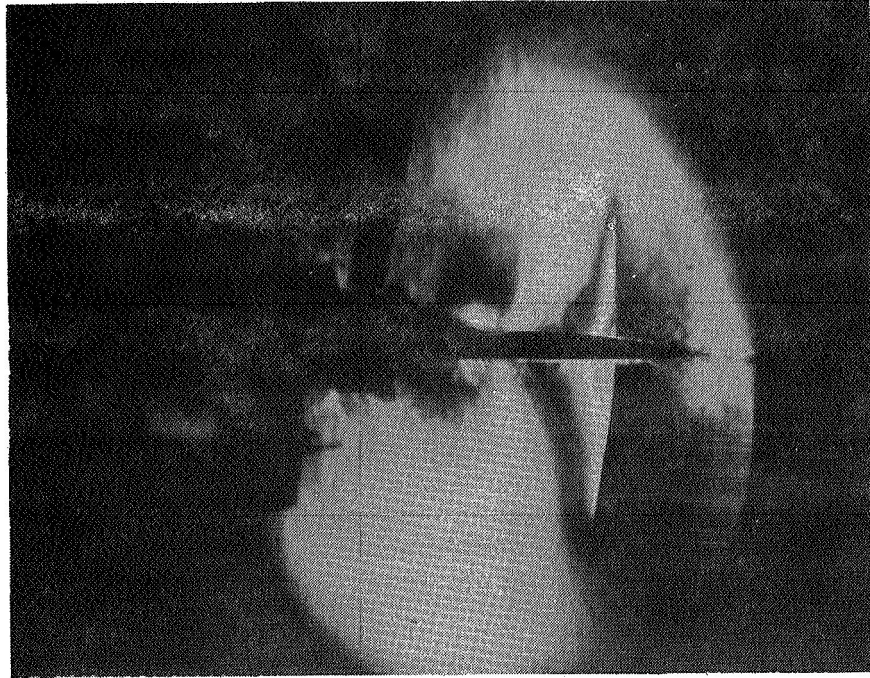
Figure 5.- Scilieren photograph: $\psi \approx 85°$, 1/7-scale UH-1H rotor without a transition strip at high tip speed.

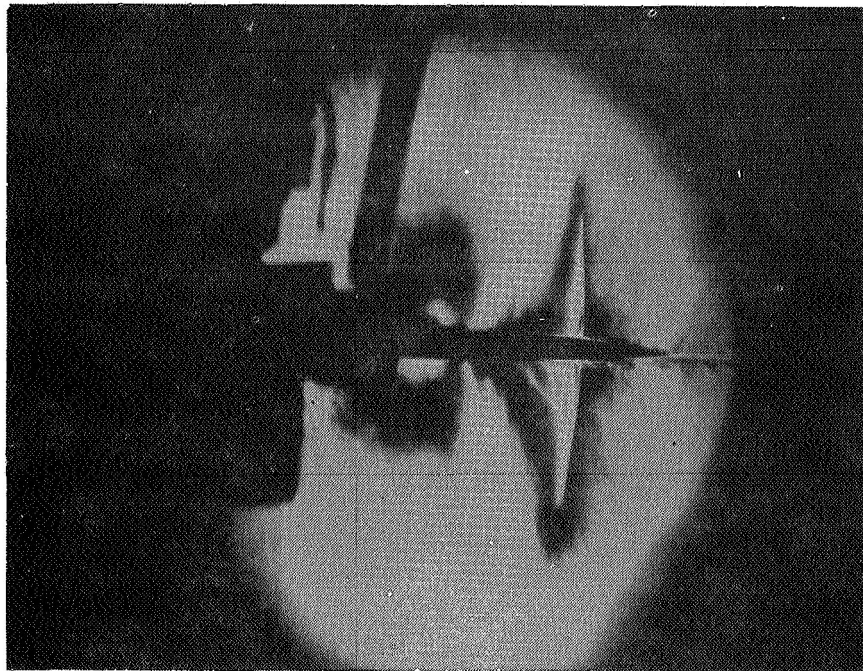Figure 6.- Schlieren photograph: $\psi \approx 85°$, roughened 1/7-scale UH-1H rotor with a transition strip at high tip speed.

DESIGN AND OPERATIONS

E. R. Wood
Hughes Helicopters

INTRODUCTION

Papers presented during this session addressed three categories. These were Design to Improve the Crews' Acoustic Environment; Design to Reduce External Noise Under Cost and Performance Constraints; and Results of External Noise Measurements During Helicopter Operations.

DESIGN TO IMPROVE ACOUSTIC ENVIRONMENT

In this area two extremely interesting papers were presented that reported on advances which promise to lead to reduction in hearing loss and improvement in flight safety. The first paper, entitled "The Effective Acoustic Environment of Army Helicopter Crewmen," by Robert T. Camp, Jr., and Ben T. Mozo, was presented by Bob Camp of the U. S. Army Aeromedical Laboratory. This paper reported on development of a new microphone transmission system which is aimed at filtering out far-field (cabin environment) noise and only accepting the near-field noise, that of the crewman's voice. The microphone accomplished this by discriminating this with respect to the difference in gradient between near- and far-field sound. Author Camp showed figures indicating that present microphones not only accept extraneous signals, but also tend to peak at 3 kHz. He also reported on the SPH-4, a new improved helmet designed to attenuate noise levels transmitted from the cabin environment to the crew member's ear.

The highlight of his presentation was a dramatic demonstration in which he played tapes of aircraft voice transmission as received by ground stations. Two of the recordings were transmissions received from pilots just prior to fatal crashes. The audience was markedly impressed by the large amount of interference noise tending to obscure the pilot's words. The point that the recordings emphasized was that during normal or emergency circumstances, present aircraft microphone systems result in transmission of a voice signal highly contaminated by aircraft noise. Author Camp then demonstrated similar transmittals using the Army's recently developed microphone system. The voice recording was clear and distinct and little interference was noted.

A related paper was that by Peter I. Wheeler, David Rawlinson, Stephen F. Pelc, and Tony P. Dorey, entitled "An Active Noise Reduction System for Aircrew Helmets." The paper was presented by Pete Wheeler of the Institute of Sound and Vibration at the University of Southampton. Wheeler reported on an Active Noise Reduction (ANR) system for air crew helmets, which is a closed-loop system that senses the sound field within the earmuff and feeds back a counter-

signal aimed to cancel out extraneous noise. Results of tests with the ANR
system were shown to have achieved a 13-dB decrease up to 2 kHz. Further,
tests conducted on 18 subjects showed a marked improvement in speech intelli-
gibility. Wheeler reported that presently under development is a new trans-
ducer for the ANR system that would yield a 25-dB attenuation up to 4 kHz.

DESIGN TO REDUCE EXTERNAL NOISE UNDER COST AND PERFORMANCE CONSTRAINTS

The paper entitled "Design of Helicopter Rotors to Noise" and authored by
Edward G. Schaeffer and Harry Sternfeld, Jr., was presented by Ed Schaeffer of
the Boeing Vertol Company. Presented were results from the initial phase of a
NASA contract. The study, when completed, will result in a general method and
sets of design charts to permit evaluation of noise and performance trade-
offs of single rotor helicopters during preliminary design.

Schaeffer reported on initial results of a parametric study. In the ana-
lysis, rotational noise was treated by the method of Lowson and Ollerhead.
Broadband noise was developed for the parametric study from a semi-empirical
equation developed by NASA. Impulsive noise is to be added later. Results to
date showed good correlation with measured whirl tower data. Application of
the prediction to variations in rotor design showed tip speed and thrust as
having the most effect on changing the PNL. A summary of findings from the
interim study is given in table I.

A second and related paper entitled "The Cost of Applying Current Heli-
copter External Noise Reduction Methods While Maintaining Realistic Vehicle
Performance" was authored by Michael A. Bowes of Kaman Aerospace Corporation.
Under contract to the FAA, Kaman has been developing methods to calculate
changes in main rotor noise reduction methods. These changes can be made
within the constraint to maintain realistic vehicle performance. The paper
reported on the results of the analysis, which consisted of three parts:
noise calculation, design and performance calculation, and cost calculation.
RASA's published noise prediction methods were applied in the study for
calculating rotational and broadband noise. Results showed that cost effective
meaningful reduction can be achieved by treating the engine exhaust duct.
Three aircraft were considered: the Hughes Model 500, the Bell Model 205, and
the Sikorsky Model S-61. Figure 1 typifies the data in the paper and shows
the calculated effect on both direct operating cost and life cycle cost with
EPNL reduction. As would be expected for higher levels of noise reduction,
the figure indicates diminishing returns.

EXTERNAL NOISE MEASUREMENTS DURING HELICOPTER OPERATIONS

The effects of helicopter operations on the aircraft's noise signature
were addressed in one paper presented during the session. The paper, entitled
"The Effect of Operations on the Ground Noise Footprints Associated With a
Large Multibladed Nonbanging Helicopter" and authored by David A. Hilton,

834

erbert R. Henderson, Domenic J. Maglieri, and William B. Bigler II, was resented by Dave Hilton of the NASA Langley Research Center. Given were esults of field noise measurements conducted for a CH-53D helicopter at NASA's OMAAR facility. The range, which is approximately 10 km in length and 1 km ide, has a provision for precise radar tracking. Positioned along the range re 38 microphones, 1.2 m in height. Hilton reported on results of level ly-bys at 152 m (500 ft) at airspeeds of 95 and 160 knots. Also, the elicopter was flown in 6° approach landings.

Results of the acoustic measurements were plotted in the form of 70 dBA ontours. Findings showed that the helicopter's acoustic footprint is quite ymmetrical. Tests were conducted for the helicopter operating in a flight egime such that blade slap or impulsive noise was absent. This reviewer was mpressed not only with the information presented with respect to the ground oise footprints, but also with the detailed information given with respect to he outstanding ROMAAR facility. This facility has the capability of cquiring pressure-time histories from the 38 position microphones and then educing these data into corresponding spectra. It provides a unique ational asset that should be made available to various government agencies r helicopter manufacturers for precise acoustic measurements of helicopters.

IMPORTANT REMAINING PROBLEMS

To summarize the session, important problems that remain follow. First, he new developments with respect to helicopter microphones and the cabin noise eduction (ANR) system for aircrew helmets should be introduced into commercial nd military helicopters as soon as possible. It appeared from the papers ddressing these subjects that we have reached the state-of-the-art where the quipment is available to do this.

With respect to the second category of papers, it is recommended that ef-orts be directed at development of means to reduce rotor noise levels without aying a price in performance. For too long, improper priority has been given o noise reduction in helicopters. This is illustrated by table II. If we onsider the commercial helicopter, those impacted are the passenger/user, he community, and the operator. With respect to their needs, the priorities ould be those given in table II. Observe that only safety and low noise evels impact all three categories.

Table III highlights the attitude which should be taken toward achieving ow noise levels if we desire an expanding helicopter market. That is, we an no longer design helicopters while neglecting noise considerations during reliminary design. Instead, low noise levels must be a primary design goal.

As depicted in table III, industry has already demonstrated that quiet elicopters can be designed. Hughes did this in the ARPA-sponsored Quiet elicopter program. But, in that case, where significant noise reductions were chieved, it was found that a price in payload had to be paid. However, the uiet Helicopter program required quieting an existing helicopter rather than

designing a low noise helicopter from the beginning. What is needed, with the assistance of NASA and the Army, is research directed at achieving practical methods for obtaining low noise level helicopters from the onset of design.

TABLE I.- INTERIM RESULTS SUMMARY OF SENSITIVITY OF PNL

TO DESIGN PARAMETER VARIATION

Parameter	Range	Sensitivity*
Tip speed	137 to 290 m/sec (450 to 950 ft/sec)	2 to 5 PNdB per 30.5 m/sec (100 ft/sec)
Thrust	11 121 to 358 876 N (2 500 to 80 000 lb)	2 PNdB per doubling of thrust
Disk loading	96.1 to 574.6 N/m^2 (2 to 12 lb/ft^2)	0.5 PNdB per 96.1 N/m^2 (2 lb/ft^2)
Number of blades per rotor	2 to 6	<0.5 PNdB per blade addition

*Based on varying parameter under study while holding all others constant.

TABLE II.- SPECIALISTS MEETING — HELICOPTER

ACOUSTICS NEEDS

PASSENGER/USER	COMMUNITY	OPERATOR
Safety	Safety	Safety
Low Noise	Low Noise	Low Noise
Low Vibration	Minimum Pollution	High Productivity
Speed	Small Space Requirements	IFR Capability
Convenience		Long Useful Life
IFR Capability		Low Vibration
Low Fare		Good Handling Qualities
		Low Operating Costs

TABLE III.- SPECIALISTS MEETING — HELICOPTER

ACOUSTICS DESIGN

- Low Noise

    - Is a primary design goal
    - Is not a secondary benefit

- Industry Can Design Quiet Helicopters

    - A price must be paid

- Needed: Practical Designs for Low Noise
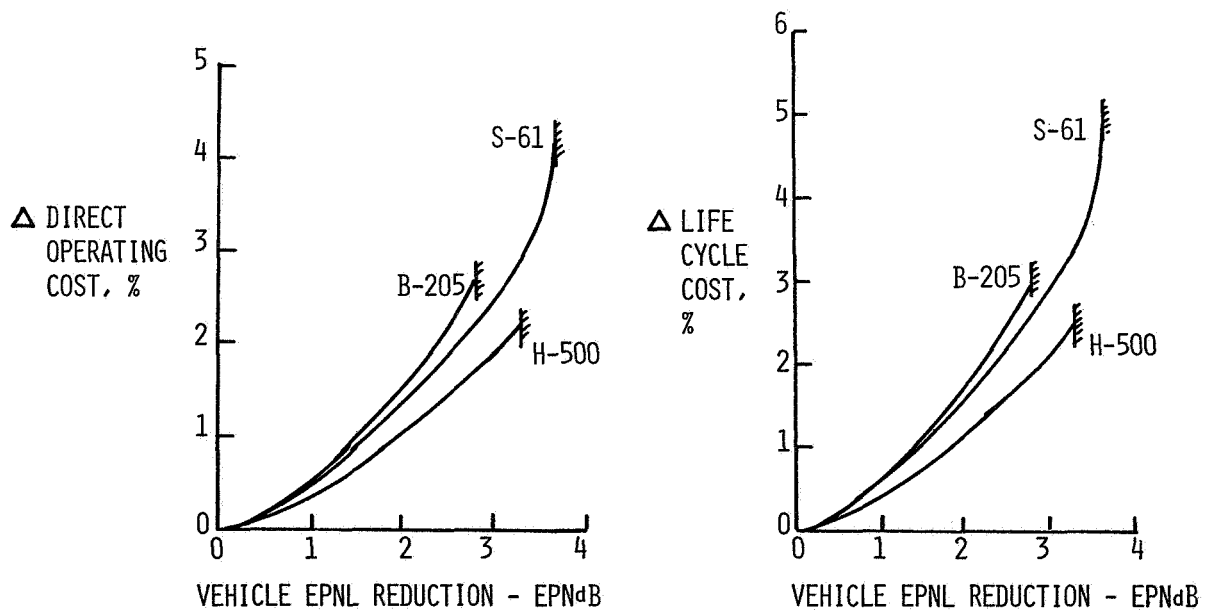
    - From start
    - Add on

Figure 1.- Direct operating cost and life cycle cost of exhaust silencing.

INTERIOR NOISE

Ronald G. Schlegel
Sikorsky Aircraft Division of United Technologies

SUMMARY

The session on helicopter interior noise covered a broad spectrum of
topics which included government service needs, improvements in helmets and
electronic noise cancellation systems, developments in electronic communica-
tions systems, development of criteria for internal noise, development of pre-
liction techniques for gearbox vibration and internal noise levels (with and
without interiors installed), demonstrated problem diagnostic and identifica-
tion techniques and lastly, several actual noise reduction programs conducted
on some recently developed helicopters. In summary, helicopter internal noise
has been identified as a significant problem which could impede the develop-
ment of the helicopter industry if cost effective methods are not found for
its reduction. Although some progress is being made on problem identification
and solution, as indicated by the papers presented at this session, an aggres-
sive attack is required now to expedite this development process.

CONFERENCE COMMENTS

At the start of the conference we heard from Mr. Charles Crawford of the
U. S. Army Aviation Research and Development Command who pointed out that "most
of our current helicopters do not meet the internal noise requirements" and
that, for the most part, the exceedances are significant and require an aggres-
sive attack to achieve the large reductions required. He also pointed out that
a service and industry committee is in the process of revising the current
military specification for internal noise and that, in all probability, the
level requirements will be even more stringent than they are now. In this
latter regard, Harry Sternfeld of Boeing Vertol told of some criteria which
he has been developing under contract with the Army which might be used in
this revised specification.

Bob Camp of the U. S. Army Aeromedical Research Labs re-emphasized the
importance of lower helicopter noise levels in helicopters, coupled with
improved helmets and communication systems, and pointed out the safety hazard
of bad communication. He noted that he and his people have demonstrated im-
proved speech intelligibility and signal-to-noise ratio. John Leverton of
Westland Helicopters and Peter Wheeler of Southhampton University each dis-
cussed work going on in the U.K. to develop better helmets and active noise
reduction systems for helmets. In summary, we appear to be making some
measurable strides to improve crew hearing conservation and speech communica-
tion in spite of the generally high noise environment inside most of our heli-
copters.

The rest of the papers at the session discussed our predictive techniques and the results of some recent programs to develop methods and solutions for lowering helicopter internal noise. Predictive techniques were shown to be largely semiempirical, requiring a fair amount of measured data on generically similar (or identical) aircraft to be used to predict treatment requirements or noise reduction techniques and benefits. Larry Levine and John DeFelice of Sikorsky discussed such a prediction program, which, in fact, gave reasonably good internal noise prediction accuracy for the helicopter evaluated, but which required past experience on transmission forced vibration levels, dynamic transfer/structural decay characteristics, and acoustic panel properties. Charts are presented to make this analysis applicable to other helicopters, but correlation in this regard has not yet been determined.

Two papers were presented, one by Bob Bossler and Mike Bowes of Kaman, the other by Bruce Murray and John Wilby of B.B.&N. which discussed measurement and analytical methods whereby one might predict source levels of a vehicle with measured data and then analytically explore possible solutions. The Kaman study dealt with the transmission source, while the B.B.&N. study dealt with defining what can be done to diagnose the sources once that noise comes into the cabin.

There were two other significant papers not yet discussed. One by Bryan Edwards and Charlie Cox of Bell, discussed case histories of noise reduction research on the Bell 214B, 206B and 222 helicopters. The other, by Messrs. Marze and D'Ambra of Aerospatiale, discussed their noise reduction program on the SA 360 and SA 365 helicopters. Both papers demonstrate the need for and payoff from a detailed, concerted and somewhat imaginative effort for noise reduction. Both programs, however, relied very heavily on an experimental and empirical approach to noise reduction.

SUMMARY OF NEEDS

A chart presented by Bob Bossler and Michael Bowes of Kaman Aerospace showed that transmission generated internal noise has been increasing at an average of 6 dB per decade in the speech interference (and hearing damage) octaves for the same horsepower generated. Figures 10 and 11 of that same paper showed that a systems approach to the problem is absolutely necessary, as methods used to alleviate one problem may aggravate response in another area.

Relative to communication systems, the basic message was that we can and must do better. As a minimum we should at least incorporate the advances offered by current state-of-the-art technology in production aircraft. As far as our predictive capability is concerned, improved detailed dynamic analysis techniques are needed to make the application of architectural room acoustics principles meaningful and allow the design of quiet aircraft from the start. As an example, we need to better know how to analytically treat gearbox isolation and structural damping. Until these more detailed analytical techniques are developed, it appears as though we must rely on combined test and analysis techniques to define and solve the problem of internal noise. Such test techniques are being developed by the individual manufacturers, but some

ssistance is needed to develop them to the point where they are generally
pplicable to a wide range of aircraft designs and then to place them in the
ublic domain.

CONCLUSION

As far as whether or not this problem of internal noise can be solved,
he papers in this session have shown the answer to be definitely yes. It is,
owever, a long, hard process and certainly not one which we can call developed
tate-of-the-art. The U. S. Government agencies which are responsible for
unding research on helicopters have been shown that there is a crying need
or helicopters to generate lower internal noise levels, but at a reasonable
enalty to vehicle performance. The tools to achieve these reductions are not
ery well developed or generally known. The helicopter industry is a small
ndustry when compared to the fixed wing industry, and can in no way afford
he sort of resources that they have been able to expend on the problem of
oise. Further, the helicopter noise generation mechanisms are generally much
ore complex. What is needed now is the commitment from government agencies
o expend the dollars and manpower to help industry solve this difficult and
emanding problem of internal noise.

Human Factors and Criteria

E. Gene Lyman
NASA Headquarters

Finally we have come full circle. Chuck Foster started the meeting off by setting the stage for the problem. We are going to specify noise rules for helicopters, and one of the issues is whether or not an impulsive noise correction factor is needed.

The Human Factors and Criteria session's major thrust was to examine the issue of annoyance, or the psychoacoustic aspect, of helicopter impulsive noise. I would like to provide some background before getting to the bottom line of this session as I saw it. Something about how human response data are used and how they fit into the general scheme of standards and other purposes. Human response data typically are used two ways.

First, one can establish noise level criteria as EPA does, based on health and welfare considerations, and they are only criteria or desirable levels. They are not standards. Or one can develop noise standards, and here the notion of "economical reasonability, technical practicability" enters into the picture.

Noise standards accomplish several purposes as I see it. One, they guide the manufacturers to minimize the clearly important adverse characteristic of the noise signal based on human response considerations. Secondly, in the broader view, they guide the development of products that meet goals to reduce environmental impact. A noise standards does not, and it was spoken to here before, assure acceptance in a community sense of the product.

Aviation has a noise unit, EPNL, for use in setting noise standards. What can we say about EPNL as it pertains to helicopters? Since something like 1969 or 1970, we can say that it has reliably failed to account for the subjective response to the impulsive noise.

Given these circumstances, several options seem open, including (1) a systematic attack on EPNL to identify any deficiencies it may have, (2) identify specific, unique features of helicopter noise to develop valid correction factors, or (3) an approach combining each of the above.

In fact the second course was chosen. Over the last several years, substantial efforts have been devoted to identifying analysis procedures that would permit a reliable correlation between the subjective judgement of helicopter noise and its impulsive signal characteristics.

Now we can get down to what we have learned in the Human Factors and Criteria session. Nothing has emerged that suggests the answers are at hand. We do know a few things. Crest factor is important, and relatively simply means are available to measure it. But the ability to predict the subjective response is relatively poor across all data sets, specifically when we examine the findings between flyover signatures and the steady-state synthesized stimuli.

In the Human Factors and Criteria session, Mr. Leverton suggested the difficulty may be due to inherent characteristics of the EPNL procedure. I believe his observation is important and should be the focus of attention over the short term. Specifically, the recent Langley flight tests at Wallops should provide important new data, and attention should be paid during its analysis to the temporal characteristics of the helicopter noise signature with the view towards understanding the implications from an EPNL point of view. Further, I think the Langley people, or others, should attempt to replicate those flyover studies in lab tests. First, to demonstrate and validate the ability to simulate important characteristics of the helicopter noise stimuli; and secondly, to provide a basis for predicting subjective response to all helicopter types.

1. Report No. NASA CP-2052, Part II	2. Government Accession No.	3. Recipient's Catalog No.
4. Title and Subtitle HELICOPTER ACOUSTICS		5. Report Date August 1978
		6. Performing Organization Code
7. Author(s)		8. Performing Organization Report No. L-12339
		10. Work Unit No. 505-03-13-15
9. Performing Organization Name and Address NASA Langley Research Center Hampton, VA 23665		11. Contract or Grant No.
		13. Type of Report and Period Covered Conference Publication
12. Sponsoring Agency Name and Address National Aeronautics and Space Administration Washington, DC 20546		14. Sponsoring Agency Code

15. Supplementary Notes

16. Abstract

This report is a compilation of papers presented at the International Specialists Symposium on Helicopter Acoustics, jointly sponsored by the American Helicopter Society, the U.S. Army Research Office, and the NASA Langley Research Center on May 22-24, 1978. Included in the topics covered are noise regulation concepts; human factors and criteria; rotor noise generation and control; design, operation and testing for noise control; helicopter noise prediction, and research tools and measurements. Exterior and interior noise problems are addressed both from the physics and engineering as well as the human factors points of view.

17. Key Words (Suggested by Author(s)) Helicopters Acoustics Noise control Human factors Noise regulations	18. Distribution Statement Distribution – Unlimited Subject Category 71

19. Security Classif. (of this report) Unclassified	20. Security Classif. (of this page) Unclassified	21. No. of Pages 450	22. Price* $14.00

National Aeronautics and
Space Administration

Washington, D.C.
20546

SPECIAL FOURTH CLASS MAIL
BOOK

U.S.MAIL

```
   2    1 1U,H,       092278 S00903DS 74073
DEPT OF THE AIR FORCE
AF WEAPONS LABORATORY
ATTN: TECHNICAL LIBRARY (SUL)
KIRTLAND AFB NM 87117
```

NASA

POSTMASTER: If Undeliverable (Section 158
Postal Manual) Do Not Return